frontiers

RESEARCH TOPICS

THE MICROBIAL NITROGEN CYCLE

Topic Editors
Bess B. Ward and Marlene M. Jensen

frontiers in MICROBIOLOGY

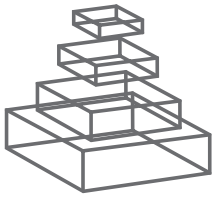

frontiers

ISSN 1664-8714
ISBN 978-2-88919-412-4
DOI 10.3389/978-2-88919-412-4

ABOUT FRONTIERS

Frontiers is more than just an open-access publisher of scholarly articles: it is a pioneering approach to the world of academia, radically improving the way scholarly research is managed. The grand vision of Frontiers is a world where all people have an equal opportunity to seek, share and generate knowledge. Frontiers provides immediate and permanent online open access to all its publications, but this alone is not enough to realize our grand goals.

FRONTIERS JOURNAL SERIES

The Frontiers Journal Series is a multi-tier and interdisciplinary set of open-access, online journals, promising a paradigm shift from the current review, selection and dissemination processes in academic publishing.
All Frontiers journals are driven by researchers for researchers; therefore, they constitute a service to the scholarly community. At the same time, the Frontiers Journal Series operates on a revolutionary invention, the tiered publishing system, initially addressing specific communities of scholars, and gradually climbing up to broader public understanding, thus serving the interests of the lay society, too.

DEDICATION TO QUALITY

Each Frontiers article is a landmark of the highest quality, thanks to genuinely collaborative interactions between authors and review editors, who include some of the world's best academicians. Research must be certified by peers before entering a stream of knowledge that may eventually reach the public - and shape society; therefore, Frontiers only applies the most rigorous and unbiased reviews.
Frontiers revolutionizes research publishing by freely delivering the most outstanding research, evaluated with no bias from both the academic and social point of view.
By applying the most advanced information technologies, Frontiers is catapulting scholarly publishing into a new generation.

WHAT ARE FRONTIERS RESEARCH TOPICS?

Frontiers Research Topics are very popular trademarks of the Frontiers Journals Series: they are collections of at least ten articles, all centered on a particular subject. With their unique mix of varied contributions from Original Research to Review Articles, Frontiers Research Topics unify the most influential researchers, the latest key findings and historical advances in a hot research area!
Find out more on how to host your own Frontiers Research Topic or contribute to one as an author by contacting the Frontiers Editorial Office: researchtopics@frontiersin.org

THE MICROBIAL NITROGEN CYCLE

Topic Editors:
Bess B. Ward, Princeton University, USA
Marlene M. Jensen, Denmark Technical University, Denmark

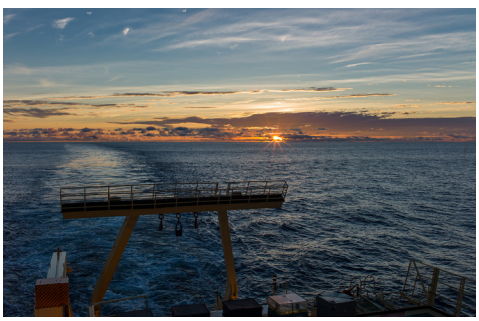

Sunrise over the Eastern Tropical South Pacific, the site of one of the three major oxygen minimum zones in the world ocean. Subsurface OMZs are the sites of intense nitrogen cycling, including the loss processes denitrification and anammox, which control the fixed N inventory of the ocean. The OMZ off Chile and Peru is overlain by some of the world's most productive waters. Incubators shown in the foreground of the photo are used in experiments to measure the rate of primary production and nitrogen fixation in surface waters. Photo credit: Qixing Ji

Nitrogen is an essential element in biological systems, and one that often limits production in both aquatic and terrestrial systems. Due to its requirement in biological macromolecules, its acquisition and cycling have the potential to structure microbial communities, as well as to control productivity on the ecosystem scale. In addition, its versatile redox chemistry is the basis of complex biogeochemical transformations that control the inventory of fixed nitrogen, both in local environments and over geological time.

Although many of the pathways in the microbial nitrogen cycle were described more than a century ago, additional fundamental pathways have been discovered only recently. These findings imply that we still have much to learn about the microbial nitrogen cycle, the organisms responsible for it, and their interactions in natural and human environments. Progress in nitrogen cycle research has been facilitated by recent rapid technological advances, especially in genomics and isotopic approaches. In this Research Topic, we reviewed the leading edge of nitrogen cycle research based on these approaches, as well as by exploring microbial processes in modern ecosystems.

Table of Contents

frontiers in
MICROBIOLOGY

EDITORIAL
published: 24 October 2014
doi: 10.3389/fmicb.2014.00553

The microbial nitrogen cycle

Bess B. Ward[1]* and Marlene M. Jensen[2]

[1] Geosciences, Princeton University, Princeton, NJ, USA
[2] Department of Environmental Engineering, Technical University of Denmark, Lyngby, Denmark
*Correspondence: bbw@princeton.edu

Edited by:
Jonathan P. Zehr, University of California, Santa Cruz, USA

Reviewed by:
Matthew Church, University of Hawaii at Manoa, USA

Keywords: nitrogen cycle, microbial ecology, nitrogen fixation, denitrification, anammox, nitrification

Nitrogen (N) is an essential element in biological systems and one that often limits production in both aquatic and terrestrial systems. Due to its requirement in biological macromolecules, its acquisition and cycling have the potential to structure microbial communities, as well as to control productivity on the ecosystem scale. In addition, its versatile redox chemistry is the basis of complex biogeochemical transformations that control the inventory of fixed (biologically available) N in local environments, on a global scale and over geological time.

Although many of the pathways in the microbial nitrogen cycle were described more than a century ago, additional fundamental pathways have been discovered only recently. These findings imply that we still have much to learn about the microbial nitrogen cycle, the organisms responsible for it and their interactions in natural and human environments. Progress in N cycle research has been facilitated by recent rapid technological advances, especially in genomics and isotopic approaches.

The papers in this issue reflect current research focus on N loss and input processes. The papers are ordered by topic beginning with N fixation, the only biological process that can increase the inventory of fixed N, Knapp (2012) reviewed the literature on the sensitivity of N fixation to dissolved inorganic N and found that neither cultured cyanobacteria nor natural assemblages are completely inhibited by the presence of inorganic N substrates. Knapp was cautious about recent reports of N fixation in subeuphotic mesopelagic waters but concluded that N fixation does occur in the presence of fixed N and in geographic ranges not usually associated with cyanobacteria, which may substantially change our understanding of the global marine N budget. Turk-Kubo et al. (2012) addressed another aspect of the regulation of N fixation and found that different types of N fixers respond differently and variably to Fe or P additions. Both N fixation rates and *nifH* gene expression indicate complex regional and taxonomic sensitivities to micronutrient limitation.

Next we include a series of papers about nitrification, a process which does not directly affect the fixed N inventory, but which links mineralization to the N loss processes by producing oxidized forms of N that can then be used as respiratory substrates. Nitrification has been the subject of increasing research interest since the discovery a decade ago that archaea were involved in ammonium oxidation. A large body of literature has since developed documenting the diversity, abundance and activity of ammonia oxidizing bacteria and archaea (AOB and AOA). For this collection, Casciotti and Buchwald (2012) reviewed knowledge about nitrification gained from the use of N and O isotopes. They found consistent support for the occurrence of nitrification in the euphotic zone, and strong evidence for nitrite reoxidation in suboxic waters. Beman et al. (2012) measured distributions of AOB and AOA in marine sediments and found evidence of their presence as well as active ammonium oxidation in sediments where oxygen was essentially undetectable. They suggest that bioturbation supplies sufficient oxygen intermittently to maintain nitrification even below the typical redox gradient in surficial sediments. Peng et al. (2013) investigated the composition of AOA assemblages in two oxygen minimum zone (OMZ) environments. Although AOA are found in abundance even in waters that contain essentially zero oxygen, active nitrification is not detected there, so Peng et al. (2013) hypothesized that AOA assemblages in oxic waters would differ from those in anoxic waters. Perhaps surprisingly, they found that AOA communities in the OMZ did not differ significantly from those in the overlying surface layer, but they found that biogeography was a significant factor in explaining community composition, as assemblages from the two OMZs (Arabian Sea and Eastern Tropical South Pacific) were significantly different. Bouskill et al. (2012) used trait based modeling to simulate and predict nitrifier community composition and nitrification rates. They found that the relatively simple metabolism of nitrifiers lends itself to such modeling, potentially allowing predictions of the response of nitrification to climate change as reflected in changing environmental parameters such as temperature, pH and substrate availability.

The next topic in the collection deals with the processes by which fixed N is lost from marine ecosystems. Low oxygen environments are of particular interest for nitrogen transformations because they are the sites of fixed N loss via denitrification and anammox. Francis et al. (2013) report on a large sequencing study in sediments of Chesapeake Bay. They found significant geographical patterns in the diversity and composition of denitrifying communities along the estuarine gradient and found that the most abundant types in the environment are only distantly related to anything in culture. Bowles et al. (2012) reported on processes controlling denitrification and the diversity of denitrifying bacteria in the sediments of Guaymas Basin. They found high rates

of denitrification associated with *Beggiatoa* mats, but even higher rates in sediments without mats. The presence of sulfide reduced denitrification rates, even though the community contained large numbers of sequences associated with taxa that are capable of linking sulfide oxidation with nitrate reduction. Kirkpatrick et al. (2012) and Fuchsman et al. (2012) report on denitrification and anammox processes and the microbes involved in those transformations in the narrow suboxic zone of the Black Sea water column. Intrusions of oxygen appear to stimulate autotrophic (i.e., sulfide linked) denitrification in the Bosporus plume, while anammox was not detected under these conditions (Fuchsman et al., 2012). In the northeastern gyre of the Black Sea, Kirkpatrick et al. (2012) found that the distribution and level of expression of denitrification genes was more variable than those of anammox genes, although both processes were consistently detected. They suggest that dynamics in the denitrifier population in response to external factors may explain the apparent decoupling between anammox and denitrification in some environments. Sokoll et al. (2012) report on the same N loss processes in the sediments of the Arabian Sea. The two processes showed opposite patterns along the gradient from shallow to deeper sediments, with the relative importance of anammox increasing from 7 to 40% of the fixed N loss at shallow and deep stations, respectively. The sediments have not previously been quantified as a site for fixed N loss in the Arabian Sea but their contribution appears to be significant.

Finally, we include a single paper on the use of nitrogen by the phytoplankton in the surface ocean. Bertrand and Allen (2012) review the evidence for vitamin B deprivation to mediate N limitation in phytoplankton. Nitrogen limitation in phytoplankton may enhance their demand for Vitamins B12 and B1. Interactions between heterotrophic bacteria, cyanobacteria and eukaryotic phytoplankton around the production and demand for vitamins may influence the timing and structure of phytoplankton blooms, including those of harmful algae.

REFERENCES

Beman, J. M., Bertics, V. J., Braunschweiler, T., and Wilson, J. M. (2012). Quantification of ammonia oxidation rates and the distribution of ammonia-oxidizing archaea and bacteria in marine sediment depth profiles from Catalina Island, California. *Front. Microbiol.* 3:263. doi: 10.3389/fmicb.2012.00263

Bertrand, E. M., and Allen, A. E. (2012). Influence of vitamin B auxotrophy on nitrogen metabolism in eukaryotic phytoplankton. *Front. Microbiol.* 3:375. doi: 10.3389/fmicb.2012.00375

Bouskill, N. J., Tang, J., Riley, W. J., and Brodie, E. L. (2012). Trait-based representation of biological nitrification: model development, testing, and predicted community composition. *Front. Microbiol.* 3:364. doi: 10.3389/fmicb.2012.00364

Bowles, M. W., Nigro, L. M., Teske, A. P., and Joye, S. B. (2012). Denitrification and environmental factors influencing nitrate removal in Guaymas Basin hydrothermally altered sediments. *Front. Microbiol.* 3:377. doi: 10.3389/fmicb.2012.00377

Casciotti, K. L., and Buchwald, C. (2012). Insights on the marine microbial nitrogen cycle from isotopic approaches to nitrification. *Front. Microbiol.* 3:356. doi: 10.3389/fmicb.2012.00356

Francis, C. A., O'Mullan, G. D., Cornwell, J. C., and Ward, B. B. (2013). Transitions in nirS-type denitrifier diversity, community composition, and biogeochemical activity along the Chesapeake Bay estuary. *Front. Microbiol.* 4:237. doi: 10.3389/fmicb.2013.00237

Fuchsman, C. A., Murray, J. W., and Staley, J. T. (2012). Stimulation of autotrophic denitrification by intrusions of the Bosporus Plume into the anoxic Black Sea. *Front. Microbiol.* 3:257. doi: 10.3389/fmicb.2012.00257

Kirkpatrick, J. B., Fuchsman, C. A., Yakushev, E., Staley, J. T., and Murray, J. W. (2012). Concurrent activity of anammox and denitrifying bacteria in the Black Sea. *Front. Microbiol.* 3:256. doi: 10.3389/fmicb.2012.00256

Knapp, A. N. (2012). The sensitivity of marine N_2 fixation to dissolved inorganic nitrogen. *Front. Microbiol.* 3:374. doi: 10.3389/fmicb.2012.00374

Peng, X., Jayakumar, A., and Ward, B. B. (2013). Community composition of ammonia-oxidizing archaea from surface and anoxic depths of oceanic oxygen minimum zones. *Front. Microbiol.* 4:177. doi: 10.3389/fmicb.2013.00177

Sokoll, S., Holtappels, M., Lam, P., Collins, G., Schlüter, M., Lavik, G., et al. (2012). Benthic nitrogen loss in the Arabian Sea off Pakistan. *Front. Microbiol.* 3:395. doi: 10.3389/fmicb.2012.00395

Turk-Kubo, K. A., Achilles, K. M., Serros, T. R. C., Ochiai, M., Montoya, J. P., and Zehr, J. P. (2012). Nitrogenase (*nifH*) gene expression in diazotrophic cyanobacteria in the Tropical North Atlantic in response to nutrient amendments. *Front. Microbiol.* 3:386. doi: 10.3389/fmicb.2012.00386

Conflict of Interest Statement: The authors declare that the research was conducted in the absence of any commercial or financial relationships that could be construed as a potential conflict of interest.

Received: 18 August 2014; accepted: 03 October 2014; published online: 24 October 2014.

*Citation: Ward BB and Jensen MM (2014) The microbial nitrogen cycle. Front. Microbiol. **5**:553. doi: 10.3389/fmicb.2014.00553*

This article was submitted to Aquatic Microbiology, a section of the journal Frontiers in Microbiology.

frontiers in
MICROBIOLOGY

ORIGINAL RESEARCH ARTICLE
published: 18 July 2012
doi: 10.3389/fmicb.2012.00257

Stimulation of autotrophic denitrification by intrusions of the Bosporus Plume into the anoxic Black Sea

Clara A. Fuchsman[1]*, James W. Murray[1] and James T. Staley[2]

[1] School of Oceanography, University of Washington, Seattle, WA, USA
[2] Department of Microbiology, University of Washington, Seattle, WA, USA

Edited by:
Bess B. Ward, Princeton University, USA

Reviewed by:
James T. Hollibaugh, University of Georgia, USA
Andreas Schramm, Aarhus University, Denmark

****Correspondence:***
Clara A. Fuchsman, School of Oceanography, University of Washington, Seattle, WA 98195-5351, USA.
e-mail: cfuchsm1@u.washington.edu

Autotrophic denitrification was measured in the southwestern coastal Black Sea, where the Bosporus Plume injects oxidized chemical species (especially O_2 and NO_3^-) into the oxic, suboxic, and anoxic layers. Prominent oxygen intrusions caused an overlap of NO_x^- and sulfide at the same station where autotrophic denitrification activity was detected with incubation experiments. Several bacteria that have been proposed to oxidize sulfide in other low oxygen environments were found in the Black Sea including SUP05, *Sulfurimonas*, *Arcobacter*, and BS-GSO2. Comparison of TRFLP profiles from this mixing zone station and the Western Gyre (a station not affected by the Bosporus Plume) indicate the greatest relative abundance of *Sulfurimonas* and *Arcobacter* at the appropriate depths at the mixing zone station. The autotrophic gammaproteobacterium BS-GSO2 correlated with ammonium fluxes rather than with sulfide fluxes and the maximum in SUP05 peak height was shallower than the depths where autotrophic denitrification was detected. Notably, anammox activity was not detected at the mixing zone station, though low levels of DNA from the anammox bacteria *Candidatus Scalindua* were present. These results provide evidence for a modified ecosystem with different N_2 production pathways in the southwest coastal region compared to that found in the rest of the Black Sea. Moreover, the same *Sulfurimonas* phylotype (BS139) was previously detected on >30 μm particles in the suboxic zone of the Western Gyre along with DNA of potential sulfate reducers, so it is possible that particle-attached autotrophic denitrification may be an overlooked N_2 production pathway in the central Black Sea as well.

Keywords: Black Sea, autotrophic denitrification, *Sulfurimonas*, Bosporus Plume, anammox

INTRODUCTION

Three processes are responsible for N_2 production under low oxygen conditions: (1) heterotrophic denitrification, which converts nitrate to N_2 using organic matter as a reductant; (2) anammox, an autotrophic process which reduces nitrite with ammonium to form N_2; and (3) autotrophic denitrification, which converts nitrate to N_2 using reduced sulfur species as a reductant. In both heterotrophic and autotrophic denitrification, nitrate is reduced using the same pathway with N_2O as an intermediate product (Sievert et al., 2008). Autotrophic denitrification has been found to be an important N_2 production pathway in anoxic water columns in the Baltic Sea (Hannig et al., 2007), the Benguela upwelling zone (Lavik et al., 2009), and Mariager Fjord, Denmark (Jensen et al., 2009).

The Black Sea is a permanently anoxic basin with a well-defined redox gradient. A 20- to 80-km wide rim current circulates around the perimeter of the Black Sea, enclosing two cyclonic gyres (Poulain et al., 2005). In most of the Black Sea, the Cold Intermediate Layer, with a characteristic core density of $\sigma_\theta \approx 14.5$, represents the lower boundary of direct communication with the surface. The suboxic zone lies between the oxic Cold Intermediate Layer and a 2000-m thick sulfidic zone. In the central Black Sea, autotrophic denitrification is generally not thought to be important. Anammox has been detected in the suboxic zone (Kuypers et al., 2003; Jensen et al., 2008), and nitrate does not co-exist with sulfide or elemental S (Luther et al., 1991; Konovalov et al., 2003; Çoban-Yildiz et al., 2006). However, the potential for S cycling in suboxic waters without the build up of sulfide has recently been demonstrated in the Chilean Oxygen Minimum Zone (Canfield et al., 2010), and DNA from potential sulfate reducers and sulfide oxidizers were found attached to large particulate matter in the Black Sea suboxic zone (Fuchsman et al., 2011).

In the southwestern Black Sea, water from the bottom layer outflow of the Bosporus Strait mixes with the overlying Cold Intermediate Layer forming the Bosporus Plume (Buessler et al., 1991; Murray et al., 1991; Ivanov and Samodurov, 2001). This plume enters the Black Sea as thin intrusions into the oxic, suboxic, and sulfidic layers (Oguz and Rozman, 1991; Konovalov et al., 2003). These intrusions inject oxygen, nitrate, and other oxidized species into the anoxic layers, where they are reduced. The rim current transports water affected by the Bosporus Plume along the coast to the east (Basturk et al., 1999; Konovalov et al., 2003; Poulain et al., 2005). From ratios of ammonium and sulfide, Konovalov and Murray (2001) calculate that 1.11×10^{12} mol of sulfide is missing from the Black Sea, and they attribute this loss to intrusions from the Bosporus Plume. They calculate that this approximates

the re-oxidation of 50% of the sulfide production (Konovalov and Murray, 2001). Most of this sulfide oxidation is due to oxygen, but oxic intrusions also oxidize ammonium to nitrate/nitrite, which in turn can oxidize sulfide. Oxygen, nitrate, and nitrite intrusions were previously described at the mixing zone station in 2001 (Konovalov et al., 2003; Fuchsman et al., 2008). In this case, an intrusion of water from the Bosporus Plume created a second maximum in nitrate (up to 3.3 μM) at depths where sulfide is usually present (Fuchsman et al., 2008). The potential for autotrophic denitrification with sulfide is clearly present in the mixing zone of the Bosporus Plume in the Black Sea.

In this paper we provide evidence for autotrophic denitrification activity in the southwestern region of the Black Sea during an intrusion event of the Bosporus Plume, which caused overlap of NO_x^- and sulfide. We examine likely denitrifying bacteria by comparing depth profiles of normalized TRFLP peak height from the mixing zone with the western central gyre.

MATERIALS AND METHODS

SAMPLING

Samples were collected using a CTD-Rosette with 10 L Niskin bottles and Sea-Bird sensors on three separate cruises in the Western Gyre of the Black Sea: (1) May 2001 at station 6 Voyage 162 leg 16 of the *R/V Knorr* (42°31′ N, 30°43.5′ E), (2) April 2003 at station 19 on Voyage 172 leg 7 of the *R/V Knorr* (42°30′ N, 31°00′ E), and (3) late March 2005 at station 2 on cruise 403 of the *R/V Endeavor* (42°30′ N, 30°45′ E). Samples were also collected in the mixing zone where the Bosporus Plume enters the Black Sea (**Figure 1**) on two cruises: Station 20 in April 2003 (41°26′ N, 29°34′ E) and Station 5 in March 2005 (41°26′ N, 29°34′ E).

NUTRIENT CONCENTRATIONS

Oxygen was measured with the classic Winkler method, and sulfide by iodometric titration (Cline, 1969). In both cases, reagents were bubbled with argon to avoid contamination by atmospheric oxygen. Nitrate, nitrite, and ammonium were analyzed shipboard using a Technicon Autoanalyzer II system (see Fuchsman et al., 2008). Nitrate was not analyzed when there was consensus that sulfide would be in the sample.

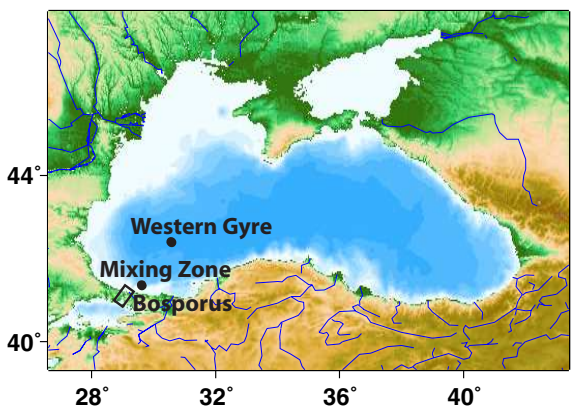

FIGURE 1 | A map of the Black Sea indicating the stations sampled in this study. This map was made with Map-It (http://woodshole.er.usgs.gov/mapit).

DNA

For DNA samples, 2 L were filtered onto 0.2 μm Millipore Sterivex filters. Samples were immediately frozen and stored at −80°C. The DNA extraction protocol was adapted from Vetriani et al. (2003) and includes 8–10 freeze thaw cycles between a dry ice/ethanol bath and a 55°C water bath followed by chemical lysis with lysozyme and proteinase K.

TRFLP

TRFLP profiles were obtained using universal bacterial primers 27F-FAM and 1517R (Vetriani et al., 2003). PCR products were amplified for 30 cycles with annealing temperature of 48°C using Fermentas PCR MasterMix. Purified PCR products (QiaQuick columns; Qiagen) were separately digested overnight with four restriction enzymes (*Hae*III, *Hpy*1881, *Msp*I, *Mnl*I) and immediately ethanol precipitated (Fuchsman et al., 2011). TRFLP data from the Western Gyre in 2005 are previously published in Fuchsman et al. (2011).

Planctomycetes-specific TRFLP profiles were obtained using primers 58F-FAM and 926R (Wang et al., 2002). Planctomycetes PCR products were amplified for 30 cycles with annealing temperature of 60°C. Purified PCR products (QiaQuick columns; Qiagen) were separately digested overnight with restriction enzymes *Hae*III, *Hpy*1881, and *Msp*I and immediately ethanol precipitated (Fuchsman et al., 2012). Planctomycetes-specific TRFLP data for the Western Gyre in 2001, 2003, and 2005 are previously published in Fuchsman et al. (2012).

In both cases, analysis was performed on a MegaBACE 1000 apparatus (Molecular Dynamics) at the University of Washington Marine Molecular Biotechnology Laboratory. Electrophoretic profiles were visualized with Dax software (Van Mierlo Software Consultancy, Netherlands).

TRFLP profiles were normalized by total peak height. If the height of a peak was below 0.3% of the total peak height, the peak was removed from further statistical analyses. TRFLP peaks were binned using frame shifting (Hewson and Fuhrman, 2006) with four frames at 0.5 bp intervals, and for each enzyme, a resemblance matrix was obtained using the Whitaker index, which takes abundance (peak height) into account (Fuchsman et al., 2011). The maximum similarity of the four frames was used to calculate the hierarchical cluster analysis (using the group average) with the Primer 6 program. Error in the resemblance matrix and significance level of the cluster diagram was determined using a Monte Carlo simulation of 50 replicates. We used the average error for both normalized peak height [±46 relative fluorescence units (rfu) where total peak height is 18,000 rfu] and base pairs (±0.08 bp) as determined by 16 sets of duplicate TRFLP profiles. The lowest similarity between Monte Carlo simulated replicates was 77% (Fuchsman et al., 2011). The average error for the Planctomycetes was ±83 rfu, where total peak height was 15,000 rfu, and ±0.06 bp as determined by 14 sets of duplicate TRFLP profiles (Fuchsman et al., 2012).

Due to the replicability of the relative peak heights and the lack of cloning bias (Rainey et al., 1994), and because each PCR was

run under the same conditions with similar extracts from the same amount of material, we were able to compare the relative abundance of the same restriction fragment (i.e., peak height) among multiple samples. However, due to PCR bias (Polz and Cavanaugh, 1998), comparison of heights among different restriction fragments was avoided. In other words, we only compare the relative abundance of a single taxon across samples and never compare the abundances of different taxa. More than one bacterial species can produce the same restriction fragment size; however, by ensuring that the shape of a fragment's relative abundance profile with depth must be supported by multiple enzymes, and by using a small bin size, that risk was reduced. Arguments supporting the similar use of fragment peak height in data from the Southern California time series station can be found in Steele et al. (2011).

Both TRFLP and pyrosequencing of the V6 region of 16S rDNA were obtained from the Western Gyre in 2005 (Fuchsman et al., 2011). Both pyrosequencing and TRFLP avoid cloning biases (Rainey et al., 1994), but still contain PCR biases (Polz and Cavanaugh, 1998; Huse et al., 2008). Despite the use of different primers, conclusions from TRFLP data and V6 tag sequences compare well and we can identify many of the same OTUs using both techniques (Fuchsman et al., 2011). Not only are depth profiles of individual OTUs similar between techniques, but similarity indices are also similar when only V6 pyrosequences with >1% relative abundance were used (Fuchsman et al., 2011).

Predicted fragment lengths for the phylotypes discussed here are shown in **Table 1**. TRFLP OTUs can represent a variety of taxonomic levels depending on the variability in the restriction sites among related phylotypes. Most of the TRFLP OTUs presented here represent a unique sequence or small group of very similar sequences. However, with the restriction enzymes used here *Arcobacter* clone BS098 (GU145483) has the same restriction sites as a wide range of *Arcobacter* members including *Arcobacter nitrofigilis* (L14627) and Black Sea sediment enrichment cultures (AJ271653-4) though they are not particularly closely related. In this paper, TRFLP OTUs are named after the phylotype that was present in the V6 pyrosequence data from the Western Gyre in 2005 (Fuchsman et al., 2011). Full length clones representing these phylotypes were amplified with TRFLP primers and digested with the restriction enzymes (Fuchsman et al., 2011). The actual length of digested clones often differ slightly from the lengths predicted *in silico*. Identifying TRFLP peaks with a database of digested clones greatly improves the reliability of peak identification. Unfortunately, we do not have a digested full length clone representing *Arcobacter* and the *in silico* prediction deviates slightly from the observed peaks (**Table 1**).

AUTOTROPHIC DENITRIFICATION ACTIVITY EXPERIMENTS

Samples for experiments were collected in 2005 at the mixing zone station at the shallowest depth where sulfide was detected ($\sigma_\theta = 16.4$; 192 m), 5 m below that depth ($\sigma_\theta = 16.46$; 197 m) and 20 m below ($\sigma_\theta = 16.52$; 212 m) as well as from a depth where no sulfide was detected ($\sigma_\theta = 16.26$; 178 m). Water was collected directly into 12.5 mL exetainers after overflowing with five times the volume of water. Vials were capped without the presence of bubbles. ^{15}N-labeled NO_3^- was added (for final concentration of 27 μM) to duplicate samples from each depth. Samples and controls were incubated at 7°C for 48 h. Experiments were stopped by addition of $HgCl_2$, and 6 mL of water was replaced by helium and equilibrated overnight. Samples were measured directly by a Finnegan Delta XL isotope ratio mass spectrometer using the Conflo system in the Stable Isotope Lab, School of Oceanography, University of Washington. After gases were measured, the remaining water was analyzed for nitrite and ammonium concentrations using the Technicon Autoanalyzer II.

RESULTS

Due to the strong stratification of the Black Sea by salinity, characteristic inflections in the water-column profiles (such as nitrate) are generally associated with specific density values regardless of when and where they were sampled, but depths vary (Murray et al., 1995). Therefore, results presented here are plotted against

Table 1 | Taxonomy and predicted fragment lengths for the phylotypes discussed in this study.

ID	Taxonomy	Accesssion	*Hae*III	*Hpy*1881	*Msp*I	*Mnl*I	Primer
JK200	*Scalindua*	DQ368308	236	530	259	NA	58F-926R
BS142	WS3	GU145525	206	——	297	144	27F-1512R
BS149	WS3	GU145532	206	——	312	144	27F-1512R
BS129	BS-GSO2	GU145512	——	——	165.3	139.2	27F-1512R
BS098	*Arcobacter*	GU145483	228	——	S:474	S:134	27F-1512R
					T:477	T:140?	
BS134	SAR324	GU145517	406	——	160.9	134	27F-1512R
BS139	*Sulfurimonas*	GU145522	——	——	465	130	27F-1512R
BS077	SUP05	GU145462	193	——	144.2	182.8	27F-1512R
BS007	SAR11 II	GU145392	292	——	147	121	27F-1512R
BS110	Marine group A	GU145495	227	290	450	286	27F-1512R
BS040	*Cytophaga*-like	GU145425	410	——	90	——	27F-1512R

16S rRNA clone PCR products were previously digested with all restriction enzymes and used to identify TRFLP peaks with a range ±0.5 bp from the length of the digested clone (Fuchsman et al., 2011) except for Arcobacter. Dashed line indicates that the enzyme did not cut the sequence within the size range examined (550 bp). NA stands for not applicable, S for in silico, and T for in TRFLP profile.

potential density (σ_θ) rather than depth (m). Densities occurred up to 75 m deeper at the mixing zone station than at the Western Gyre station and varied up to 15 m between years at the Western Gyre (**Figure A1** in Appendix).

CHEMISTRY

A station where the Bosporus Plume enters and mixes with the Black Sea was occupied in late April 2003 and in March 2005 (**Figure 1**). Oxygen, sulfide, and nutrient data from this mixing station are compared to data from the Western Gyre in **Figures 2** and **3**. In 2003, the Western Gyre and Mixing Zone stations had similar oxygen profiles above $\sigma_\theta = 15.9$, but there was an intrusion of oxygen at $\sigma_\theta = 16.15$ at the mixing zone. In 2003, sulfide was first detected at $\sigma_\theta = 16.05$ (81 m) in the Western Gyre, while in the mixing zone, sulfide became detectable above $\sigma_\theta = 16.4$ (192 m; **Figure 2**). Nitrate maximum concentrations were similar between stations in 2003, and nitrite concentrations remained below 0.05 μM (**Figure 3**). In 2005, the oxygen concentrations in the mixing zone station were greatly elevated. Oxygen was measured down to $\sigma_\theta = 16.3$ (7 μM, 180 m; **Figure 2**). Nitrate was 0.5 μM at $\sigma_\theta = 16.3$ while nitrite had a maximum of 0.18 μM and was still elevated at $\sigma_\theta = 16.4$ (192 m; **Figure 3**). Sulfide was not detected at 16.3 on the two casts at this station but was 12 μM just 6 m deeper on the cast not shown here. Given the detection limit for sulfide (3 μM), it is possible that nitrate and sulfide overlapped at this station. In any case, the flux of sulfide to $\sigma_\theta = 16.3$ was 303 μmol m^{-2} day^{-1}, so both nitrate and sulfide were available at this depth.

In the Western Gyre, oxygen extended deeper in the water column in 2005 than in other years. The top of the suboxic zone, defined as <10 μM O_2, was at $\sigma_\theta = 15.38$ (72 m) in 2001, $\sigma_\theta = 15.6$ (61 m) in 2003, and $\sigma_\theta = 15.65$ (78 m) in 2005. Higher oxygen concentrations at the Western Gyre in 2005 are due to a transitory lens of colder, more highly oxygenated water that appeared in the $\sigma_\theta = 15.4$–15.6 range. On March 29th and 30th, the lens of more oxygenated water increased to 22 μM oxygen at $\sigma_\theta = 15.6$ and then decreased to 12 μM at $\sigma_\theta = 15.6$. When microbial samples were collected in 2001, oxygen concentrations (**Figure 2**) decreased from the top of the suboxic zone to near the detection limit at $\sigma_\theta = 15.85$ and then increased to 2–4 μM from $\sigma_\theta = 15.92$–16.05.

Ammonium was consistently present in the lower suboxic zone at both stations and during all years. However ammonium fluxes at $\sigma_\theta = 16.0$ (calculated with diffusion coefficients from Ivanov and Samodurov, 2001) varied between stations and years with the lowest fluxes (190 μmol m^{-2} day^{-1}) at the mixing zone station in 2003 and the western gyre in 2001 and the highest fluxes (330 and 310 μmol m^{-2} day^{-1}) from the mixing zone station in 2005 and from the western gyre in 2003. In 2005, the Western Gyre in 2005 had an intermediate flux (270 μmol m^{-2} day^{-1}).

EVIDENCE FOR AUTOTROPHIC DENITRIFICATION

In incubation experiments at the mixing zone station in 2005, where ^{15}N-labeled NO_3^- was added, enriched $\delta^{30}N_2$, indicative of denitrification, was found in all sulfidic samples but $\delta^{30}N_2$ was not enriched in the non-sulfidic sample [$\sigma_\theta = 16.26$ (178 m; **Figure 4**)]. The amount of enriched N_2 increased with depth from an enrichment of 590‰ at $\sigma_\theta = 16.4$ (192 m) to an enrichment of 9800% at $\sigma_\theta = 16.52$ (212 m). In the ^{15}N-nitrate enriched samples from the sulfidic zone, there was substantial build up of nitrite, up to 18 μM at $\sigma_\theta = 16.46$ (197 m; **Figure 4**) while ammonium concentrations were not different from controls.

Formation of $\delta^{29}N_2$ from ^{15}N - NO_3^- enriched experiments is usually used to denote anammox activity. No enrichment in $\delta^{29}N_2$ was detected in the non-sulfidic sample ($\sigma_\theta = 16.26$), though ammonium was available from the ambient water, indicating that the anammox process was not occurring at that depth even though nitrite and ammonium were present. In the sulfidic zone, $\delta^{29}N_2$ was enriched by 1‰ compared to controls. The relative abundance of *Candidatus Scalindua*, the genus of anammox bacteria in the Black Sea (Kirkpatrick et al., 2006), was low but present at $\sigma_\theta = 16.4$ (**Figure 3**). However, the enrichment in $\delta^{29}N_2$ could also be from denitrification using small amounts of unspiked NO_x^- or N_2O.

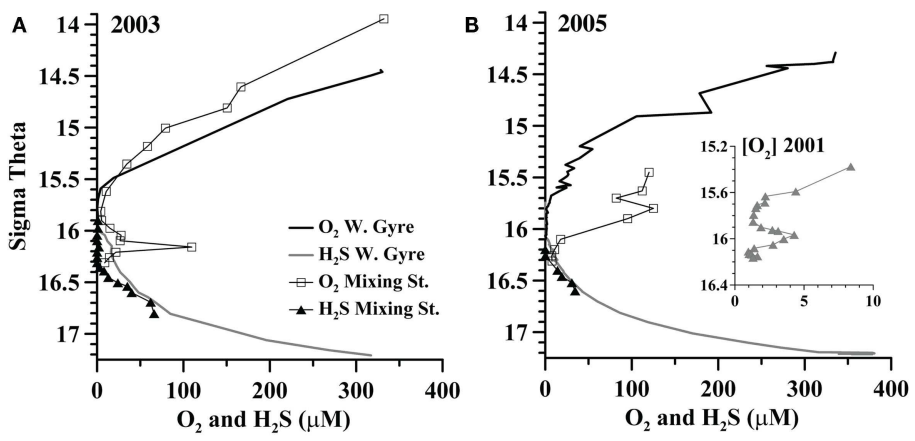

FIGURE 2 | A comparison between oxygen and sulfide in the Western Gyre and mixing zone stations in (A) 2003 and (B) 2005. Inset: oxygen from the Western Gyre in 2001 during an intrusion event.

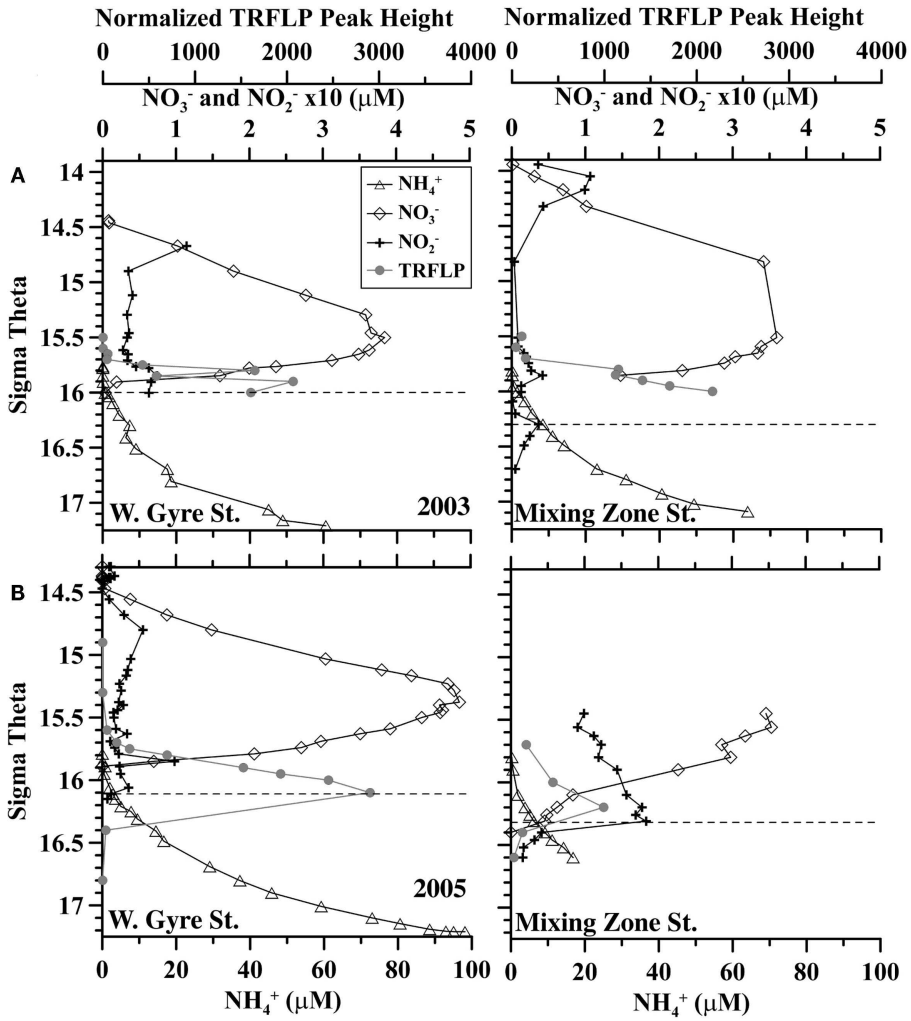

FIGURE 3 | Comparison of nitrate (diamonds), nitrite (crosses), ammonium (triangles), and *Scalindua* normalized TRFLP peak height (gray circles) between the Western Central Gyre and Mixing zone site in (A) 2003 and (B) 2005. Shallowest detection of sulfide is indicated by dashed lines. Average error in normalized peak height is ±83 rfu.

BACTERIAL COMMUNITY

A Spearman Rank correlation between environmental ($[O_2]$, $[H_2S]$, $[NO_3^-]$, $[NH_4^-]$, $[NO_2^-]$, [PMn]) and biological (TRFLP) data indicated that a combination of nitrate, ammonium, and particulate manganese best explained all the bacterial data ($R = 0.698$). Oxygen was not found to be a significant factor, likely because samples with 82 and 5 μM oxygen have similar bacterial communities. However, if instead, the samples are binned into groups >4 μM oxygen, <4 μM oxygen, and sulfidic (see symbols in **Figure 5**), an ANOSIM analysis indicates that oxygen is a significant factor determining the differences in the bacterial communities ($R = 0.460$, $p = 0.001$). In a pairwise test, the >4 μM oxygen and <4 μM oxygen communities were different ($R = 0.316$, $p = 0.001$). The bacterial community does not seem to react linearly to oxygen, but instead to have a threshold.

The community at the mixing site and the central gyre were fundamentally similar. At some depths, the community at the mixing zone has >60% similarity with the Whittaker index to communities at the western central gyre (**Figure 5**). However, there are some significant differences, especially in the sulfidic samples. We directly compared mixing zone station samples from 2005 to the same density at the central gyre station at two depths using the *Msp*I, *Mnl*I, and *Hae*III restriction enzymes with a cutoff of 3% total peak height to reduce noise (**Figure 6**). At $\sigma_\theta = 16.0$, a density surface which contained no oxygen in the Western Gyre (97 m) and 47 μM oxygen at the mixing zone station in 2005 (166 m), the relative abundance of SAR11 clusters II phylotype BS007 was greater in the mixing zone station (**Figure 6**). The relative abundance of potential sulfur cycling bacteria *Sulfurimonas* phylotype BS139 and SUP05 BS077 phylotype along with unidentified *Msp*I peak 498 was also greater at the mixing zone station. The *Hae*III enzyme does not cut *Sulfurimonas* phylotypes, allowing Cytophaga phylotype BS040 to creep above the 3% total peak height threshold for that enzyme. At $\sigma_\theta = 16.4$, a density surface which is in the sulfate

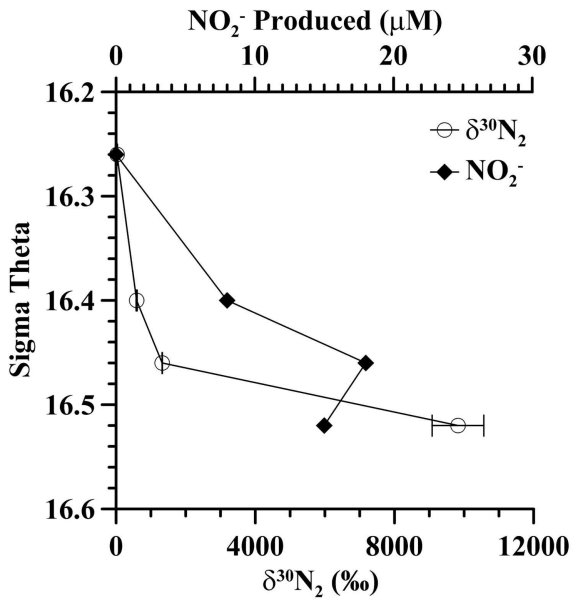

FIGURE 4 | Autotrophic denitrification activity at the mixing zone station in 2005 as indicated by $^{30}N_2$ production (circles) during incubations with ^{15}N-labeled nitrate. Nitrite was also formed during the incubation (diamonds). Error bars indicate duplicate measurements.

reduction zone in the Western Gyre (141 m) but where autotrophic denitrification was detected at the mixing zone station (192 m), potential S oxidizers SUP05 BS077, *Sulfurimonas* BS139, *Arcobacter* BS098, and unidentified *Msp*I peak 91/Mnl peak 254 pair had much higher normalized peak height in the mixing zone station compared to the Western Gyre (**Figure 6**). For the *Hae*III enzyme, peak 206 representing the Black Sea WS3 group and unidentified peak 339 also had higher normalized peak height for the mixing station. The 206 cut site from *Hae*III represents multiple WS3 phylotypes that are separate peaks when different restriction enzymes were used. Two WS3 phylotypes have been identified by TRFLP in the sulfidic zone of the Black Sea (Fuchsman et al., 2011, supplemental).

When we look at all profiles over five stations instead of just the two depths in 2005, we see that the relative abundances of BS139 from the *Sulfurimonas* genus of epsilonproteobacteria, BS077 from the SUP05 group of gammaproteobacteria, BS098 from the *Arcobacter* genus of epsilonproteobacteria, and unidentified *Msp*I peak 91/Mnl peak 254 pair are clearly greater in the mixing zone station (**Figures 7** and **8**). Peaks 91/254 are in fact only seen in the mixing zone station in 2005 (**Figure 8**). Contrastingly, both group WS3 and peak 339 (*Hae*III) have maxima in the sulfidic zone in the Western gyre (**Figure 8**), implying that their presence at the mixing zone station is not due to the intrusions there.

This dataset also allows us to examine variability in the bacterial community within the Western Gyre. Upper suboxic zone samples ($\sigma_\theta = 15.5$–15.7) from the Western Gyre in 2003 are included in the Suboxic cluster while upper suboxic zone samples from 2001 and 2005 are included in the Hypoxic cluster (**Figure 5**), perhaps due to the influence of oxygen intrusions in 2001 and 2005. In the deep suboxic zone, samples from 2001 clustered in a separate subcluster from samples from 2003 and 2005 (**Figure 5**). There was an oxygen intrusion into the deep suboxic zone in 2001 (**Figure 2**) and the particulate manganese maximum was also deeper. The maximum in particulate manganese at the Western Gyre varied $\sigma_\theta = 16.05$ in 2001 (Konovalov et al., 2003) to $\sigma_\theta = 15.8$–15.85 in 2003 and 2005 (Trowborst et al., 2006; Fuchsman et al., 2011).

PLANCTOMYCETES COMMUNITY

The members of the Planctomycetes community at the mixing station were similar to those described in Fuchsman et al. (2012) with 60–70% community similarity to samples from the Western Gyre. *Msp*I peak 263, representing WS3 bacteria, had high peak height in the sulfidic mixing zone samples from 2005, corroborating information from the bacterial primers. At the mixing zone station, *Scalindua* peak height increased with depth starting at $\sigma_\theta = 15.7$ in 2003, while in 2005 *Scalindua* peak height had a maximum at $\sigma_\theta = 16.2$ (**Figure 3**). At $\sigma_\theta = 16.0$, in the mixing zone station, *Scalindua* normalized peak height was significantly lower in 2005 than in 2003 (**Figure 3**).

The chemical parameters that most strongly correlated with the Planctomycetes community similarity among samples (Spearman Rank correlation) were nitrate, ammonium, and sulfide ($R = 0.730$ when combined), but ammonium and nitrate without sulfide explained most of the data ($R = 0.729$). Oxygen concentration was not found to be an important variable. However, the bacterial communities generally cluster by the presence of >3 or <3 μM oxygen or sulfide (ANOSIM $R = 0.386$, $p = 0.001$) supporting the importance of an oxygen threshold.

DISCUSSION

In the southwestern coastal Black Sea, intrusions from the Bosporus Plume inject oxygen, nitrate, and other oxidized species into the sulfidic layer (Konovalov et al., 2003). In 2005, there was abundant evidence of intrusions at the mixing zone station. Oxygen, usually only measurable to around $\sigma_\theta = 15.8$, was measured down to $\sigma_\theta = 16.3$ (**Figure 2**). Nitrate and nitrite were also unusually elevated at $\sigma_\theta = 16.3$ and nitrite concentrations were still elevated at $\sigma_\theta = 16.4$ (**Figure 3**). Sulfide was not detected at 16.3 (detection limit 3 μM), but the flux of sulfide to $\sigma_\theta = 16.3$ was 303 μmol m^{-2} day^{-1}, so both nitrate and sulfide were available. In experiments at the mixing zone station in 2005, where ^{15}N-labeled NO_3^- was added, enriched $\delta^{30}N_2$ was found in all sulfidic samples but not in the non-sulfidic sample ($\sigma_\theta = 16.26$; **Figure 4**). This implies autotrophic denitrification activity with sulfide as an electron donor. If we convert these enrichments to experimental rates, they range from 4 nM N day^{-1} at $\sigma_\theta = 16.4$ to 10 nM N day^{-1} at $\sigma_\theta = 16.46$ and 78 nM N day^{-1} at $\sigma_\theta = 16.52$. These rates are an order of magnitude lower than experiments with comparable nitrate concentrations in Mariager Fjord (Jensen et al., 2009). These experimental rates do not represent *in situ* rates because nitrate additions (27 μM) were much higher than the largest values seen *in situ* (~3 μM; Fuchsman et al., 2008). Additionally, the positive dependence of autotrophic denitrification on sulfide concentration and the large accumulation of nitrite in the experiments (18 μM) are both consistent with trends seen

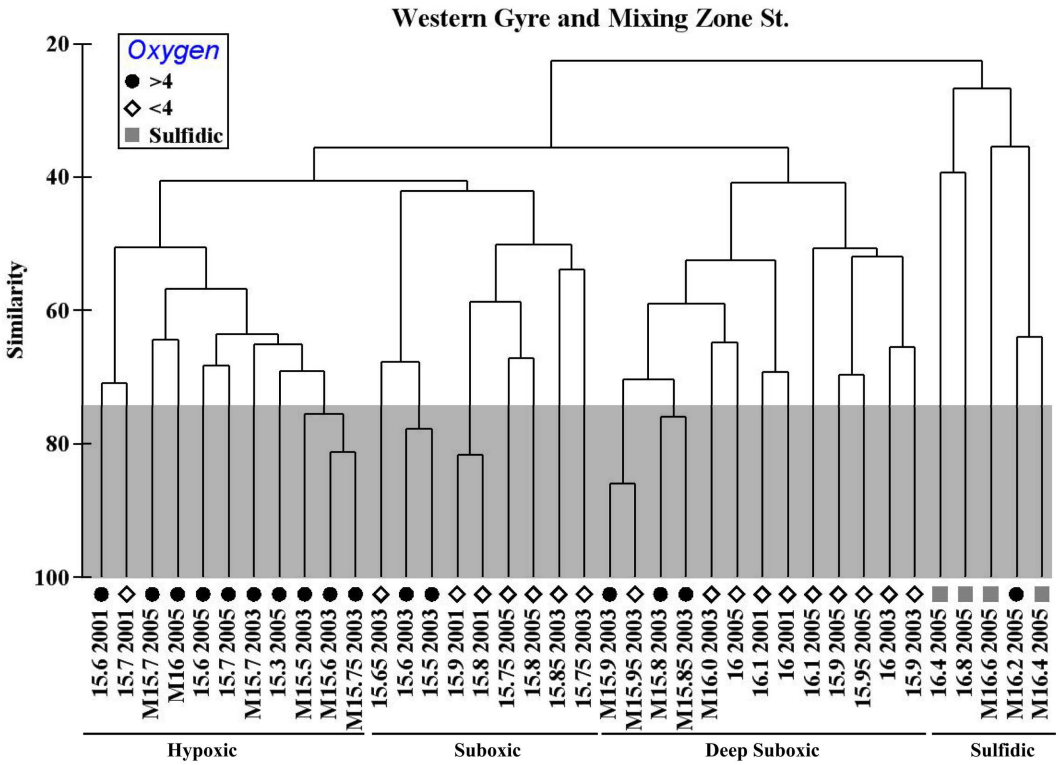

FIGURE 5 | Hierarchical cluster of the bacterial community as determined by TRFLP data (*Msp*I) from Western Gyre in 2001, 2003, and 2005 and Mixing Zone Site in 2003 and 2005. Samples are named by the sigma theta and year where they were obtained. M indicates mixing zone station. Symbols indicate oxygen concentrations: >4 μM O_2 (circle), <4 μM O_2 (diamond), sulfidic (square). Error was determined using a Monte Carlo simulation; nodes within the gray box are not significantly different (e.g., $\sigma_\theta = 15.5$–15.75 from the 2003 mixing zone site).

in Mariager Fjord, Denmark (Jensen et al., 2009) and may be due to sulfide limitation. The accumulation of nitrite could also be due to the slower kinetics of nitrite reduction compared to nitrate reduction (Jensen et al., 2009) or to bacteria that merely perform the first step of nitrate reduction (Zumft, 1997). However, the consumption of five moles of sulfide for every two moles of nitrate (Jensen et al., 2009) indicates that sulfide limitation was likely in all of the experiments, but would have been especially important in the $\sigma_\theta = 16.4$ experiment (14 μM H_2S). While not indicating *in situ* rates, these experiments do indicate the ability of the bacterial community in the sulfidic zone of the mixing station to reduce nitrate when it becomes available, likely through intrusions from the Bosporus Plume.

Though the highest denitrification activity was seen at $\sigma_\theta = 16.52$ with the addition of nitrate (**Figure 4**), it seems more likely that *in situ* rates at the time of sampling were higher between $\sigma_\theta = 16.3$ and 16.4 where *in situ* nitrate/nitrite were naturally present (**Figure 3**). We also have DNA samples from $\sigma_\theta = 16.4$. The relative abundances of BS139 from the *Sulfurimonas* genus of epsilonproteobacteria, BS077 from the SUP05 group of gammaproteobacteria, BS098 from the *Arcobacter* genus of epsilonproteobacteria, and unidentified *Msp*I peak 91/Mnl peak 254 pair are all clearly greater at $\sigma_\theta = 16.4$ of the mixing zone station in 2005 compared to the Western Gyre (**Figure 6**). Members of the *Candidatus* genus *Scalindua*, known to mediate the anammox reaction but typically missed by universal bacterial primers, were also present at $\sigma_\theta = 16.4$ at the mixing zone. Additionally, a labeled bicarbonate stable isotope probing experiment at the chemosynthesis maximum in the upper sulfidic zone of the central Black Sea in 2007, attributed autotrophic activity not only to members of the genus *Sulfurimonas* and the SUP05 (Glaubitz et al., 2010), found to be enriched in the mixing zone station in this study, but also to members of the BS-GSO2 group of gammaproteobacteria (Glaubitz et al., 2010). In the following section we examine these six bacteria to determine which was the most likely to mediate N_2 production in the mixing zone site in 2005.

ANAMMOX

Sequences of potential anammox bacteria in the Black Sea are of the *Candidatus Scalindua* genus (Kirkpatrick et al., 2006). In the mixing zone station in 2005, *Scalindua* peak height had a maximum at $\sigma_\theta = 16.2$ (**Figure 3**). This maximum was much reduced from the maximum at the same station in 2003 and from the Western Gyre in 2005 (**Figure 3**). Anammox activity was not detected at the mixing zone station in 2005, though only one depth was examined. However, that depth did correspond to the maximum in *Scalindua* peak height. *Scalindua* DNA at the mixing zone station may be remnants from previous activity, or *Scalindua* may be mediating Fe or Mn oxide reduction (van de Vossenberg et al., 2008).

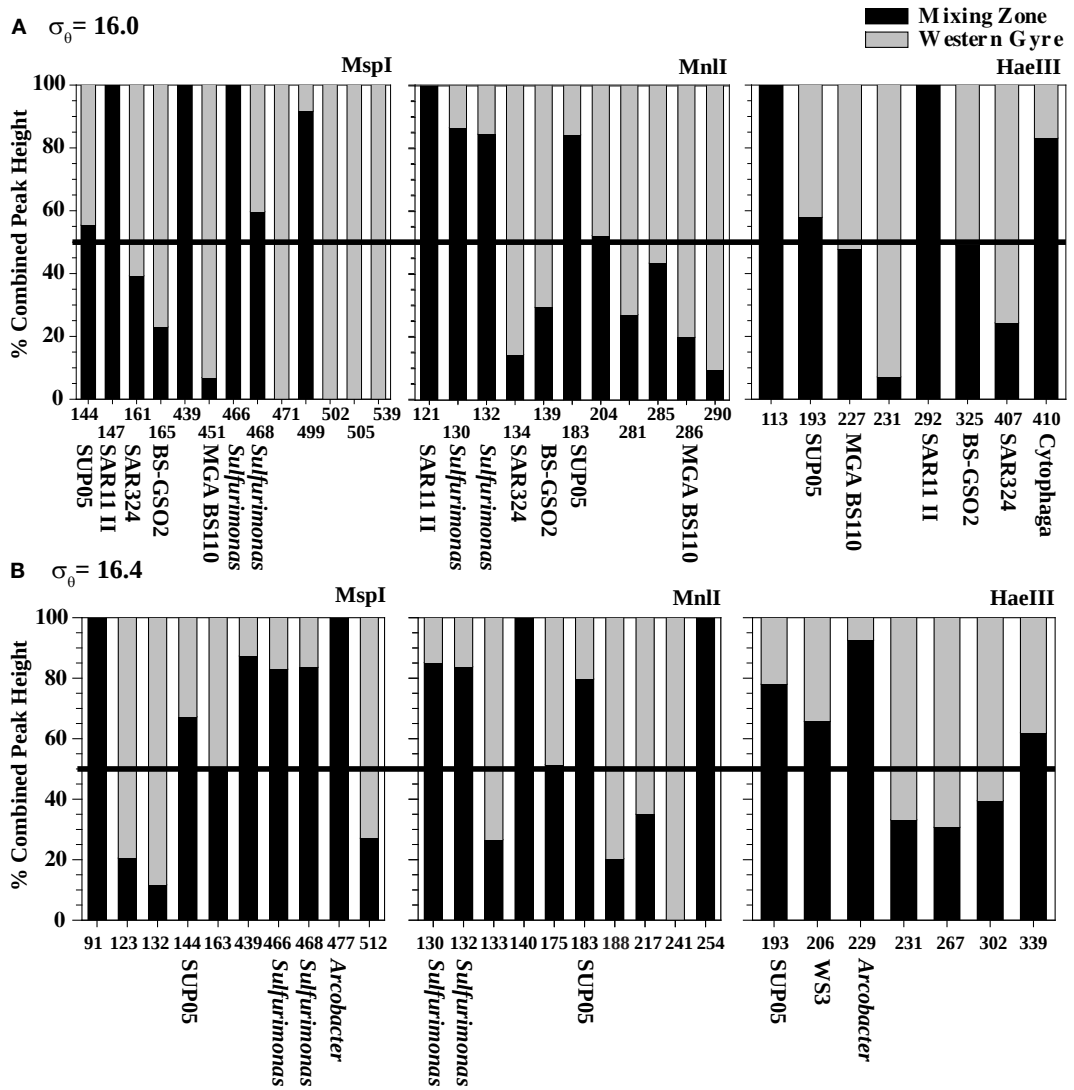

FIGURE 6 | A comparison of TRFLP chromatograms from (A) $\sigma_\theta = 16.0$ and (B) $\sigma_\theta = 16.4$ for three restriction enzymes at the Mixing Zone Station (black) and the Western Gyre (gray) where the *x*-axis displays different TRFLP peaks and the *y*-axis is the percent of peak height associated with each chromatogram. The black line at 50% indicates where the relative peak height is the same at each station. Only peaks with normalized peak height above 3% of the total peak height are shown.

SUP05

A metagenome of SUP05 bacteria from Saanich Inlet, a seasonally anoxic fjord on Vancouver Island, Canada indicated that the SUP05 group of gammaproteobacteria had the ability to autotrophically oxidize sulfur compounds and also contain genes for the production of N_2O (Walsh et al., 2009). Subsequently, SUP05 phylotypes were shown to be autotrophic in the upper sulfidic zone of the central Black Sea (Glaubitz et al., 2010). Transcripts of sulfur oxidizing genes from the SUP05 group have also been detected in the Chilean Oxygen Minimum Zone (Stewart et al., 2012). Altogether, this evidence could suggest a potential for autotrophic denitrification. Normalized TRFLP peak height for BS077 (the dominant SUP05 phylotype in the Black Sea) was much greater in the mixing zone stations than in the Western Central Gyre stations. However, phylotype BS077 had a maximum peak height at $\sigma_\theta = 16.2$ in the 2005 mixing zone station, which was shallower than the depths where autotrophic denitrification was detected (**Figure 7**).

BS-GSO2

A second group of uncultured gammaproteobacteria, BS-GSO2, was implicated in autotrophic activity in the upper sulfidic zone of both the Black and the Baltic Seas (Glaubitz et al., 2009, 2010) and linked to autotrophic denitrification in the Benguela upwelling zone (Lavik et al., 2009). Autotrophic activity in these sulfidic zones implies this group might be involved in sulfur oxidation (Glaubitz et al., 2009, 2010). BS129 (the dominant BS-GSO2 phylotype in the Black Sea) was identified in all years and stations but its relative abundance was greater in the Western Gyre than in the mixing zone station in 2005 (**Figure 8**). At the mixing station in 2005, BS129

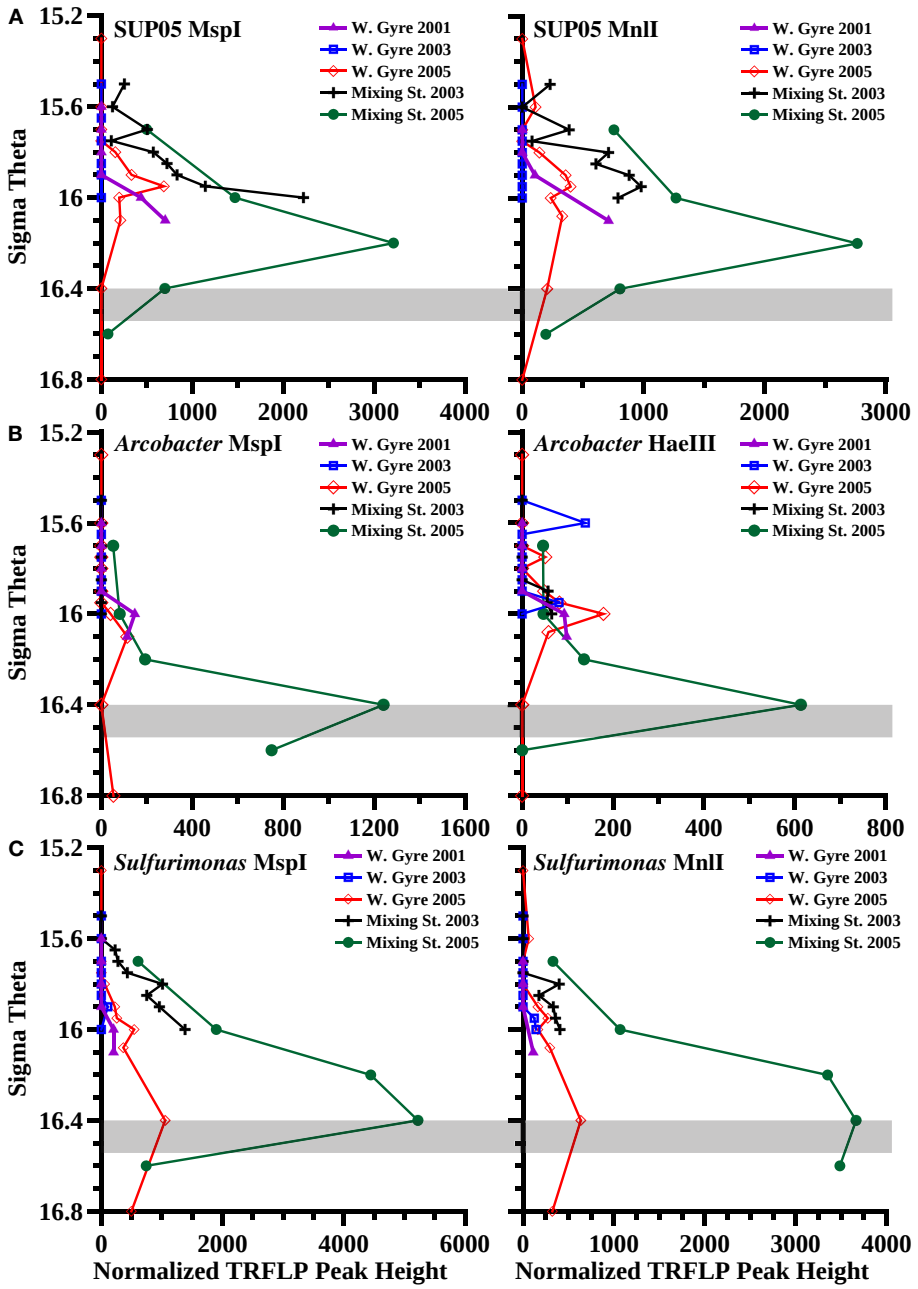

FIGURE 7 | TRFLP peak height depth profiles of autotrophic denitrification candidates that are enriched at the mixing zone station in 2005, obtained using multiple restriction enzymes, for the five stations: (A) Black Sea SUP05 phylotype BS077, (B) *Arcobacter* phylotype BS098, (C) Black Sea *Sulfurimonas* phylotype BS139. The gray box indicates the range of autotrophic denitrification activity seen in the Mixing Zone station in 2005 (**Figure 4**).

had a maximum peak height at $\sigma_\theta = 16.2$, and its relative peak height was greatly reduced at $\sigma_\theta = 16.4$, where autotrophic denitrification activity was detected (**Figure 8**). In fact, the normalized peak height for BS129 at $\sigma_\theta = 16.0$ appears to be anti-correlated with ammonium flux (**Figure 8**; $p = 0.004$ for *Msp*I). Normalized TRFLP peak height was greatest at the mixing zone station in 2003 and the Western Gyre in 2001 where ammonium fluxes were lowest. BS129 peak height was lowest in the Western Gyre in 2003 and the mixing zone station in 2005, both of which had high ammonium fluxes. Interestingly, an unknown gammaproteobacterium was found to mediate ammonium oxidation in the lower suboxic zone (Lam et al., 2007). Therefore, considering its correlation with ammonium fluxes, depth profile (**Figure 8**), and ability to fix carbon (Glaubitz et al., 2010), BS129 seems a likely candidate for autotrophic ammonium oxidation, but not autotrophic denitrification.

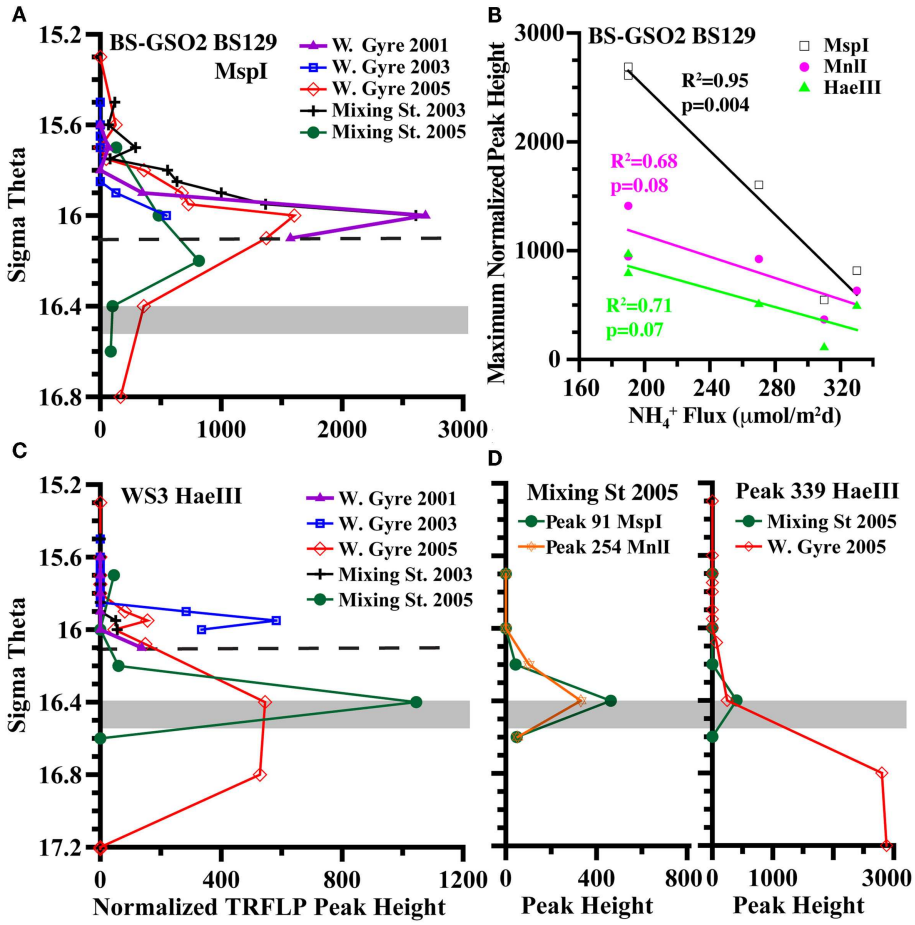

FIGURE 8 | Examination of autotrophic denitrification candidates (A) TRFLP peak height depth profiles of BS-GSO2 phylotype BS129, (B) the inverse correlation of BS129 peak height with ammonium fluxes at $\sigma_\theta = 16.0$ at all five stations with a comparison between restriction enzymes, (C) TRFLP peak height depth profiles of WS3, and (D) depth profiles of unidentified peak 91 from digestion with *Msp*I and peak 254 from digestion with *Mnl*I and peak 339 from digestion with *Hae*III. Dashed line indicates a typical depth for the shallowest detection of sulfide in the Western Gyre. The gray box indicates the range of autotrophic denitrification activity seen in the Mixing Zone station in 2005 (**Figure 4**).

ARCOBACTER

In the Benguela upwelling zone the epsilonproteobacteria *Arcobacter* were found at depths where autotrophic denitrification occurred (Lavik et al., 2009). *Arcobacter sulfidicus* has been found to autotrophically oxidize sulfide with oxygen forming elemental S mats (Wirsen et al., 2002; Sievert et al., 2007). *Arcobacter* phylotypes have been associated with such mats at sulfidic/oxic boundaries at hydrothermal vents, cold seeps, and the sediment water interface (Taylor and Wirsen, 1997; Moussard et al., 2006; Grunke et al., 2011). The *Arcobacter* depth profile in the Black Sea (**Figure 7**) would be consistent with either autotrophic denitrification or microaerophilic sulfide oxidation. The cultured representative, *A. sulfidicus,* which is closely related to BS098 found in the Black Sea (**Figure 9**), is microaerophilic and is incapable of oxidizing sulfide with nitrate (Wirsen et al., 2002). Some *Arcobacter* species can reduce nitrate heterotrophically (Heylen et al., 2006) but these isolates are not closely related to BS098 (**Figure 9**). Other *Arcobacter* enrichment cultures from sediments, such as Black Sea sediments (Thamdrup et al., 2000), have been found to reduce manganese oxides with acetate (Vandieken et al., 2012). The maximum in particulate manganese at the mixing zone station in 2005 is at $\sigma_\theta = 16.3$ (B. Tebo, personal communication). The versatility of the *Arcobacter* genus makes predictions of the activity of the species at the mixing zone station particularly difficult.

SULFURIMONAS

Members of the *Sulfurimonas* genus of Epsilonproteobacteria have been associated with autotrophic denitrification in the marine environment; many known strains of *Sulfurimonas* from hydrothermal vents and marine sediments can carry out autotrophic denitrification (Gevertz et al., 2000; Takai et al., 2006), and environmental clones affiliated with the genus have been extracted from marine sediments and correlated with active autotrophic denitrification (Shao et al., 2009; Zhang et al., 2009). *Sulfurimonas* phylotype GD17 has been found to mediate autotrophic denitrification in the Baltic Sea (Brettar et al., 2006). Black Sea sequences are closely related to GD17 from the Baltic Sea as well as to *Sulfurimonas denitrificans* (Glaubitz et al., 2010;

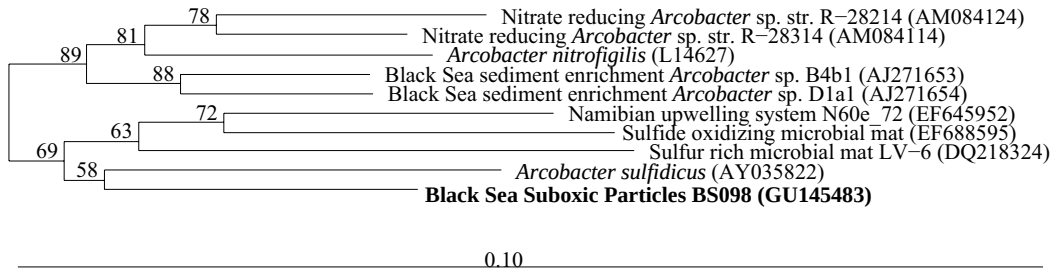

FIGURE 9 | A bootstrapped (1000) neighbor joining phylogenetic tree of relevant members of the *Arcobacter* genus was created in arb after aligning to a master database using NAST (greengenes.lbl.gov). The *Arcobacter* sequence from the Black Sea suboxic zone is in bold.

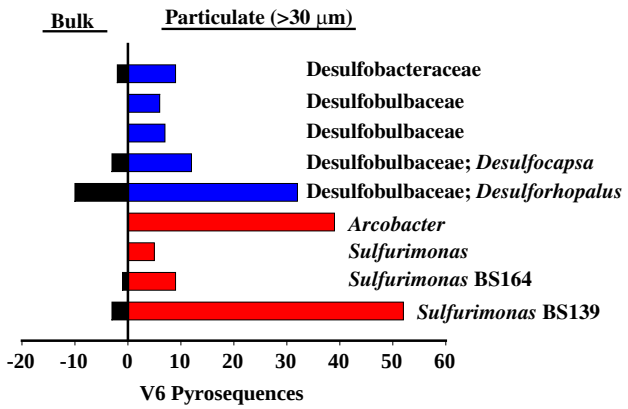

FIGURE 10 | Examples of potential sulfate reducers (blue) or sulfide oxidizers (red) enriched in particulate sample (30 μm filter) from $\sigma_\theta = 15.8$ in the Western Gyre in 2005 compared to a bulk sample from the same depth, as determined from V6 pyrosequences (data from Fuchsman et al., 2011, supplemental).

Fuchsman et al., 2011). The normalized TRFLP peak height of *Sulfurimonas* phylotype BS139 was up to 10 times greater in the mixing zone stations than in the Western Central Gyre stations (**Figure 7**). The phylotype BS139 had a maximum peak height from $\sigma_\theta = 16.2$–16.4 in the 2005 mixing zone station and still had significant abundance at $\sigma_\theta = 16.6$ (**Figure 7**). Thus the *Sulfurimonas* peak spanned the depths where autotrophic denitrification activity was detected (**Figure 4**) and remains the leading candidate for mediating autotrophic denitrification.

Sulfurimonas was also enriched at $\sigma_\theta = 16.2$. The presence of *Sulfurimonas* DNA at the Western Gyre site in 2005, 2007, and 1988 (Vetriani et al., 2003; Glaubitz et al., 2010) also implies *Sulfurimonas* can live at depths where sulfide is not detectable. There are two possible explanations for this. First, the depth profile for thiosulfate, another potential electron source for autotrophic bacteria (Takai et al., 2006) is unknown in the Black Sea during this time period. Second, pyrosequences of the V6 variable region of 16S rRNA identical to *Sulfurimonas* phylotype BS139 were also present in the particulate fraction in the suboxic zone in Western Gyre of the Black Sea, along with a *Desulfobacter* phylotype BS105 (GU145490) and pyrosequences from potential sulfate reducers from the Desulfobulbaceae and Desulfuromonadales families (**Figure 10**; data from Fuchsman et al., 2011). Many but not all cultured members of these families are sulfate reducers (e.g., Finster et al., 1994; Hoeft et al., 2004; Tarpgaard et al., 2006; Vandieken et al., 2006). *Arcobacter* V6 pyrosequences were also found on the particulate material and BS098 was sequenced from the particulates (Fuchsman et al., 2011). If *Sulfurimonas* phylotype BS139 or *Arcobacter* phylotype BS098 are indeed responsible for autotrophic denitrification in the mixing zone station, their presence on large particles in the nitrate-rich suboxic zone of the Western Gyre indicates that autotrophic denitrification may be fed by sulfate reduction inside sinking aggregates. This form of denitrification could easily have been missed in experiments by Jensen et al. (2008) due to the patchy nature of sinking particulate matter and the hydrodynamics of Niskin bottles (Altabet et al., 1992).

CONCLUSION

Chemical profiles indicate that nitrate and sulfide may have co-existed at the mixing zone station in 2005 (**Figures 2** and **3**). ^{15}N - NO_3^- tracer experiments indicate autotrophic denitrification occurred in the sulfidic zone at this station (**Figure 4**). Though SUP05 and BS-GSO2 bacteria are autotrophic and have been found in sulfidic environments (Glaubitz et al., 2009, 2010; Lavik et al., 2009; Walsh et al., 2009), their depth profiles are not consistent with autotrophic denitrification at this station. Instead the depth profile for BS-GSO2 phylotype BS129 correlated with ammonium fluxes. In contrast, *Sulfurimonas* BS139, *Arcobacter* BS098, and unidentified *Msp*I peak 91/Mnl peak 254 pair have their greatest relative abundance in the zone where autotrophic denitrification was detected (**Figure 7**). Out of these three bacteria, we consider the Black Sea *Sulfurimonas* to be the most likely candidate for this denitrification because many *Sulfurimonas* species have previously been found to mediate autotrophic denitrification (Gevertz et al., 2000; Brettar et al., 2006; Takai et al., 2006). Evidence for the involvement of *Arcobacter* and peak 91 is less clear.

For most of the Black Sea, both anammox (Kuypers et al., 2003; Jensen et al., 2008) and heterotrophic denitrification (Fuchsman et al., 2008) are the important nitrogen loss pathways. Biogeochemical modeling indicates that autotrophic denitrification from overlapping depth profiles of nitrate and sulfide may only contribute 1% to nitrogen loss in the central Black Sea (Konovalov et al., 2008). However, where the Bosporus enters the Black Sea,

autotrophic denitrification appears to be more important, and autotrophic denitrification associated with sinking particles has not yet been quantified. Future work should investigate these possibilities in order to better constrain the role of autotrophic denitrification in the Black Sea's nitrogen cycle.

ACKNOWLEDGMENTS

We would like to thank Barbara Paul for collecting DNA samples from 2001. We would like to thank S. Tugrul, T. Uysal, B. Paul, S. Konovalov, A. Romanov, E. Yakushev, B. Tebo for nutrient, manganese, and oxygen data. We would like to thank Sergey Konovalov for help planning the autotrophic denitrification experiment, and Paul Quay for use of the mass spectrometer. Thank you to G. Rocap, W. Brazelton, and the reviewers for manuscript edits. Funding was provided by OCE 0081118, MCB0132101, OCE0649223. Clara A. Fuchsman was supported by an IGERT traineeship in Astrobiology under NSF grant 05-04219.

REFERENCES

Altabet, M. A., Bishop, J. K. B., and McCarthy, J. J. (1992). Differences in particulate nitrogen concentration and isotopic composition for samples collected by bottles and large-volume pumps in gulfstream warm-core rings and the Sargasso Sea. *Deep Sea Res. A* 39, S405–S417.

Basturk, O., Yakushev, E. V., Tugrul, S., Salihoglu, I. (1999) "Characteristic chemical features and biogeochemical cycles in the Black Sea," in *Environmental Degradation of the Black Sea: Challenges and Remedies*, eds S. Besiktepe, U. Unluata, and A. Bologa (Dordrecht: Kluwer Academic Publishers), 43–59.

Brettar, I., Labrenz, M., Flavier, S., Botel, J., Christen, R., and Hofte, M. G. (2006). Identification of a *Thiomicrospira denitrificans* like epsilon proteobacteria as a catalyst for autotrophic denitrification in the central Baltic Sea. *Appl. Environ. Microbiol.* 72, 1364–1372.

Buessler, K. O., Livingston, H. D., and Casso, S. A. (1991). Mixing between oxic and anoxic waters of the Black Sea as traced by Chernobyl cesium isotopes. *Deep Sea Res. A* 38, S725–S746.

Canfield, D. E., Stewart, F. J., Thamdrup, B., De Brabandere, L., Dalsgaard, T., Delong, E. F., Revsbech, N. P., and Ulloa, O. (2010). A cryptic sulfur cycle in oxygen-minimum-zone waters off the Chilean coast. *Science* 330, 1375–1378.

Cline, J. D. (1969). Spectrophotometric determination of hydrogen sulfide in natural waters. *Limnol. Oceanogr.* 14, 454–458.

Çoban-Yildiz, Y., Fabbri, D., Baravelli, V., Vassura, I., Yilmas, A., Tugrul, S., and Eker-Develi, E. (2006). Analytical pyrolysis of suspended particulate organic matter from the Black Sea water column. *Deep Sea Res. Part II Top. Stud. Oceanogr.* 53, 1856–1874.

Finster, K., Bak, F., and Pfennig, N. (1994). *Desulfuromonas acetexigens* sp. Nov., a dissimilatory sulfur-reducing eubacterium from anoxic freshwater sediments. *Arch. Microbiol.* 161, 328–332.

Fuchsman, C. A., Kirkpatrick, J. B., Brazleton, W. J., Murray, J. W., and Staley, J. T. (2011). Metabolic strategies of free-living and aggregate associated bacterial communities inferred from biological and chemical profiles in the Black Sea suboxic zone. *FEMS Microbiol. Ecol.* 78, 586–603.

Fuchsman, C. A., Konovalov, S. K., and Murray, J. W. (2008). Concentration and natural stable isotope profiles of nitrogen species in the Black Sea. *Mar. Chem.* 111, 90–105.

Fuchsman, C. A., Staley, J. T., Oakley, B. B., Kirkpatrick, J. B., and Murray, J. W. (2012). Free-living and aggregate-associated Planctomycetes in the Black Sea. *FEMS Microbiol. Ecol.* 80, 402–418.

Gevertz, D., Telang, A. J., Voordouw, G., and Jenneman, G. E. (2000). Isolation and characterization of strains CVO and FWKO B, two novel nitrate-reducing, sulfide oxidizing bacteria isolated from oil field brine. *Appl. Environ. Microbiol.* 66, 2491–2501.

Glaubitz, S., Labrenz, M., Jost, G., and Jurgens, K. (2010). Diversity of active chemolithoautotrophic prokaryotes in the sulfidic zone of a Black Sea pelagic redoxcline as determined by rRNA-based stable isotope probing. *FEMS Microbiol. Ecol.* 74, 32–41.

Glaubitz, S., Lueders, T., Abraham, W. R., Jost, G., Jurgens, K., and Labrenz, M. (2009). C-13-isotope analyses reveal that chemolithotrophic Gamma- and Epsilonproteobacteria feed a microbial foodweb in a pelagic redoxcline of the central Baltic Sea. *Environ. Microbiol.* 11, 326–337.

Grunke, S., Felden, J., Lichtschlag, A., Girnth, A. C., De Beer, D., Wenzhofer, F., and Boetius, A. (2011). Niche differentiation among mat-forming, sulfide-oxidizing bacteria at cold seeps of the Nile Deep ea Fan (Eastern Mediterranean Sea). *Geobiology* 9, 330–348.

Hannig, M., Lavik, G., Kuypers, M. M. M., Woebken, D., Martens-Habbena, W., and Jurgens, K. (2007). Shift from denitrification to anammox after inflow events in the central Baltic Sea. *Limnol. Oceanogr.* 52, 1336–1345.

Hewson, I., and Fuhrman, J. A. (2006). Improved strategy for comparing microbial assemblage fingerprints. *Microb. Ecol.* 51, 147–153.

Heylen, K., Vanparys, B., Wittebolle, L., Verstraete, W., Boon, N., and De Vos, P. (2006). Cultivation of denitrifying bacteria: optimization of isolation conditions and diversity study. *Appl. Environ. Microbiol.* 72, 2637–2643.

Hoeft, S. E., Kulp, T. R., Stolz, J. F., Hollibaugh, J. T., and Oremland, R. S. (2004). Dissimilatory arsenate reduction with sulfide as an electron donor: experiments with Mono Lake water and isolation of strain MLMS-1, a chemoautotrophic arsenate respirer. *Appl. Environ. Microbiol.* 70, 2741–2747.

Huse, S. M., Dethlefsen, L., Huber, J. A., Welch, D. M., Relman, D. A., and Sogin, M. L. (2008). Exploring microbial diversity and taxonomy using SSU rRNA hypervariable tag sequencing. *PLoS Genet.* 4, e1000255. doi:10.1371/journal.pgen.1000255

Ivanov, L. I., and Samodurov, A. S. (2001). The role off lateral fluxes in ventilation of the Black Sea. *J. Mar. Syst.* 31, 159–174.

Jensen, M. M., Kuypers, M. M. M., Lavik, G., and Thamdrup, B. (2008). Rates and regulation of anaerobic ammonium oxidation and denitrification in the Black Sea. *Limnol. Oceanogr.* 53, 25–36.

Jensen, M. M., Petersen, J., Dalsgaard, T., and Thamdrup, B. (2009). Pathways, rates and regulation of N2 production in the chemocline of an anoxic basin, Mariager Fjord, Denmark. *Mar. Chem.* 113, 102–113.

Kirkpatrick, J., Oakley, B., Fuchsman, C., Srinivasan, S., Staley, J. T., and Murray, J. W. (2006). Diversity and distribution of Planctomycetes and related bacteria in the suboxic zone of the Black Sea. *Appl. Environ. Microbiol.* 72, 3079–3083.

Konovalov, S. K., Fuchsman, C. A., Murray, J. W., and Belokopitov, V. N. (2008). Models of the distribution of nitrogen species and isotopes in the water column of the Black Sea. *Mar. Chem.* 111, 105.

Konovalov, S. K., Luther, G. W. III, Friederich, G. E., Nuzzio, D. B., Tebo, B. M., Murray, J. W., Oguz, T., Glazer, B., Trouwborst, R. R., Clement, B., Murray, K. J., and Romanov, A. S. (2003). Lateral injection of oxygen with the Bosporus Plume-fingers of oxidizing potential in the Black Sea. *Limnol. Oceanogr.* 48, 2369–2376.

Konovalov, S. K., and Murray, J. W. (2001). Variations in the chemistry of the Black Sea on time-scales of decades (1960–1995). *J. Mar. Syst.* 31, 217–243.

Kuypers, M. M. M., Sliekers, A. O., Lavik, G., Schmid, M., Jorgensen, B. B., Kuenen, J. G., Sinninghe Damste, J. S., Strous, M., and Jetten, M. S. M. (2003). Anaerobic ammonium oxidation by anammox bacteria in the Black Sea. *Nature* 422, 608–611.

Lam, P., Jensen, M. M., Lavik, G., McGinnis, D. F., Muller, B., Schubert, C. J., Amann, R., Thamdrup, B., and Kuypers, M. M. M. (2007). Linking crenarchaeal and bacterial nitrification to anammox in the Black Sea. *Proc. Natl. Acad. Sci. U.S.A.* 104, 7104–7109.

Lavik, G., Stuhrmann, T., Bruchert, V., Van der Plas, A., Mohrholz, V., Lam, P., Mussmann, M., Fuchs, B. M., Amann, R., Lass, U., and Kuypers, M. M. M. (2009). Detoxification of sulphidic African shelf waters by blooming chemolithotrophs. *Nature* 457, 581–585.

Luther, G. W. III, Church, T. M., and Powell, D. (1991). Sulfur speciation and sulfide oxidation in the water column of the Black Sea. *Deep Sea Res. A* 38, S1121–S1137.

Moussard, H., Corre, E., Cambon-Bonavita, M., Fouquet, Y., and Jeanthon, C. (2006). Novel uncultured epsilonproteobacteria dominate a filamentous sulphur mat from the 13N hydrothermal vent field, East Pacific Rise. *FEMS Microbiol. Ecol.* 58, 449–463.

Murray, J. W., Codispoti, L. A., Friederich, G. E. (1995) "Oxidation-reduction environments: the suboxic zone in the Black Sea" in *Aquatic Chemistry: Interfacial and Interspecies Processes. Advances in Chemistry Series*, Vol. 224, eds C. P. Huang, C. R. O'Melia, and J. J. Morgan (Washington DC: American Chemical Society), 157–176.

Murray, J. W., Top, Z., and Özsoy, E. (1991). Hydrographic properties and ventilation of the Black Sea. *Deep Sea Res. A* 38, S663–689.

Oguz, T., and Rozman, L. (1991). Characteristics of the Mediterranean underflow in the southwestern Black Sea continental shelf/slope region. *Oceanol. Acta* 14, 433–444.

Polz, M. F., and Cavanaugh, C. M. (1998). Bias in template-to-product ratios in multitemplate PCR. *Appl. Environ. Microbiol.* 64, 3724–3730.

Poulain, P., Barbanti, R., Motyzhev, S., and Zatsepin, A. (2005). Statistical description of the Black Sea near-surface circulation using drifters in 1999–2003. *Deep Sea Res. Part I Oceanogr. Res. Pap.* 52, 2250–2274.

Rainey, F. A., Ward, N., Sly, L. I., and Stackebrandt, E. (1994). Dependence on the taxon composition of clone libraries for PCR amplified, naturally occurring 16S rDNA, on the primer pair and the cloning system used. *Experientia* 50, 796–797.

Shao, M., Zhang, T., and Fang, H. H. P. (2009). Autotrophic denitrification and its effect on metal speciation during marine sediment remediation. *Water Res.* 43, 2961–2968.

Sievert, S. M., Scott, K. A., Klotz, M. G., Chain, P. S. G., Hauser, L. J., Hemp, J., Hugler, M., Land, M., Lapidus, A., Larimer, F. W., Lucas, S., Malfatti, S. A., Meyer, F., Paulsen, I. T., Ren, Q., and Simon, J. (2008). Genome of Epsilonproteobacterial chemolithoautotroph *Sulfurimonas denitrificans*. *Appl. Environ. Microbiol.* 74, 1145–1156.

Sievert, S. M., Wierings, E. B. A., Wirsen, C. O., and Taylor, C. D. (2007). Growth and mechanism of filamentous-sulfur formation by *Candidatus Arcobacter sulfidicus* in opposing oxygen-sulfide gradients. *Environ. Microbiol.* 9, 271–276.

Steele, J. A., Countway, P. D., Xia, L., Vigis, P. D., Beman, J. M., Kim, D. Y., Chow, C. T., Sachdeva, R., Jones, A. C., Schwalbach, M. S., Rose, J. M., Hewson, I., Patel, A., Sun, F., Caron, D. A., and Fuhrman, J. A. (2011). Marine bacterial, archaeal and protistan association networks reveal ecological linkages. *ISME J.* 5, 1414–1425.

Stewart, F. J., Ulloa, O., and DeLong, E. F. (2012). Microbial metatranscriptomics in a permanent marine oxygen minimum zone. *Environ. Microbiol.* 14, 23–40.

Takai, K., Suzuki, M., Nakagawa, S., Miyazaki, M., Suzuki, Y., Inagaki, F., and Horikoshi, K. (2006). *Sulfurimonas paralvinellae* sp nov., a novel mesophilic, hydrogen- and sulfur-oxidizing chemolithoautotroph within the Epsilonproteobacteria isolated from a deep-sea hydrothermal vent polychaete nest, reclassification of *Thiomicrospira denitrificans* as *Sulfurimonas denitrificans* comb, nov and emended description of the genus *Sulfurimonas*. *Int. J. Syst. Evol. Microbiol.* 56, 1725–1733.

Tarpgaard, I. H., Boetius, A., and Finster, K. (2006). *Desulfobacter psychrotolerans* sp. nov., a new psychrotolerant sulfate-reducing bacterium and descriptions of its physiological response to temperature changes. *Antonie Van Leeuwenhoek* 89, 109–124.

Taylor, C. D., and Wirsen, C. O. (1997). Microbiology and ecology of filamentous sulfur formation. *Science* 277, 1483–1485.

Thamdrup, B., Rossello-Mora, R., and Amann, R. (2000). Microbial manganese and sulfate reduction in Black Sea shelf sediments. *Appl. Environ. Microbiol.* 66, 2888–2897.

Trowborst, R. E., Clement, B. G., Tebo, B. M., Glazer, B. T., and Luther, G. W. III. (2006). Soluble Mn(III) in suboxic zones. *Science* 313, 1955–1957.

van de Vossenberg, J., Rattray, J. E., Geerts, W., Kartal, B., van Niftrik, L., van Donselaar, E. G., Sinninghe Damste, J. S., Strous, M., and Jetten, M. S. M. (2008). Enrichment and characterization of marine anammox bacteria associated with global nitrogen gas production. *Environ. Microbiol.* 10, 3120–3129.

Vandieken, V., Mussmann, M., Niemann, H., and Jorgensen, B. B. (2006). *Desulfuromonas svalbardensis* sp. Nov. and *Desulfuromonas ferrireducens* sp. Nov., psychrophilic, Fe(III) reducing bacteria isolated from Arctic sediments, Svalbard. *Int. Syst. Evol. Microbiol.* 56, 1133–1139.

Vandieken, V., Pester, M., Finke, N., Hyun, J., Friedrich, M. W., Loy, A., and Thamdrup, B. (2012). Three manganese oxide-rich marine sediments harbor similar acetate-oxidizing manganese-reducing bacteria. *ISME J.* doi:10.1038/ismej.2012.41

Vetriani, C., Tran, H. V., and Kerkhof, L. J. (2003). Fingerprinting microbial assemblages from the oxic/anoxic chemocline of the Black Sea. *Appl. Environ. Microbiol.* 69, 6481–6488.

Walsh, D. A., Zaikova, E., Howes, C. G., Song, Y. C., Wright, J. J., Tringe, S. G., Tortell, P. D., and Hallam, S. J. (2009). Metagenome of a versatile chemolithoautotroph from expanding oceanic dead zones. *Science* 326, 578–582.

Wang, J., Jenkins, C., Webb, R. I., and Fuerst, J. A. (2002). Isolation of Gemmata-like and Isophaera-like bacteria from soil and freshwater. *Appl. Environ. Microbiol.* 68, 417–422.

Wirsen, C. O., Sievert, S. M., Cavanaugh, C. M., Molyneaux, S. J., Ahman, A., Taylor, L. T., DeLong, E. F., and Taylor, C. D. (2002). Characterization of an autotrophic sulfide-oxidizing marine *Arcobacter* sp. that produces filamentous sulfur. *Appl. Environ. Microbiol.* 68, 316–325.

Zhang, M., Zhang, T., Shao, M. F., and Fang, H. H. P. (2009). Autotrophic denitrification in nitrate-induced marine sediments remediation and *Sulfurimonas denitrificans* like bacteria. *Chemosphere* 76, 677–682.

Zumft, W. G. (1997). Cell biology and molecular basis of denitrification. *Microbiol. Mol. Biol. Rev.* 61, 533.

Conflict of Interest Statement: The authors declare that the research was conducted in the absence of any commercial or financial relationships that could be construed as a potential conflict of interest.

Received: 20 January 2012; accepted: 30 June 2012; published online: 18 July 2012.
Citation: Fuchsman CA, Murray JW and Staley JT (2012) Stimulation of autotrophic denitrification by intrusions of the Bosporus Plume into the anoxic Black Sea. Front. Microbio. ***3****:257. doi: 10.3389/fmicb.2012.00257*
This article was submitted to Frontiers in Aquatic Microbiology, a specialty of Frontiers in Microbiology.

APPENDIX

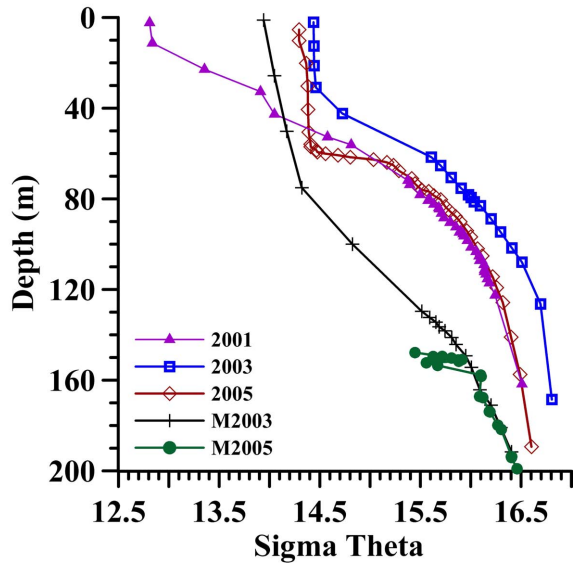

FIGURE A1 | The density (sigma theta) of the top 200 m for each station discussed in this paper: the Western Gyre in 2001 (purple triangles), 2003 (blue squares), and 2005 (red diamonds) and at the mixing zone station in 2003 (black crosses) and 2005 (green circles).

frontiers in
MICROBIOLOGY

ORIGINAL RESEARCH ARTICLE
published: 19 July 2012
doi: 10.3389/fmicb.2012.00256

Concurrent activity of anammox and denitrifying bacteria in the Black Sea

***John B. Kirkpatrick*[1,2]*, *Clara A. Fuchsman*[1], *Evgeniy Yakushev*[3], *James T. Staley*[4] and *James W. Murray*[1]**

[1] *School of Oceanography, University of Washington, Seattle, WA, USA*
[2] *Graduate School of Oceanography and Center for Dark Energy Biosphere Investigations, University of Rhode Island, Narragansett, RI, USA*
[3] *Norwegian Institute for Water Research, Oslo, Norway*
[4] *Department of Microbiology, University of Washington, Seattle, WA, USA*

Edited by:
Bess B. Ward, Princeton University, USA

Reviewed by:
Bonnie X. Chang, Princeton University, USA
Mark Trimmer, Queen Mary University of London, UK

****Correspondence:***
John B. Kirkpatrick, Graduate School Oceanography, University of Rhode Island, Narragansett Bay Campus, South Ferry Road, Narragansett, RI, 02882, USA.
e-mail: jbk@gso.uri.edu

After the discovery of ANaerobic AMMonium OXidation (anammox) in the environment, the role of heterotrophic denitrification as the main marine pathway for fixed N loss has been questioned. A 3 part, 15 month time series investigating nitrite reductase (*nirS*) mRNA transcripts at a single location in the Black Sea was conducted in order to better understand the activity of anammox and denitrifying bacteria. Here we show that both of these groups were active, as well as being concurrent in the lower suboxic zone over this time span. Their distributions, however, differed in that only expression of denitrification-type *nirS* was seen in the upper suboxic zone, where geochemistry was variable. Depth profiles covering the suboxic zone showed that the four groups of anammox-type sequences were expressed consistently in the lower suboxic zone, and were consistent with anammox 16 S rDNA gene profiles. By contrast, denitrifier-type *nirS* sequence groups were mixed; some groups exhibited consistent expression in the lower suboxic zone, while others appeared less consistent. Co-occurrence of both anammox and denitrifier expression was common and ongoing. Both types of transcripts were also found in samples with low concentrations of sulfide ($>2\,\mu M$). Six major groups of denitrifier-type *nirS* transcripts were identified, and several groups of denitrifier-type *nirS* transcripts were closely related to sequences from the Baltic Sea. An increase in denitrifier-type *nirS* transcript diversity and depth range in October 2007 corresponded to a small increase in mixed layer net community productivity (NCP) as measured by O_2/Ar gas ratios, as well as to an increase in N_2 concentrations in the suboxic zone. Taken together, the variations in expression patterns between anammox and denitrification provide one possible explanation as to how near instantaneous rate measurements, such as isotope spike experiments, may regularly detect anammox activity but underreport denitrification.

Keywords: anammox, denitrification, Black Sea, nirS, nitrogen, gene expression

INTRODUCTION

Fixed nitrogen loss from marine systems balances N fixation, thereby exerting a long-term control over primary productivity and therefore climate (Altabet et al., 1995, 1999; Ganeshram et al., 1995), as well as anthropogenic influences. Loss of fixed N occurs via two microbial pathways: denitrification and the more recently discovered anammox process (ANaerobic AMMonium OXidation). While both require nitrite (NO_2^-), heterotrophic denitrification is reliant on organic C while anammox requires ammonium (NH_4^+). Since the discovery of environmental anammox in marine sediments (Thamdrup and Dalsgaard, 2002) and the water column (Dalsgaard et al., 2003; Kuypers et al., 2003), many groups have debated the relative role of these two processes in the environment. Anammox organisms have now been documented in many water column marine oxygen minimum zones (OMZs), and isotope labeling experiments have even shown in some cases a complete lack of denitrification (Schmid et al., 2007; Jensen et al., 2008; Lam et al., 2009). Other labeling studies have pointed towards a dominant contribution from denitrifiers (Ward et al., 2009), while DNA-based methods have suggested the potential for considerable variation in levels of heterotrophic denitrification (Jayakumar et al., 2009a). Conclusions regarding the dominance of one pathway over the other have thus been varied and conflicting (Lam et al., 2007; Schmid et al., 2007; Fuchsman et al., 2008; Lam et al., 2009; Ward et al., 2009; Bulow et al., 2010; Jensen et al., 2011). It has also been shown that it is possible to construct an N cycle where the role of heterotrophic denitrification is entirely replaced by Dissimilatory Nitrite Reduction to Ammonium (DNRA) coupled with anammox (Lam et al., 2009; Jensen et al., 2011).

The Black Sea is well suited for investigations of these processes, as it is permanently anoxic at depth and contains a well-defined suboxic zone ($O_2 < 10\,\mu M$, no detectable H_2S; **Figure 1**) sandwiched between shallow oxic and deeper sulfidic waters (Murray et al., 1995). Nonetheless, there has been no consensus there as to the relative contributions of anammox and

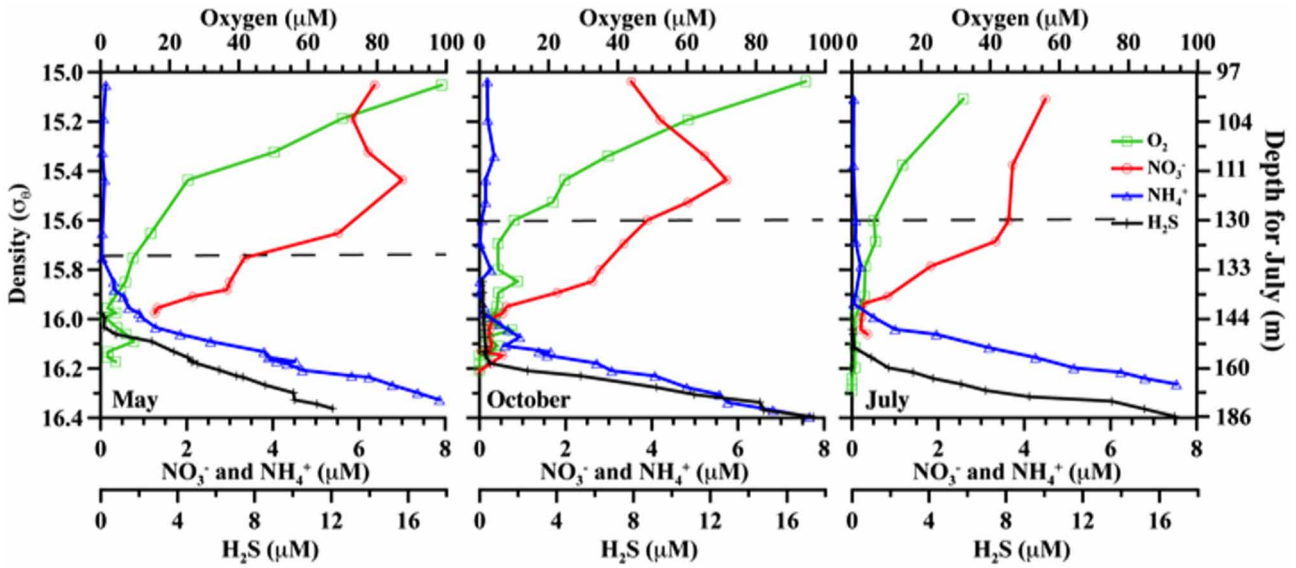

FIGURE 1 | Comparative chemical profiles for the three different cruises. Markers indicate discrete samples. Plots are versus density as absolute depths are less consistent. For reference, July 2008 also includes absolute depth in m, but note this measure only applies to the right panel. From left to right, panels are for May 2007; October 2007; and July 2008. Horizontal dashed lines indicate the upper boundary of the suboxic zone ($O_2 = 10\,\mu M$).

denitrification to N_2 production (Lam et al., 2007; Fuchsman et al., 2008; Jensen et al., 2008). Some incubation experiments with Black Sea water have shown the absence of denitrification activity (Lam et al., 2007). However, the presence of both denitrifying and anammox bacteria in the Black Sea's suboxic zone have also been documented (Kirkpatrick et al., 2006; Oakley et al., 2007). In order to better understand the *in situ* activity of these organisms and its variability, we investigated transcription of metabolic genes, as a proxy for bacterial activity, from three different cruises in different seasons.

MATERIALS AND METHODS

Field sampling was conducted in the northeastern Black Sea at 44° 25′ N, 37° 30′ E, onboard the *R/V Akvanavt* and *R/V Ashamba* (mean water depth >1000 m), for three time points: May 2007, October 2007, and July 2008. Data is graphed versus potential density (σ_θ, kg m^{-3}), measured by SeaBird CTD package attached to the sampling rosette. Density was used to take into account spatial and temporal effects, which may alter the absolute depth of a feature in meters. For example, the oxycline may appear tens of meters shallower or deeper at different times and/or stations, but can be consistently found at the same density range (Murray et al., 1995). Samples were taken for the suboxic zone, roughly $15.6 \leq \sigma_\theta \leq 16.1$ (**Figure 1**; includes July 2008 depth comparison).

NUTRIENTS, DISSOLVED GASES, AND PRODUCTIVITY

Dissolved oxygen and hydrogen sulfide were measured onshore the night after daytime sampling, using standard techniques (Grasshoff et al., 1983). Nutrients were also measured (NO_3^-, NO_2^-, NH_4^+), with conventional chemical techniques and utilizing an autoanalyzer (Fuchsman et al., 2008). Dissolved gases were collected in evacuated 250 mL glass cylinders with $HgCl_2$ pre-added, transported to the University of Washington, and measured by a Finnegan Delta XL isotope ratio mass spectrometer as per Fuchsman et al. (2008) and Emerson et al. (1999). A known amount of ^{36}Ar was added to the samples (Nicholson et al., 2010). $\delta^{18}O$-O_2 values were corrected for addition of ^{36}Ar. $\delta^{18}O$-H_2O was measured using an automated Micromass 903 mass spectrometer with CO_2 equilibration system at the Quaternary Research Center, University of Washington. Net community productivity (NCP) calculations based on O_2/Ar were calculated as per equation (2) of Stanley et al. (2010);

$$NCP = \Delta(O_2/Ar)[O_2]_{eq}\,\rho\,k$$

where $[O_2]_{eq}$ is O_2 equilibrium concentration (calculated from CTD temperature and salinity data), ρ is the measured density from the CTD, and k is the gas transfer velocity. Gas exchange parameters were estimated via the parameterizations of Nightingale et al. (2000), using 14 day averaged QuikSCAT wind products. This calculation assumes a well-mixed layer, negligible impact from advection or cross-diapycnal mixing (upwelling), and a steady state system.

RNA SAMPLING AND ANALYSIS

Different versions of nitrite reductase (*nirS*) mRNA transcripts corresponding to denitrification and anammox organisms [specifically, "*Candidatus* Scalindua"-type (Lam et al., 2009)] were extracted, reverse transcribed, amplified and sequenced. Samples for RNA analysis were taken every 0.1 density level from $\sigma_\theta = 15.5$ to 16.1, filtered directly from Niskin bottles onto 0.2 μm Millipore Sterivex™ filters, and fixed with RNALater® within 30 min of the start of filtration. October 2007 was unusual in that opportunistic RNA sampling extended deeper, to $\sigma_\theta = 16.3$. Filters were incubated for ∼1 h, frozen, shipped

on dry ice to the University of Washington, and ultimately stored at −80°C. RNA extraction was conducted similar to Poretsky et al. (2005), and reverse-transcribed with random primers using the Fermentas Maxima® kit. Amplification of Scalindua-type *nirS* was performed with primers Scnir372F and Scnir845R (Lam et al., 2009). For conventional *nirS* several primer sets were tried (Braker et al., 1998; Michotey et al., 2000; Throbäck et al., 2004; see discussion). The primary results presented here are the nirS1F/6R primers of Braker et al. (1998) amplified as per Santoro et al. (2006) but using Fermentas DreamTaq™ 2x Mastermix with BSA added to 1x concentration, because it returned *nirS* type sequences for the largest number of samples. Attempts were also made to amplify different version of nitrite reductase (*nirK*) for all samples, but because amplification was at best erratic, and failed outright in the majority of cases, those results are not considered here. Scalindua-type products, uniformly single-banded, were cleaned with a Qiagen PCR Clean-up Kit, while other *nirS* products were commonly multi-banded and therefore gel-purified (Fermentas GeneJet™ Gel Purification Kit). Cloning was conducted with the StrataClone PCR Cloning Kit, and sequenced at the High-Throughput Genomics Unit (www.htseq.org). Sequences were hand-checked and amino acid translation was performed with Transeq (European Bioinformatics Institute), related protein sequences added for reference from GenBank (National Center for Biotechnology Information), and alignments performed with ClustalX. Bootstrapped data sets (Phylip's seqboot, 100 replicates) were analyzed for maximum likelihood phylogeny with Phylip (Felsenstein, 2005), and consensus tree branch lengths subsequently determined via protein maximum likelihood (JTT algorithm; Jones et al., 1992). Final tree visualization was accomplished using the program FigTree (http://tree.bio.ed.ac.uk/). Genbank accession numbers are JX102246—JX102470.

TRFLP

DNA was extracted using a combination of standard freeze-thaw and enzymatic lysis methods, followed by phenol-chloroform extraction and spin-column purification (Qiagen) (Fuchsman et al., 2012). Amplification was obtained using Planctomycetes primers 58F (labeled) and 926R (Wang et al., 2002). PCR products were amplified for 30 cycles at 60°C (Fuchsman et al., 2012). Column purified PCR products were digested separately overnight with restriction enzymes *HaeIII*, *Hpy1881*, *MspI*, and immediately precipitated with ethanol. Fragment analysis was performed on a MegaBACE 1000 apparatus (Molecular Dynamics) at the University of Washington Marine Molecular Biotechnology Laboratory. Electrophoretic profiles were visualized with Dax software (Van Mierlo Software Consultancy, The Netherlands). TRFLP profiles were normalized downward by total peak height. Scalindua was identified as peak 236 using *HaeIII*, peak 530 using *HpyI881*, and peak 260 using *MspI*.

RESULTS

Nutrients (O_2, H_2S, NO_3^-, NH_4^+) are given in **Figure 1**. Oxygen penetration was deepest in May 2007 and shallowest in July 2008, affecting the apparent range of the suboxic zone (defined as $O_2 <$ 10 μM, H_2S undetectable; appx. $15.7 \leq \sigma_\theta \leq 16.1$). Nitrate concentrations were highest at the top of the suboxic zone (max between 4.5 and 7 μM), but nitrate was detectable until at least $\sigma_\theta = 16.0$. Nitrite was below 0.1 μM for all seasons, with a small peak around in the suboxic zone and migrating slightly in a similar fashion to oxygen (**Figure 2**). Ammonium concentrations

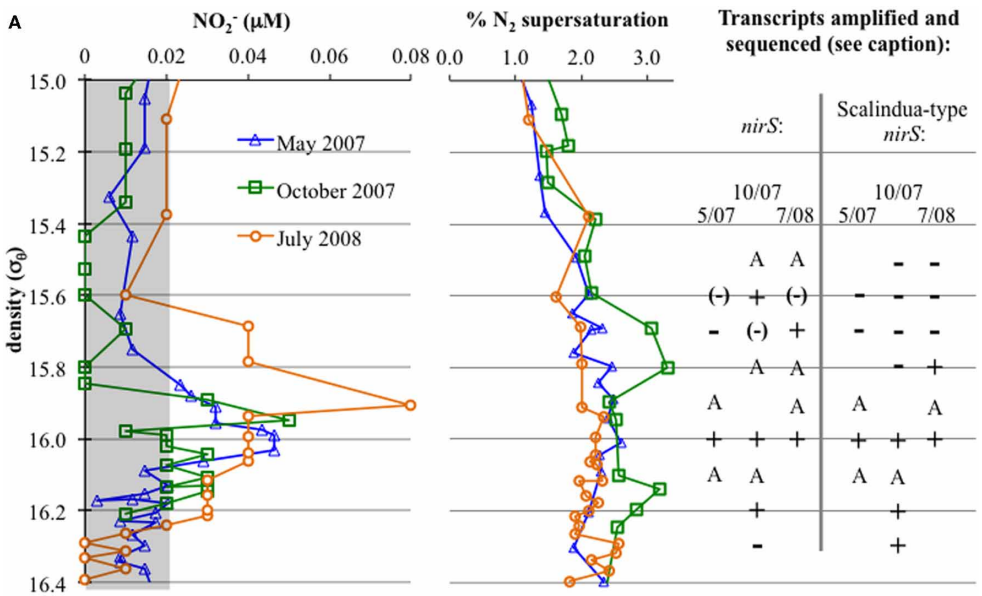

FIGURE 2 | Left: NO_2^- concentrations, with a gray box indicating values at or below detection limit. **Right:** First, N_2 supersaturation (from N_2/Ar ratio compared to calculated values for saturation); N_2 is produced *in situ* in the lower suboxic zone. To the right, detection of gene transcripts: "A" indicates amplification without sequencing confirmation, while "+" indicates amplification and sequencing confirmation. "−" indicates no amplification, while "(–)" indicates bands were apparent but sequencing resulted in non-specific sequences (generally, 23S ribosomal sequences).

were highest in the sulfidic zone, but became negligible around $\sigma_\theta = 16.0$ in October 2007 and July 2008 and at 15.8 in May 2007 (**Figure 1**). N_2 supersaturation generally increased with depth and reached a broad maximum in the suboxic zone (**Figure 2**). N_2 supersaturation was greatest in October 2007 with a maximum at $\sigma_\theta = 15.7$–15.8.

Anammox and denitrifying mRNA transcripts were detected in all three sample sets (**Figure 2**). Note however, that deep RNA samples ($\sigma_\theta = 16.2$ and 16.3), extending into the sulfidic zone, were only available for October 2007. Considering first anammox, Scalindua-type *nirS* appeared localized to the lower suboxic zone ($\sigma_\theta = 15.8$), a distribution almost invariant for the time period sampled and coincident with a stable maxima in dissolved N_2 (**Figure 2**). Four sequence groups were detected (**Figure 3**). Groups II and III were detected across a broad depth range (**Figure 4**), while group I was relatively shallow ($15.8 \leq \sigma_\theta \leq 16.0$) and group IV was relatively deep ($16.0 \leq \sigma_\theta \leq 16.3$). TRFLP of Scalindua 16S rDNA from May and October 2007

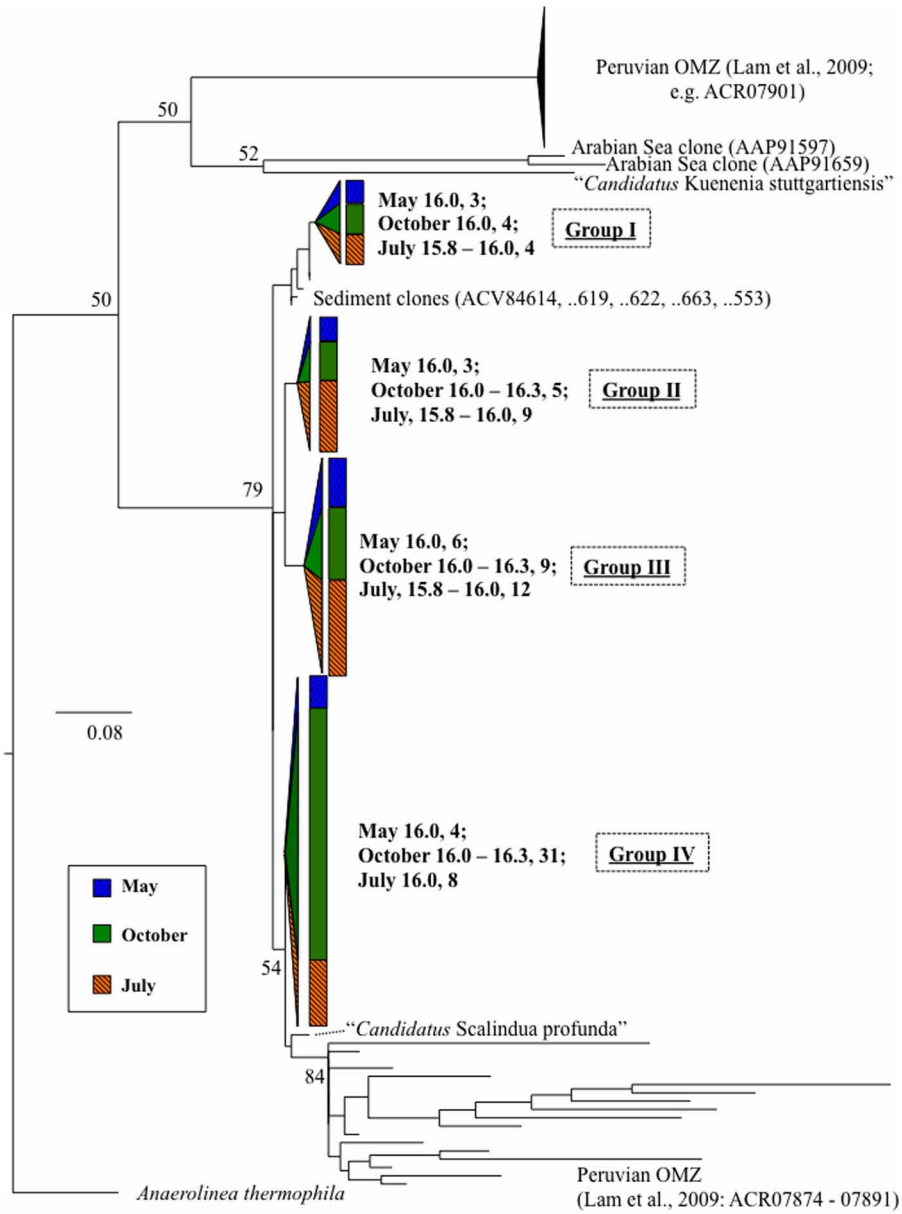

FIGURE 3 | Scalindua-type *nirS* expression, in bold, as detected with primers Scnir372F and Scnir845R (Lam et al., 2009). Numbers indicate density, followed by number of clones. References include cultured strains (in italics), and environmental clones. "*Candidatus* Scalindua" is from van de Vossenberg et al. (2012). Tree was constructed from amino acid sequences (~160 aa), bootstrapped (100 replicates; nodes present >50% noted) and analyzed for maximum likelihood phylogeny with Phylip (Felsenstein, 2005). Scale bar indicates branch length as calculated by protein maximum likelihood (Jones-Taylor-Thornton algorithm; Jones et al., 1992). Wedge and bar sizes are proportional to clone library composition.

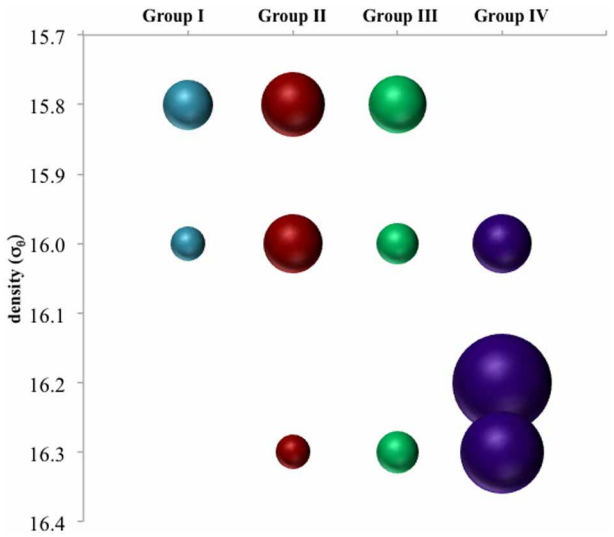

FIGURE 4 | Depth breakdown of groups noted in Figure 3. Area of bubbles are proportional to percentage of clone library sequences for a given depth found in a given group.

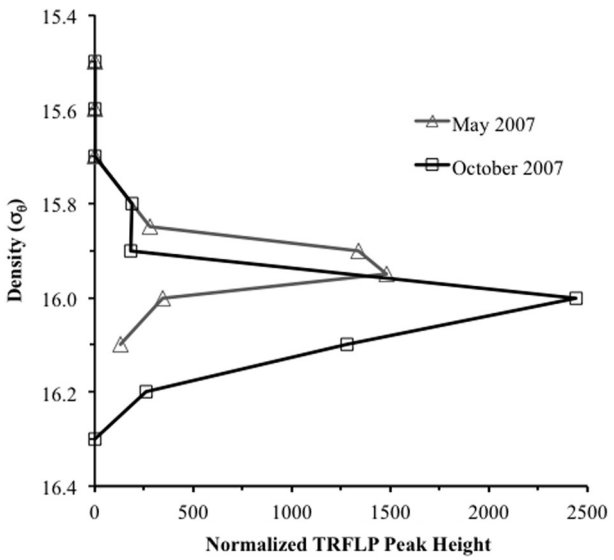

FIGURE 5 | Terminal restriction fragment length polymorphism (TRFLP) profile of "*Candidatus* Scalindua" 16S ribosomal DNA for May and October 2007. Products were amplified using Planctomycetes specific primers 58F and 926R, and peak identification obtained with enzymes *HaeIII, Hpy1881, MspI*. Profiles were normalized downward by total peak height.

ranged from $\sigma_\theta = 15.8$ to 16.2 with a maximum at $\sigma_\theta = 15.95$ in May and $\sigma_\theta = 16.0$ in October (**Figure 5**).

Conventional *nirS* expression was also continually present in the lower suboxic zone and continued into the upper sulfidic zone (**Figure 2**). Six major groups, as well as a variety of singletons, were found using the nirS1F/6R primer set and are labeled in **Figure 6** for ease of discussion. Groups I, IV, and VI were expressed in a consistent pattern similar to anammox (**Figure 7**). Other groups and singletons were more dynamic, with varying depth ranges and/or seasons in which they were detected. Unlike anammox, however, some expression was detected in the upper suboxic zone ($\sigma_\theta = 15.6$, 15.7; **Figures 2**, **7**). Groups I, V, and VI were related to Baltic Sea samples (Hannig et al., 2006). Groups II and IV contained no closely related database sequences, while Group III had an Arabian Sea analog (Jayakumar et al., 2009b). Finally, *Marinobacter hydrocarbonoclasticus* was the sole described species closely related to sequences from these clone libraries.

Amplification with a second primer set for conventional *nirS* expression, cd3aF/R3cd (Throbäck et al., 2004), was only detected in the lower suboxic zone ($\sigma_\theta \geq 15.9$). Groups I, III, and VI from the nirS1F/6R primer set results were also found with cd3aF/R3cd (**Figure 8**).

We used dissolved gases to estimate NCP in the surface mixed layer. NCP, effectively oxygen production in excess of consumption, was calculated from O_2/Ar (Stanley et al., 2010; **Figure 9A**). NCP for the three cruises showed small but significant difference, with May 2007 and July 2008 having lower values (28 and 26 mmol O_2 m^{-2} d^{-1}) and October 2007 showing slightly elevated NCP (31 mmol O_2 m^{-2} d^{-1}). $\delta^{18}O$-O_2 was also measured, which can show negative deviations if photosynthetic production is great enough to drive the below equilibrium levels (Quay et al., 1993). Unlike May 2007 and July 2008, October 2007 exhibited a large negative deviation in $\delta^{18}O$-O_2 immediately below the mixed layer, concordant with a 52% supersaturation of O_2 relative to Ar (Ar used to normalize for physical processes; **Figure 10**).

DISCUSSION

ANAMMOX-TYPE EXPRESSION

Anammox-type *nirS* was first used as a process-specific sequence type in the Peruvian OMZ (Lam et al., 2009). All of the sequences amplified in this Black Sea study were monophyletic with Peruvian OMZ sequences, in turn closely allied to the environmental anammox clade, "*Candidatus* Scalindua" (Lam et al., 2009; van de Vossenberg et al., 2012) (**Figure 3**). For comparison, anammox-type 16S rDNA was also analyzed (**Figure 5**). The observed distribution of this anammox-type *nirS* was consistent with this ribosomal DNA based distribution, as well as previous data sets (Kuypers et al., 2003; Kirkpatrick et al., 2006; Fuchsman et al., 2012). The presence of anammox bacteria in the lower suboxic zone may be due to the flux of ammonium from the sulfide zone that affects these depths. Although amplification of sequence types not involved in the anammox process cannot be ruled out, both the sequence data and depth distribution similarity lend credence to the applicability of these products as process specific markers.

Phylogenetically, expressed anammox-type *nirS* sequences fell into four highly similar groups (**Figure 3**). Distance between these Black Sea groups was less than between sequences from the Peruvian OMZ. It may be that a relatively small subset of marine anammox bacteria are adapted to the brackish waters of the Black Sea (suboxic zone salinity ∼20–21) as compared to the Peruvian OMZ; this is consistent with previous 16S-based approaches (Schmid et al., 2007).

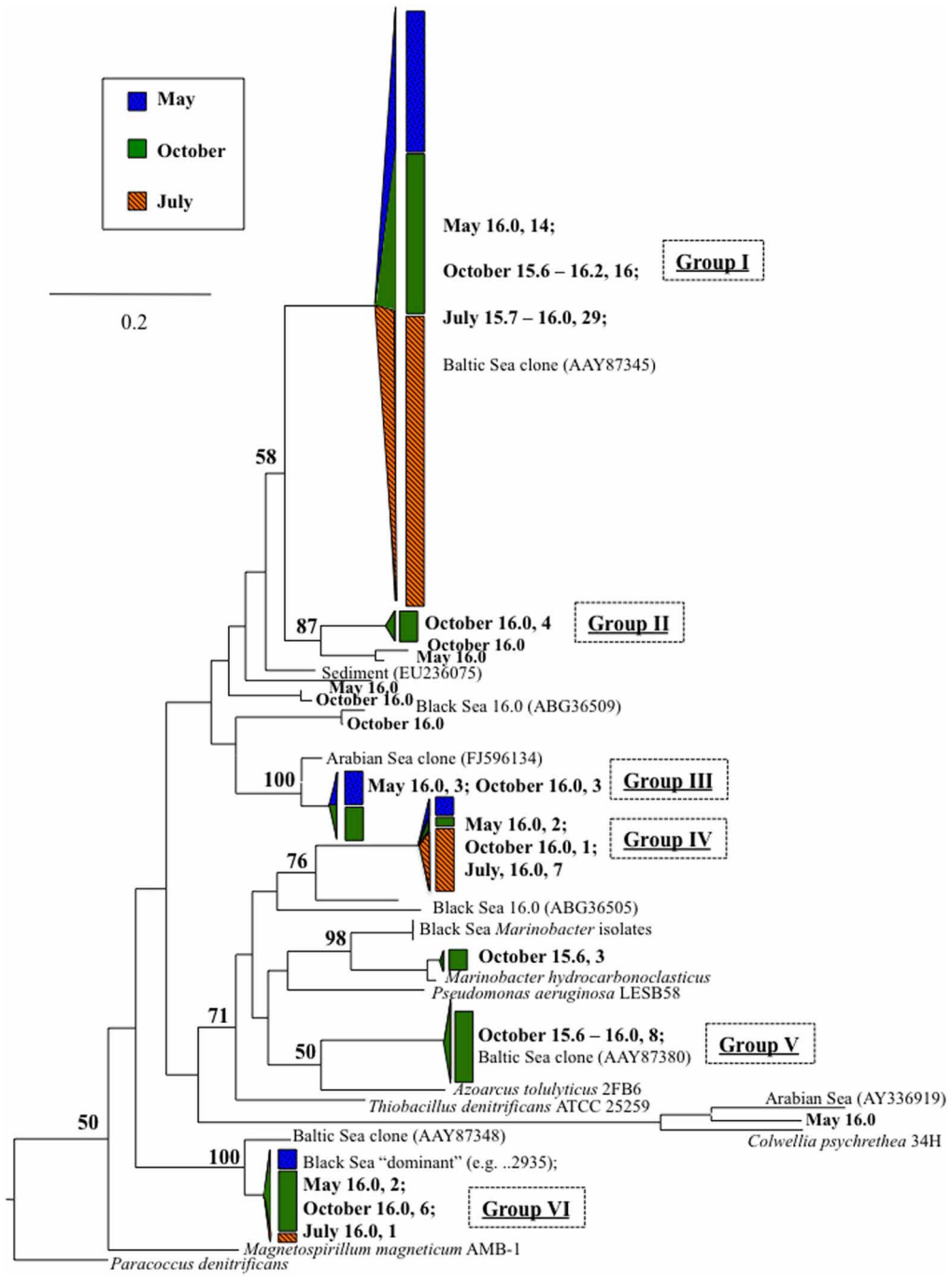

FIGURE 6 | *nirS* expression as detected with degenerate primers nirS1F/6R (Braker et al., 1998). Numbers indicate density, followed by number of clones. References include cultured strains (in italics), Baltic Sea environmental clones (Hannig et al., 2006), and DNA-based sequences previously obtained from the Black Sea (Oakley et al., 2007). Tree was constructed from amino acid sequences (~290 aa) as per **Figure 3**.

There appeared to be little difference between time points for the anammox-type *nirS* data, suggesting that these organisms were consistently transcribing this *nirS*-type gene. The single exception was July 2008, the only time that amplification could be detected as shallow as $\sigma_\theta = 15.8$, though only a few sequences could be retrieved (**Figure 2**). This was also the time of shallowest oxygen penetration (**Figure 1**). Between groups, the only variation appeared to be associated with differences in depth. Group I expression was only detected for $15.8 \geq \sigma_\theta \geq 16.0$ and Group IV was found for $16.0 \geq \sigma_\theta \geq 16.3$; Groups II and III were found variously across the whole range (**Figure 4**). Interestingly, for the one sample set which extended into the sulfidic zone (October

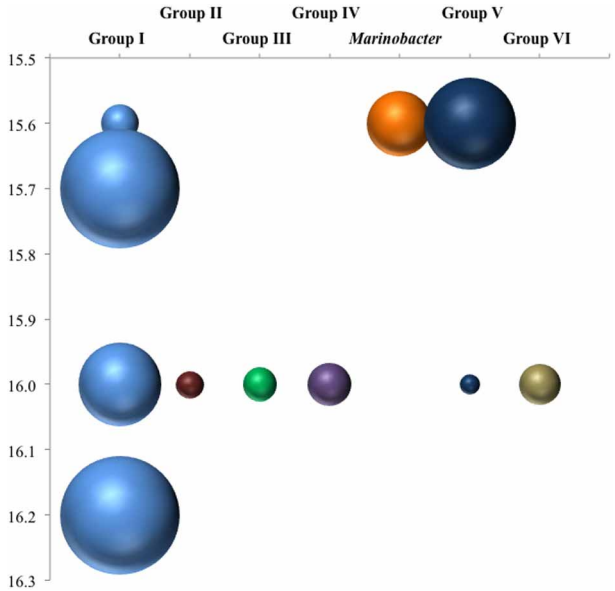

FIGURE 7 | Depth breakdown of groups noted in Figure 6. Areas of bubbles are proportional to percentage of clone library sequences for a given depth found in a given group.

2007) anammox activity could still be detected as deep as $\sigma_\theta = 16.3$, where $H_2S \geq 10\,\mu M$. Evidence for the presence of anammox bacteria coincident with low levels of sulfide has been previously found in the Black Sea (Wakeham et al., 2007; Fuchsman et al., 2012). This suggests some sulfide tolerance for Groups II, III, and IV. Theoretically, these groups could be actively involved in S-linked processes (Kalyuzhnyi et al., 2006), provided that a flux of NO_3^- or NO_2^- penetrates down to these density surfaces. While this is speculative, it is known that NO_2^- levels for $\sigma_\theta \geq 16.2$ were below the detection limit for October 2007, when deep activity was sampled (**Figure 2**). Other explanations for anammox activity require a supply of nitrite such as horizontal advection (Stunzhas and Yakushev, 2006) or *in situ* production with sparse oxidants such as trace levels of MnOx; a fast sinking mechanism to import active cells and their mRNA; or perhaps the utilization of abundant sulfate as the ultimate electron acceptor (Liu et al., 2008). While the specific adaptations of the four different anammox types are speculative, it is nonetheless apparent that there are some micro-heterogenities in this population.

DENITRIFICATION AND RELATION TO ENVIRONMENTAL FACTORS

Expression patterns of denitrification appeared more complex than anammox. October 2007 stands out in this data set due several factors, including deeper samples that were not available for the other two timepoints. Even excluding these samples, however, several "intermittent" groups were detected in October 2007 that were not found other times. Denitrifiers in the upper suboxic zone ($\sigma_\theta = 15.6$) were not only active, unlike other seasons, but included *Marinobacter* and Group V phylotypes not found at other times (**Figures 6**, **7**). Group V contains sequences up to 100% similar to a sequence known from the Baltic Sea's upper, oxic waters (AAY87380; Hannig et al., 2006), suggesting a tolerance for relatively oxidizing conditions. The *Marinobacter*-type sequences were distinct from strains previously isolated from the Black Sea (bootstrap support 98%) (Oakley et al., 2007). July 2008 also had transcripts at a relatively shallow density surface ($\sigma_\theta = 15.7$), but unlike the varied phylogeny of October 2007, the shallower July expression was only an extension of consistent, deeper Group I activity. This was perhaps in response to the shoaling of the oxycline (**Figure 1**).

Interestingly, October 2007 surface waters exhibited relatively high biological productivity (**Figure 9A**). October 2007 also had a large dissolved oxygen minimum below the mixed layer (**Figure 10**), suggestive of enhanced productivity, though assessing a rate to this deeper production is problematic. Although the linkage is indirect, if either mixed layer or deeper productivity resulted in sinking organic matter, this could have impacted heterotrophic denitrification. October 2007 was also unusual in the detection of elevated N_2 supersaturation levels, indicative of biological N_2 production, in both the upper suboxic zone ($15.6 \leq \sigma_\theta \leq 15.8$) and the upper sulfidic layer ($16.1 \leq \sigma_\theta \leq 16.25$) (**Figure 2**). Part of this N_2 build-up was potentially a result of these intermittently detected denitrifiers, particularly in the upper suboxic zone ($\sigma_\theta < 15.8$) where anammox type *nirS* expression was not found for our three time points. The deeper N_2 peak ($\sigma_\theta = 16.1$–16.2) was found at the transition from suboxic to sulfidic zones, and nutrient profiles (**Figure 1**) are suggestive of deeper H_2S consumption in October; it is possible that autotrophic denitrification could also have been enhanced at this time.

Looking at the diversity of denitrifiers, the Shannon-Wiener index for the suboxic zone also peaked in October (**Figure 9B**; $H'_{May} = 1.4$, $H'_{Oct} = 1.9$, $H'_{Jul} = 0.6$). This is excluding the deep samples unique to the October cruise. In October, when the N_2 build-up had both a shallow and a deep peak (**Figure 2**), $\sigma_\theta = 15.6$ in the upper suboxic zone had some *nirS* expression not seen other times (**Figure 7**), in addition to the consistent deep expression. This multiplicity of apparent niches was one of the drivers of diversity in October. If in fact greater productivity led to C export which stimulated denitrification at depth, this would be consistent with other studies that have linked organic C input to changes in denitrification activity (Engström et al., 2005; Fuchsman et al., 2008; Ward et al., 2008, 2009).

Many denitrifier groups, on the other hand, seem more similar to the detected anammox expression in that their expression was detected regularly between seasons and in the lower suboxic zone. These "consistent" denitrifiers include an unknown type (Group IV), a Group that was previously known from Black Sea clone libraries as the "dominant" type (Oakley et al., 2007)—here, Group VI—and a third type (Group I) identical to a different Baltic Sea clone, this one from suboxic waters (AAY87345; Hannig et al., 2006). Transcripts of this Baltic Sea type were found into the sulfidic layer. Whether this represents autotrophic or heterotrophic denitrification is unknown. While there were some sequences shared with Baltic Sea studies, it is notable that the consistent expression pattern typical of Black Sea groups I, IV, and VI discussed here are different from the temporal changes documented in the Baltic Sea (Hannig et al., 2007).

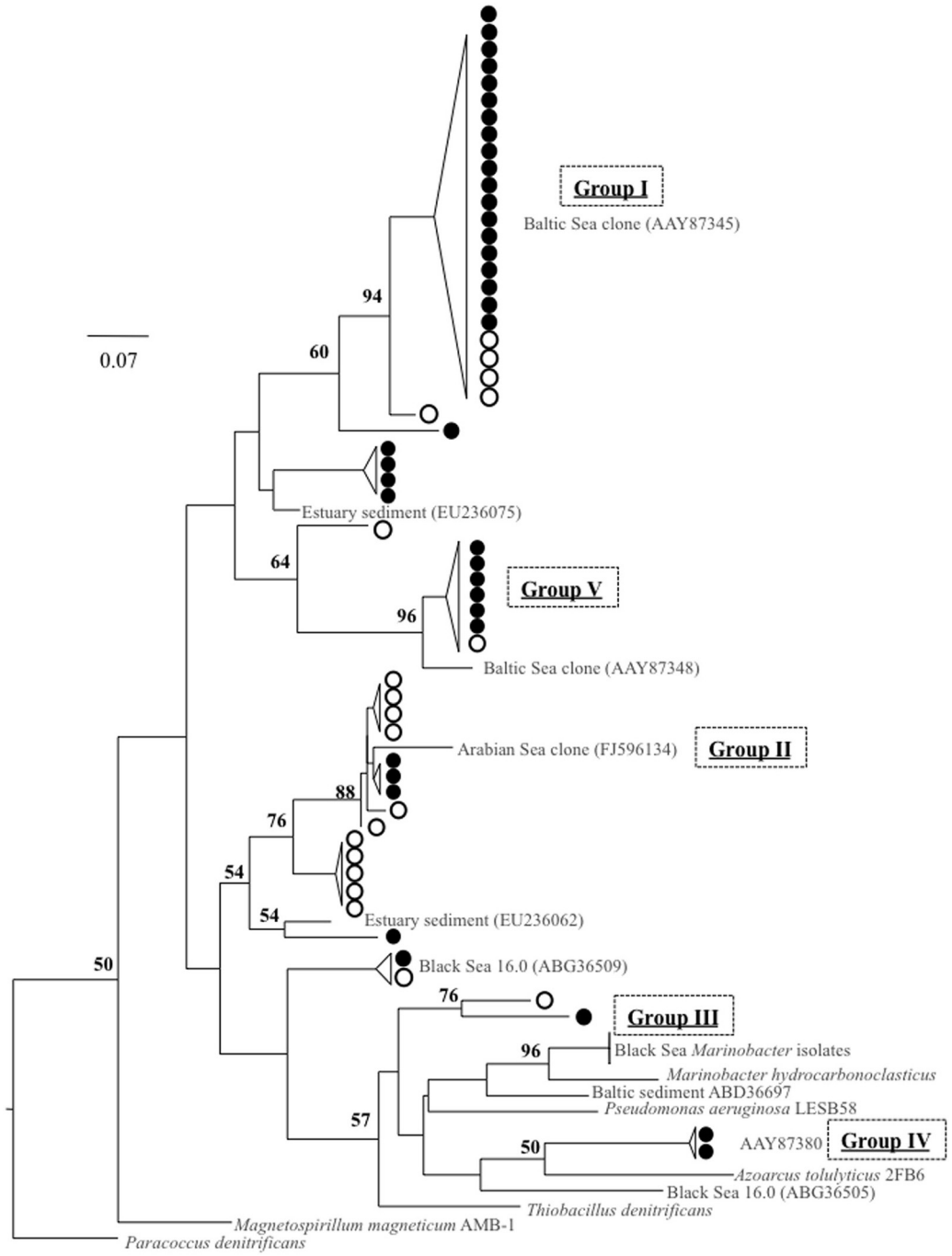

FIGURE 8 | Clone library comparison tree for two different primer pairs: nirS1F/6R, indicated by filled circles, and cd3aF/R3cd, in empty circles. All are from October 2007, $\sigma_\theta = 16.0$ or 16.2. References, in gray, include cultured strains (in italics), Baltic Sea environmental clones (Hannig et al., 2006), and DNA-based sequences previously obtained from the Black Sea (Oakley et al., 2007). Tree was constructed from amino acid sequences (~140 aa, necessarily shorter than other alignments) as per **Figure 3**.

Denitrification was indicated in the Baltic mainly in instances where the suboxic zone was compressed or absent and nitrate and sulfide overlapped, with the establishment of a stable suboxic zone favoring anammox (Hannig et al., 2007). Measurable levels of nitrate and sulfide do not commonly overlap in the Black Sea (Murray et al., 1995), though as noted above and in **Figure 1** some variability was observed in this study. Several lines of published evidence point toward autotrophic metabolism by ε- and γ-proteobacteria in the sulfidic zone, including the autotrophic denitrifier *Sulfurimonas* (Grote et al., 2008; Glaubitz et al., 2010).

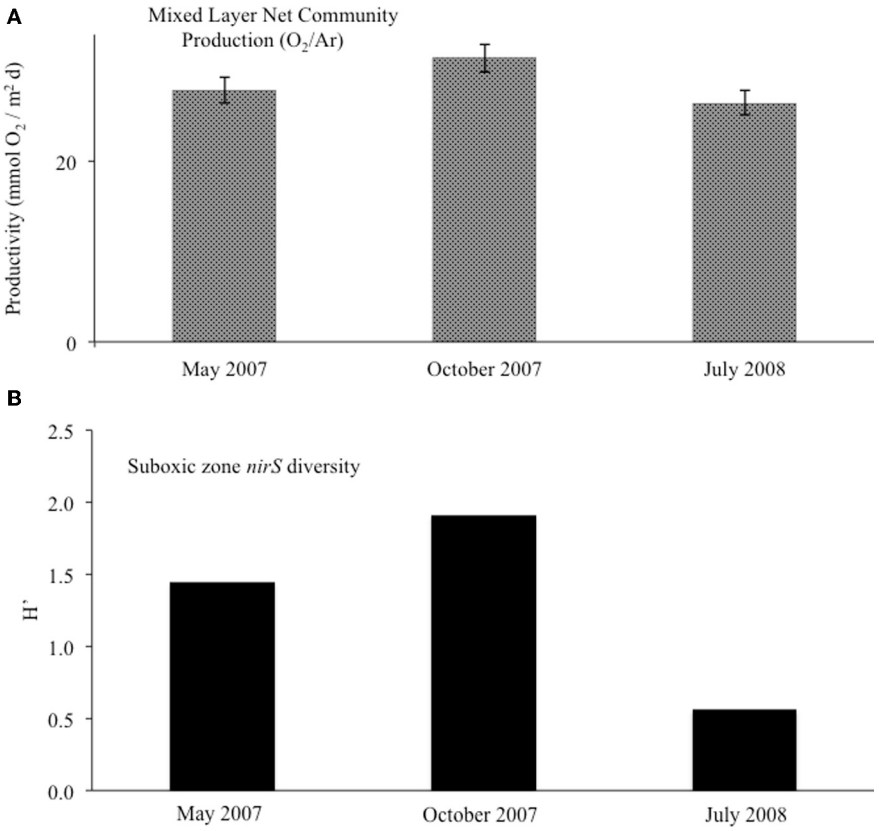

FIGURE 9 | (A) For the surface mixed layer, net community productivity calculated with O_2/Ar measurements. Error bars for NCP were calculated from averages of mixed layer O_2/Ar ($n = 4$). **(B)** Suboxic zone ($15.6 \leq \sigma_\theta \leq 16.0$) clone library diversity, as calculated with the Shannon-Wiener index.

In the case of *Sulfurimonas*, primer mismatch could have prevented detection of mRNA transcripts by our methods; see primer bias considerations, below.

CONCURRENT DENITRIFICATION AND ANAMMOX ACTIVITY

Both denitrification and anammox type *nirS* expression were consistently detected at the same density surfaces in the lower suboxic zone. This occurs despite the fact that they have different metabolic requirements, and in spite of the restricted, relatively stable environment formed by the redox gradient; this seems to indicate that conditions are conducive for both processes to persist simultaneously. As both require nitrite, a competitive playoff between the two processes is often assumed (e.g., Hannig et al., 2007; Bulow et al., 2010; Lam et al., 2011). Our data set suggests that this may not be the case, with the ongoing activity of both processes more similar to the balanced activity seen in Skagerrak sediments (Thamdrup and Dalsgaard, 2002) or the waters of Golfo Dulce (Dalsgaard et al., 2003).

PRIMER BIAS CONSIDERATIONS

Regarding primer sets, it should be noted that the *nirS* primer set used here (nirS1F/nirS6R), while degenerate, is not considered universal (Throbäck et al., 2004). Nitrite reductase genes, here focusing on *nirS*, are fairly diverse and exhibit significant sequence divergence, making whole-community analysis difficult and subject to bias. A fairly comprehensive analysis of different primer sets was conducted in 2004 for cultured organisms and soil samples (Throbäck et al., 2004). Studies of ocean OMZs have commonly relied on nirS1F/6R (Braker et al., 1998) or cd3aF/R3cd (Michotey et al., 2000; Throbäck et al., 2004). In order to assess possible primer pair bias in our data sets, products of both primer sets were analyzed. It must be noted that while we could compare between primer sets and samples, it is difficult to infer what other potential sequences were missed entirely. There could have been a large number of organisms contributing to the mRNA pool that remained undetected due to primer mismatches, including *Sulfurimonas*, which has previously been detected in the Black Sea (Grote et al., 2008). Compared to the Braker primers (Braker et al., 1998), we found *Sulfurimonas denitrificans DSM1* to have 6 mismatches and one deletion over the 18 bp of nirS1F and 10 mismatches over the 16 bp of nirS6R. Regardless of what was missed, given the data at hand it was possible to compare data produced by these two primer sets in an effort to understand what relative biases may have been present.

While nirS1F/6R amplified sequences throughout the suboxic zone, albeit intermittently for the upper suboxic zone (**Figure 2**), cd3aF/R3cd amplification was only successful in the lower suboxic zone ($\sigma_\theta \geq 15.9$). This suggests that the upper suboxic zone community may be "missed" not only because of changes in activity but also due to poor amplification if analyzed with a different

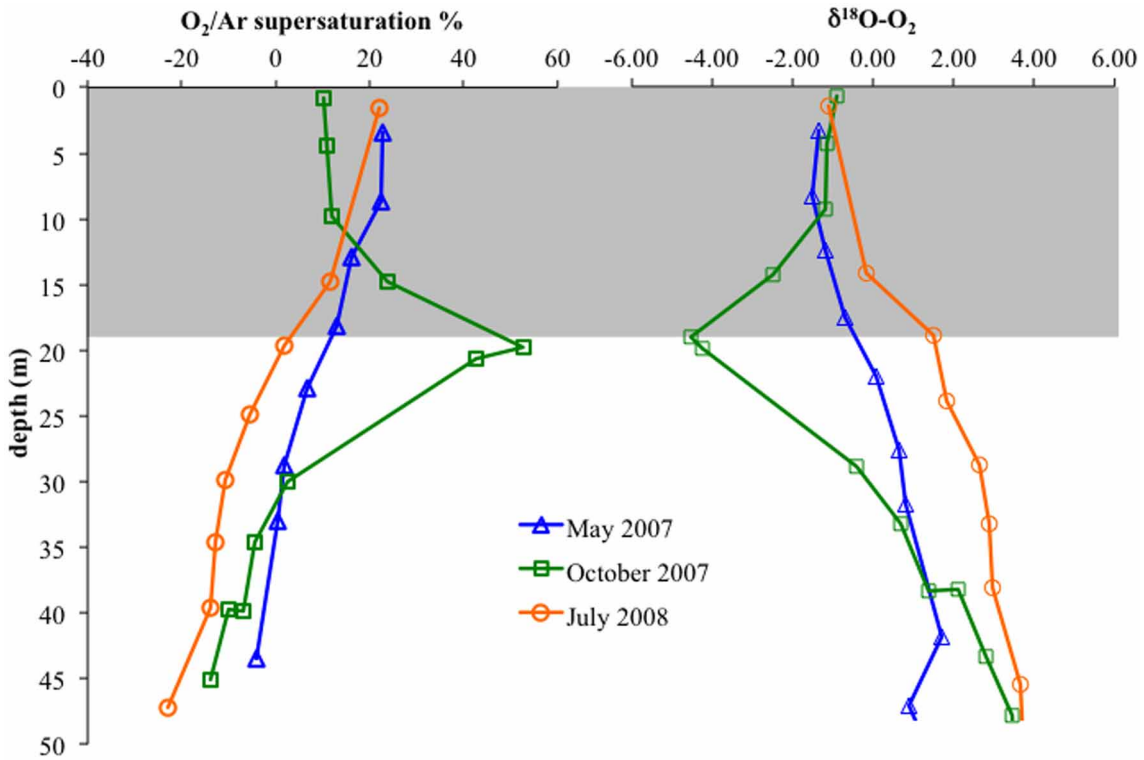

FIGURE 10 | Left: O_2/Ar supersaturation versus depth in the upper 50 m for May 2007, October 2007, and July 2008. **Right:** $\delta^{18}O$-O_2 versus depth. Gray box indicates average mixed layer depths.

primer set. This was further indicated by analyzing the entire nirS1F/6R data set (all depths) for mismatches to the cd3aF/R3cd priming site, both of which are internal to the amplicon produced by nirS1F/6R. 73% of nirS1F/6R clones mismatched the cd3aF primer, and 99% mismatched R3cd. The same analysis for nirS1F or 6R binding sites is not possible, as both sites are outside of the amplicons produced by cd3aF/R3cd.

In order to check for systematic discrimination of specific phyla by the different primer sets, sequences of both for October samples $\sigma_\theta = 16.0$ and 16.2 were obtained (**Figure 8**). It is important to note that ribosomal contamination was intermittently found in both data sets. This contamination, typically found in the absence of *nirS* template, was detected when sequences contained multiple stop codons and could not be aligned; it was confirmed with BLAST searches to the Genbank database. For nirS1F/6R this only happened in the upper suboxic zone. This was true even when bands of the proper size were excised and purified from the agarose gel and even when, additionally, mRNA purification of the RNA extract (MICROBExpress©, Ambion) was conducted before reverse transcription. This suggests that qPCR methods cannot be easily applied to these primer sets. Considering phylogeny, groups I, II, and V were present in both data sets, suggesting fairly good overlap between primer products (**Figure 8**). While it is not easy to make conclusions about groups that were not present, due to sampling depth, overall diversity of the two different data sets is similar (Shannon-Wiener index of 1.6 for 1F/6R, 1.8 for cd3aF/R3cd). In summary, while no clade-specific bias appeared when comparing sequences from successfully amplified PCR products of both primer sets for the same depths, for other depths nirS1F/6R was the only primer set that produced any *nirS*-type sequences at all. This suggests that, for some marine environments such as OMZs, cd3aF/R3cd may undersample diversity.

CONCLUSIONS

Our results, based on analysis of dissimilatory nitrite reductase (*nirS*) expression over three sampling seasons, revealed that both denitrification and anammox were consistently found in the lower suboxic zone, for three sample sets spanning15 months. Consistent *nirS*-expression was localized to the lower suboxic zone, and included both anammox and conventional denitrification type genes. Intermittent *nirS* expression was detected in the upper suboxic zone ($\sigma_\theta \leq 15.7$) and varied between sampling times, perhaps in response to environmental variables such as oxygen and organic C input. This connection is inferred, and not proven; other studies are required to directly investigate this linkage. The fluctuating response of some denitrifiers appears not just the opportunistic response of phylotypes otherwise routinely active at other depths, but characteristic of several groups that were not found to be active at other times, within the acknowledged limitations of sampling and sequencing for this study. This underscores the problematic nature of making global N budgets based on instantaneous measurements of rate or activity, and points toward the necessity of time-integrated approaches in

order to resolve conflicting estimates. Further work is needed to directly examine the interplay between surface productivity and deeper denitrification, resolve inconsistencies between methods based on *in situ* parameters versus incubations, and to understand the ongoing activity and interplay of anammox, heterotrophic denitrification, and autotrophic denitrification.

ACKNOWLEDGMENTS

This work was supported by grants NSF OCE-0751617, NSF IGERT 05-04219, NSF OISE 0637845, NSF OISE 0637866, and CRDF GCP-15123. The May 2007 cruise was also supported by the Lewis and Clark Astrobiology Travel Grant to Clara A. Fuchsman. We thank the staff of the Laboratory of Marine Chemistry of the Southern Branch of Shirshov Institute of Oceanology RAS (Ghelendzhik). We are indebted to Barbara Paul for essential aid in field and laboratory work, as well as Alexander Novigatsky, Alexander Filippov, Alexander Egorov, Nikolay Pimenov, and Oleg Podymov for help collecting samples. Thank you to Paul Quay, Steve Emerson, and Eric Steig for use of lab space and equipment.

REFERENCES

Altabet, M. A., Francois, R., Murray, D. W., and Prell, W. L. (1995). Climate-related variations in denitrification in the Arabian Sea from sediment 15N/14N ratios. *Nature* 373, 506–509.

Altabet, M. A., Murray, D. W., and Prell, W. L. (1999). Climatically linked oscillations in Arabian Sea denitrification over the past 1 m.y.: implications for the marine N cycle. *Paleoceanography* 14, 732–743.

Braker, G., Fesefeldt, A., and Witzel, K. P. (1998). Development of PCR primer systems for amplification of nitrite reductase genes (nirK and nirS) to detect denitrifying bacteria in environmental samples. *Appl. Environ. Microbiol.* 64, 3769–3775.

Bulow, S. E., Rich, J. J., Naik, H. S., Pratihary, A. K., and Ward, B. B. (2010). Denitrification exceeds anammox as a nitrogen loss pathway in the Arabian Sea oxygen minimum zone. *Deep-Sea Res.* 57(Pt 1), 384–393.

Dalsgaard, T., Canfield, D. E., Petersen, J., Thamdrup, B., and Acuña-González, J. (2003). N2 production by the anammox reaction in the anoxic water column of Golfo Dulce, Costa Rica. *Nature* 422, 606–608.

Emerson, S., Stump, C., Wilbur, D. O., and Quay, P. (1999). Accurate measurement of O_2, N_2, and Ar gases in water and the solubility of N_2. *Mar. Chem.* 64, 337–347.

Engström, P., Dalsgaard, T., Hulth, S., and Aller, R. C. (2005). Anaerobic ammonium oxidation by nitrite (anammox): implications for N_2 production in coastal marine sediments. *Geochim. Cosmochim. Acta* 69, 2057–2065.

Felsenstein, J. (1989). PHYLIP – Phylogeny Inference Package (Version 3.2). *Cladistics* 5, 164–166.

Fuchsman, C. A., Murray, J. W., and Konovalov, S. K. (2008). Concentration and natural stable isotope profiles of nitrogen species in the Black Sea. *Mar. Chem.* 111, 90–105.

Fuchsman, C. A., Staley, J. T., Oakley, B. B., Kirkpatrick, J. B., and Murray, J. W. (2012). Free-living and aggregate-associated Planctomycetes in the Black Sea. *FEMS Microbiol. Ecol.* 80, 402–416.

Ganeshram, R. S., Pedersen, T. F., Calvert, S. E., and Murray, J. W. (1995). Large changes in oceanic nutrient inventories from glacial to interglacial periods. *Nature* 376, 755–758.

Glaubitz, S., Labrenz, M., Jost, G., and Jürgens, K. (2010). Diversity of active chemolithoautotrophic prokaryotes in the sulfidic zone of a Black Sea pelagic redoxcline as determined by rRNA-based stable isotope probing. *FEMS Microbiol. Ecol.* 74, 32–41.

Grasshoff, K., Ehrhardt, M., and Kreming, K. (eds). (1983). *Methods of Seawater Analysis*. Third comp. Weinheim/New York/Chichester/Brisbane/Singapore/Tor onto: Wiley-VCH.

Grote, J., Jost, G., Labrenz, M., Herndl, G. J., and Jürgens, K. (2008). Epsilonproteobacteria represent the major portion of chemoautotrophic bacteria in sulfidic waters of pelagic redoxclines of the Baltic and Black Seas. *Appl. Environ. Microbiol.* 74, 7546–7551.

Hannig, M., Braker, G., Dippner, J., and Jürgens, K. (2006). Linking denitrifier community structure and prevalent biogeochemical parameters in the pelagial of the central Baltic Proper (Baltic Sea). *FEMS Microbiol. Ecol.* 57, 260–271.

Hannig, M., Lavik, G., Kuypers, M. M. M., Woebken, D., Martens-Habbena, W., and Jürgens, K. (2007). Shift from denitrification to anammox after inflow events in the central Baltic Sea. *Limnol. Oceanogr.* 52, 1336–1345.

Jayakumar, A., O'Mullan, G. D., Naqvi, S. W. A., and Ward, B. B. (2009a). Denitrifying bacterial community composition changes associated with stages of denitrification in oxygen minimum zones. *Microb. Ecol.* 58, 350–362.

Jayakumar, A., Naqvi, S. W. A., and Ward, B. B. (2009b). Distribution and relative quantification of key genes involved in fixed nitrogen loss from the Arabian Sea oxygen minimum zone. *Geophs. Monogr. Ser.* 185, 187–203.

Jensen, M. M., Kuypers, M. M. M., Lavik, G., and Thamdrup, B. (2008). Rates and regulation of anaerobic ammonium oxidation and denitrification in the Black Sea. *Limnol. Oceanogr.* 53, 23–36.

Jensen, M. M., Lam, P., Revsbech, N. P., Nagel, B., Gaye, B., Jetten, M. S. M., and Kuypers, M. M. M. (2011). Intensive nitrogen loss over the Omani Shelf due to anammox coupled with dissimilatory nitrite reduction to ammonium. *ISME J.* 5, 1660–1670.

Jones, D. T., Taylor, W. R., and Thornton, J. M. (1992). The rapid generation of mutation data matrices from protein sequences. *Comput. Appl. Biosci.* 8, 275–282.

Kalyuzhnyi, S., Gladchenko, M., Mulder, A., and Versprille, B. (2006). DEAMOX–new biological nitrogen removal process based on anaerobic ammonia oxidation coupled to sulphide-driven conversion of nitrate into nitrite. *Water Res.* 40, 3637–3645.

Kirkpatrick, J. B., Oakley, B. B., Fuchsman, C. A., Srinivasan, S., Staley, J. T., and Murray, J. W. (2006). Diversity and distribution of Planctomycetes and related bacteria in the suboxic zone of the Black Sea. *Appl. Environ. Microbiol.* 72, 3079–3083.

Kuypers, M. M. M., Sliekers, A. O., Lavik, G., Schmid, M., Jørgensen, B. B., Kuenen, J. G., Sinninghe Damsté, J. S., Strous, M., and Jetten, M. S. M. (2003). Anaerobic ammonium oxidation by anammox bacteria in the Black Sea. *Nature* 422, 608–611.

Lam, P., Jensen, M. M., Lavik, G., McGinnis, D. F., Müller, B., Schubert, C. J., Amann, R., Thamdrup, B., and Kuypers, M. M. M. (2007). Linking crenarchaeal and bacterial nitrification to anammox in the Black Sea. *Proc. Natl. Acad. Sci. U.S.A.* 104, 7104–7109.

Lam, P., Lavik, G., Jensen, M. M., van de Vossenberg, J., Schmid, M., Woebken, D., Gutiérrez, D., Amann, R., Jetten, M. S. M., and Kuypers, M. M. M. (2009). Revising the nitrogen cycle in the Peruvian oxygen minimum zone. *Proc. Natl. Acad. Sci. U.S.A.* 106, 4752–4757.

Lam, P., Jensen, M. M., Kock, A., Lettmann, K. A., Plancherel, Y., Lavik, G., Bange, H. W., and Kuypers, M. M. M. (2011). Origin and fate of the secondary nitrite maximum in the Arabian Sea. *Biogeosciences* 8, 1565–1577.

Liu, S., Yang, F., Gong, Z., Meng, F., Chen, H., Xue, Y., and Furukawa, K. (2008). Application of anaerobic ammonium-oxidizing consortium to achieve completely autotrophic ammonium and sulfate removal. *Bioresour. Technol.* 99, 6817–6825.

Michotey, V., Méjean, V., and Bonin, P. (2000). Comparison of methods for quantification of cytochrome cd(1)-denitrifying bacteria in environmental marine samples. *Appl. Environ. Microbiol.* 66, 1564–1571.

Murray, J. W., Codispoti, L. A., and Friedrich, G. E. (1995). "Oxidation-reduction environments: the suboxic zone in the Black Sea," in *Aquatic Chemistry: Interfcial and Interspecies Processess*, eds C. P., Huang, C. R. O'Melia, and J. J. Morgan (San Francisco, CA: American Chemical Society), 157–176.

Nicholson, D., Emerson, S., Caillon, N., Jouzel, J., and Hamme, R. C. (2010). Constraining ventilation during deepwater formation using deep ocean measurements of the dissolved gas ratios 40 Ar/ 36 Ar, N 2 /Ar, and Kr/Ar. *J. Geophys. Res.* 115, C11015.

Nightingale, P. D., Malin, G., Law, C. S., Watson, A. J., Liss, P. S., Liddicoat, M. I., Boutin, J., and Upstill-Goddard, R. C. (2000). *In situ* evaluation of air-sea gas exchange parameterizations using novel conservative and volatile tracers. *Glob. Biogeochem. Cycles* 14, 373–387.

Oakley, B. B., Francis, C. A., Roberts, K. J., Fuchsman, C. A., Srinivasan, S., and Staley, J. T. (2007). Analysis of nitrite reductase (nirK and nirS) genes and cultivation reveal depauperate community of denitrifying bacteria in the Black Sea suboxic zone. *Environ. Microbiol.* 9, 118–130.

Poretsky, R. S., Bano, N., Buchan, A., Lecleir, G., Kleikemper, J., Pickering, M., Pate, W. M., Moran, M. A., and Hollibaugh, J. T. (2005). Analysis of microbial gene transcripts in environmental samples. *Appl. Environ. Microbiol.* 71, 4121–4126.

Quay, P. D., Emerson, S., Wilbur, D. O., Stump, C., and Knox, M. (1993). The $\delta^{18}O$ of dissolved O_2 in the surface waters of the subarctic Pacific: a tracer of biological productivity. *J. Geophys. Res.* 98, 8447–8458.

Santoro, A. E., Boehm, A. B., and Francis, C. A. (2006). Denitrifier community composition along a nitrate and salinity gradient in a coastal aquifer. *Appl. Environ. Microbiol.* 72, 2102–2109.

Schmid, M. C., Risgaard-Petersen, N., van de Vossenberg, J., Kuypers, M. M., Lavik, G., Petersen, J., Hulth, S., Thamdrup, B., Canfield, D., Dalsgaard, T., Rysgaard, S., Sejr, M. K., Strous, M., den Camp, H. J., and Jetten, M. S. (2007). Anaerobic ammonium-oxidizing bacteria in marine environments: widespread occurrence but low diversity. *Environ. Microbiol.* 9, 1476–1484.

Stanley, R. H. R., Kirkpatrick, J. B., Cassar, N., Barnett, B. A., and Bender, M. L. (2010). Net community production and gross primary production rates in the western equatorial Pacific. *Glob. Biogeochem. Cycles* 24, 1–17.

Stunzhas, P. A., and Yakushev, E. V. (2006). Fine hydrochemical structure of the redox zone in the black sea according to the results of measurements with an open oxygen sensor and with bottle samplers. *Oceanology* 46, 629–641.

Thamdrup, B., and Dalsgaard, T. (2002). Production of N_2 through anaerobic ammonium oxidation coupled to nitrate reduction in marine sediments. *Appl. Environ. Microbiol.* 68, 1312–1318.

Throbäck, I. N., Enswall, K., Jarvis, Å., and Hallin, S. (2004). Reassessing PCR primers targeting nirS, nirK and nosZ genes for community surveys of denitrifying bacteria with DGGE. *FEMS Microbiol. Ecol.* 49, 401–417.

van de Vossenberg, J., Woebken, D., Maalcke, W. J., Wessels, H. J., Dutilh, B. E., Kartal, B., Janssen-Megens, E. M., Roeselers, G., Yan, J., Speth, D., Gloerich, J., Geerts, W., van der Biezen, E., Pluk, W., Francoijs, K. J., Russ, L., Lam, P., Malfatti, S. A., Tringe, S. G., Haaijer, S. C., Op den Camp, H. J., Stunnenberg, H. G., Amann, R., Kuypers, M. M., and Jetten, M. S. (2012). The metagenome of the marine anammox bacterium "Candidatus Scalindua profunda" illustrates the versatility of this globally important nitrogen cycle bacterium. *Environ. Microbiol*. doi: 10.1111/j.1462-2920.2012.02774.x. [Epub ahead of print].

Wakeham, S. G., Amann, R., Freeman, K., Hopmans, E., Jørgensen, B. B., Putnam, I., Schouten, S., Sinninghedamste, J., Talbot, H., and Woebken, D. (2007). Microbial ecology of the stratified water column of the Black Sea as revealed by a comprehensive biomarker study. *Org. Geochem.* 38, 2070–2097.

Wang, J., Jenkins, C., Webb, R. I., and Fuerst, J. A. (2002). Isolation of Gemmata-Like and Isosphaera-Like Planctomycete Bacteria from Soil and Freshwater. *Appl. Environ. Microbiol.* 68, 417–422.

Ward, B. B., Tuit, C., Jayakumar, A., Rich, J. J., Moffett, J., Wajih, S., and Naqvi, A. (2008). Organic carbon, and not copper, controls denitrification in oxygen minimum zones of the ocean. *Deep-Sea Res.* 55(Pt I), 1672–1683.

Ward, B. B., Devol, A. H., Rich, J. J., Chang, B. X., Bulow, S. E., Naik, H. S., Pratihary, A. K., and Jayakumar, A. (2009). Denitrification as the dominant nitrogen loss process in the Arabian Sea. *Nature* 461, 78–81.

Conflict of Interest Statement: The authors declare that the research was conducted in the absence of any commercial or financial relationships that could be construed as a potential conflict of interest.

Received: 14 February 2012; accepted: 29 June 2012; published online: 19 July 2012.

Citation: Kirkpatrick JB, Fuchsman CA, Yakushev E, Staley JT and Murray JW (2012) Concurrent activity of anammox and denitrifying bacteria in the Black Sea. Front. Microbio. ***3****:256. doi: 10.3389/fmicb.2012.00256*

This article was submitted to Frontiers in Aquatic Microbiology, a specialty of Frontiers in Microbiology.

frontiers in
MICROBIOLOGY

ORIGINAL RESEARCH ARTICLE
published: 28 November 2012
doi: 10.3389/fmicb.2012.00395

Benthic nitrogen loss in the Arabian Sea off Pakistan

Sarah Sokoll[1]*, Moritz Holtappels[1], Phyllis Lam[1], Gavin Collins[2], Michael Schlüter[3], Gaute Lavik[1] and Marcel M. M. Kuypers[1]

[1] Biogeochemistry Department, Max Planck Institute for Marine Microbiology, Bremen, Germany
[2] Microbiology, School of Natural Sciences, National University of Ireland, Galway, Ireland
[3] Geosciences, Marine Geochemistry, Alfred Wegener Institute, Bremerhaven, Germany

Edited by:
Hongyue Dang, China University of Petroleum, China

Reviewed by:
Susannah Green Tringe, DOE Joint Genome Institute, USA
Zhe-Xue Quan, Fudan University, China

***Correspondence:**
Sarah Sokoll, Biogeochemistry Department, Max Planck Institute for Marine Microbiology, Celsiusstrasse 1, D-28359 Bremen, Germany.
e-mail: ssokoll@mpi-bremen.de

A pronounced deficit of nitrogen (N) in the oxygen minimum zone (OMZ) of the Arabian Sea suggests the occurrence of heavy N-loss that is commonly attributed to pelagic processes. However, the OMZ water is in direct contact with sediments on three sides of the basin. Contribution from benthic N-loss to the total N-loss in the Arabian Sea remains largely unassessed. In October 2007, we sampled the water column and surface sediments along a transect cross-cutting the Arabian Sea OMZ at the Pakistan continental margin, covering a range of station depths from 360 to 1430 m. Benthic denitrification and anammox rates were determined by using ^{15}N-stable isotope pairing experiments. Intact core incubations showed declining rates of total benthic N-loss with water depth from 0.55 to 0.18 mmol N m^{-2} day^{-1}. While denitrification rates measured in slurry incubations decreased from 2.73 to 1.46 mmol N m^{-2} day^{-1} with water depth, anammox rates increased from 0.21 to 0.89 mmol N m^{-2} day^{-1}. Hence, the contribution from anammox to total benthic N-loss increased from 7% at 360 m to 40% at 1430 m. This trend is further supported by the quantification of *cd*$_1$-containing nitrite reductase (*nirS*), the biomarker functional gene encoding for cytochrome *cd*$_1$-Nir of microorganisms involved in both N-loss processes. Anammox-like *nirS* genes within the sediments increased in proportion to total *nirS* gene copies with water depth. Moreover, phylogenetic analyses of NirS revealed different communities of both denitrifying and anammox bacteria between shallow and deep stations. Together, rate measurement and *nirS* analyses showed that anammox, determined for the first time in the Arabian Sea sediments, is an important benthic N-loss process at the continental margin off Pakistan, especially in the sediments at deeper water depths. Extrapolation from the measured benthic N-loss to all shelf sediments within the basin suggests that benthic N-loss may be responsible for about half of the overall N-loss in the Arabian Sea.

Keywords: Arabian Sea, benthic N-loss, anammox, denitrification, qPCR, *nirS*

INTRODUCTION

The Arabian Sea is the semi-enclosed, north-western part of the Indian Ocean. Connected with the Red Sea and the Persian Gulf, it also receives discharge from some of the largest rivers in the world and is fringed by amongst the densest human populations. Although covering only 1% of the ocean surface, the Arabian Sea accounts for ∼5% of the global phytoplankton production, which has characteristic seasonal variability driven by two monsoons each year (Marra and Barber, 2005; Wiggert et al., 2005). Owing to the high seasonal surface production, high respiration in subsurface waters along with slow ventilation produces a pronounced oxygen minimum zone (OMZ) at depths between ∼100 and 1000 m. This OMZ is associated with a high nitrogen deficit (Codispoti et al., 2001; Deutsch et al., 2001) and a strong secondary nitrite maximum found at similar depths, which have been attributed to high pelagic N-loss activities therein (Naqvi, 1994; Naqvi et al., 2006; Ward et al., 2009). Due to its size, the Arabian Sea OMZ is assumed to be one of the biggest pelagic N-sinks, with annual estimated rates varying between ∼30 and 60 Tg N $year^{-1}$ (Bange et al., 2000; Codispoti et al., 2001; Devol et al., 2006).

On the other hand, N-loss processes also occur in marine sediments. In fact, benthic N-loss is believed to contribute ∼50–70% of global oceanic N-loss (Codispoti et al., 2001; Galloway et al., 2004; Gruber, 2004). Because of the geographical configuration of the Arabian Sea, OMZ waters therein impinge on the sediments along the continental margins off the coasts of India, Pakistan as well as Oman. Consequently, any *in situ* N-transformations within the OMZ waters would undoubtedly affect the N-budget of the sediments, and vice versa. Nevertheless, despite the obvious importance of benthic N-loss in the Arabian Sea, benthic N-loss activities have hardly been assessed, and thus estimates of the benthic contribution to the N-deficit and overall N-loss in the Arabian Sea remain poorly constrained. Based on depth-integrated primary production rates (Seitzinger and Giblin, 1996), Bange et al. (2000) estimated that shelf and margin sediments may account for 17% of the N-loss in the Arabian Sea; or up to 26% estimated by Schwartz et al. (2009) from the changes in N_2:Ar and nitrate consumption rates in Arabian Sea sediments. No direct measurements have been made, however, to distinguish the benthic N-loss pathways, nor have the

potential interactions with overlying OMZ waters been much considered.

In general, two processes are known to remove nitrogen from marine systems: the N_2O and N_2 production via canonical denitrification $NO_3^- \rightarrow NO_2^- \rightarrow NO \rightarrow N_2O \rightarrow N_2$ and the N_2 production by anaerobic ammonium oxidation (anammox, $NH_4^+ + NO_2^- \rightarrow N_2$). In marine environments, anammox activities were first detected in sediments (Dalsgaard and Thamdrup, 2002; Thamdrup and Dalsgaard, 2002), and later in the suboxic water columns of the Black Sea (Kuypers et al., 2003) and Golfo Dulce, Costa Rica (Dalsgaard et al., 2003). Since then anammox bacteria have been found in marine habitats ranging from the Arctic sea ice (Rysgaard et al., 2004) to deep sea hydrothermal vents (Byrne et al., 2009). In sediments, anammox has been shown to contribute up to 80% to the N_2 production (Dalsgaard et al., 2005), but anammox rates measured by ^{15}N stable isotope pairing experiments in sediments underlying a major OMZ to our knowledge have never been made before.

The reduction of nitrite to nitric oxide is an essential step in both anammox and denitrification, and is mediated by specific nitrite reductases (Nir; Schalk et al., 2000; Strous et al., 2006; Kartal et al., 2011). In general, two different types of nitrite reductases are known to occur, the copper-(NirK), and the cd_1-containing nitrite reductase (NirS), but organisms harbor either of the reductases. The *nirK* genes are not only present in denitrifiers, but also known to occur in nitrifiers and therefore not suitable for the quantification of denitrifiers. Hence, genes encoding for the (*nirS*) are more commonly used as biomarkers for denitrifiers (Jayakumar et al., 2004; Castro-Gonzalez et al., 2005; Tiquia et al., 2006; Dang et al., 2009) and found to be more abundant in general and in an estuary system (Abell et al., 2010). Meanwhile, anammox bacteria also use a NirS, which is phylogenetically distinct from denitrifier NirS. Thus, *nirS* can be a useful biomarker to distinguish between denitrifiers and anammox bacteria, as evidenced by studies in the Peruvian and Arabian Sea pelagic OMZs (Lam et al., 2009).

In this study, we determined N-loss rates of denitrification and anammox in surface sediments at the continental margin off Pakistan via ^{15}N-stable isotope experiments in intact core and slurry incubations. The relative abundances of denitrifying and anammox bacteria in the sediment were quantified based on their respective *nirS* genes and their phylogenies were further evaluated to characterize the benthic microbial communities at various station depths. In order to explore the potential interaction between benthic and OMZ N-loss rates, stations with water depths between 360 and 1430 m were sampled. Accordingly, sediments at one station lay below the OMZ, while the others were within OMZ waters.

MATERIALS AND METHODS

SAMPLING PROCEDURES AND CHEMICAL ANALYSES

Sampling was conducted during the *R/V Meteor* cruise M74/2, on 7th to 28th October 2007, in the Arabian Sea over the Pakistan shelf (Makran region, **Figure 1**). Four stations ranging from 360 to 1430 m were selected for detailed sampling and sediment incubations. (Please note, that original station names have been shortened for simplicity, from, e.g. GeoB12204 to station 04). Dissolved oxygen and temperature of the water column were measured with

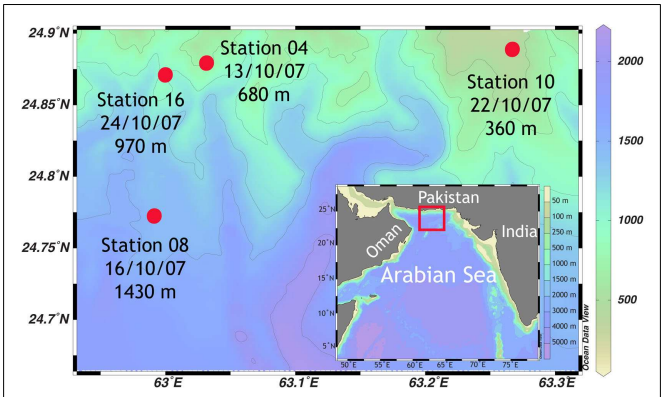

FIGURE 1 | Sampling area of the *R/V Meteor* cruise M74/2 in October 2007, in the Makran region at the Pakistan continental margin. Color scale on the right denotes water depth.

a conductivity-temperature-depth (CTD) probe, equipped with an oxygen sensor (Sea Bird Electronics). The oxygen concentration was calibrated against Winkler titration. Water samples were taken with a CTD-rosette. On ship board, concentrations of ammonium and nitrite were measured fluorometrically (Holmes et al., 1999) and photometrically (Grasshoff and Johannsen, 1972), respectively. Additional subsamples were stored at −20°C for later analyses for ammonium, nitrate, nitrite, and phosphate in a shore based laboratory using an autoanalyzer (TRAACS 800, Bran & Luebbe).

Sediment cores were taken with a multicorer (MUC) equipped with eight acrylic liners (10 cm diameter). Subsamples for molecular analyses were taken directly from MUC cores at 2 cm intervals from the surface down to 8 cm. DNA samples were stored at −80°C, shipped on dry ice and kept at −80°C until DNA extraction. Pore water extraction was conducted on board, sediment cores were sliced in a resolution of 0.5 cm (sediment depth 0–1 cm), 1 cm (sediment depth 2–5 cm), and 4 cm (sediment depth 5–0 cm), and pore water was squeezed out of the sediment slices with a pore water press (Schlüter, 1990). Pore water samples for nitrate and nitrite were kept frozen until measurement with a chemiluminescence NO_x analyzer (Thermo Environmental Instruments, Inc; Braman and Hendrix, 2002) in a shore based laboratory. For analyses of dissolved iron and sulfide, sediment cores were sampled on board with rhizomes at 1 cm (sediment depth 0–5 cm) and 2 cm intervals (sediment depth 5–30 cm). Subsequently the obtained pore water was analyzed for Fe^{2+} and HS^- on board according to Grasshoff et al. (1999) and Cline (1969). Concentrations of organic carbon and nitrogen were determined by combustion/gas chromatography (Carlo Erba NA-1500 CNS analyzer) of dried sediment samples after acidification with 3 mol l^{-1} phosphoric acid in a shore based laboratory.

INCUBATION EXPERIMENTS

Benthic denitrification and anammox rates were determined from N_2 production of ^{15}N-labeled slurry and intact core incubations. Rates from slurry incubations were used to calculate the contribution of anammox and denitrification to the total N-loss. Furthermore, volumetric rates from slurry incubations were integrated

over the nitrate penetration depth to derive areal N-loss rates. Areal rates were also estimated from intact core incubations according to the revised isotope pairing technique (rIPT) detailed in Risgaard-Petersen et al. (2003).

Intact core incubations

Sediment cores (10 cm diameter) were subsampled with 3.6 cm diameter liners and the overlying water was adjusted to a height of 12.5 cm above sediment surface. $^{15}NO_3^-$ (Campro Scientific GmbH) was added to a final concentration of 50 μmol l^{-1} in the overlying water, which was constantly mixed with magnetic stirrers. After pre-incubation for 8–12 h, the cores were sealed with rubber stoppers and incubated without gas phase in the dark at *in situ* temperature (6–16°C). Five time points were taken at ∼0, 2, 6, 10, and 15 h after the cores have been sealed. At each time point, three cores were randomly selected and sacrificed by first removing the rubber stopper and injecting 1 ml of 50% (w/v) zinc chloride to the overlying water to precipitate any free sulfide. Then the first 6 cm of the sediment were mixed with the overlying water. A subsample of the slurry was transferred into 12 ml gas tight sterile glass vials (Exetainer®, Labco), poisoned with 100 μl of saturated $HgCl_2$ solution to stop biological activity and kept at room temperature in the dark until further processing.

Slurry incubations

Vertical distributions of denitrification and anammox rates within the sediment were estimated from slurry incubation experiments in gas tight bags made of plastic-laminated aluminum-foil (Gao et al., 2009). Briefly, MUC sediment cores were sliced in 2 cm intervals between 0 and 8 cm depth. Each slice (volume of ∼160 cm^3) was transferred into a gas tight bag that was subsequently heat-sealed from all sides. To prepare the slurry, 200 ml of degassed bottom water, taken from the overlying water in the MUC cores, was injected through a gas tight port into the bag. The residual air was removed from the bag and the slurry was thoroughly mixed. After pre-incubating the bags for 2 h, to remove potential air-contamination introduced by the sub-sampling, ^{15}N-labeled substrates were injected into the bags and the slurries were again thoroughly mixed. Incubations were performed in the dark at *in situ* temperatures. In Experiment 1, $^{15}NH_4^+$ and $^{14}NO_2^-$ were added to the slurries to final concentrations of 200 and 100 μmol l^{-1}, respectively. Furthermore, allylthiourea (ATU) was added to a final concentration of 86 μmol l^{-1} (Ginestet et al., 1998) to inhibit possible bacterial ammonia oxidation. In Experiment 2, $^{15}NO_3^-$ was added to the slurries to a final concentration of 200 μmol l^{-1}. For both experiments, a subsample of 6 ml was drawn from the bags immediately after tracer addition, transferred into sterile gas tight glass vials (Exetainer®, Labco) and fixed with 100 μl of saturated $HgCl_2$ solution. Between five and seven subsamples were drawn from the bags during the subsequent 26–28 h. The exetainers containing the subsamples were kept and shipped upside down in the dark at room temperature.

In the laboratory, a 2 ml helium headspace was introduced into the 12 ml exetainer of the whole core incubations while a headspace of 1 ml was used for the 6 ml exetainer of the slurries. The exetainers were shaken vigorously to allow N_2 to equilibrate between the headspace and the liquid phase. The N_2 isotope ratio ($^{28}N_2$, $^{29}N_2$, and $^{30}N_2$) of the headspace was determined by gas chromatography-isotopic ratio mass spectrometry (VG Optima, Micromass) by direct injections from the headspace according to Kuypers et al. (2005). Concentrations of $^{30}N_2$ and $^{29}N_2$ were normalized to $^{28}N_2$ and calculated as excess relative to air according to Holtappels et al. (2011). N_2 production rates were calculated from the $^{29}N_2$ and $^{30}N_2$ increase over time. Only production with a significant linear slope ($p < 0.05$) over time without delay was used for further calculations.

Calculation of N-loss in the sediment slurries

In Experiment 1, the anammox pathway ($NH_4^+ + NO_2^- \rightarrow N_2$) combines either $^{14}NH_4^+$ or $^{15}NH_4^+$ with $^{14}NO_2^-$ to form $^{28}N_2$ and $^{29}N_2$. Anammox activity was indicated when the production of $^{29}N_2$ ($p^{29}N_2$) was measured without any production of $^{30}N_2$ ($p^{30}N_2$). The production of $^{30}N_2$ was not detected in our samples, only a small amount of $^{30}N_2$ production was measured at station 16, depth 2–4 cm. The total N_2 production via anammox in Experiment 1 [$A_{(Ex1)}$] was calculated from:

$$A_{(Ex1)} = \frac{p^{29}N_2}{F_{NH_4^+}} \quad (1)$$

where $F_{NH_4^+}$ is the labeling percentage of the ^{15}N-substrate ($F_{NH_4^+} = {}^{15}NH_4^+/({}^{14}NH_4^+ + {}^{15}NH_4^+)$). For Experiment 1, $F_{NH_4^+}$ was calculated from the measured $^{14}NH_4^+$-concentrations in bottom waters and pore waters and the known addition of $^{15}NH_4^+$.

In Experiment 2, the addition of $^{15}NO_3^-$ to background concentrations of $^{14}NO_3^-$ and $^{14}NH_4^+$ would produce $^{28}N_2$ and $^{29}N_2$ via anammox and $^{28}N_2$, $^{29}N_2$, and $^{30}N_2$ via denitrification. Thus, the production of $^{30}N_2$ ($p^{30}N_2$) indicates active denitrification. The total N_2 production by denitrification in Experiment 2 [$D_{(Ex2)}$] was calculated according to Thamdrup and Dalsgaard (2002) from $p^{30}N_2$:

$$D_{(Ex2)} = \frac{p^{30}N_2}{\left(F_{NO_3^-}\right)^2} \quad (2)$$

where $F_{NO_3^-}$ is the labeling percentage of nitrate ($F_{NO_3^-} = {}^{15}NO_3^-/({}^{14}NO_3^- + {}^{15}NO_3^-)$). In Experiment 2, both, anammox and denitrification produce $^{29}N_2$. To calculate anammox from Experiment 2, Eq. 1 is modified to: $A_{(Ex2)} = (p^{29}N_2 - p^{29}N_{2(Den)})/F_{NO_3^-}$, where $p^{29}N_{2(Den)}$ is the $^{29}N_2$ production via denitrification. With $p^{29}N_{2(Den)} = 2\ p^{30}N_2(1 - F_{NO_3^-})/F_{NO_3^-}$ (Thamdrup and Dalsgaard, 2002), we derive:

$$A_{(Ex2)} = \left(p^{29}N_2 - 2\frac{\left(1 - F_{NO_3^-}\right)}{F_{NO_3^-}}p^{30}N_2\right) \cdot \frac{1}{F_{NO_3^-}} \quad (3)$$

Results from slurry incubations indicated the presence of NO_3^--storing organisms releasing intracellular $^{14}NO_3^-$ in the course of the experiment (for further details, see discussion). An estimate of $F_{NO_3^-}$ on the basis of measured $^{14}NO_3^-$ bottom water and pore

water concentrations was therefore not possible. Instead, we calculated $F_{NO_3^-}$ from Eq. 3 by inserting the measured $p^{29}N_2$ and $p^{30}N_2$ and by assuming $A_{(Ex1)} = A_{(Ex2)}$. The derived $F_{NO_3^-}$ value, in the following referred to as $^*F_{NO_3^-}$, was then used to estimate denitrification according to Eq. 2. For sediments without the release of stored nitrate we expected $F_{NO_3^-}$ equals $^*F_{NO_3^-}$, whereas $^*F_{NO_3^-} < F_{NO_3^-}$ indicated an additional source of $^{14}NO_3^-$, which was not dissolved initially in the pore water. We denoted the additional nitrate as excess $^{14}NO_3^-$ that was calculated from $^*F_{NO_3^-}$, $F_{NO_3^-}$ and the known concentration of $^{15}NO_3^-$ in the slurry:

$$\text{Excess}^{14}NO_3^- = {}^{15}NO_3^- \left(\frac{1}{{}^*F_{NO_3^-}} - \frac{1}{F_{NO_3^-}} \right) \quad (4)$$

Calculation of N-loss in intact sediment cores

From the slurry incubation, the contribution of anammox to the total N-loss was estimated as $ra = A_{(Ex1)}/[A_{(Ex1)} + D_{(Ex2)}]$. The total N-loss due to denitrification and anammox was calculated according to Risgaard-Petersen et al. (2003) from ra and the production of $^{30}N_2$ and $^{29}N_2$ in the core incubations:

$$N - \text{loss} = 2 \cdot \frac{(1 - ra)\ R^{29} - ra}{2 - ra} \cdot \left[p^{29}N_2 + p^{30}N_2 \left(1 - \frac{(1 - ra)\ R^{29} - ra}{2 - ra} \right) \right] \quad (5)$$

where R^{29} is the ratio between the $^{29}N_2$ and $^{30}N_2$ production.

DETECTION AND PHYLOGENETIC ANALYSES OF DENITRIFIER AND ANAMMOX *nirS* GENES

The biomarker functional gene *nirS*, encoding the cd_1-containing nitrite reductase, for both denitrifiers and marine anammox bacteria were targeted using qualitative and quantitative analyses. Nucleic acids were extracted from the sediment layers corresponding to those used for rate measurements (0–2, 2–4, 4–6, and 6–8 cm, respectively), by applying the UltraClean™Soil DNA Isolation Kit (MO BIO Labratories, Inc.) according to the manufacturer's instructions. Triplicate DNA extractions were made for each sample to reduce bias through the extraction procedure and pooled together through purification with the Wizard® Genomic DNA Purification Kit (Promega GmbH). DNA was stored in 10 mM Tris-HCl at −80°C until further analyses. The concentrations of the DNA in the samples were measured spectrophotometrically with a NanoDrop instrument (Thermo Fisher Scientific Inc.).

Denitrifier *nirS* gene fragments were PCR amplified with the primers cd3aF/R3cd (5′-GTSAACGTSAAGGARACSGG-3′ (Michotey et al., 2000)/5′-GASTTCGGRTGSGTCTTGA-3′; Throback et al., 2004). The primers Scnir372F/Scnir845R (5′-TGTAGCCAGCATTGTAGCGT-3′/5′-TCAAGCCAGACCCATTTGCT-3′; Lam et al., 2009) were used to target the specific *nirS* for marine anammox bacteria, so far believed to all fall into the *Candidatus* Scalindua clade. PCR reactions were performed with the Master *Taq* Kit (5 Prime) on a thermal cycler (Eppendorf AG) and were examined with gel electrophoresis on 1% LE agarose gels (Biozym Scientific GmbH).

Subsequently, clone libraries were constructed from PCR amplicons of correct sizes. The PCR products were purified with the QIAquick PCR Purification Kit (QIAGEN) and the cloning reactions were performed with the TOPO TA Cloning® Kit for sequencing (pCR4 vector) with One Shot® TOP10 chemically competent *E. coli* cells (Invitrogen GmbH). Clones were screened for correct inserts by performing PCR with the primers M13F/M13R (5′-GTAAAACGACGGCCAG-3′/5′-CAGGAAACAGCTATGAC-3′), the number of non-nirS sequences was ≤2 per library. PCR products of the correct size were sequenced using the dye terminator sequencing method (Sanger et al., 1977) with the BigDye® Terminator v3.1 Cycle Sequencing Kit (Applied Biosystems, Inc.) and the T7 primer (5′-TAATACGACTCACTATAGGG-3′). Sequencing was performed on an ABI3730 capillary sequencer system (ABI) according to the manufacturer's protocol. For the primers cd3aF/R3cd, sequence length used for phylogenetic analyses was ∼400 bp, while for primers Scnir372F/Scnir845R sequences had a minimum length of 440 bp.

Sequences were initially processed using BioEdit (Hall, 1999), aligned with ClustalW (Thompson et al., 1994) and screened for NirS encoding genes in the GenBank using the BLAST searches (Altschul et al., 1997). Mothur (Schloss et al., 2009) was used to calculate a similarity cut-off for operational taxonomic units (OTUs) based on nucleic acids of ≥95% and rarefaction curves. The screened sequences were imported into the ARB software package for phylogenetic analyses (Ludwig et al., 2004). Phylogenetic analyses were performed according to the amino acid sequences translated from the obtained sequences, together with some related sequences retrieved from GenBank. Phylogenetic trees were calculated based on the algorithms of maximum likelihood and maximum parsimony. Bootstrapped analyses of 100 resamplings were conducted. The sequences were deposited in GenBank under the accession numbers KC111208 to KC111421.

QUANTITATIVE PCR

Both denitrifier- and *Scalindua*-specific *nirS* genes were further quantified with real-time PCR, using the primers cd3aF/R3cd (Michotey et al., 2000) and Scnir372F/Scnir845R (Lam et al., 2009), which result in amplicons of 425 and 473 bp, respectively. The reactions were performed on an iQ5 cycler (Bio-Rad Laboratories GmbH) with the *Power*SYBR® Green Master Mix (Applied Biosystems Inc.), as previously described (Lam et al., 2009; Jensen et al., 2011). All samples and non-template controls were analyzed as triplicate and the standards were analyzed in every qPCR run. The specificities of PCR amplicons were checked with subsequent melt curve analyses, as well as with 2% agarose gel electrophoresis.

RESULTS

HYDRO- AND GEOCHEMISTRY

The compiled oxygen concentration profiles of the four investigated stations revealed an OMZ with a vertical expanse of ∼900 m (**Figure 2**). Within the oxycline (50–100 m), oxygen concentrations decreased from ∼200 to ∼5 μmol O_2 l^{-1}. From 200 to 300 m, an intrusion of Persian Gulf Water, identified by higher salinity

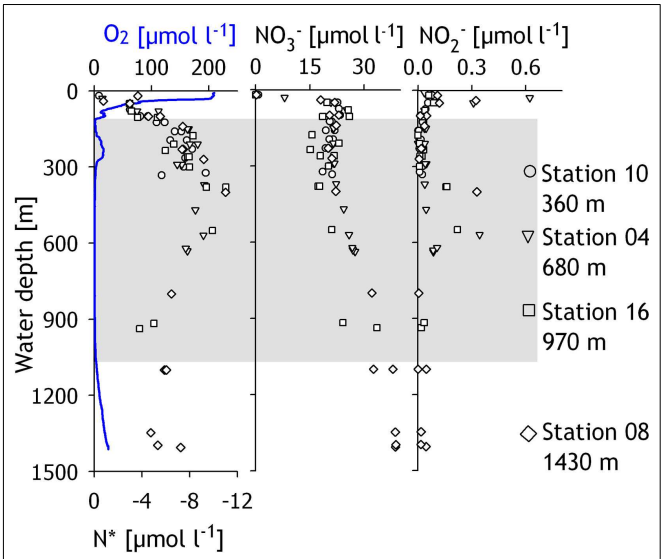

FIGURE 2 | Concentrations of dissolved oxygen, N*, nitrate and nitrite, in the water column of the Pakistan continental margin in the Arabian Sea, with data compiled from all four sampling stations. N* was calculated according to Gruber and Sarmiento (1997). The shaded region depicts the extent of the oxygen minimum zone, while the different symbols denote the data points from different sampled stations.

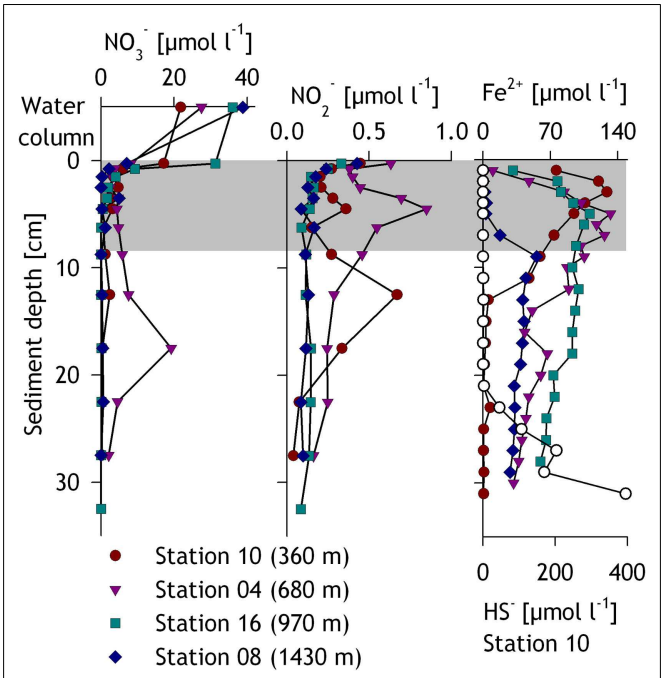

FIGURE 3 | Pore water profiles for nitrate, nitrite, iron, and sulfide for the investigated stations. The gray zone indicates the layers sampled for slurry incubations and DNA extraction, while the zone immediately above in the first panel represents the water column or bottom water. Samples for nitrate concentrations in the bottom water were retrieved from the bottom-most CTD sample. Sulfide was only measurable at and thus shown for station 10.

(Shetye et al., 1994), led to increased oxygen concentrations of up to 16 µmol O_2 l^{-1}. At 300 m, oxygen concentrations dropped below the detection limit (~1 µmol O_2 l^{-1}) and increased again below ~900 m water depth. Bottom water oxygen concentrations of 23 µmol O_2 l^{-1} were measured at the deepest station (1430 m), whereas no oxygen was detectable in the bottom water of the three shallower stations. Concentrations of ammonium were low throughout the water column (<0.1 µmol NH_4^+ l^{-1}, data not shown). Nitrite concentrations were close to the detection limit of 0.01 µmol NO_2^- l^{-1} but peaked at distinct depths to maximum concentrations of 0.7 µmol NO_2^- l^{-1} at 30 m depth and 0.33 µmol l^{-1} between 400 and 600 m (**Figure 2**). Nitrate was depleted in the surface waters but increased below the oxycline (**Figure 2**) so that bottom water concentrations increased from 22 µmol NO_3^- l^{-1} at the shallowest station to 39 µmol NO_3^- l^{-1} at the deepest station. The nitrogen deficit, calculated according to Gruber and Sarmiento (1997) as $N^* = [NH_4^+]+[NO_2^-]+[NO_3^-]-16^*[PO_4^{3-}]+2.9$, was zero in surface waters (**Figure 2**), then decreased to −11 µmol N l^{-1} between 300 and 600 m depth and rose slightly to −7 µmol N l^{-1} below 800 m depth.

Within the sediments, the pore water was analyzed for the upper ~30 cm (**Figure 3**). Nitrate concentrations in the first 0.5 cm of the sediment ranged from 7 to 31 µmol NO_3^- l^{-1} and dropped sharply to <3 µmol NO_3^- l^{-1} below. Similar to nitrate, nitrite generally declined within the upper centimeters from ~0.5 µmol NO_2^- l^{-1} at the surface to 0.2 µmol NO_2^- l^{-1} below 2 cm. Significant subsurface maxima of nitrate (19 µmol NO_3^- l^{-1} at 17.5 cm, station 04) and nitrite (up to 0.9 µmol NO_2^- l^{-1}, stations 10 and 04) were sometimes found at the shallower stations. Concentrations of dissolved Fe^{2+} increased from 0.2 µmol l^{-1} at the surface to maximum concentrations ranging from 55 to 133 µmol l^{-1} at 5–9 cm depth and decreased within the layers below (**Figure 3**). Sulfide was detected only at the shallowest station 10 below 23 cm sediment depth where it increased with depth to a maximum of ~400 µmol HS^- l^{-1} at the lowermost sampled layer (31 cm, **Figure 3**).

Organic carbon and nitrogen contents were measured in the sediment layers corresponding to the slurry incubations (**Table 1**). Within the OMZ, the organic carbon content (% of dry weight) in the surface sediment layer increased from 1.6% at 360 m to 2.4% at 970 m, but decreased again to 1.7% below the OMZ at 1430 m. Although organic carbon and nitrogen contents decreased within sediment depth at all stations, there was no clear trend for C:N ratios with sediment depth. However, the C:N ratios were slightly enhanced with station depth within the OMZ (C:N = 8–9 at 680 and 970 m), compared to the shallowest and deepest stations (C:N = 7–8).

BENTHIC N-LOSS RATES

Benthic N-loss activity was detected in both sediment slurries and intact sediment cores. In the intact core incubations, total benthic N-loss rates increased within the OMZ waters from 0.39 mmol N m^{-2} day^{-1} at 360 m to a maximum of 0.52 mmol N m^{-2} day^{-1} at 680 m (**Figure 5A**). At the lower

Table 1 | Organic carbon and nitrogen, C:N ratios, N-loss rates, and gene copy numbers of the investigated sediment layers.

Station	Sediment depth [cm]	Organic carbon [% dry wt]	Organic nitrogen [% dry wt]	C:N [mol:mol]	Excess nitrate [nmol (cm sed)$^{-3}$]	DNA [ng DNA (mg dry sed)$^{-1}$]
10	0–2	1.6	0.26	7.2	95.8	4.92 ± 0.03
	2–4	1.5	0.23	7.8	22.2	3.69 ± 0.23
	4–6	1.5	0.21	8.2	12.3	3.47 ± 0.23
	6–8	1.2	0.21	7.1	n.d.	3.05 ± 0.24
04	0–2	2.2	0.31	8.4	110.6	9.18 ± 0.65
	2–4	2.0	0.28	8.1	23.6	5.04 ± 0.59
	4–6	1.9	0.25	8.8	3.1	6.42 ± 0.84
	6–8	1.8	0.26	8.1	n.d.	3.96 ± 0.33
16	0–2	2.4	0.31	9.0	222.0	5.08 ± 0.14
	2–4	2.1	0.28	8.6	n.d.	5.61 ± 0.49
	4–6	2.0	0.27	8.7	n.d.	4.43 ± 0.43
	6–8	1.3	0.19	8.0	n.d.	3.12 ± 0.41
08	0–2	1.7	0.24	8.3	111.6	6.48 ± 0.41
	2–4	1.6	0.23	7.8	n.d.	5.13 ± 0.21
	4–6	1.4	0.21	7.9	n.d.	5.62 ± 0.40
	6–8	1.2	0.19	7.4	n.d.	2.70 ± 0.08

n.s., not significant; n.d., not detectable; sed, sediment.

boundary of the OMZ, rates decreased to 0.22 mmol N m^{-2} day^{-1} (970 m) and were the lowest at 1430 m (0.18 mmol N m^{-2} day^{-1}). The relative contribution of denitrification and anammox to the total N-loss was estimated from slurry incubations. Denitrification rates in intact sediment cores ranged between 0.11 and 0.46 mmol N m^{-2} day^{-1}, while anammox rates increased from 0.03 mmol N m^{-2} day^{-1} at the shallowest station to 0.07 mmol N m^{-2} day^{-1} at the deepest station (**Figure 5A**).

There were strong indications of the release of intracellular $^{14}NO_3^-$ during the slurry incubations. The release of stored $^{14}NO_3^-$ was most apparent in the NO_3^- measurements in the $HgCl_2$-fixed subsamples from the initial time point (T_0). NO_3^--concentrations at T_0 were significantly above the total sum of NO_3^- in the bottom water, pore water, and ^{15}N-amendment combined, thus indicating an excess of $^{14}NO_3^-$ in the slurry. Unfortunately, the true labeling percentage ($F_{NO_3^-}$) during the slurry incubation could not be determined from these subsamples, since any residual intracellular nitrate would have been released after poisoning with $HgCl_2$. For this reason, $^*F_{NO_3^-}$ was calculated from Eq. 3 (see Materials and Methods) and subsequently the excess concentrations of $^{14}NO_3^-$ were calculated according to Eq. 4. Excess nitrate was calculated for all depths with denitrification rates (**Table 1**) and generally decreased with sediment depth. Excess nitrate ranged between 222 nmol N (cm^3 sediment)$^{-1}$ in the surface at station 16 and 3.1 nmol N (cm^3 sediment)$^{-1}$ in 4–6 cm at station 04.

In slurry incubations, both denitrification and anammox rates generally decreased with increasing sediment depth (**Figures 4A,B**). Due to insignificant $^{29}N_2$ and $^{30}N_2$ production, denitrification rates could not be obtained for 6–8 cm at all stations and 4–6 cm at stations 16 and 08. Denitrification rates at the sediment surface (0–2 cm layer) decreased with increasing water depth, from 136 nmol N cm^{-3} day^{-1} at 360 m to 73 nmol N cm^{-3} day^{-1} at 1430 m (**Figure 4A**). Anammox rates in surface sediments were lower than denitrification rates. However, in contrast to denitrification rates, anammox rates increased with water depth from 10 nmol N cm^{-3} day^{-1} at 360 m to 45 nmol N cm^{-3} day^{-1} at 1430 m (**Figure 4B**). Anammox and denitrification rates from slurry incubations were integrated down to the nitrate penetration depth of 2 cm (**Figure 5B**), which represents a rather conservative estimate, given that nitrate was found deeper in the sediment at some stations. Integrated denitrification rates decreased from 2.7 (±0.07) mmol m^{-2} day^{-1} at 360 m to 1.5 (±0.17) mmol m^{-2} day^{-1} at 1430 m. Anammox rates on the other hand increased with water depth from 0.21 (±0.03) mmol m^{-2} day^{-1} at 360 m to 0.89 (±0.04) mmol m^{-2} day^{-1} at the deepest station. As a result, the relative contribution of anammox to total N-loss increased with water depth from 7% at the shallowest station to 38% at the deepest station (**Figure 5C**).

DETECTION OF *nirS* GENES FROM DENITRIFIERS AND ANAMMOX BACTERIA

The presence of microorganisms mediating the denitrification and anammox processes was verified by the detection of their respective biomarker functional genes *nirS*. Altogether, 225 denitrifier *nirS* sequences were obtained, and they formed 114 OTUs that could be grouped into seven clusters (**Figure 6**; **Table A1** in Appendix). The *nirS* sequences from the Pakistan continental margin are diverse, and show clustering pattern that seems to be depth-related: certain clusters are dominated by sequences from the two shallow stations (10 and 04), while others are dominated by sequences from the two deeper stations (16 and 08). The majority of the sequences derived from stations 10 and 04 are found in clusters D2 (33 sequences) and D3 (49 sequences), to which the contributions from the deep stations (08 and 16) are considerably lower (only 13 sequences for D2 and 6 for D3). Meanwhile, clusters D1, D4, D5, and D6 seemed to be dominated by sequences from the deeper stations (08 and 16), with 41, 29, 6, and 9 sequences, respectively. Although the cd3aF–R3cd primer pair amplified predominantly

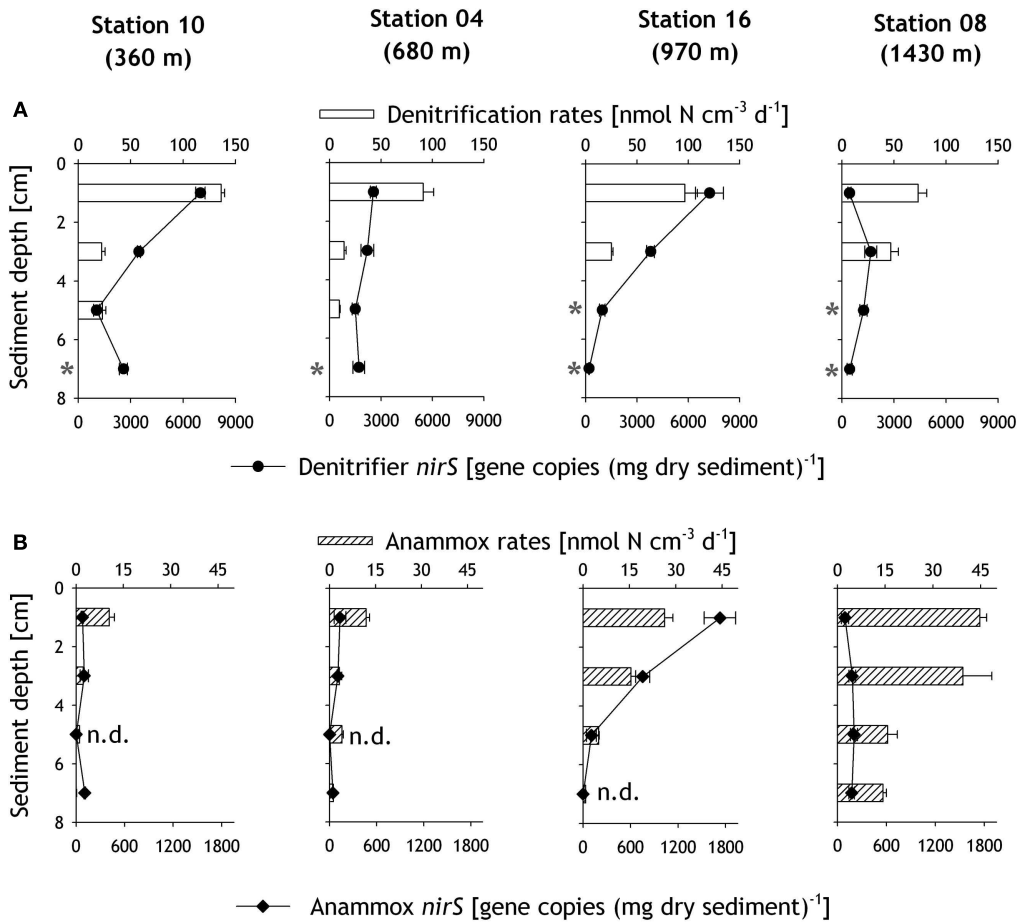

FIGURE 4 | Denitrification (A) and anammox (B) rates determined from slurry incubation experiments, along with the corresponding gene copy numbers of denitrifier *nirS* (A) and anammox *nirS* (B) quantified by real-time qPCR in the sediments. The asterisks mark the incubations that showed insignificant $^{15}N–N_2$ production. Abbreviations: "n.d." refers to non-detectable anammox *nirS* gene copy numbers.

denitrifier *nirS* genes, two sequences (OTU 04nir375) obtained from station 04 (680 m) were found to be more closely affiliated with the freshwater anammox bacterium *Candidatus* "Kuenenia stuttgartiensis" in cluster D7, with a similarity of 73% based on amino acid sequence. It should be noted that cluster D7 also includes cultured species like *Halomonas campisalis* and *Methylomirabilis oxyfera*, which share up to 59 and 69% amino acid sequence similarity, respectively, to the Arabian Sea D7 sequences obtained in this study.

A total of 109 OTUs from 241 anammox *nirS* sequences were retrieved from the Pakistani margin sediments (**Figure 7**), and they formed three clusters that might also carry some water-depth-related pattern, though not as obvious as for the denitrifier *nirS* sequences. Cluster S1 and S3, closely related to OTUs from the Arabian Sea water column, were dominated by sequences from deep stations (16 and 08) with 33 sequences compared to 17 and 22 sequences from the shallow stations (10 and 04). In contrast, cluster S2 affiliated with OTUs from the Peruvian water column seemed to have similar contributions from both shallow and deep stations.

QUANTIFICATION OF DENITRIFIER- AND ANAMMOX-*nirS* GENES

Consistent with benthic N-loss rate measurements, the anammox *nirS* genes were generally less abundant than denitrifier *nirS* genes (**Figures 4A,B**). Both *nirS* gene copy numbers showed a decreasing trend with sediment depth. Amongst all stations, the highest denitrifier *nirS* gene abundance of 7245 ± 813 gene copies $(\text{mg dry sediment})^{-1}$ was detected in the surface sediment layer at station 16 (970 m), whereas the lowest denitrifier *nirS* abundance of 439 ($\pm$90) gene copies $(\text{mg dry sediment})^{-1}$ was detected in the uppermost 2 cm at the deepest station 08.

The abundance of anammox *nirS* genes was usually an order of magnitude lower than that of the denitrifier *nirS* (**Figure 4B**), and was often found to be close to the detection limit. Similar to the denitrifier *nirS* genes, the highest numbers of anammox *nirS* genes were also detected at station 16, ranging from 1728 ± 198 gene copies $(\text{mg dry sediment})^{-1}$ in the surface to undetectable at 6–8 cm. Although the highest rates of anammox were measured in the slurry incubation experiment at station 08, only low gene copy numbers of anammox *nirS*, in the range of 93 ± 44 to 203 ± 44 gene copies $(\text{mg dry sediment})^{-1}$, were detected.

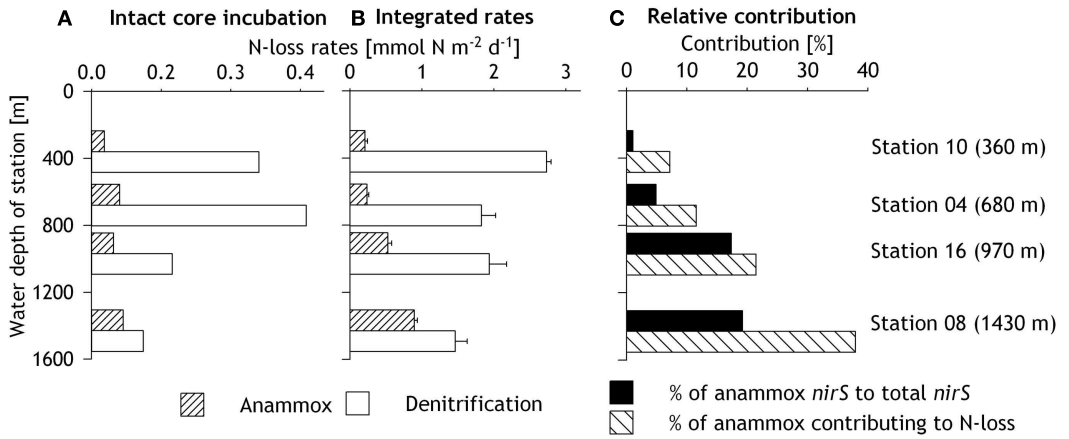

FIGURE 5 | (A) Anammox and denitrification rates measured in intact core incubation experiments, using the rIPT method described by Risgaard-Petersen et al. (2003). **(B)** Areal depth-integrated rates of anammox and denitrification measured in slurry incubations for the uppermost 2 cm of the sediment. **(C)** Contribution of anammox to the total benthic N-loss of the slurry incubations and the ratio of anammox *nirS* gene copy numbers to total *nirS* gene copy numbers in the surface layer (0–2 cm) of the sediment.

The relative contribution of the anammox *nirS* to the total *nirS* gene copy numbers in the uppermost 2 cm increased with water depth from 1% at 360 m to 19% at station 16 (**Figure 5C**). These results are consistent with depth-integrated rates, which show an increase of anammox contribution to total N-loss with increasing water depth.

DISCUSSION

BENTHIC N-LOSS DUE TO DENITRIFICATION

Consistent with previous benthic N-loss studies from other continental slopes, e.g., the North Atlantic (Trimmer and Nicholls, 2009), denitrification along the Pakistan margin was shown to be the primary N_2 production process, as measured in slurry incubation experiments and further corroborated by the abundance of the biomarker functional gene *nirS*. Measurements of benthic N-loss rates in the Arabian Sea are rare and so far estimates from direct sediment incubations using ^{15}N labeled substrates have not been reported. Schwartz et al. (2009) estimated benthic denitrification rates across the Pakistan continental margin to be 0.40–3.78 mmol N m^{-2} day^{-1}. However, these estimates were based on nitrate uptake measurements that would have included the nitrate uptake by nitrate-storing organisms (e.g., sulfur bacteria, foraminifera) as well as the dissimilatory nitrate reduction to ammonium (DNRA). In contrast, N_2 production rates (determined as the N_2/Ar ratio) from the same study were lower (0.05–0.13 mmol N m^{-2} day^{-1}) than the total N-loss rates we measured with the intact core incubation experiments (0.18–0.52 mmol N m^{-2} day^{-1}).

Denitrification rates have been determined for the continental shelf sediments off central Chile, where seasonal hypoxia develops each year (Farías et al., 2004). The measured benthic denitrification rates of 0.6–2.9 mmol N m^{-2} day^{-1} are similar in magnitude to those estimated for the sediments underlying the Peruvian OMZ (0.2–2 mmol N m^{-2} day^{-1}) based on modeled pore water fluxes (Bohlen et al., 2011). In comparison, the denitrification rates measured in our intact core incubations for the Pakistan margin (0.11–0.46 mmol N m^{-2} day^{-1}) were at the lower end of those estimates for the Chilean and Peruvian sediments, while the integrated rates based on slurry incubations (1.46–2.73 mmol N m^{-2} day^{-1}) lay within the upper range. The actual *in situ* N-loss rates on the Pakistan margin are likely somewhere between these two sets of obtained rates – as the amended substrates in the slurry incubations could have stimulated additional N-loss activity, while intact cores might have underestimated N-loss activity due to insufficient diffusion of the ^{15}N-labeled substrates into deeper sediment layers. Moreover, intact core incubations could not account for any potential denitrification by nitrate-storing organisms (e.g., foraminifera) as would be discussed below. Therefore, rates derived from slurry incubations may be closer to reality than those from intact core incubations.

Several lines of observations collectively indicate the likely presence of nitrate-storing organisms in the sediments of the Pakistani margin. Firstly, high production of $^{29}N_2$ relative to $^{30}N_2$ was measured in the $^{15}NO_3^-$ incubations, which did not agree with the calculated labeling percentage and the measured anammox rates. Secondly, nitrate concentrations in the T_0 subsamples of the slurry incubations exceeded the sum of bottom water, pore water and ^{15}N-nitrate. Thirdly, subsurface maxima of pore water nitrate/nitrite, similar to those previously observed at the Pakistani margin (Woulds et al., 2009), were found during this study. These various findings combined suggest that intracellular NO_x^- had been released during the pore water squeezing and during the mixing of sediment slurries.

Nitrate-storing sulfur bacteria, such as *Thioploca* spp. and *Beggiotoa* spp., have been associated with high pore water nitrate concentrations (Fossing et al., 1995). However, despite the lack of detailed microscopic or molecular analyses to confirm their absence, these mat-forming sulfur bacteria were not visible to naked eyes in the collected samples. Besides, sulfide was only detectable at the shallowest station (station 10) and only below 23 cm, while there were high concentrations of Fe^{2+} at all other stations that indicated the absence of free sulfide. Given such low

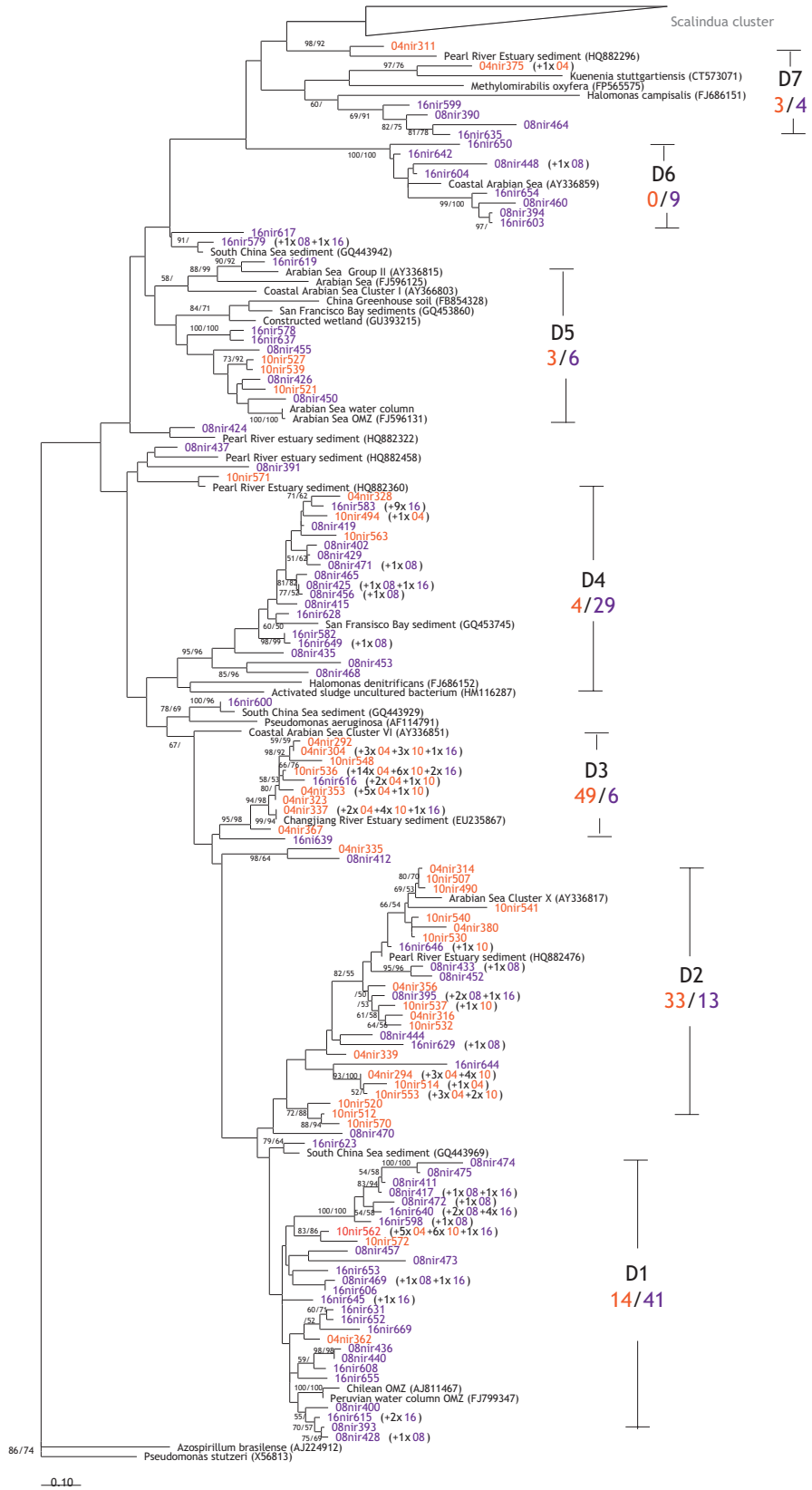

FIGURE 6 | Continued

FIGURE 6 | Phylogenetic reconstruction of the denitrifier NirS based on amino acids sequences translated from gene sequences. Sequences were retrieved from clone libraries constructed for sediments of all stations based on maximum likelihood and maximum parsimony algorithms. Bootstrapped values of >50% are shown for maximum likelihood/maximum parsimony. Indicated in black are the related reference sequences obtained from GenBank. Labeling of sequences: station = 04, 08, 10, or 16, "nir" = amplicons from primers cd3aF/R3cd, or "sc" = amplicons from primers Scnir372F/Scnir845R, followed by unique sequence number. Numbers in parentheses are the numbers of sequences represented by the same OTU with ≥95% nucleic acids sequence similarity. OTUs from the shallow stations are in orange red, while OTUs from deep stations are in purple. D1–D7 indicate the different clusters identified in this study, while the ratio below gives the ratio of sequences from shallow stations (10 and 04) to the deeper stations (08 and 16).

availability (or lack) of electron donor for their energy production, it was thus unlikely for these sulfur bacteria to thrive in the sediments examined. On the other hand, nitrate storage of up to 80% of the total benthic nitrate pool has been described for foraminifera in sediments (Risgaard-Petersen et al., 2006; Glud et al., 2009), including the Peruvian OMZ (Piña-Ochoa et al., 2010). Indeed, living foraminifera had been found particularly in the first cm of sediments underlying the OMZ at the Pakistan margin (Schumacher et al., 2007), which agrees well with the enhanced excess nitrate concentrations calculated for the uppermost sediment layer in our samples. The mean excess nitrate concentration in our study was ∼135 nmol (cm^3 sediment)$^{-1}$, equivalent to twice as much as that reported in the anoxic zone of Gullmar Fjord, Sweden [∼60 nmol (cm^3 sediment)$^{-1}$; Risgaard-Petersen et al., 2006].

Denitrification from the stored NO_3^- by foraminifera would lead to false denitrification estimates if the intracellular labeling percentage ($F_{NO_3^-}$) was not known. However, the increased NO_3^- concentrations in the slurry subsamples at T_0 suggest that the stored $^{14}NO_3^-$ was released into the pore water when the slurry was mixed at the start of the experiment. Thus, a subsequent uptake of NO_3^- from the pore water would lead to an intracellular $F_{NO_3^-}$ that is close to the pore water $F_{NO_3^-}$. Furthermore, the linear increase of $^{29}N_2$ and $^{30}N_2$ with time indicates that either intracellular $F_{NO_3^-}$ did not change over time or that the N_2 production by foraminifera was minor, as was also observed in other regions (Glud et al., 2009). Nonetheless, nitrate-storing foraminifera would potentially lead to an underestimation of N-loss by intact core incubations, since the unlabeled intracellular nitrate was not accounted for. In order to fully explain the source of excess nitrate observed, additional sample collection and analyses, including some shipboard microscopic examination of live cells, would be necessary to especially target the nitrate-storing sulfur bacteria and foraminifera at the point of sampling. These were unfortunately unavailable in our current study and should be further investigated.

The dominance of denitrification in benthic N-loss in the Pakistan margin sediments is strongly supported by the high abundance of denitrifier *nirS* genes. Moreover, the gene copy numbers generally followed similar decreasing trends as the rates measured in slurry incubation within the sediments (**Figure 4**). Exceptions were noted particularly in the topmost layer(s) at the deepest station (station 8), and these could potentially be due to nucleic acid extraction efficiency or biases, and/or the presence of PCR inhibitors. In addition, the primers used only target *nirS*, while any occurrence of the *nirK* genes would not have been accounted for. Although there are also primers designed for *nirK*, those currently available may also target those of nitrifiers. Consequently, quantification of *nirK* in addition to that of *nirS* would likely overestimate denitrifier abundance instead. Future refinement of primer designs, or the assessment of multiple biomarker genes in parallel, may help shed light on the true quantitative distribution of denitrifiers in the environment. Compared to previous studies in various sediments, most of which also focused on denitrifier *nirS* and found gene copy numbers ranging from ca. 0.6×10^3 copies (mg sediment)$^{-1}$ at the mouth of the Colne estuary (Smith et al., 2007) to 27.2×10^3 copies (mg sediment)$^{-1}$ at the mouth of the Rhône River (Michotey et al., 2000), denitrifier *nirS* abundance at the Pakistan margin [$0.2–6.9 \times 10^3$ copies (mg sediment)$^{-1}$] lay within the same range.

In agreement with studies addressing *nirS* genes in the water column of the Arabian Sea (Jayakumar et al., 2004; Bulow et al., 2008), the denitrifier *nirS* community seems to be very diverse (Chao1 richness estimate = 327). However, diversity seems to vary amongst the stations (Chao1 richness estimates of 48–239 were calculated), though the rarefaction analyses indicate that the sequences obtained from the two deeper stations may not be sufficient to represent the full denitrifier diversity therein (**Figures A1A,B** in Appendix). Phylogenetic analyses revealed some apparent differences in the shallow versus deep denitrifying communities, with certain clusters dominated by sequences from shallow stations, while others by sequences from the deeper stations (**Figure 5**). As suggested in other studies (Liu et al., 2003; Dang et al., 2009), such a clustering pattern could result from the adaptation of specific denitrifying communities to different environmental conditions that vary with water depth, such as oxygen, carbon, and nitrate availabilities.

It is particularly interesting to find an OTU amplified with the primers targeting denitrifier *nirS* genes, to be related to the *Ca.* "K. stuttgartiensis" (73% similarity, **Figure 6**). *Ca.* "K. stuttgartiensis" is an anammox bacterium known to occur in freshwater (Jetten et al., 2003), though capable of adapting to higher salinity (Kartal et al., 2006), it has never been found in marine environments thus far. In the same cluster (D7), between the Scalindua cluster and a cluster (D6) affiliated with a sequence from the Arabian Sea water column (Jayakumar et al., 2004), sequences from the deep stations are most closely affiliated with the halophilic bacteria *H. campisalis* (Mormile et al., 1999) and *M. oxyfera*, a freshwater methanotroph that denitrifies via an alternative pathway (Ettwig et al., 2010). The interesting NirS phylogeny of the cluster D7 may indicate that these organisms were no ordinary denitrifiers, yet their exact metabolic pathways remain to be determined. Recent studies from a hydrothermal vent system (Byrne et al., 2009) and an estuary (Dang et al., 2010) report the presence of anammox bacteria, other

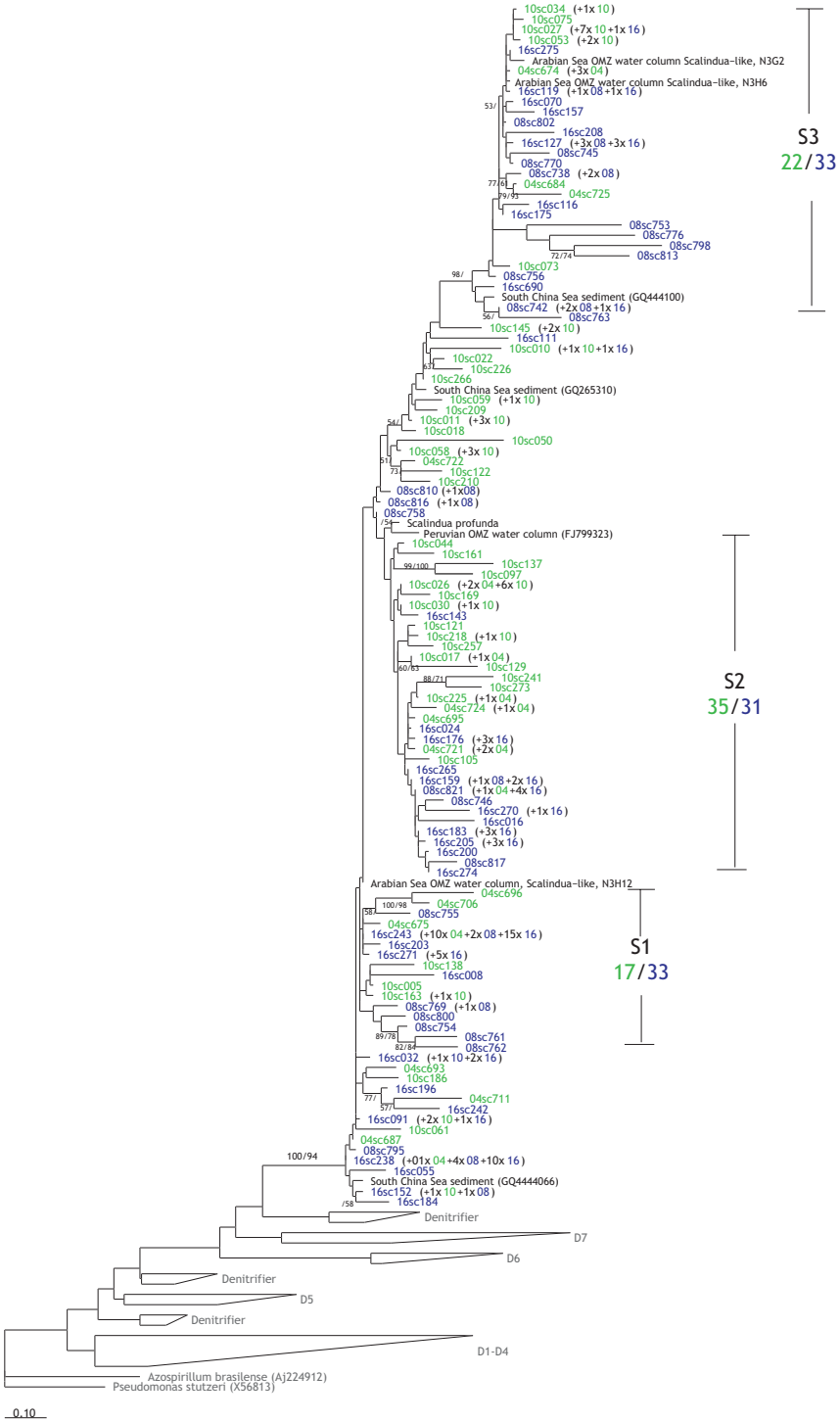

FIGURE 7 | Phylogenetic reconstruction of the anammox (Scalindua) NirS based on amino acids sequences. In blue are the OTUs from the deep stations (08 and 16), while the green sequences were obtained from the shallow stations (10 and 04). Please refer to **Figure 6** for additional information regarding the sequence labels in tree.

than *Candidatus* "Scalindua." These results together with the finding of the OTU related to *Ca.* "K. stuttgartiensis" in this study may hint toward a different type of anammox bacteria, although the abundance seems to be very low. Further studies need to be conducted to verify the occurrence of anammox bacteria, other than *Candidatus* "Scalindua" in the marine environment.

BENTHIC N-LOSS VIA ANAMMOX

This study provides the first direct measurement of anammox activity in the sediments of the Arabian Sea, or any OMZs. The very recent study by Bohlen et al. (2011) in the Peruvian OMZ estimated benthic anammox rates based on modeled pore water fluxes of up to 0.43 mmol N m^{-1} day^{-1} for an anoxic station at 376 m, with lower rates at deeper as well as shallower stations. In general, anammox rates according to intact core incubations at the Pakistan continental margin are much lower (0.003–0.007 mmol N m^{-1} day^{-1}) than the estimates from the Peruvian OMZ. The integrated anammox rates based on slurry incubations, on the other hand, are comparable (0.21 mmol N m^{-1} day^{-1}) on the Pakistan margin at a similar water depth (360 m) and reached as high as 0.89 mmol N m^{-1} day^{-1} at the deepest sampled station (1430 m). In congruence with the rate measurements, anammox Scalindua-like *nirS* genes could be detected at all stations and are in lower abundance than the denitrifier *nirS* genes. The anammox *nirS* gene abundance [undetectable to 1.7×10^3 copies (mg sediment)$^{-1}$] detected at the Pakistan margin were an order of magnitude lower than those detected in deep sea sediments of South China Sea [up to $44.1(\pm 3.3) \times 10^3$ copies (mg sediment)$^{-1}$; Li et al., 2011] in which the same primers were used as in the current study.

Because the *nirS* gene is present as a single copy in anammox bacteria, according to the sequenced genomes of both the freshwater *Ca.* "K. stuttgartiensis" (Strous et al., 2006) and marine *Candidatus* "Scalindua profunda" (van de Vossenberg et al., 2008), potential cell specific activity may be calculated from the anammox rates measured in slurry incubations and the anammox *nirS* gene copies quantified. Taking station 16 that lay within the OMZ as an example, cell specific anammox rates were calculated to be 10–24 fmol N $cell^{-1}$ day^{-1}, which was highly similar to those estimated for the Arabian Sea OMZ waters (1.6–25 fmol N day^{-1} $cell^{-1}$) over the Omani Shelf (Jensen et al., 2011). However, likely lower DNA extraction efficiency in sediments has probably led to underestimated anammox *nirS* gene copy numbers particularly for the deepest station, which in turn would result in overestimated cell specific rates, and so are not presented here. In addition, a recent study reported the occurrence of *nirK* instead of *nirS* gene in a freshwater anammox bacterium from a bioreactor (Hira et al., 2012). Although *nirK*-containing anammox bacteria have not been found in the marine environment to date, such possibility cannot be eliminated and the quantification of *nirS* genes alone might have underestimated the anammox bacterial abundance. In future studies, the recently discovered gene *hzsA*, encoding hydrazine synthase (Harhangi et al., 2012), might be a reasonable alternative or additional biomarker gene for the quantification of anammox bacteria, since it is also present as a single copy in the genomes analyzed until now.

According to the phylogenetic reconstruction of Scalindua NirS (**Figure 6**), three different clusters could be identified and the diversity of the community (Chao1 richness estimate = 275), though lower than the diversity of the denitrifier NirS (**Figures A1A,C** in Appendix), seems to be higher compared to those found in the water column OMZ of the Arabian Sea (Chao1 richness estimate = 8; Jensen et al., 2011) and Peru (Chao1 richness estimate = 43; Lam et al., 2009). The higher diversity could have been caused by more distinct segregation of the organisms in the sediments compared to the water column. Similar to the denitrifier NirS tree, sequences from the deep stations appeared to predominate in two clusters, presumably due to their different adaptations to environmental conditions as mentioned earlier for the denitrifiers.

ANAMMOX CONTRIBUTION INCREASED WITH WATER DEPTH

In agreement with other studies (Engström et al., 2009; Trimmer and Nicholls, 2009; Bohlen et al., 2011), we found an increasing contribution of anammox to the total benthic N-loss with increasing water depth. At a water depth of 1430 m, the contribution of anammox was the highest (38%) and similar to the mean anammox contribution of 37% measured by Glud et al. (2009) at comparable water depths (1450 m) in a basin with low oxygen concentrations ($\sim$60 μmol O_2 l^{-2}) off Japan (Sagami Bay). Even at the Washington margin with water depths >2700 m, the contribution of anammox to total N-loss was found to be 40% on average (Engström et al., 2009). These studies, all based on ^{15}N incubation experiments, suggest a consistent contribution of $\sim$40% of anammox to the benthic N-loss at sites with water depths >1400 m in different regions across global oceans. Earlier studies, as summarized by Trimmer and Engström (2011), observed a decrease in both denitrification and anammox rates with increasing water depth, such that the overall increase in anammox contribution to total N-loss with water depth was attributed to less decrease in anammox activity relative to denitrification. In contrast, this study shows an increase of potential anammox activity in the slurry incubation experiments from 0.21 to 0.89 mmol N m^{-2} day^{-1} with station depth, while denitrification rates decreased from 2.7 to 1.5 mmol N m^{-2} day^{-1}. This trend was further corroborated by the relative increase in anammox *nirS* gene copy abundance with the water depth (**Figure 7**).

Although anammox rates and cell abundance increase with water depth, it is unlikely that water depth or rather pressure itself is a direct regulating factor for the anammox contribution, since bacterial communities and denitrifiers in particular are able to cope with high pressure very well (Tamegai et al., 1997). More likely than pressure are factors that correlate with depth, such as temperature, organic carbon content, and nitrate concentration. Trimmer and Nicholls (2009) attributed the increase of anammox contribution to total N-loss, amongst other factors, to the bottom water temperature. Experiments with different incubation temperatures suggested, that anammox might be more compatible with lower temperatures (Dalsgaard and Thamdrup, 2002). This could also be the case here as the measured bottom water temperature at the Pakistan margin decreased with the water depth from 15.7°C at the shallowest station to 6.1°C at the deep station. On the other hand, it is generally believed that temperature and metabolic rates correlate (Gillooly et al., 2001, 2002; Savage et al., 2004) such that temperature is unlikely the responsible factor for the increase in anammox rates with depth at the Pakistan margin.

Organic carbon concentrations usually decrease with water depth and therefore it is hypothesized in some studies (Nicholls and Trimmer, 2009) that a decrease in benthic carbon content favors the chemolithoautotrophic anammox process. In the meantime, denitrifiers seem to proliferate particularly in reactive

sediments where the lability as well as content of organic matter are higher (Engström et al., 2005), due to their possibly stronger competition for nitrite as electron acceptor when the electron donors (i.e., organic matter) are abundant. However, at the Pakistan margin, benthic organic carbon content of surface sediments did not show a decreasing trend with water depth, but increased within the core OMZ. It has been suggested that downslope redistribution of shelf sediments and increased preservation of organic carbon under anoxic conditions have caused the high organic carbon content in the core OMZ (Schott et al., 1970). Indeed, the highest organic carbon content was found along with the highest C:N ratio at the bottom of the OMZ (station 16), which hints toward the assumption that the organic matter is more refractory. Unlike the dependence of heterotrophic denitrifiers on the availability of labile organic carbon, anammox bacteria can fix their own organic carbon and therefore likely have an advantage at the deeper stations, where the supply of organic carbon from the surface is lower due to probably reduced primary production with distance to the coast and/or greater extent remineralization in the water column reaching those depths.

Anammox activity depends on sufficient supplies of NO_x^- (Dalsgaard and Thamdrup, 2002), which acts as the electron acceptor for the anammox reaction. The highest anammox rates were measured at the deepest station, where nitrate concentration was almost twice as high ($\sim$39 μmol l^{-1}) as at the shallow station in the upper OMZ ($\sim$22 μmol l^{-1}). Moreover, oxygen was present which could have stimulated nitrification and thus could enhance the availability of NO_x^- in the sediments. The high nitrate concentrations and to a lesser extent the more refractory organic carbon at the deeper stations could have led to incomplete denitrification (i.e., nitrate reduction to nitrite) and an overall increased availability of NO_x^- for anammox (Dalsgaard et al., 2005). This would be particularly important for deeper sediment layers, where NO_x^- availability is usually low. This postulation would be in good agreement with the high rates measured in deeper layers at station 08 (**Figure 4B**), the deepest station with the highest nitrate concentration and oxic overlying bottom water.

CONTRIBUTION OF BENTHIC N-LOSS TO THE N-DEFICIT IN THE ARABIAN SEA

In general, the water column of the central Arabian Sea is believed to be an important sink for fixed nitrogen in global oceans as indicated by a prominent N-deficit (Naqvi, 1994; Naqvi et al., 2006; Ward et al., 2009). Recent studies on the water column N-loss in the Arabian Sea OMZ could not agree on the dominant pathway, denitrification or anammox, responsible for the N-loss therein, and much variability has been found in the measured rates (Ward et al., 2009; Jensen et al., 2011; Lam et al., 2011). Ward et al. (2009) measured pelagic denitrification of up 25.4 nmol N_2 l^{-1} day^{-1} in the central Arabian Sea. In contrast, pelagic N-loss rates measured during the cruise for this study at the same stations on the Pakistan margin (data not shown here) as well as in the central Arabian Sea (Jensen et al., 2011) immediately before this study were very low (0–0.04 nmol N l^{-1} day^{-1}). These direct rate measurements together may suggest that the Arabian Sea harbors distinct regions of seasonally high N-loss (Lam et al., 2011), rather than being an area of uniformly and persistently high N-loss activity throughout the year. While the water column seems to be subject to seasonal variations in N-loss due to the supply of substrates from the surface and removal by sinking particles, benthic N-loss is likely less seasonally dependant, since organic carbon concentrations integrate over a longer period of time. Hence, consistently high benthic N-loss may have contributed significantly to the N-deficit signals in the water column where the OMZ water impinges on the Pakistani margin.

Naqvi et al. (2006) calculated that an area of 1.15 m $\times$ 10^{12} m of seafloor in the Arabian Sea is affected by oxygen concentrations of $<$22 μmol O_2 l^{-1}. Since we measured N-loss at four stations across the OMZ with bottom water O_2 concentrations of 0–23 μmol l^{-1}, an extrapolation of average fluxes to the area estimated by Naqvi et al. appears reasonable. The mean rates measured in the slurry incubations in this study would result in an annual N removal as high as 14.7 Tg N year^{-1} (range between 12.3 and 17.0 Tg N year^{-1}). Similar rates via denitrification of 1.1–10.5 Tg N year^{-1} were estimated for the continental shelves of the Arabian Sea by Schwartz et al. (2009). Based on primary production rates, Bange et al. (2000) estimated the N-loss from shelf sediments (0–200 m) to be 6.8 Tg N year^{-1} and as much as 33 Tg N year^{-1} were attributed to pelagic denitrification. Accordingly, shelf sediments would account for only 17% to the total N-loss in the Arabian Sea. Nonetheless, these estimates did not include sediments at water depths deeper than 200 m, which also contribute to the N-loss in the Arabian Sea. Therefore, sediments likely contribute more to the total N-loss in the Arabian Sea than previously assumed.

Furthermore, N-loss rates measured in the central Arabian Sea of 0.3–0.6 mmol N m^{-2} day^{-1} (Jensen et al., 2011) are comparable to benthic N-loss rates measured in this study. An extrapolation of these rates to the area of the Arabian Sea to the north of 6°N (4.93×10^{12} m^2; Bange et al., 2000) would result in an annual pelagic N-loss of 7.6–15 Tg N year^{-1}, which is similar to a recently published estimate for pelagic N-loss in the Arabian Sea of 12–16 Tg N year^{-1} (DeVries et al., 2012). Compared to the mean benthic N-loss calculated from our data (14.7 Tg N year^{-1}) with only the shelf sediments included, water column and the sediments might contribute more or less equally to the N-loss in the Arabian Sea.

CONCLUSION

Benthic N-loss due to anammox increased with water depth on the Pakistan margin and the contribution of anammox to total N-loss seemed to co-vary with temperature and nitrate concentrations in the bottom water. Compared to shallow sediments, anammox bacteria seem to be more successful in deeper sediments, as anammox accounted for almost 40% to the total benthic N-loss at 1430 m water depth. The shift from a denitrifier-dominated heterotrophic system in shallow sediments, to a system in which the autotrophic anammox process plays a more important role in sediments at deeper water depths, could also be coupled to the availability of labile organic carbon. Owing to their chemolithoautotrophic lifestyle, anammox bacteria could have a competitive advantage over denitrifiers in deeper sediments due to their lesser dependence on the often seasonally fluctuating primary production in surface waters for sources of electron donor and carbon. Extrapolation from our data suggests that benthic N-loss could account for up to

half of the total N-loss in the Arabian Sea as a whole, and may thus have contributed to the N-deficits in the water column, though further investigations during different seasons are necessary to fully evaluate the role of sediments in the annual marine N-loss. Since human populations and anthropogenic atmospheric N deposition (Duce et al., 2008) have been increasing in the Arabian Sea, primary production therein would likely be enhanced further in the near future, possibly resulting in higher oxygen consumption and thus an expansion of the OMZ. What additional positive and negative feedbacks may ensue, and how the overall nitrogen as well as the intimately linked carbon cycles might respond in this key region of global biogeochemical cycling, cannot be fully evaluated without taking the interacting benthic and pelagic fluxes into due consideration.

ACKNOWLEDGMENTS

We are very thankful for the technical support and analyses by G. Klockgether, D. Franzke, M. Meier, I. Vieweg, A. Schipper, S. Kühn, and for the excellent cooperation with captain and crew of *R/V Meteor* M74/2. We thank K. Zonneveld and S. Kasten for providing the equipment and fruitful discussions. Funding from DFG-Research Center/Excellence Cluster "The Ocean in the Earth System" (MARUM) and the Max Planck Society are gratefully acknowledged.

REFERENCES

Abell, G. C. J., Revill, A. T., Smith, C., Bissett, A. P., Volkman, J. K., and Robert, S. S. (2010). Archaeal ammonia oxidizers and nirS-type denitrifiers dominate sediment nitrifying and denitrifying populations in a subtropical macrotidal estuary. *ISME J.* 4, 286–300.

Altschul, S. F., Madden, T. L., Schaffer, A. A., Zhang, J. H., Zhang, Z., Miller, W., et al. (1997). Gapped BLAST and PSI-BLAST: a new generation of protein database search programs. *Nucleic Acids Res.* 25, 3389–3402.

Bange, H. W., Rixen, T., Johansen, A. M., Siefert, R. L., Ramesh, R., Ittekkot, V., et al. (2000). A revised nitrogen budget for the Arabian Sea. *Global Biogeochem. Cycles* 14, 1283–1297.

Bohlen, L., Dale, A. W., Sommer, S., Mosch, T., Hensen, C., Noffke, A., et al. (2011). Benthic nitrogen cycling traversing the Peruvian oxygen minimum zone. *Geochim. Cosmochim. Acta* 75, 6094–6111.

Braman, R. S., and Hendrix, S. A. (2002). Nanogram nitrite and nitrate determination in environmental and biological materials by vanadium (III) reduction with chemiluminescence detection. *Anal. Chem.* 61, 2715–2718.

Bulow, S. E., Francis, C. A., Jackson, G. A., and Ward, B. B. (2008). Sediment denitrifier community composition and nirS gene expression investigated with functional gene microarrays. *Environ. Microbiol.* 10, 3057–3069.

Byrne, N., Strous, M., Crepeau, V., Kartal, B., Birrien, J.-L., Schmid, M., et al. (2009). Presence and activity of anaerobic ammonium-oxidizing bacteria at deep-sea hydrothermal vents. *ISME J.* 3, 117–123.

Castro-Gonzalez, M., Braker, G., Farias, L., and Ulloa, O. (2005). Communities of nirS-type denitrifiers in the water column of the oxygen minimum zone in the eastern South Pacific. *Environ. Microbiol.* 7, 1298–1306.

Cline, J. D. (1969). Spectrophotometric determination of hydrogen sulfide in natural waters. *Limnol. Oceanogr.* 14, 454–458.

Codispoti, L. A., Brandes, J. A., Christensen, J. P., Devol, A. H., Naqvi, S. W. A., Paerl, H. W., et al. (2001). The oceanic fixed nitrogen and nitrous oxide budgets: moving targets as we enter the anthropocene? *Sci. Mar.* 65, 85–105.

Dalsgaard, T., Canfield, D. E., Petersen, J., Thamdrup, B., and Acuna-Gonzalez, J. (2003). Anammox is a significant pathway of N2 production in the anoxic water column of Golfo Dulce, Costa Rica. *Nature* 422, 606–608.

Dalsgaard, T., and Thamdrup, B. (2002). Factors controlling anaerobic ammonium oxidation with nitrite in marine sediments. *Appl. Environ. Microbiol.* 68, 3802–3808.

Dalsgaard, T., Thamdrup, B., and Canfield, D. E. (2005). Anaerobic ammonium oxidation (anammox) in the marine environment. *Res. Microbiol.* 156, 457–464.

Dang, H., Chen, R., Wang, L., Guo, L., Chen, P., Tang, Z., et al. (2010). Environmental factors shape sediment anammox bacterial communities in hypernutrified Jiaozhou Bay, China. *Appl. Environ. Microbiol.* 76, 7036–7047.

Dang, H., Wang, C., Li, J., Li, T., Tian, F., Jin, W., et al. (2009). Diversity and distribution of sediment NirS-encoding bacterial assemblages in response to environmental gradients in the eutrophied Jiaozhou Bay, China. *Microb. Ecol.* 58, 161–169.

Deutsch, C., Gruber, N., Key, R., Sarmiento, J. L., and Ganachaud, A. (2001). Denitrification and N2 fixation in the Pacific Ocean. *Global Biogeochem. Cycles* 15, 483–506.

Devol, A. H., Naqvi, S. W. A., and Codispoti, L. A. (2006). "Nitrogen cycling in the suboxic waters of the Arabian sea," in *NATO Science Series IV Earth and Environmental Sciences: 64, Past and Present Water Column Anoxia*, ed. L. Neretin (Amsterdam: IOS Press and Kluwer Academic Publishers in conjunction with the NATO Scientific Affairs Division), 283–310.

DeVries, T., Deutsch, C., Primeau, F., Chang, B., and Devol, A. (2012). Global rates of water-column denitrification derived from nitrogen gas measurements. *Nat. Geosci.* 5, 547–550.

Duce, R. A., Laroche, J., Altieri, K., Arrigo, K. R., Baker, A. R., Capone, D. G., et al. (2008). Impacts of atmospheric anthropogenic nitrogen on the open ocean. *Science* 320, 893–897.

Engström, P., Dalsgaard, T., Hulth, S., and Aller, R. C. (2005). Anaerobic ammonium oxidation by nitrite (anammox): implications for N2 production in coastal marine sediments. *Geochim. Cosmochim. Acta* 69, 2057–2065.

Engström, P., Penton, C. R., and Devol, A. H. (2009). Anaerobic ammonium oxidation in deep-sea sediments off the Washington margin. *Limnol. Oceanogr.* 54, 1643–1652.

Ettwig, K. F., Butler, M. K., Le Paslier, D., Pelletier, E., Mangenot, S., Kuypers, M. M. M., et al. (2010). Nitrite-driven anaerobic methane oxidation by oxygenic bacteria. *Nature* 464, 543–548.

Farías, L., Graco, M., and Ulloa, O. (2004). Temporal variability of nitrogen cycling in continental-shelf sediments of the upwelling ecosystem off central Chile. *Deep Sea Res. Part II Top. Stud. Oceanogr.* 51, 2491–2505.

Fossing, H., Gallardo, V. A., Jorgensen, B. B., Huttel, M., Nielsen, L. P., Schulz, H., et al. (1995). Concentration and transport of nitrate by the mat-forming sulfur bacterium Thioploca. *Nature* 374, 713–715.

Galloway, J. N., Dentener, F. J., Capone, D. G., Boyer, E. W., Howarth, R. W., Seitzinger, S. P., et al. (2004). Nitrogen cycles: past, present, and future. *Biogeochemistry* 70, 153–226.

Gao, H., Schreiber, F., Collins, G., Jensen, M. M., Kostka, J. E., Lavik, G., et al. (2009). Aerobic denitrification in permeable Wadden sea sediments. *ISME J.* 4, 417–426.

Gillooly, J. F., Brown, J. H., West, G. B., Savage, V. M., and Charnov, E. L. (2001). Effects of size and temperature on metabolic rate. *Science* 293, 2248–2251.

Gillooly, J. F., Charnov, E. L., West, G. B., Savage, V. M., and Brown, J. H. (2002). Effects of size and temperature on developmental time. *Nature* 417, 70–73.

Ginestet, P., Audic, J. M., Urbain, V., and Block, J. C. (1998). Estimation of nitrifying bacterial activities by measuring oxygen uptake in the presence of the metabolic inhibitors allylthiourea and azide. *Appl. Environ. Microbiol.* 64, 2266–2268.

Glud, R. N., Thamdrup, B., Stahl, H., Wenzhoefer, F., Glud, A., Nomaki, H., et al. (2009). Nitrogen cycling in a deep ocean margin sediment (Sagami Bay, Japan). *Limnol. Oceanogr.* 54, 723–734.

Grasshoff, K., and Johannsen, H. (1972). New sensitive and direct method for automatic determination of ammonia in sea-water. *ICES J. Mar. Sci.* 34, 516–521.

Grasshoff, K., Kremling, K., and Ehrhardt, M. (1999). *Methods of Seawater Analysis.* Weinheim: Wiley-VCH Verlag GmbH.

Gruber, N. (2004). "The dynamics of the marine nitrogen cycle and its influence on atmospheric CO_2 variations," in *NATO Science Series IV Earth and Environmental Sciences: 40, The Ocean Carbon Cycle and Climate*, eds M. Follows and T. Oguz (Dordrecht: Kluwer Academic Publishers), 97–148.

Gruber, N., and Sarmiento, J. L. (1997). Global patterns of marine nitrogen fixation and denitrification. *Global Biogeochem. Cycles* 11, 235–266.

Hall, T. A. (1999). BioEdit: a user-friendly biological sequence alignment editor and analysis program for Windows 95/98/NT. *Nucleic Acids Symp. Ser.* 41, 95–98.

Harhangi, H. R., Le Roy, M., Van Alen, T., Hu, B.-L., Groen, J., Kartal, B., et al. (2012). Hydrazine synthase, a unique phylomarker with which to study the presence and biodiversity of anammox bacteria. *Appl. Environ. Microbiol.* 78, 752–758.

Hira, D., Toh, H., Migita, C. T., Okubo, H., Nishiyama, T., Hattori, M., et al. (2012). Anammox organism KSU-1 expresses a NirK-type copper-containing nitrite reductase instead of a NirS-type with cytochrome cd(1). *FEBS Lett.* 586, 1658–1663.

Holmes, R. M., Aminot, A., Kerouel, R., Hooker, B. A., and Peterson, B. J. (1999). A simple and precise method for measuring ammonium in marine and freshwater ecosystems. *Can. J. Fish. Aquat. Sci.* 56, 1801–1808.

Holtappels, M., Lavik, G., Jensen, M. M., and Kuypers, M. M. M. (2011). "(15)N-labeling experiments to dissect the contributions of heterotrophic denitrification and anammox to nitrogen removal in the OMZ waters of the ocean," in *Methods in Enzymology: Research on Nitrification and Related Processes*, Vol. 486, Part A, ed. M. Klotz (San Diego: Elsevier Academic Press Inc.), 223–251.

Jayakumar, D. A., Francis, C. A., Naqvi, S. W. A., and Ward, B. B. (2004). Diversity of nitrite reductase genes (nirS) in the denitrifying water column of the coastal Arabian Sea. *Aquat. Microb. Ecol.* 34, 69–78.

Jensen, M. M., Lam, P., Revsbech, N. P., Nagel, B., Gaye, B., Jetten, M. S. M., et al. (2011). Intensive nitrogen loss over the Omani Shelf due to anammox coupled with dissimilatory nitrite reduction to ammonium. *ISME J.* 5, 1660–1670.

Jetten, M. S. M., Sliekers, O., Kuypers, M., Dalsgaard, T., van Niftrik, L., Cirpus, I., et al. (2003). Anaerobic ammonium oxidation by marine and freshwater planctomycete-like bacteria. *Appl. Microbiol. Biotechnol.* 63, 107–114.

Kartal, B., Koleva, M., Arsov, R., van der Star, W., Jetten, M. S. M., and Strous, M. (2006). Adaptation of a freshwater anammox population to high salinity wastewater. *J. Biotechnol.* 126, 546–553.

Kartal, B., Maalcke, W. J., de Almeida, N. M., Cirpus, I., Gloerich, J., Geerts, W., et al. (2011). Molecular mechanism of anaerobic ammonium oxidation. *Nature* 479, 127–130.

Kuypers, M. M. M., Lavik, G., Woebken, D., Schmid, M., Fuchs, B. M., Amann, R., et al. (2005). Massive nitrogen loss from the Benguela upwelling system through anaerobic ammonium oxidation. *Proc. Natl. Acad. Sci. U.S.A.* 102, 6478–6483.

Kuypers, M. M. M., Sliekers, A. O., Lavik, G., Schmid, M., Jorgensen, B. B., Kuenen, J. G., et al. (2003). Anaerobic ammonium oxidation by anammox bacteria in the Black Sea. *Nature* 422, 608–611.

Lam, P., Jensen, M. M., Kock, A., Lettmann, K. A., Plancherel, Y., Lavik, G., et al. (2011). Origin and fate of the secondary nitrite maximum in the Arabian sea. *Biogeosciences* 8, 1565–1577.

Lam, P., Lavik, G., Jensen, M. M., van de Vossenberg, J., Schmid, M., Woebken, D., et al. (2009). Revising the nitrogen cycle in the Peruvian oxygen minimum zone. *Proc. Natl. Acad. Sci. U.S.A.* 106, 4752–4757.

Li, M., Ford, T., Li, X., and Gu, J.-D. (2011). Cytochrome cd1-containing nitrite reductase encoding gene nirS as a new functional biomarker for detection of anaerobic ammonium oxidizing (Anammox) bacteria. *Environ. Sci. Technol.* 45, 3547–3553.

Liu, X. D., Tiquia, S. M., Holguin, G., Wu, L. Y., Nold, S. C., Devol, A. H., et al. (2003). Molecular diversity of denitrifying genes in continental margin sediments within the oxygen-deficient zone off the Pacific coast of Mexico. *Appl. Environ. Microbiol.* 69, 3549–3560.

Ludwig, W., Strunk, O., Westram, R., Richter, L., Meier, H., Yadhukumar, et al. (2004). ARB: a software environment for sequence data. *Nucleic Acids Res.* 32, 1363–1371.

Marra, J., and Barber, R. T. (2005). Primary productivity in the Arabian sea: a synthesis of JGOFS data. *Prog. Oceanogr.* 65, 159–175.

Michotey, V., Mejean, V., and Bonin, P. (2000). Comparison of methods for quantification of cytochrome cd1-denitrifying bacteria in environmental marine samples. *Appl. Environ. Microbiol.* 66, 1564–1571.

Mormile, M. R., Romine, M. F., Garcia, T., Ventosa, A., Bailey, T. J., and Peyton, B. M. (1999). Halomonas campisalis sp nov., a denitrifying, moderately haloalkaliphilic bacterium. *Syst. Appl. Microbiol.* 22, 551–558.

Naqvi, S. W. A. (1994). Denitrification processes in the Arabian sea. *Proceedings of the Indian Academy of Sciences – Earth and Planetary Sciences* 103, 279–300.

Naqvi, S. W. A., Naik, H., Pratihary, A., D'Souza, W., Narvekar, P. V., Jayakumar, D. A., et al. (2006). Coastal versus open-ocean denitrification in the Arabian sea. *Biogeosciences* 3, 621–633.

Nicholls, J. C., and Trimmer, M. (2009). Widespread occurrence of the anammox reaction in estuarine sediments. *Aquat. Microb. Ecol.* 55, 105–113.

Piña-Ochoa, E., Høgslund, S., Geslin, E., Cedhagen, T., Revsbech, N. P., Nielsen, L. P., et al. (2010). Widespread occurrence of nitrate storage and denitrification among Foraminifera and Gromiida. *Proc. Natl. Acad. Sci. U.S.A.* 107, 1148–1153.

Risgaard-Petersen, N., Langezaal, A. M., Ingvardsen, S., Schmid, M. C., Jetten, M. S. M., Op den Camp, H. J. M., et al. (2006). Evidence for complete denitrification in a benthic foraminifer. *Nature* 443, 93–96.

Risgaard-Petersen, N., Nielsen, L. P., Rysgaard, S., Dalsgaard, T., and Meyer, R. L. (2003). Application of the isotope pairing technique in sediments where anammox and denitrification coexist. *Limnol. Oceanogr. Methods* 1, 63–73.

Rysgaard, S., Glud, R. N., Risgaard-Petersen, N., and Dalsgaard, T. (2004). Denitrification and anammox activity in Arctic marine sediments. *Limnol. Oceanogr.* 49, 1493–1502.

Sanger, F., Nicklen, S., and Coulson, A. R. (1977). DNA sequencing with chain-terminating inhibitors. *Proc. Natl. Acad. Sci. U.S.A.* 74, 5463–5467.

Savage, V. M., Gillooly, J. F., Brown, J. H., West, G. B., and Charnov, E. L. (2004). Effects of body size and temperature on population growth. *Am. Nat.* 163, 429–441.

Schalk, J., de Vries, S., Kuenen, J. G., and Jetten, M. S. M. (2000). Involvement of a novel hydroxylamine oxidoreductase in anaerobic ammonium oxidation. *Biochemistry* 39, 5405–5412.

Schloss, P. D., Westcott, S. L., Ryabin, T., Hall, J. R., Hartmann, M., Hollister, E. B., et al. (2009). Introducing mothur: open-source, platform-independent, community-supported software for describing and comparing microbial communities. *Appl. Environ. Microbiol.* 75, 7537–7541.

Schlüter, M. (1990). "Zur Frühdiagenese von organischem Kohlenstoff und Opal in Sedimenten des südlichen und östlichen Weddellmeeres: geochemische Analyse und Modellierung=Early diagenesis of organic carbon and opal in sediments of the southern and eastern Weddell Sea: geochemical analysis and modelling," in *Berichte zur Polarforschung (Reports on Polar Research)*, Bremerhaven: Alfred Wegener Institute for Polar and Marine Research.

Schott, W., von Stackelberg, U., Eckhardt, F. J., Mattiat, B., Peters, J., and Zobel, B. (1970). Geologische Untersuchungen an Sedimenten des indisch-pakistanischen Kontinentalrandes (Arabisches Meer). *Int. J. Earth Sci.* 60, 264–275.

Schumacher, S., Jorissen, F. J., Dissard, D., Larkin, K. E., and Gooday, A. J. (2007). Live (Rose Bengal stained) and dead benthic foraminifera from the oxygen minimum zone of the Pakistan continental margin (Arabian Sea). *Mar. Micropaleontol.* 62, 45–73.

Schwartz, M. C., Woulds, C., and Cowie, G. L. (2009). Sedimentary denitrification rates across the Arabian Sea oxygen minimum zone. *Deep Sea Res. Part II Top. Stud. Oceanogr.* 56, 324–332.

Seitzinger, S., and Giblin, A. (1996). Estimating denitrification in North Atlantic continental shelf sediments. *Biogeochemistry* 35, 235–260.

Shetye, S., Gouveia, A., and Shenoi, S. (1994). Circulation and water masses of the Arabian Sea. *J. Earth Syst. Sci.* 103, 107–123.

Smith, C. J., Nedwell, D. B., Dong, L. F., and Osborn, A. M. (2007). Diversity and abundance of nitrate reductase genes (narG and napA), nitrite reductase genes (nirS and nrfA), and their transcripts in estuarine sediments. *Appl. Environ. Microbiol.* 73, 3612–3622.

Strous, M., Pelletier, E., Mangenot, S., Rattei, T., Lehner, A., Taylor, M. W., et al. (2006). Deciphering the evolution and metabolism of an anammox bacterium from a community genome. *Nature* 440, 790–794.

Tamegai, H., Li, L., Masui, N., and Kato, C. (1997). A denitrifying bacterium from the deep sea at 11,000-m depth. *Extremophiles* 1, 207–211.

Thamdrup, B., and Dalsgaard, T. (2002). Production of N2 through anaerobic ammonium oxidation coupled to nitrate reduction in marine sediment. *Appl. Environ. Microbiol.* 68, 1312–1318.

Thompson, J. D., Higgins, D. G., and Gibson, T. J. (1994). Clustal-W – improving the sensitivity of progressive multiple sequence alignment through sequence weighting, position-specific gap penalties and weight matrix choice. *Nucleic Acids Res.* 22, 4673–4680.

Throback, I. N., Enwall, K., Jarvis, A., and Hallin, S. (2004). Reassessing PCR primers targeting nirS, nirK and nosZ genes for community surveys of denitrifying bacteria with DGGE. *FEMS Microbiol. Ecol.* 49, 401–417.

Tiquia, S. M., Masson, S. A., and Devol, A. (2006). Vertical distribution of nitrite reductase genes (nirS) in continental margin sediments of the Gulf of Mexico. *FEMS Microbiol. Ecol.* 58, 464–475.

Trimmer, M., and Engström, P. (2011). "Distribution, activity, and ecology of anammox bacteria in aquatic environments," in *Nitrification*, eds B. Ward, D. Arp, and M. Klotz (Washingtopn: American Society for Microbiology), 201–235.

Trimmer, M., and Nicholls, J. C. (2009). Production of nitrogen gas via anammox and denitrification in intact sediment cores along a continental shelf to slope transect in the North Atlantic. *Limnol. Oceanogr.* 54, 577–589.

van de Vossenberg, J., Rattray, J. E., Geerts, W., Kartal, B., van Niftrik, L., van Donselaar, E. G., et al. (2008). Enrichment and characterization of marine anammox bacteria associated with global nitrogen gas production. *Environ. Microbiol.* 10, 3120–3129.

Ward, B. B., Devol, A. H., Rich, J. J., Chang, B. X., Bulow, S. E., Naik, H., et al. (2009). Denitrification as the dominant nitrogen loss process in the Arabian Sea. *Nature* 461, 78–81.

Wiggert, J. D., Hood, R. R., Banse, K., and Kindle, J. C. (2005). Monsoon-driven biogeochemical processes in the Arabian Sea. *Prog. Oceanogr.* 65, 176–213.

Woulds, C., Schwartz, M. C., Brand, T., Cowie, G. L., Law, G., and Mowbray, S. R. (2009). Pore water nutrient concentrations and benthic nutrient fluxes across the Pakistan margin OMZ. *Deep Sea Res. Part II Top. Stud. Oceanogr.* 56, 333–346.

Conflict of Interest Statement: The authors declare that the research was conducted in the absence of any commercial or financial relationships that could be construed as a potential conflict of interest.

Received: 09 July 2012; paper pending published: 09 August 2012; accepted: 29 October 2012; published online: 28 November 2012.

Citation: Sokoll S, Holtappels M, Lam P, Collins G, Schlüter M, Lavik G and Kuypers MMM (2012) Benthic nitrogen loss in the Arabian Sea off Pakistan. Front. Microbio. ***3****:395. doi: 10.3389/fmicb.2012.00395*

This article was submitted to Frontiers in Aquatic Microbiology, a specialty of Frontiers in Microbiology.

APPENDIX

Table A1 | Range of similarities (%) between the different clusters identified in the NirS phylogenetic trees, based on amino acid sequences.

	Denitrifier or *Kuenenia*-like									*Scalindua*-like			
	D1	**D2**	**D3**	**D4**	**D5**	**D6**	**D7**	***Kuenenia stuttgartiensis***	***Methylomirabilis oxyfera***	**S1**	**S2**	**S3**	***Scalindua profunda***
D1													
D2	82–54												
D3	82–60	76–56											
D4	70–47	71–53	70–54										
D5	74–51	70–55	70–56	72–55									
D6	59–38	60–47	58–44	62–47	63–48								
D7	58–38	58–43	59–41	58–46	61–45	66–48							
Kuenenia stuttgartiensis	61–48	60–53	61–54	62–55	62–53	60–51	73–38						
Methylomirabilis oxyfera	58–42	58–49	55–45	59–52	60–54	62–47	69–42	56					
S1	62–39	61–42	57–39	63–44	66–47	66–46	60–44	61–51	64–56				
S2	61–41	62–44	57–40	65–43	68–48	65–49	63–44	61–50	66–54	94–57			
S3	66–38	62–37	59–36	65–38	67–44	65–41	63–42	59–44	64–49	85–52	84–50		
Scalindua profunda	60–49	61–52	57–47	64–54	65–57	64–56	62–45	51	60	94–77	95–77	82–64	

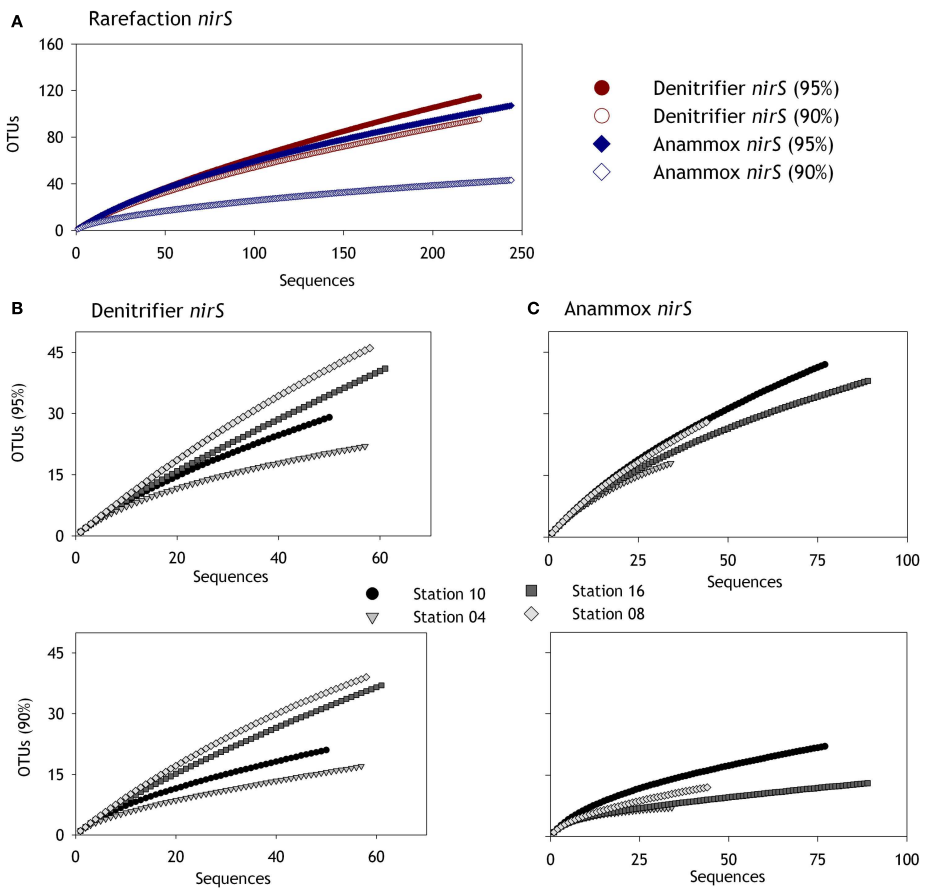

FIGURE A1 | Rarefaction curves for denitrifier and anammox (Scalindua) nirS sequences based on 95% and 90% nucleotide sequences cut offs. (A) Shows rarefaction curves over all sampled stations, **(B)** shows the denitrifier *nirS* rarefaction curves separately for each sampled station, and **(C)** the corresponding curves for anammox (Scalindua) *nirS*.

frontiers in
MICROBIOLOGY

ORIGINAL RESEARCH ARTICLE
published: 25 October 2012
doi: 10.3389/fmicb.2012.00377

Denitrification and environmental factors influencing nitrate removal in Guaymas Basin hydrothermally altered sediments

Marshall W. Bowles[1†], Lisa M. Nigro[2], Andreas P. Teske[2] and Samantha B. Joye[1]*

[1] Aquatic Microbial Biogeochemistry Laboratory, Department of Marine Sciences, University of Georgia, Athens, GA, USA
[2] Department of Marine Sciences, The University of North Carolina at Chapel Hill, Chapel Hill, NC, USA

Edited by:
Bess B. Ward, Princeton University, USA

Reviewed by:
Xiao-Hua Zhang, Ocean University of China, China
Alyson E Santoro, University of Maryland Center for Environmental Science, USA

***Correspondence:**
Samantha B. Joye, Aquatic Microbial Biogeochemistry Laboratory, Department of Marine Sciences, University of Georgia, Room 220, Marine Sciences Building, Athens, GA 30602-3636, USA.
e-mail: mjoye@uga.edu

†Present address:
Marshall W. Bowles, MARUM Center for Marine Environmental Sciences, University of Bremen, Bremen, Germany.

We measured potential nitrate removal and denitrification rates in hydrothermally altered sediments inhabited by *Beggiatoa* mats and adjacent brown oil stained sediments from the Guaymas Basin, Gulf of California. Sediments with *Beggiatoa* maintained slightly higher rates of potential denitrification than did brown sediments at 31.2 ± 12.1 versus 21.9 ± 1.4 μM N day^{-1}, respectively. In contrast, the nitrate removal rates in brown sediments were higher than those observed in mat-hosting sediments at 418 ± 145 versus 174 ± 74 μM N day^{-1}, respectively. Additional experiments were conducted to assess the responses of denitrifying communities to environmental factors [i.e., nitrate, sulfide, and dissolved organic carbon (DOC) concentration)]. The denitrifying community had a high affinity for nitrate (K_m = 137 ± 91 μM NO_3^-), in comparison to other environmental communities of denitrifiers, and was capable of high maximum rates of denitrification (V_{max} = 1164 ± 153 μM N day^{-1}). The presence of sulfide resulted in significantly lower denitrification rates. Microorganisms with the potential to perform denitrification were assessed in these sediments using the bacterial 16S rRNA gene and nitrous oxide reductase (*nosZ*) functional gene libraries. The bacterial 16S rRNA gene clone library was dominated by Epsilonproteobacteria (38%), some of which (e.g., *Sulfurimonas* sp.) have a potential for sulfide-dependent denitrification. The *nosZ* clone library did not contain clones similar to pure culture denitrifiers; these clones were most closely associated with environmental clones.

Keywords: denitrification, nitrogen cycle, *Beggiatoa*

INTRODUCTION

In anoxic environments, nitrate serves as an energy-rich electron acceptor for microbial terminal metabolism and its complete reduction generates either dinitrogen or ammonium. In the hydrothermally altered surficial sediments of Guaymas Basin, nitrate is abundant (highest 40 μM; McHatton et al., 1996 and references therein) and nitrate-concentrating *Beggiatoa* mats cover vast areas of sediment surface. Mat-hosting sediments are sites of rigorous coupled nitrogen–carbon–sulfur cycling (Teske and Nelson, 2006 and references therein). Dissimilatory processes, such as sulfate reduction and anaerobic methane oxidation, have been studied frequently in Guaymas Basin sediments, including mat-hosting sites (Elsgard et al., 1994; Weber and Jørgensen, 2002; Kallmeyer and Boetius, 2004; Holler et al., 2011; Biddle et al., 2012). However, nitrate dynamics and dissimilatory pathways of nitrate reduction, such as denitrification, have not been explored.

Environmental conditions are postulated to control the dominant dissimilatory nitrate reduction pathways expressed in sediments and therefore which product(s) accumulate (Brunet and Garcia-Gil, 1996; Burgin and Hamilton, 2007; Porubsky et al., 2009). In Guaymas Basin, abundant stocks of thermally-derived organic carbon and reduced substrates, including sulfide, can influence nitrate reduction pathways. Complex organic carbon can support heterotrophic dissimilatory denitrification (DNF) and fermentative dissimilatory nitrate reduction to ammonium (DNRA; Burgin and Hamilton, 2007; Widdel and Rabus, 2001). Sulfide can have a stimulatory or inhibitory effect on nitrate reduction – depending on the pathway employed – and hence may affect the products of nitrate reduction (Joye, 2002). Sulfide can also fuel the activity of some autotrophic denitrifiers (e.g., *Sulfurimonas denitrificans*) and some nitrate reducers capable of DNRA use sulfide as an electron donor. Sulfide inhibition can reduce denitrification rates and stimulate nitrous oxide production because nitrous oxide reductase, the enzyme catalyzing the reduction of nitrous oxide to dinitrogen, is sensitive to sulfide (Brunet and Garcia-Gil, 1996; Joye, 2002; Porubsky et al., 2009). The absence of the nitrous oxide reductase gene could also result in N_2O production in the environment. The abundance of reduced carbon substrates and sulfide are not considered conducive for anaerobic ammonium oxidation (ANAMMOX; Burgin and Hamilton, 2007), so this pathway was not examined in this study.

Microorganisms capable of complete or incomplete DNF exist across the microbial tree of life. Previous studies of the molecular ecology of Guaymas Basin sediments focused on general prokaryotic, sulfate reducing, or methane cycling populations (Teske et al., 2002; Dhillon et al., 2003; Dhillon et al., 2005; Biddle et al., 2012). In Guaymas bacterial clone libraries, potential nitrogen cycling members of Gammaproteobacteria related to bacterial

mat species (e.g., *Beggiatoa*) and of Epsilonproteobacteria (Teske et al., 2002; Dhillon et al., 2003) were observed. These groups of nitrate-utilizing bacteria can use sulfide as an electron donor, and are thought to produce dinitrogen as the end product of their metabolism (Sievert et al., 2003; Sweerts et al., 1990). However, some members of Gammaproteobacteria reduce nitrate to ammonium (Høgslund et al., 2009; Otte et al., 1999). The functional gene responsible for the final step of DNF (*nosZ*) reflects the dinitrogen producers present.

Working under the assumption that DNF and nitrate removal were active in Guaymas Basin sediments, we tested the impact of varying nitrate, sulfide, and dissolved organic carbon concentrations on NO_3^- cycling processes, and describe the diversity of the *nosZ* functional genes in Guaymas sediments. First, we describe and compare potential nitrate removal and DNF rates in *Beggiatoa* mat hosting sediments versus adjacent brown sediments lacking *Beggiatoa* mat biomass. Then, from similar *Beggiatoa* mat hosting sediments, we report how denitrifying bacteria responded to changes in nitrate, sulfide, and dissolved organic carbon (DOC) concentration. Finally, we describe the microbial communities performing nitrous oxide reduction using specific functional genes for this step (*nosZ*), complemented by bacterial 16S rRNA gene surveys.

MATERIALS AND METHODS

SAMPLE COLLECTION AND TREATMENT

Sediments were collected from Guaymas Basin, Gulf of California, by the manned submersible *DSV Alvin* during research cruises in 2008 and 2009. From the 2008 expedition, cores were collected from a dense *Beggiatoa* mat and surrounding sediments, within the area named "Megamat" (*DSV* Alvin-Dives 4490 and 4492; 27°0.459N, 111°24.526W; December 14 and 16, 2008). During the 2009 expedition, several sediment cores within a dense *Beggiatoa* mat were collected (*DSV* Alvin- Dive 4572; December 3, 2009). All sediments were collected at approximately 2000 meters below sea level with upper sediment horizons near 4°C, but typically temperatures increased to >80°C by 20 cm below the sediment water interface. Sediment cores were stored at 4°C until use in laboratory experiments (within 2 weeks).

For sediments sampled in 2008, experiments were conducted on cores either hosting *Beggiatoa* mat (hereafter, mat) at the surface or brown sediment lacking visible mat (hereafter, brown). The brown sediment was sulfidic within millimeters of the sediment surface and was oil-stained over its entire depth. Rates of potential DNF and nitrate removal were measured as described by Bowles and Joye (2011). Briefly, sediment was collected from the 0–6 cm horizon and mixed with an Ar purged artificial porewater mixture [APW (mM): NaCl, 491, $MgCl_2$*$6H_2O$, 24, $CaCl_2$*$2H_2O$, 1.6, KH_2PO_4, 0.03, KCl, 11, $NaHCO_3$, 5] in a 2:1 ratio. The APW and sediment mixture was then centrifuged. The supernatant APW was poured off, fresh APW was added to reconstitute the initial volume, then the sample was gently mixed. This process was repeated three times to obtain a known amount of dissolved constituents in the porewater prior to starting the rate experiments. Before dispensing the slurry into individual culture tubes, the slurry was bubbled with 0.09% Ar and a balance of He for 1 h. Individual culture tubes containing 15 mL of slurry were sealed with butyl rubber stoppers without a headspace (Orcutt et al., 2005). All samples were next injected with 100 μL of concentrated DOC with equimolar carbon from lactate and acetate to achieve a final concentration of 2 mM DOC. Then samples were injected with enriched nitrate ($K^{15}NO_3$, 99% Cambridge Isotope Laboratories®) to a final concentration of 100 μM. Samples were constantly shaken (75 rpm) and incubated at 40°C, a temperature representing the approximate average for the upper 6 cm. Prior to injection with $^{15}NO_3^-$ and DOC, samples were pre-incubated at 40°C for 48 h to reacclimatize microorganisms to quasi *in situ* temperatures. Incubations were terminated (for triplicate sub-samples) at each time point (0, 5, 13, and 26 h) by centrifugation at 500 rpm for 15 minutes, after which porewater was sampled immediately for dissolved gases (i.e., dinitrogen as $^{29}N_2$ and $^{30}N_2$). Briefly, dinitrogen was sampled on a membrane inlet mass spectrometer (MIMS) with minimum detection limit <5 nM and precision of standard measurement of <0.5% (Kana et al., 1998). After gas sampling, the remaining porewater was filtered (0.2 μm), and samples for determination of dissolved components nitrate (NO_3^-), and nitrite (NO_2^-), were collected and subsequently measured. The preservation and analytical methods used for dissolved constituents were described previously (Bowles and Joye, 2011). Briefly, samples for dissolved constituents were refrigerated (4°C) until measurement on an Antek 7050 with chemiluminescence detection (NO_x) and on a spectrophotometer (NO_2^-; Joye et al., 2004). The detection limit for NO_x was approximately 150 nM and precision was <5%, while the NO_2^- detection limit was 50 nM and the precision was 2%.

NITRATE, SULFIDE, AND DOC EXPERIMENTS

To investigate the response of nitrogen cycle dynamics to environmental factors, we used cores collected from a site occupied by dense *Beggiatoa* mat. Prior to these experiments, the mat was gently removed from the sediment surface to reduce background nitrate levels because Guaymas *Beggiatoa* vacuoles often contain 50–100 mM NO_3^- (McKay et al., 2012). For this sampling the upper 3 cm of the sediment from three sediment cores was collected and a slurry was generated, as described above. We used three separate treatments to analyze the physiological response of the mixed community of nitrate reducers: (1) nitrate, (2) sulfide, and (3) DOC treatments at concentrations of 0, 100, 500, 1000, 5000 μM. The sediment slurry was mixed with APW, purged, and rinsed as described previously for potential DNF rate assays. All treatments were run in triplicate. For the individual treatments, 100 μL of the concentrated respective component was added to achieve the target concentration. In the nitrate treatment, samples were injected with 100 μL of a DOC solution (equimolar C from lactate, acetate, and glucose) to yield 1 mM DOC. After purging the nitrate ($K^{15}NO_3$, 99% Cambridge Isotope Laboratories®) with 0.09% Ar and a balance of He, an aliquot was injected into samples so that the target concentration was reached. The pH of the sulfide treatment was adjusted by addition of an equimolar amount of He purged hydrochloric acid applied directly to sulfide solution, and subsequently the sample was tested to ensure that the desired pH was maintained (Teske and Nelson, 2006). For the DOC treatment, carbon was added as equimolar C from lactate, acetate, and glucose. In sulfide and DOC treatments, 100 μL

of nitrate (^{15}N) was injected to equal the final concentration of 1 mM. Immediately following the injection, samples were placed on a shaker table at 75 rpm at 4°C and allowed to incubate for 5 h. A lower temperature was used on these experiments because the temperature of the surficial sediments used was comparable to the ambient bottom seawater.

After the incubation, tubes were centrifuged and sampled as described above. Immediately after the incubation subsamples for dissolved gases were collected ($^{30}N_2$, $^{29}N_2$, and N_2O). Measurement of N_2O was conducted for the nitrate and DOC treatments; the N_2O samples from the sulfide treatment were unfortunately contaminated. The concentration of N_2O was measured with a gas chromatograph equipped with an electron capture detector with a detection limit of around 20 ppb in the headspace analysis, which gave a detection limit of ~9 nM at 5% precision (Porubsky et al., 2009). Briefly, 1 mL of media sample was collected after centrifugation and injected into a He purged headspace vial closed with a butyl rubber stopper and containing a pellet of NaOH. After gas sampling, the artificial porewater was filtered (0.2 μm) and a sample was collected for NO_x and NO_2^- concentration determination. Methods used to preserve and analyze the dissolved constituents were described previously.

MOLECULAR ANALYSIS

DNA extraction, primer design, and polymerase chain reaction

Approximately 0.5 g of wet sediment was used for DNA extraction with the MOBIO® (Carlsbad, CA) Ultrapure Soil DNA extraction kit following the manufacturer's protocol. The PCR master mix consisted of (25 μL): 2μL of template DNA, 0.25 μL of forward, and reverse primers (100 μmol L^{-1}), 0.75 μL of bovine serum albumin (10 mg/mL), 0.12 μL of GoTaq Taq polymerase (Promega™), and the balance of the volume as sterile H_2O. The PCR cycle for 16S rRNA bacterial gene region began with an initial denaturation of 10 min at 94°C followed by 30 cycles of 1.5 min of denaturation at 94°C, 30 s of annealing at 55°C, 30 s of elongation at 72°C, ending with 7 min of elongation at 72°C. The 16S rRNA gene region of bacteria was amplified using the primer B27f (AGAGTTTGATCCTGGCTCAG) and UNI1392r (ACGGGCGGTGTGTRCA; Orphan et al., 2001a,b).

The gene catalyzing the reduction of N_2O to N_2, nitrous oxide reductase, *nosZ* is highly diverse (Scala and Kerkhof, 1999). Primers *nosZ661f* (CGGCTGGGGGCTGACCAA) and *nosZ1773r* (ATRTCGATCARCTGBTCGTT) were used to amplify the region 661–1773, with positions relative to *Pseudomonas stutzeri* (Scala and Kerkhof, 1999). For PCR amplification of the ~1,100 base pair *nosZ* gene, a denaturation of 5 min at 94°C was used and followed by 35 cycles of 30 s of denaturation at 94°C, 1.5 min of annealing at 56°C, 2 min of elongation at 72°C, ending with 7 min of elongation at 72°C (Scala and Kerkhof, 1999).

Cloning

All PCR products were verified to contain the gene of interest based on the size of the amplicon, and subsequently purified using a Qiagen Gel Extraction Kit, as specified by the manufacturer. The PCR products were then ligated into a pCR4 vector (Invitrogen) and transformed into *Escherichia coli* according to manufacturer's specifications. All colonies were screened for ampicillin resistance and lacZ expression. Sequencing was commenced at the M13F primer within the pCR4 vector.

Phylogenetic analysis

The 16S rRNA gene sequences were screened first using blastn (NCBI), and next were aligned using the *S*ilva *In*cremental *A*ligner (SINA; Pruesse et al., 2007). For *nosZ* gene analysis, sequences were converted to amino acids and verified to be on the correct reading frame using the open reading frame (ORF) finder (NCBI). The *nosZ* functional gene was aligned using Clustal W and the alignment (196 amino acids) was then manually edited (Larkin et al., 2007). After alignment, all 16S rRNA gene clones (600 nucleotides) were tested for chimeras using Bellerophon (Huber et al., 2004). Following the chimera check, sequences were imported to ARB and the quality of the alignment was verified and manually adjusted in ARB_EDIT (Ludwig et al., 2004). Mega5 was used to create 16S rRNA gene and *nosZ* phylogenetic trees (Tamura et al., 2011). Phylogenetic trees for 16S rRNA were made by neighbor joining, with a Jukes–Cantor model for distance correction, and the tree was verified by bootstrap analysis ($n = 1000$). The *nosZ* tree was created using amino acid translations (197 amino acids) using minimum evolution with complete deletion and verification by bootstrap analysis ($n = 1000$). The cutoff for operational taxonomic units (OTUs) for bacterial 16S rRNA genes was 97%, and since divergence and hence OTUs are not established for *nosZ*, sequences are shown with identical sequences removed. All bacterial 16S rRNA gene OTUs were established using mothur (Schloss et al., 2009).

RESULTS

POTENTIAL DENITRIFICATION RATES IN MAT AND BROWN SEDIMENTS

Over the course of a 26-h incubation, mat and brown sediments consumed all added $^{15}NO_3^-$ (110 ± 33 μM at time zero and <1 μM at 26 h); nitrite was not detected at any time point (**Figure 1A**). In brown sediments without mat, nitrate concentrations at the start of the incubation were 108 (±29) μM and the amended nitrate was exhausted (<1 μM) after only 13 h (**Figure 1B**). Potential denitrification, tracked as accumulation of $^{30}N_2$ and $^{29}N_2$, was observed in as little as 5 h in both types of sediment. The majority of $^{15}NO_3^-$ was converted to $^{30}N_2$, with only a minor fraction (<2 μM) ending up as $^{29}N_2$. In mat sediments, 16.2 (±6.4) μM $^{30}N_2$ accumulated by 13 h. Relatively more $^{30}N_2$, 22.4 (±1.4) μM, accumulated in brown sediments after 26 h.

Potential denitrification is defined as the sum of $^{30}N_2$ and $^{29}N_2$ formation rates. Linear portions of nitrate consumption and $^{30}N_2$ and $^{29}N_2$ formation curves were used to estimate nitrate removal rates and potential denitrification rates, respectively. In mat sediments, over the first 13 h of the incubation, the rate of nitrate removal was 174 (±74) μM N day^{-1}. In brown sediments, the first 5 h were used to estimate a nitrate removal rate of 418 (±145) μM N day^{-1}. Integrated areal rates of nitrate removal were 435 and 1045 μmol m^{-2} h^{-1} in mat and brown sediments, respectively. Potential denitrification accounted for only a small fraction of nitrate removal in both mat and brown sediments. In mat sediments, potential denitrification rates were estimated over the first 13 h to be 31.2 (±12.1) μM N day^{-1}. Potential denitrification rates were slightly lower in brown sediments at 21.9

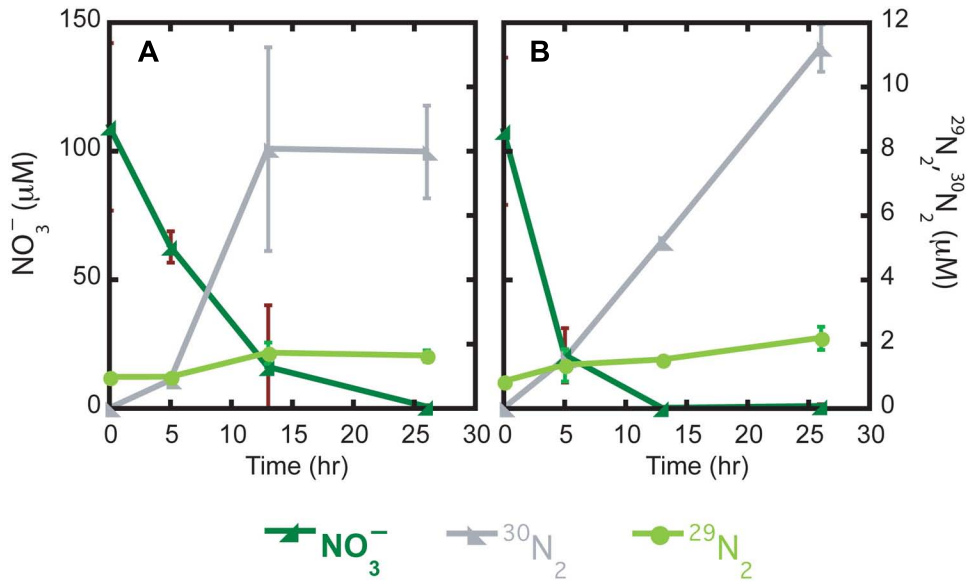

FIGURE 1 | Time series incubations of mat (A) and brown (B) sediments with the substrate (NO_3^-, μM) and products ($^{29}N_2$ and $^{30}N_2$, μM) plotted against time (h).

(±1.4) μM N day^{-1}, but this difference was not statistically significant. Integrated areal rates of potential denitrification were 78 and 54 μmol m^{-2} h^{-1} in mat and brown sediments, respectively.

DENITRIFICATION KINETICS AND INFLUENCES OF SULFIDE AND DOC

Nitrate, sulfide, and DOC amendment generated different responses of the nitrate utilizing populations in Guaymas Basin sediments. The NO_x^- consumption levels were the highest in the nitrate treatment of 5000 μM at 675 μM NO_x^- consumed (ΔNO_x^-; **Figure 2A**). In the nitrate treatment at 1000 μM and at all DOC concentration treatments, the nitrate removal levels were roughly ~300 μM NO_x^- (**Figures 2A,C**). With respect to increases in concentrations of nitrate, sulfide, and DOC, nitrate consumption levels increased, decreased, or did not change, respectively (**Figure 2**).

The proportion of $^{15}NO_3^-$ converted to $^{30}N_2$ and $^{29}N_2$ was summed to generate the μM N as N_2 and is presented as the potential denitrification rate (**Figure 2**). In the nitrate treatment, maximum denitrification was observed at 500 μM with 243 (±6.1) μM N converted to dinitrogen, corresponding to a DNF rate of

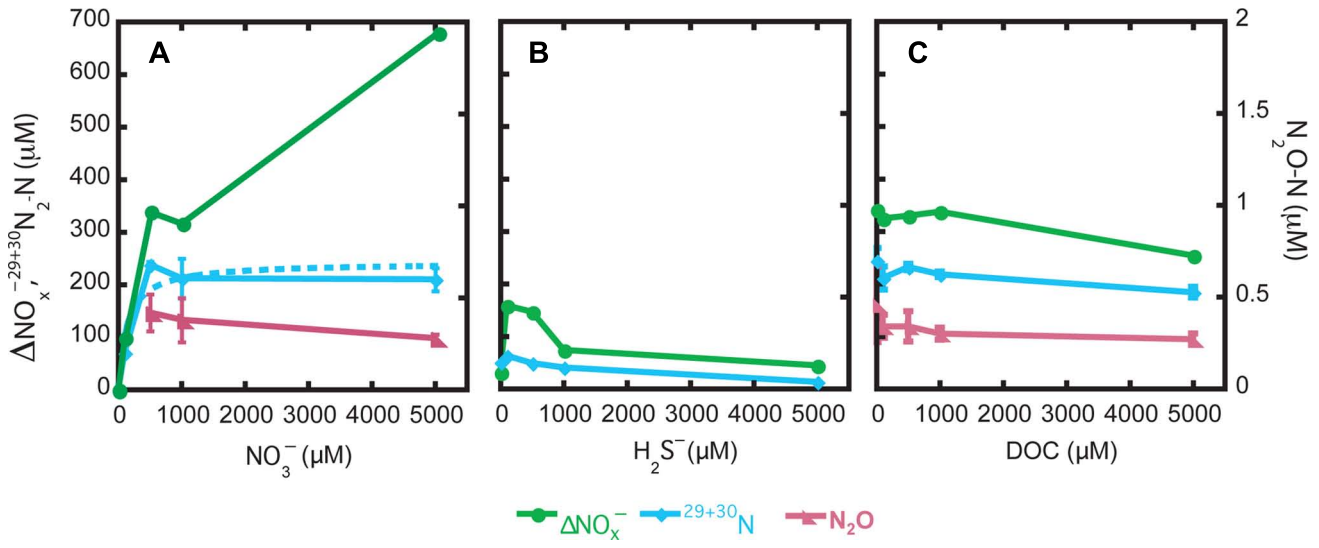

FIGURE 2 | Environmental influences of nitrate (A), sulfide (B), and DOC (C) on denitrification and nitrogen species end products.

1166 μM N d^{-1}. A Michaelis–Menten equation was fit to the data ($r^2 = 0.91$) from the nitrate treatments resulting in a maximum denitrification rate (V_{max}) of 1164 (±153) μM N day^{-1} and half-saturation constant (K_m) of 137 (±91) μM NO_3^- for the endogenous denitrifying community (**Figure 2A**). In the sulfide amended samples, much less N_2 formation was observed relative to the nitrate or DOC treatments. The most N_2 formed in the sulfide treatment was at the concentration of 100 μM, at 61 (±1) μM N as N_2. Denitrification slowed as sulfide concentration rose above 100 μM H_2S. In the DOC treatment, rates of denitrification to N_2 varied little, from 178 (±10) to 238 (±24) μM N day^{-1}, with no observable trends in response versus DOC concentration.

In the nitrate and DOC treatments, N_2O was measured to determine if there was N_2O accumulation in response to the specific treatments. In the nitrate and DOC treatments, N_2O accumulation was high relative to typical environmental levels (range of 0.2–0.4 μM N as N_2O; **Figures 2A,C**). The exception was the nitrate treatment with no nitrate added and with 100 μM nitrate wherein N_2O was not detected.

In order to assess the pathways or fates of nitrate in Guaymas Basin sediments, percentages of total nitrate consumption converted to N_2 or N_2O relative to nitrate removed (e.g., assimilation, storage, or other processes DNRA and anaerobic ammonium oxidation, ANAMMOX) were determined. The fraction of nitrate converted to N_2 represents the sum of $^{30}N_2$ and $^{29}N_2$ and the proportion classified as nitrate removed is the balance of nitrate consumption not occurring as N_2 or N_2O (where N_2O data was available). In general, as nitrate concentrations increased, the fraction of nitrate converted to N_2 decreased, from ∼75 to 32% (**Table 1**). Systematic changes in the fraction of N_2 formation observed were not influenced by sulfide or DOC treatments; note that gaseous N formation in the sulfide treatment does not include N_2O. In the DOC treatment the fraction of nitrate converted to N_2O appeared to decrease slightly with respect to DOC concentration from 0.14 to 0.11% (**Table 1**).

MOLECULAR CENSUS OF BACTERIA AND POSSIBLE DENITRIFIERS

Bacterial 16S rRNA gene and nosZ functional genes

Cloning and sequencing of PCR-amplified 16S rRNA and *nosZ* genes from sediments used in the nitrate, sulfide, and DOC experiments suggested that the sediments maintained a microbiological capacity for denitrification. The 16S rRNA bacterial gene clone library ($n = 77$ clones total) was dominated by Epsilonproteobacteria (38%), Bacteroidetes (21%), Deltaproteobacteria (8%), and Gammaproteobacteria (7%). Within the Epsilonproteobacteria most clones were affiliated with the genus Sulfurovum (27%) or Sulfurimonas (6%; percentages are relative to the entire 16S library). Many of the clones were highly similar to Epsilonproteobacteria clones previously detected in Guaymas Basin sediments (**Figure 3**). In addition to the occurrence of 16S rRNA gene clones potentially relevant to denitrification, we also characterized the nitrous oxide reductase functional gene from these sediments. A total of 20 *nosZ* functional genes were retrieved. Of these, two sequences reflected multiple identical clones, leaving 10 unique sequences (**Figure 4**). The Guaymas Basin sequences were dissimilar from all pure culture *nosZ*, and similar to *nosZ* functional genes extracted from continental margin sediments (Scala and Kerkhof, 1999).

DISCUSSION

BACTERIAL MATS AS NITROGEN CYCLE HOT SPOTS

Bacterial mats are considered areas of intensified nitrogen cycling (Teske and Nelson, 2006; Bourbonnais et al., 2012). Significant accumulations of thick (∼3 cm) bacterial mats (*Beggiatoa* sp.) thrive at the surface of Guaymas Basin hydrothermal sediments and these mats concentrate up to mM levels of nitrate inside their vacuoles (Jannasch et al., 1989; McHatton et al., 1996; McKay et al., 2012). Given the high concentration of nitrate in mat-forming vacuolate sulfur bacteria and their abundance along surficial sediments in the Guaymas Basin, we postulated that nitrate cycling processes like nitrate reduction would be stimulated in mat-hosting sediments. Surprisingly, denitrification and nitrate removal rates were high in both Guaymas Basin mat-hosting sediments and brown sediments that lacked mats. Rates of potential denitrification were somewhat higher in sediments that hosted bacterial mats, versus the brown sediments adjacent to mats. However, nitrate removal rates were faster in brown sediments relative to mat sediments. Collectively these data suggest that while denitrifying communities might be more prominent in mat sediments, other nitrate removal processes are predominant in brown sediments. Other nitrate removal processes in brown sediments could include DNRA, ANAMMOX, and assimilation by endogenous prokaryotes. The lack of any nitrite or $^{29}N_2$ accumulation, which would be the reactant and product of ANAMMOX,

Table 1 | Percent of end products observed in samples amended with nitrate, sulfide, and DOC for all concentration levels.

Concentration (μM)	NO_3^- (%)			H_2S (%)			DOC (%)		
	Removal	$^{29}+^{30}N_2$	N_2O	Removal	$^{29}+^{30}N_2$	N_2O	Removal	$^{29}+^{30}N_2$	N_2O
0	ND	ND	ND	24.5	75.5	NA	27.7	72.1	0.1
100	25.1	74.9	ND	60.0	40.0	NA	34.7	65.2	0.1
500	27.5	72.4	0.1	66.4	33.6	NA	29.3	70.6	0.1
1000	30.1	69.8	0.1	44.6	55.4	NA	34.7	65.2	0.1
5000	67.7	32.2	0.04	68.7	31.3	NA	27.4	72.5	0.1

ND, not determined; NA, not available.

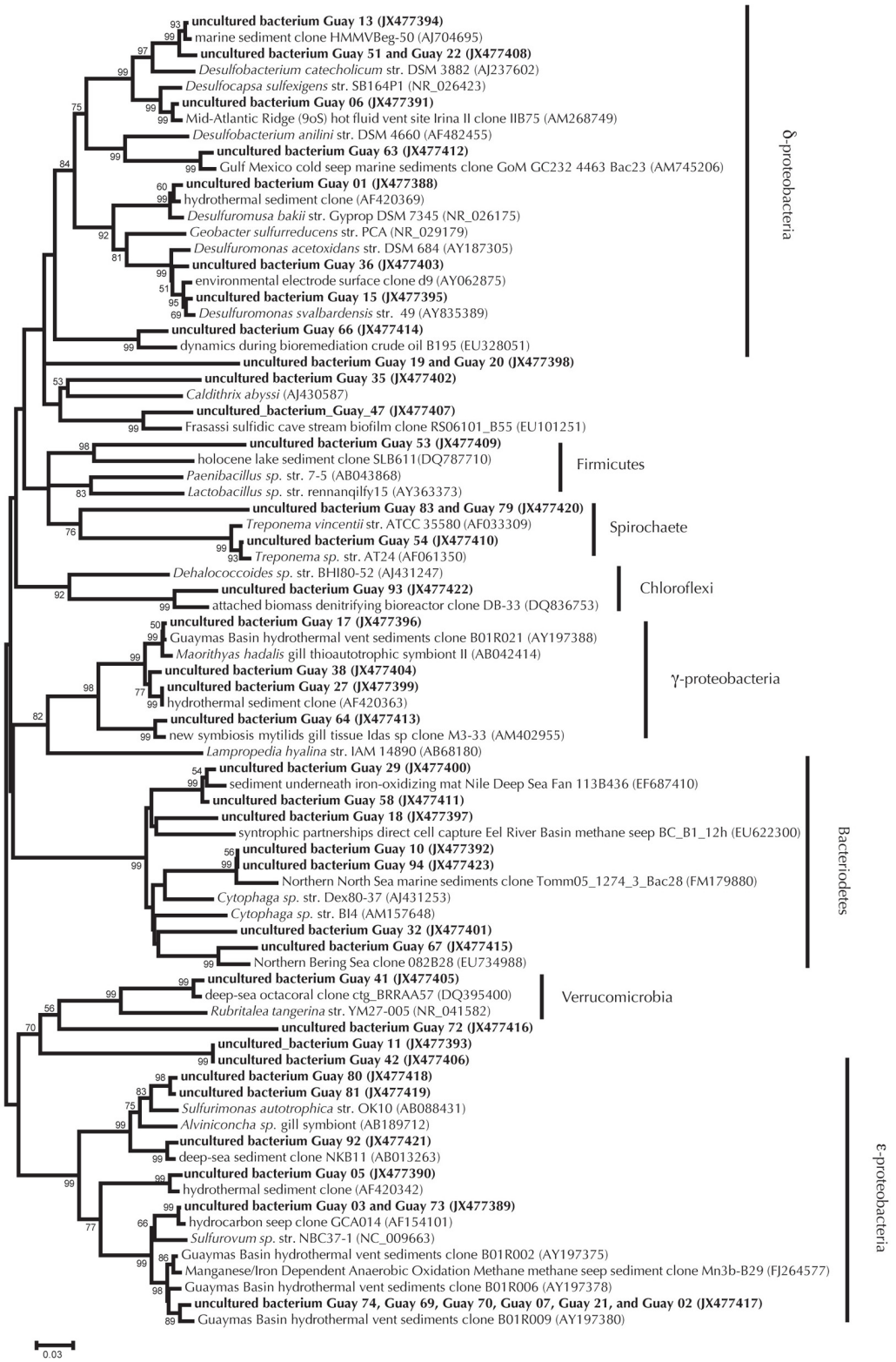

FIGURE 3 | 16S rRNA bacterial gene phylogeny of Guaymas Basin environmental clones relative to pure culture and other environmental clones. Environmental clones from this work appear as bold text, pure cultures are italicized, and environmental clones from other environments appear as normal text. Neighbor joining method was used to generate a tree with a Jukes–Cantor correction of evolutionary distance. Bootstrap values for branches occurring for >50% of 1000 iterations are reported. Scaling of the phylogenetic tree is based on an evolutionary distance of 0.03.

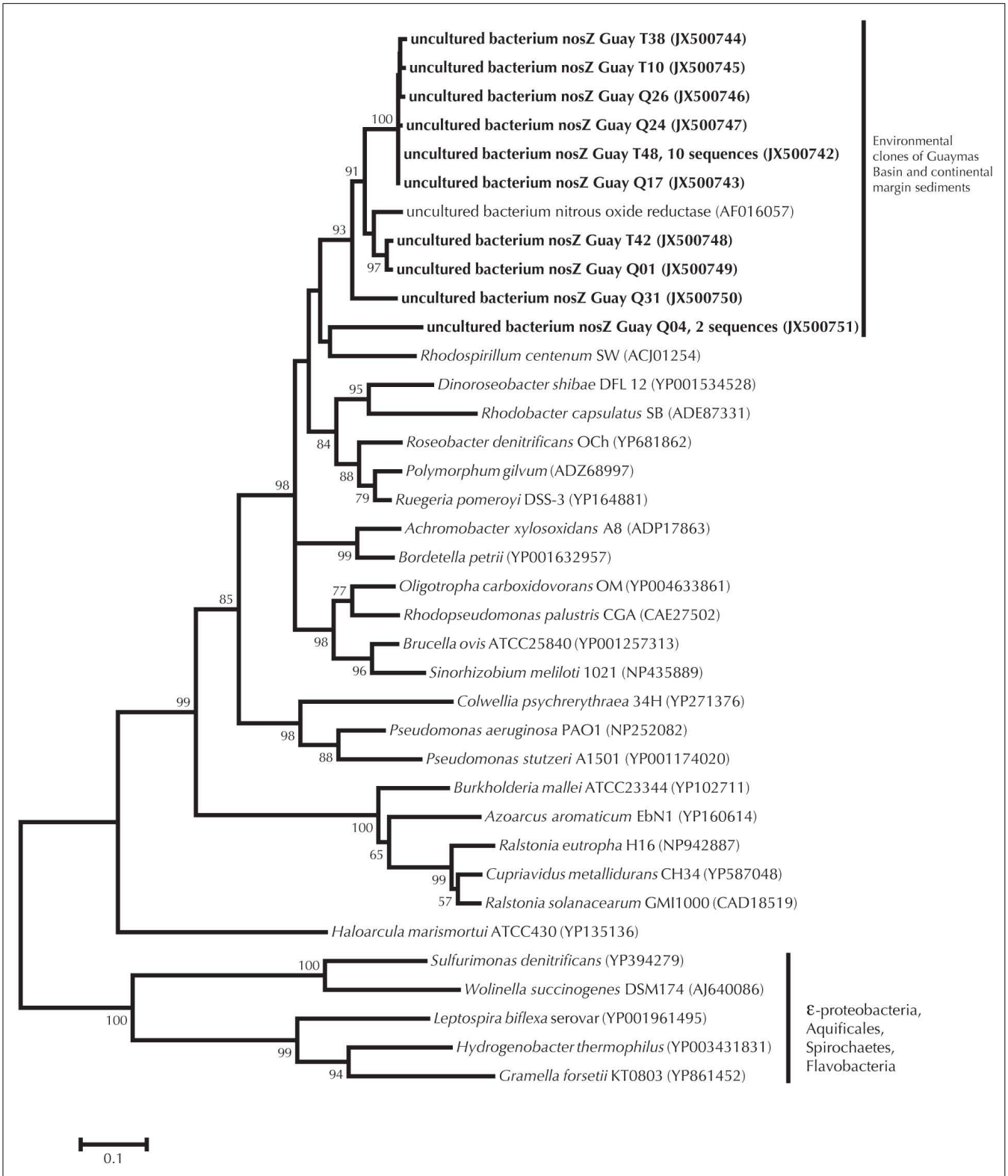

FIGURE 4 | *nosZ* phylogeny of Guaymas Basin environmental clones relative to environmental clones from continental margin sediments and pure culture data. Minimum evolution method was used to generate the phylogeny, with a Poisson correction of evolutionary distance. Bootstrap values for branches occurring for >50% of 1000 iterations are reported. Scaling of the phylogenetic tree is based on an evolutionary distance of 0.10.

respectively, suggests that its occurrence is limited in these sediments, assuming of course that there was no stored nitrate or nitrite present in *Beggiatoa* during experiments. Furthermore, available evidence suggests that in sulfidic sediments, DNRA rather than ANAMMOX is the favored process (Burgin and Hamilton, 2007). Nitrogen assimilation can be performed by numerous heterotrophic and autotrophic organisms and might also contribute to nitrate removal (Allen et al., 2001). Therefore we postulate that DNRA and possibly assimilation are most likely the leading nitrate removal processes in brown sediments.

Few measurements of rates of nitrogen related processes exist in deep-sea sediments (Zopfi et al., 2001; Preisler et al., 2007; Høgslund et al., 2009; Bowles and Joye, 2011). In mat-hosting Gulf of Mexico cold seep sediments, potential denitrification rates were 32 μM N day^{-1}; virtually the same rate as observed in Guaymas Basin mat sediments. Deeper (>6 cm) cold seep sediments not directly associated with mat material had a lower rate that was similar to brown sediments from Guaymas Basin. However, nitrate removal from Guaymas Basin sediments were an order magnitude faster than those measured in Gulf of Mexico cold seep sediments (Bowles and Joye, 2011). Integrated areal rates of potential denitrification (78 and 54 μmol m^{-2} h^{-1}) in Guaymas Basin sediments were similar to rates measured in coastal and eutrophic environments (range: 3.5–1067 μmol m^{-2} h^{-1}; Seitzinger, 1988). The areal integrated rate of nitrate removal in Guaymas Basin of 1045 μmol m^{-2} h^{-1} was very high and similar to the highest reported denitrification rate from sediments in the Tejo estuary (1067 μmol m^{-2} h^{-1}; Seitzinger, 1988). In highly eutrophic Eckernförde Bay on the German Baltic coast, Preisler et al. (2007) performed a stable isotopic tracer rate ($^{15}NO_3^-$) analyses and found *Beggiatoa*-associated nitrate removal was only about 6.5 μmol m^{-2} h^{-1}, which amounts to a minor fraction of the rates observed in sediments of Guaymas Basin. Collectively these data suggest that in addition to the activity of *Beggiatoa*, other sediment microorganisms rigorously metabolize nitrate in organic carbon rich sediments.

ENVIRONMENTAL FACTORS: NITRATE, SULFIDE, AND DOC

Nitrate, sulfide, and DOC concentrations influenced the rates and end products of nitrate reduction (**Figure 2**; **Table 1**). Nitrate utilizing communities in Guaymas Basin sediments reduced nitrate rapidly (high V_{max}) to N_2, with a high affinity for nitrate (relatively low K_m), in comparison to other endogenous communities in other environments (V_{max} = 422 μM N_2−N cm^{-3} day^{-1}, K_m = 344 μM; Oren and Blackburn, 1979). Sulfide clearly influenced the production of dinitrogen; N_2 production rates plummeted and may have resulted in the production of substantial amounts of N_2O (**Figure 2B**). But, we were unfortunately unable to measure N_2O in the sulfide treatments. Finally, microbial communities displayed a limited response to the availability of labile DOC, as observed in consistent potential DNF rates and N_2O accumulation over a range of DOC concentrations.

DENITRIFICATION KINETICS AND NITRATE CONCENTRATION EFFECTS

Data from kinetic experiments on mixed environmental sediment populations performing denitrification are not common (e.g., Oren and Blackburn, 1979; Garcia-Ruiz et al., 1998). In the most relevant dataset from Kysing Fjord (Denmark) sediments, the community K_m was 344 μM nitrate and V_{max} was 422 μM N day^{-1} (Oren and Blackburn, 1979). The microorganisms within Guaymas Basin sediments maintained a higher affinity for nitrate and were able to perform denitrification at a higher maximum rate. This feature may be related to the presence of autotrophic, or sulfide-dependent denitrifiers and heterotrophic populations that utilize endogenous particulate organic carbon. For example, low K_m values (3–161 μM) for nitrate in sulfidic bioreactors have been observed (Zeng and Zhang, 2005). In enrichments for sulfide oxidizing communities of denitrifiers, Shao et al. (2011) observed V_{max} values up to 700 μM h^{-1}. Molecular results also support our findings, as Guaymas sediments contained functional genes associated with heterotrophic denitrification (*nosZ*) as well as some Epsilonproteobacteria typically associated with sulfide dependent denitrification within 16S clone libraries.

Another environmental ramification of enhanced nitrate availability is the potential for a higher proportion of N_2O production relative to N_2 during denitrification (Tiedje, 1988). Increasing amounts of nitrous oxide production as a function of nitrate concentrations have been observed in environmental samples and in pure cultures (Sacks and Barker, 1952; Blackmer and Bremner, 1978; Joye, 2002). However Shao et al. (2011) recently observed no relationship between extremely high levels of nitrate (80 mM) and N_2O production. We did not observe substantial increases in the proportion of N_2O formed in Guaymas Basin sediments up to 5000 μM NO_3^-.

SULFIDE AND DENITRIFICATION

Nitrogen related processes are often subject to substantial influences from sulfides; nitrogen fixation (e.g., Marino et al., 2003), denitrification (e.g., Joye, 2002), and nitrification (Joye and Hollibaugh, 1995) are all influenced by sulfide concentration. Denitrification to N_2 often slows substantially or ceases at relatively low sulfide concentrations, and sulfide might be a contributing factor to the observed accumulation of N_2O in anoxic marine sediments (Sørensen, 1978; Joye, 2002). In Guaymas Basin sediments we observed low rates of potential denitrification in the presence of sulfide. The production of dinitrogen is limited by the sulfide-induced inhibition of nitrous oxide reductase (*nosZ*; Sørensen et al., 1980) or by limitation of denitrifiers by sulfide in general (Joye, 2002). Some pure culture data (*Aeromonas* sp., *Vibrio* sp., and *Pseudomonas fluorescens*) and environmental assays suggest that nitrous oxide reductase is already significantly inhibited at low sulfide concentrations of 100–300 μM (Sørensen et al., 1980; Senga et al., 2006). In contrast to relatively low inhibitory concentrations of sulfide observed in pure cultures, some environmental studies have reported evidence of nitrous oxide reductase inhibition (nitrous oxide accumulation) at much higher sulfide concentrations of 1–2.5 mM (Brunet and Garcia-Gil, 1996; Senga et al., 2006).

A paradoxical feature of denitrification in sulfidic sediments is that some microorganisms are able to use sulfide as an electron donor for denitrification. Perhaps it is the rigorous activity of sulfide utilizing denitrifying microorganisms that supports denitrification at high sulfide concentrations (2.5 mM) in some environments, such as Lake Shinji (Japan; Senga et al., 2006). The

Guaymas sediments investigated here and previously investigated sediments from the same site hosted Epsilonproteobacteria (here ∼38%; Teske et al., 2002; Dhillon et al., 2003) and cultured representatives of this group can likely use sulfide as an electron donor (Takai et al., 2003). Considering the high environmental concentrations of sulfide and nitrate, it is surprising that the endogenous denitrifier community in Guaymas Basin sediments was not more tolerant of sulfide.

DISSOLVED ORGANIC CARBON ADDITION

The addition of labile DOC is thought to support high denitrification rates and might also support production of N_2O (Tiedje, 1988). Though functional gene analysis of *nosZ* suggests the activity of heterotrophic denitrifying communities, we did not observe any stimulation of denitrification rates in response to increases in labile carbon concentration (DOC). These data suggest that heterotrophic metabolism to N_2 was important, though other denitrification pathways (autotrophic) must also contribute substantially to the total observed rate. Another distinct possibility is that these communities are adapted to high DOC levels in the natural environment and the addition here was insufficient to stimulate potential denitrification rates. In soils, additions of glucose decreased N_2O production (Weier et al., 1993). In Guaymas sediments, despite large additions of DOC, N_2O accumulation did not systematically change.

COMPLEX NITROGEN CYCLING COMMUNITIES

Molecular microbiological data are indicative of autotrophic and heterotrophic denitrification (**Figures 3 and 4**). Though not quantitative, the domination of clone libraries by Epsilonproteobacteria related to Sulfurovum and Sulfurimonas implies the presence and activity of an autotrophic denitrifying population in Guaymas sediments (Shao et al., 2010). The Epsilonproteobacteria clones outnumbered Deltaproteobacteria, which are largely sulfate reducers. Though elevated rates of sulfate reduction are often measured in this environment, the quantitative and qualitative data presented here (e.g., measured rates of denitrification and nitrate removal and molecular data) underscore the importance of nitrogen related processes (Elsgard et al., 1994; **Figure 3**) in this habitat as well.

The amino acid composition of *nosZ* within sulfide utilizing microorganisms is dissimilar to that of other organisms, corresponding to the outgroup in **Figure 4**. Traditional primers used for *nosZ* do not capture the Epsilonproteobacteria *nosZ* functional genes (see Sievert et al., 2003 and discussion therein). However utilizing the traditional *nosZ* primers (Scala and Kerkhof, 1999), we observed an outgroup of environmental samples similar to *nosZ* isolated from continental margin sediments (Scala and Kerkhof, 1999; **Figure 4**). The relationship of Guaymas *nosZ* clones with continental margins could be because the primers developed by Scala and Kerkhof (1999) target specific types of denitrifiers or because the recovered sequences reflect microorganisms that are general heterotrophic denitrifiers.

NITRATE REMOVAL

An observation similar between Guaymas and cold seep sediments (Bowles and Joye, 2011) is that a great fraction of NO_3^- added is not recovered or accounted for. Though termed nitrate removal we speculate that this component is largely composed of DNRA and assimilation. Detecting both processes can be difficult and made more complex by the fact that DNRA and assimilation can be related. Ammonium generated by DNRA can be directly assimilated into biomass representing an interconnected series of pathways, from nitrate to biomass. Measuring DNRA in Guaymas Basin sediments was complicated by high background levels of ammonium (100s μM to >10 mM; Simoneit et al., 1992). Though sediments were rinsed prior to the experiments, ammonium levels during these incubations were still 100s of μM owing to high initial concentrations and potentially ammonium absorption to sediment particles (data not shown). In high activity sediments such as Guaymas Basin sediments we speculate that assimilation alone could also play a large role in nitrate removal. Carbon assimilation has been directly measured in Guaymas Basin sediments and these rates are substantial at about 4000 μM C day^{-1} (Joye and Samarkin, unpublished results). If we assume stoichiometric uptake of nitrogen by prokaryotes (C:N ∼1:0.24; Whitman et al., 1998), then the demand for nitrogen comes to approximately 960 μM N day^{-1}. This estimate from previous measurements of C assimilation shows that nitrate assimilation is the correct order of magnitude to account for all of the nitrate that was not recovered. In addition, this estimate would only include nitrogen incorporation from autotrophic microorganisms, and has to be regarded as conservative since it does not include heterotrophic nitrogen assimilation processes in carbon rich environments (Allen et al., 2001).

CONCLUSION

Denitrification is carried out by the endogenous prokaryotic communities in Guaymas Basin sediments. Denitrification rates are high in comparison to those observed in other environments and rates and endpoints are influenced by environmental factors, most notably sulfide. In molecular surveys of denitrifying bacteria from Guaymas Basin the potential for both heterotrophic and autotrophic, sulfide based, denitrification was observed. Future studies should further document the presence of nitrate in these environments, contained within *Beggiatoa* and free nitrate, in order to understand the importance of denitrification in this type of environment, relative to other processes. Additionally, quantification of heterotrophic and autotrophic gene transcripts should be performed to better constrain carbon and sulfur interrelations in these complex settings.

ACKNOWLEDGMENTS

We thank the R/V *Atlantis* and HOV *Alvin* crews for exemplary work and unflagging support during our dives in Guaymas Basin, Jennifer Biddle, Vladimir Samarkin, and all the participants of the Guaymas Basin cruise science parties for collecting and providing samples for these analyses. We also thank the two reviewers whose suggestions greatly improved this manuscript. This research was supported by grants from the U.S. National Science Foundation (OCE 0959337 to Samantha B. Joye and OCE 0647633 to Andreas P. Teske).

REFERENCES

Allen, A. E., Booth, M. G., Frischer, M. E., Verity, P. G., Zehr, J. P., and Zani, S. (2001). Diversity and detection of nitrate assimilation genes in marine Bacteria. *Appl. Environ. Microbiol.* 67, 5343–5348.

Biddle, J. F., Cardman, Z., Mendlovitz, H., Albert, D., Lloyd, K. G., Boetius, A., et al. (2012). Anaerobic oxidation of methane at different temperature regimes in Guaymas Basin hydrothermal sediments. *ISME J.* 6, 1018–1031.

Blackmer, M., and Bremner, J. M. (1978). Inhibitory effect of nitrate on reduction of N_2O to N_2 by soil microorganisms. *Soil Biol. Biochem.* 10, 187–191.

Bourbonnais, A., Lehmann, D. A., and Juniper, S. K. (2012). Subseafloor nitrogen transformations in diffuse hydrothermal vent fluids of the Juan de Fuca Ridge evidenced by the isotopic composition of nitrate and ammonium. *Geochem. Geophys. Geosysts.* 13, Q02T01. doi: 10.1029/2011GC003863 [Epub ahead of print].

Bowles, M. W., and Joye, S. B. (2011). High rates of denitrification and nitrate removal in cold seep sediments. *ISME J.* 5, 565–567.

Brunet, R. C., and Garcia-Gil, L. J. (1996). Sulfide-induced dissimilatory nitrate reduction to ammonia in anaerobic freshwater sediments. *FEMS Microbiol. Ecol.* 21, 131–138.

Burgin, A. J., and Hamilton, S. K. (2007). Have we overemphasized the role of denitrification in aquatic ecosystems? A review of nitrate removal pathways. *Front. Ecol. Environ.* 5, 89–96.

Dhillon, A., Lever, M., Lloyd, K. G., Albert, D. B., Sogin, M. L., and Teske, A. (2005). Methanogen diversity evidenced by molecular characterization of methyl coenzyme M reductase A (mcrA) genes in hydrothermal sediments of the Guaymas Basin. *Appl. Environ. Microbiol.* 71, 4592–4601.

Dhillon, A., Teske, A., Dillon, J., Stahl, D. A., and Sogin, M. L. (2003). Molecular characterization of sulfate-reducing bacteria in the Guaymas Basin. *Appl. Environ. Microbiol.* 69, 2765–2772.

Elsgard, L., Isaksen, M. I., Jørgensen, B. B., Alayse, A.-M., and Jannasch, H. W. (1994). Microbial sulfate reduction in deep-sea sediments at the Guaymas basin hydrothermal vent area: influence of temperature and substrates. *Geochim. Cosmochim. Acta* 58, 3335–3343.

Garcia-Ruiz, R., Pattinson, S. N., and Whitton, B. A. (1998). Kinetic parameters of denitrification in a River Continuum. *Appl. Environ. Microbiol.* 64, 2533–2538.

Høgslund, S., Revsbech, N. P., Kuenen, G., Jørgensen, B. B., Gallardo, V. A., Vossenberg, J. V. D., et al. (2009). Physiology and behaviour of marine *Thioploca*. *ISME J.* 3, 647–657.

Holler, T., Widdel, F., Knittel, K., Amann, R., Kellermann, M. Y., Hinrichs, K.-U., et al. (2011). Thermophilic anaerobic oxidation of methane by marine microbial consortia. *ISME J.* 5,1946–1956.

Huber, T., Faulkner, G., and Hugenholtz, P. (2004). Bellerophon: a program to detect chimeric sequences in multiple sequence alignments. *Bioinformatics* 20, 2317–2319.

Jannasch, H. W., Nelson, D. C., and Wirsen, C. O. (1989). Massive natural occurrence of unusually large bacteria (*Beggiatoa* sp.) at a hydrothermal deep-sea vent site. *Nature* 342, 834–836.

Joye, S. B. (2002). "Denitrification in the marine environment," in *Encyclopedia of Environmental Microbiology*, ed. G. Collins (New York: John Wiley & Sons, Inc.), 1010–1019.

Joye, S. B., Boetius, A., Orcutt, B. N., Montoya, J. P., Schulz, H. N., Erickson, M. J., et al. (2004). The anaerobic oxidation of methane and sulfate reduction in sediments from Gulf of Mexico cold seeps. *Chem. Geol.* 205, 219–238.

Joye, S. B., and Hollibaugh, J. T. (1995). Influence of sulfide inhibition of nitrification on nitrogen regeneration in sediments. *Science* 270, 623–625.

Kallmeyer, J., and Boetius, A. (2004). Effects of temperature and pressure on sulfate reduction and anaerobic oxidation of methane in hydrothermal sediments of Guaymas Basin. *Appl. Environ. Microbiol.* 70, 1231–1233.

Kana, T. M., Sullivan, M. B., Cornwell, J. C., and Groszkowski, K. M. (1998). Denitrification in estuarine sediments determined by membrane inlet mass spectrometry. *Limnol. Oceanogr.* 43, 334–339.

Larkin, M. A., Blackshields, G., Brown, N. P., Chenna, R., McGettigan, P. A., McWilliam, H., et al. (2007). Clustal W and Clustal X version 2.0. *Bioinformatics* 23, 2947–2948.

Ludwig, W., Strunk, O., Westram, R., Richter, L., Meier, H., Yadhukumar, A., et al. (2004). ARB: a software environment for sequence data. *Nucleic Acids Res.* 32, 1363–1371.

Marino, R., Howarth, R. W., Chan, F., Cole, J. J., and Likens, G. E. (2003). Sulfide inhibition of molybdenum-dependent nitrogen fixation by planktonic cyanobacteria under seawater conditions: a non-reversible effect. *Aquat. Biodivers.* 171, 277–293.

McHatton, S. C., Barry, J. P., Jannasch, H. W., and Nelson, D. C. (1996). High nitrate concentrations in vacuolate autotrophic marine *Beggiatoa* spp. *Appl. Environ. Microbiol.* 62, 954–958.

McKay, L. J., MacGregor, B. J., Biddle, J. F., Mendlovitz, H. P., Hoer, D., Lipp, J. S., et al. (2012). Spatial heterogeneity and underlying geochemistry of phylogenetically diverse orange and white Beggiatoa mats in Guaymas Basin hydrothermal sediments. *Deep Sea Res.* 67, 21–31.

Orcutt, B., Boetius, A., Elvert, M., Samarkin, V., and Joye, S. B. (2005). Molecular biogeochemistry of sulfate reduction, methanogenesis and the anaerobic oxidation of methane at Gulf of Mexico cold seeps. *Geochim. Cosmochim. Acta* 69, 4267–4281.

Oren, A., and Blackburn, T. H. (1979). Estimation of sediment denitrification rates at *in situ* nitrate concentration. *Appl. Environ. Microbiol.* 37, 174–176.

Orphan, V. J., Hinrichs, K. U., Ussler, W., Paull, C. K., Taylor, L. T., Sylva, S. P., et al. (2001a). Comparative analysis of methane-oxidizing Archaea and sulfate-reducing bacteria in anoxic marine sediments. *Appl. Environ. Microbiol.* 67, 1922–1934.

Orphan, V. J., House C. H., Hinrichs K.-U., McKeegan K. D., and DeLong E. F. (2001b). Methane-consuming Archaea revealed by directly coupled isotopic and phylogenetic analysis. *Science* 293, 484–487.

Otte, S., Kuenen, J. G., Nielsen, L. P., Paerl, H. P., Zopfi, J., Schulz, H. N., et al. (1999). Nitrogen, carbon, and sulfur metabolism in natural *Thioploca* samples. *Appl. Environ. Microbiol.* 65, 3148–3157.

Porubsky, W. P, Weston, N. B., and Joye, S. B. (2009). Interactions between benthic primary production, denitrification and dissimilatory nitrate reduction to ammonium in intertidal sediments. *Estuar. Coast. Shelf Sci.* 83, 392–402.

Preisler, A., de Beer, D., Lichschlag, A., Lavik, G., Boetius, A., and Jørgensen, B. B. (2007). Biological and chemical sulfide oxidation in a Beggiatoa inhabited marine sediment. *ISME J.* 1, 341–353.

Pruesse, E., Quast, C., Knittel, K., Fuchs, B. M., Ludwig, W., Peplies, J., et al. (2007). SILVA: a comprehensive online resource for quality checked and aligned ribosomal RNA sequence data compatible with ARB. *Nucleic Acids Res.* 35, 7188–7196.

Sacks, L. E., and Barker, H. A. (1952). Substrate oxidation and nitrous oxide utilization in denitrification. *J. Bacteriol.* 64, 247–252.

Scala, D. J., and Kerkhof, L. J. (1999). Diversity of nitrous oxide reductase (*nosZ*) genes in continental shelf sediments. *Appl. Environ. Microbiol.* 65, 1681–1687.

Schloss, P. D., Westcott, S. L., Ryabin, T., Hall, J. R., Hartmann, M., Hollister, E. B., et al. (2009). Introducing mothur: open-source, platform-independent, community-supported software for describing and comparing microbial communities. *Appl. Environ. Microbiol.* 75, 7537–7541.

Seitzinger, S. P. (1988). Denitrification in freshwater and coastal marine ecosystems: ecological and geochemical significance. *Limnol. Oceanogr.* 33, 702–724.

Senga, Y., Mochida, K., Fukumori, R., Okamoto, N., and Seiki, Y. (2006). N_2O accumulation in estuarine and coastal sediments: the influence of H_2S on dissimilatory nitrate reduction. *Estuar. Coast. Shelf Sci.* 67, 231–238.

Shao, M.-F., Zhang, T., and Fang, H. (2010). Sulfur-driven autotrophic denitrification: diversity, biochemistry, and engineering applications. *Appl. Microbiol. Biotechnol.* 88, 1027–1042.

Shao, M.-F., Zhang, T., Fang, H., and Li, X. (2011). The effect of nitrate concentration on sulfide-driven autotrophic denitrification in marine sediment. *Chemosphere* 83, 1–6.

Sievert, S. M., Scott, K. M., Klotz, M. G., Chain, P. S. G., Hauser, L. J., Hemp, J., et al. (2003). Genome of the epsilonproteobacterial chemolithoautotroph *Sulfurimonas denitrificans*. *Appl. Environ. Microbiol.* 74, 1145–1156.

Simoneit, B. R. T., Leif, R. N., Sturz, A. A., Sturdivant, A. E., and Gieskes, J. M. (1992). Geochemistry of shallow sediments in Guaymas Basin, Gulf of California: hydrothermal gas and oil migration and effects of mineralogy. *Org. Geochem.* 18, 765–784.

Sørensen, J. (1978). Occurence of nitric and nitrous oxides in a coastal marine sediment. *Appl. Environ. Microbiol.* 36, 809–813.

Sørensen, J., Tiedje, J. M., and Firestone, R. B. (1980). Inhibition by sulfide of nitric and nitrous oxide reduction by denitrifying *Pseudomonas fluorescens*. *Appl. Environ. Microbiol.* 39, 105–108.

Sweerts, J. P. R. A., De Beer, D., Nielsen, L. P., Verdouw, H., Van den Heuvel, J. C., Cohen, Y., et al. (1990). Denitrification by sulfur oxidizing *Beggiatoa* spp. mats on freshwater sediments. *Nature* 344, 762–763.

Takai, K., Inagaki, F., Nakagawa, S., Hirayama, H., Nunoura, T., Sako, Y., et al. (2003). Isolation and phylogenetic diversity of members of previously uncultivated ε-Proteobacteria in deep-sea hydrothermal vents. *FEMS Microbiol. Lett.* 218, 167–174.

Tamura, K., Peterson, D., Peterson, N., Stecher, G., Nei, M., and Kumar, S. (2011). MEGA5: molecular evolutionary genetics analysis using maximum likelihood, evolutionary distance, and maximum parsimony methods. *Mol. Biol. Evol.* 28, 2731–2739.

Teske, A., Hinrichs, K.-U., Edgcomb, V., Gomez, A. V., Kysela, D., Sylva, S. P., et al. (2002). Microbial diversity of hydrothermal sediments in the Guaymas Basin: evidence for anaerobic methanotrophic communities. *Appl. Environ. Microbiol.* 68, 1994–2007.

Teske, A., and Nelson, D. C. (2006). *The Genera Beggiatoa and Thioploca Prokaryotes*, Vol. 3. New York: Springer, 784–810.

Tiedje, J. M. (1988). "Ecology of denitrification and dissimilatory nitrate reduction to ammonium," in *Biology of Anaerobic Microorganisms*, ed. A. J. B. Zehnder (New York: John Wiley), 197–244.

Weber, A., and Jørgensen, B. B. (2002). Bacterial sulfate reduction in hydrothermal sediments of the Guaymas Basin, Gulf of California, Mexico. *Deep Sea Res.* 49, 827–841.

Weier, K. L., Macrae, I. C., and Myers, R. J. K. (1993). Denitrification in a clay soil under pasture and annual crop: estimation of potential losses using intact soil cores. *Soil Biol. Biochem.* 25, 991–997.

Whitman, W. B., Coleman, D. C., and Wiebe, W. J. (1998). Prokaryotes: the unseen majority. *Proc. Natl. Acad. Sci. U.S.A.* 95, 6578–6583.

Widdel, F., and Rabus, R. (2001). Anaerobic biodegradation of saturated and aromatic hydrocarbons. *Curr. Opin. Biotechnol.* 12, 259–276.

Zeng, H., and Zhang, C. (2005). Evaluation of kinetic parameters of a sulfur-limestone autotrophic denitrification biofilm process. *Water Res.* 39, 4941–4952.

Zopfi, J., Kjaer, T., Nielsen, L. P., and Jørgensen, B. B. (2001). Ecology of *Thioploca* spp.: nitrate and sulfur storage in relation to chemical microgradients and influence of *Thioploca* spp. on the sedimentary nitrogen cycle. *Appl. Environ. Microbiol.* 67, 5530–5537.

Conflict of Interest Statement: The authors declare that the research was conducted in the absence of any commercial or financial relationships that could be construed as a potential conflict of interest.

Received: 08 July 2012; paper pending published: 03 August 2012; accepted: 03 October 2012; published online: 25 October 2012.

Citation: Bowles MW, Nigro LM, Teske AP and Joye SB (2012) Denitrification and environmental factors influencing nitrate removal in Guaymas Basin hydrothermally altered sediments. Front. Microbio. ***3****:377. doi: 10.3389/fmicb.2012.00377*

This article was submitted to Frontiers in Aquatic Microbiology, a specialty of Frontiers in Microbiology.

frontiers in MICROBIOLOGY

ORIGINAL RESEARCH ARTICLE
published: 30 August 2013
doi: 10.3389/fmicb.2013.00237

Transitions in *nirS*-type denitrifier diversity, community composition, and biogeochemical activity along the Chesapeake Bay estuary

Christopher A. Francis[1,2]*, Gregory D. O'Mullan[2,3], Jeffrey C. Cornwell[4] and Bess B. Ward[2]

[1] Department of Environmental Earth System Science, Stanford University, Stanford, CA, USA
[2] Department of Geosciences, Princeton University, Princeton, NJ, USA
[3] School of Earth and Environmental Sciences, Queens College, City University of New York, Flushing, NY, USA
[4] University of Maryland Center for Environmental Science, Horn Point Laboratory, Cambridge, MD, USA

Edited by:
Marlene M. Jensen, University of Southern Denmark, Denmark

Reviewed by:
Hongyue Dang, Xiamen University, China
Phyllis Lam, University of Southampton, UK

***Correspondence:**
Christopher A. Francis, Department of Environmental Earth System Science, Stanford University, 473 Via Ortega, Y2E2 Bldg Rm. 140, Stanford, CA 94305-4216, USA
e-mail: caf@stanford.edu

Chesapeake Bay, the largest estuary in North America, can be characterized as having steep and opposing gradients in salinity and dissolved inorganic nitrogen along the main axis of the Bay. In this study, the diversity of *nirS* gene fragments (encoding cytochrome cd_1-type nitrite reductase), physical/chemical parameters, and benthic N_2-fluxes were analyzed in order to determine how denitrifier communities and biogeochemical activity vary along the estuary salinity gradient. The *nir*S gene fragments were PCR-amplified, cloned, and sequenced from sediment cores collected at five stations. Sequence analysis of 96–123 *nirS* clones from each station revealed extensive overall diversity in this estuary, as well as distinct spatial structure in the *nirS* sequence distributions. Both *nirS*-based richness and community composition varied among stations, with the most dramatic shifts occurring between low-salinity (oligohaline) and moderate-salinity (mesohaline) sites. For four samples collected in April, the *nirS*-based richness, nitrate concentrations, and N_2-fluxes all decreased in parallel along the salinity gradient from the oligohaline northernmost station to the highest salinity (polyhaline) station near the mouth of the Bay. The vast majority of the 550 *nirS* sequences were distinct from cultivated denitrifiers, although many were closely related to environmental clones from other coastal and estuarine systems. Interestingly, 8 of the 172 OTUs identified accounted for 42% of the total *nirS* clones, implying the presence of a few dominant and many rare genotypes, which were distributed in a non-random manner along the salinity gradient of Chesapeake Bay. These data, comprising the largest dataset to investigate *nirS* clone sequence diversity from an estuarine environment, also provided information that was required for the development of *nirS* microarrays to investigate the interaction of microbial diversity, environmental gradients, and biogeochemical activity.

Keywords: denitrification, nitrite reductase, *nir*S, estuary

INTRODUCTION

Denitrification, the dissimilatory reduction of nitrate and nitrite to gaseous products (NO, N_2O, N_2) under suboxic conditions, is a major biological loss term for fixed nitrogen from terrestrial and aquatic ecosystems to the atmosphere (Devol, 2008). In estuarine sediments, denitrification is capable of removing significant quantities (>50%) of nitrate from the water column, providing a sink for nitrogen, and thereby playing an important role in ameliorating the degree of eutrophication in waters subjected to external (agricultural or urban) N inputs (Seitzinger et al., 2006; reviewed by Boynton and Kemp, 2008). The anaerobic oxidation of ammonium to nitrogen gas (anammox) also contributes to the loss of fixed nitrogen in aquatic systems, particularly in suboxic water columns (Dalsgaard et al., 2003; Kuypers et al., 2003, 2005; Francis et al., 2007; Lam et al., 2009; Ward et al., 2009), but anammox is thought to be less quantitatively significant in estuaries (Risgaard-Petersen et al., 2004; Trimmer et al., 2005), including the Chesapeake Bay (Rich et al., 2008). Sedimentary denitrification is supported both by nitrate diffusing from the overlying water and by nitrate produced by nitrification within the sediment (Kemp et al., 1990; Jensen et al., 1993, 1994). These coupled processes are quantitatively important in the nitrogen budgets of estuarine and continental shelf sediments (Christensen et al., 1987; Cornwell et al., 1999). Considering the tremendous importance of denitrification in estuarine systems, it is critical to understand the distribution, diversity, and biogeochemical activity of the underlying denitrifier communities within estuaries.

Because the metabolic potential for denitrification is widespread among many phylogenetically unrelated groups, including over 50 different genera, a 16S rRNA-based approach is not generally appropriate for characterizing complex denitrifying communities. Instead, the functional genes encoding key metalloenzymes in the denitrification pathway have proven

to be useful molecular markers for denitrifying organisms. In particular, nitrite reductase (NiR) catalyzes the first committed step to a gaseous product (Zumft, 1997), distinguishing true (gas-producing) denitrifiers from nitrate-respiring microbes (including those that perform dissimilatory nitrate or nitrite reduction to ammonium; DNRA). NiR occurs in two distinct forms that are structurally different but apparently functionally equivalent: NirS, containing iron (cytochrome-cd_1); and NirK, containing copper (spectroscopic types I and II). Due to the critical role of nitrite reductase in the dentrification pathway, the *nirK* and *nirS* genes have been most frequently targeted for molecular diversity studies in many environments, including soils (Prieme et al., 2002; Rösch et al., 2002; Sharma et al., 2005; Smith and Ogram, 2008); groundwater (Yan et al., 2003); wastewater (Yoshie et al., 2004); suboxic water columns (Jayakumar et al., 2004, 2009; Castro-González et al., 2005; Oakley et al., 2007); and coastal and marine sediments (Braker et al., 2000, 2001; Liu et al., 2003; Santoro et al., 2006). To date, however, the molecular diversity of estuarine nitrite reductase genes has only been explored in detail within a few systems (Nogales et al., 2002; Hannig et al., 2006; Dang et al., 2009; Abell et al., 2010; Mosier and Francis, 2010). Recent studies of bacterial ammonia monooxygenase subunit A (*amoA*) genes have revealed a pattern of ammonia oxidizer diversity correlated with salinity, as well as distinct communities in freshwater and high salinity estuarine environments (Francis et al., 2003; Bernhard et al., 2005; Ward et al., 2007; Mosier and Francis, 2008). While similar patterns might be expected for the distribution of denitrification genes along the estuary, denitrifier diversity might also be related to the distribution of suboxic environments and denitrification rates, which in turn depend on the availability of key factors like organic carbon, oxygen, and nitrate.

In the present study, we explore the distribution and diversity of cytochrome cd_1-type nitrite reductase (*nirS)* sequences in sediments of the Chesapeake Bay. This is the largest estuary in North America, and denitrification is a critical component of the N cycle, which is dominated by sediment N transformations. We have previously examined ammonia-oxidizing (AO) communties in these sediments (Francis et al., 2003), and the abundance and expression of key *nirS*-type genotypes at three sites in this estuary (Bulow et al., 2008). Here the fine-scale diversity, community composition, and phylogeny of *nirS* sequences at five stations were analyzed, along with *in situ* benthic N_2-flux rates, in order to explore spatial variability in estuarine denitrifier diversity and function. The data described in this study are also significant because it represents the largest clone library-based survey of *nirS* sequence diversity in an estuary and the dataset has been used to develop a *nirS* microarray that can more efficiently investigate the interaction of microbial diversity, environmental factors, and biogeochemical activity.

MATERIALS AND METHODS

SITE DESCRIPTION

The Chesapeake Bay drains a watershed of 166,000 km^2 and fills a dendritic river valley system consisting of a main channel and 7 main rivers, including the Choptank River, a subestuary that contributes roughly 1% of the total freshwater to the bay. Five stations (**Figure 1**) were chosen to represent the range of salinity and environmental conditions encountered along the estuarine gradient, from nearly freshwater (oligohaline; CB1, CT1) to mesohaline (CB2, CT2) to polyhaline (CB3).

COLLECTION AND N_2-FLUX ANALYSIS OF INTACT SEDIMENT CORES

Sediments were collected from upper (CT1) and lower Choptank River (CT2) stations, as well as mainstem Chesapeake Bay stations (CB1, CB2, CB3; **Figure 1**) using a box core sampling device deployed from either a small boat or a research vessel in April 2001 (Francis et al., 2003). Sediment samples collected in July 2000 from the upper Choptank River (CT1) were also analyzed in this study, to provide some basis for comparison with the other stations, because a subsample for molecular analysis from CT1 in April 2001 was not available. As reported previously (Francis et al., 2003), bottom water conditions measured at each sampling site are displayed in **Table 1**. Bottom water temperature, salinity and dissolved O_2 were determined with a Sea-Bird CTD or a YSI 600 sonde equipped with an oxygen electrode. Nutrient concentrations were determined on using an automated analyzer (Parsons et al., 1984) on samples collected from Niskin bottles (CB1, CB2, CB3) or using a diaphragm pump (CT1, CT2).

Benthic N_2-fluxes were measured in subcores collected from the box cores as described previously (Kana et al., 2006). For each site, three subcores in 6.35 cm i.d. acrylic core liners (~15 cm of sediment and 15 cm of overlying water) were submersed in an incubator bath of oxic bottom water from the core sampling

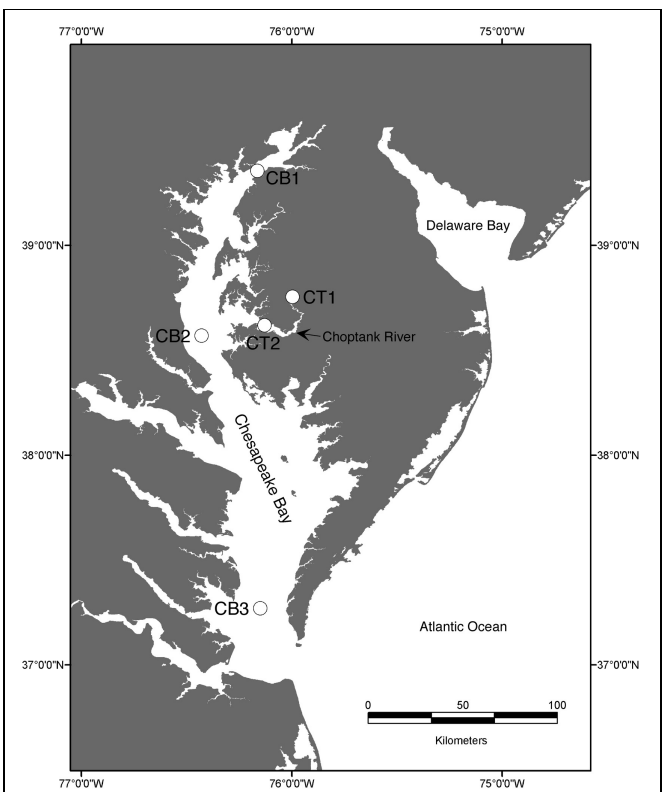

FIGURE 1 | Map of the Chesapeake Bay sampling stations.

Table 1 | Bottom water environmental parameters and N_2-flux rates for Chesapeake Bay samples analyzed in this study.

Station	Sampling date	Water depth (m)	Temp (°C)	Salinity (psu)	NH_4^+ (μM)	NO_3^- (μM)	O_2 (μM)	N_2-N flux (μmol m^{-2} h^{-1})
CT1	July 2000	5.5	27	0.3	5	44	NA	0
CT1	April 2001	5.5	7	0.0	11	188	NA	149 ± 51
CT2	April 2001	7	8	14.5	7	22	NA	101 ± 13
CB1	April 2001	10	6.7	4.4	10	83	278	172 ± 6
CB2	April 2001	17.5	7.2	18.7	7	22	247	20 ± 24
CB3	April 2001	11	8.7	23.6	4	3	306	8 ± 13

NA, Not available.

site, and held overnight with continual aeration and circulation of the overlying water with bath water. Sediment cores and a water-only control core were capped with O-ring fitted stirring tops and incubated in the dark at *in situ* (±2°C) temperatures (see **Table 1**). When samples were withdrawn at various times during the incubation, replacement bottom water was supplied through a port in the stirring top, using gravity head pressure to fill vials and syringes. Solute samples were filtered using 25 mm diameter, 0.45 μm cellulose acetate syringe filters. Water for dissolved gas analysis was collected in ∼7 ml ground glass test tubes that were filled through a small tube placed in the bottom of the vial to minimize gas exchange. Samples were preserved with 10 ml 50% saturated $HgCl_2$ and stored at near ambient bottom water temperature until analysis.

Incubations were sampled for solutes and gases four times over a time course of 4–8 h, depending on the degree of oxygen depletion. Oxygen concentrations were occasionally monitored using an oxygen electrode early in the incubation, to determine incubation time intervals such that oxygen did not fall below 50% of air saturation by the final time point.

A quadrupole mass spectrometer with a silicone membrane inlet (Kana et al., 1994, 1998) was used for the analysis of N_2 and O_2 in flux samples. The N_2:Ar ratios were corrected for any changes due to decreasing O_2 concentrations (Kana and Weiss, 2004). Nitrate was analyzed via segmented flow analysis after Cd reduction, and ammonium was manually analyzed using the phenol hypochlorite colorimetric method (Parsons et al., 1984). Benthic N_2 fluxes were calculated from the linear regression of the rate of change of N_2 concentrations. At the end of the flux measurements, the cores were subsampled using cut-off 5-cc syringes. The sediment was frozen immediately in liquid nitrogen and stored on dry ice or at −80°C until DNA extraction.

Pcr AMPLIFICATION AND CLONING OF *nirS* GENE FRAGMENTS

DNA was extracted from replicate ∼0.25 g sediment subsamples (0–0.5 cm depth interval) using the FastDNA SPIN kit for soil (MP Biomedicals), as described in Francis et al. (2003). *nirS* gene fragments (∼840–890 bp) were amplified from pooled sediment DNA extracts using the PCR primers (nirS1F and nirS6R) and conditions described by Braker et al. (1998). Products were visualized by electrophoresis in 1.2% agarose gels stained with ethidium bromide. Triplicate PCR reactions were pooled, gel-purified using the QIAquick gel extraction kit (Qiagen), and cloned into the pCR2.1 vector using the TOPO-TA cloning kit (Invitrogen). Insert-containing transformants were transferred to 96-well plates containing LB broth (with 50 μg/ml kanamycin) and grown overnight at 37°C. Clones were screened directly for the presence of inserts by PCR using T7 and M13R vector primers. Sediment DNA extracts were also screened multiple times using two different *nirK* primer sets, nirK1F/nirK5R (Braker et al., 1998) as well as Cunir3/Cunir4 (Casciotti and Ward, 2001), but no consistent amplification was observed (except for the positive control DNA templates).

SEQUENCING, RICHNESS AND PHYLOGENETIC ANALYSIS OF *nirS* SEQUENCES

Sequencing of both strands of T7/M13 PCR products was performed using ABI 310 and 3100 capillary sequencers (PE Applied Biosystems). Nucleotide sequences were assembled, edited, and aligned using Sequencher™ v.4.2 (GeneCodes Corp.), and translated using MacClade (Maddison and Maddison, 2003). Two different types of phylogenetic analysis were performed, based on nucleotide and amino acid alignments, respectively. The *nirS* nucleotide alignment (of 550 sequences) was used to define operational taxonomic units (OTUs) on the basis of DNA sequence identity. Distance matrices based on this nucleotide alignment were generated using the PAUP software package. To compare the relative *nirS* richness within each clone library, rarefaction analysis was performed. For this analysis, OTUs were defined as *nirS* sequence groups in which sequences differed by ≤5% using the furthest neighbor method in the MOTHUR program (Schloss et al., 2009).

Deduced amino acid sequences of 550 *nirS* PCR products (after removal of the primer sequences) from the Chesapeake Bay were aligned with representative database sequences (as of July 2012) using ClustalX (Thompson et al., 1997), edited in MacClade, and subjected to phylogenetic analysis. A total of 280 amino acid positions were used in the phylogenetic analysis (shorter database sequences were not included). Neighbor-joining and parsimony trees were constructed based on amino acid alignments using the PAUP software package. Bootstrap analysis was used to estimate the reliability of phylogenetic reconstructions (1000 replicates).

STATISTICAL ANALYSES

Correlation analysis of environmental variables (e.g., NH_4^+, NO_3^-, and salinity) was performed in JMP (SAS Institute, 2002). Extrapolated richness [Abundance-based Coverage Estimators (ACE) and Chao1] and classical diversity (Shannon and

Simpson's index) estimates were computed using MOTHUR (Schloss et al., 2009). PC-ORD software version 4.01 (McCune and Medford, 1999) was used for multivariate analyses of OTU and environmental data. OTU data were normalized for each site by dividing the number of clones per OTU by the total number of clones sequenced from the site. Environmental data were normalized by dividing the value for each variable at each site by the maximum observed value across sites. Cluster analyses (McCune and Grace, 2002), based on Sorenson distances, were performed for both OTU and environmental matrices. A Mantel Test (Smouse et al., 1986) was used to compare the significance of the observed cluster structure to the structure determined from 1000 randomizations of the matrices.

NUCLEOTIDE SEQUENCE ACCESSION NUMBERS

The GenBank accession numbers of the *nirS* sequences from cultivated denitrifiers and environmental clones used for comparison are displayed in **Figure 2**. The 550 *nirS* sequences reported in this study have been deposited in GenBank under accession numbers DQ675693 to DQ676242.

RESULTS AND DISCUSSION

ENVIRONMENTAL GRADIENTS ALONG THE ESTUARY

The five Chesapeake Bay stations have been described previously in general terms (Francis et al., 2003) and the specific bottom water conditions at the time of sampling for this study are detailed in **Table 1**. Along the longitudinal transect from the North Bay (CB1) to South Bay (CB3) station in April 2001 (**Figure 1**), the salinity increased from 4.4 to 23.6 psu (**Table 1**). While NH_4^+ concentration decreased gradually from 10 to 4 μM, concentrations of NO_3^-—the primary electron acceptor for denitrification and generally an indicator of agricultural or urban runoff in estuarine systems—exhibited a much steeper gradient along this same transect, decreasing from 83 to 3 μM. Similar opposing gradients of salinity and inorganic nitrogen were observed from the oligohaline upper station of the Choptank River (CT1) to the mesohaline lower Choptank station (CT2) (**Table 1**). The overall physical/chemical conditions at the two mesohaline stations, CT2 and CB2, were quite similar, with identical levels of NO_3^- and NH_4^+ and salinities of 14.5 and 18.7 respectively. Key differences between the environmental conditions at CT1 in July 2000 and April 2001 were temperature (27°C and 7°C, respectively) and NO_3^- concentration (44 μM and 188 μM, respectively). Oxic conditions were present in the bottom waters of all stations at the time of sediment sampling. Nitrate concentration and salinity were negatively correlated (Spearman $\rho = -0.93$; $p = 0.008$). Cluster analysis of the sites based on normalized values of salinity, nitrate, and ammonium resulted in the formation of two distinct groups (**Figure 3**). The first group was comprised of CB1 and CT1 and the second group comprised of CB2, CT2, and CB3. The two most similar sites were CB2 and CT2.

BENTHIC N_2 FLUXES

The N_2-fluxes measured in sediment cores collected from five stations in April 2001 were negatively correlated to salinity (Spearman $\rho = -0.90$; $p = 0.037$), ranging from a high of 172 μmol N $m^{-2}h^{-1}$ at CB1 to a low of 8 μmol N $m^{-2}h^{-1}$ at CB3 (**Table 1**). Although this trend also generally paralleled the nitrate gradient along the Bay, the benthic N_2-fluxes at the two mesohaline sites were quite different (CT2 rates were 5-fold greater than at CB2), despite identical (22 μM) bottom water nitrate concentrations. This difference could be due to greater coupling to nitrification at CT2, where the sediments do not experience seasonal anoxia. In contrast, the sediments at the much deeper CB2 station (18-m vs. 7-m depth at CT2) are exposed to seasonally anoxic conditions and have higher levels of pore water hydrogen sulfide (Cornwell and Sampou, 1995), which can inhibit both nitrification and denitrification (Joye and Hollibaugh, 1995). Interestingly, benthic N_2-fluxes were undetectable at the upper Choptank River station, CT1, during July 2000, but were quite high in April 2001 (**Table 1**). These spatial differences, plus seasonal differences illustrated by a wide range of rates at a single site (CT1), highlight the extensive variability often associated with microbial nitrogen transformations in estuarine systems (Cowan and Boynton, 1996; Boynton and Kemp, 2008). The benthic N_2 fluxes reported here represent the sum of both conventional denitrification and anammox. However, anammox has been shown to account for only 10-20% of the total benthic N_2 flux at stations CB1, CT1, and CT2, (Rich et al., 2008), and was undetectable at the low-nitrate station CB3. These findings are consistent with previous studies of anammox in other estuarine systems (Risgaard-Petersen et al., 2004; Trimmer et al., 2005), and suggest that denitrification is the dominant N-removal process within Chesapeake Bay sediments.

ANALYSIS OF *nirS* RICHNESS IN CHESAPEAKE BAY SEDIMENTS

PCR amplification of *nirS* gene fragments was obtained from sediment DNA extracts from all five stations. Clone libraries were subsequently generated for each station, and 96 to 123 clones per library were completely sequenced (~840–890 bp), resulting in an overall database of 550 *nirS* sequences from the Chesapeake Bay estuary. This represents the most extensive clone library-based sequencing effort, to date, of *nirS* sequences from any system, let alone an estuary. Since *nirK* could not be reliably amplified (i.e., PCR results ranged from faint, non-specific, or multiple bands to no amplification) from all five of these sediment DNA extracts using several primer combinations (Braker et al., 1998; Casciotti and Ward, 2001), and *nirK* has been shown to be far less abundant than *nirS* in other estuarine systems (Abell et al., 2010; Mosier and Francis, 2010), we focused our efforts here on *nirS* diversity.

To compare the relative *nirS*-based denitrifier richness between stations, rarefaction analysis was performed on the *nirS* sequences from using a 5% cutoff at the DNA level to define an OTU (**Figure 4**). Rarefaction analysis indicated the greatest *nirS* richness in the low-salinity upper Choptank River (CT1) and North Bay (CB1) libraries, and the lack of significant curvature after >95 clones suggests that that the diversity of distinct *nirS* sequences is not yet saturated in these two libraries. By far the lowest richness was observed in the South Bay (CB3) library, while intermediate levels were observed at the two mesohaline stations, CT2 and CB2. Overall, the rarefaction curves illustrate a rather striking

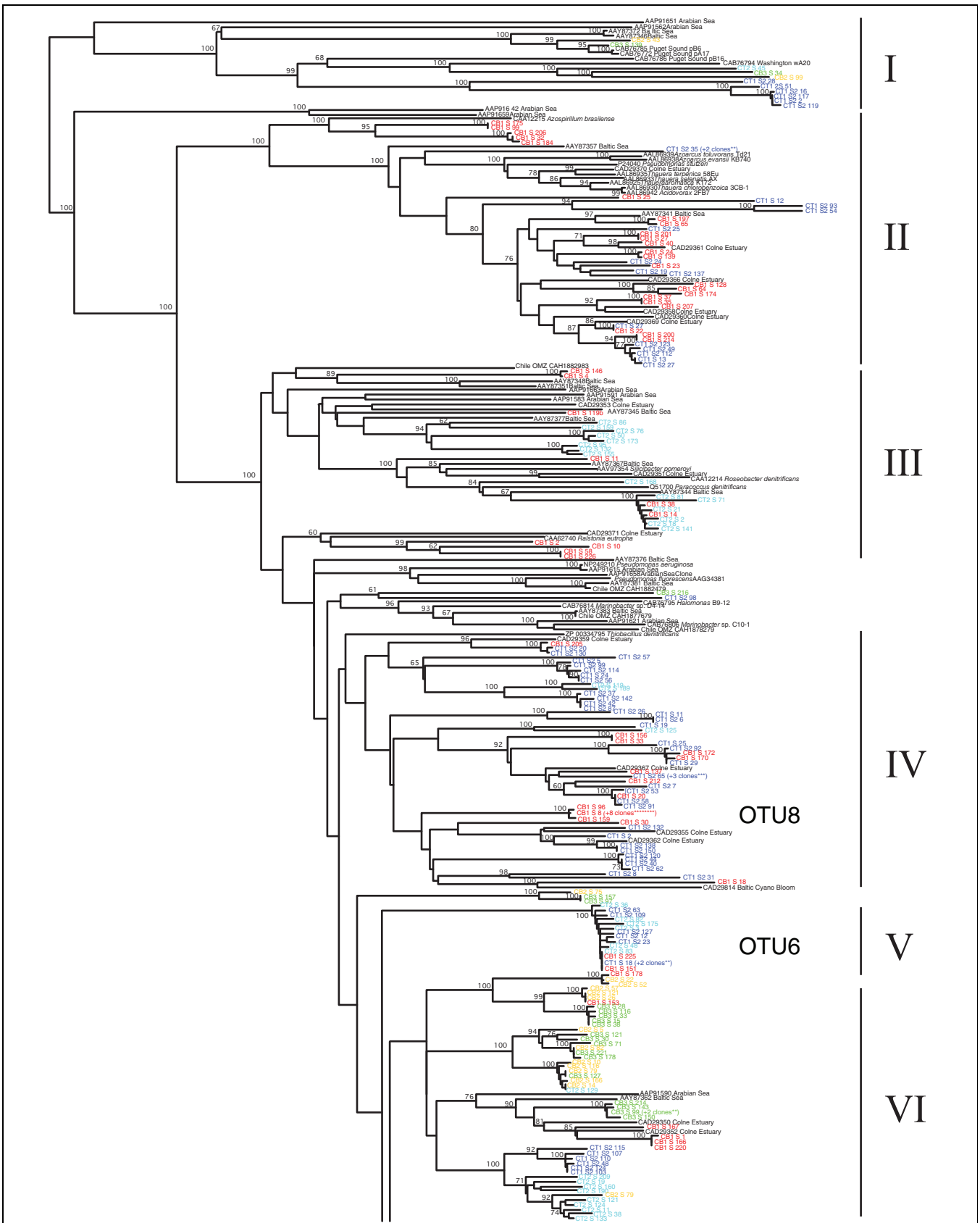

FIGURE 2 | Continued

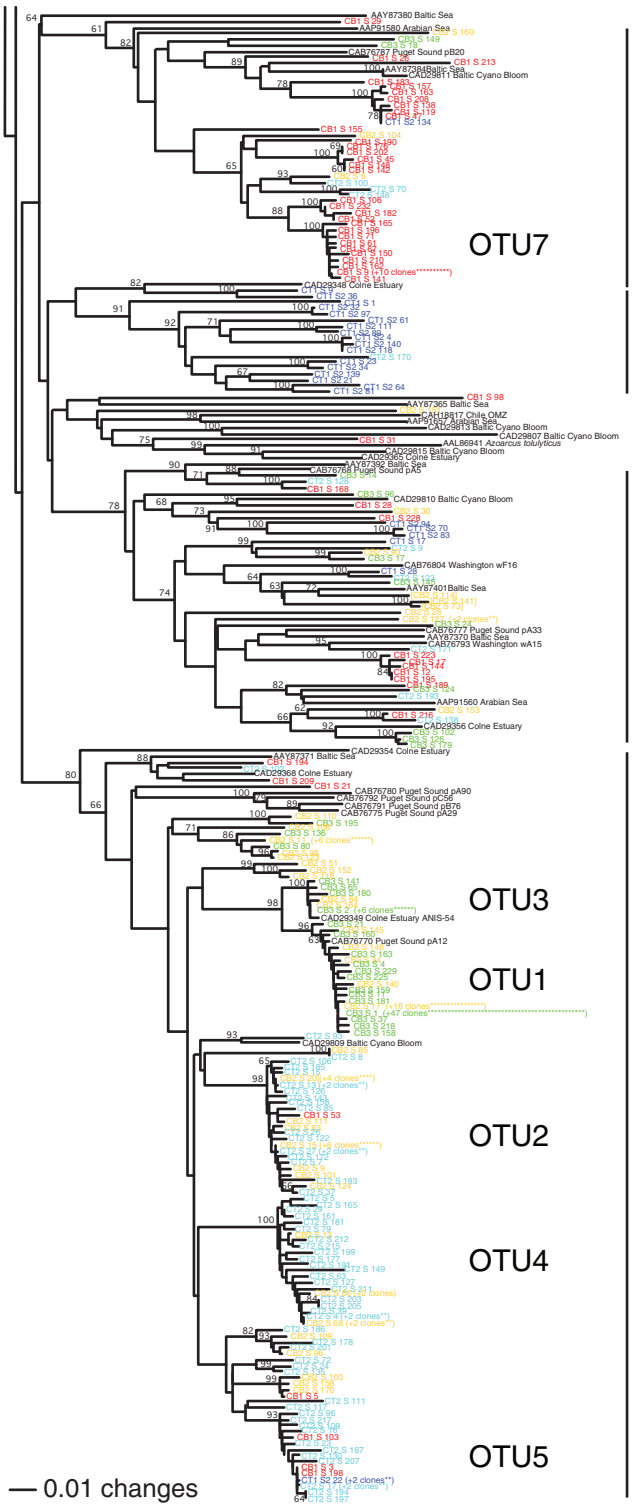

FIGURE 2 | Neighbor-joining phylogenetic tree of deduced NirS amino acid sequences (280 positions considered) from Chesapeake Bay sediments. Bootstrap values (≥60%) are shown at the branch points. Sequences from the present study are shown in color by station (CB1, red; CB2, yellow; CB3, green; CT1, blue; CT2, aqua). Database sequences are shown in black along with the corresponding GenBank accession numbers. The number of clones identical at the amino acid level is indicated in parentheses (only for those sequences occurring >2 times within a clone library). Roman numerals refer to the ten clusters discussed in the text, all of which were also present in the parsimony tree (not shown). Clusters of NirS sequences corresponding to the 8 major nucleotide-based OTUs (defined according to 5% nucleotide sequence difference using the farthest neighbor method) are also indicated.

trend among these sites spanning the estuarine salinity gradient, in which *nirS* richness decreased as salinity increased along the estuary (**Figure 4** and **Table 2**). This trend is consistent with a previous study reporting that *nirS* diversity was inversely correlated with salinity in a wastewater treatment plant (Yoshie et al., 2004).

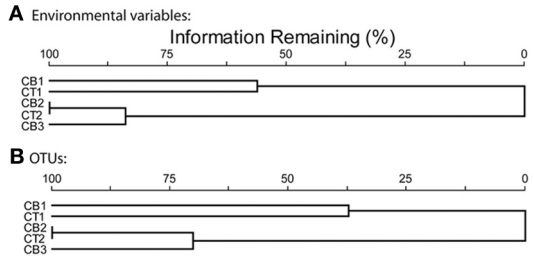

FIGURE 3 | Cluster analyses of five Chesapeake Bay sites based on relativized data using Sorenson distances. (A) ammonium, nitrate and salinity data, **(B)** OTU distribution data, defined according to 5% nucleotide sequence difference using the farthest neighbor method.

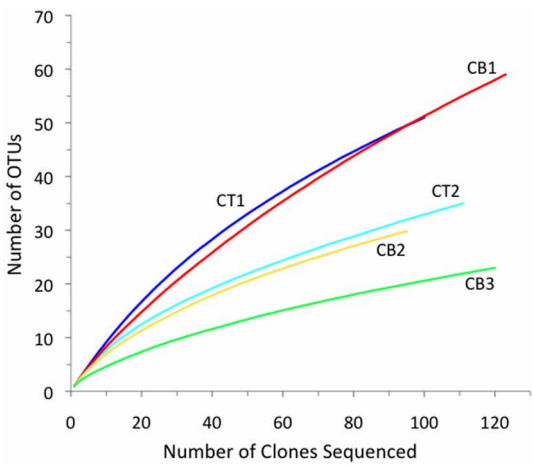

FIGURE 4 | Rarefaction curves displaying observed OTU richness versus the number of *nirS* clones sequenced from each of five Chesapeake Bay sediment samples. OTUs were defined according to 5% nucleotide sequence difference using the furthest neighbor method.

Interestingly, no clear trends in *nirS* richness across estuarine salinity gradients were observed in Huntington Beach (Santoro et al., 2006) or San Francisco Bay (SFB; Mosier and Francis, 2010); however, both *nirS* abundance and denitrification potential activity were correlated with salinity in SFB, further highlighting the significance of this environmental factor in large North American estuaries.

The freshwater/oligohaline stations (CT1 and CB1) had the greatest total number of OTUs that were found exclusively at one site (**Table 2**). Interestingly, using the same OTU definition (5% cutoff), betaproteobacterial *amoA* richness was also greatest in the North Bay (CB1) but the lowest and essentially identical levels of richness were detected at the two mesohaline stations, CT2 and CB2, and intermediate levels at CT1 and CB3 (Francis et al., 2003). Thus, the relative richness/diversity of denitrifying and AO communities (based on functional genes) may be influenced differently by physical/chemical parameters, such as salinity and oxygen. It is clear that salinity has a direct, if imperfectly understood, effect on ammonia oxidizer diversity and activity (De Bie et al., 2001; Caffrey et al., 2003; Francis et al., 2003; Bernhard et al., 2005, 2007; Ward et al., 2007; Mosier and Francis, 2008); however, it is worth noting that some studies have found other factors (e.g., pH) to be important in structuring estuarine AO communities (Dang et al., 2010). Nitrate, which covaries with salinity in this system, and organic matter flux may be more important for denitrifiers. Given the limited number of samples (5) in this study, we are not able to untangle the potentially complex influence of these factors with our data; nevertheless, the pattern of changing *nirS* diversity along the salinity gradient is striking.

Although rarefaction analysis is useful for comparing the relative observed richness among clone libraries, it is not intended to predict the actual community richness (i.e., total number of OTUs) within the original samples (Hughes et al., 2001). Therefore, we also utilized several non-parametric richness estimators and diversity indices to analyze the *nirS* clone library data (**Table 2**). The extrapolated richness estimates (Chao1 and ACE) were generally much higher (∼2–3-fold) than the observed richness within a given library. For example, the total number of observed *nirS* OTUs within our dataset (172 OTUs) represented only 37 to 48% of the number of OTUs predicted by ACE and Chao1, respectively. Overall, the predicted *nirS* richness values basically exhibited the same trend from high to low richness

Table 2 | Richness and diversity statistics for *nirS* clone libraries from five Chesapeake Bay sediment samples.

Station	No. of clones	No. of OTUs	Unique OTUs*	ACE†	Chao1†	Shannon	Simpson's
CT1	100	51	44	97	95	3.69	0.02
CT2	111	35	25	126	88	2.98	0.07
CB1	123	59	45	139	116	3.54	0.05
CB2	96	30	18	82	57	2.75	0.10
CB3	120	23	17	80	46	1.79	0.35
Combined	550	172		468	360	4.24	0.04

†*ACE and Chao1 are non-parametric estimators which predict the total number of OTUs in the original sample.*

**OTUs detected in only 1 of the 5 Chesapeake Bay sediment samples.*

along the estuarine gradient that was revealed through rarefaction analysis. The classical ecological diversity indices (Shannon and Simpson's) also supported this trend.

ANALYSIS OF OTU DISTRIBUTIONS

The number of OTUs shared between sites represents one measure of site similarity (**Table 3**). CT1 and CB1 had the greatest number of site-specific OTUs, while CB2 and CB3 had the greatest degree of overlap in OTU occurrence. A second measure of site similarity is the frequency of shared OTUs among sites. OTUs representing a large portion of the sequenced clones (i.e., the most abundant sequences within the clone libraries) have a large impact on this second measure of site similarity. Eight of the 172 *nirS* OTUs detected in the Chesapeake Bay accounted for 232 (42%) of the total sequences (**Figure 5**). Of these eight abundant OTUs, only two were unique to a particular site (OTUs 7 and 8 from CB1), while the remaining six each included sequences from two or more sites, as well as sequences from a mesohaline site. All 8 major OTUs corresponded to distinct phylogenetic clusters in the NirS amino acid tree in **Figure 2**. OTU1 contained the greatest number of sequences, including 71 CB3 and 20 CB2 sequences (**Figure 5**). The other 164 OTUs were mostly rare, 101 of which were represented by only a single *nirS* sequence (i.e., singletons).

In order to quantify the distribution of OTUs across sites, including information from both the number of shared OTUs and the relative frequency of OTUs, a cluster analysis based on normalized OTU distribution was performed. This analysis revealed the same two station groups that had been identified in the cluster analysis of environmental data above (**Figure 3**). The first group was comprised of CB1 and CT1 and the second group contained CB2, CT2, and CB3 (**Figure 3**). The mesohaline sites, CB2 and CT2, were most similar in terms of both OTUs and environmental characteristics. A Mantel test indicated that the correspondence of OTU distribution and environmental variables was significant ($p = 0.006$). The observed clustering of environmental variables and sampling sites suggests a relationship between environmental factors and OTU distribution. However, the rather limited number of samples (5) ultimately limits our statistical power to definitively determine the impact of particular factors on the distribution of *nirS*-type denitrifier populations. While it is not always feasible (or desirable) to generate massive PCR clone libraries for the extensive number of samples necessary to perform more robust statistical approaches (e.g., non-metric multidimensional scaling), the extensive *nirS* dataset described in this study allowed the development of a microarray (Bulow et al., 2008) that can now be used to easily screen a much larger number of samples (e.g., Jayakumar et al., in press).

Table 3 | Shared *nirS* OTUs from five Chesapeake Bay sediment samples.

Station	No. of OTUs shared with site:				
	CT1	CT2	CB1	CB2	CB3
CT1	–	2	7	0	0
CT2		–	6	5	1
CB1			–	4	0
CB2				–	6
CB3					–

PHYLOGENETIC ANALYSIS OF CHESAPEAKE BAY *nirS* SEQUENCES

In addition to comparing the relative richness and OTU distribution of *nirS* sequences, we examined the phylogenetic relationships of these sequences (**Figure 2**). The deduced amino acid sequences of the 550 *nirS* clones from Chesapeake Bay sediments showed only 35–85% identity to sequences of cultivated denitrifying strains. Instead, the majority of the sequences fell into phylogenetic clusters comprised primarily of Chesapeake Bay sequences and, in some cases, closely related marine and estuarine environmental clones (**Figure 2**).

For the purposes of this discussion, we have grouped the sequences into 10 broadly defined clusters/regions of the tree. As suggested by the extensive richness of *nirS* OTUs associated with the two oligohaline stations, CT1 and CB1, the sequences from these sites were distributed among numerous branches throughout the tree (**Figure 2**). However, even the less abundant sequences and OTUs exhibited substantial overlap between CB1 and CT1, as might be expected from the similarity in physical/chemical characteristics of CB1 and CT1. In fact, many sequences from these stations fell into similar regions or clusters of the phylogenetic tree, including two large clusters (II and IV) in the upper region of the tree (**Figure 2**) comprised almost exclusively of CT1 and CB1 sequences. Interestingly, all but one of the mRNA *nirS* clones recovered from the low-salinity, hyper-nutrified (1 mM nitrate) Hythe site, located at the head of the River Colne estuary (Nogales et al., 2002), also fell into these clusters, several of which were >95% identical to these Chesapeake sequences. The similar salinity regimes at these two geographically-distinct upper estuarine sites, despite considerably higher nitrate concentrations in the Colne estuary, support the importance of salinity (or an environmental factor that co-varies

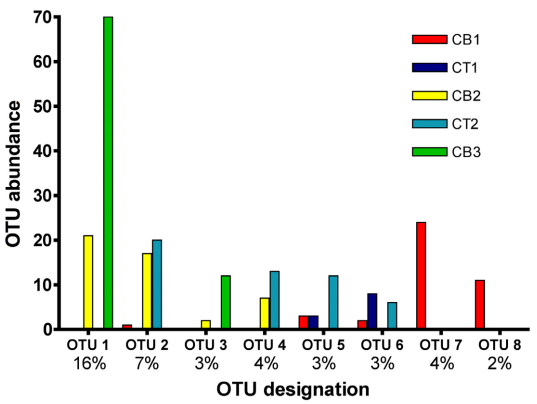

FIGURE 5 | Histogram of the eight most common OTUs from the five Chesapeake Bay *nirS* clone libraries. OTUs were considered common if the total abundance of an OTU was ≥2% of the total number of *nirS* clones analyzed (550). The x-axis lists the OTU designation (8 of 172 OTUs are displayed), as well as the percentage of total sequences that each OTU comprises.

with salinity) as a key determinant in structuring denitrifying communities. Furthermore, the *nirS* sequences in Clusters II and IV apparently correspond to "low-salinity" groups of estuarine denitrifiers.

In addition to the "low-salinity" sequence types, the remaining CT1 and CB1 sequences were dispersed throughout the tree, either in discrete site-specific clusters or within clusters of sequences from other CB sites, possibly corresponding to denitrifiers that have a wide salinity tolerance. In addition to those CT1 and CB1 sequences that fell broadly into similar clusters, 13-19% of the sequences in each library were essentially identical (>99% amino acid identity) to sequences from the other site. In the absence of clone library analysis from CT1 in April 2001, comparisons between CB1 and CT1 unavoidably combine temporal and spatial variation. Even less overlap was observed in the *amoA* sequence types recovered from these two sites (Francis et al., 2003), perhaps reflecting differences in how salinity influences the composition of AO and denitrifying communities. Despite similar conditions, these upper bay and river sites experience quite different allochthonous inputs (urban vs. agricultural, respectively), which likely include microbes as well as nutrients, and these factors may interact with the physiological response to salinity.

While only three CT2 sequences fell into the two "low-salinity" clusters (II and IV), more than half (59 of 111 sequences) of the CT2 sequences fell into three distinct but closely related subclusters within cluster X (corresponding largely to OTU2, 4, and 5 from **Figure 5**). Cluster X contains a small number of CT1 and CB1 sequences, but is clearly dominated by sequences from mesohaline and polyhaline sites. Interestingly, there was considerable overlap between sequences from CT2 and CB2, as well as CB2 and CB3, but virtually no overlap between CT2 and CB3 (**Figure 2**) (also demonstrated in **Figure 5** and **Table 3**).

The mesohaline CB2 station represents the transition zone between the North and South Bay sites, as well as the junction between the mainstem of the Bay and the Choptank River. Like the transition from CT1 to CT2, a shift in both denitrifier richness (**Figure 4** and **Table 2**) and community composition (**Figure 2**) occurred between CB1 and CB2. Although the "true" (e.g., 16S rRNA-based) phylogenetic affiliations of denitrifiers cannot usually be determined based on *nirS* functional gene sequences alone, it is tempting to speculate that the shift in *nirS* sequence types from CB1 to CB2 in part reflects a major overall compositional shift in the sedimentary microbial communities between the oligohaline stations and mesohaline stations. Indeed, the transition from oligohaline to mesohaline conditions in estuarine systems is often accompanied by dramatic shifts in microbial community structure (De Bie et al., 2001), and the Chesapeake Bay estuary is no exception. Using 16S rRNA probes to enumerate the main groups of *Proteobacteria* by fluorescence *in situ* hybridization (FISH), Bouvier and del Giorgio (2002) found consistent community shifts between the upper and lower Choptank River (CT) regions. *Betaproteobacteria* were abundant in the freshwater stations, but were rare in the lower river and the opposite pattern was observed for *Alphaproteobacteria*. The switch occurred at approximately the location of our station CT2, suggesting that a shift in the community structure of proteobacterial denitrifiers might also be expected between the two river stations, CT1 and CT2 (Taroncher-Oldenburg et al., 2003), and possibly CB1 and CB2.

Perhaps the most striking feature of the phylogenetic tree (**Figure 2**) is the large cluster of 83 closely-related CB3 sequences (and 23 CB2 sequences) within cluster X (corresponding to OTU1 and OTU3 in **Figure 5**), which share 95–100% amino acid identity to sequences of RT-PCR and PCR clones recovered from meso- to poly-haline sites within the River Colne estuary (Nogales et al., 2002) and Puget Sound (Braker et al., 2000), respectively. Within the OTU1 subcluster, 47 CB3 clones (represented by CB3-S-1) and 17 CB2 clones (represented by CB2-S-17) were 100% identical. Interestingly, these sequences also shared >99% identity with mRNA clones obtained from Narragansett Bay sediment mesocosms (Fulweiler et al., 2013). The remarkable similarity between these dominant mid- and South Chesapeake Bay sequences and sequences from multiple geographically-distinct estuaries suggests that these *nirS* genotypes may be ubiquitous in mesohaline to polyhaline (15–30 psu) sedimentary environments. Furthermore, using a *nirS* microarray, developed using sequences from this study, Bulow et al. (2008) demonstrated that sequences corresponding to the dominant CB3 *nirS* genotypes (OTU1) as well as the major CT2/CB2 sequence type (OTU2) within Cluster X were the most abundant (DNA) *and* most actively expressed (mRNA) within both CB2 and CB3 sediments. It is worth highlighting that 5 of the 8 most abundant nucleotide-based OTUs identified in the present study (**Figure 5**) correspond to well-defined clusters of NirS amino acid sequences within Cluster X (**Figure 2**), all of which are distinct from known cultivated denitrifiers. The microarray format used by Bulow et al. (2008) is capable of distinguishing *nirS* sequences that differ by 13–15% sequence identity (Taroncher-Oldenburg et al., 2003). Thus it is likely that 70-mer probes based on OTU1 and OTU2 sequences (defined based on a 5% identity cutoff) would collectively detect sequences corresponding to all 5 major OTUs within Cluster X. The microarray results verify that not only are these Cluster X sequences most abundant in Chesapeake Bay, but they also represent the most active groups.

Although the vast majority of sequences from the Chesapeake Bay were either site-specific or clustered with sequences from sites with similar physical/chemical characteristics, 5–10% of the cloned sequences from all five sites fell into one large well-supported phylogenetic cluster (IX). This cluster also included 10 clones from a number of different environments, including sediments from the River Colne estuary, Puget Sound, and Washington continental margin, as well as water column depths within the Baltic Sea and the coastal Arabian Sea oxygen minimum zone. The only cultivated member of this cluster is *Azoarcus tolulyticus*, a nitrogen-fixing betaproteobacterium that can degrade toluene under denitrifying conditions (Zhou et al., 1995; Song and Ward, 2002). This cluster is thus not only widely distributed geographically, but also among several different kinds of estuarine and marine environments.

The most divergent nitrite reductase sequences obtained in this study, sharing only 35–40% amino acid identity with the nearest cultivated denitrifier sequence, fell into Cluster I along with related sequences from several other marine and

sedimentary environments. These distinct sequences represented 2% of the total 550 *nirS* sequences in this study, comprising 6% of the CT1 clones, and 1–2% of three other libraries, but were not found in the CB1 library. Although Cluster I sequences are quite distinct from most known NirS sequences, there appears to be conservation of key amino acid residues known to be critical for function. For example, Histidine 352 (*P. aeruginosa* numbering), which serves as a heme-d_1 ligand in the active site of cytochrome-cd_1 nitrite reductase enzymes, was conserved among Cluster I and all other sequences in this study.

CONCLUSIONS

This study has revealed extensive and unprecedented *nirS* diversity within Chesapeake Bay estuarine sediments, with the vast majority of 550 sequences falling into numerous novel phylogenetic clusters, lineages, and OTUs, many of which may represent estuarine-specific sequence types. Both the benthic N_2 fluxes and *nirS* gene sequences were non-randomly distributed in relation to the physical/chemical parameters observed across the five estuarine sites. While salinity was most obviously related to the benthic N_2 fluxes and observed diversity patterns, covariation of key parameters and the limited number of sampling sites makes it difficult to definitively determine the importance of individual environmental factors in this study. A clear shift in *nirS* phylogeny and richness occurred between the freshwater and mesohaline stations, where the steepest environmental gradients were also observed. In contrast, the transition from the mesohaline mid-Bay station to the polyhaline South Bay station was less pronounced, with considerable overlap observed in *nirS* sequence types and fairly comparable richness. Sequences were not evenly distributed among the stations, however, and some dominant *nirS* genotypes (within clone libraries) were identified, especially at CB3, the most "marine" site. The eight most abundant OTUs accounted for 42% of the total sequences, consistent with the idea that *nirS*-type denitrifiers exhibit a typical "species" abundance curve, with a few very common types and many rare ones. The dominant *nirS* genotypes identified here are not obviously affiliated with known denitrifying strains, which implies that we know very little about a group of organisms that are numerically-dominant (and active in gene expression) in this system and ubiquitous in estuarine systems in general. Recent advances in high-throughput sequencing technology will undoubtedly allow future studies to more thoroughly survey the diversity of *nirS* sequences, and microarray technologies will allow a larger number of samples to be investigated so that interactions with complex environmental factors can be better understood. However, further cultivation and/or metagenomic investigations will ultimately be required to determine the phylogenetic and physiological nature of these estuarine denitrifier groups.

ACKNOWLEDGMENTS

This research was supported in part by an NSF Biocomplexity research grant to Bess B. Ward. (OCE-9981482) and an NSF Postdoctoral Research Fellowship in Microbial Biology to Christopher A. Francis (DBI-0102106). We thank Jeff Alexander, Mike Owens, and Lora Pride for field and laboratory assistance.

REFERENCES

Abell, G. C. J., Revill, A. T., Smith, C., Bissett, A. P., Volkman, J. K., and Robert, S. S. (2010). Archaeal ammonia oxidizers and *nirS*-type denitrifiers dominate sediment nitrifying and denitrifying populations in a subtropical macrotidal estuary. *ISME J.* 4, 286–300. doi: 10.1038/ismej.2009.105

Bernhard, A. E., Donn, T., Giblin, A. E., and Stahl, D. A. (2005). Loss of diversity of ammonia-oxidizing bacteria correlates with increasing salinity in an estuary system. *Environ. Microbiol.* 7, 1289–1297. doi: 10.1111/j.1462-2920.2005.00808.x

Bernhard, A. E., Tucker, J., Giblin, A. E., and Stahl, D. A. (2007). Functionally distinct communities of ammonia-oxidizing bacteria along an estuarine salinity gradient. *Environ. Microbiol.* 9, 1439–1447. doi: 10.1111/j.1462-2920.2007.01260.x

Bouvier, T. C., and del Giorgio, P. A. (2002). Compositional changes in free-living bacterial communities along a salinity gradient in two temperate estuaries. *Limnol. Oceanogr.* 47, 453–470. doi: 10.4319/lo.2002.47.2.0453

Boynton, W. R., and Kemp, M. (2008). "Estuaries," in *Nitrogen in the Marine Environment, 2nd Edn.*, eds D. G. Capone, D. A. Bronk, M. R. Mullholland, and E. J. Carpenter (New York, NY: Academic Press), 809–866.

Braker, G., Ayala-del-Rio, H. L., Devol, A. H., Fesefeldt, A., and Tiedje, J. M. (2001). Community structure of denitrifiers, Bacteria, and Archaea along redox gradients in Pacific Northwest marine sediments by terminal restriction fragment length polymorphism analysis of amplified nitrite reductase (*nirS*) and 16S rRNA genes. *Appl. Environ. Microbiol.* 67, 1893–1901. doi: 10.1128/AEM.67.4.1893-1901.2001

Braker, G., Fesefeldt, A., and Witzel, K. P. (1998). Development of PCR primer systems for amplification of nitrite reductase genes (*nirK* and *nirS*) to detect denitrifying bacteria in environmental samples. *Appl. Environ. Microbiol.* 64, 3769–3775.

Braker, G., Zhou, J., Wu, L., Devol, A. H., and Tiedje, J. M. (2000). Nitrite reductase genes (*nirK* and *nirS*) as functional markers to investigate diversity of denitrifying bacteria in Pacific Northwest marine sediment communities. *Appl. Environ. Microbiol.* 66, 2096–2104. doi: 10.1128/AEM.66.5.2096-2104.2000

Bulow, S. E., Francis, C. A., Jackson, G. A., and Ward, B. B. (2008). Sediment denitrifier community composition and *nirS* gene expression investigated with functional gene microarrays. *Environ. Microbiol.* 10, 3057–3069. doi: 10.1111/j.1462-2920.2008.01765.x

Caffrey, J. M., Harrington, N., Solem, I., and Ward, B. B. (2003). Biogeochemical processes in a small California estuary. 2. Nitrification activity, community structure and role in nitrogen budgets. *Mar. Ecol. Prog. Ser.* 248, 27–40. doi: 10.3354/meps248027

Casciotti, K. L., and Ward, B. B. (2001). Dissimilatory nitrite reductase genes from autotrophic ammonia-oxidizing bacteria. *Appl. Environ. Microbiol.* 67, 2213–2221. doi: 10.1128/AEM.67.5.2213-2221.2001

Castro-González, M., Braker, G., Farías, L., and Ulloa, O. (2005). Communities of *nirS*-type denitrifiers in the water column of the oxygen minimum zone in the eastern South Pacific. *Environ. Microbiol.* 7, 1298–1306. doi: 10.1111/j.1462-2920.2005.00809.x

Christensen, J. P., Smethie W. M. Jr., and Devol, A. H. (1987). Benthic nutrient regeneration and denitrification on the Washington continental shelf. *Deep-Sea Res.* 34, 1027–1047. doi: 10.1016/0198-0149(87)90051-3

Cornwell, J. C., Kemp, W. M., and Kana, T. M. (1999). Denitrification in coastal ecosystems: methods, environmental controls, and ecosystem level controls, a review. *Aquat. Ecol.* 33, 41–54. doi: 10.1023/A:1009921414151

Cornwell, J. C., and Sampou, P. A. (1995). "Environmental controls on iron sulfide mineral formation in a coastal plain estuary," in *Geochemical Transformations of Sedimentary Sulfur*, eds M. A. Vairavamurthy, and M. A. A. Schoonen (Washington, DC: American Chemical Society), 224–242. doi: 10.1021/bk-1995-0612.ch012

Cowan, J. L. W., and Boynton, W. R. (1996). Sediment-water oxygen and nutrient exchanges along the longitudinal axis of Chesapeake Bay: seasonal patterns controlling factors and ecological significance. *Estuaries* 19, 562–580. doi: 10.2307/1352518

Dalsgaard, T., Canfield, D. E., Petersen, J., Thamdrup, B., and Cuna-Gonzalez, J. (2003). N2 production by the anammox reaction in the anoxic water column of Golfo Dulce, Costa Rica. *Nature* 422, 606–608. doi: 10.1038/nature01526

Dang, H., Li, J., Chen, R., Wang, L., Guo, L., Zhang, Z., et al. (2010). Diversity, abundance, and spatial distribution of sediment ammonia-oxidizing betaproteobacteria in response to environmental gradients and coastal eutrophication in Jiaozhou Bay, China. *Appl. Environ. Microbiol.* 76, 4691–4702. doi: 10.1128/AEM.02563-09

Dang, H. Y., Wang, C. Y., Li, J., Li, T. G., Tian, F., Jin, W., et al. (2009). Diversity and distribution of sediment *NirS*-encoding bacterial assemblages in response to environmental gradients in the eutrophied Jiaozhou Bay, China. *Microb. Ecol.* 58, 161–169. doi: 10.1007/s00248-008-9469-5

De Bie, M. J., Speksnijder, A. G., Kowalchuk, G. A., Schuurman, T., Zwart, G., Stephen, J. R., et al. (2001). Shifts in the dominant populations of ammonia-oxidizing ß-subclass *Proteobacteria* along the eutrophic Shelde estuary. *Aquat. Microb. Ecol.* 23, 225–236. doi: 10.3354/ame023225

Devol, A. H. (2008). "Denitrification including anammox," in *Nitrogen in the Marine Environment, 2nd Edn.*, eds D. G. Capone, D. A. Bronk, M. R. Mullholland, and E. J. Carpenter (New York, NY: Academic Press), 263–302.

Francis, C. A., Beman, J. M., and Kuypers, M. M. M. (2007). New processes and players in the nitrogen cycle: the microbial ecology of anaerobic and archaeal ammonia oxidation. *ISME J.* 1, 19–27. doi: 10.1038/ismej.2007.8

Francis, C. A., O'Mullan, G. D., and Ward, B. B. (2003). Diversity of *amoA* ammonia monooxygenase genes across environmental gradients in Chesapeake Bay sediments. *Geobiology* 1, 129–140. doi: 10.1046/j.1472-4669.2003.00010.x

Fulweiler, R. W., Brown, S. M., Nixon, S. W., and Jenkins, B. D. (2013). Evidence and a conceptual model for the co-occurrence of nitrogen fixation and denitrification in heterotrophic marine sediments. *Mar. Ecol. Prog. Ser.* 482, 57–68. doi: 10.3354/meps10240

Hannig, M., Braker, G., Dippner, J., and Jurgens, K. (2006). Linking denitrifier community structure and prevalent biogeochemical parameters in the pelagial of the central Baltic Proper (Baltic Sea). *FEMS Microbiol. Ecol.* 57, 260–271. doi: 10.1111/j.1574-6941.2006.00116.x

Hughes, J. B., Hellmann, J. J., Rocketts, T. H., and Bohannan, B. J. M. (2001). Counting the uncountable: statistical approaches to estimating microbial diversity. *Appl. Environ. Microbiol.* 67, 4399–4406. doi: 10.1128/AEM.67.10.4399-4406.2001

Jayakumar, D. A., Francis, C. A., Naqvi, S. W. A., and Ward, B. B. (2004). Diversity of nitrite reductase genes (*nirS*) in the denitrifying water column of the coastal Arabian Sea. *Aquat. Microb. Ecol.* 34, 69–78. doi: 10.3354/ame034069

Jayakumar, D. A., Naqvi, S. W. A., and Ward, B. B. (2009). "Distribution and relative quantification of key genes involved in fixed nitrogen loss from the Arabian Sea oxygen minimum zone," in *Indian Ocean Biogeochemical Processes and Ecological Variability*, eds J. D. Wiggert, and R. R. Hood (Washington, DC: American Geophysical Union), 187–203. doi: 10.1029/2008GM000730

Jayakumar, A., Peng, X., and Ward, B. B. (in press). Community composition of bacteria involved in fixed nitrogen loss in the water column of two major oxygen minimum zones in the ocean. *Aqua. Microb. Ecol.* doi: 10.3354/ame01654

Jensen, K., Revsbech, N. P., and Nielsen, L. P. (1993). Microscale distribution of nitrification activity in sediment determined with a shielded microsensor for nitrate. *Appl. Environ. Microbiol.* 59, 3287–3296.

Jensen, K., Sloth, N. P., Risgaard-Petersen, N., Rysgaard, S., and Revsbech, N. P. (1994). Estimation of nitrification and denitrification from microprofiles of oxygen and nitrate in model sediment systems. *Appl. Environ. Microbiol.* 60, 2094–2100.

Joye, S. B., and Hollibaugh, J. T. (1995). Influence of sulfide inhibition of nitrification on nitrogen regeneration in sediments. *Science* 270, 623–625. doi: 10.1126/science.270.5236.623

Kana, T. M., Cornwell, J. C., and Zhong, L. J. (2006). Determination of denitrification in the Chesapeake Bay from measurements of N2 accumulation in bottom water. *Estuaries Coasts* 29, 222–231. doi: 10.1007/BF02781991

Kana, T. M., Darkangelo, C., Hunt, M. D., Oldham, J. B., Bennett, G. E., and Cornwell, J. C. (1994). Membrane inlet mass spectrometer for rapid high-precision determination of N_2, O_2, and Ar in environmental water samples. *Anal. Chem.* 66, 4166–4170. doi: 10.1021/ac00095a009

Kana, T. M., Sullivan, M. B., Cornwell, J. C., and Groszkowski, K. (1998). Denitrification in estuarine sediments determined by membrane inlet mass spectrometry. *Limnol. Oceanogr.* 42, 334–339. doi: 10.4319/lo.1998.43.2.0334

Kana, T. M., and Weiss, D. L. (2004). Comment on "Comparison of isotope pairing and N2:ar methods for measuring sediment denitrirification" By, B.D. Eyre, S., Rysgaard, and P. Bondo Christensen. 2002. Estuaries 25, 1077-1087." *Estuaries* 27, 173–176. doi: 10.1007/BF02803571

Kemp, W. M., Sampou, P., Caffrey, J., Mayer, M., Henriksen, K., and Boynton, W. R. (1990). Ammonia recycling versus denitrification in Chesapeake Bay sediments. *Limnol. Oceanogr.* 35, 1545–1563. doi: 10.4319/lo.1990.35.7.1545

Kuypers, M. M. M., Lavik, G., Woebken, D., Schmid, M., Fuchs, B. M., Amann, R., et al. (2005). Massive nitrogen loss from the Benguela upwelling system through anaerobic ammonium oxidation. *Proc. Natl. Acad. Sci. U.S.A.* 102, 6478–6483. doi: 10.1073/pnas.0502088102

Kuypers, M. M. M., Sliekers, A. O., Lavik, G., Schmid, M., Jørgensen, B. B., Kuenen, J. G., et al. (2003). Anaerobic ammonium oxidation by annamox bacteria in the Black Sea. *Nature* 422, 608–611. doi: 10.1038/nature01472

Lam, P., Lavik, G., Jensen, M. M., van de Vossenberg, J., Schmid, M., Woebken, D., et al. (2009). Revising the nitrogen cycle in the Peruvian oxygen minimum zone. *Proc. Natl. Acad. Sci. U.S.A.* 106, 4752–4757. doi: 10.1073/pnas.0812444106

Liu, X., Tiquia, S. M., Holguin, G., Wu, L., Nold, S. C., Devol, A. H., et al. (2003). Molecular diversity of denitrifying genes in continental margin sediments within the oxygen-deficient zone off the Pacific coast of Mexico. *Appl. Environ. Microbiol.* 69, 3549–3560. doi: 10.1128/AEM.69.6.3549-3560.2003

Maddison, D. R., and Maddison, W. P. (2003). *MacClade 4: Analysis of Phylogeny and Character Evolution, Version 4.06*. Sunderland, MA: Sinauer Associates.

McCune, B., and Grace, J. B. (2002). *Analysis of Ecological Communities*. Gleneden Beach, OR: MjM Software Design.

McCune, B., and Medford, M. J. (1999). *PC-ORD: Multivariate Analysis of Ecological Data, Version 4*. Gleneden Beach, OR: MjM Software Design.

Mosier, A. C., and Francis, C. A. (2008). Relative abundance of ammonia-oxidizing archaea and bacteria in the San Francisco Bay estuary. *Environ. Microbiol.* 10, 3002–3016. doi: 10.1111/j.1462-2920.2008.01764.x

Mosier, A. C., and Francis, C. A. (2010). Denitrifier abundance and activity across the San Francisco Bay estuary. *Environ. Microbiol. Rep.* 2, 667–676. doi: 10.1111/j.1758-2229.2010.00156.x

Nogales, B., Timmis, K. N., Nedwell, D. B., and Osborn, A. M. (2002). Detection and diversity of expressed denitrification genes in estuarine sediments after reverse transcription-PCR amplification from mRNA. *Appl. Environ. Microbiol.* 68, 5017–5025. doi: 10.1128/AEM.68.10.5017-5025.2002

Oakley, B. B., Francis, C. A., Roberts, Fuchsman, C., Srinivasan, S., and Staley, J. T. (2007). Analysis of nitrite reductase (*nirK* and *nirS*) genes and cultivation reveal depauperate community of denitrifying bacteria unique to the Black Sea suboxic zone. *Environ. Microbiol.* 9, 118–130. doi: 10.1111/j.1462-2920.2006.01121.x

Parsons, T. R., Maita, Y., and Lalli, C. M. (1984). *A Manual of Chemical and Biological Methods for Seawater Analysis*. Elmsford, NY: Pergamon Press.

Prieme, A., Braker, G., and Tiedje, G. M. (2002). Diversity of nitrite reductase (*nirK* and *nirS*) gene fragments in forested upland and wetland soils. *Appl. Environ. Microbiol.* 68, 1893–1900. doi: 10.1128/AEM.68.4.1893-1900.2002

Rich, J. J., Dale, O. R., Song, B. K., and Ward, B. B. (2008). Anaerobic ammonium oxidation (anammox) in Chesapeake Bay sediments. *Microb. Ecol.* 55, 311–320. doi: 10.1007/s00248-007-9277-3

Risgaard-Petersen, N., Meyer, R. L., Schmid, M. C., Jetten, M. S. M., Enrich-Prast, A., Rysgaard, S., et al. (2004). Anaerobic ammonia oxidation in an estuarine sediment. *Aquat. Microb. Ecol.* 36, 293–304. doi: 10.3354/ame036293

Rösch, C., Mergel, A., and Bothe, H. (2002). Biodiversity of denitrifying and dinitrogen-fixing bacteria in an acid forest soil. *Appl. Environ. Microbiol.* 68, 3818–3829. doi: 10.1128/AEM.68.8.3818-3829.2002

Santoro, A. E., Boehm, A. B., and Francis, C. A. (2006). Denitrifier community composition along a nitrate and salinity gradient in a coastal aquifer. *Appl. Environ. Microbiol.* 72, 2102–2109. doi: 10.1128/AEM.72.3.2102-2109.2006

SAS Institute. (2002). *JMP User's Guide*. Cary, NC: SAS Institute.

Schloss, P. D., Westcott, S. L., Ryabin, T., Hall, J. R., Hartmann, M., Hollister, E. B., et al. (2009). Introducing MOTHUR: open-source, platform-independent, community-supported software for describing and comparing microbial communities. *Appl. Environ. Microbiol.* 75, 7537–7541. doi: 10.1128/AEM.01541-09

Seitzinger, S., Harrison, J. A., Bohlke, J. K., Bouwman, A. F., Lowrance, R., Peterson, B., et al. (2006). Denitrification across landscapes and waterscapes: a synthesis. *Ecol. Appl.* 16, 2064–2090. doi: 10.1890/1051-0761(2006)016[2064:DALAWA]2.0.CO;2

Sharma, S., Aneja, M. K., Mayer, J., Munch, J. C., and Schloter, M. (2005). Diversity of transcripts of nitrite reductase genes (*nirK* and *nirS*) in rhizospheres of grain legumes. *Appl. Environ. Microbiol.* 71, 2001–2007. doi: 10.1128/AEM.71.4.2001-2007.2005

Smith, J. M., and Ogram, A. (2008). Genetic and functional variation in denitrifier populations along a short-term restoration chronosequence. *Appl. Environ. Microbiol.* 74, 5615–5620. doi: 10.1128/AEM.00349-08

Smouse, P. E., Long, J. C., and Sokal, R. R. (1986). Multiple regression and correlation extensions of the Mantel Test of matrix correspondence. *Syst. Zool.* 35, 627–632. doi: 10.2307/2413122

Song, B., and Ward, B. B. (2002). Nitrite reductase genes in halobenzoate degrading denitrifying bacteria. *FEMS Microbiol. Ecol.* 43, 349–357. doi: 10.1111/j.1574-6941.2003.tb01075.x

Taroncher-Oldenburg, G., Griner, E. M., Francis, C. A., and Ward, B. B. (2003). Oligonucleotide microarray for the study of functional gene diversity of the nitrogen cycle in the environment. *Appl. Environ. Microbiol.* 69, 1159–1171. doi: 10.1128/AEM.69.2.1159-1171.2003

Thompson, J. D., Gibson, T. J., Plewniak, F., Jeanmougin, F., and Higgins, D. G. (1997). The ClustalX windows interface: flexible strategies for multiple sequence alignment aided by quality analysis tools. *Nucleic Acid Res.* 24, 4876–4882. doi: 10.1093/nar/25.24.4876

Trimmer, M., Nicholls, J. C., Morley, N., Davies, C. A., and Aldridge, J. (2005). Biphasic behavior of anammox regulated by nitrite and nitrate in an estuarine sediment. *Appl. Environ. Microbiol.* 71, 1923–1930. doi: 10.1128/AEM.71.4.1923-1930.2005

Ward, B. B., Devol, A. H., Rich, J. J., Chang, B. X., Bulow, S. E., Naik, H., et al. (2009). Denitrification as the dominant nitrogen loss process in the Arabian Sea. *Nature* 461, 78–82. doi: 10.1038/nature08276

Ward, B. B., Eveillard, D., Kirshtein, J. D., Nelson, J. D., Voytek, M. A., and Jackson, G. A. (2007). Ammonia-oxidizing bacterial community composition in estuarine and oceanic environments assessed using a functional gene microarray. *Environ. Microbiol.* 9, 2522–2538. doi: 10.1111/j.1462-2920.2007.01371.x

Yan, T., Fields, M. W., Wu, L., Zu, Y., Tiedje, J. M., and Zhou, J. (2003). Molecular diversity and characterization of nitrite reductase gene fragments (*nirK* and *nirS*) from nitrate- and uranium-contaminated groundwater. *Environ. Microbiol.* 5, 13–24. doi: 10.1046/j.1462-2920.2003.00393.x

Yoshie, S., Noda, N., Tsuneda, S., Hirata, A., and Inamori, Y. (2004). Salinity decreases nitrite reductase gene diversity in denitrifying bacteria of wastewater treatment systems. *Appl. Environ. Microbiol.* 70, 3152–3157. doi: 10.1128/AEM.70.5.3152-3157.2004

Zhou, J., Fries, M. R., Chee-Sanford, J., and Tiedje, J. M. (1995). Phylogenetic analyses of a new group of denitrifiers capable of anaerobic growth on toluene and description of *Azoarcus tolulyticus* sp. nov. *Int. J. Syst. Bacteriol.* 45, 500–506. doi: 10.1099/00207713-45-3-500

Zumft, W. G. (1997). Cell biology and molecular basis of denitrification. *Microbiol. Mol. Biol. Rev.* 61, 533–616.

Conflict of Interest Statement: The authors declare that the research was conducted in the absence of any commercial or financial relationships that could be construed as a potential conflict of interest.

Received: 18 July 2012; accepted: 30 July 2013; published online: 30 August 2013.
*Citation: Francis CA, O'Mullan GD, Cornwell JC and Ward BB (2013) Transitions in nirS-type denitrifier diversity, community composition, and biogeochemical activity along the Chesapeake Bay estuary. Front. Microbiol. **4**:237. doi: 10.3389/fmicb.2013.00237*
This article was submitted to Aquatic Microbiology, a section of the journal Frontiers in Microbiology.

frontiers in
MICROBIOLOGY

ORIGINAL RESEARCH ARTICLE
published: 02 November 2012
doi: 10.3389/fmicb.2012.00386

Nitrogenase (*nifH*) gene expression in diazotrophic cyanobacteria in the Tropical North Atlantic in response to nutrient amendments

Kendra A. Turk-Kubo[1]*, Katherine M. Achilles[1,2], Tracy R. C. Serros[1], Mari Ochiai[1,3], Joseph P. Montoya[4] and Jonathan P. Zehr[1]

[1] *Department of Ocean Sciences, University of California at Santa Cruz, Santa Cruz, CA, USA*
[2] *Southwest Fisheries Science Center, NOAA Fisheries Service, La Jolla, CA, USA*
[3] *Center for Marine Environmental Studies, Ehime University, Matsuyama, Ehime, Japan*
[4] *School of Biology, Georgia Institute of Technology, Atlanta, GA, USA*

Edited by:
Bess B. Ward, Princeton University, USA

Reviewed by:
Mark Moore, University of Southampton, UK
Amal Jayakumar, Princeton University, USA

****Correspondence:***
Kendra A. Turk-Kubo, Department of Ocean Sciences, University of California Santa Cruz, 1156 High Street, Santa Cruz, CA 95064, USA.
e-mail: kturk@ucsc.edu

The Tropical North Atlantic (TNAtl) plays a critical role in the marine nitrogen cycle, as it supports high rates of biological nitrogen (N_2) fixation, yet it is unclear whether this process is limited by the availability of iron (Fe), phosphate (P) or is co-limited by both. In order to investigate the impact of nutrient limitation on the N_2-fixing microorganisms (diazotrophs) in the TNAtl, trace metal clean nutrient amendment experiments were conducted, and the expression of nitrogenase (*nifH*) in cyanobacterial diazotrophs in response to the addition of Fe, P, or Fe+P was measured using quantitative PCR. To provide context, N_2 fixation rates associated with the $<10\,\mu m$ community and diel *nifH* expression in natural cyanobacterial populations were measured. In the western TNAtl, *nifH* expression in *Crocosphaera*, *Trichodesmium*, and *Richelia* was stimulated by Fe and Fe+P additions, but not by P, implying that diazotrophs may be Fe-limited in this region. In the eastern TNAtl, *nifH* expression in unicellular cyanobacteria UCYN-A and *Crocosphaera* was stimulated by P, implying P-limitation. In equatorial waters, *nifH* expression in *Trichodesmium* was highest in Fe+P treatments, implying co-limitation in this region. Nutrient additions did not measurably stimulate N_2 fixation rates in the $<10\,\mu m$ fraction in most of the experiments, even when upregulation of *nifH* expression was evident. These results demonstrate the utility of using gene expression to investigate the physiological state of natural populations of microorganisms, while underscoring the complexity of nutrient limitation on diazotrophy, and providing evidence that diazotroph populations are slow to respond to the addition of limiting nutrients and may be limited by different nutrients on basin-wide spatial scales. This has important implications for our current understanding of controls on N_2 fixation in the TNAtl and may partially explain why it appears to be intermittently limited by Fe, P, or both.

Keywords: nitrogenase, P-limitation, Fe-limitation, UCYN-A, UCYN-B, *Trichodesmium*, diazotrophs, nitrogen fixation

INTRODUCTION

Nitrogen (N_2) fixation is an important component of the marine N_2 cycle, as it serves as a source for biologically available N_2 and can relieve N-limitation experienced by microbial communities living in oligotrophic regimes, in turn supporting a significant percentage of new production (Gruber and Galloway, 2008). High rates of biological N_2 fixation (BNF) have been reported in the oligotrophic Tropical North Atlantic (TNAtl; Voss et al., 2004), and some estimates indicate that N_2 fixation may support a large percentage of the export production in this region (Gruber and Sarmiento, 1997). Evidence indicates that these high BNF rates are influenced by Saharan dust deposition to surface waters in the TNAtl, which delivers dissolved iron (Fe) and to a lesser extent phosphorus (P; Mills et al., 2004), nutrients which are essential for the growth and activity microorganisms with the metabolic capability of N_2 fixation, termed diazotrophs.

It remains unclear whether BNF in the TNAtl is ultimately limited by the availability of Fe, P or is co-limited by both. Several studies have argued that high fluxes of Fe-rich Saharan dust in to the TNAtl drive P-limitation of diazotrophy (Sanudo-Wilhelmy et al., 2001). More recently, Moore et al. (2009) correlate the different magnitudes of N_2 fixation in the North and South Atlantic to Fe inputs rather than P availability, and ultimately argues that on large spatial scales, N_2 fixation is limited by Fe in the Atlantic Ocean. However, direct experimental measurements of the response of N_2 fixation to P or Fe additions in the TNAtl is limited to a study conducted by Mills et al. (2004), in which N_2 fixation was only stimulated by the addition of both Fe and P,

or by Saharan dust (presumed to have both) in the easternmost part of the basin.

A diverse community of diazotrophs has been described in this ocean basin that includes *Trichodesmium*, unicellular cyanobacteria (UCYN-A and *Crocosphaera*, also referred to as UCYN-B), and the heterocystous symbiont *Richelia* associated with diatoms *Rhizosolenia clevi* (sometimes abbreviated as Het-1, but will be referred to as RR herein) and *Hemiaulus hauckii* (Het-2, HR herein; Langlois et al., 2008; Foster et al., 2009; Goebel et al., 2010). Goebel et al. (2010) reported on the spatial and depth distribution of these cyanobacterial phylotypes across the TNAtl, determined using quantitative polymerase chain reaction (qPCR) assays targeting a gene in the nitrogenase operon, *nifH*, and used a subset of this *nifH*-based abundance data in a diagnostic model to predict contributions of several phylotypes to N_2 fixation in these waters. *Trichodesmium* was the dominant diazotroph at most of the stations surveyed, and the resulting model suggests that it is also responsible for a majority of the N_2 fixed in these waters. However, in the easternmost stations around the Cape Verde Islands, abundances of the uncultivated unicellular cyanobacteria, UCYN-A, exceeded those of *Trichodesmium*, suggesting that UCYN-A may be the most important contributor to N_2 fixation rates in this region. A separate study in the vicinity of the Cape Verde Islands, reported that *nifH* expression in UCYN-A was consistently higher (per L of seawater) than in other diazotrophs, including *Trichodesmium* (Turk et al., 2011). Together with the studies of Langlois et al. (2008) there is an emerging pattern of distinct spatial variability of the dominant diazotrophs in the TNAtl. However, there is a paucity of data on the expression of *nifH* in these phylotypes throughout this basin, and more importantly, there have been no direct measurements of how additions of Fe and P to natural populations of diazotrophs in the TNAtl impact the expression of *nifH* in individual cyanobacterial phylotypes (which can be considered a proxy for active N_2-fixing activity).

The biological reduction of N_2 to biologically available N is energetically expensive and has high Fe requirements, due to the use of Fe as a cofactor in the nitrogenase enzyme. Furthermore, the efficiency of microorganisms in utilizing Fe appears to be strain-specific (Berman-Frank et al., 2007). Recent advances in metagenomic techniques have provided insight into the metabolic potential of several cultivated diazotrophs. For example, the recently sequenced genomes of *Trichodesmium erythraeum* IMS101 and *Crocosphaera watsonii* WH8501 indicate that these diazotrophs have significant differences in their capabilities to acquire and use different species of dissolved organic P (DOP) (Dyhrman and Haley, 2006; Dyhrman et al., 2006). It follows that in natural populations of diazotrophs, the availability of Fe and P will have different impacts on N_2 fixation based on the diazotrophic taxa present.

This study extends the findings of Goebel et al. (2010) by investigating the spatial variability of *nifH* expression associated with the same natural populations of cyanobacterial diazotrophs using reverse transcription (RT)-qPCR assays. BNF rates associated with the small size-fraction ($<10\,\mu m$) of these natural populations were also measured using $^{15}N_2$ tracer assays (Montoya et al., 1996). To investigate the nutrient limitations of diazotrophy in this ocean basin, five trace-metal clean bottle incubations were conducted over 36–48 h periods, with additions of Fe, inorganic phosphorus, and a combination of both (Fe+P). Both qPCR and RT-qPCR assays were used to determine changes in *nifH*-based abundances and *nifH* expression in five cyanobacterial phylotypes in response to these experimental conditions, and BNF rates for the small size-fraction were also measured. This study is one of the first attempts to use targeted functional gene expression to investigate the response to nutrient additions in natural assemblages of marine microorganisms.

MATERIALS AND METHODS

CRUISE TRACK, CTD AND DIEL SAMPLING

Samples were collected during a 2006 Trans-Atlantic cruise aboard the R/V *Seward Johnson* (**Figure 1**). The eastbound leg of the cruise began in Barbados, and transited southeast into Amazon plume-influenced waters, then east to the Cape Verde Islands. The westbound leg of the cruise transited southwest from the Cape Verde Islands to the Equator, then transited northwest through Amazon plume-influenced waters again, back to Barbados. Samples were collected for the quantification of daytime and nighttime *nifH* expression in natural cyanobacterial populations, and for the corresponding N_2 fixation rates, using Niskin bottles mounted in a rosette coupled to a conductivity temperature depth (CTD) instrument from the surface (between 5–15 m), the deep chlorophyll max (DCM; between 65–125 m depth), and depth of the oxygen minimum (between 150–200 m). Seawater from Niskin bottles was collected into HCl-cleaned polycarbonate bottles with HCl-cleaned tubing. If the CTD was deployed within 2 h of local noon or midnight, samples were collected directly from the Niskin bottles, and immediately filtered and frozen (as described below). In some cases, this was not possible, and the water was collected into 4 L bottles and incubated at surface seawater temperatures with shading to approximate the appropriate light intensity until harvested at local noon/midnight. All samples for molecular analyses were filtered using a Masterflex peristaltic pump (Cole Parmer, Vernon Hills, IL) and size-fractionated onto a

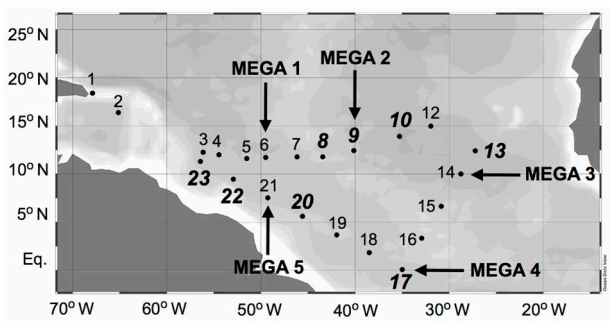

FIGURE 1 | Cruise track of SJ0609 aboard R/V *Seward Johnson* in September 2006. Diel *nifH* expression is reported from stations italicized in bold. MEGA nutrient addition experiments were performed at stations designated with arrows.

25 mm diameter 10 μm pore-size polyester filter (GE Osmotics, Minnetonka, MN) and a 25 mm 0.2 μm Supor filter (Paul Corp., Port Washington, NY), held in parallel swinnex filter holders (Millipore, Billarica, MA). Filters for RNA samples were transferred into microcentrifuge tubes containing 0.1 and 0.5 mm diameter glass beads (BioSpec Products, Bartsville, OK) and 400 μL RLT buffer (Qiagen, Germantown, MD, USA) with 1% (v/v) betamercaptoethanol (BME), immediately frozen in liquid N_2, and kept at −80°C until extraction. Filters for DNA samples were also flash frozen in liquid N_2 after being transferred in to microcentrifuge tubes containing 500 μL TE buffer and glass beads and stored at −80°C. Samples were also taken and analyzed for inorganic nutrient concentrations (nitrate+nitrite, phosphate, and silicate) and chlorophyll *a*, and the methods used for sampling and analysis along with the resulting data was reported in Goebel et al. (2010).

NUTRIENT ENRICHMENT (MEGA) EXPERIMENTAL SET-UPS

At stations 6, 9, 14, 17, and 21, large volumes of surface water were collected for nutrient enrichment experiments (called the "MEGA" experiments). These MEGA experiments were conducted using trace metal clean techniques throughout the entire sampling process. The seawater, pumped from approximately 10 m using acid-washed tubing, was collected directly into large acid-washed mixing carboys within a laminar-flow trace metal clean working area. For each of the five MEGA experiments, the seawater was subsequently dispensed into 4-L acid-washed polycarbonate bottles. The 4 L bottles were designated for sampling at various time intervals (0, 12, 24, 36, and 48 hours) and with different nutrient amendments (control, Fe, P, and Fe+P). For MEGA experiments 1–4, Fe bottles were amended with $FeCl_3$ (dissolved in 0.01 N HCl) for a final concentration of 10 nM of added Fe and P bottles were amended with KH_2PO_4 (stock solution previously eluted through a Chelex-100 column to remove trace metals) for a final concentration of 200 nM of added PO_4. As the Amazon River plume influenced nutrient levels at Station 21, final concentrations of Fe and P were increased to 50 nM and 2 μM, respectively, in MEGA5. Time zero bottles were sampled immediately. The remaining bottles were placed in spectrally corrected blue deck-board incubators that were continuously flushed with surface seawater to maintain the proper temperature until ready for sample processing. Samples for RNA extraction and $^{15}N_2$ rate measurements were collected from duplicate bottles at each time point and for each type of nutrient enrichment; samples for DNA extraction were collected from triplicate bottles. DNA and RNA samples were filtered (500–2000 mL depending on time point) as described above. RNA samples were collected at every time point whereas DNA samples were only collected at 0, 24, and 48 h.

$^{15}N_2$ RATE MEASUREMENTS

Rates of N_2 fixation were measured using tracer additions of $^{15}N_2$ gas following the general protocol of Montoya et al. (1996). In brief, incubation bottles were filled to the point of overflowing, while carefully excluding bubbles, then 2 mL of $^{15}N_2$ gas at 1 atm pressure was added using a gas-tight syringe. The bottles were incubated under simulated *in situ* conditions in a flowing seawater incubator on deck for 12, 24, 36, or 48 h, and were terminated by gentle pressure filtration through a 10 μm Nitex screen and a precombusted GF/F filter (small size fraction material). Material collected on the 10 μm screens (large size fraction material) was rinsed off and transferred to a precombusted GF/C filter. Filters were dried at 60°C on board the ship then stored over desiccant for analysis ashore.

All isotope measurements were carried out by continuous-flow isotope ratio mass spectrometry using a Micromass Optima interfaced to a CE Instruments NC2500 elemental analyzer for online combustion and purification of organic N_2. All isotope abundances were corrected for instrument and blank effects as described in Montoya (2008), and rates were calculated using the mass balance approach of Montoya et al. (1996).

NUCLEIC ACID EXTRACTIONS AND cDNA GENERATION

DNA from bottle incubations was extracted using the modified DNeasy Plant kit (Qiagen) method described in Moisander et al. (2008) with the following modifications: the glass beads were added to autoclaved bead-beating tubes prior to sampling; freeze-thaw cycles used liquid N_2 rather than an ethanol/dry ice slurry; and the final elution volume was 50 μL. DNA extracts were stored at −20°C. This is the same protocol used to process the complementary samples presented in Goebel et al. (2010), which are used to provide context for this study. DNA extracts were quantified using the Quant-iT™ PicoGreen® kit assay kit (Invitrogen, Carlsbad, CA, USA) and measured using a SpectraMax M2e spectrophotometer (Molecular Devices, Sunnyvale, CA, USA).

RNA extractions were performed using a modified RNeasy Plant Mini kit (Qiagen) protocol. To ensure that extractions were carried out in an RNase-free environment all surfaces and pipettors were cleaned with RNase Zap solution (Invitrogen). Prior to extractions, a DNAse I working solution was made from an RNase-free DNAse I stock (RNase-free DNase set; Qiagen), by adding 10 μL of the stock (2.73 units μL^{-1}) to 70 μL Buffer RDD for each sample. Bead-beating tubes containing filters frozen RLT/BME were thawed on ice and agitated in a bead-beater twice for 2 min each, cooling on ice between bead-beatings (Mini-Beadbeater-96; Biospec Inc., Bartlesville, OK, USA). Filters were removed using sterile needles and discarded. Samples were then centrifuged for 2 min, and the supernatant was transferred into a new sterile 2-mL microfuge tube. 250 μL of 100% ethanol was added to the supernatant, and then samples were gently mixed by inversion and transferred onto RNeasy Mini spin columns. Spin columns were centrifuged for 15 s, and the flow through was discarded. 350 μL of RW1 buffer was then added to each spin column, and after another centrifugation step for 15 s the flow through was discarded. DNA was removed using an on-column DNase digestion step where 80 μL of the DNAse I working solution was added directly to the spin column and incubated at room temperature for 1 h. After DNase digestion, an additional 350 μL of buffer RWI was added to the spin column, followed by another centrifugation step for 15 s. RNA retained on the column was cleaned with two consecutive additions of 500 μL RPE buffer and centrifugation for 15 s followed by an additional 2-min centrifugation to dry columns. RNA was eluted into sterile 1.5 mL microfuge tubes by adding 50 μL RNase-free

water to the column, letting sit at room temperature for 1 min and then centrifuging for 2 min. All centrifugation steps were carried out at 8000 × *g*. RNA extracts were quantified using the Quant-it™ RiboGreen® RNA assay kit (Invitrogen), according to manufacturer's guidelines. RNA extracts were stored at −80°C. Complementary DNA (cDNA) was generated from RNA extracts via RT using the SuperScript™ III First Strand Synthesis System for RT-qPCR (Invitrogen) as described for RT-qPCR reactions in Turk et al. (2011).

QUANTITATIVE PCR ASSAYS FOR ABUNDANCE (qPCR) AND EXPRESSION (RT-qPCR)

Quantitative PCR (qPCR) and RT quantitative PCR (RT-qPCR) were used to quantify *nifH* gene copies and *nifH* transcripts, respectively, from five different cyanobacterial phylotypes that have been detected in the TNAtl (Langlois et al., 2008; Goebel et al., 2010; Turk et al., 2011) described in **Table 1**.

All qPCR reactions used reaction conditions, plate set-up, instrumentation, thermocycling parameters, and approach to calculating *nifH* transcripts/gene copies L^{-1} according to methods described in Goebel et al. (2010).

Taking into consideration the dilutions made during the RT reactions, the volume of nucleic acid extractions, and the volume of seawater filtered, the limit of detection (LOD) and limit of quantitation (LOQ) for the RT-qPCR reactions in this study were between 32–63 and 250–500 *nifH* transcripts L^{-1} seawater, respectively. The LODs and LOQs were slightly lower (13–25 and 100–200 *nifH* copies L^{-1}) in the qPCR analysis of DNA extracts. For both qPCR and RT-qPCR analyses, samples were designated as "detected not quantified" (DNQ) where the detected signal was greater than the LOD, but fell below the LOQ.

For cDNA samples, each RT and no-RT sample was screened for inhibition using the UCYN-A primer/probe set by spiking the reaction with a 10^5 standard and determining the percent efficiency. No inhibition was observed. For a majority of the samples, no-RTs did not amplify, indicating that the DNase step successfully removed all DNA present. In the several samples where amplification was observed in the no-RTs, the *nifH* transcripts reaction^{-1} were always in the range of DNQs, and were subtracted from the *nifH* transcripts reaction^{-1} calculated for the RT amplification.

In order to discuss *nifH* expression per N_2-fixing cell in natural diazotrophic populations, the following assumptions were made: DNQs were estimated to be 100 *nifH* copies L^{-1} for DNA and 250 *nifH* copies L^{-1} for RNA; UCYN-A, -B, and *Trichodesmium* were assumed to have one gene per N_2-fixing cell; and the RR phylotype was assumed to have four vegetative cells per heterocyst, and the HR phylotype was assumed to have three vegetative cells per heterocyst (Foster and Zehr, 2006).

Where possible, a Student's *t*-test (homoscedastic, 2-tailed) was used to determine the statistical significance of differences between control and treatment incubations ($p < 0.05$) in both abundance (qPCR) and expression (RT-qPCR) data from the MEGA experiments. It is important to note, however, conditions of normality cannot be verified with replicates, and that in many cases, expression and/or abundance data in control incubations were either UD or DNQ, which represents real information that cannot be included in a *t*-test.

RESULTS

NITROGENASE GENE EXPRESSION IN NATURAL POPULATIONS OF CYANOBACTERIA IN THE TROPICAL NORTH ATLANTIC

In order to investigate the diel *nifH* expression in natural populations of cyanobacterial diazotrophs in the TNAtl, we used a combination of direct sampling from the CTD and shipboard incubations at eight stations along the SJ0609 transit (**Figure 1**). These stations spanned a range of environmental conditions (**Table 2**), from waters with low salinities (<35 ppt) resulting from the Amazon River plume (Stations 20, 22, and 23), to the oligotrophic waters surrounding the Cape Verde Islands (Stations 10 and 13), and equatorial waters with detectable $NO_3 + NO_2$ and PO_4 at the surface, characteristic of equatorial upwelling (Station 17). Diel *nifH* expression was determined for UCYN-A, UCYN-B, *Trichodesmium*, HR and RR using RT-qPCR assays. In addition to considering the absolute *nifH* transcripts L^{-1} for each phylotype at three depths in the photic zone (**Figure 2**), daytime and nighttime expression data was also normalized to represent the number of transcripts associated with each N_2-fixing cell (**Figure 3**), which had been used as a proxy for which diazotrophs are most actively expressing *nifH* (Zehr et al., 2007). This required dividing the *nifH* transcript copies L^{-1} by the *nifH* gene copies L^{-1} reported by Goebel et al. (2010), which were determined from complementary sampling efforts at these stations, and the assumptions outlined in the method

Table 1 | Cyanobacterial *nifH* qPCR and RT-qPCR targets.

Cyanobacterial target	References	Genbank accession no. of standard	Efficiency (E)	Size fraction
UCYN-A	Church et al., 2005	AF059642	102%	0.2–10 μm
UCYN-B	Moisander et al., 2010	DQ481411	88%	0.2–10 μm
Trichodesmium	Church et al., 2005	DQ404414	94%	>10 μm
Richelia in *R. clevi* (RR)	Church et al., 2005	DQ225757	98%	>10 μm
Richelia in *H. hauckii* (HR)	Foster et al., 2007	DQ225753	98%	>10 μm

The efficiency (E) of each assay was determined using the formula $E = 10^{-1/m} - 1$, where m is the slope from the linear regression applied to standards with 10^0–10^7 gene copies reaction^{-1}. All DNA and RNA samples were size fractionated, and the target size fraction for each phylotype is indicated. Abbreviations: UCYN-A, uncultivated unicellular cyanobacteria group A; UCYN-B, uncultivated unicellular cyanobacteria group B.

Table 2 | SJ0609 station information, environmental and experimental parameters for all stations and depths sampled for both diel investigations and MEGA experiments.

Station	Lat. (ddm)	Long. (ddm)	depth (m)	Temp (°C)	Salinity (psu)	chl *a* ($\mu g\ L^{-1}$)	$NO_3 + NO_2$ (μM)	PO_4 (μM)	$Si(OH)_4$ (μM)	Time of $^{15}N_2$ gas injection in BNF rate incubations (hh:mm)
6	**11.712**	**−49.486**	**5**	**27.5**	**36.1**	**0.13**	**bd**	**bd**	**bd**	**na**
8	11.787	−43.447	5	27.4	36.1	0.11	0.01	bd	bd	03:15
			75	25.5	36.3	0.42	0.10	bd	0.01	
			200	13.1	35.5	bd	nm	nm	nm	
9	**12.434**	**−40.135**	**5**	**26.4**	**36.4**	**nm**	**bd**	**bd**	**bd**	14:50/**09:20–13:27***
			96	22.4	36.8	0.47	0.08	0.04	0.01	
			200	13.3	35.5	nm	24.42	1.43	7.78	
10	13.921	−35.284	15	26.0	36.4	0.02	bd	bd	bd	04:30
			125	21.0	37.0	0.12	3.57	0.11	bd	
			200	15.7	36.0	0.01	19.61	0.86	3.30	
13	12.413	−27.247	5	26.9	36.2	0.07	0.01	bd	bd	16:55
			65	21.7	35.9	0.43	0.04	bd	1.13	
			200	12.2	35.3	bd	24.61	1.54	9.26	
14	**10.000**	**−28.772**	**5**	**27.2**	**36.0**	**nm**	**0.05**	**bd**	**0.01**	**12:00–15:30***
17	**0.081**	**−34.991**	**5**	**26.8**	**36.2**	**0.20**	**0.48**	**0.58**	**bd**	04:20/**13:06–00:48***
			75	25.5	36.5	0.37	1.26	0.59	bd	
			200	13.3	35.3	nm	14.11	1.27	8.61	
20	5.601	−45.598	5	28.6	33.0	0.30	0.15	0.13	5.23	03:15
			70	26.7	36.3	0.62	0.14	0.10	0.07	
			150	12.7	35.4	0.01	19.74	1.42	8.49	
21	**7.531**	**−49.260**	**5**	**28.8**	**32.8**	**0.24**	**nm**	**nm**	**nm**	**12:51–15:30***
22	9.467	−52.93	5	28.3	34.7	nm	nm	nm	nm	na
			73	25.0	36.6	nm	1.18	0.48	1.75	
			150	15.6	35.9	nm	0.29	1.37	6.52	
23	11.303	−56.443	5	28.4	32.9	nm	nm	nm	nm	00:10
			76	26.9	36.2	nm	nm	nm	nm	
			160	20.5	36.8	nm	nm	nm	nm	

Stations where MEGA experiments were conducted are in shaded rows with bold text, and the time of $^{15}N_2$ gas tracer injection for associated BNF rate measurements is marked with an asterisk (*). Abbreviations: na, not applicable; nm, not measured; bd, below detection limit.

section for the ratio of vegetative and heterocystous cells in the HR and RR. In general, the highest *nifH* expression for the unicellular cyanobacterial phylotypes UCYN-A and UCYN-B was measured in the eastern part of the basin (Stations 9, 10, and 13), and highest *nifH* expression for the heterocystous cyanobacterial symbionts was measured along the southern cruise track in the western part of the basin (Station 22). *Trichodesmium nifH* expression was measured at all eight stations (**Figure 2**).

UCYN-A was found to be actively expressing *nifH* around mid-day at a depth of 15 m at Station 10, with 39 *nifH* transcripts N_2-fixing $cell^{-1}$, and also had elevated levels of expression at night at this station and depth (**Figure 2**). Although UCYN-B was detected in DNA samples in surface waters at Station 10 (Goebel et al., 2010), expression of *nifH* from UCYN-A accounted for all of the characterized transcripts in both the daytime and nighttime samples. The observation of *nifH* expression during the day is consistent with what we now know about the photoheterotrophic metabolism of UCYN-A (Zehr et al., 2008; Tripp et al., 2010). However, measuring high transcript numbers during the night is contrary to diel observations made at station ALOHA, where *nifH* expression was not observed in the dark (Zehr et al., 2007).

UCYN-B *nifH* expression was observed exclusively at night in surface waters at Station 9 (5 m) and at the DCM at Station 13 (65 m). This supports previous observations, in both cultures and in the environment, that UCYN-B temporally separates N_2 fixation to protect the nitrogenase from oxygen evolved during oxygenic photosynthesis (Church et al., 2005; Zehr et al., 2007; Shi et al., 2010). Although *nifH*-based abundances are generally considered a proxy for the dominant diazotrophs in a given sample, such assumptions can be incorrect when comparing *nifH*-based abundance data with *nifH* transcript data. This is evident in surface samples from Station 9, where no UCYN-B was detected using *nifH*-based abundances (implying UCYN-B abundance was <63 *nifH* copies L^{-1}, the LOD for this qPCR assay; Goebel et al., 2010), yet *nifH* transcripts from UCYN-B were the predominant contributor to the overall *nifH* pool characterized at 5 m

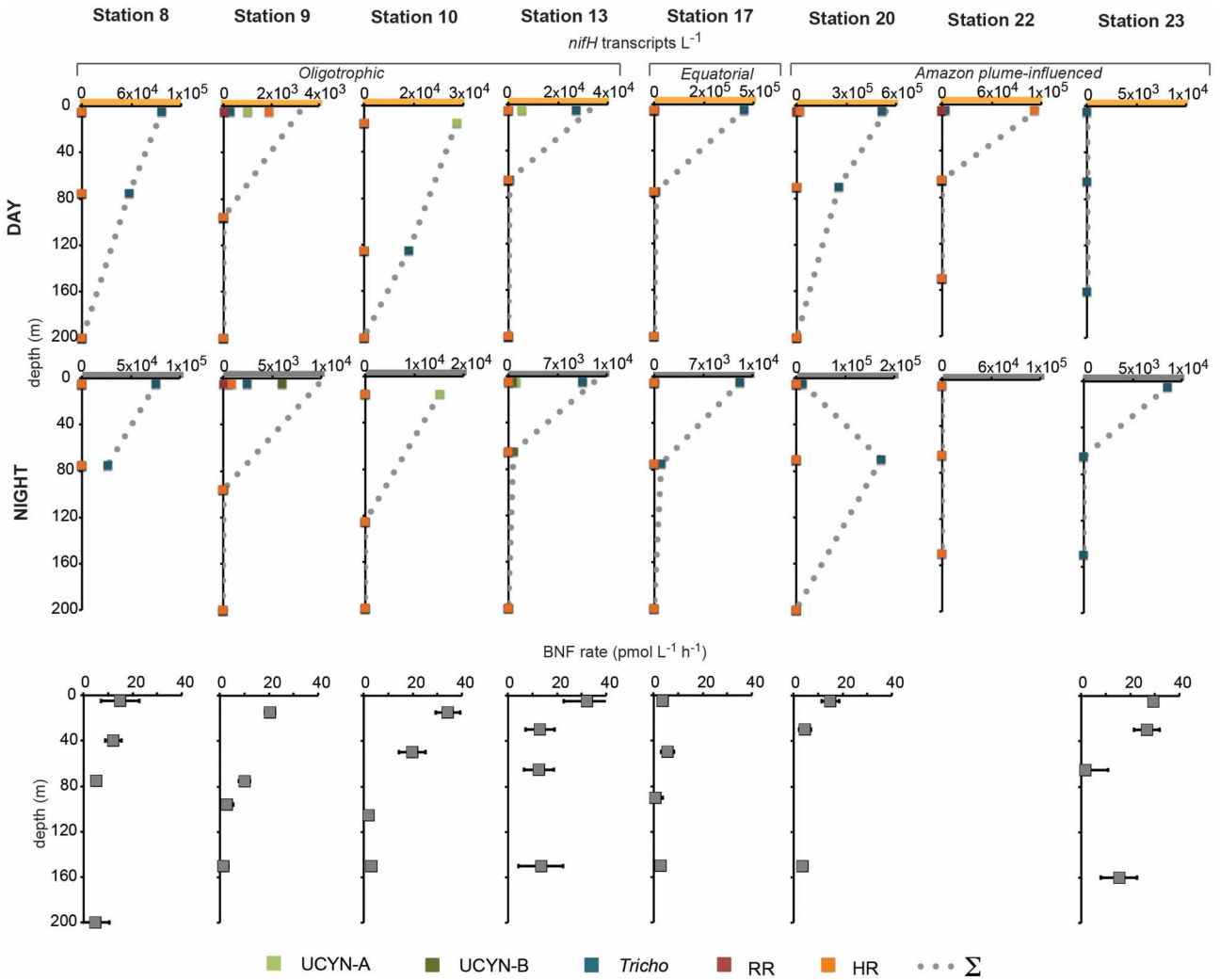

FIGURE 2 | Daytime and nighttime *nifH* expression and BNF rates associated with the <10 μm size-fraction in natural populations of diazotrophs. No BNF rates were measured at Station 22. Note the different scales on the x-axis of *nifH* expression data, and the y-axis for BNF rate depths. Abbreviations: UCYN-A, uncultivated unicellular cyanobacteria group A; UCYN-B, uncultivated unicellular cyanobacteria group B; *Tricho*, *Trichodesmium*; RR, *Richelia* in *Rhizosolenia* (Het-1); HR, *Richelia* in *Hemiaulus* (Het-2); and Σ, sum of all *nifH* transcripts L^{-1} for both size-fractions quantified at each station and depth.

(**Figure 2**), even representing the highest normalized *nifH* transcripts N_2-fixing cell^{-1} among all the samples and diazotrophs characterized in this study (**Figure 3**).

Trichodesmium was the most abundant phylotype across this ocean basin (Goebel et al., 2010) and *nifH* transcripts were consistently high, with the notable exception of having low copy numbers and expression in surface waters at Station 10. However, when transcripts were normalized to *nifH* gene copies (reported from complementary samples in Goebel et al. (2010)), normalized transcripts from *Trichodesmium* were consistently low (**Figure 3**), less than 10 *nifH* transcripts N_2-fixing cell^{-1}. The highest normalized *nifH* expression measurements were found midday at Station 10 (125 m), Station 13 (5 m), and Station 17 (5 m). At station ALOHA, normalized gene expression for *Trichodesmium* has been measured to be an order of magnitude greater (∼100 transcripts gene^{-1}; Zehr et al., 2007).

As described for UCYN-B, *nifH*-based abundances (from DNA samples) do not always predict *Trichodesmium* nitrogenase activity. For example, at Station 13, it appeared that UCYN-A was the dominant diazotroph in surface waters using *nifH*-based abundances (4.6×10^4 *nifH* copies L^{-1}; Goebel et al., 2010). However, it appears that *Trichodesmium* may be the most active N_2-fixing organism, as a majority of the *nifH* transcripts quantified from these surface waters were from *Trichodesmium* (2.4×10^4 *Trichodesmium nifH* transcripts L^{-1}, compared to 4.8×10^3 UCYN-A *nifH* transcripts L^{-1}; **Figure 2**).

RR *nifH* expression was highest at midday in surface waters at Station 20 at 3.6×10^3 *nifH* transcripts L^{-1}. Despite being

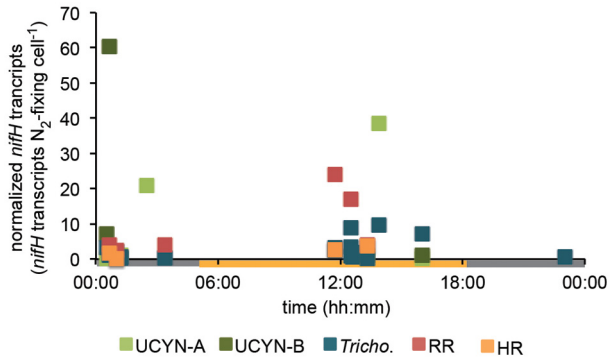

FIGURE 3 | Diel *nifH* expression normalized to the abundance of each phylotype. Expression data across all stations was pooled, and transcript numbers were normalized to each N_2-fixing cell using *nifH*-based abundances at each station reported in Goebel et al. (2010), and assumptions outlined in the methods section. DNQs for DNA and RNA were changed to 100 and 250 *nifH* copies/transcripts L^{-1} for these calculations, respectively.

two-orders of magnitude lower than *Trichodesmium nifH* transcripts, normalized *nifH* transcripts N_2-fixing cell^{-1} in this sample were the highest measured in this study for non-unicellular cyanobacterial diazotrophs (24 *nifH* transcripts N_2-fixing cell^{-1}; **Figure 3**). This indicates that although RR may be less abundant than *Trichodesmium*, its contribution to the fixed N pool in this region may be just as important, if not more important, than *Trichodesmium*. RR and *Trichodesmium* were the only two phylotypes with detectable expression in the warm equatorial waters at Station 17 (4.2×10^2 and 4.3×10^5 *nifH* transcripts L^{-1}, respectively). RR was either not detected or had low abundances at all other stations and depths. However, it should be noted that RR abundances and expressions were not measured for Stations 22 and 23, a region of the Atlantic basin heavily influenced by the Amazon plume where abundant RR and HR have previously been documented (Foster et al., 2007).

HR *nifH* transcripts were detected in both daytime and nighttime surface samples at Stations 9 and 20 and in the daytime surface sample at Station 22. At Stations 9 and 20, the normalized transcript abundance was low, at <4 *nifH* transcripts N_2-fixing cell^{-1}. At Station 9, *nifH* transcripts from HR accounted for a majority of the transcript pool for the daytime sample (**Figure 2**), despite being lower in abundance than UCYN-A (1.5×10^3 and 5.6×10^3 *nifH* copies L^{-1} for HR and UYCN-A respectively; Goebel et al., 2010). It is important to note that the highest measured *nifH* transcripts for HR were in surface waters at Station 22 (1.1×10^5 *nifH* transcripts L^{-1}), but no DNA was analyzed for this sample, so the normalized expression cannot be determined. Both RR and HR *nifH* expression are positively correlated with temperature ($r^2 = 0.27$, $p = 0.01$ and $r^2 = 0.20$, $p = 0.03$, respectively), and negatively correlated with salinity ($r^2 = 0.18$, $p = 0.04$ and $r^2 = 0.26$, $p = 0.01$, respectively), but these correlations, though significant, are weak. In the case of RR, these results contradict those reported in Foster et al. (2009) from a region farther south (the eastern equatorial Atlantic), where the correlation between RR and temperature was negative.

BIOLOGICAL NITROGEN FIXATION RATES IN THE TROPICAL NORTH ATLANTIC

BNF rates associated with the small size-fraction were generally highest in surface waters at the oligotrophic stations and reached their highest rates at the easternmost Stations 10 and 13, at 34.3 ± 5.0 pmol L^{-1} h^{-1} (15 m), and 32.3 ± 5.0 pmol L^{-1} h^{-1} (5 m), respectively. They were also comparably high at Station 23 (26.7 ± 5.3 pmol L^{-1} h^{-1}; 30 m) where no *nifH* expression from UCYN-A or UCYN-B was quantified (**Figure 2**). BNF rates were lowest throughout the photic zone at the equatorial Station 17 (between 0.6 and 5.7 pmol L^{-1} h^{-1}). At most stations, the biomass collected in the large size fraction (>10 μm) was too small to provide a robust measurement of isotope content and N_2-fixation activity, therefore, only the small-size fraction data is reported here.

The overall UCYN-A *nifH* expression does show a significant positive correlation with integrated BNF rates associated with the small size-fraction ($r^2 = 0.33$, $p = 0.0005$). However, HR *nifH* expression showed the strongest correlation with integrated BNF rates ($r^2 = 0.40$ and $p = 0.002$), across all the stations sampled. This correlation between a diatom-diazotroph association (DDA) and integrated BNF rates assumed to be associated with much smaller cells is surprising and difficult to interpret given that the *nifH* expression was quantified from the 10 μm filter, and was not measured on the 0.2 μm filter, which is a common practice for these DDAs. There have been several reports of free-living planktonic heterocystous cyanobacteria (e.g., Gómez et al., 2005) that might contribute to BNF rates in this size-fraction, but it is assumed that the *Richelia* phylotype targeted by this qPCR assay lives within the host diatom frustule. This correlation might also result from either the physical disruption of the HR association during filtration, or the rapid incorporation and excretion of ^{15}N by HR in the 10 μm size fraction, followed up by assimilation into particulate N of smaller microorganisms, an effect which has been reported for *Trichodesmium* (Mulholland et al., 2006). Due to the technical approaches used to measure BNF rates in this and other studies, discussed in detail below, the values reported here are likely underestimates.

NITROGENASE GENE EXPRESSION IN RESPONSE TO NUTRIENT AMENDMENT EXPERIMENTS

Sets of five trace-metal clean bottle incubations, called the "MEGA" experiments, were conducted at select stations (**Figure 1**) to investigate nutrient limitations of diazotrophy in major cyanobacterial phylotypes across the TNAtl Ocean basin. Three experiments were conducted on diazotrophic communities in oligotrophic waters (MEGA1—Station 6; MEGA2—Station 9; and MEGA3—Station 14), one in equatorial water with evidence of upwelling (MEGA4—Station 17) and one from the lower salinity, higher-nutrient Amazon-plume influenced waters (MEGA5—Station 21).

Results from each experiment will be discussed in detail below; however, some general findings were consistent across all experiments. Enhanced *nifH* expression in cyanobacteria associated with the small size-fraction (UCYN-A and UCYN-B) rarely correlated with a stimulation of BNF rates in these experiments, which were carried out over a relatively short time period (between

36–48 h), as the intent was to capture the first order changes evident in gene expression. Despite this lack in response, BNF rates measured in controls from MEGA experiments were almost always higher than those measured for the *in situ* communities discussed above. It is also important to note that an increase in population size for any given diazotroph throughout the duration of these experiments (as inferred from an increase in *nifH* gene copies L^{-1} in DNA extracts) was rare, even in cases where stimulation of *nifH* expression with respect to the control was measured. Finally, diazotroph *nifH*-based abundances from time zero samples correlate well with those reported at the same station in Goebel et al. (2010).

MEGA1

Conducted at Station 6, where the low salinity lens from the Amazon River plume is no longer detected, the diazotrophic community in MEGA1 was dominated by *Trichodesmium* and HR based on the *nifH*-based abundances in time zero samples, and UCYN-B, *Trichodesmium* and HR were all showing signs of active regulation of the *nif* operon based on the detectable expression of *nifH* in time zero samples. UCYN-A was determined to be present at low abundances in time zero samples (**Figure 5**), but there was no detection of *nifH* expression at any point in the experiment, and based on the decrease in *nifH* abundances by $t = 48$ h, it appears that this small population of UCYN-A dwindled to below detection limits, or crashed all together. UCYN-B *nifH* expression appeared to be stimulated in the Fe treatment at $t = 48$ h, despite being present at low abundances in this treatment, which is somewhat surprising as $t = 48$ h was taken during the day (**Figure 4**), and without sampling at the peak of *nifH* nighttime expression it is difficult to interpret these results. Furthermore, UCYN-B *nifH*-based abundances increased in the Fe+P treatment, but it is impossible to determine if there were different factors driving UCYN-B growth and N_2-fixing activity in this experiment. *Trichodesmium* was present at high abundances in the control and all three treatments ($\sim 10^5$ cells L^{-1}; **Figure 5**) and was actively transcribing *nifH* at the onset of the experiment; however, none of the nutrient additions appeared to stimulate *nifH* expression (**Figure 4**). Although RR was not expressing *nifH* at the beginning of this experiment, elevated *nifH* expression, with respect to the $t = 48$ h control was measured in the Fe treatment alone, which implies that during the course of the experiment, RR began to regulate the *nif* operon in the presence of Fe. No BNF rates were available from this experiment.

MEGA2

In MEGA 2, conducted at Station 9, the diazotrophic community was comprised predominantly of UCYN-A, *Trichodesmium*, and HR (**Figure 5**; Goebel et al., 2010). Although RR was not detected in time zero samples, *nifH*-based abundances in $t = 48$ h samples indicate that they were present in low abundances in the P and Fe treatments as well as the control. UCYN-B was also detected at low abundances in time zero samples, but the Fe+P treatment stimulated a measurable increase in *nifH*-based abundances by $t = 48$ h, from 6.7×10^2 *nifH* copies L^{-1} to 1.5×10^4 *nifH* copies L^{-1}. As with MEGA1, the sampling time at the end of the experiment occurred during the daytime, so no information about the stimulation of *nifH* expression in UCYN-B was obtained in this experiment. Expression of *nifH* in UCYN-A, *Trichodesmium*, HR and RR was stimulated in the P treatment, increasing by 10^3–10^4 *nifH* transcripts L^{-1} with respect to the control expression (which was UD or DNQ for all phylotypes; **Figure 4**). There was also an increase in *nifH* expression in the Fe treatments for *Trichodesmium*, HR and RR, but it was consistently about an order of magnitude less than the P response. BNF rates at $t = 12$ h did not show any measurable response to any of the three treatments, and rates associated with the $t = 48$ h samples were unavailable (**Figure 6**). As discussed in detail below, it is possible that a lack of measureable response in the first 12 h results from incomplete dissolution of the $^{15}N_2$ tracer gas which was injected into BNF rate incubations during the daytime (**Table 2**).

MEGA3

In the easternmost region of the TNAtl, near the Cape Verde Islands, the prevalence of UCYN-A and UCYN-B has been reported (Langlois et al., 2008; Goebel et al., 2010; Turk et al., 2011), and it is hypothesized that these unicellular diazotrophs may contribute to a significant portion of the fixed N in this area. At Station 14, the source waters for the MEGA3 experiment, the most abundant diazotroph in time zero waters was UCYN-A at 4.0×10^4 *nifH* gene copies L^{-1}. UCYN-B was present below detection limits of the qPCR assay at time zero. RR was the second most abundant diazotroph at 1.2×10^3 *nifH* copes L^{-1}, which is in contrast to *nifH*-based abundances reported in Goebel et al. (2010), where RR was not detected at this station. *Trichodesmium* and HR were both present at approximately 10^2 *nifH* copies, L^{-1}. Only UCYN-A and *Trichodesmium* had detectable *nifH* expression in time zero samples. The *nifH* expression from unicellular diazotrophs was stimulated in P treatments in the $t = 24$ h daytime sampling (UCYN-A) and the $t = 36$ h nighttime sampling (UCYN-B). At the $t = 48$ h sampling however, very low numbers of *nifH* transcripts associated with UCYN-A were quantified, and no response to the treatments was observed. The opposite is true for *Trichodesmium*; no *nifH* expression response was quantified in the $t = 24$ h sampling, but in the $t = 48$ h sampling, a significant response in *nifH* expression was seen in all treatments (**Figure 4**, Fe, $p = 0.04$; P, $p = 0.003$, and Fe+P, $p = 0.0002$). This was accompanied by a decrease in UCYN-A *nifH*-based abundances in all treatments, and an increase in *Trichodesmium nifH*-based abundances in both the Fe+P and P treatments between time zero and $t = 48$ h samples. These results indicate that UCYN-A was able to respond more quickly to P additions than the other diazotrophs, and that in P-replete conditions, UCYN-A *nifH* transcription was stimulated more quickly than in *Trichodesmium*, HR and RR. BNF rates for MEGA3 were determined for $t = 12$ h (except P), $t = 24$ h, $t = 36$ h and $t = 48$ h (**Figure 6**). For a majority of the samples, no measurable difference in BNF was measured between the control and treatments. The only measurable stimulation in BNF rate was seen in the $t = 36$ h sample for the P treatment, which corresponds with the increased response in *nifH* transcription by UCYN-A and UCYN-B in the first 36 h of this experiment.

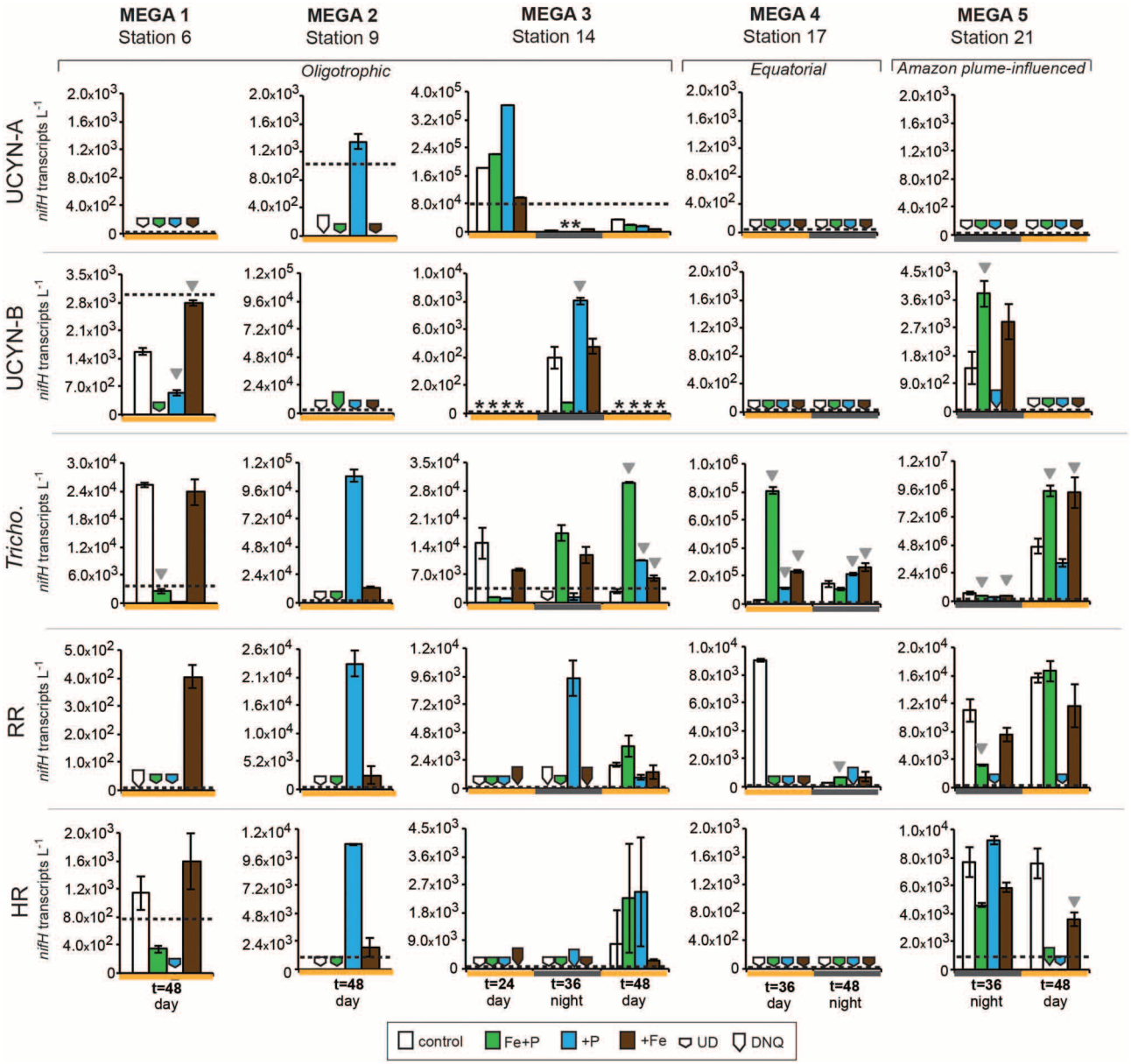

FIGURE 4 | Expression of *nifH* in response to nutrient additions in the MEGA experiments. Quantified *nifH* transcripts L^{-1} in time zero samples in each experiment for each phylotype is marked with a dotted line. UCYN-A and UCYN-B *nifH* transcripts L^{-1} were quantified from 0.2 μm filters; *Tricho*, RR, and HR *nifH* transcripts L^{-1} were quantified from 10 μm filters. Error bars indicate the standard error, where possible. Significant differences between control and treatment (Student's *t*-test, $p < 0.05$) are marked with a grey triangle. Missing data is marked with an asterisk (*). Note the different scales used for the y-axis. Abbreviations: UD, undetected; DNQ, detected not quantified.

MEGA4

In the equatorial waters at Station 17, the diazotrophic community was composed almost entirely of *Trichodesmium* (**Figure 5** and Goebel et al., 2010), although RR was also detected at low abundances in time zero samples (2.2×10^2 *nifH* copies L^{-1}). Neither *Trichodesmium* nor RR had detectable *nifH* expression at time zero, but this is likely due to the nighttime sampling, therefore it is not possible to determine whether these populations were actively regulating the *nif* operon at the onset of MEGA4. It is reasonable to assume, however, that the *Trichodesmium* was active, as *nifH* expression was measured in the natural population (**Figure 2**) at this station. Both the P and Fe additions stimulated small increases in *Trichodesmium nifH* transcripts L^{-1}, but a much larger increase in *nifH* expression was seen in the Fe+P treatment (**Figure 4**), implying that N_2 fixation by *Trichodesmium* in this region may be co-limited by both Fe and P. However, by the end of the incubation, *Trichodesmium* abundances were significantly higher in Fe treatments ($p = 0.02$; **Figure 5**). Even

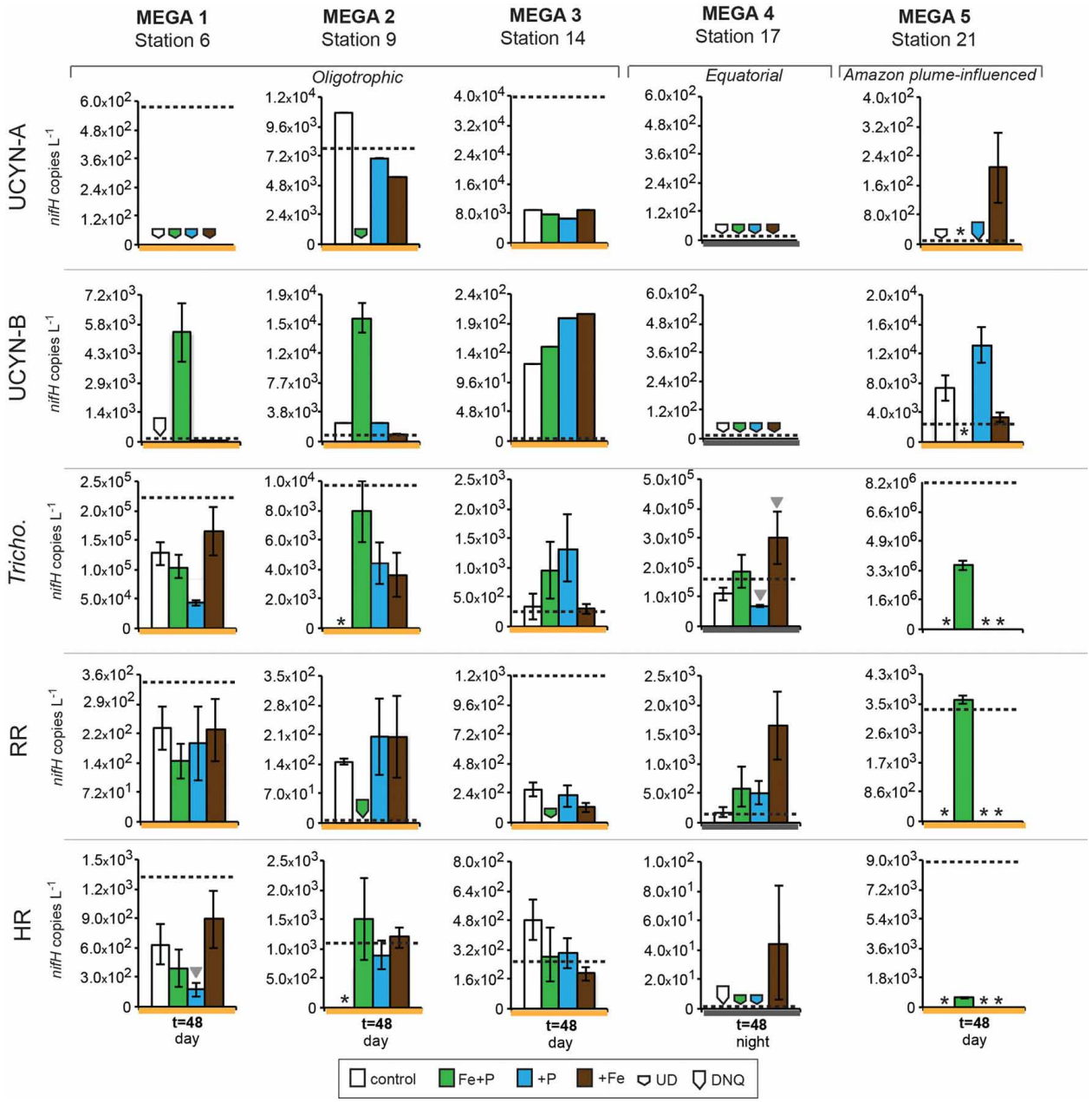

FIGURE 5 | Changes in *nifH*-based abundances in response to nutrient additions in the MEGA experiments between time zero and $t = 48$ h samplings. Quantified *nifH* copies L^{-1} in time zero samples in each experiment for each phylotype is marked with a dotted line. UCYN-A and UCYN-B *nifH* copies L^{-1} were quantified from 0.2 μm filters; *Tricho*, RR, and HR *nifH* copies L^{-1} were quantified from 10 μm filters. Error bars indicate the standard error, where possible. Significant differences between control and treatment (Student's *t*-test, $p < 0.05$) are marked with a grey triangle. Missing data is marked with an asterisk (*). Note the different scales used for the y-axis. Abbreviations: UD, undetected; DNQ, detected not quantified.

though unicellular diazotrophs were not detected at this station, BNF rates associated with the <10 μm fraction in MEGA4 were comparable, and in some cases higher, than the rates measured in MEGA3. Furthermore, there was a measurable stimulation of BNF rates associated with the Fe treatment in $t =$ 36 h samples (**Figure 6**). There are several potential explanations for the measurement of these rates in the small size fraction, including the presence of unicellular cyanobacterial phylotypes or heterotrophic diazotrophs not targeted by these qPCR assays, or the incorporation of ^{15}N by organisms in the small size fraction that was originally fixed then released as reduced N by *Trichodesmium*, which has been shown to occur on very short time scales (<12 h) in the Gulf of Mexico (Mulholland et al., 2006). It is also possible that measured rates in the small size fraction result from the disruption of *Trichodesmium* filaments during filtering and size fractionation. Previous studies have

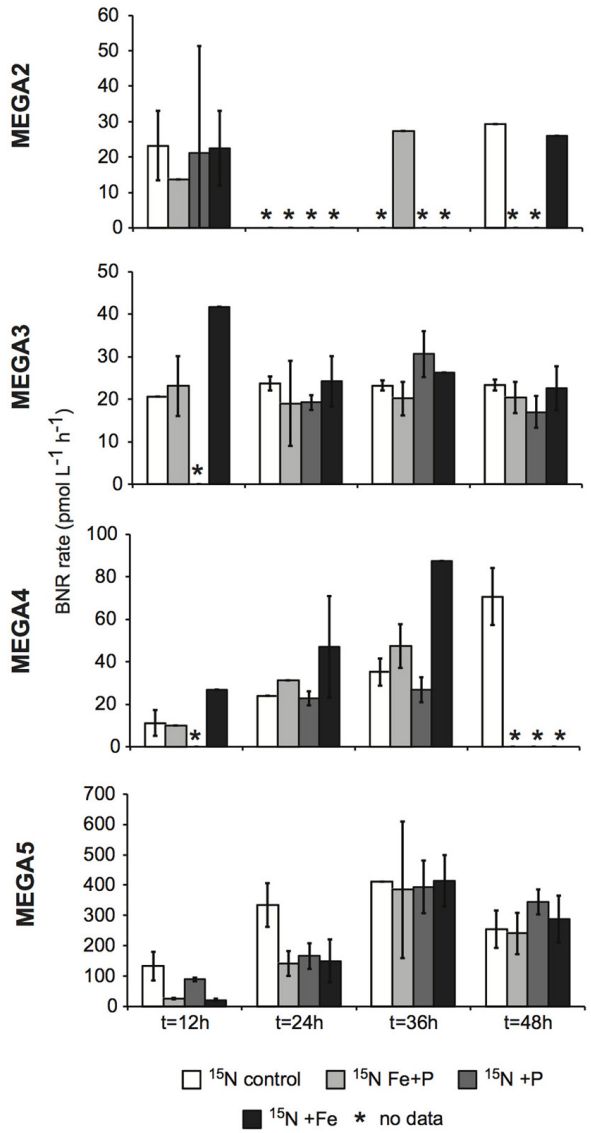

FIGURE 6 | Biological N_2 fixation rates associated with the <10 μm size-fraction in response to nutrient additions in the MEGA experiments. BNF rates were measured using the $^{15}N_2$ tracer method. Error bars indicate the standard deviation for two replicates, where possible. Missing data is marked with an asterisk (*). Note the different scales used for the y-axis.

Table 3 | Size-fractionated *Trichodesmium nifH* qPCR results from natural populations along this cruise track from 5 m DNA samples reported in (Goebel et al., 2010), and estimated BNF fixation rates associated with disrupted *Trichodesmium* colonies measured as part of the small size fraction.

Station	*Tricho. nifH* copies L^{-1} <10 μm fraction	*Tricho. nifH* copies L^{-1} >10 μm fraction	*Tricho. nifH* copies L^{-1} Σ	Estimated BNF rate (pmol L^{-1} d^{-1}) of disrupted *Tricho.* in <10 μm fraction
6	1.2E + 04	3.6E + 05	3.8E + 05	238
8	4.8E + 02	1.8E + 05	1.8E + 05	10
9	2.1E + 01	1.5E + 03	1.6E + 03	0
10*	0.0E + 00	1.6E + 03	1.6E + 03	0
13	2.9E + 02	3.1E + 03	3.4E + 03	6
14	1.0E + 00	2.1E + 02	2.1E + 02	0
17	5.4E + 03	4.3E + 04	4.8E + 04	107
20	1.4E + 03	2.0E + 05	2.0E + 05	29
21	6.1E + 04	1.1E + 06	1.2E + 06	1216
22	nm	nm	na	na
23	1.2E + 04	nm	1.2E + 04	240

The assumed cell specific N_2 fixation rate is 20 fmol N $cell^{-1}$ hr^{-1} (Capone, 2001), and it is assumed that single Trichodesmium filaments and colonies have the same cell-specific rates. Station 10 (*) data is reported from 30 m depth. Abbreviations: Tricho., Trichodesmium; nm, not measured; na, not applicable.

visually documented the breakage of *Trichodesmium* filaments in the filtration process (Letelier and Karl, 1996), an observation consistent with the reported detection of *Trichodesmium nifH* in the small size fraction using qPCR-based approaches (Zehr et al., 2007; Moisander et al., 2008). Goebel et al. (2010) conducted qPCR analysis of both size fractions on the natural population of *Trichodesmium* along this cruise track, and reported abundances as the combined total of both size fractions. In surface waters (5 m) at Station 17, 11% of the total *nifH* copies L^{-1} were found in the small size-fraction (5.4×10^3 out of a total of 4.8×10^4 *nifH* copies L^{-1}; **Table 3**). If the detection of *Trichodesmium nifH* in the 0.2–10 μm fraction results from disrupted colonies that were fixing N at previously reported cell-specific rates (20 fmol N $cell^{-1}$ h^{-1}; Capone, 2001), and that the same disruption effect occurred in the filtration for rate measurements, it follows that the cells captured in this size fraction would appear to have incorporated $^{15}N_2$ at a rate of approximately 100 pmol L^{-1} h^{-1}, which could account for the measured rates (**Table 3**), despite this N actually being fixed in the >10 μm community.

MEGA5

MEGA5 was the only nutrient amendment experiment conducted in Amazon Plume-influenced waters (Station 21). *Trichodesmium* dominated the diazotrophic community in this experiment (8.2×10^6 *nifH* copies L^{-1}), although UCYN-B, RR and HR were also present in abundances on the order of 10^3 *nifH* copies L^{-1} (**Figure 5**). UCYN-A was not detected in qPCR assays at time zero, but was present in the Fe treatment at $t = 48$ h, however, no UCYN-A *nifH* transcripts were detected in this experiment. Both UCYN-B and *Trichodesmium nifH* expression was stimulated with respect to control treatments in Fe+P and Fe treatments (**Figure 4**). Nutrient amendments did not appear to stimulate *nifH* expression in RR or HR. Although stimulation of UCYN-B *nifH* expression in Fe and Fe+P treatments was not reflected in the BNF rates, it is notable that the highest BNF rates in this study were measured from this experiment, reaching as high as 400 pmol L^{-1} h^{-1} (**Figure 6**). As described above for MEGA4, based on the high abundances of *Trichodesmium* in time zero samples, the most likely explanation

is that colonies or single *Trichodesmium* filaments were disrupted during filtration and captured on the GF/F filter as part of the small size fraction. Estimated BNF rates based on the *Trichodesmium nifH* qPCR analysis of the small size-fraction in the natural population of *Trichodesmium* (Goebel et al., 2010), using assumptions described above and in **Table 3**, support this hypothesis.

DISCUSSION

DIEL *nifH* GENE EXPRESSION AND BNF RATES IN NATURAL POPULATIONS OF CYANOBACTERIA

This is the first study to quantify daytime and nighttime *nifH* expression of key cyanobacterial phylotypes in the natural populations of diazotrophs in the TNAtl. This builds upon, and is complementary to, the *nifH* gene-based abundances for these same phylotypes reported by Goebel et al. (2010). Gene expression provides information on the activity or physiological status of cells, since detection of transcripts implies active gene transcription. Although the expression of *nifH* cannot be directly linked to N-limitation or active N_2 fixation, transcripts are not long-lived, thus detection of *nifH* transcripts indicates the organisms are alive, and that they are regulating expression of the nitrogenase operon.

Trichodesmium nifH transcripts comprised a majority of the total *nifH* transcript pool quantified in this study, and were the most abundant transcript (by many orders of magnitude) measured at five out of the eight stations (**Figure 2**). This study provides further evidence that *Trichodesmium* is the most widespread diazotroph in this ocean basin. However, another important outcome of this study is that *nifH* gene-based abundances do not always predict which diazotroph is actively transcribing *nifH* (and presumably fixing N_2), as discussed above.

Trichodesmium consistently had low normalized *nifH* transcripts (<10 *nifH* transcripts N_2-fixing cell^{-1}; **Figure 3**), and it is unclear whether this reflects the TNAtl *Trichodesmium* population, or is an artifact of sampling times or extraction techniques. The ratio of *Trichodesmium nifH* transcripts to *nifH* gene-based abundances was also generally low in a study conducted south of this study site in the East Equatorial Atlantic (Foster et al., 2007), which utilized similar DNA/RNA extraction, cDNA generation and RT-qPCR techniques. In contrast, in two studies from the North Pacific Subtropical Gyre, normalized *nifH* transcripts were measured as high as 10^2–10^3 *nifH* transcripts per *nifH* gene copy (Church et al., 2005; Zehr et al., 2007). These two studies used a different DNA extraction technique, making direct comparisons to this study difficult. More importantly, however, the diel sampling resolution in Church et al. (2005) was much greater, and it is clear that in the North Pacific Subtropical Gyre, normalized *nifH* transcripts are >10 *nifH* cDNA copies gene copy^{-1} roughly between 04:00 and noon (local time), and vary over a 72-h period. A more high-resolution diel sampling scheme with TNAtl populations is ultimately needed to inform our interpretations, but it is reasonable to assume that that the peak of *nifH* transcription in *Trichodesmium* occurred in the early morning and was missed due to the sampling scheme.

BNF rates associated with the <10 μm size-fraction are not commonly measured. Using complementary methods in the South Pacific, Moisander et al. (2010) reported maximum BNF rates associated with environmental samples dominated by UCYN-A and UCYN-B of 4500 pmol L^{-1} h^{-1}, and 26 pmol L^{-1} h^{-1}, respectively. Kitajima et al. (2009) also measured significantly higher rates associated with the small size-fraction in the Western North Pacific (between 42–541 pmol L^{-1} h^{-1}), but these numbers were acquired using the acetylene reduction assay, thus are considered gross N_2 fixation rates, rather than net N_2 fixation rates, like those measured by the $^{15}N_2$ gas tracer method.

There are two important sources of underestimation in the BNF measurements reported in this and other studies. First, the amount of ^{15}N incorporated into particulate N in the small size fraction was determined using the material captured on a GF/F filter, after being prefiltered using a 10 μm filter. Therefore the BNF rates reported are associated with organisms between 0.7 μm and 10 μm, while the *nifH* abundance and expression data includes microorganisms as small as 0.2 μm. Our best estimates for the diameter of a UCYN-A cell is 0.62 ± 0.17 μm (Thompson et al., 2012) and there is no reason to assume that the UCYN-A present in this study remained attached to it's recently identified picoeukaryote host (see "discussion" below), therefore it is likely that some of the ^{15}N-labeled particluate N fixed by UCYN-A passed through the GF/F filter. Despite this discrepency, using GF/F filters remains a standard technique in this field, even in studies that endeavor to compare these measurements to the abundance of unicellular diazotrophs (e.g., Bonnet et al., 2009; Sohm et al., 2011; Großkopf et al., 2012; Halm et al., 2012).

The second source of underestimation is evidenced in a series of recent studies that report a significant and variable underestimation of BNF rates measured using the $^{15}N_2$ gas tracer method resulting from the slow dissolution of gaseous $^{15}N_2$ into the water phase (Mohr et al., 2010; Großkopf et al., 2012; Wilson et al., 2012). According to Mohr et al. (2010), based on results from experiments using *Crocosphaera* cultures, the most extreme underestimation of BNF rates using the $^{15}N_2$ gas tracer technique occurs if the spike of $^{15}N_2$ gas is initiated just as an organism is beginning to fix N_2. Thus, $^{15}N_2$ gas introduction in the early morning may most egregiously underestimate BNF rates associated with *Trichodesmium*, UCYN-A, HR, and RR which fix N_2 during daylight hours while BNF rates associated with UCYN-B will be most compromised by $^{15}N_2$ gas introduction in the late evening. Furthermore, there is some evidence that in natural communities where unicellular cyanobacteria or heterotrophs are the most abundant diazotrophs, the degree of underestimation of BNF rates is far greater than when *Trichodesmium* is the most abundant diazotroph, possibly as a result of different buoyancies (Großkopf et al., 2012).

The current study was conducted prior to the findings of Mohr et al. (2010), and without performing parallel bubble and dissolved seawater incubations, such as those in Wilson et al. (2012) and Großkopf et al. (2012), it is impossible to address the degree to which the BNF rates reported in this study are underestimated. However, it is reasonable to assume that BNF rates measured at Stations 9 and 10, where unicellular cyanobacterial transcripts dominated the *nifH* expression (**Figure 2**), are most heavily underestimated. At Stations 9 and 10, $^{15}N_2$ gas introduction in the rate incubations occurred at 14:50 and 04:30,

respectively (**Table 2**). Therefore, at both stations the timing of the gas introduction likely resulted in a significant underestimate of the BNF rate associated with UCYN-B (Station 9) and UCYN-A (Station 10), which may have impacted the overall BNF rate, presented here as an hourly average over a 24 h period.

MEGA EXPERIMENTS INDICATE THAT FE AND P LIMITATIONS ON DIAZOTROPHY ARE SPATIALLY HETEROGENEOUS AND PHYLOTYPE-SPECIFIC

The MEGA experiments are among the first to investigate the response of a natural assemblage of marine microorganisms to the addition of limiting nutrients by quantifying changes in functional gene expression (using RT-qPCR). Similar experiments have been conducted to study the response of diazotrophs to inorganic P additions in the oligotrophic North Pacific (Zehr et al., 2007) and the Great Barrier Reef (Hewson et al., 2007), but this is the first study to focus on *nifH* expression in the diazotrophic population in the TNAtl, and to use trace-metal clean techniques so that Fe responses could be investigated. Although there are several recent examples of using high throughput sequencing or microarray techniques to analyze the (meta)transcriptional responses of communities of marine microorganisms to experimental manipulations (e.g., Smith et al., 2010; Shi et al., 2011), these approaches are currently limited in the qualitative nature of their data.

It is important to note that one underlying assumption of the MEGA experiments is that the diazotrophs were actively regulating the *nif* operon—an assumption that is supported by the measurement of *nifH* transcripts in the natural diazotroph assemblage (discussed above) and in time zero samples. Although 48 h incubations may not be long enough to regularly see shifts in diazotroph abundances (via qPCR) or stimulation of BNF rates, it is assumed that the changes in *nifH* expression (via RT-qPCR) that might result from P, Fe, or Fe+P additions are possible because the community is N-limited overall and that diazotrophs are active but might be experiencing either P- or Fe-stress. Conversely, measuring no response in *nifH* expression during the course of a treatment might ultimately mean that the phylotype was not N-limited at the time, in addition to not being P- and/or Fe-limited.

The MEGA experiments revealed a distinct spatial pattern of *nifH* expression response to Fe, P, and Fe+P amendments, with Fe limitation of *nifH* expression in the western basin of the TNAtl, and P limitation of the unicellular diazotrophs in the eastern basin. This appears to contradict the findings of Sohm et al. (2008), who reported the quickest turnover of the P pool in the western part of the basin, which is considered a proxy for P-limitation. This contradiction may be reflective of the differences between nutrient limitation for the microbial community as a whole and that of a specific taxonomic group, like the diazotrophs. In addition to this spatial trend, there appear to be phylotype-specific responses, which strongly suggests that P and Fe (co-)limitation of diazotrophy is extremely heterogeneous on short time scales. Furthermore, over the time scale of these experiments, stimulation of BNF rates associated with the $<10\,\mu$m size fraction and increases in diazotroph abundances were rarely measured, implying that diazotroph abundances are slow to respond to changing nutrient conditions. It is important to note however, that the above discussion of underestimation in these rate measurements due to the use of GF/F filters and the $^{15}N_2$ gas tracer method, are applicable to the MEGA experiments as well. A summary of the MEGA experimental results can be found in **Table 4**.

nifH expression responses to Fe/P additions in unicellular diazotrophs UCYN-A and UCYN-B

One of the most unexpected results of these nutrient amendment experiments is that increases of *nifH* expression in UCYN-A were observed only in P treatments. Fe additions did not

Table 4 | Synthesis of MEGA experimental results, indicating the nutrient stress conditions that can be inferred.

	MEGA1				MEGA2				MEGA3				MEGA4				MEGA5			
	Present[a]	Active N-fix[b]	Fe-response[c]	P-response[d]	Present[a]	Active N-fix[b]	Fe-response[c]	P-sesponse[d]	Present[a]	Active N-fix[b]	Fe-response[c]	P-response[d]	Present[a]	Active N-fix[b]	Fe-response[c]	P-sesponse[d]	Present[a]	Active N-fix[b]	Fe-response[c]	P-response[d]
UCYN-A	+	nd	nd	nd	+	+	−	+	+	+	−	+	−	nd	nd	nd	−	nd	nd	nd
UCYN-B	−	+	+[e]	−	+	+	na[e]	na[e]	−	na[e]	−	+	−	nd	nd	nd	+	na[e]	+	−
Tricho.	+	+	−	−	+	+	+	+	+	+	+	+	+	+	+	+	+	−	+	−
RR	+	−	+	−	−	−	+	+	+	−	+	+[f]	+	−	+	−	+	−	−	−
HR	+	+	−	−	+	+	+	+	+	−	−	+	−	nd	nd	nd	+	+	−	+

"+" Indicates that the phylotype was present or exhibiting the specified response; "−" Indicates that the phylotype was not present or no response was detected. Abbreviations: nd, nifH expression not detected; na, not applicable (UCYN-B nifH expression during the day).

[a] Detection of nifH from phylotype in DNA (qPCR) at time zero.

[b] Detection of expression of nifH from phylotype (RT-qPCR) at time zero.

[c] Increased expression of nifH from phylotype (RT-qPCR) at time zero with respect to the control upon addition of Fe.

[d] Increased expression of nifH from phylotype (RT-qPCR) at time zero with respect to the control upon addition of P.

[e] Sample collected during the day.

[f] Expression response at night.

stimulate the expression of *nifH* in UCYN-A, despite having stimulatory effects for other diazotrophs in the same samples (e.g., *Trichodesmium* in MEGA2 and MEGA3; **Figure 4**). There were detectable (0.74 ± 0.01 nM) concentrations of Fe in surface waters at nearby Station 13 at the time of MEGA3 (Goebel et al., 2010), and it is reasonable to assume that UCYN-A was able to fulfill its Fe demands with this ambient Fe in the first 24 h. Nonetheless, these findings raise interesting questions about the specific Fe demands and acquisition strategies of UCYN-A, especially given that *Trichodesmium* appears to be co-limited by Fe and P in this experiment (see "discussion" below). The two experiments where UCYN-A *nifH* expression response to P treatments (MEGA2 and MEGA3) were conducted in waters where concentrations of soluble reactive P (SRP) were low (<25 nM), while DOP was much higher (>200 nM) (Sohm et al., 2008), which may play a role in the apparent P-limitation of UCYN-A N_2 fixation in these waters. Analysis of the recently sequenced genome of UCYN-A (Tripp et al., 2010) revealed that UCYN-A lacks important genes required for the hydrolysis of organic phosphates (compounds with a C-O-P bond) and utilization of phosphonates (compounds with a C-P bond), such as alkaline phosphatase (*phoA*), and genes in the phosphonate lyase pathway (*phnC-P*), therefore, based on our current understanding of this organism, it appears unlikely that UCYN-A is able to directly utilize components of the DOP pool. However, there is now evidence that UCYN-A forms a mutualistic association with a unicellular picoeukaryote prymnesiophyte (Thompson et al., 2012), and it is now unclear whether UCYN-A has a free-living state, thus the potential relevance of UCYN-As metabolic strategies (or lack there-of) is complicated by the paucity of information about the nature of this association, and the Fe and P acquisition strategies and requirements of its prymnesiophyte partner. In spite of these unknowns, observations from MEGA3 support the possibility that the UCYN-A/prymnesiophyte symbiosis, may have a competitive advantage in low SRP water, and may be able to outcompete *Trichodesmium*, RR and HR for inputs of inorganic P in the short term.

In MEGA1 and MEGA5, both conducted in the western part of the TNAtl basin, there was no indication that P availability had an impact on nitrogenase activity in UCYN-B. In contrast, UCYN-B *nifH* expression appeared to be responsive solely to the addition of Fe (**Figure 4**). At Station 21 (MEGA5), due to the influence of the Amazon River plume, the concentration of SRP was ∼60 nM, which was among the highest measured concentrations by Sohm et al. (2008) during this cruise. It therefore seems likely that high SRP concentrations in surface waters were fulfilling the P demands of UCYN-B, driving N_2 fixation in UCYN-B to Fe-limitation (despite concentrations of Fe in surface waters of 1.89 ± 0.03 nM; Goebel et al., 2010), which was relieved upon the addition of Fe.

It is less evident what factors might play a role in the stimulation of UCYN-B *nifH* expression by Fe at Station 6 (MEGA1), but Sohm et al. (2008) did report high concentrations of DOP along the northern leg of this cruise track, including Station 6. Although little is known about the exact chemical composition of the DOP pool, it is likely comprised partially of phosphomonoesters. Based on observations made from the genome analysis of a cultivated strain of UCYN-B, *Crocosphaera watsonii* WH8501, it is clear that at least some strains of UCYN-B have the genetic capability to utilize these compounds as a P source (Dyhrman and Haley, 2006), which may explain why *nifH* expression in UCYN-B responded to Fe, not P additions in MEGA1. It is important to note that this Fe stimulation was seen in samples taken during the daytime, and UCYN-B is known transcribe *nifH* at highest rates during the night.

However, like UCYN-A, *nifH* expression in UCYN-B is stimulated by the addition of P, and not Fe, in the easternmost experiment (MEGA3), despite comparable concentrations of DOP in these waters. This stimulation of *nifH* expression in UCYN-A and UCYN-B is reflected in the BNF rates measured in the small size-fraction, where a small increase time-averaged over the first 36 h is measured (**Figure 6**). It is possible that the differences in UCYN-B response between Station 6 and Station 14 are a result of different DOP pool compositions, or even strain differences in UCYN-B across the ocean basin not detected using the *nifH* qPCR assay, which broadly targets cultivated *Crocosphaera* strains and many environmental phylotypes characterized using degenerate *nifH* PCRs, but may not capture all phylotypes.

Although it was rare to observe *nifH*-based abundances of these diazotrophs increase throughout the duration of these experiments, UCYN-B increased in population size between time zero and $t = 36/48$ h samplings in all of the MEGA experiments in which it was detected (MEGA1–3 and MEGA5; **Figure 5**). In some experiments, growth was seen in different treatments than those where *nifH* expression was stimulated (e.g., MEGA5, **Figures 4**, **5**) or where no *nifH* expression was observed at all (e.g., MEGA2, **Figures 4**, **5**). The observation of decoupled growth and *nifH* expression might be explained by UCYN-B preferentially growing on other N sources, and/or natural grazing of UCYN-B being suppressed with respect to the other diazotrophs.

nifH expression responses to Fe/P additions in Trichodesmium

Like UCYN-B, *nifH* expression in *Trichodesmium* exhibited distinct spatial patterns in response to Fe, P, and Fe+P additions. In the Amazon River plume influenced experiment, MEGA5, *nifH* expression was stimulated in Fe and Fe+P treatments, while at Station 9 (MEGA2) the most prominent response in *nifH* expression was seen in the P treatments. Furthermore, *Trichodemsium* exhibited potential co-limitation of N_2 fixation in the eastern (MEGA3) and in equatorial waters (MEGA4).

This is the first study that directly documents the Fe-limitation of N_2 fixation activity in natural populations of *Trichodesmium* in the Amazon River plume using molecular techniques to our knowledge. Work by Webb et al. (2007) in the western Atlantic, showed stimulation of N_2 fixation by the addition of dissolved inorganic P, not Fe. Together with the lack of evidence of extreme Fe deficiency (as evidenced by the production of an Fe deficiency protein, *IdiA*), they concluded that P-limitation of diazotrophy was in effect in this region. However, this study also documented heterogeneity in *Trichodemsium* P-stress responses, potentially

explained by observations that P-stress was rarely observed in colonies with "tuft" morphologies.

As discussed above, results from MEGA3 indicate that there was a delay in *Trichodesmium nifH* expression response to the input of inorganic P, as *nifH* expression at the $t = 24$ h sampling was lower in the three treatments than in the control. In the $t = 48$ h sampling, however, response was seen in all three treatments, with the greatest response in the Fe+P treatment (**Figure 4**). This may be, in part, a function of the ability of *Trichodesmium* colonies to physically acquire P, which have a much larger cell to volume ratio and diffusive boundary layer thickness than UCYN-A/prymnesiophyte symbiont cells, which may drive diffusion limitation of nutrient acquisition, an effect that has been demonstrated to be an underlying factor in phytoplankton size distributions in the oligotrophic ocean (Chisholm, 1992).

Trichodesmium was the dominant diazotroph in the only equatorial upwelling waters sampled (Station 17); it was present at relatively high abundances at time zero samples in MEGA4 (1.7×10^5 *nifH* copies L^{-1}), and active diel expression was measured in corresponding samples (**Figure 3**). However, *Trichodesmium nifH* expression showed a significant response to all treatments (Fe, $p = 0.002$; P, $p = 0.004$, and Fe+P, $p = 0.001$), and appeared to be co-limited by P and Fe at this station as well (**Figure 4**). Inorganic P concentrations were high in surface waters at Station 17 (**Table 2**; and Sohm et al., 2008) due to upwelling, so the fact that *Trichodesmium nifH* expression was stimulated in the P and Fe+P treatment is unexpected, although it is important to note that the *nifH*-based abundances imply that growth was limited by Fe availability (**Figure 5**).

nifH expression responses to Fe/P additions in RR and HR

Despite the presence of RR in four of the five MEGA experiments (as determined via *nifH* qPCR at time zero; **Figure 5**), the data available indicate that it was not actively regulating the *nif* operon at the onset of most of these experiments. MEGA1 is the only experiment where no inferences can be made about the starting condition of the RR population, as time zero samples were taken at night, and no complementary data is available for the diel *nifH* expression of RR at this station. Over the course of these experiments, however, the expression of *nifH* was often measured in some or all of the treatments, indicating that RR began to transcribe the *nif* operon in the bottles. In Amazon Plume influenced waters (MEGA5), the RR population begins to express *nifH* in some of the treatments, but did not appear to be limited by Fe or P. In MEGA1, this onset of *nifH* expression was coupled to Fe-stress, and to P-stress in MEGA2. Like *Trichodesmium*, there is some indication that RR might be experiencing co-limitation of Fe+P in MEGA 3, as Fe and P additions alone did not result in an increase in *nifH* expression. In contrast, the natural population of HR was more likely to actively transcribing *nifH* than RR, as evidenced by detection of *nifH* samples in time zero samples, and in the natural diazotoph assemblage at Station 9 and Station 22 (**Figures 4** and **2**).

There is very little known about the Fe and P acquisition strategies and requirements of *Richelia* strains associated with either *R. clevi* or *H. hauckii*, and though these experiments provide some insight into the nutrient-stressed state of these populations in the TNAtl, further research is required to understand the metabolic potential of *Richelia* to use P-compounds, its Fe requirements, and the extent to which its diatom host impacts these requirements.

CONCLUSIONS

This study is the first to report the daytime and nighttime *nifH* expression in natural populations of diazotrophs in the TNAtl, and for the most part, the dominant diazotrophs characterized by Goebel et al. (2010) were predictive of which organisms were actively regulating the *nif* operon at each of the stations measured. However, it is important to note that there were exceptions, and in those cases, DNA-based approaches alone would have not predicted which phylotypes were actively expressing *nifH*, thus likely fixing N_2.

This is also one of the first studies to quantify the expression of a target gene in response to nutrient amendments within complex microbial assemblages in the marine environment. These findings indicate that gene expression can be used as a measure of changes in the activity of a community, especially over short timescales where changes in biomass are not expected. In the TNAtl, the MEGA experiments not only revealed that cyanobacterial diazotrophs within a single community can sometimes respond differently to the same nutrient amendment, which emphasizes the importance of the metabolic capabilities of the individual organisms, but also that diazotrophs in the western region of the TNAtl responded primarily to Fe additions, while responding primarily to P additions in eastern waters. Further research is required to understand whether this phenomena exists year round, or whether it is heavily influenced by the seasonality of the Amazon River flow, to what extent these diazotrophs are actually experiencing P or Fe limitation and/or starvation, and to what extent the availability of Fe and different P compounds drive the diazotrophic community structure in the TNAtl. However, these findings underscore the importance of understanding the diazotroph community structure when considering whether a region is Fe or P limited.

ACKNOWLEDGMENTS

The authors would like to acknowledge the captain and crew of the R/V Seward Johnson for their support during SJ0609, Dr. Mak Saito and his research group for providing support with trace metal clean procedures and supplies, and members of the Zehr Lab including Amanda Morrison, Ryan Paerl, Katie London, Irina Shilova (formerly Ilichyan), and Mary Hogan for their valuable support in collecting samples and discussions during the writing of this manuscript. We also thank Jason Landrum, Samantha Allen, Julie Gonzalez, Bibiana Garcia, and other members of the Montoya Lab for their assistance with the nutrient and N_2-fixation assays. This study was supported by the Gordon and Betty Moore Foundation Marine Microbiology Initiative and by award OCE0425363 (Jonathan P. Zehr) and OCE0425583 (Joseph P. Montoya) from the National Science Foundation.

REFERENCES

Berman-Frank, I., Quigg, A., Finkel, Z. V., Irwin, A. J., and Haramaty, L. (2007). Nitrogen-fixation strategies and Fe requirements in cyanobacteria. *Limnol. Oceanogr.* 52, 2260–2269.

Bonnet, S., Biegala, I. C., Dutrieux, P., Slemons, L. O., and Capone, D. G. (2009). Nitrogen fixation in the western equatorial Pacific: rates, diazotrophic cyanobacterial size class distribution, and biogeological significance. *Global Biogeochem. Cycles* 23, GB3012.

Capone, D. G. (2001). Marine nitrogen fixation: what's the fuss? *Curr. Opin. Microbiol.* 4, 341–348.

Chisholm, P. (1992). "Phytoplankton size," in *Primary Productivity and Biogeochemical Cycles in the Sea,* eds P. G. Falkowski and A. D. Woodhead (New York, NY: Plenum Press), 213–237.

Church, M. J., Jenkins, B. D., Karl, D. M., and Zehr, J. P. (2005). Vertical distributions of nitrogen-fixing phylotypes at Stn ALOHA in the oligotrophic North Pacific Ocean. *Aquat. Microb. Ecol.* 38, 3–14.

Church, M. J., Short, C. M., Jenkins, B. D., Karl, D. M., and Zehr, J. P. (2005). Temporal patterns of nitrogenase gene (*nifH*) expression in the oligotrophic North Pacific Ocean. *Appl. Environ. Microbiol.* 71, 5362–5370.

Dyhrman, S. T., Chappell, P. D., Haley, S. T., Moffett, J. W., Orchard, E. D., Waterbury, J. B., et al. (2006). Phosphonate utilization by the globally important marine diazotroph *Trichodesmium*. *Nature* 439, 68–71.

Dyhrman, S. T., and Haley, S. T. (2006). Phosphorus scavenging in the unicellular marine diazotroph *Crocosphaera watsonii*. *Appl. Environ. Microbiol.* 72, 1452–1458.

Dyhrman, S. T., Haley, S. T., Birkeland, S. R., Wurch, L. L., Cipriano, M. J., and McArthur, A. G. (2006). Long serial analysis of gene expression for gene discovery and transcriptome profiling in the widespread marine coccolithophore *Emiliania huxleyi*. *Appl. Environ. Microbiol.* 72, 252–260.

Foster, R. A., Subramaniam, A., Mahaffey, C., Carpenter, E. J., Capone, D. G., and Zehr, J. P. (2007). Influence of the Amazon River plume on distributions of free-living and symbiotic cyanobacteria in the western tropical north Atlantic Ocean. *Limnol. Oceanogr.* 52, 517–532.

Foster, R. A., Subramaniam, A., and Zehr, J. P. (2009). Distribution and activity of diazotrophs in the Eastern Equatorial Atlantic. *Environ. Microbiol.* 11, 741–750.

Foster, R. A., and Zehr, J. P. (2006). Characterization of diatom-cyanobacteria symbioses on the basis of *nifH*, *hetR*, and 16S rRNA sequences. *Environ. Microbiol.* 8, 1913–1925.

Goebel, N. L., Turk, K. A., Achilles, K. M., Paerl, R., Hewson, I., and Morrison, A. E. (2010). Abundance and distribution of major groups of diazotrophic cyanobacteria and their potential contribution to N_2 fixation in the tropical Atlantic Ocean. *Environ. Microbiol.* 12, 3272–3289.

Gómez, F., Furuya, K., and Takeda, S. (2005). Distribution of the cyanobacterium *Richelia intracellularis* as an epiphyte of the diatom *Chaetoceros compressus* in the western Pacific Ocean. *J. Plankton Res.* 27, 323–330.

Großkopf, T., Mohr, W., Baustiam, T., Schunck, H., Gill, D., and Kuypers, M. M. M. (2012). Doubling of marine dinitrogen-fixation rates based on direct measurements. *Nature* 488, 361–364.

Gruber, N., and Galloway, J. N. (2008). An Earth-system perspective of the global nitrogen cycle. *Nature* 451, 293–296.

Gruber, N., and Sarmiento, J. L. (1997). Global patterns of marine nitrogen fixation and denitrification. *Global Biogeochem. Cycles* 11, 235–266.

Halm, H., Lam, P., Ferdelman, T. G., Lavik, G., Dittmar, T., and LaRoche, J. (2012). Heterotrophic organisms dominate nitrogen fixation in the South Pacific Grye. *ISME J.* 6, 1238–1249.

Hewson, I., Moisander, P. H., Morrison, A. E., and Zehr, J. P. (2007). Diazotrophic bacterioplankton in a coral reef lagoon: phylogeny, diel nitrogenase expression and response to phosphate enrichment. *ISME J.* 1, 78–91.

Kitajima, S., Furuya, K., Hashihama, F., Takeda, S., and Kanda, J. (2009). Latitudinal distribution of diazotrophs and their nitrogen fixation in the tropical and subtropical western North Pacific. *Limnol. Oceanogr.* 54, 537–547.

Langlois, R. J., Hummer, D., and LaRoche, J. (2008). Abundances and distributions of the dominant *nifH* phylotypes in the Northern Atlantic Ocean. *Appl. Environ. Microbiol.* 74, 1922–1931.

Letelier, R. M., and Karl, D. M. (1996). Role of *Trichodesmium* spp. in the productivity of the subtropical North Pacific Ocean. *Mar. Ecol. Prog. Ser.* 133, 263–273.

Mills, M. M., Ridame, C., Davey, M., La Roche, J., and Geider, R. J. (2004). Iron and phosphorus co-limit nitrogen fixation in the eastern tropical North Atlantic. *Nature* 429, 292–294.

Mohr, W., Grosskopf, T., Wallace, D. W. R., and LaRoche, J. (2010). Methodological underestimation of oceanic nitrogen fixation rates. *PLoS ONE* 5:e12583. doi: 10.1371/journal.pone.0012583

Moisander, P. H., Beinart, R. A., Hewson, I., White, A. E., Johnson, K. S., and Carlson, C. A. (2010). Unicellular cyanobacterial distributions broaden the oceanic N_2 fixation domain. *Science* 327, 1512–1514.

Moisander, P. H., Beinart, R. A., Voss, M., and Zehr, J. P. (2008). Diversity and abundance of diazotrophic microorganisms in the South China Sea during intermonsoon. *ISME J.* 2, 954–967.

Montoya, J. P. (2008). "Nitrogen stable isotopes in marine environments," in *Nitrogen in the Marine Environment, 2nd Edn.* eds D. Capone, E. Carpernter, and M. Mulholland (Burlington, MA: Academic Press), 1277–1302.

Montoya, J. P., Voss, M., Kahle, P., and Capone, D. G. (1996). A simple, high-precision, high-sensitivity tracer assay for N_2 fixation. *Appl. Environ. Microbiol.* 62, 986–993.

Moore, C. M., Mills, M. M., Achterberg, E. P., Geider, R. J., LaRoche, J., and Lucas, M. I. (2009). Large-scale distribution of Atlantic nitrogen fixation controlled by iron availability. *Nat. Geosci.* 2, 867–871.

Mulholland, M. R., Bernhardt, P. W., Heil, C. A., Bronk, D. A., and O'Neil, J. M. (2006). Nitrogen fixation and release of fixed nitrogen by *Trichodesmium* spp. in the Gulf of Mexico. *Limnol. Oceanogr.* 51, 1762–1776.

Sanudo-Wilhelmy, S. A., Kustka, A. B., Gobler, C. J., Hutchins, D. A., Yang, M., and Lwiza, K. (2001). Phosphorus limitation of nitrogen fixation by *Trichodesmium* in the central Atlantic Ocean. *Nature* 411, 66–69.

Shi, T., Ilikchyan, I. N., Rabouille, S., and Zehr, J. P. (2010). Genome-wide analysis of diel gene expression in the unicellular N_2-fixing cyanobacterium *Crocosphaera watsonii* WH (8501). *ISME J.* 4, 621–632.

Shi, Y., Tyson, G. W., Eppley, J. M., and DeLong, E. F. (2011). Integrated metatranscriptomic and metagenomic analyses of stratified microbial assemblages in the open ocean. *ISME J.* 5, 999–1013.

Smith, M. W., Herfort, L., Tyrol, K., Suciu, D., Campbell, V., and Crump, B. C. (2010). Seasonal changes in bacterial and archaeal gene expression patterns across salinity gradients in the Columbia River coastal margin. *PLoS ONE* 5:e13312. doi: 10.1371/journal.pone.0013312

Sohm, J. A., Hilton, J. A., Noble, A. E., Zehr, J. P., Saito, M. A., and Webb, E. A. (2011). Nitrogen fixation in the South Atlantic Gyre and the Benguela Upwelling System. *Geophys. Res. Lett.* 38, L16608.

Sohm, J. A., Mahaffey, C., and Capone, D. G. (2008). Assessment of relative phosphorus limitation of *Trichodesmium* spp. in the North Pacific, North Atlantic, and the north coast of Australia. *Limnol. Oceanogr.* 53, 2495–2502.

Thompson, A. W., Foster, R. A., Krupke, A., Carter, B. J., Musat, N., and Vaulot, D. (2012). Unicellular cyanobacterium symbiotic with a single-celled Eukaryotic alga. *Science* 337, 1546–1550.

Tripp, H. J., Bench, S. R., Turk, K. A., Foster, R. A., Desany, B. A., and Niazi, F. (2010). Metabolic streamlining in an open ocean nitrogen-fixing cyanobacterium. *Nature* 464, 90–94.

Turk, K. A., Rees, A. P., Zehr, J. P., Pereira, N., Swift, P., and Shelley, R. (2011). Nitrogen fixation and nitrogenase (*nifH*) expression in tropical waters of the eastern North Atlantic. *ISME J.* 5, 1201–1212.

Voss, M., Croot, P., Lochte, K., Mills, M., and Peeken, I. (2004). Patterns of nitrogen fixation along 10N in the tropical Atlantic. *Geophys. Res. Lett.* 31, L23S09.

Webb, E. A., Jakuba, R. W., Moffett, J. W., and Dyhrman, S. T. (2007). Molecular assessment of phosphorus and iron physiology in Trichodesmium populations from the western Central and western South Atlantic. *Limnol. Oceanogr.* 52, 2221–2232.

Wilson, S. T., Böttjer, D., Church, M. J., and Karl, D. M. (2012). Comparative assessment of nitrogen fixation methodologies, conducted in the oligotrophic North Pacific Ocean. *Appl. Environ. Microbiol.* 78, 6516–6523.

Zehr, J. P., Bench, S. R., Carter, B. J., Hewson, I., Niazi, F., and Shi, T.

(2008). Globally distributed uncultivated oceanic N_2-fixing cyanobacteria lack oxygenic photosystem II. *Science* 322, 1110–1112.

Zehr, J. P., Montoya, J. P., Jenkins, B. D., Hewson, I., Mondragon, E., and Short, C. M. (2007). Experiments linking nitrogenase gene expression to nitrogen fixation in the North Pacific subtropical gyre. *Limnol. Oceanogr.* 52, 169–183.

Conflict of Interest Statement: The authors declare that the research was conducted in the absence of any commercial or financial relationships that could be construed as a potential conflict of interest.

Received: 11 April 2012; accepted: 17 October 2012; published online: 02 November 2012.

*Citation: Turk-Kubo KA, Achilles KM, Serros TRC, Ochiai M, Montoya JP and Zehr JP (2012) Nitrogenase (nifH) gene expression in diazotrophic cyanobacteria in the Tropical North Atlantic in response to nutrient amendments. Front. Microbio. **3**:386. doi: 10.3389/fmicb.2012.00386*

This article was submitted to Frontiers in Aquatic Microbiology, a specialty of Frontiers in Microbiology.

frontiers in
MICROBIOLOGY

REVIEW ARTICLE
published: 19 October 2012
doi: 10.3389/fmicb.2012.00374

The sensitivity of marine N_2 fixation to dissolved inorganic nitrogen

Angela N. Knapp*

Rosenstiel School of Marine and Atmospheric Sciences, University of Miami, Miami, FL, USA

Edited by:
Bess B. Ward, Princeton University, USA

Reviewed by:
Scott D. Wankel, Harvard University, USA
Shawn R. Campagna, University of Tennessee, Knoxville, USA

****Correspondence:***
Angela N. Knapp, Rosenstiel School of Marine and Atmospheric Science, University of Miami, 4600 Rickenbacker Cswy, Miami, FL 33149, USA.
e-mail: aknapp@rsmas.miami.edu

The dominant process adding nitrogen (N) to the ocean, di-nitrogen (N_2) fixation, is mediated by prokaryotes (diazotrophs) sensitive to a variety of environmental factors. In particular, it is often assumed that consequential rates of marine N_2 fixation do not occur where concentrations of nitrate (NO_3^-) and/or ammonium (NH_4^+) exceed 1 μM because of the additional energetic cost associated with assimilating N_2 gas relative to NO_3^- or NH_4^+. However, an examination of culturing studies and *in situ* N_2 fixation rate measurements from marine euphotic, mesopelagic, and benthic environments indicates that while elevated concentrations of NO_3^- and/or NH_4^+ can depress N_2 fixation rates, the process can continue at substantial rates in the presence of as much as 30 μM NO_3^- and/or 200 μM NH_4^+. These findings challenge expectations of the degree to which inorganic N inhibits this process. The high rates of N_2 fixation measured in some benthic environments suggest that certain benthic diazotrophs may be less sensitive to prolonged exposure to NO_3^- and/or NH_4^+ than cyanobacterial diazotrophs. Additionally, recent work indicates that cyanobacterial diazotrophs may have mechanisms for mitigating NO_3^- inhibition of N_2 fixation. In particular, it has been recently shown that increasing phosphorus (P) availability increases diazotroph abundance, thus compensating for lower per-cell rates of N_2 fixation that result from NO_3^- inhibition. Consequently, low ambient surface ocean N:P ratios such as those generated by the increasing rates of N loss thought to occur during the last glacial to interglacial transition may create conditions favorable for N_2 fixation and thus help to stabilize the marine N inventory on relevant time scales. These findings suggest that restricting measurements of marine N_2 fixation to oligotrophic surface waters may underestimate global rates of this process and contribute to uncertainties in the marine N budget.

Keywords: N2 fixation, diazotroph, inhibition, sensitivity, nitrate, ammonium

INTRODUCTION

Phytoplankton growing in the sunlit surface ocean (euphotic zone) produce organic matter via photosynthesis at a rate of ~50 Pg C $year^{-1}$ (Westberry et al., 2008), and thus play an important role in the global carbon (C) cycle. However, phytoplankton growth in the euphotic zone is commonly limited by the availability of nutrients such as nitrogen (N); consequently, the processes that add and remove N to and from the ocean, respectively, influence the C cycle and thus climate. Unlike the physical processes that supply other biologically necessary elements like phosphorus (P) and iron (Fe) to the ocean (such as atmospheric deposition and fluvial inputs), the dominant process adding N to the ocean, di-nitrogen (N_2) fixation, is unique in that it is biologically mediated. While N_2 gas is unavailable to most organisms, certain groups of prokaryotes known as diazotrophs have the enzymatic ability to reduce dissolved N_2 to ammonium (NH_4^+) and assimilate it into their biomass. The ultimate fate of N in diazotrophic biomass is to be cycled into more bio-available forms, including nitrate (NO_3^-), that serve as the primary source of assimilative N for non-diazotrophic phytoplankton and bacteria in the ocean. In spite of the fundamental importance of N_2 fixation in the global C cycle and in supporting the base of the food web, the locations and rates of N_2 fixation in the ocean are poorly known.

Uncertainty in the rates of marine N_2 fixation contributes to ambiguity as to whether the modern marine N budget is balanced. Some estimates suggest that rates of N fluxes to the ocean only compensate for one third to one half of the fluxes of N out of the ocean (Codispoti et al., 2001; Codispoti, 2007), while constraints from paleoceanographic and modeling studies indicate that the marine N budget has been balanced to within ~10% over at least the Holocene (Brandes and Devol, 2002; Deutsch et al., 2004). Assuming that the marine N budget is essentially balanced, the discrepancy in N flux estimates requires that rates of marine N_2 fixation are underestimated and/or that rates of N loss are overestimated. The constraint of an approximately balanced marine N budget also implies that there are feedback mechanisms allowing N_2 fixation and denitrification, the dominant pathway by which N is lost from the ocean, to respond to each other on relatively short (i.e., ≤1000 years) timescales. Currently, both the size of the fluxes of N to and from the ocean, as well as the nature of potential feedback mechanisms that maintain a balanced marine N budget, remain ill-defined.

While improved knowledge of the marine N cycle requires a multifaceted approach, characterizing the physical and chemical sensitivities of marine diazotrophs to various environmental conditions provides constraints on regions of the ocean that may support diazotrophy. A better understanding of the sensitivities of marine diazotrophs may also reveal mechanisms by which marine N_2 fixation can respond to changes in rates of marine denitrification. However, our ability to describe the sensitivities of N_2 fixation depends on the degree to which we understand and have characterized the diversity of marine diazotrophs, an understanding presently limited by the small number of marine diazotrophs isolated for manipulative culture-based experiments.

The majority of marine N_2 fixation has historically been attributed to the filamentous, non-heterocystous cyanobacteria *Trichodesmium* spp. resident in the warm, stratified, and nutrient-depleted regions of the surface ocean (Carpenter, 1983; Capone et al., 1997, 2005). However, the past decade has seen a number of challenges to the paradigm that N_2 fixation by *Trichodesmium* spp., especially in the tropical North Atlantic, is the primary source of N to the global ocean. For example, molecular tools have identified novel diazotrophs present in environments with physical and/or chemical characteristics different from their more well-studied counterparts in tropical and subtropical seas (Zehr et al., 2001, 2008; Montoya et al., 2004; Langlois et al., 2008; Moisander et al., 2010; Fernandez et al., 2011). Additionally, indirect evidence such as remote sensing (Westberry et al., 2005; Westberry and Siegel, 2006) and geochemical modeling (Deutsch et al., 2007) describes geographic distributions of N_2 fixers, including *Trichodesmium* spp., that differs from our expectation of oligotrophic dominance. Finally, a number of both *in situ* and culture-based studies challenge some long-held notions of diazotrophic sensitivities to nutrients, including the degree to which inorganic N inhibits N_2 fixation. All of these findings raise the possibility that the geographic distribution and sensitivities of marine diazotrophs may be different than previously thought. As recognition of both the breadth of oceanic conditions supportive of diazotrophy and the diversity of marine diazotrophs increases, so too does the possibility that considerable rates of N_2 fixation occur in environments beyond the surface waters of the oligotrophic gyres. If so, global marine N_2 fixation rates may be greater than previously estimated.

In spite of an incomplete knowledge of marine diazotroph diversity, environmental and culture-based observations can establish criteria consistent with diazotrophic success. Environmental factors that are known to regulate marine diazotrophy include light (Carpenter et al., 1993; Milligan et al., 2007; Breitbarth et al., 2008), temperature (Chen et al., 1998; Breitbarth et al., 2007; Stal, 2009), oxygen (Robson and Postgate, 1980; Capone and Budin, 1982; Stal and Heyer, 1987), and metal availability (Rueter et al., 1990; Berman-Frank et al., 2001; Kustka et al., 2003; Chappell and Webb, 2010; Saito et al., 2011). Here, the sensitivity of marine diazotrophs to dissolved inorganic N (DIN), in particular NO_3^- and NH_4^+, is evaluated, and evidence for the inhibition of N_2 fixation by DIN in (1) the euphotic zone, (2) the sub-euphotic zone, and (3) benthic marine environments, is reviewed. In particular, the question of whether significant rates of N_2 fixation can occur when ambient DIN concentrations are significant, i.e., $\geq 1\,\mu M$, is examined. The findings of this review are that: (1) reports of substantial rates of N_2 fixation in euphotic and benthic environments with $\geq 1\,\mu M$ DIN indicate that elevated DIN does not necessarily preclude large N_2 fixation fluxes; (2) certain benthic marine diazotrophs may be less sensitive to chronic exposure to elevated concentrations of DIN than diazotrophs in the euphotic zone; (3) while benthic N_2 fixation is widespread and can occur at significant rates, global estimates are poorly known, likely contributing significant uncertainty to global estimates of marine N_2 fixation fluxes, and, (4) euphotic zone diazotrophs may respond to changes in ambient N:P ratios, providing a potential mechanism for diazotrophs to respond to changes in denitrification rates and thus to stabilize the marine N inventory. These findings are investigated below.

NUTRIENT INHIBITION OF EUPHOTIC ZONE N_2 FIXATION

There are three primary lines of evidence for the inhibition of marine N_2 fixation by inorganic N. The first results from circumstances associated with the origins of marine diazotrophic research. Before molecular tools became widely available, our understanding of marine diazotrophs was largely limited to the study of macroscopic cyanobacteria that could be readily identified and manipulated in field and culture-based studies. The most conspicuous and well-studied marine diazotroph, *Trichodesmium* spp., has predominantly been observed in warm, nutrient depleted regions of the surface ocean (Carpenter, 1983; Capone et al., 1997, 2005). The association of *Trichodesmium* spp. with these environmental characteristics, and the strong bias of studies of marine diazotrophs towards *Trichodesmium* spp., has perhaps unintentionally lead to the expectation that other marine diazotrophs will share the same environmental preferences. The second line of evidence for DIN inhibition of N_2 fixation comes from calculations showing that it requires ~25% more energy to reduce N_2 (87 kcal) than NO_3^- (69 kcal) to NH_4^+ (Falkowski, 1983). Together with the majority of field observations of diazotrophs from nutrient-depleted tropical surface waters, this additional energetic cost has lead to the assumption that significant rates of N_2 fixation do not occur in marine environments with $\geq 1\,\mu M$ DIN.

The third line of evidence for the inhibition of N_2 fixation by DIN comes from culture studies of marine diazotrophs that test the effects of short-term and/or chronic exposure to NO_3^- and NH_4^+ (e.g., Ohki et al., 1991; Mulholland and Capone, 1999; Mulholland et al., 2001; Fu and Bell, 2003; Holl and Montoya, 2005) (**Table 1**) (the numerous studies of DIN inhibition of fresh water diazotrophs are not reviewed here). These studies have demonstrated that NH_4^+ is more effective at inhibiting N_2 fixation than NO_3^- (Ohki and Fujita, 1982; Ohki et al., 1991; Mulholland et al., 2001), presumably because of the larger energetic cost associated with assimilating N_2 vs. NH_4^+ than with assimilating N_2 vs. NO_3^-. Additionally, these studies have shown that chronic exposure to both NO_3^- and NH_4^+ more strongly inhibits N_2 fixation than does short-term (i.e., less than 24 h) exposure (Ohki et al., 1991; Mulholland et al., 2001; Fu and Bell,

Table 1 | Reports of the inhibition of N_2 fixation by combined N for marine diazotrophs.

Diazotroph	Experimental condition	Form of combined N	Concentration of added combined N	Concentration of P	Duration of exposure	% inhibition of N_2 fixation compared to no-DIN control	References
Trichodesmium thiebautii, natural populations	Field manipulations	Chloramphenicol	10 μg mL^{-1}	Ambient surface seawater	0–7 h	28% inhibition when added before/early in photoperiod	Capone et al., 1990
Trichodesmium thiebautii, natural populations	Field manipulations	Chloramphenicol	10 μg mL^{-1}	Ambient surface seawater	0–5 h	Stimulated N_2 fixation when added in late afternoon	Capone et al., 1990
Trichodesmium thiebautii, natural populations	Field manipulations	NH_4^+	100 μM	Ambient surface seawater	0–7 h	60% inhibition	Capone et al., 1990
Trichodesmium sp. NIBB 1067	Batch culture	NO_3^-	2 mM	3.2 μM	7 h	0% inhibition	Ohki et al., 1991
Trichodesmium sp. NIBB 1067	Batch culture	NH_4^+	20 μM	3.2 μM	7 h	0% inhibition	Ohki et al., 1991
Trichodesmium sp. NIBB 1067	Batch culture	urea	500 μM	3.2 μM	3 h	Some inhibition	Ohki et al., 1991
Trichodesmium sp. NIBB 1067	Batch culture	NO_3^-	2 mM	3.2 μM	Multiple generations	100% inhibition	Ohki et al., 1991
Trichodesmium sp. NIBB 1067	Batch culture	NH_4^+	20 μM	3.2 μM	Multiple generations	100% inhibition	Ohki et al., 1991
Trichodesmium sp. NIBB 1067	Batch culture	urea	500 μM	3.2 μM	Multiple generations	100% inhibition	Ohki et al., 1991
Trichodesmium sp. NIBB 1067	Batch culture	NO_3^-	150 μM	3.2 μM	Multiple generations	75% inhibition	Mulholland et al., 1999
Trichodesmium sp. NIBB 1067	Batch culture	urea	30 μM	3.2 μM	Multiple generations	66% inhibition	Mulholland et al., 1999
Trichodesmium spp. natural populations	Field manipulations	NH_4^+	1 and 5 μM	Ambient surface seawater	23 h	20% inhibition for 1 μM and 53% inhibition for 5 μM	Mulholland et al., 2001
Trichodesmium spp. natural populations	Field manipulations	NH_4^+	10 μM	Ambient surface seawater	0–23 h	28% inhibition after 1–2 h, 99% inhibition after 23 h	Mulholland et al., 2001
Trichodesmium spp. natural populations	Field manipulations	Glutamate	5 μM	Ambient surface seawater	23 h	33% inhibition	Mulholland et al., 2001
Trichodesmium spp. natural populations	Field manipulations	Glutamate	10 μM	Ambient surface seawater	0–23 h	5% inhibition after 1–2 h, 99% inhibition after 23 h	Mulholland et al., 2001
Trichodesmium spp. natural populations	Field manipulations	Glutamine	5 μM	Ambient surface seawater	23 h	89% inhibition	Mulholland et al., 2001
Trichodesmium spp. natural populations	Field manipulations	Glutamine	10 μM	Ambient surface seawater	0–23 h	29% inhibition after 1–2 h, 99% inhibition after 23 h	Mulholland et al., 2001
Trichodesmium sp. NIBB 1067	Batch culture	NO_3^-	1 μM	3.2 μM	1–6 h	0% inhibition	Mulholland et al., 2001
Trichodesmium sp. NIBB 1067	Batch culture	NO_3^-	10 μM	3.2 μM	1–6 h	40% inhibition	Mulholland et al., 2001

(Continued)

Table 1 | Continued

Diazotroph	Experimental condition	Form of combined N	Concentration of added combined N	Concentration of P	Duration of exposure	% inhibition of N_2 fixation compared to no-DIN control	References
Trichodesmium sp. NIBB 1067	Batch culture	NH_4^+	1 μM	3.2 μM	2 and 4 h	0% inhibition	Mulholland et al., 2001
Trichodesmium sp. NIBB 1067	Batch culture	NH_4^+	10 μM	3.2 μM	2 and 4 h	90–99% inhibition after 4 h	Mulholland et al., 2001
Trichodesmium sp. NIBB 1067	Batch culture	Glutamate	1 or 10 μM	3.2 μM	2 and 4 h	0% inhibition after 4 h	Mulholland et al., 2001
Trichodesmium sp. NIBB 1067	Batch culture	Glutamine	1 or 10 μM	3.2 μM	2 and 4 h	Up to 50% inhibition after 2 and 4 h	Mulholland et al., 2001
Trichodesmium sp. GBRTRLI101	Batch culture	NH_4^+	2 μM	3 μM	3 generations	0% inhibition	Fu and Bell, 2003
Trichodesmium sp. GBRTRLI101	Batch culture	NH_4^+	10 μM	3 μM	1 generation	0% inhibition	Fu and Bell, 2003
Trichodesmium sp. GBRTRLI101	Batch culture	NH_4^+	10 μM	3 μM	5 generations	86% inhibition	Fu and Bell, 2003
Trichodesmium sp. GBRTRLI101	Batch culture	NO_3^-	10 μM	3 μM	1 generation	0% inhibition	Fu and Bell, 2003
Trichodesmium sp. GBRTRLI101	Batch culture	NO_3^-	10 μM	3 μM	5 generations	75% inhibition	Fu and Bell, 2003
Trichodesmium sp. GBRTRLI101	Batch culture	Urea	10 μM	3 μM	1 generation	0% inhibition	Fu and Bell, 2003
Trichodesmium sp. GBRTRLI101	Batch culture	Urea	10 μM	3 μM	5 generations	66% inhibition	Fu and Bell, 2003
Trichodesmium sp. IMS101	Continuous culture	NO_3^-	0.5–20 μM	10 μM	0–12 h (added just prior to initiation of light cycle)	Up to 35% inhibition up to 5 μM, ≥10 μM apparently saturates at 70% inhibition	Holl and Montoya, 2005
Trichodesmium sp. IMS101	Batch culture	NO_3^-	100 μM	50 μM	2 weeks	100% inhibition	Milligan et al., 2007
Trichodesmium sp. IMS101	Batch culture	NO_3^-	100 μM (semi-continuous re-supply of 100 μM NO_3^-)	50 μM	1, 3, or 6 days	~60% inhibition at 1 day, 100% inhibition at 3 and 6 days	Sandh et al., 2011
Crocosphaera sp. WH8501	Batch culture	NO_3^-	0.2–10 μM	50 μM	90 min prior to initiation of dark period	5% inhibition up to 1 μM, 24% inhibition at 5 μM, 12% inhibition at 10 μM	Dekaezemacker and Bonnet, 2011
Crocosphaera sp. WH0003	Batch culture	NO_3^-	0.2–10 μM	50 μM	90 min prior to initiation of dark period	14% inhibition at 0.2 μM; 11% inhibition at 1 μM, 4% inhibition at 5 μM	Dekaezemacker and Bonnet, 2011
Crocosphaera sp. WH8501	Batch culture	NH_4^+	0.2–10 μM	50 μM	90 min prior to initiation of dark period	Up to 12% inhibition up to 5 μM; 38% inhibition at 10 μM	Dekaezemacker and Bonnet, 2011
Crocosphaera sp. WH0003	Batch culture	NH_4^+	0.2–10 μM	50 μM	90 min prior to initiation of dark period	21% inhibition at 1 μM, 41% inhibition at 5 μM, and 80% inhibition at 10 μM	Dekaezemacker and Bonnet, 2011

(Continued)

Table 1 | Continued

Diazotroph	Experimental condition	Form of combined N	Concentration of added combined N	Concentration of P	Duration of exposure	% inhibition of N_2 fixation compared to no-DIN control	References
Trichodesmium sp. IMS101	Batch culture	NO_3^-	8 μM	0.5 μM	≥10 generations	90% inhibition*	Knapp et al., 2012
Trichodesmium sp. IMS101	Batch culture	NO_3^-	5 and 16 μM	1 μM	≥10 generations	72% inhibition at 5 μM and 85% inhibition at 16 μM*	Knapp et al., 2012
Crocosphaera sp. WH8501	Batch culture	NO_3^-	8 μM	0.5 μM	≥10 generations	79% inhibition*	Knapp et al., 2012
Crocosphaera sp. WH8501	Batch culture	NO_3^-	5 and 16 μM	1 μM	≥10 generations	71% inhibition at 5 μM and 85% inhibition at 16 μM*	Knapp et al., 2012

** Indicates the degree of inhibition when N_2 fixation rates are normalized per trichomes or cells; N_2 fixation is significantly less inhibited when N_2 fixation rates are normalized to chl a content for Trichodesmium sp., but not for Crocosphaera sp.*

2003; Milligan et al., 2007; Dekaezemacker and Bonnet, 2011; Sandh et al., 2011; Knapp et al., 2012) (**Table 1**). Supporting these observations of depressed N_2 fixation rates, physiological changes in *Trichodesmium* have also been documented when cultures are grown with NO_3^- as a source of assimilative N instead of dissolved N_2 gas. After chronic exposure of *Trichodesmium* cultures to 100 μM NO_3^- (Milligan et al., 2007) demonstrated a down-regulation of Mehler activity relative to cultures grown on N_2 gas, while (Sandh et al., 2011) found an inhibition of nitrogenase expression and diazocyte development. These effects of NO_3^- on diazotroph physiology suggest that chronic exposure to DIN has a greater impact on N_2 fixation rates than does short-term exposure.

The relatively small impact on N_2 fixation rates by short-term exposure to NO_3^- (**Table 1**) has implications for proposed mechanisms for diazotrophs to acquire limiting nutrients such as P. For example, short-term exposure to DIN could take place during the vertical migration of *Trichodesmium* spp. (Capone et al., 1990) showed that nitrogenase in *Trichodesmium* spp. is synthesized each morning prior to the initiation of nitrogenase activity. Consequently, the downward migration of *Trichodesmium* spp. at night (Villareal and Carpenter, 1990) to acquire P (Villareal and Carpenter, 2003) at the top of the nutricline (where NO_3^- is also present) might not strongly depress peak daytime N_2 fixation rates in *Trichodesmium* spp. if exposure to NO_3^- is brief and occurs at night before new nitrogenase is synthesized. While studies of the effects of DIN inhibition on marine diazotrophs have largely been restricted to *Trichodesmium* spp., recent culturing work suggests that *Crocosphaera* has similar sensitivities to short-term vs. chronic NO_3^- exposure (Dekaezemacker and Bonnet, 2011; Knapp et al., 2012). Given the similarity in response of *Trichodesmium* and *Crocosphaera* spp. and the limited genetic divergence in nitrogenase amino acid sequences in marine diazotrophic cyanobacteria (Zehr, 2011), the smaller effect of short-term vs. long-term DIN exposure on N_2 fixation rates may be common among other diazotrophic cyanobacteria as well.

Culturing studies clearly show that DIN *can* inhibit N_2 fixation; however most inhibition studies have been performed with concentrations of N and/or P in the culture media that exceed those typically found in the euphotic zone (**Table 1**). This discrepancy between nutrient concentrations in the environment and in cultures leaves open the possibility that culturing studies overestimate the degree to which DIN inhibits N_2 fixation in the environment. Recent culturing work using concentrations of NO_3^- and PO_4^{3-} typically found in the euphotic zone show that chronic exposure of *Trichodesmium* and *Crocosphaera* to 5 to 16 μM NO_3^- depresses N_2 fixation rates relative to cultures grown with no NO_3^-, but that N_2 fixation did not stop even in cultures amended with as much as 16 μM NO_3^- (Knapp et al., 2012). Moreover, the same work showed that higher concentrations of PO_4^{3-} can offset NO_3^- inhibition of per-cell N_2 fixation rates by increasing diazotroph abundance. Consequently, the volume-integrated rate of N_2 fixation in treatments grown with 5.0 μM NO_3^- and 1.0 μM PO_4^{3-} was comparable to the volume-integrated rate of N_2 fixation in treatments not amended with NO_3^- and grown with 0.5 μM PO_4^{3-} (Knapp et al., 2012).

The finding of increased diazotroph abundance as a function of increasing P availability is consistent with the well-recognized role that P availability plays in regulating the biomass of microbes [e.g., (Elser et al., 2007; Loladze and Elser, 2011; Scott et al., 2012)]. Investigations into variability in phytoplankton biomass N:P ratios indicate that P is preferentially used to create new biomass (e.g., in DNA) whereas N is required both for the production of new biomass as well as for the production of proteins, especially associated with resource acquisition (Klausmeier et al., 2004; Loladze and Elser, 2011). Consequently, the results of (Knapp et al., 2012) documenting a two- to three-fold greater abundance of both the diazotrophs *Crocosphaera watsonii* and *Trichodesmium erythraeum* in batch cultures grown with 1.0 vs. 0.5 μM PO_4^{3-} are perhaps unsurprising. What is surprising is that the increase in diazotrophic biomass was sufficient to offset the lower per-trichome rates of N_2 fixation resulting from inhibition by 5.0 μM NO_3^-. This work shows that NO_3^- present at typical

surface ocean concentrations does not necessarily preclude N_2 fixation fluxes comparable to those observed in NO_3^--depleted environments, and suggests that field and numerical modeling investigations of marine N_2 fixation that exclude surface ocean environments with $\geq 1\,\mu M$ NO_3^- may overlook potentially significant regions of N_2 fixation.

Additionally, the work of (Knapp et al., 2012) identifies a potential mechanism for euphotic zone diazotrophs to respond to changes in surface ocean concentrations of NO_3^- and PO_4^{3-}. Specifically, while it has been assumed that low ambient N:P ratios (a condition created by denitrification occurring below the euphotic zone) would stimulate higher rates of N_2 fixation (Haug et al., 1998; Deutsch et al., 2004), no mechanism has been proposed for how a diazotroph would sense and respond favorably to lower N:P ratios. The results of Knapp et al. (2012) describe how the separate physiological effects of relatively high concentrations of P (i.e., increased diazotroph abundance) and relatively low concentrations of N (i.e., lessened NO_3^- inhibition of N_2 fixation) together can create conditions that can support significant N_2 fixation fluxes. While relatively low N and high P concentrations have distinct effects on diazotrophs, combining these effects results in a perceived advantage for diazotrophs growing in environments with low ambient N:P ratios and may provide a feedback mechanism for diazotrophs to respond to increases in denitrification and thus help stabilize the marine N inventory. This finding also has implications for diazotroph biogeography, and suggests that significant abundances and/or N_2 fixation fluxes may not be restricted to oligotrophic surface waters such as the North Atlantic, but may occur in more nutrient-replete regions of the surface ocean such as the surface waters overlying ODZs where rates of N loss are high.

Indeed, these culture-based results are consistent with recent field observations by (Fernandez et al., 2011; Sohm et al., 2011) who document N_2 fixation rates of 0.1–7.5 nmol N L^{-1} d^{-1} in surface ocean waters with 5–20 μM NO_3^- (**Table 2**), although molecular analyses indicate that this fixation was carried out by diazotrophs other than *Trichodesmium* or *Crocospahera* spp. These rates of N_2 fixation in NO_3^--replete coastal waters are comparable to the range in N_2 fixation rates measured at Station ALOHA in the North Pacific gyre of 0.5–11 nmol N L^{-1} d^{-1} (Church et al., 2009) and where surface NO_3^- concentrations are consistently $\leq$100 nM (Fujieki et al., 2011). Similarly, (Halm et al., 2012) found higher euphotic zone rates of N_2 fixation in regions of the South Pacific gyre with higher concentrations of NO_3^- (as well as PO_4^{3-}) compared to more oligotrophic regions of the gyre, i.e., average N_2 fixation rates of 1.5 ± 0.3 nmol N L^{-1} d^{-1} vs. 0.4 ± 0.3 nmol N L^{-1} d^{-1}, respectively. These N_2 fixation rate measurements are supported by numerous other field observations documenting significant abundances of and/or N_2 fixation by diazotrophs including *Trichodesmium* spp. in other near-shore locations (Lenes et al., 2001; White et al., 2007; Rodier and Le Borgne, 2008; Grosse et al., 2010; Rodier and Le Borgne, 2010; Bombar et al., 2011) (**Table 2**).

These reports of substantial rates of N_2 fixation in NO_3^--bearing surface waters, especially in upwelling and coastal regions, underscore the potential bias of prior field campaigns documenting N_2 fixation predominantly in the nutrient-depleted oligotrophic gyres, and suggest that N_2 fixation may have a broader geographic distribution in marine euphotic waters that episodically and/or chronically have significant DIN concentrations. Indeed, the strains of *Trichodesmium erythraeum* commonly used in culture studies, i.e., NIBB1067 and IMS101, were collected from the coastal waters of Japan and North Carolina, respectively (Ohki and Fujita, 1982; Prufert-Bebout et al., 1993), where surface water DIN concentrations are at least episodically elevated. That *Trichodesmium* spp. are frequently found in coastal waters that can have relatively high DIN concentrations is relevant considering that recent remote sensing (Westberry and Siegel, 2006) and geochemical modeling (Deutsch et al., 2007) studies have predicted high abundances of diazotrophs and/or rates of N_2 fixation in regions of the surface ocean with NO_3^- concentrations consistently $\geq 5\,\mu M$ (Garcia et al., 2010). The results reviewed here suggest that NO_3^- is not as inhibitive of N_2 fixation by euphotic-zone diazotrophs as previously thought, especially if P and the necessary trace metals are abundant, and have implications for field studies documenting marine N_2 fixation fluxes as well as for the parameterization of N_2 fixation in models.

NUTRIENT INHIBITION OF MESOPELAGIC N_2 FIXATION

While there are only a handful of reports of N_2 fixation occurring in the mesopelagic (i.e., sub-euphotic) water column, advances in molecular techniques capable of identifying diazotrophs and the improved sensitivity of mass spectrometers for detecting the incorporation of labeled $^{15}N_2$ into suspended particulate organic N (PN_{susp}) have improved our ability to evaluate N_2 fixation in this environment. It is expected that N_2 fixation in this portion of the water column would be carried out by diazotrophs that have substantially different physiologies than those living in the euphotic zone: mesopelagic diazotrophs require a different energy source than their photosynthetic counterparts, they need to tolerate lower temperatures, and due to the higher concentrations of NO_3^- below the base of the euphotic zone, they would also presumably be less inhibited by NO_3^-. Perhaps unsurprisingly then, diazotrophs collected from meso- and bathypelagic waters contain *nifH* sequences distinct from euphotic zone diazotrophs. In samples collected from the deep North Pacific (Mehta et al., 2003, 2005) identified a number of *nifH* sequences associated with methanogens and anaerobic sulfate reducers from hydrothermal vent systems, and was able to document growth and N_2 fixation in a culture of thermophilic archeal methanogens (Mehta and Baross, 2006). (Hewson et al., 2007) identified *nifH* genes in samples collected throughout the water column of the Sargasso Sea and detected *nifH* in meso- and abyssopelagic samples more consistently than in euphotic zone samples, suggesting the potential for diazotrophy below the euphotic zone. However, (Hewson et al., 2007) recovered *nifH* sequences of the cyanobacterial diazotrophs *Trichodesmium thiebautii* and *Crocosphaera watsonii* at 250 and 1000 m, respectively, demonstrating that the *nifH* associated with diazotrophs active in other environments persists upon transport to the deep ocean in a reasonably robust form, as has been recently reported for RuBisCO (Orellana and Hansell, 2012). However, (Hewson

Table 2 | Reported rates of N_2 fixation in euphotic, mesopelagic, and benthic marine environments with significant (i.e., ≥1 μM) ambient concentrations of NO_3^- and/or NH_4^+.

Location	Depth	Diazotroph	N_2 fixation rate	N_2 fixation method	Ambient [NO_3^-]	Ambient [PO_4^{3-}]	References
EUPHOTIC ZONE							
Eastern Tropical North Atlantic	48 m	Unidentified, whole water incubation	0.7 nmol N L^{-1} h^{-1}	$^{15}N_2$ assimilation	10 μM	0.6 μM	Voss et al., 2004
Mekong River plume, mesohaline station	Surface*	*Trichodesmium* spp.	1.13 nmol N L^{-1} h^{-1}	$^{15}N_2$ assimilation	12.4 μM	0.7 μM	Grosse et al., 2010; Bombar et al., 2011
Benguela upwelling	8 m	Unidentified, whole water incubation	7.5 nmol N L^{-1} d^{-1}	$^{15}N_2$ assimilation	21 μM	1.5 μM	Sohm et al., 2011
Eastern Tropical South Pacific	Surface*	Whole water incubation, 2005	0.089 nmol N L^{-1} d^{-1}	$^{15}N_2$ assimilation	7.8 μM	1.2 μM	Fernandez et al., 2011
Eastern Tropical South Pacific	Surface*	Whole water incubation, 2007	0.66 nmol N L^{-1} d^{-1}	$^{15}N_2$ assimilation	5.5 μM	0.68 μM	Fernandez et al., 2011
MESOPELAGIC							
Eastern Tropical South Pacific	400 m	Cluster I and III phylotypes	1.27 nmol N L^{-1} d^{-1}	$^{15}N_2$ assimilation	>9.3 μM	>1.0 μM	Fernandez et al., 2011
California Borderland Basins	500 m	Heterotrophic Alpha- and Gammaproteobacteria, putative sulfate reducing bacteria	0.07 μmol m^{-3} d^{-1} total; <10 μm fraction 0.1 μmol m^{-3} d^{-1}, >10 μm fraction 0.01 μmol m^{-3} d^{-1}	$^{15}N_2$ assimilation	32 μM	4 μM	Hamersley et al., 2011
California Borderland Basins	850 m	Heterotrophic Alpha- and Gammaproteobacteria, putative sulfate reducing bacteria	0.07 μmol m^{-3} d^{-1} total; <10 μm fraction 0.08 μmol m^{-3} d^{-1}; >10 μm fraction 0.00 μmol m^{-3} d^{-1}	$^{15}N_2$ assimilation	32 μM	4 μM	Hamersley et al., 2011

(Continued)

Table 2 | Continued

Location	Sediment depth	Diazotroph	N_2 fixation rate	N_2 fixation method	Ambient $[NO_3^-]$	Ambient $[NH_4^+]$	Ambient $[PO_4^{3-}]$	References
BENTHIC								
Waccasassa estuary, FL, USA	Upper 2–5 cm	*Clostridium* spp.	0.64 – 6.0 ng N g^{-1} hr^{-1}	Acetylene reduction	NR	0.06 mg N g–1	NR	Brooks et al., 1971
Continental Shelf Sediments, Upper Cook Inlet, AK, USA	Upper 0–5 cm	NR	0.3 μg atoms N m^{-2} hr^{-1}*#	Acetylene reduction	29 μM	127 μM	NR	Haines et al., 1981
Continental Shelf Sediments, Norton Sound, AK, USA	Upper 0–5 cm	NR	0.8 μg atoms N m^{-2} hr^{-1}*#	Acetylene reduction	7 μM	177 μM	NR	Haines et al., 1981
Zostera marina seagrass sediments, Long Island, NY, USA	Upper 12 cm	NR	1.6 nmol C_2H_2 cm^{-2} hr^{-1}	Acetylene reduction	NR	116 μM	NR	Capone, 1982
Tomales Bay, CA, USA	Upper 1 cm	*Microcoleous* sp., *Lyngbya* sp., *Oscillatoria* sp., *Spirulina* sp.	3 mmol N m^{-2} d^{-1}*#	Acetylene reduction	1 μM	3 μM	1.9 μM	Joye and Paerl, 1993
Transplanted Spartina marsh, NC, USA	Upper 1 cm	Heterocystous and non-heterocystous cyanobacteria	37 mg N m^{-2} d^{-1}#	Acetylene reduction	NR	18–83 μM	NR	Currin et al., 1996
Seagrass meadow, France	Upper 5 cm	Sulfate reducing bacteria	0.1–7.3 mg N m^{-2} d^{-1}	Acetylene reduction	NR	190 μM	NR	Welsh et al., 1996
Mangrove sediments, Twin Cays, Belize	Upper 1 cm	Heterocystous and not-heterocystous cyanobacteria, sulfate reducing bacteria	0–1.21 mmol N d^{-1}#	Acetylene reduction	1.0 μM	12–250 μM	0.4–1.9 μM	Lee and Joye, 2006
Corpus Christi Bay, TX, USA	Upper 15–20 cm	NR	0–75 μmol N m^{-2} hr^{-1}#	Net N_2 fluxes using MIMS	≤1 μM	≤1 μM	0.2–1.6 μM	McCarthy et al., 2008
Catalina Harbor sediments, CA, USA	Upper 0–10 cm	Sulfate reducing bacteria, cyanobacteria	0.1–8.0 mmol N m^{-2} d^{-1}	Acetylene reduction	NR	50–100 μM	NR	Bertics et al., 2010
Eutrophic estuary, Waquoit Bay, MA, USA	Upper 20 cm	NR	0–0.77 mmol N m^{-2} hr^{-1}#	Net N_2 fluxes using benthic flux chamber and MIMS	<1 μM	10–40 μM	NR	Rao and Charette, 2012

*The units for N_2 fixation rates as well as concentration are taken from the original publication. * Indicates average value for N_2 fixation rate, NO_3^- concentration, and/or PO_4^{3-} concentration; # Indicates that denitrification was documented simultaneously in the same sediments; NR indicates not reported.*

et al., 2007) also detected *nifH* expression in some mesopelagic samples, indicating some diazotrophs may be active in this NO_3^--rich environment. Similarly, (Jayakumar et al., 2012) found both *nifH* DNA and cDNA sequences associated with strictly anaerobic proteobacteria in samples collected from the oxygen minimum zone of the Arabian Sea, also indicating potential activity of diazotrophs in sub-euphotic zone waters.

In addition to the molecular studies described above, two recent reports document relatively low rates of N_2 fixation in mesopelagic samples collected from coastal environments. In the NO_3^--rich coastal waters of the Eastern Tropical South Pacific (ETSP), (Fernandez et al., 2011) measured N_2 fixation both in the euphotic zone and in mesopelagic waters, including in the core of the local oxygen deficient zone (ODZ) where they reported rates of 1.3 nmol N L^{-1} d^{-1} (**Table 2**). While (Fernandez et al., 2011) recovered numerous *nifH* sequences, they amplified no cyanobacterial phylotypes in surface or subsurface waters; instead most of the *nifH* sequences aligned with Cluster I, and to a lesser extent, Cluster III *nifH* genes, including representatives of anaerobic sulfate reducers. In mesopelagic samples collected in the California Borderland Basins (i.e., San Pedro and Santa Monica Basins) (Hamersley et al., 2011) report similar N_2 fixation rates of 0.07 μmol N m^{-3} d^{-1} (**Table 2**). The most common *nifH* phylotype recovered by (Hamersley et al., 2011) was from the UCYN-A group found both in surface and mesopelagic samples. Additionally, (Hamersley et al., 2011) recovered heterotrophic *nifH* sequences in mesopelagic samples from Cluster I as well as a number of Cluster III sequences that correspond to strict anaerobes, including alpha- and gamma-proteobacteria, as well as sulfate reducing bacteria (SRB). While both (Fernandez et al., 2011; Hamersley et al., 2011) suggest that diazotrophy in these mesopelagic environments may be associated with oxygen deficiency, the similarity of some mesopelagic *nifH* sequences to those of diazotrophs found both in surface waters and in benthic environments (see below) raises the possibility that some of the diazotrophs recovered in these near-shore mesopelagic samples are introduced via sinking particles (from the euphotic zone) or via nepheloid layer from sediments to the water column further offshore. Given that a number of the phylotypes collected by (Hamersley et al., 2011) are similar to sequences from microbial mats and/or to cultivated strains of strict anaerobes, a condition not met in the water column of the San Pedro Basin where ambient oxygen concentrations are ∼11 μM, it raises the possibility that sedimentary microbes are resuspended and then detected in mesopelagic waters.

The determination of N_2 fixation rates in mesopelagic waters presents unique analytical challenges as it depends on the incorporation of $^{15}N_2$ by living, active diazotrophs into particulate organic matter that can then be analyzed by combustion on an isotope ratio mass spectrometer (Montoya et al., 1996). Even with increasingly sensitive instrumentation, the concentration of PN_{susp} in mesopelagic waters is extremely low. Thus, even with "large volume," i.e., 4 L, incubations and given a typical detection limit of ∼1.4 μmol N for GC-MS systems commonly used to analyze these samples (e.g., http://stableisotopefacility.ucdavis.edu/), a PN_{susp} concentration of ∼0.35 μM is required to generate a signal above typical analytical detection limits. Since most open-ocean PN_{susp} concentrations are only this high within the euphotic zone, and then decrease sharply in the mesopelagic (i.e., PN_{susp} concentrations at 300 m at BATS and HOT are 0.05 μM) (Michaels and Knap, 1996; Fujieki et al., 2011), even larger volume incubations and/or more sensitive analytical approaches are required to reliably to detect N_2 fixation rates in these waters. While PN_{susp} concentrations in mesopelagic waters of near-shore environments are higher than those in the oligotrophic ocean, e.g., (Hamersley et al., 2011) report PN_{susp} of 0.23 and 0.25 μM for their samples collected at 500 and 850 m, respectively, ensuring that mesopelagic samples have sufficient PN_{susp} to generate a signal above detection limits remains a significant challenge for documenting mesopelagic N_2 fixation rates. Moreover, it is not clear that improving incubation techniques to increase $^{15}N_2$ gas solubility (Mohr et al., 2010) will improve the ability to measure mesopelagic N_2 fixation rates, as this modification does not increase the initial quantity of PN_{susp} in a mesopelagic sample. Given the very low PN_{susp} concentration in mesopelagic waters, great care must be taken to quantify blanks for these incubations and to demonstrate that N_2 fixation rates generated by these methods contain a sufficient quantity of N to exceed analytical detection limits. Consequently, it may be warranted to view the water-column integrated mesopelagic N_2 fixation rates of 55 μmol N m^{-2} d^{-1} in the California Borderland Basins (Hamersley et al., 2011) and 5.4 ± 2.4 μmol N m^{-2} d^{-1} in the ETSP (Fernandez et al., 2011), and their potential to help resolve global marine N budget imbalances, as provisional estimates until supporting measurements confirm the activity of N_2 fixation in mesopelagic environments. If these early reports of relatively low N_2 fixation rates in sub-euphotic zone waters (**Table 2**) are broadly characteristic of mesopelagic environments, they may be the consequence of NO_3^- inhibition. A better understanding of the capacity of mesopelagic environments to support diazotrophy will benefit from methodological and analytical improvements of *in situ* N_2 fixation rate measurements, as well as successful culturing of microbes recovered from these environments.

NUTRIENT INHIBITION OF BENTHIC MARINE N_2 FIXATION

From intertidal cyanobacterial mats to dark muds, and from low to high latitudes, numerous reports from diverse marine ecosystems demonstrate that benthic diazotrophy is widespread (Capone, 1983 and references therein). N_2 fixation in marine sediments has received renewed attention based on evidence that the net flux of N_2 gas in certain coastal sediments may have changed from efflux, via denitrification, to influx, via N_2 fixation, potentially forced by climate change (Fulweiler et al., 2007). Due to the high concentrations of NO_3^- and/or NH_4^+ that can accumulate as a result of organic matter degradation, N_2 fixation in benthic environments presents perhaps the greatest challenge to the expectation for DIN to inhibit diazotrophy. **Table 2** includes the small subset of all studies documenting benthic marine N_2 fixation that reported both N_2 fixation rates as well as concentrations of ambient NO_3^- and/or NH_4^+ that exceeded 1 μM. While the culture-based studies described above indicate that NH_4^+ significantly depresses N_2 fixation rates in *Trichodesmium* and *Crocosphaera* spp.,

rates of 7–521 μmol N m^{-2} d^{-1} have been documented in seagrass-bearing, NH_4^+-rich (190 μM) sediments on the French coast (Welsh et al., 1996). Similar rates have been reported in other NH_4^+-rich benthic environments, including mangrove sediments (Lee and Joye, 2006) and in coastal sediments from Alaska (Haines et al., 1981) to California (Bertics et al., 2010) to Florida (Brooks et al., 1971), indicating that benthic N_2 fixation can occur at considerable rates in spite of high ambient NH_4^+ concentrations.

Given that the highest rates of N loss in the ocean occur in marine sediments (Brandes and Devol, 2002), it is perplexing that both N_2 fixation and denitrification have frequently been observed in the same sediments (Haines et al., 1981; Slater and Capone, 1984; Joye and Paerl, 1993; Currin et al., 1996; An and Joye, 2001; Gardner et al., 2006; Lee and Joye, 2006; Fulweiler et al., 2007; McCarthy et al., 2008; Bertics et al., 2012; Rao and Charette, 2012). Indeed, *Azospirillum*, a bacteria associated with seagrasses (Patriquin, 1978) is thought to carry out both denitrification and N_2 fixation (Bothe et al., 1981). These observations raise the question: if N_2 fixation is an energetically costly process whose role is to provide a source of assimilatory N to the ecosystem, and if diazotrophs are inhibited by DIN, why does N_2 fixation happen at significant rates in benthic environments rich in DIN and that also support denitrification?

Benthic diazotrophy has been investigated with a variety of biological and geochemical tools that together indicate that benthic N_2 fixation is carried out by a diverse suite of microbes at environmentally significant rates (**Table 2**). Many benthic N_2 fixation rates have been measured using acetylene reduction, and concerns have been raised regarding its use in these environments because of the capacity for acetylene to inhibit other microbial processes including denitrification, methanogenesis, methane oxidation, sulfate reduction, nitrification, and even N_2 fixation [(Capone, 1983) and references therein]. In spite of these and other more general concerns regarding the limitation of methods to measure absolute rates of benthic microbial processes, including the high degree of spatial heterogeneity due to microsites and steep geochemical gradients on millimeter spatial scales, benthic diazotrophy has been validated using $^{15}N_2$ assimilation (Patriquin and Knowles, 1972; Burris, 1976; Carpenter et al., 1978; Capone and Budin, 1982; Dekas et al., 2009) and net N_2 gas flux measurements made using membrane inlet mass spectrometry (MIMS) (An and Joye, 2001; Gardner et al., 2006; Fulweiler et al., 2007; McCarthy et al., 2008; Rao and Charette, 2012). Based on visual identification of diazotrophs and differences in N_2 fixation rates between light and dark incubations, cyanobacteria are thought to contribute to N_2 fixation fluxes in intertidal microbial mat consortia (Joye and Paerl, 1993; Currin et al., 1996; An et al., 2001; Lee and Joye, 2006). Additionally, a number of benthic studies have used molybdate amendment experiments to inhibit sulfate reduction and have simultaneously inhibited N_2 fixation in the same sediments; such experiments have been used to attribute N_2 fixation in certain benthic marine environments to SRB (Gandy and Yoch, 1988; Welsh et al., 1996; Nielsen et al., 2001; Burns et al., 2002; Steppe and Paerl, 2002; Bertics et al., 2010). Molecular tools have also verified the presence of *nif* genes, and thus the metabolic potential for N_2 fixation, in various benthic marine microbes including in SRB (Burns et al., 2002; Steppe and Paerl, 2002, 2005; Dekas et al., 2009; Bertics et al., 2010, 2012), anaerobic methane-oxidizing archaea (Dekas et al., 2009), and benthic cyanobacteria (Steppe and Paerl, 2005; Bertics et al., 2010).

Previous studies provide some insight into the role of DIN in regulating N_2 fixation and denitrification in some benthic environments. Specifically, (Joye and Paerl, 1993, 1994) established seasonality in patterns of N_2 fixation and denitrification in Tomales Bay, CA sediments that are consistent with studies documenting DIN inhibition of N_2 fixation. (Joye and Paerl, 1993, 1994) observed that when ambient benthic DIN concentrations were relatively low, N_2 fixation rates were high and denitrification rates were low, but when runoff or other sources introduced NO_3^- to sediments, denitrification rates increased and N_2 fixation rates decreased. These observations from Tomales Bay indicate both that denitrification is NO_3^- limited and that N_2 fixation is inhibited by NO_3^-. The sensitivity of benthic N_2 fixation and denitrification rates to changes in ambient DIN concentration in Tomales Bay has been replicated in manipulated core studies and observed in other benthic N cycling studies. For example, in the estuarine sands of Waquoit Bay, MA (Rao and Charette, 2012) documented net N_2 fixation, and suggested that denitrification occurring elsewhere in the estuary removes DIN, permitting N_2 fixation to proceed downstream. Similarly, in a study of N_2 fixation rates associated with seagrass roots in a French estuary (Welsh et al., 1996) observed peak N_2 fixation rates when ambient NH_4^+ concentrations reached their annual minima of 190 μM, relative to the peak concentration of 290 μM.

Many of these studies also document complex interactions between oxygen, DIN, and/or organic carbon, and their relationship with N_2 fixation and/or denitrification rates in benthic environments. For example, (Fulweiler et al., 2007) attributed a change from net denitrification to net N_2 fixation in Narragansett Bay, RI sediments to a decrease in the organic matter flux to the sediments due to diminished winter-spring blooms in the Bay. (Fulweiler et al., 2007) tested this hypothesis, observing a change from net N_2 fixation to net denitrification after adding organic matter to incubated sediment cores that had previously shown net N_2 fixation. In the past, benthic remineralization of winter-spring bloom material in Narragansett Bay provided a source of DIN to the sediment and overlying water column, which is nutrient-poor in summers; presumably the reduction in the magnitude of the organic matter flux to Narragansett Bay sediments corresponds to a reduced DIN flux to the sediments, and is proposed by Fulweiler et al. (2007) to be the cause of the switch to net N_2 fixation from net denitrification.

Observations of decreased rates of benthic N_2 fixation when ambient DIN concentrations increase, either because of runoff or remineralization, are generally consistent with the observations described above that show that DIN inhibits, but does not stop, pelagic diazotrophy. However, the observations of decreased benthic N_2 fixation rates when DIN concentrations increase are *not* consistent with other observations of high rates of benthic N_2

fixation in dark, NH_4^+-rich environments [e.g., (Haines et al., 1981; Capone, 1982; Welsh et al., 1996; Bertics et al., 2010)]. Some previous studies of benthic N_2 fixation have suggested that oxygen and organic carbon availability also play a role in mitigating DIN inhibition (Yoch and Whiting, 1986; McGlathery et al., 1998). Another explanation for why N_2 fixation may occur at considerable rates in DIN-rich benthic environments invokes a role for N_2 fixation that is entirely different from providing a source of assimilatory N to the ecosystem. Specifically, there is evidence that in the presence of high concentrations of NH_4^+ benthic N_2 fixation can serve as a sink for excess electrons to help bacteria achieve redox balance, especially in the absence of a viable Calvin–Benson–Bassham pathway (Joshi and Tabita, 1996; Tichi and Tabita, 2000). Ultimately, sensitivity studies of benthic diazotrophs to these parameters are limited by the lack of isolated diazotrophs for manipulative culture studies.

A better understanding of the sensitivities of the diverse suite of benthic diazotrophs to oxygen, organic carbon and DIN is critical for refining models of benthic N cycling, and in particular determining whether marine sediments are a net source or sink of fixed N to the marine environment. While marine sediments are normally considered a net sink for fixed N (Seitzinger, 1988), a variety of reports show that some benthic environments can be a net source of bioavailable N at least on seasonal timescales, if not annually, as well (Currin et al., 1996; Lee and Joye, 2006; Fulweiler et al., 2007; McCarthy et al., 2008). Moreover, if environmental conditions change to favor diazotrophy (e.g., Fulweiler et al., 2007), it is plausible that even if marine sediments do not overwhelmingly become a source of fixed N, they might at least not be as large of a sink as previously thought. Benthic N_2 fixation deserves more attention as it is a poorly constrained term in the global marine N budget; the process is not always included in marine N budget estimates, although (Capone, 1983) estimated it may contribute 15 Tg N $year^{-1}$, which would increase some estimates of N fluxes to the marine environment by 10–15% (Brandes and Devol, 2002).

CONCLUSIONS

Rates of the dominant fluxes of N to and from the ocean are highly uncertain, leaving open the question of whether the modern marine N budget is balanced. Some estimates suggest that rates of N fluxes to the ocean only compensate for one-third to one-half of the fluxes of N out of the ocean (Codispoti et al., 2001; Codispoti, 2007), while paleoceanographic and modeling studies require a balanced N budget, implying that either rates of N_2 fixation are underestimated, and/or that rates of N loss are overestimated (Brandes and Devol, 2002; Deutsch et al., 2004). One potential liability in previous estimates of N fluxes to the ocean is the assumption that the highest rates of marine N_2 fixation occur in the warm, nutrient-depleted regions of the surface ocean. However, culture and field evidence reviewed here indicates that low concentrations of NO_3^- and/or NH_4^+ ($\leq$1 μM) are not a strict requirement for high rates of marine N_2 fixation, and that numerical models using this as a criteria for significant diazotroph abundance and/or N_2 fixation fluxes may not accurately represent diazotroph sensitivities to DIN. Generally, the best-studied cyanobacterial diazotrophs show little inhibition by short-term exposure to inorganic N. Instead, depressed rates of N_2 fixation occur after long-term exposure of diazotrophs to elevated concentrations of DIN, although long-term exposure does not necessarily stop N_2 fixation. Recent field and culturing work has shown that NO_3^- concentrations commonly found in marine surface waters, i.e., up to 20 μM, do not preclude rates of N_2 fixation comparable to those measured in the NO_3^--depleted surface waters of the North Pacific gyre (Fernandez et al., 2011; Sohm et al., 2011). Moreover, field and culture evidence suggests that well-studied cyanobacterial diazotrophs such as *Trichodesmium* spp. are more tolerant of NO_3^- than previously assumed, especially when P is relatively abundant. Together with molecular evidence documenting novel diazotrophs in cooler euphotic zone waters [e.g., (Needoba et al., 2007; Moisander et al., 2010)], these observations imply that surface waters other than those in the warm, nutrient-poor oligotrophic gyres may support substantial rates of N_2 fixation, and that overlooking these potential diazotrophic contributions may compound uncertainties in the marine N budget, as well as modeled estimates of global marine diazotroph distributions and rates of N_2 fixation.

While the nascent case for significant N_2 fixation fluxes by mesopelagic diazotrophs is ambiguous, it is clear that N_2 fixation occurs in diverse benthic environments at significant rates in the presence of DIN concentrations in excess of 100 μM. Benthic N_2 fixation is peculiar in that it presents the strongest challenge to DIN inhibition of N_2 fixation, and because it often occurs in environments that also support high rates of N loss via denitrification and/or anammox. While traditionally it has been thought that benthic environments represent a net loss of bioavailable N from the marine ecosystem, previous work has shown that the net flux of N_2 gas to or from the sediments varies seasonally, and may be sensitive to environmental perturbations that may accelerate due to anthropogenic activities. These observations underscore the importance of developing and testing models of what controls benthic N_2 fixation (and denitrification) to generate more robust estimates of benthic N fluxes.

Our current understanding of the sensitivity of even the most well studied marine diazotrophs is incomplete, and we have considerably more to learn about diazotrophs that have only recently been identified using molecular tools. These are critical uncertainties to resolve if we are to understand how the marine N inventory can remain balanced on 100–1000 year time scales. Better constraints of diazotroph sensitivities will help us understand N cycle changes in the past, and to predict future changes as atmospheric carbon dioxide concentrations and temperatures increase and potentially stimulate N_2 fixation by *Trichodesmium* (Breitbarth et al., 2007; Hutchins et al., 2007; Levitan et al., 2007; Ramos et al., 2007; Levitan et al., 2010), if not other diazotrophs as well.

ACKNOWLEDGMENTS

D. A. Hansell and two reviewers provided comments that improved this manuscript. This work was funded by NSF grants OCE-0850905 and OCE-0933076.

REFERENCES

An, S., and Joye, S. B. (2001). Enhancement of coupled nitrification-denitrification by benthic photosynthesis in shallow estuarine sediments. *Limnol. Oceanogr.* 46, 62–74.

An, S. M., Gardner, W. S., and Kana, T. (2001). Simultaneous measurement of denitrification and nitrogen fixation using isotope pairing with membrane inlet mass spectrometry analysis. *Appl. Environ. Microbiol.* 67, 1171–1178.

Berman-Frank, I., Cullen, J. T., Shaked, Y., Sherrell, R. M., and Falkowski, P. G. (2001). Iron availability, cellular iron quotas, and nitrogen fixation in Trichodesmium. *Limnol. Oceanogr.* 46, 1249–1260.

Bertics, V. J., Sohm, J. A., Magnabosco, C., and Ziebis, W. (2012). Denitrification and nitrogen fixation dynamics in the area surrounding an individual ghost shrimp (*Neotrypaea californiensis*) burrow system. *Appl. Environ. Microbiol.* 78, 3864–3872.

Bertics, V. J., Sohm, J. A., Treude, T., Chow, C. E. T., Capone, D. G., Fuhrman, J. A., et al. (2010). Burrowing deeper into benthic nitrogen cycling: the impact of bioturbation on nitrogen fixation coupled to sulfate reduction. *Mar. Ecol. Prog. Ser.* 409, 1–15.

Bombar, D., Moisander, P. H., Dippner, J. W., Foster, R. A., Voss, M., Karfeld, B., et al. (2011). Distribution of diazotrophic microorganisms and nifH gene expression in the Mekong River plume during intermonsoon. *Mar. Ecol. Prog. Ser.* 424, U39–U55.

Bothe, H., Klein, B., Stephan, M. P., and Dobereiner, J. (1981). Transformations of inorganic nitrogen by Azospirillum spp. *Arch. Microbiol.* 130, 96–100.

Brandes, J. A., and Devol, A. H. (2002). A global marine-fixed nitrogen isotopic budget: implications for holocene nitrogen cycling. *Global Biogeochem. Cycles* 16. doi: 10.1029/2001GB001856

Breitbarth, E., Oschlies, A., and Laroche, J. (2007). Physiological constraints on the global distribution of Trichodesmium–effect of temperature on diazotrophy. *Biogeosciences* 4, 53–61.

Breitbarth, E., Wohlers, J., Klaes, J., Laroche, J., and Peeken, I. (2008). Nitrogen fixation and growth rates of Trichodesmium IMS-101 as a function of light intensity. *Mar. Ecol. Prog. Ser.* 359, 25–36.

Brooks, R. H., Brezonik, P. L., Putnam, H. D., and Keirn, M. A. (1971). Nitrogen fixation in an estuarine environment–Waccasassa on Florida Gulf Coast. *Limnol. Oceanogr.* 16, 701–710.

Burns, J. A., Zehr, J. P., and Capone, D. G. (2002). Nitrogen-fixing phylotypes of Chesapeake Bay and Neuse River estuary sediments. *Microb. Ecol.* 44, 336–343.

Burris, R. H. (1976). Nitrogen fixation by blue-green algae of the lizard island area of the great barrier reef. *Aust. J. Plant Physiol.* 3, 41–51.

Capone, D. G. (1982). Nitrogen-fixation (acetylene-reduction) by rhizosphere sediments of the Eelgrass Zostera-Marina. *Mar. Ecol. Prog. Ser.* 10, 67–75.

Capone, D. G. (1983). "Benthic nitrogen fixation," in *Nitrogen in the Marine Environment*, eds E. J. Carpenter and D. G. Capone (New York, NY: Academic Press), 105–137.

Capone, D. G., and Budin, J. M. (1982). Nitrogen-fixation associated with rinsed roots and rhizomes of the Eelgrass Zostera-Marina. *Plant Physiol.* 70, 1601–1604.

Capone, D. G., Burns, J. A., Montoya, J. P., Subramaniam, A., Mahaffey, C., Gunderson, T., et al. (2005). Nitrogen fixation by Trichodesmium spp.: an important source of new nitrogen to the tropical and subtropical North Atlantic Ocean. *Global Biogeochem. Cycles* 19. doi: 10.1029/2004GB002331

Capone, D. G., Oneil, J. M., Zehr, J., and Carpenter, E. J. (1990). Basis for diel variation in nitrogenase activity in the marine planktonic cyanobacterium Trichodesmium-Thiebautii. *Appl. Environ. Microbiol.* 56, 3532–3536.

Capone, D. G., Zehr, J. P., Paerl, H. W., Bergman, B., and Carpenter, E. J. (1997). Trichodesmium, a globally significant marine cyanobacterium. *Science* 276, 1221–1229.

Carpenter, E. J. (1983). "Nitrogen fixation by marine Oscillatoria (Trichodesmium) in the world's oceans," in *Nitrogen in the Marine Environment*, eds D. G. Capone and E. J. Carpenter (New York, NY: Academic Press), 65–103.

Carpenter, E. J., Oneil, J. M., Dawson, R., Capone, D. G., Siddiqui, P. J. A., Roenneberg, T., et al. (1993). The tropical diazotrophic phytoplankter Trichodesmium - biological characteristics of 2 common species. *Mar. Ecol. Prog. Ser.* 95, 295–304.

Carpenter, E. J., Vanraalte, C. D., and Valiela, I. (1978). Nitrogen-fixation by algae in a massachusetts salt-marsh. *Limnol. Oceanogr.* 23, 318–327.

Chappell, P. D., and Webb, E. A. (2010). A molecular assessment of the iron stress response in the two phylogenetic clades of Trichodesmium. *Environ. Microbiol.* 12, 13–27.

Chen, Y. B., Dominic, B., Mellon, M. T., and Zehr, J. P. (1998). Circadian rhythm of nitrogenase gene expression in the diazotrophic filamentous nonheterocystous Cyanobacterium Trichodesmium sp strain IMS101. *J. Bacteriol.* 180, 3598–3605.

Church, M. J., Mahaffey, C., Letelier, R. M., Lukas, R., Zehr, J. P., and Karl, D. M. (2009). Physical forcing of nitrogen fixation and diazotroph community structure in the North Pacific subtropical gyre. *Global Biogeochem. Cycles* 23. doi: 10.1029/2008GB003418

Codispoti, L. A. (2007). An oceanic fixed nitrogen sink exceeding 400 Tg Na-1 vs the concept of homeostasis in the fixed-nitrogen inventory. *Biogeosciences* 4, 233–253.

Codispoti, L. A., Brandes, J. A., Christensen, J. P., Devol, A. H., Naqvi, S. W. A., Paerl, H. et al. (2001). The oceanic fixed nitrogen and nitrous oxide budgets: moving targets as we enter the anthropocene? *Sci. Mar.* 65, 85–105.

Currin, C. A., Joye, S. B., and Paerl, H. W. (1996). Diel rates of N-2-fixation and denitrification in a transplanted Spartina alterniflora marsh: implications for N-flux dynamics. *Estuar. Coast. Shelf Sci.* 42, 597–616.

Dekaezemacker, J., and Bonnet, S. (2011). Sensitivity of N-2 fixation to combined nitrogen forms (NO3- and NH4+) in two strains of the marine diazotroph Crocosphaera watsonii (Cyanobacteria). *Mar. Ecol. Prog. Ser.* 438, 33–46.

Dekas, A. E., Poretsky, R. S., and Orphan, V. J. (2009). Deep-sea archaea fix and share nitrogen in methane-consuming microbial consortia. *Science* 326, 422–426.

Deutsch, C., Sarmiento, J. L., Sigman, D. M., Gruber, N., and Dunne, J. P. (2007). Spatial coupling of nitrogen inputs and losses in the ocean. *Nature* 445, 163–167.

Deutsch, C., Sigman, D. M., Thunell, R. C., Meckler, A. N., and Haug, G. H. (2004). Isotopic constraints on glacial/interglacial changes in the oceanic nitrogen budget. *Global Biogeochem. Cycles* 18. doi: 10.1029/2003GB002189

Elser, J. J., Bracken, M. E. S., Cleland, E. E., Gruner, D. S., Harpole, W. S., Hillebrand, H., et al. (2007). Global analysis of nitrogen and phosphorus limitation of primary producers in freshwater, marine and terrestrial ecosystems. *Ecol. Lett.* 10, 1135–1142.

Falkowski, P. G. (1983). "Enzymology of Nitrogen Assimilation," in *Nitrogen in the Marine Environment*, eds E. J. Carpenter and D. G. Capone (New York, NY: Academic Press), 839–868.

Fernandez, C., Farias, L., and Ulloa, O. (2011). Nitrogen fixation in denitrified marine waters. *PLoS ONE* 6:e20539. doi: 10.1371/journal.pone.0020539

Fu, F. X., and Bell, P. R. F. (2003). Factors affecting N-2 fixation by the cyanobacterium Trichodesmium sp GBR-TRLI101. *FEMS Microbiol. Ecol.* 45, 203–209.

Fujieki, L. A., Santiago-Mandujano, F., Lethaby, P., Lukas, R., and Karl, D. M. (2011). *Hawaii Ocean Time-series Data Report 20: 2008*, University of Hawaii, Honolulu, HI, USA.

Fulweiler, R. W., Nixon, S. W., Buckley, B. A., and Granger, S. L. (2007). Reversal of the net dinitrogen gas flux in coastal marine sediments. *Nature* 448, 180–182.

Gandy, E. L., and Yoch, D. C. (1988). Relationship between nitrogen-fixing sulfate reducers and fermenters in salt-marsh sediments and roots of Spartina-Alterniflora. *Appl. Environ. Microbiol.* 54, 2031–2036.

Garcia, H. E., Locarnini, R. A., Boyer, T. B., Antonov, J. I., Zweng, M. M., Baranova, O. K., et al. (2010). "Nutrients (phosphate, nitrate, silicate)," in *World Ocean Atlas 2009*, ed S. Levitus (Washington, DC: US Government Printing Office), 398.

Gardner, W. S., Mccarthy, M. J., An, S. M., Sobolev, D., Sell, K. S., and Brock, D. (2006). Nitrogen fixation and dissimilatory nitrate reduction to ammonium (DNRA) support nitrogen dynamics in Texas estuaries. *Limnol. Oceanogr.* 51, 558–568.

Grosse, J., Bombar, D., Hai Nhu, D., Lam Ngoc, N., and Voss, M. (2010). The Mekong River plume fuels nitrogen fixation and determines phytoplankton species distribution in the South China Sea during low- and high-discharge season. *Limnol. Oceanogr.* 55, 1668–1680.

Haines, J. R., Atlas, R. M., Griffiths, R. P., and Morita, R. Y. (1981). Denitrification and nitrogen-fixation in alaskan continental-shelf sediments. *Appl. Environ. Microbiol.* 41, 412–421.

Halm, H., Lam, P., Ferdelman, T. G., Lavik, G., Dittmar, T., Laroche, J., et al. (2012). Heterotrophic

organisms dominate nitrogen fixation in the South Pacific Gyre. *ISME J.* 6, 1238–1249.

Hamersley, M. R., Turk, K. A., Leinweber, A., Gruber, N., Zehr, J. P., Gunderson, T., et al. (2011). Nitrogen fixation within the water column associated with two hypoxic basins in the Southern California Bight. *Aquat. Microb. Ecol.* 63, 193–205.

Haug, G. H., Pedersen, T. F., Sigman, D. M., Calvert, S. E., Nielsen, B., and Peterson, L. C. (1998). Glacial/interglacial variations in production and nitrogen fixation in the Cariaco Basin during the last 580 kyr. *Paleoceanography* 13, 427–432.

Hewson, I., Moisander, P. H., Achilles, K. M., Carlson, C. A., Jenkins, B. D., Mondragon, E. et al. (2007). Characteristics of diazotrophs in surface to abyssopelagic waters of the Sargasso Sea. *Aquat. Microb. Ecol.* 46, 15–30.

Holl, C. M., and Montoya, J. P. (2005). Interactions between nitrate uptake and nitrogen fixation in continuous cultures of the marine diazotroph Trichodesmium (Cyanobacteria). *J. Phycol.* 41, 1178–1183.

Hutchins, D. A., Fu, F. X., Zhang, Y., Warner, M. E., Feng, Y., Portune, K., et al. (2007). CO2 control of Trichodesmium N-2 fixation, photosynthesis, growth rates, and elemental ratios: Implications for past, present, and future ocean biogeochemistry. *Limnol. Oceanogr.* 52, 1293–1304.

Jayakumar, A., Al-Rshaidat, M. M. D., Ward, B. B., and Mulholland, M. R. (2012). Diversity, distribution and expression of diazotroph nifH genes in oxygen deficient waters of the Arabian Sea. *FEMS Microbiol. Ecol.* doi: 10.1111/j.1574-6941.2012.01430.x. [Epub ahead of print].

Joshi, H. M., and Tabita, F. R. (1996). A global two component signal transduction system that integrates the control of photosynthesis, carbon dioxide assimilation, and nitrogen fixation. *Proc. Natl. Acad. Sci. U.S.A.* 93, 14515–14520.

Joye, S. B., and Paerl, H. W. (1993). Contemporaneous nitrogen-fixation and denitrification in intertidal microbial mats - rapid response to runoff events. *Mar. Ecol. Prog. Ser.* 94, 267–274.

Joye, S. B., and Paerl, H. W. (1994). Nitrogen cycling in microbial mats–rates and patterns of denitrification and nitrogen-fixation. *Mar. Biol.* 119, 285–295.

Klausmeier, C. A., Litchman, E., Daufresne, T., and Levin, S. A. (2004). Optimal nitrogen-to-phosphorus stoichiometry of phytoplankton. *Nature* 429, 171–174.

Knapp, A. N., Dekaezemacker, J., Bonnet, S., Sohm, J. A., and Capone, D. G. (2012). Sensitivity of Trichodesmium and Crocosphaera abundance and N2 fixation rates to varying NO3- and PO43- concentrations in batch cultures. *Aquat. Microb. Ecol.* 66, 223–236.

Kustka, A. B., Sanudo-Wilhelmy, S. A., Carpenter, E. J., Capone, D., Burns, J., and Sunda, W. G. (2003). Iron requirements for dinitrogen- and ammonium-supported growth in cultures of Trichodesmium (IMS 101): comparison with nitrogen fixation rates and iron: carbon ratios of field populations. *Limnol. Oceanogr.* 48, 1869–1884.

Langlois, R. J., Huemmer, D., and Laroche, J. (2008). Abundances and distributions of the dominant nifH phylotypes in the Northern Atlantic Ocean. *Appl. Environ. Microbiol.* 74, 1922–1931.

Lee, R. Y., and Joye, S. B. (2006). Seasonal patterns of nitrogen fixation and denitrification in oceanic mangrove habitats. *Mar. Ecol. Prog. Ser.* 307, 127–141.

Lenes, J. M., Darrow, B. P., Cattrall, C., Heil, C. A., Callahan, M., Vargo, G. A., et al. (2001). Iron fertilization and the Trichodesmium response on the West Florida shelf. *Limnol. Oceanogr.* 46, 1261–1277.

Levitan, O., Brown, C. M., Sudhaus, S., Campbell, D., Laroche, J., and Berman-Frank, I. (2010). Regulation of nitrogen metabolism in the marine diazotroph Trichodesmium IMS101 under varying temperatures and atmospheric CO(2) concentrations. *Environ. Microbiol.* 12, 1899–1912.

Levitan, O., Rosenberg, G., Setlik, I., Setlikova, E., Grigel, J., Klepetar, J., et al. (2007). Elevated CO(2) enhances nitrogen fixation and growth in the marine cyanobacterium Trichodesmium. *Glob. Change Biol.* 13, 531–538.

Loladze, I., and Elser, J. J. (2011). The origins of the Redfield nitrogen-to-phosphorus ratio are in a homoeostatic protein-to-rRNA ratio. *Ecol. Lett.* 14, 244–250.

McCarthy, M. J., McNeal, K. S., Morse, J. W., and Gardner, W. S. (2008). Bottom-water hypoxia effects on sediment-water interface nitrogen transformations in a seasonally hypoxic, shallow bay (Corpus christi bay, TX, USA). *Estuar. Coast.* 31, 521–531.

McGlathery, K. J., Risgaard-Petersen, N., and Christensen, P. B. (1998). Temporal and spatial variation in nitrogen fixation activity in the eelgrass Zostera marina rhizosphere. *Mar. Ecol. Prog. Ser.* 168, 245–258.

Mehta, M. P., and Baross, J. A. (2006). Nitrogen fixation at 92 degrees C by a hydrothermal vent archaeon. *Science* 314, 1783–1786.

Mehta, M. P., Butterfield, D. A., and Baross, J. A. (2003). Phylogenetic diversity of nitrogenase (nifH) genes in deep-sea and hydrothermal vent environments of the Juan de Fuca ridge. *Appl. Environ. Microbiol.* 69, 960–970.

Mehta, M. P., Huber, J. A., and Baross, J. A. (2005). Incidence of novel and potentially archaeal nitrogenase genes in the deep Northeast Pacific Ocean. *Environ. Microbiol.* 7, 1525–1534.

Michaels, A. F., and Knap, A. H. (1996). Overview of the US JGOFS Bermuda Atlantic time-series study and the hydrostation S program. *Deep Sea Res. Part II Top. Stud. Oceanogr.* 43, 157–198.

Milligan, A. J., Berman-Frank, I., Gerchman, Y., Dismukes, G. C., and Falkowski, P. G. (2007). Light-dependent oxygen consumption in nitrogen-fixing cyanobacteria plays a key role in nitrogenase protection. *J. Phycol.* 43, 845–852.

Mohr, W., Grosskopf, T., Wallace, D. W. R., and Laroche, J. (2010). Methodological underestimation of oceanic nitrogen fixation rates. *PLoS ONE* 5:e12583. doi: 10.1371/journal.pone.0012583

Moisander, P. H., Beinart, R. A., Hewson, I., White, A. E., Johnson, K. S., Carlson, C. A., et al. (2010). Unicellular cyanobacterial distributions broaden the oceanic N(2) fixation domain. *Science* 327, 1512–1514.

Montoya, J. P., Holl, C. M., Zehr, J. P., Hansen, A., Villareal, T. A., and Capone, D. G. (2004). High rates of N-2 fixation by unicellular diazotrophs in the oligotrophic Pacific Ocean. *Nature* 430, 1027–1031.

Montoya, J. P., Voss, M., Kahler, P., and Capone, D. G. (1996). A simple, high-precision, high-sensitivity tracer assay for N-2 fixation. *Appl. Environ. Microbiol.* 62, 986–993.

Mulholland, M. R., and Capone, D. G. (1999). Nitrogen fixation, uptake and metabolism in natural and cultured populations of Trichodesmium spp. *Mar. Ecol. Prog. Ser.* 188, 33–49.

Mulholland, M. R., Ohki, K., and Capone, D. G. (1999). Nitrogen utilization and metabolism relative to patterns of N(2) fixation in cultures of Trichodesmium NIBB1067. *J. Phycol.* 35, 977–988.

Mulholland, M. R., Ohki, K., and Capone, D. G. (2001). Nutrient controls on nitrogen uptake and metabolism by natural populations and cultures of Trichodesmium (Cyanobacteria). *J. Phycol.* 37, 1001–1009.

Needoba, J. A., Foster, R. A., Sakamoto, C., Zehr, J. P., and Johnson, K. S. (2007). Nitrogen fixation by unicellular diazotrophic cyanobacteria in the temperate oligotrophic North Pacific Ocean. *Limnol. Oceanogr.* 52, 1317–1327.

Nielsen, L. B., Finster, K., Welsh, D. T., Donelly, A., Herbert, R. A., De Wit, R., et al. (2001). Sulphate reduction and nitrogen fixation rates associated with roots, rhizomes and sediments from Zostera noltii and Spartina maritima meadows. *Environ. Microbiol.* 3, 63–71.

Ohki, K., and Fujita, Y. (1982). Laboratory culture of the pelagic blue-green-alga Trichodesmium-Thiebautii–conditions for unialgal culture. *Mar. Ecol. Prog. Ser.* 7, 185–190.

Ohki, K., Zehr, J. P., Falkowski, P. G., and Fujita, Y. (1991). Regulation of nitrogen-fixation by different nitrogen-sources in the marine nonheterocystous Cyanobacterium Trichodesmium sp Nibb1067. *Arch. Microbiol.* 156, 335–337.

Orellana, M. V., and Hansell, D. A. (2012). Ribulose-1, 5-bisphosphate carboxylase/oxygenase (RuBisCO): a long-lived protein in the deep ocean. *Limnol. Oceanogr.* 57, 826–834.

Patriquin, D. (1978). "Nitrogen fixation (acetylene reduction) associated with cord grass, Spartina alterniflora Loisel," in *Environmental Role of Nitrogen-Fixing Blue-Green Algae and Asymbiotic Bacteria*, ed U. Granhall (Stockholm: Ecological Bulletin), 20–27.

Patriquin, D., and Knowles, R. (1972). Nitrogen fixation in rhizosphere of marine angiosperms. *Mar. Biol.* 16, 49–58.

Prufert-Bebout, L., Paerl, H. W., and Lassen, C. (1993). Growth, nitrogen-fixation, and spectral attenuation in cultivated Trichodesmium species. *Appl. Environ. Microbiol.* 59, 1367–1375.

Ramos, J. B. E., Biswas, H., Schulz, K. G., Laroche, J., and Riebesell, U. (2007). Effect of rising atmospheric carbon dioxide on the marine nitrogen fixer Trichodesmium. *Global Biogeochem. Cycles* 21. doi: 10.1029/2006GB002898

Rao, A. M. F., and Charette, M. A. (2012). Benthic nitrogen fixation in an eutrophic estuary affected by groundwater discharge. *J. Coast. Res.* 28, 477–485.

Robson, R. L., and Postgate, J. R. (1980). Oxygen and hydrogen in biological nitrogen-fixation. *Annu. Rev. Microbiol.* 34, 183–207.

Rodier, M., and Le Borgne, R. (2008). Population dynamics and environmental conditions affecting Trichodesmium spp. (filamentous cyanobacteria) blooms in the south-west lagoon of New Caledonia. *J. Exp. Mar. Biol. Ecol.* 358, 20–32.

Rodier, M., and Le Borgne, R. (2010). Population and trophic dynamics of Trichodesmium thiebautii in the SE lagoon of New Caledonia. Comparison with T. erythraeum in the SW lagoon. *Mar. Pollut. Bull.* 61, 349–359.

Rueter, J. G., Ohki, K., and Fujita, Y. (1990). The effect of iron nutrition on photosynthesis and nitrogen-fixation in cultures of Trichodesmium (Cyanophyceae). *J. Phycol.* 26, 30–35.

Saito, M. A., Bertrand, E. M., Dutkiewicz, S., Bulygin, V. V., Moran, D. M., Monteiro, F. M., et al. (2011). Iron conservation by reduction of metalloenzyme inventories in the marine diazotroph *Crocosphaera watsonii*. *Proc. Natl. Acad. Sci. U.S.A.* 108, 2184–2189.

Sandh, G., Ran, L., Xu, L., Sundqvist, G., Bulone, V., and Bergman, B. (2011). Comparative proteomic profiles of the marine cyanobacterium Trichodesmium erythraeum IMS101 under different nitrogen regimes. *Proteomics* 11, 406–419.

Scott, T., Cotner, J., and Lapara, T. (2012). Variable stoichiometry and homeostatic regulation of bacterial biomass elemental composition. *Front. Microbiol.* 3:42. doi: 10.3389/fmicb.2012.00042

Seitzinger, S. P. (1988). Denitrification in fresh-water and coastal marine ecosystems–ecological and geochemical significance. *Limnol. Oceanogr.* 33, 702–724.

Slater, J., and Capone, D. G. (1984). Effects of metals on nitrogen-fixation and denitrification in slurries of anoxic saltmarsh sediment. *Mar. Ecol. Prog. Ser.* 18, 89–95.

Sohm, J. A., Hilton, J. A., Noble, A. E., Zehr, J. P., Saito, M. A., and Webb, E. A. (2011). Nitrogen fixation in the South Atlantic Gyre and the Benguela Upwelling System. *Geophys. Res. Lett.* 38. doi: 10.1029/2011GL048315

Stal, L. J., and Heyer, H. (1987). Dark anaerobic nitrogen-fixation (acetylene-reduction) in the cyanobacterium *Oscillatoria sp. FEMS Microbiol. Ecol.* 45, 227–232.

Stal, L. J. (2009). Is the distribution of nitrogen-fixing cyanobacteria in the oceans related to temperature? *Environ. Microbiol.* 11, 1632–1645.

Steppe, T. F., and Paerl, H. W. (2002). Potential N-2 fixation by sulfate-reducing bacteria in a marine intertidal microbial mat. *Aquat. Microb. Ecol.* 28, 1–12.

Steppe, T. F., and Paerl, H. W. (2005). Nitrogenase activity and nifH expression in a marine intertidal microbial mat. *Microb. Ecol.* 49, 315–324.

Tichi, M. A., and Tabita, F. R. (2000). Maintenance and control of redox poise in Rhodobacter capsulatus strains deficient in the Calvin-Benson-Bassham pathway. *Arch. Microbiol.* 174, 322–333.

Villareal, T. A., and Carpenter, E. J. (1990). Diel buoyancy regulation in the marine diazotrophic cyanobacterium Trichodesmium-Thiebautii. *Limnol. Oceanogr.* 35, 1832–1837.

Villareal, T. A., and Carpenter, E. J. (2003). Buoyancy regulation and the potential for vertical migration in the oceanic cyanobacterium Trichodesmium. *Microb. Ecol.* 45, 1–10.

Voss, M., Croot, P., Lochte, K., Mills, M., and Peeken, I. (2004). Patterns of nitrogen fixation along 10N in the tropical Atlantic. *Geophys. Res. Lett.* 31. doi: 10.1029/2004GL020127

Welsh, D. T., Bourgues, S., Dewit, R., and Herbert, R. A. (1996). Seasonal variations in nitrogen-fixation (acetylene reduction) and sulphate-reduction rates in the rhizosphere of Zostera noltii: nitrogen fixation by sulphate reducing bacteria. *Mar. Biol.* 125, 619–628.

Westberry, T., Behrenfeld, M. J., Siegel, D. A., and Boss, E. (2008). Carbon-based primary productivity modeling with vertically resolved photoacclimation. *Global Biogeochem. Cycles* 22. doi: 10.1029/2007GB003078

Westberry, T. K., and Siegel, D. A. (2006). Spatial and temporal distribution of Trichodesmium blooms in the world's oceans. *Global Biogeochem. Cycles* 20. doi: 10.1029/2005GB002673

Westberry, T. K., Siegel, D. A., and Subramaniam, A. (2005). An improved bio-optical model for the remote sensing of Trichodesmium spp. blooms. *J. Geophys. Res. Oceans* 110. doi: 10.1029/2004JC002517

White, A. E., Prahl, F. G., Letelier, R. M., and Popp, B. N. (2007). Summer surface waters in the Gulf of California: prime habitat for biological N-2 fixation. *Global Biogeochem. Cycles* 21. doi: 10.1029/2006GB002779

Yoch, D. C., and Whiting, G. J. (1986). Evidence for Nh4+ switch-off regulation of nitrogenase activity by bacteria in salt-marsh sediments and roots of the grass Spartina-Alterniflora. *Appl. Environ. Microbiol.* 51, 143–149.

Zehr, J. P. (2011). Nitrogen fixation by marine cyanobacteria. *Trends Microbiol.* 19, 162–173.

Zehr, J. P., Bench, S. R., Carter, B. J., Hewson, I., Niazi, F., Shi, T., et al. (2008). Globally distributed uncultivated oceanic N(2)-fixing cyanobacteria lack oxygenic photosystem II. *Science* 322, 1110–1112.

Zehr, J. P., Waterbury, J. B., Turner, P. J., Montoya, J. P., Omoregie, E., Steward, G. F., et al. (2001). Unicellular cyanobacteria fix N-2 in the subtropical North Pacific Ocean. *Nature* 412, 635–638.

Conflict of Interest Statement: The author declares that the research was conducted in the absence of any commercial or financial relationships that could be construed as a potential conflict of interest.

Received: 08 July 2012; accepted: 02 October 2012; published online: 19 October 2012.

*Citation: Knapp AN (2012) The sensitivity of marine N_2 fixation to dissolved inorganic nitrogen. Front. Microbio. **3**:374. doi: 10.3389/fmicb.2012.00374*

This article was submitted to Frontiers in Aquatic Microbiology, a specialty of Frontiers in Microbiology.

frontiers in
MICROBIOLOGY

ORIGINAL RESEARCH ARTICLE
published: 24 July 2012
doi: 10.3389/fmicb.2012.00263

Quantification of ammonia oxidation rates and the distribution of ammonia-oxidizing *Archaea* and *Bacteria* in marine sediment depth profiles from Catalina Island, California

J. M. Beman[1]*, Victoria J. Bertics[2,3], Thomas Braunschweiler[2†] and Jesse M. Wilson[1]

[1] School of Natural Sciences, University of California, Merced, Merced, CA, USA
[2] Department of Biological Sciences and Wrigley Institute for Environmental Studies, University of Southern California, Los Angeles, CA, USA
[3] Department of Marine Biogeochemistry, Helmholtz Centre for Ocean Research Kiel, Kiel, Germany

Edited by:
Bess B. Ward, Princeton University, USA

Reviewed by:
Zhe-Xue Quan, Fudan University, China
Andreas Schramm, Aarhus University, Denmark

****Correspondence:***
J. M. Beman, School of Natural Sciences and Sierra Nevada Research Institute, University of California, Merced, 5200 North Lake Road, Merced, CA 95343, USA.
e-mail: jmbeman@gmail.com

†Present address:
Thomas Braunschweiler, Institute of Microbiology, Swiss Federal Institute of Technology Zürich, Zürich, Switzerland.

Microbial communities present in marine sediments play a central role in nitrogen biogeochemistry at local to global scales. Along the oxidation–reduction gradients present in sediment profiles, multiple nitrogen cycling processes (such as nitrification, denitrification, nitrogen fixation, and anaerobic ammonium oxidation) are active and actively coupled to one another – yet the microbial communities responsible for these transformations and the rates at which they occur are still poorly understood. We report pore water geochemical (O_2, NH_4^+, and NO_3^-) profiles, quantitative profiles of archaeal and bacterial *amoA* genes, and ammonia oxidation rate measurements, from bioturbated marine sediments of Catalina Island, California. Across triplicate sediment cores collected offshore at Bird Rock (BR) and within Catalina Harbor (CH), oxygen penetration (0.24–0.5 cm depth) and the abundance of *amoA* genes (up to 9.30×10^7 genes g^{-1}) varied with depth and between cores. Bacterial *amoA* genes were consistently present at depths of up to 10 cm, and archaeal *amoA* was readily detected in BR cores, and CH cores from 2008, but not 2007. Although detection of DNA is not necessarily indicative of active growth and metabolism, ammonia oxidation rate measurements made in 2008 (using isotope tracer) demonstrated the production of oxidized nitrogen at depths where *amoA* was present. Rates varied with depth and between cores, but indicate that active ammonia oxidation occurs at up to 10 cm depth in bioturbated CH sediments, where it may be carried out by either or both ammonia-oxidizing *archaea* and *bacteria*.

Keywords: nitrification, *amoA*, sediments, bioturbation, *archaea*

INTRODUCTION

Marine sediments are Earth's largest microbial habitat, harboring an estimated 10^{31} microbial cells with a total biomass rivaling that of all plants (Whitman et al., 1998). Sedimentary microbial communities play a substantial role in global biogeochemical cycles of carbon (C), nitrogen (N), and sulfur (S) – nearly 50% of N removal from the ocean, for instance, occurs in sediments (Codispoti et al., 2001; Deutsch et al., 2011). Coastal sediments are particularly significant sites for N cycling due to human influence on the global N cycle: agricultural fertilizer use and fossil fuel combustion have more than doubled the amount of N flowing through terrestrial ecosystems, yet over 50% of this N is removed in aquatic and coastal ecosystems before it reaches the sea (Seitzinger et al., 2006; Gruber and Galloway, 2008). The overall size of the N sink in sediments (where N is converted by anaerobic microbial processes into gaseous forms that may flux out of the system) is nonetheless poorly constrained, leading to debate about whether the oceanic N cycle is currently in balance (e.g., Codispoti et al., 2001; Gruber and Galloway, 2008; Deutsch et al., 2011). In order for these outputs to occur via denitrification – which is thought to dominate N loss in sediments at water depths <100 m (Kuypers et al., 2006; Francis et al., 2007) – N must be present in oxidized forms such as nitrite (NO_2^-) or nitrate (NO_3^-). This is also the case for N loss via anaerobic ammonium oxidation (anammox), as anammox uses NO_2^- as an electron acceptor (Strous et al., 2006). Dissolved ammonium (NH_4^+) must therefore first be oxidized, or reduced N present within organic material must be regenerated and subsequently oxidized, before N can be removed anaerobically.

The oxidation of reduced N occurs via the two-step process of nitrification: ammonia-oxidizing archaea (AOA) and bacteria (AOB) oxidize reduced NH_3/NH_4^+ to NO_2^-, and nitrite-oxidizing bacteria (NOB) oxidize nitrite to NO_3^- (Francis et al., 2007; Erguder et al., 2009). Given the importance of nitrification to sedimentary and global N cycling, AOA and AOB have been studied extensively in estuarine and coastal sediments (Freitag and Prosser, 2003; Mortimer et al., 2004; Bernhard et al., 2005; Francis et al., 2005; Beman and Francis, 2006; Bernhard et al., 2007; Mosier and Francis, 2008; Abell et al., 2010; Wankel et al., 2011) using 16S rRNA or the ammonia monooxygenase subunit A gene (*amoA*)

as molecular markers. Most of these studies have targeted surface sediments, and few have examined variability in nitrifier distributions and activity with depth. Surprisingly, Freitag and Prosser (2003) and Mortimer et al. (2004) detected AOB 16S rRNA at depths of up to 40 cm in sediments from Loch Duich in Scotland; based on this observation and detectable rates of nitrification down to 8 cm depth, Mortimer et al. (2004) argue that this is evidence of "anoxic nitrification," possibly coupled to manganese reduction. Dollhopf et al. (2005) also showed that sediment bioturbation supplies oxygen to AOB present at 6 cm depth in salt marsh sediments.

In contrast to AOB, however, the depth distribution of the recently discovered AOA in sediments is largely unknown. Sulfide inhibits sedimentary nitrification (Joye and Hollibaugh, 1995), but Erguder et al. (2009) argue that AOA tolerate higher concentrations of sulfide than AOB based in part on their presence in sulfidic sediments (Caffrey et al., 2007). In an underground coastal aquifer, Santoro et al. (2008) found that AOA and AOB appear to shift in relative dominance based on salinity and ammonium concentrations (Santoro et al., 2008). Based on pyrosequencing of 16S rRNA, AOA comprised 35% of archaeal sequences in an oxic coral reef sediment sample, but formed a smaller proportion (<10%) of the archaeal community in an anoxic sample (Gaidos et al., 2011). Few other data are available from sediments. Quantifying the distribution of AOA relative to AOB and in relation to nitrification rates may therefore enhance our understanding of sedimentary N biogeochemistry, as no study has collected sediment depth profiles of AOA, AOB, and ammonia oxidation rates in parallel.

The purpose of this study was consequently to quantify AOA, AOB, and ammonia oxidation rates in sediment cores from Catalina Island, California, USA (**Figure 1**). In a previous

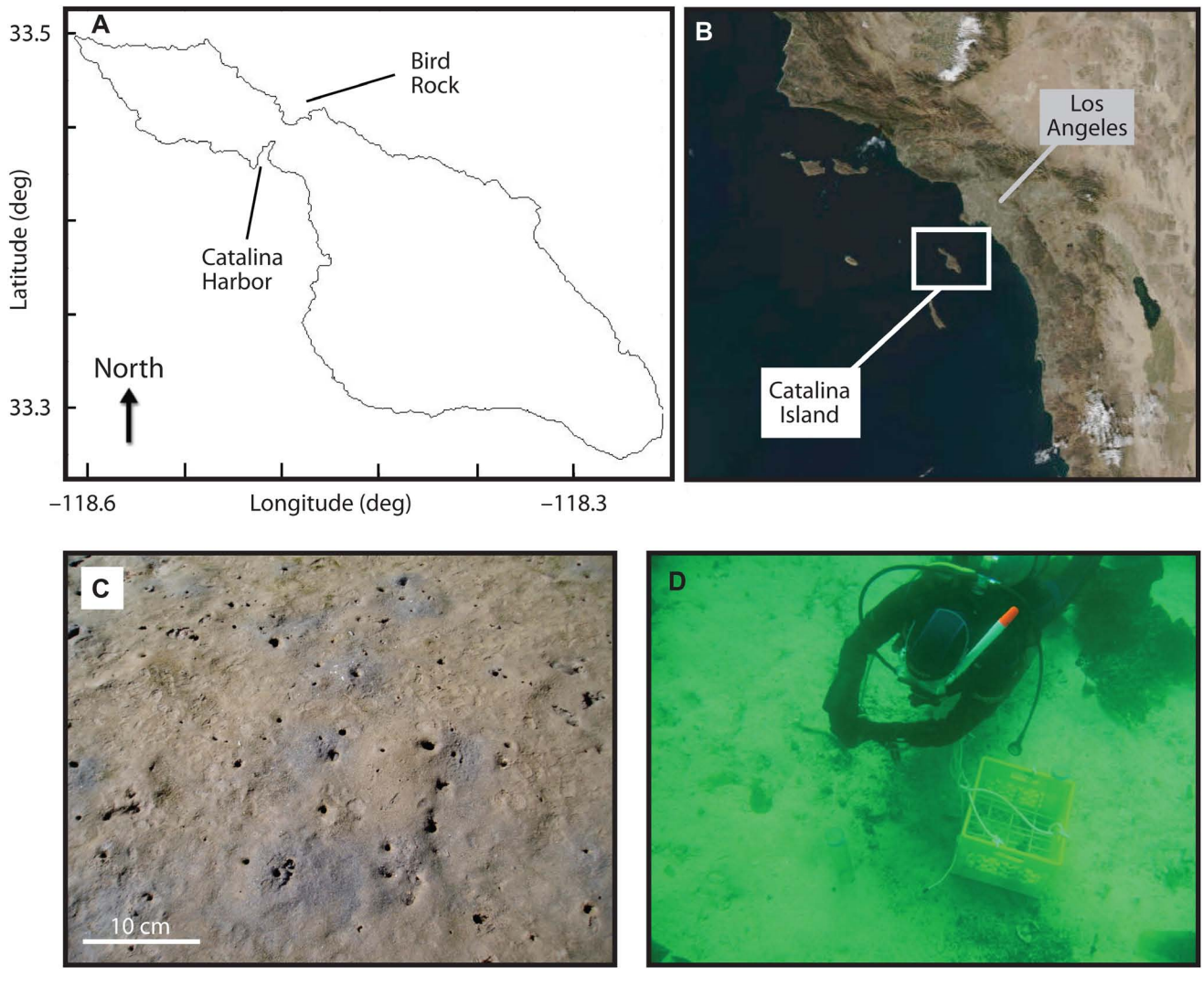

FIGURE 1 | Location of Catalina Island along the coast of California **(B)**, and of Catalina Harbor and Bird Rock sampling locations **(A)**. Catalina Harbor sediment sampling location is shown in **(C)** with scale bar at lower left, and collection of Bird Rock sediments is shown in **(D)**. Burrow density at Catalina Harbor in 2008 was ~120 burrow opening per square meter.

study of Catalina Island sediments, Bertics and Ziebis (2009) detected increases in pore water nitrate where decreases in pore water ammonium concentrations were also observed; canonical correspondence analysis revealed that changes in the microbial community with sediment depth were correlated to changes in ammonium concentrations – indicating that ammonium is a key factor influencing microbial communities in Catalina Island sediments. In the present study, AOA and AOB *amoA* genes were quantified in sectioned, triplicate cores collected at two locations, and cores were collected during two sampling periods at one of these locations. Coupled biogeochemical measurements included microsensor oxygen profiles, measurements of dissolved nitrogen in pore waters, and nitrification rate measurements using ^{15}N isotopically labeled ammonium. Measurable rates of nitrification were found throughout two cores, and both AOA and AOB *amoA* genes were present at depths of up to 10 cm.

MATERIALS AND METHODS

SITE DESCRIPTION

Samples were collected from two locations on or near Catalina Island, California, USA. The first site, "Catalina Harbor" (CH; 33° 27.080′N, 118° 29.293′W), was a shallow (<2 m) intertidal lagoon in CH on the western side of the island (**Figure 1**). The lagoon was a low energy, highly bioturbated area consisting of muddy sand with the majority of grains being <500 μm (Bertics et al., 2010). The two most abundant burrowing macrofauna were the bay ghost shrimp *Neotrypaea californiensis*, Dana, 1854 (Crustacea: Decapoda: Thalassinidea) and the Mexican fiddler crab *Uca crenulata*, Lockington, 1877 (Crustacea: Decapoda: Ocypodoidea). *N. californiensis* inhabits intertidal areas stretching from Alaska to Baja California, and is known to build complex branching burrows that extend to ∼76 cm depth and have several openings to the surface (MacGinitie, 1934; Brenchley, 1981; Swinbanks and Murray, 1981). *U. crenulata* is found from Santa Barbara, California to Central Mexico and typically maintains simple J-shaped burrows with a single entrance and that extend to a depth of ∼20 cm; *U. crenulata* frequently leaves these burrows during low tide to forage on algae, bacteria, and detritus on the sediment surface (Zeil et al., 2006).

The second site, "Bird Rock" (BR; 33° 25.788′N, 118° 30.314′W), was located 1.5 km off the eastern shore the island in ca. 20 m of water. This site consisted of regions with boulders lying on top of more permeable sandy and gravel sediment (Nelson and Vance, 1979), and regions of rocky outcrops – the largest of which extends out of the water and forms a small island named BR. The sandy region where sampling occurred supported dense patches of the giant kelp *Macrocystis pyrifera* and other brown algae, along with associated meio- and macrofaunal communities. Typical water velocities in the area range from 1 to 7 m s^{-1} and the swell surrounding BR ranges from 1 to 3 m in height (Morrow and Carpenter, 2008), making this site an area of high tidal activity in contrast to CH.

SAMPLE COLLECTION

In 2007, sediment samples from CH were collected on 19 November during high tide, as a minimum of 10 cm of water above the sediment was required to allow for coring, while samples from BR were collected on 21 November below the sea surface via SCUBA in an area near a large rock formation. At both sites, sediment samples were collected using 5 cm diameter, 39 cm length acrylic cores; three intact sediment cores of 5–25 cm sediment depth were collected at each site, and cores were placed in an ice chest at ambient temperature for transport back to the laboratory. In 2008, six sediment cores were collected in approximately the same location in CH as was sampled in 2007, with three parallel cores collected for ^{15}N measurements on 14 April, and three parallel cores collected for nutrient measurement, oxygen measurements, and DNA sampling on 15 April.

Following oxygen analyses (see below), each of the nine cores was sub-sampled for ammonium and nitrate concentration analyses and DNA extraction. One-centimeter slices were taken from each core starting at the surface down to 10 cm for the CH cores (CH1–CH6) and 5 cm for the BR cores (BR1–BR3). BR cores extended to a depth of only 5 cm owing to the difficulty in obtaining longer cores from porous sediments via SCUBA. Pore water was collected from each 1-cm slice by centrifugation (10 min at 5000 × *g*) using 50 ml Macrosep® Centrifugal Devices (Pall Corporation, Life Sciences) flushed with nitrogen gas. The recovered pore water (∼3 ml) was immediately frozen at −20°C for later determination of dissolved nitrogen compounds.

PORE WATER AMMONIUM AND NITRATE ANALYSES AND MICROSENSOR OXYGEN PROFILES

Pore water ammonium concentrations were determined by flow injection analysis modified for small sample volumes (Hall and Aller, 1992); 50 μl of pore water was injected for each sediment slice in triplicate. The sum of nitrate and nitrite was determined spectrophotometrically after reduction of samples with spongy cadmium (Jones, 1984). One milliliter of pore water from the respective core slices was used for the colorimetric analysis of nitrite concentrations, and nitrite + nitrate concentrations (after reduction) on a spectrophotometer (Strickland and Parsons, 1972).

Each of the nine intact cores was analyzed for oxygen content on the vertical axis using a Unisense oxygen microsensor – a miniaturized amperometric sensor with a guard electrode (Revsbech and Jørgensen, 1986; Unisense© 2007). For each core, three high-resolution microprofiles of oxygen were measured in vertical intervals of 200–250 μm using Clark-type amperometric oxygen sensors (Revsbech and Jørgensen, 1986; Revsbech, 1989; Unisense©, Aarhus, Denmark) following a two-point calibration. Sensors were attached to computer-controlled motorized micromanipulators (Märzhäuser, Wetzlar, Germany) and driven vertically into the sediment in micrometer steps. Signals were amplified and transformed to millivolt (mV) by a two-channel picoammeter (PA 2000; Unisense©) and directly recorded on a computer using the software Profix® (Unisense©).

DNA EXTRACTION AND QUANTIFICATION AND QUANTITATIVE PCR ANALYSES

For DNA extraction, ca. 500 mg of sediment from each 1 cm depth interval was stored at −80°C, and DNA was extracted from 200 to

700 mg of sediment using the ZR Soil Microbe DNA Kit (Zymo Research, Irvine, CA, USA; 2007 samples) or the MP Biomedicals FastDNA Spin Kit for Soil (MP Biomedicals, Solon, OH, USA; 2008 samples). DNA was quantified using the PicoGreen assay and the manufacturer's protocol (Life Technologies Corporation, Carlsbad, CA, USA).

Quantitative PCR (qPCR) analyses were identical to those used by Beman et al. (2012). Archaeal *amoA* qPCR assays used the following reaction chemistry: 12.5 μL SYBR Premix F (Epicentre Biotechnologies, Madison, WI, USA), 2 mM $MgCl_2$, 0.4 μM of each primer, 1.25 units AmpliTaq polymerase (Life Technologies Corporation, Carlsbad, CA, USA), 40 ng μL^{-1} BSA (Life Technologies Corporation, Carlsbad, CA, USA), and 1 ng DNA in a final volume of 25 μL. β-AOB were quantified using the same reaction chemistry but without additional $MgCl_2$. Primers (and relevant references for primer sequences), cycling conditions, qPCR standards, standard curve correlation coefficients, and PCR efficiencies are listed in **Table 1**. All qPCR assays were performed on a Stratagene MX3005P qPCR system (Agilent Technologies, La Jolla, CA, USA).

$^{15}NH_4^+$ OXIDATION RATE MEASUREMENTS

Ammonia oxidation rates were measured by injecting 99 atom percent (at%) $^{15}NH_4^+$ solution to a concentration of 33 μmol L^{-1} through small silicone-sealed holes drilled into the acrylic core cylinder. The accumulation of ^{15}N label in the oxidized $NO_2^- + NO_3^-$ pool was measured after incubation for ~24 h. The $\delta^{15}N$ value of N_2O produced from $NO_2^- + NO_3^-$ using the "denitrifier method" (Sigman et al., 2001) was measured using methods described in Popp et al. (1995) and Dore et al. (1998): N_2O produced from $NO_2^- + NO_3^-$ was transferred from the reaction vial, cryofocused, separated from other gases using a 0.32 mm i.d. × 25 m PoraPLOT-Q capillary column at room temperature, and introduced into ion source MAT252 mass spectrometer through a modified GC-C I interface. Isotopic reference materials (USGS-32, NIST-3, and UH $NaNO_3$) bracketed every 12–16 samples and $\delta^{15}N$ values measured on-line were linearly correlated ($r^2 = 0.996$–0.999) with accepted reference material $\delta^{15}N$ values.

Initial at% enrichment of the substrate at the beginning of the experiment ($n_{NH_4^+}$, see Eq. 1) was calculated by isotope mass balance based on NH_4^+ concentrations assuming that the ^{15}N activity of unlabeled NH_4^+ was 0.3663 at% ^{15}N. Rates of ammonia oxidation ($^{15}R_{ox}$) were calculated using an equation modified from Ward et al. (1989):

$$^{15}R_{ox} = \frac{(n_t - n_{oNO_x^-}) \times [NO_3^- + NO_2^-]}{(n_{NH_4^+} - n_{oNH_4^+}) \times t}, \quad (1)$$

where n_t is the at% ^{15}N in the $NO_3^- + NO_2^-$ pool measured at time t, $n_{oNO_x^-}$, is the measured at% ^{15}N of unlabeled $NO_3^- + NO_2^-$, $n_{oNH_4^+}$ is the initial at% enrichment of NH_4^+ at the beginning of the experiment, $n_{NH_4^+}$ is at% ^{15}N of NH_4^+, and $[NO_3^- + NO_2^-]$ is the concentration of the NO_x^- pool. All statistical analyses were conducted in MATLAB.

RESULTS

MICROSENSOR OXYGEN PROFILES AND PORE WATER DISSOLVED NITROGEN CONCENTRATIONS

Oxygen concentrations in overlying water were similar in both CH and BR sediments in 2007 (typically 150–210 μM), but oxygen concentrations declined to 0 μM at a depth of 2400 μm in CH cores (**Figure 2**), whereas more permeable BR sediments contained >114 μM O_2 at 2400 μm, and oxygen was detectable down to a depth of 5000 μm (0.5 cm; **Figures 2A–C**). In CH cores collected in 2008, oxygen penetrated up to 3000 μm, consistent with what was observed in 2007. There was substantial variation among measurements made in individual cores, however, and among many of the cores. For example, triplicate measurements in BR core 1 (**Figure 2A**), CH core 1 (**Figure 2D**), and CH core 6 (**Figure 2I**) exhibit high variation, and measured oxygen profiles differed across cores collected at the same time in the same sampling location.

Dissolved nitrogen in pore water also differed between the two sampling locations, but displayed consistent patterns between sampling periods in CH (**Figure 3**). In BR pore water, ammonium (NH_4^+) was maximal at 1 cm and declined from 28 to 9.9 μM moving into the sediments. Combined nitrate and nitrite ($NO_3^- + NO_2^-$) concentrations exhibited moderate variation with depth in BR cores, ranging from 23 to 33 μM. CH sediments differed from BR in absolute values and observed trends of dissolved nitrogen with depth: in 2007, NH_4^+ increased with depth, from 23 to >100 μM; $NO_3^- + NO_2^-$ was typically low in CH pore water and reached a maximum value of 14 μM at 1 cm, plateaued at 10–12 μM from 4 to 6 cm, and was below 3.5 μM from 2 to 3 and 7

Table 1 | Primers (and relevant references for primer sequences) cycling conditions used for qPCR, qPCR standards and standard curve correlation coefficients, and qPCR efficiencies.

Assay	Primers (reference)	Cycling conditions	qPCR standard	r^2	Efficiency (%)
Archaeal *amoA*	Arch-amoAF and Arch-amoAR (Francis et al., 2005)	95°C (4 min); 30× of 95°C (30 s), 53°C (45 s), 72°C (60 s with detection step); dissociation curve	Clone GOC-G-60-9 (GenBank accession no. EU340472) dilution series	0.989–0.994	83.1–101
Betaproteobacterial *amoA*	amoAF and amoA2R (Rotthauwe et al., 1997)	95°C (5 min); 40× of 94°C (45 s), 56°C (30 s), 72°C (60 s), detection step at 81°C (7 s); dissociation curve	Clone HB_A_0206_G01 (GenBank accession no. EU155190) dilution series	0.973–0.998	85.7–109

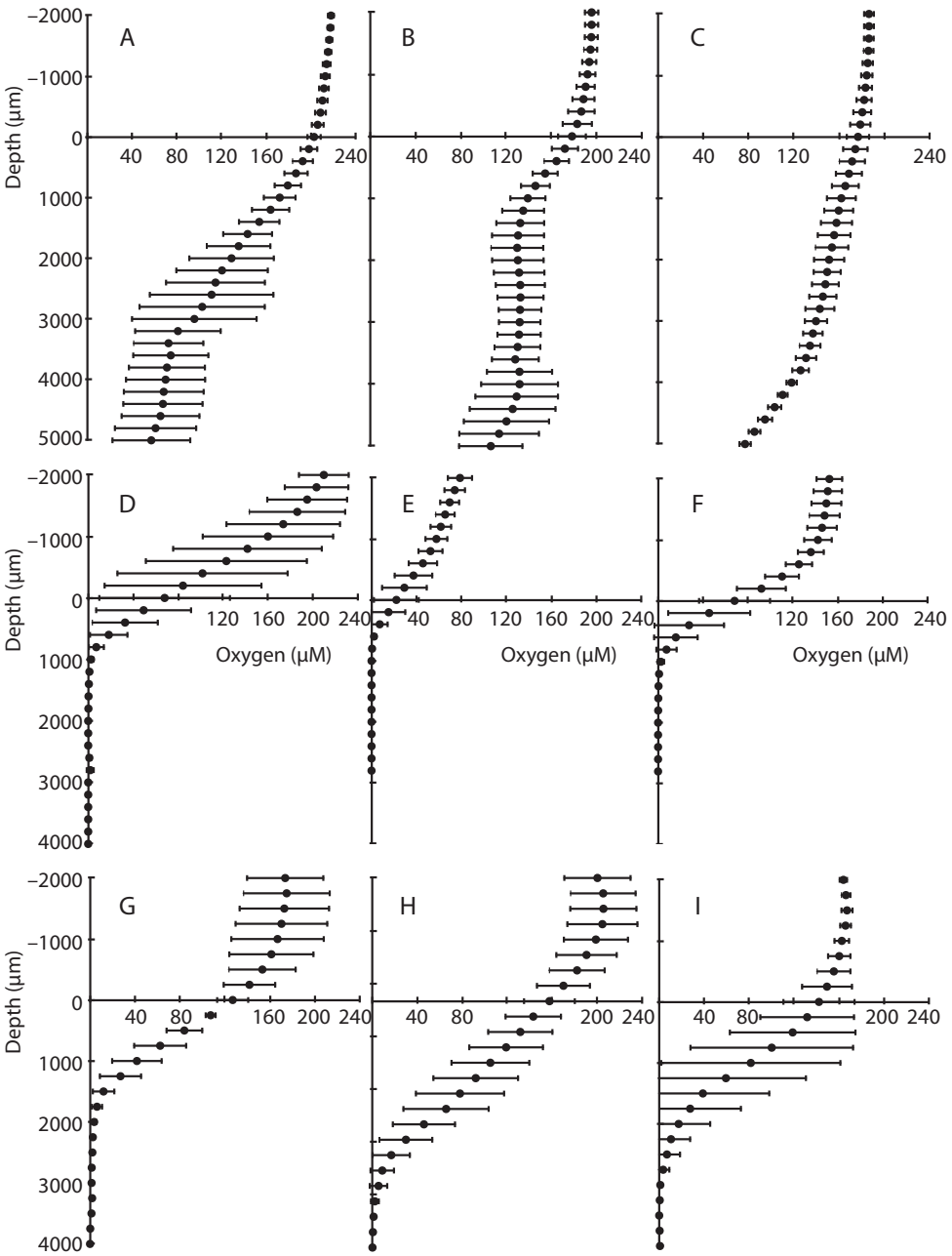

FIGURE 2 | Microsensor profiles of oxygen in sediment cores. Data from Bird Rock cores from **(A–C)**, and Catalina Harbor cores from 2007 **(D–F)** and 2008 **(G–I)** are shown; vertical axis depicts depth in sediment (0 µm depth represents the sediment surface and negative values represent overlying water) and the horizontal axis displays oxygen concentrations in micromolar. Error bars denote one standard deviation of triplicate microsensor profiles taken for each core.

to 10 cm. The same overall pattern was observed in CH sediments in 2008: NH_4^+ increased from 6.6 to 76 µM with depth whereas $NO_3^- + NO_2^-$ concentrations were always less than 10 µM, and exceeded 5 µM only at 2, 5, and 6 cm depth in the cores. On average, concentrations of both NH_4^+ and $NO_3^- + NO_2^-$ were lower in 2008 compared with 2007, but these differences were not significant owing to variability between replicate cores. Inter-core variability was generally much higher for $NO_3^- + NO_2^-$ than NH_4^+ in both 2007 and 2008: $NO_3^- + NO_2^-$ varied from 3.3 to 33 µM at 6 cm depth in 2007, and from 2.6 to 15 µM at 5 cm depth in 2008.

QUANTIFICATION OF AOA AND AOB

To examine whether ammonia oxidizers were present in these sediments, we extracted DNA and quantified the abundance of AOA and AOB based on *amoA* genes. AOA *amoA* genes, AOB *amoA*

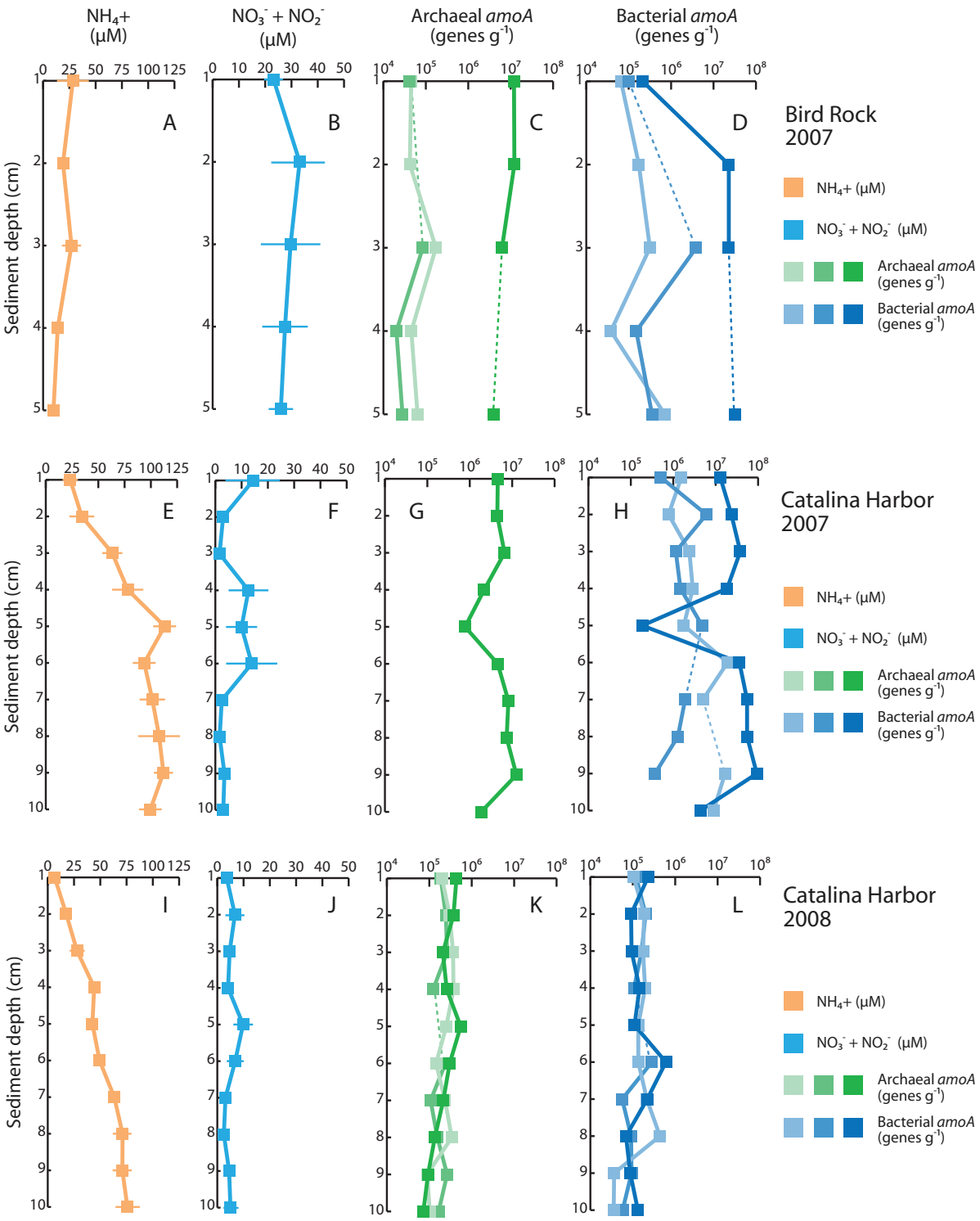

FIGURE 3 | Sediment profiles of dissolved inorganic nitrogen and ammonia oxidizers. Average pore water [NH_4^+] is shown for Bird Rock in 2007 **(A)**, Catalina Harbor in 2007 **(E)**, and Catalina Harbor in 2008 **(I)**, and pore water [$NO_3^- + NO_2^-$] is shown for Bird Rock **(B)**, Catalina Harbor in 2007 **(F)**, and Catalina Harbor in 2008 **(J)**. Archaeal *amoA* genes (g-sediment^{-1}) are shown for individual cores collected at Bird Rock **(C)**, Catalina Harbor in 2007 **(G)**, and Catalina Harbor in 2008 **(K)**. Bacterial *amoA* genes (g-sediment^{-1}) are shown for individual cores collected at Bird Rock **(D)**, Catalina Harbor in 2007 **(H)**, and Catalina Harbor in 2008 **(L)**. In **(C–L)**, dashed lines denote depths were data values are omitted due to qPCR inhibition of samples, and color shading denotes different cores. Light green/light blue denotes BR1 **(C,D)**, CH1 **(G,H)**, and CH4 **(K,L)**; "mid" green/"mid" blue denotes BR2 **(C,D)**, CH2 **(G,H)**, and CH5 **(K,L)**; dark green/dark blue denotes BR3 **(C,D)**, CH3 **(G,H)**, and CH6 **(K,L)**. In **(G)**, archaeal *amoA* was only detectable in one core.

genes, or both, were present in all samples from all depths, sampling locations, and time points (**Figure 3**). AOB *amoA* genes were quantified in every sample collected in 2007 at CH and BR, whereas AOA were undetectable in two of three CH cores collected in 2007, and were present at lower abundance in two of three BR cores. Both AOB and AOA *amoA* genes varied with depth in BR and CH cores: AOA *amoA* genes ranged from 4.01×10^6 to 1.22×10^7 genes g^{-1} in BR core 3 and 2.03×10^4 to 1.73×10^5 genes g^{-1} in cores 1 and 2 (**Figure 3**), while AOB *amoA* genes ranged from 6.55×10^4 to 3.26×10^7 genes g^{-1} in the BR cores. AOA and AOB *amoA* genes were highly variable across the replicate cores, however, and this pattern held for CH cores from both 2007 and 2008: for most sediment depths, the coefficient of variation among replicate cores was >1. This is clearly indicative of heterogeneity and patchiness in *amoA* genes in these sediments, and most striking is that fact that AOA *amoA* genes were undetected in two sediment cores collected at CH in 2007, but were detected in the third replicate separated by <50 cm. Another possibility is that the *amoA* primers did not successfully amplify the archaeal *amoA* sequence types present in these samples; if so, this indicates that entirely different AOA communities inhabit these cores, and is consistent with heterogeneity and patchiness of *amoA* genes in Catalina sediments.

When AOA *amoA* genes were quantified in the CH3 core collected in 2007, they were correlated with *amoA* genes from AOB ($r^2 = 0.936$, $P < 0.001$) with an AOB:AOA slope of 7.78 (**Figure 3**). It is unlikely that this correlation is an artifact of different DNA extraction efficiencies for different depths, as DNA was extracted from 0.15 to 0.25 g of sediment at each core depth and yielded 316–741 ng of DNA, while both AOA and AOB *amoA* genes varied by more than an order of magnitude. In 2008, AOA and AOB *amoA* genes were more weakly related ($r^2 = 0.49$–0.55, $P < 0.05$) in two of the cores, and uncorrelated in the third ($r^2 = 0.03$, $P > 0.05$). As these relationships indicate, we observed relatively little variability in AOB *amoA*:AOA *amoA* ratios with core depth in BR and CH sediments, yet there were obvious differences between cores, sampling locations, and sampling periods in the relative dominance of AOB and AOA *amoA* genes. With a lone exception, AOB *amoA* was 1.9–46 times more abundant than AOA *amoA* in all BR samples (at 1 cm depth in BR core 3 AOA *amoA* was more numerous), while the ratio of AOB to AOA *amoA* ranged from 0.24 (5 cm depth) to 8.6 (4 cm depth) in the CH3 core collected in 2007. AOA *amoA* was not amplifiable in CH cores 1 and 2 from 2007 and AOB *amoA* was therefore present in substantial greater amounts. In contrast, AOA *amoA* genes were more abundant than AOB in the 2008 CH cores, with AOA *amoA*:AOB *amoA* ratios ranging from 0.86 to 2.9 in CH core 4, 0.77 to 2.9 in CH core 5, and 0.5 to 5.1 in CH core 6.

δ^{15}N AND NITRIFICATION RATE PROFILES

δ^{15}N of $NO_3^- + NO_2^-$ in pore water was measured following a 24 h incubation of intact cores collected in 2008 to calculate $^{15}NH_4^+$ oxidation rates. δ^{15}N of $NO_3^- + NO_2^-$ in CH core 5 exhibited only modest enrichment, ranging from 13.8‰ at the surface to 54.0‰ at 10 cm depth (**Figure 4B**). This pattern is typical for sediments (e.g., Lehmann et al., 2007) where denitrification at depth preferentially removes isotopically light N, enriching the remaining $NO_3^- + NO_2^-$ pool in ^{15}N. Because the values we observed are in the range expected for sedimentary denitrification, this suggests that little or no ammonia oxidation occurred in this core (we enriched the $^{15}NH_4^+$ pool to 76.7 at%). Instead, the measured values effectively represent *in situ* δ^{15}N of $NO_3^- + NO_2^-$, and these values were used to calculate $^{15}NH_4^+$ oxidation rates in the other cores. (Two exceptions were the lower δ^{15}N values measured at 7 and 9 cm depth, where we instead linearly interpolated the *in situ* δ^{15}N values.) In contrast to the δ^{15}N values observed in CH core 5, δ^{15}N of $NO_3^- + NO_2^-$ in pore water exceeded 330‰ in CH cores 4 and 6 (**Figures 4A,C**). Pore water δ^{15}N was highly variable throughout each core, and between both cores, and spiked at several depth intervals – indicating that labeled $^{15}NH_4^+$ was being oxidized relatively deep within the CH4 and CH6 cores (**Figures 4D,E**). $^{15}NH_4^+$ oxidation rate profiles showed maxima at 6 cm in CH4, and at 3 cm in CH6, where rates were also elevated at 5 and 7 cm (**Figure 4**). In both cores, $^{15}NH_4^+$ oxidation rates were readily detectable at 9 cm depth. Rates ranged from 0 to 7.15 nmol L^{-1} day^{-1} in CH4 and 0 to 18.3 nmol L^{-1} day^{-1} in CH6.

DISCUSSION

GEOCHEMISTRY OF CATALINA SEDIMENTS

Oxygen typically penetrates only a few millimeters into coastal sediments owing to rapid consumption during organic matter degradation, or chemical re-oxidation of reduced compounds (Revsbech et al., 1980; Gundersen and Jørgensen, 1990). However, the depth of oxygen penetration can be increased via bioturbation/bioirrigation (Aller, 1982; Ziebis et al., 1996a; Bertics and Ziebis, 2009), sediment permeability and increased bottom water flow velocity, and/or increased wave action (Booij et al., 1991; Precht et al., 2004). Sediment topography features that generate pressure differences can also lead to advective transport of oxygenated water into the sediment (Ziebis et al., 1996b). At BR, sediments contained >114 μM O_2 at 2400 μm and oxygen was detectable down to a depth of 5000 μm (0.5 cm; **Figures 2A–C**). This is consistent with oxygen transport via advective processes several centimeters into the sediment, especially given the porous nature of these coarse BR sediments. In contrast, in CH sediments, oxygen was not detected below 2400 μm in 2007 (**Figures 2D–F**) and 3000 μm in 2008 (**Figures 2G–I**) – suggesting that oxygen diffuses to a consistent depth at CH. An important caveat to this is the fact that macrofauna can transport oxygen more than 50 cm deep (Ziebis et al., 1996a) and bioturbation has been shown to transfer oxygen multiple centimeters deep into CH sediments (Bertics and Ziebis, 2009). The presence of bioturbation is therefore a likely explanation for the variation within and among many of the CH cores – e.g., CH core 1 (**Figure 2D**) and CH core 6 (**Figure 2I**).

$NO_3^- + NO_2^-$ profiles also differed between BR and CH sediments, in that high concentrations (>20 μM) were seen throughout BR cores while concentrations reached a maximum value of 14 μM at 1 cm in CH cores from 2007 and were always less than 10 μM in cores from 2008. However, several subsurface peaks of $NO_3^- + NO_2^-$ occurred in CH in both 2007 and 2008, and may reflect either (1) transport of oxidized compounds into the sediment via bioturbation, or (2) production of $NO_3^- + NO_2^-$ in the sediment via the activity of nitrifying bacteria and archaea

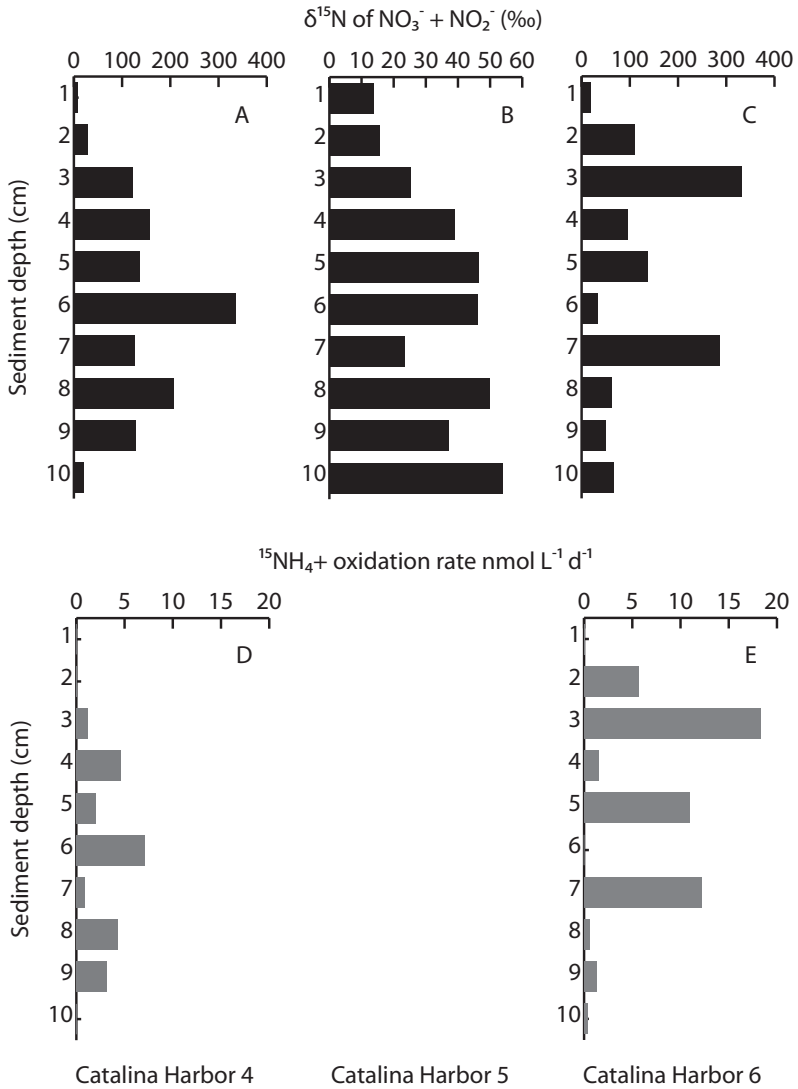

FIGURE 4 | Measured $\delta^{15}N$ of pore water $NO_3^- + NO_2^-$ following incubation with added $^{15}NH_4^+$ label **(A–C)**, and $^{15}NH_4^+$ oxidation rates **(D,E)** in Catalina Harbor in 2008. Note differences in scales in **(A–C)**; oxidation rates were not calculated in Catalina Harbor core 5 owing to the lack of clear isotopic enrichment.

(i.e., *in situ* nitrification). CH cores displayed the typical increase in NH_4^+ that is expected with increasing sediment depth due to microbial remineralization of organic material. Concentrations of both NH_4^+ and $NO_3^- + NO_2^-$ were on average lower in 2008 when compared with 2007 – although these differences were not significant owing to variability between replicate cores. A decrease in recruitment of shrimp and a decrease in microbial mat formation was previously observed in these sediments from 2007 to 2008 (Bertics et al., 2010) and may explain this shift in sediment geochemistry. Hence interannual variability in geochemical conditions and microbial activity can occur in CH, but it occurs against a backdrop of substantial spatial variability.

ABUNDANCE OF AOA AND AOB IN CATALINA SEDIMENTS

Ammonia-oxidizing archaea and AOB were also highly variable in Catalina Island sediments based on the abundance of *amoA* genes. DNA extracted from sediments may not be derived from active or viable microorganisms – indeed, it is possible to recover ancient DNA from sediment cores (Coolen and Overmann, 1998) – yet the presence of, and variability in, oxidized nitrogen at 4–6 cm depth in CH cores is indicative of active production. We assessed this using direct biogeochemical measurements (see below) rather than extraction of RNA, yielding quantitative rates rather than relative levels of gene expression. Our DNA data are nevertheless consistent with other studies profiling AOB in sediments:AOB DNA has been detected at 40 cm depth in Loch Duich sediments (Freitag and Prosser, 2003; Mortimer et al., 2004), 6 cm depth in salt marsh sediments (Dollhopf et al., 2005), and at least 2 cm depth in estuarine sediments from Plum Island Sound (Bernhard et al., 2007), where potential nitrification was measured at up to 4 cm. In these studies, AOB typically ranged from 10^4 to 10^7 *amoA* genes g^{-1}, and our data are similar (3.6×10^4 to 9.3×10^7 *amoA*

genes g^{-1}). However, in addition to AOB, we report *amoA* genes from AOA at up to 5 cm depth in BR sediment cores, and 10 cm depth in CH sediment cores, where they ranged from 7.2×10^4 to 1.3×10^7 genes g^{-1}.

Previous studies have shown that although AOA and AOB are presumably functionally equivalent, their relative dominance varies across gradients of salinity present in sediments (Caffrey et al., 2007; Mosier and Francis, 2008; Santoro et al., 2008). Studies in soils suggest that pH (Nicol et al., 2008) and NH_4^+ concentrations (reviewed by Erguder et al., 2009) also alter the relative abundance of AOA and AOB – more specifically, an exceptionally high affinity for ammonia benefits AOA when NH_4^+ concentrations are low (Martens-Habbena et al., 2009). While we observed relatively little variability in AOB *amoA*:AOA*amoA* ratios with depth in BR and CH sediments, AOB *amoA* genes were more abundant in BR sediments and CH sediments from 2007, while AOA *amoA* genes were more abundant than AOB in the 2008 CH cores. Different DNA extraction kits were used for CH sediments collected in 2007 and 2008, and it is possible that the MP Biomedicals kit (used in 2008) is less effective in extracting bacterial DNA and so explains the differences observed between the two sampling periods. When comparing measured values, however, 2008 values lie within the range of AOB and AOA *amoA* gene abundances observed across both sites in 2007; this argues against extraction bias, as one would expect much lower or higher numbers for one or both of the genes. In any case, the evidence for interannual variability in ammonia oxidizer populations is mixed, given that: (1) measured NH_4^+ values are still far in excess of K_m value (123 nM) for the lone cultured marine AOA, *Nitrosopumilus maritimus* (Martens-Habbena et al., 2009), while K_m values for some AOB are as low as 10 μM (Casciotti et al., 2003 and references therein), and (2) high spatial variation within these sediments might obscure temporal trends. Put another way, our data do not conclusively indicate whether AOA or AOB are more dominant in these sediments, but are indicative of substantial spatial variation and possibly temporal variation as well. This parallels our geochemical results, but there was little correspondence between AOA and AOB and nutrient and rate data: no significant correlations were observed in the 2007 data (all $P > 0.05$), whereas AOA were negatively correlated with NH_4^+ – and positively correlated with NO_2^- – in 2008 (**Table 2**).

NITRIFICATION IN CATALINA SEDIMENTS

Ammonia oxidation rate measurements indicated that AOA and AOB were actively nitrifying throughout two of the three collected cores in 2008. Modest enrichment in the CH5 core suggests that although we recovered *amoA* genes, either this DNA was not derived from living organisms, or these organisms were inactive during our incubation. Evidence for the later includes the relatively low $\delta^{15}N$ values measured at 7 and 9 cm depth, as in a previous study conducted in the same location in 2008, Bertics et al. (2010) found the highest rates of nitrogen fixation at depth of 7 and 9 cm in the most bioturbated location they sampled. Hence one possible explanation for the "light" $\delta^{15}N$ of $NO_3^- + NO_2^-$ at these depths is the oxidation of recently fixed nitrogen, i.e., while ammonia oxidation appeared inactive at the time of our sampling, it may have been previously active within or near these sediment layers. Another explanation for these local minima in the pore water profile is that this represents NO_3^- and/or NO_2^- of differing $\delta^{15}N$ that is present in groundwater.

In the CH4 and CH6 cores, $^{15}NH_4^+$ oxidation rates were readily detectable at most depths up 9 cm in both cores, and up to 10 cm depth in the CH6 core. Relatively few ^{15}N-based rate measurements have been conducted within sediments (Ward, 2008), but our experimental approach was similar to that used by Mortimer et al. (2004) and our measured rates (0–18.3 nmol L^{-1} day^{-1}) were similar to values of 4.86–89.6 nmol L^{-1} day^{-1} measured at 2–6 and 10–12 cm depth in Loch Duich (Mortimer et al., 2004). However, our measurements were much lower than the maximum rates measured at 0–2 cm in Loch Duich (1.6×10^6 nmol L^{-1} day^{-1}) and most other measurements in the literature (Ward, 2008). These results therefore capture active $^{15}NH_4^+$ oxidation at depths of up to 10 cm in Catalina Island sediments, but also indicate that rates are generally low and variable with depth and between replicate cores.

One possible explanation for measurable ammonia oxidation at depth is the periodic supply of oxygen to aerobic nitrifiers: previous work has shown that alteration of sediment by

Table 2 | Correlation coefficients (r^2) for comparisons between qPCR data, nutrient concentrations, and $^{15}NH_4^+$ oxidation rates averaged across triplicate cores collected in Catalina Harbor in 2008.

	Log AOA *amoA*	AOA *amoA*	Log AOB *amoA*	AOB *amoA*	$[NH_4^+]$	$[NO_2^-]$	$[NO_3^-]$	$^{15}NH_4^+$ oxidation rate
Log AOA *amoA*			0.19	0.07	0.55*	0.44*	0.22	0.28
AOA *amoA*			0.09	0.02	0.48*	0.54*	0.36	0.26
Log AOB *amoA*					0.08	0.03	0.01	0.06
AOB *amoA*					0.02	0.02	0.01	0.02
NH_4^+						0.30	0.03	0.02
NO_2^-							0.41*	0.01
NO_3^-								0.10

*$P < 0.05$.

macrofauna can alter redox chemistry and microbial communities in CH sediments (Bertics and Ziebis, 2009, 2010; Bertics et al., 2010), and burrows were present in the majority of the cores we collected. Previous work by Dollhopf et al. (2005) in fact showed that nitrification rates and AOB abundance were related to burrow abundance. Abiotic "anoxic nitrification" (Mortimer et al., 2004) may also explain oxidation of ammonia at up to 9 cm depth – however, AOB have been detected at greater depths in other sedimentary environments, and *amoA* genes from both AOB and AOA were readily quantified where active ammonia oxidation was also measured. As a result, our findings are consistent with previous work indicating that bioturbation sustains nitrification by providing periodic intrusions of oxygen (Dollhopf et al., 2005; Ward, 2008, and references therein).

Hydrogen sulfide is a confounding issue for nitrification in sediments because it can completely inhibit nitrification (e.g., Joye and Hollibaugh, 1995); yet in spite of relatively high sulfate reduction rates occurring in CH sediments (Bertics and Ziebis, 2010), pore water hydrogen sulfide was not previously detected (Bertics and Ziebis, 2009), possibly because dissolved sulfide reacts with the high levels of iron (Bertics and Ziebis, 2009), leading to the precipitation of iron sulfides (Berner, 1970). Hydrogen sulfide may also be oxidized by sulfide oxidizers present in nearby sediments (Meyers et al., 1987) – in fact, hydrogen sulfide is oxidized by organisms using nitrate as an electron acceptor in oceanic oxygen minimum zones (Canfield et al., 2010). Some combination of these processes likely explains the lack of sulfide inhibition of ammonia oxidation in cores CH4 and CH6.

However, the variation in $^{15}NH_4^+$ oxidation rates that we observed (e.g., between cores and with depth) may stem from production of hydrogen sulfide: similar to the rate measurements reported here, sulfate reduction rates are heterogeneous in CH bioturbated sediments, with areas having sulfate reduction rates of 790 nmol SO_4^{2-} cm^{-3} day^{-1} separated by only 3–5 cm from areas displaying rates of <5 nmol SO_4^{2-} cm^{-3} day^{-1} (Bertics and Ziebis, 2010). It is therefore possible that in some patches of CH sediment, high sulfate reduction rates inhibit nitrification, while in other areas, low sulfate reduction rates allow for the presence of nitrification – thereby explaining the high levels of variation in nitrification rates seen between replicate cores in CH. This hypothesis is supported by Gilbert et al. (1998), in which the authors found that bioturbation led to the close presence of oxic and anoxic microenvironments, which in turn strengthened the proximity and exchanges between nitrification and denitrification in sediments.

Our results are consistent with ammonia oxidation being broadly but patchily distributed in marine sediments, where this key process may be coupled to anaerobic N cycling and loss. The high degree of heterogeneity observed for substrates, products, genes, and biogeochemical activity – laterally, with depth, and through time – demonstrates that sedimentary N cycling is extraordinarily complex. Understanding this complexity and variability will be critical for balancing the N cycle in an era of global change (Gruber and Galloway, 2008; Beman et al., 2011).

ACKNOWLEDGMENTS

This work was supported by NSF grants OCE 08-24997 (to J. M. Beman and Brian Popp) and 10-34943 (to J. M. Beman), and the Eugene Cota Robles Fellowship (awarded to Jesse M. Wilson). We thank Susan Alford, C. J. Bradley, Jackie Mueller, Natalie Walsgrove, and Elizabeth Gier for assistance in preparing and analyzing samples, and Brian Popp for access to the Stable Isotope Biogeochemistry lab at the University of Hawaii. We also wish to thank Jed Fuhrman and Wiebke Ziebis for helpful discussions, and the Wrigley Marine Science Center on Catalina Island for supporting field work.

REFERENCES

Abell, G. C. J., Revill, A. T., Smith, C., Bissett, A. P., Volkman, J. K., and Robert, S. S. (2010). Archaeal ammonia oxidizers and nirS-type denitrifiers dominate sediment nitrifying and denitrifying populations in a subtropical macrotidal estuary. *ISME J.* 10, 286–300.

Aller, R. C. (1982). "The effects of macrobenthos on chemical properties of marine sediment and overlying water," in *Animal–Sediment Relations (2): Topics in Geobiology*, eds P. L. McCall and M. J. S. Tevesz (New York, NY: Plenum Press), 53–96.

Beman, J. M., Chow, C., King, A. L., Feng, Y., Fuhrman, J. A., Andersson, A., Bates, N. R., Popp, B. N., and Hutchins, D. A. (2011). Global declines in oceanic nitrification rates as a consequence of ocean acidification. *Proc. Natl. Acad. Sci. U.S.A.* 108, 208–213.

Beman, J. M., and Francis, C. A. (2006). Diversity of ammonia-oxidizing archaea and bacteria in the sediments of a hypernutrified subtropical estuary: Bahía del Tóbari, Mexico. *Appl. Environ. Microbiol.* 72, 7767–7777.

Beman, J. M., Popp, B. N., and Alford, S. E. (2012). Quantification of ammonia oxidation rates and ammonia-oxidizing archaea and bacteria at high resolution in the Gulf of California and eastern tropical North Pacific Ocean. *Limnol. Oceanogr.* 57, 711–726.

Bernhard, A. E., Donn, T., Giblin, A. E., and Stahl, D. A. (2005). Loss of diversity of ammonia-oxidizing bacteria correlates with increasing salinity in an estuary system. *Environ. Microbiol.* 7, 1289–1297.

Bernhard, A. E., Tucker, J., Giblin, A. E., and Stahl, D. A. (2007). Functionally distinct communities of ammonia-oxidizing bacteria along an estuarine salinity gradient. *Environ. Microbiol.* 9, 1439–1447.

Berner, R. A. (1970). Sedimentary pyrite formation. *Am. J. Sci.* 268, 1–23.

Bertics, V. J., Sohm, J. A., Treude, T., Chow, C. -E., Capone, D. G., Fuhrman, J. A., and Ziebis, W. (2010). Burrowing deeper into benthic nitrogen cycling: the impact of bioturbation on nitrogen fixation coupled to sulfate reduction. *Mar. Ecol. Prog. Ser.* 409, 1–15.

Bertics, V. J., and Ziebis, W. (2009). Biodiversity of benthic microbial communities in bioturbated coastal sediments is controlled by geochemical microniches. *ISME J.* 3, 1269–1285.

Bertics, V. J., and Ziebis, W. (2010). Bioturbation and the role of microniches for sulfate reduction in coastal marine sediments. *Environ. Microbiol.* 12, 3022–3034.

Booij, K., Helder, W., and Sundby, B. (1991). Rapid redistribution of oxygen in a sandy sediment induced by changes in the flow velocity of the overlying water. *Neth. J. Sea Res.* 28, 149–165.

Brenchley, G. A. (1981). Disturbance and community structure, an experimental study of bioturbation in marine soft-bottom environments. *J. Mar. Res.* 39, 767–790.

Caffrey, J. M., Bano, N., Kalanetra, K., and Hollibaugh, J. T. (2007). Ammonia oxidation and ammonia-oxidizing bacteria and archaea from estuaries with differing histories of hypoxia. *ISME J.* 1, 660–662.

Canfield, D. E., Stewart, F. J., Thamdrup, B., De Brabandere, L., Dalsgaard, T., Delong, E. F., Revsbech, N. R., and Ulloa, O. (2010). A cryptic sulfur cycle in oxygen-minimum–zone waters off the Chilean coast. *Science* 330, 1375–1378.

Casciotti, K. L., Sigman, D. M., and Ward, B. B. (2003). Linking diversity and stable isotope fractionation in ammonia-oxidizing bacteria. *Geomicrobiol. J.* 20, 335–353.

Codispoti, L. A., Brandes, J. A., Christensen, J. P., Devol, A. H., Naqvi, S. W. A., Paerl, H. W., and Yoshinari,

T. (2001). The oceanic fixed nitrogen and nitrous oxide budgets: moving targets as we enter the anthropocene. *Sci. Mar.* 65, 85–105.

Coolen, M. J. L., and Overmann, J. (1998). Analysis of subfossil molecular remains of purple sulfur bacteria in a lake sediment. *Appl. Environ. Microbiol.* 64, 4513–4521.

Deutsch, C., Brix, H., Ito, T., Frenzel, H., and Thompson, L. (2011). Climate-forced variability of ocean hypoxia. *Science* 333, 336–339.

Dollhopf, S. L., Hyun, J., Smith, A. C., Adams, H. J., O'Brien, S., and Kostka, J. E. (2005). Quantification of ammonia-oxidizing bacteria and factors controlling nitrification in salt marsh sediments. *Appl. Environ. Microbiol.* 71, 240–246.

Dore, J. E., Popp, B. N., Karl, D. M., and Sansone, F. J. (1998). A large source of atmospheric nitrous oxide from subtropical North Pacific surface waters. *Nature* 396, 63–66.

Erguder, T. H., Boon, N., Wittebolle, L., Marzorati, M., and Verstraete, W. (2009). Environmental factors shaping the ecological niches of ammonia-oxidizing archaea. *FEMS Microbiol. Rev.* 33, 855–869.

Francis, C. A., Beman, J. M., and Kuypers, M. M. M. (2007). New processes and players in the nitrogen cycle: the microbial ecology of anaerobic and archaeal ammonia oxidation. *ISME J.* 1, 19–27.

Francis, C. A., Roberts, K. J., Beman, J. M., Santoro, A. E., and Oakley, B. B. (2005). Ubiquity and diversity of ammonia-oxidizing archaea in water columns and sediments of the ocean. *Proc. Natl. Acad. Sci. U.S.A.* 102, 14683–14688.

Freitag, T. E., and Prosser, J. I. (2003). Community structure of ammonia-oxidizing bacteria within anoxic marine sediments. *Appl. Environ. Microbiol.* 69, 1359–1371.

Gaidos, E., Rusch, A., and Ilardo, M. (2011). Ribosomal tag pyrosequencing of DNA and RNA from benthic coral reef microbiota: community spatial structure, rare members and nitrogen-cycling guilds. *Environ. Microbiol.* 13, 1138–1152.

Gilbert, F., Stora, G., and Bonin, P. (1998). Influence of bioturbation on denitrification activity in Mediterranean coastal sediments: an *in situ* experimental approach. *Mar. Ecol. Prog. Ser.* 163, 99–107.

Gruber, N., and Galloway, J. N. (2008). An Earth-system perspective of the global nitrogen cycle. *Nature* 451, 293–296.

Gundersen, J. K., and Jørgensen, B. B. (1990). Microstructure of diffusive boundary layers and the oxygen uptake of the sea floor. *Nature* 345, 604–607.

Hall, P. O. J., and Aller, R. C. (1992). Rapid, small-volume, flow injection analysis for Σ CO2 and NH4+ in marine and freshwaters. *Limnol. Oceanogr.* 37, 1113–1119.

Jones, M. N. (1984). Nitrate reduction by shaking with cadmium: alternative to cadmium columns. *Water Res.* 18, 643–646.

Joye, S. B., and Hollibaugh, J. T. (1995). Influence of sulfide inhibition of nitrification on nitrogen regeneration in sediments. *Science* 270, 623–625.

Kuypers, M. M. M., Lavik, G., and Thamdrup, B. (2006). "Anaerobic ammonium oxidation in the marine environment," in *Past and Present Water Column Anoxia*, ed. L. Neretin (Dordrecht, Netherlands: Springer), 311–335.

Lehmann, M. F., Sigman, D. M., McCorkle, D. C., Granger, J., Hoffmann, S., Cane, G., and Brunelle, B. G. (2007). The distribution of nitrate 15N/14N in marine sediments and the impact of benthic nitrogen loss on the isotopic composition of oceanic nitrate. *Geochim. Cosmochim. Acta* 71, 5384–5404.

MacGinitie, G. E. (1934). The natural history of *Callianassa californiensis* Dana. *Amer. Midland Nat.* 15, 166–177.

Martens-Habbena, W., Berube, P. M., Urakawa, H., de la Torre, J. R., and Stahl, D. A. (2009). Ammonia oxidation kinetics determine niche separation of nitrifying archaea and bacteria. *Nature* 461, 976–979.

Meyers, M. B., Fossing, H., and Powell, E. N. (1987) Microdistribution of interstitial meiofauna, oxygen and sulfide gradients, and the tubes of macro-infauna. *Mar. Ecol. Prog. Ser.* 35, 223–241.

Morrow, K., and Carpenter, R. (2008). Shallow kelp canopies mediate macroalgal composition: effects on the distribution and abundance of *Corynactis californica* (Corallimorpharia). *Mar. Ecol. Prog. Ser.* 361, 119–127.

Mortimer, R. J. G., Harris, S. J., Krom, M. D., Freitag, T. E., Prosser, J. I., Barnes, J., Anschutz, P., Hayes, P. J., and Davies, I. M. (2004). Anoxic nitrification in marine sediments. *Mar. Ecol. Prog. Ser.* 276, 37–52.

Mosier, A. C., and Francis, C. A. (2008). Relative abundance and diversity of ammonia-oxidizing archaea and bacteria in the San Francisco Bay estuary. *Environ. Microbiol.* 10, 3002–3016.

Nelson, B. V., and Vance, R. R. (1979). Diel foraging patterns of the sea urchin *Centrostephanus coronatus* as a predator avoidance strategy. *Mar. Biol.* 51, 251–258.

Nicol, G. W., Leininger, S., Schleper, C., and Prosser, J. I. (2008). The influence of soil pH on the diversity, abundance and transcriptional activity of ammonia oxidizing archaea and bacteria. *Environ. Microbiol.* 10, 2966–2978.

Popp, B. N., Sansone, F. J., Rust, T. M., and Merritt, D. A. (1995). Determination of concentration and carbon isotopic composition of dissolved methane in sediments and nearshore waters. *Anal. Chem.* 67, 405–411.

Precht, E., Franke, U., Polerecky, L., and Huettel, M. (2004). Oxygen dynamics in permeable sediments with wave-driven pore water exchange. *Limnol. Oceanogr.* 49, 693–705.

Revsbech, N. P. (1989). An oxygen electrode with a guard cathode. *Limnol. Oceanogr.* 28, 474–478.

Revsbech, N. P., and Jørgensen, B. B. (1986). "Microelectrodes: their use in microbial ecology," in *Advances in Microbial Ecology*, ed. K. C. Marshall (New York, NY: Plenum Press), 293–352.

Revsbech, N. P., Sorensen, J., Blackburn, T. H., and Lomholt, J. P. (1980). Distribution of oxygen in marine sediments measured with microelectrodes. *Limnol. Oceanogr.* 25, 403–411.

Rotthauwe, J. H., Witzel, K. P., and Liesack, W. (1997). The ammonia monooxygenase structural gene *amoA* as a functional marker: molecular fine-scale analysis of natural ammonia-oxidizing populations. *Appl. Environ. Microbiol.* 63, 4704–4712.

Santoro, A. E., Francis, C. A., De Sieyes, N. R., and Boehm, A. B. (2008). Shifts in the relative abundance of ammonia-oxidizing bacteria and archaea across physicochemical gradients in a subterranean estuary. *Environ. Microbiol.* 10, 1068–1079.

Seitzinger, S., Harrison, J. A., Bohlke, J. K., Bouwman, A. F., Lowrance, R., Peterson, B., Tobias, C., and Drecht, G. V. (2006). Denitrification across landscapes and waterscapes: a synthesis. *Ecol. Appl.* 16, 2064–2090.

Sigman, D. M., Casciotti, K. L., Andreani, M., Barford, C., Galanter, M., and Böhlke, J. K. (2001). A bacterial method for the nitrogen isotopic analysis of nitrate in seawater and freshwater. *Anal. Chem.* 73, 4145–4153.

Strickland, J. H., and Parsons, T. R. (1972). *A Practical Handbook of Seawater Analysis*, 2nd Edn. Ottawa: Fisheries Research Board of Canada.

Strous, M., Pelletier, E., Mangenot, S., Rattei, T., Lehner, A., Taylor, M. W., Horn, M., Daims, H., Bartol-Marvel, D., Wincker, P., Barbe, V., Fonknechten, N., Vallenet, D., Segurens, B., Schenowitz-Truong, C., Médigue, C., Collingro, A., Snel, B., Dutilh, B. E., Op den Camp, H. J. M., van der Drift, C., Cirpus, I., van de Pas-Schoonen, K. T., Harhangi, H. R., van Niftrik, L., Schmid, M., Keltjens, J., van de Vossenberg, J., Kartal, B., Meier, H., Frishman, D., Huynen, M. A., Mewes, H., Weissenbach, J., Jetten, M. S. M., Wagner, M., and Le Paslier, D. (2006). Deciphering the evolution and metabolism of an anammox bacterium from a community genome. *Nature* 440, 790–794.

Swinbanks, D. D., and Murray, J. W. (1981). Biosedimentological zonation of boundary bay tidal flats, Fraser River Delta, British Columbia. *Sedimentology* 28, 201–237.

Wankel, S. D., Mosier, A. C., Hansel, C. M., Paytan, A., and Francis, C. A. (2011). Spatial variability in nitrification rates and ammonia-oxidizing microbial communities in the agriculturally impacted Elkhorn Slough estuary, California. *Appl. Environ. Microbiol.* 77, 269–280.

Ward, B. B. (2008). "Nitrification in marine systems," in *Nitrogen in the Marine Environment*, eds D. G. Capone, D. Bronk, M. Mulholland, and E. J. Carpenter (San Diego, CA: Academic Press), 199–261.

Ward, B. B., Kilpatrick, K. A., Renger, E. H., and Eppley, R. W. (1989). Biological nitrogen cycling in the nitracline. *Limnol. Oceanogr.* 34, 493–513.

Whitman, W. B., Coleman, D. C., and Wiebe, W. J. (1998). Prokaryotes: the unseen majority. *Proc. Natl. Acad. Sci. U.S.A.* 95, 6578–6583.

Zeil, J., Hemmi, J. M., and Backwell, P. R. Y. (2006). Quick guide to Fiddler crabs. *Curr. Biol.* 16, 40–41.

Ziebis, W., Forster, S., Huettel, M., and Jørgensen, B. B. (1996a). Complex burrows of the mud shrimp *Callianassatruncata* and their geochemical impact in the seabed. *Nature* 382, 619–622.

Ziebis, W., Huettel, M., and Forster, S. (1996b). Impact of biogenic sediment topography on oxygen fluxes in permeable seabeds. *Mar. Ecol. Prog. Ser.* 140, 227–237.

Conflict of Interest Statement: The authors declare that the research was conducted in the absence of any commercial or financial relationships that

could be construed as a potential conflict of interest.

Received: 04 May 2012; accepted: 04 July 2012; published online: 24 July 2012.
Citation: Beman JM, Bertics VJ, Braunschweiler T and Wilson JM (2012) Quantification of ammonia oxidation rates and the distribution of ammonia-oxidizing archaea and bacteria in marine sediment depth profiles from Catalina Island, California. Front. Microbio. ***3****:263. doi: 10.3389/fmicb. 2012.00263*

This article was submitted to Frontiers in Aquatic Microbiology, a specialty of Frontiers in Microbiology.

frontiers in
MICROBIOLOGY

ORIGINAL RESEARCH ARTICLE
published: 18 October 2012
doi: 10.3389/fmicb.2012.00364

Trait-based representation of biological nitrification: model development, testing, and predicted community composition

Nicholas J. Bouskill[1]*, Jinyun Tang[2], William J. Riley[2] and Eoin L. Brodie[1]

[1] *Ecology Department, Earth Sciences Division, Lawrence Berkeley National Laboratory, Berkeley, CA, USA*
[2] *Climate Science Department, Earth Sciences Division, Lawrence Berkeley National Laboratory, Berkeley, CA, USA*

Edited by:
Bess B. Ward, Princeton University, USA

Reviewed by:
J. Michael Beman, University of California, Merced, USA
Daniel Laughlin, University of Waikato, New Zealand

****Correspondence:***
Nicholas J. Bouskill, Ecology Department, Earth Sciences Division, Lawrence Berkeley National Laboratory, Berkeley, CA 94720, USA.
e-mail: njbouskill@lbl.gov

Trait-based microbial models show clear promise as tools to represent the diversity and activity of microorganisms across ecosystem gradients. These models parameterize specific traits that determine the relative fitness of an "organism" in a given environment, and represent the complexity of biological systems across temporal and spatial scales. In this study we introduce a *micro*bial community *trait*-based modeling framework (MicroTrait) focused on *nit*rification (MicroTrait-N) that represents the ammonia-oxidizing bacteria (AOB) and ammonia-oxidizing archaea (AOA) and nitrite-oxidizing bacteria (NOB) using traits related to enzyme kinetics and physiological properties. We used this model to predict nitrifier diversity, ammonia (NH_3) oxidation rates, and nitrous oxide (N_2O) production across pH, temperature, and substrate gradients. Predicted nitrifier diversity was predominantly determined by temperature and substrate availability, the latter was strongly influenced by pH. The model predicted that transient N_2O production rates are maximized by a decoupling of the AOB and NOB communities, resulting in an accumulation and detoxification of nitrite to N_2O by AOB. However, cumulative N_2O production (over 6 month simulations) is maximized in a system where the relationship between AOB and NOB is maintained. When the reactions uncouple, the AOB become unstable and biomass declines rapidly, resulting in decreased NH_3 oxidation and N_2O production. We evaluated this model against site level chemical datasets from the interior of Alaska and accurately simulated NH_3 oxidation rates and the relative ratio of AOA:AOB biomass. The predicted community structure and activity indicate (a) parameterization of a small number of traits may be sufficient to broadly characterize nitrifying community structure and (b) changing decadal trends in climate and edaphic conditions could impact nitrification rates in ways that are not captured by extant biogeochemical models.

Keywords: nitrogen cycle, models, biological, geochemistry, mathematical modeling, nitrification

INTRODUCTION

Understanding the interaction between ecology and biogeochemistry is an important frontier in environmental microbiology. Temporal separation between cellular activity and trace gas flux measurement has hampered efforts to connect, in field studies, the composition, structure, and activity of microbial communities to the biogeochemical processes they catalyze. Given the importance of prokaryotic diversity for ecosystem function (Kassen et al., 2000), a greater understanding of how microbial communities assemble, interact with the changing environment over time is clearly required.

The application of next generation sequencing technology is continually improving our understanding of the spatial and temporal distribution of microorganisms (Caporaso et al., 2012), while metabolomics and proteomics can help contextualize biological interactions with the environment and clarify relationships within and between microbial functional groups (Kujawinski, 2011; Schneider et al., 2012). In contrast, theoretical approaches in microbial ecology have lagged significantly behind these methodological developments (Prosser et al., 2007). Unlike macrofaunal ecology (Webb et al., 2010), mathematical relationships are not routinely applied to explore the implications behind experimental observations. The theoretical background to expand numerical approaches in environmental microbiology could well follow the trait-based approach implemented in models of marine autotrophic phytoplankton (Litchman and Klausmeier, 2008; Follows and Dutkiewicz, 2011). These models have been shown to be valuable tools for understanding how communities assemble (Follows et al., 2007; Litchman et al., 2007), how they change over time (Litchman and Klausmeier, 2006), and the interdependencies between community dynamics and biogeochemistry (Dutkiewicz et al., 2009).

In the current study we expand the trait-based approach to study a critical component of the nitrogen cycle, nitrification. Nitrification, the oxidation of ammonia to nitrite and then nitrate, is a rate-limiting step in the microbially mediated N cycle (Ward, 2008). Nitrification alters the distribution of inorganic N in soil and bridges the input of NH_3 from N-fixation or organic

matter (OM) decomposition to its loss as N_2O or N_2 gas via denitrification. In addition, nitrification is closely linked to the carbon cycle as nitrifier activity determines the relative concentration of two major plant and microbial nitrogen sources: ammonia and nitrate. The availability of these two nutrients in turn affects N mineralization rates, soil OM decomposition, denitrification, plant-productivity, and N-loss through leaching or gas efflux.

The initial step of nitrification ($NH_3 \rightarrow NO_2$) is catalyzed by a phylogenetically restricted group of beta- and gammaproteobacteria (Kowalchuk and Stephen, 2001) and members of the thaumarchaea (Brochier-Armanet et al., 2008). The distribution and abundance of ammonia-oxidizing bacteria (AOB) and ammonia-oxidizing archaea (AOA) in soils and sediments show broad patterns related to substrate (i.e., NH_3) concentration (Erguder et al., 2009; Wertz et al., 2011), pH (He et al., 2007); (Nicol et al., 2008), OM concentrations (Könneke et al., 2005), dissolved oxygen (Bouskill et al., 2012), and temperature (Avrahami and Bohannan, 2007; Tourna et al., 2008). In addition, while studies of the ecology and biogeochemical importance of the AOA are still nascent, certain ecological trends are evident, such as the ability to nitrify at low pH and grow under oligotrophic substrate concentrations (Erguder et al., 2009; Nicol et al., 2011).

The nitrite-oxidizing bacteria (NOB) belonging to five genera (Nitrobacter, Nitrospira, Nitrococcus, Nitrospina, and Nitrotoga) catalyze the second major step of nitrification ($NO_2 \rightarrow NO_3$). Few NOB have been isolated from soil and the extent of ecophysiological kinetic data for NOB significantly lags that of AOB. Additionally, PCR primers targeting the functional gene involved in nitrite oxidation (nitrite oxidoreductase) have only recently become available (Vanparys et al., 2007), which has hindered studies of NOB ecology and environmental distribution. Spatial coupling of the two reactions (NH_3 and NO_2 oxidation) is well known (Okabe et al., 1999; Schramm et al., 1999) and reduces the likelihood that toxic NO_2 will accumulate in soils. However, these two oxidative processes can, and often do, become spatially or temporally uncoupled by fluctuating redox or low NO_2 concentrations selecting against NOB activity, resulting in NO_2 accumulation. In the following section, we briefly introduce the concept of disaggregating microbial functional groups by specific traits and discuss previous attempts to apply these ideas to microbial ecosystems.

TRAIT-BASED MICROBIAL MODELS

Ecosystem activity is closely aligned to the structure and function of endemic microbial communities. These communities catalyze the bulk of biogeochemical reactions related to OM decomposition and nutrient transformations. Although the majority of ecosystem models acknowledge the contribution of prokaryotes in determining the rate of C and N cycling, these models have mainly focused their mechanistic representation on the role physical processes play in regulating biogeochemical cycles. Microbial transformations are often implicitly represented (e.g., Manzoni and Porporato, 2009, and references therein; Parton et al., 1987; Jenkinson and Coleman, 2008) using a specified turnover time for various pools of soil OM (e.g., slow, intermediate, and fast turnover pools). To our knowledge, no modeling frameworks applied at regional or larger scales attempt to represent how the dynamic nature of microbial diversity and activity affects biogeochemical cycling of C, N, or other compounds.

A deterrent to the explicit representation of microbial community dynamics is a lack of understanding of how microbial communities assemble and respond to changing environmental conditions. Microbial communities are extraordinarily diverse, with thousands of different taxa seemingly inhabiting the same environment (Gans et al., 2005; Delong et al., 2006). This diversity can be attributed to a small subset of microorganisms being selected for by the prevailing environmental conditions (Hutchinson, 1961). Selection can be due to a combination of genomic and physiological traits that elevate the fitness of some organisms over their competitors. Therefore, functional diversity is a transient ecosystem property, and as environmental conditions change over time so can microbially mediated reaction rates (e.g., Carney et al., 2007). These changes can have important implications for ecosystem model structure and parameterization.

Trait-based modeling approaches have been reviewed elsewhere (McGill et al., 2006; Green et al., 2008; Webb et al., 2010) and previously applied in ecology (Laughlin, 2011). In microbiology, these models have been used to depict communities of functionally important groups (Allison, 2012) and address questions that field and laboratory experiments are unable to sufficiently answer (Monteiro et al., 2011). These trait-based approaches have attempted to numerically characterize key physiological parameters that contribute toward an ecological strategy.

Nitrifiers are ideal candidates for building and refining trait-based models. They are autotrophic with a simple metabolism largely defined by central physiological processes, such as substrate acquisition (NH_3 and NO_2) and substrate use efficiency (number of moles of substrate required to fix one mole of CO_2). Several decades of ecophysiological studies using different nitrifiers have produced a wealth of data that can be used to mathematically characterize different nitrifier guilds. While heterotrophic organisms can also carry out nitrification (Schimel et al., 1984), at the present time, too little is understood about the distribution, importance and physiology of these organisms (De Boer and Kowalchuk, 2001). Therefore, in this manuscript we describe the development of a *micro*bial community *trait*-based modeling framework (MicroTrait) to simulate the physiology and ecology of autotrophic *nit*rifiers (MicroTrait-N), including an explicit representation of the rates of NH_3 and NO_2 oxidation, N_2O production, and nitrogen pool transformations. We apply MicroTrait-N to examine predicted patterns in nitrifier community diversity and activity across several geochemical gradients.

MATERIALS AND METHODS

EMERGENT COMMUNITY ECOSYSTEM MODEL DESCRIPTION (MICROTRAIT-N)

MicroTrait-N resolves intra-functional group diversity of the nitrifier populations (AOB, AOA, NOB) by parameterizing multiple guilds spanning a range in the trait-space (**Figure 1**). Although this nitrifier model will be integrated in an ecosystem model that allows for a wide range of interactions (Tang et al., submitted), we focus here on resolving nitrifier diversity in a competitive environment

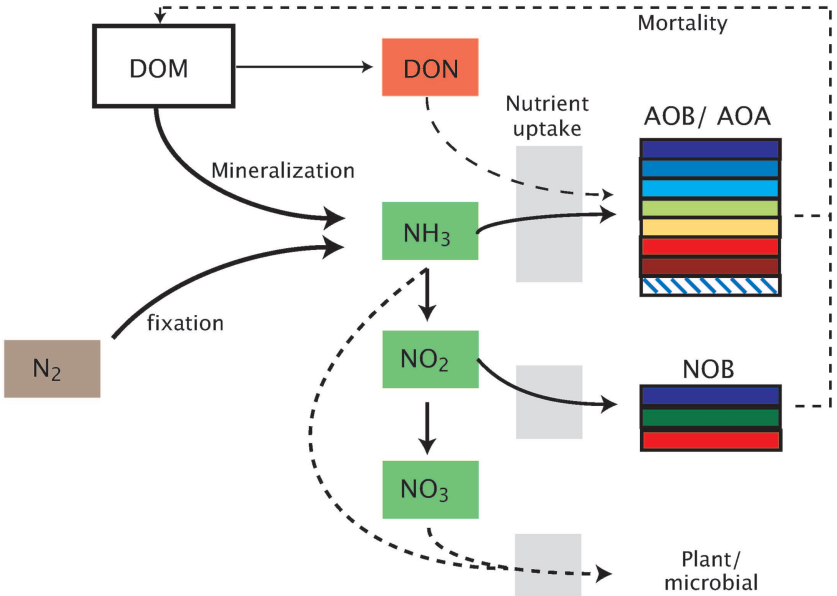

FIGURE 1 | Schematic representation of the model. Model abbreviations. DOM, dissolved organic matter; DON, dissolved organic nitrogen; AOB/AOA, ammonia-oxidizing bacteria/archaea; NOB, nitrite-oxidizing bacteria.

across a range of conditions, including pH, O_2, substrate type (NH_3 or urea), and temperature. Our approach is general enough that it can be applied to nitrifier populations in freshwater and aquatic environments and flexible enough to be used within soil pores. The model is written in Matlab (Matlab R2011b, Natick, MA, USA).

Our guild approach simulates seven lineages of Betaproteobacterial AOB as individual guilds, three NOB guilds, and one AOA guild. The smaller number of NOB and AOA guilds reflects the lack of relevant ecophysiological studies of these groups. Intra-guild diversity is parameterized by allowing a range of values for each trait (**Table 1**), based on previous ecophysiology studies (Loveless and Painter, 1968; Suzuki, 1974; Suzuki et al., 1974; Drozd, 1976; Belser, 1979; Belser and Schmidt, 1979; Glover, 1985; Keen and Prosser, 1987; Prosser, 1989; Nishio and Fujimoto, 1990; Verhagen and Laanbroek, 1991; Laanbroek and Gerards, 1993; Jiang and Bakken, 1999; Schramm et al., 1999; Gieseke et al., 2001; Koops and Pommerening Röser, 2001; Cébron et al., 2003; Martens-Habbena et al., 2009; Schreiber et al., 2009). Further information concerning the derivation of trait values is given in the supplemental material. Given the paucity of within-guild information, we assumed a uniform probability density of trait values across each trait range. We can increase the number of guilds as more information becomes available to distinguish intra-guild diversity. We performed several types of simulations investigating the role of pH, temperature, decoupling nitrite, and ammonia oxidation, and pulsed NH_3 inputs, by: (1) using the mean value of each trait; (2) performing Monte Carlo (MC) simulations to account for intra-guild diversity; and (3) running the model in equilibrium and dynamic steady state cycle modes to characterize the impact of temporal forcing variation on predicted emergent microbial community structure.

REPRESENTING AUTOTROPHY

In the model, the biomass of each nitrifier guild is represented with five variables: (1) total cell biomass (denoted B_T, which may represent the ammonia-oxidizing organism (AOO, i.e., AOB + AOA) as B_{TA} or the NOB, B_{TN}); (2) carbon biomass (B_C); (3) nitrogen biomass (B_N); (4) Cellular quotas for carbon (Q_C); and (5) cellular quotas for nitrogen (Q_N). The latter two are defined relative to total biomass (i.e., $Q_C = B_C/B_T$; $Q_N = B_N/B_T$). Carbon biomass increases by fixing CO_2 through the ribulose-bisphosphate enzyme using energy produced during the oxidation of either NH_3 or NO_2 (**Figure 1**). Cell division of the AOO and NOB is governed by Droop kinetics (Droop, 1973):

$$d^i_{B,j} = \max\left(1 - \frac{Q^{\min}_{B,j}}{Q^i_{B,j}}, 0\right) \quad (1)$$

where $Q^i_{B,j}$ represents the biomass quota (i.e., Q_C or Q_N) of the ith guild for the jth element. Here j represents either C or N. The minimum quota for carbon is 1 and for nitrogen is 1/13.2 (according to the Redfield Ratio). The carbon and nitrogen constraints are then applied to regulate the cell division rate (D_B) with Liebig's law of the minimum (van der Ploeg, 1999):

$$D_B = \mu^B_{\max} \min\{d_i\} B_T \quad (2)$$

where $\mu^B_{\max}\left(d^{-1}\right)$ is the nitrifier maximum specific growth rate (**Table 1**). Ammonia oxidation in AOO is modeled with Briggs–Haldane kinetics (Koper et al., 2010):

$$V^{NH_3}_{AOB} = V^{NH_3}_{\max} \frac{[NH_3]}{K^{NH_3}_M + [NH_3]\left(\frac{1+[NH_3]}{K^{NH_3}_i}\right)} \frac{[O_2]}{K^{O_2}_M + [O_2]} B_{TA} \quad (3)$$

Table 1 | Trait values across the different guilds.

GUILD	DON	$V_{max}^{NH_3}$ (day^{-1})	$K_M^{NH_3}$ (μM)	μmax (day^{-1})	$K_M^{O_2}$ (μM)	R_{CN}	Temperature optimum (K)	Phylogenetic affiliation
AOB(1)	–	0.38–1.1	30–61	0.02–0.09	6.9–17.6	0.04–0.08	290–95	*Nitrosomonas europaea*
AOB(2)	–	0.24	14–43	0.01–0.06	3.6–12.4	0.08–0.09	287–99	*Nitrosomonas communis*
AOB(3)	+	0.4–0.9	19–46	0.04*	4.2–14	0.06*	287–99	*Nitrosomonas nitrosa*
AOB(4) AOB(5)	+	0.4–0.8	1.9–4.2	0.06–0.08	1.4–4.7	0.02–0.05	287–99	*Nitrosomonas oligotropha*
	+	1.0–1.04	50–52	0.018	11–23	0.04–0.07	287–99	*Nitrosomonas marina*
AOB(6)	+	0.8–1.2	42–59	0.04*	11–23	0.02–0.03	275–86	*Nitrosomonas cryotolerans*
AOB(7)	+	0.42–0.9	1.4–11	0.07–0.08	0.7–1.2	0.06	285–99	*Nitrosospira* spp.
AOA	?	0.4–0.8	0.01–0.02	0.09–0.11	0.015	0.05	285–99	*Nitrosopumilus maritimus*
NOB(1)	–	0.8–1.9	4–10	0.3–0.7	40–80	0.01–0.03	285–95	*Nitrospina* spp.
NOB(2)	–	2–3.2	45–260	0.8–1.0	60–120	0.04–0.07	275–302	*Nitrobacter* spp.
NOB(3)	–	0.4–4	24–120	0.5–0.7	35–70	0.03–0.06	273–84	–

*Column headers represent the following; DON, ability to use dissolved organic nitrogen ("?" indicates the ability to use DON is unknown. In this case the guild is assumed to be unable to use DON); $V_{MAX}^{NH_3}$, maximal substrate uptake rate; $K_M^{NH_3}$, half saturation constant for NH_3; μ_{MAX}, maximum growth rate; $K_M^{O_2}$, half saturation constant for O_2, R_{CN}, substrate use efficiency, ratio of NH_3 moles required to fix one mole of CO_2, *indicates this value has not been measured and it's derivation is based on an average across the values for different guilds.*

Here, $V_{\max}^{\mathrm{NH_3}}$ $\left(\mathrm{MS}^{-1}\right)$ is the maximum substrate (NH_3) uptake rate, K_{M} is the half saturation constant for NH_3 or O_2 (μM; **Table 1**), and $K_i^{\mathrm{NH_3}}$ is the NH_3 inhibition constant for AOB (μM; **Table 1**). Substrate concentrations are in M (mol L^{-1}). CO_2 uptake follows Michaelis–Menten kinetics:

$$V_{AOB}^{\mathrm{CO_2}} = V_{\max}^{\mathrm{CO_2}} \frac{[\mathrm{CO_2}]}{K_m^{\mathrm{CO_2}} + [\mathrm{CO_2}]} \tag{4}$$

where $V_{\max}^{\mathrm{CO_2}}$ is guild-specific and depends on energy yielded by ammonia oxidation and the efficiency of CO_2 fixed relative to NH_3 oxidized:

$$V_{\max}^{\mathrm{CO_2}} = \frac{Y_{\mathrm{N}}^{\mathrm{CO_2}} V_{\max}^{\mathrm{NH_3}}}{Q_{\mathrm{N}}} \max\left(1 - \frac{r_{\mathrm{CN}} - r_{\mathrm{CN}}^{\min}}{r_{\mathrm{CN}}^{\max} - r_{\mathrm{CN}}^{\min}}, 0\right) \tag{5}$$

where $Y_{\mathrm{N}}^{\mathrm{CO_2}}$ (unitless) is the guild-specific substrate use efficiency (number of moles of NH_3 oxidized per mole of CO_2 fixed, **Table 1**) and represents the C:N ratio (i.e., the Redfield ratio; Redfield, 1958) of each nitrifier guild and $r_{\mathrm{CN}}^{\min} = 6.6$ and $r_{\mathrm{CN}}^{\max} = 13.2$, which are use to reflect the autotrophic nature of the nitrifiers.

Growth of the *i*th AOB biomass over time is calculated as:

$$\frac{dB_{\mathrm{TA}}^{i}}{dt} = \mu_{\max}^{i} \min\{d_i\} \mathrm{B}_{\mathrm{TA}}^{i} - \Delta B_{\mathrm{TA}}^{\mathrm{i}} - \frac{1}{4}\left(D_{\mathrm{A}}^{\mathrm{NO_2}} + D_{\mathrm{A}}^{\mathrm{NO}}\right) \tag{6}$$

Here, Δ (s^{-1}) is the first order microbial mortality rate and D_{A} is biomass loss (M s^{-1}) attributable to the detoxification of NO_2 following the uncoupling of AOB and NOB mediated reactions (see below). Total biomass loss is the sum of that required to convert $NO_2 \rightarrow NO$ and $NO \rightarrow N_2O$, and the 1/4 represents the stoichiometric relationship between biomass and NO_2 detoxification (i.e., $4NO_2 + CH_2O \rightarrow 4NO + CO_2 + 3H_2O$; $8NO + 2CH_2O \rightarrow 4N_2O + 2CO_2 + 2H_2O$).

The NOB gains energy to fix CO_2 to biomass via the oxidation of $NO_2 \rightarrow NO_3$. NO_2 uptake rate is modeled by:

$$V_{\mathrm{NOB}}^{\mathrm{NO_2}} = V_{\max}^{\mathrm{NO_2}} \frac{[\mathrm{NO_2}]}{K_M^{\mathrm{NO_2}} + [\mathrm{NO_2}]} \frac{[\mathrm{O_2}]}{K_M^{\mathrm{O_2}} + [\mathrm{O_2}]} B_{\mathrm{TN}} \tag{7}$$

where the different terms in Eq. 7 are analogous to those in Eq. 3. The uptake of CO_2 occurs via the same pathway as for AOO (Eqs 4 and 5) and the biomass of the *i*th NOB guild varies as:

$$\frac{dB_{\mathrm{TN}}^{\mathrm{i}}}{dt} = \mu_{\max}^{i} \min\{d_{\mathrm{i}}\} B_{\mathrm{TN}}^{i} - \Delta B_{\mathrm{TN}}^{i} \tag{8}$$

NITROUS OXIDE PRODUCTION

N_2O is produced by AOO via two distinct pathways: (1) decomposition of the hydroxylamine intermediate and (2) the likely more significant mechanism of NO_2 detoxification (**Figure A1** in Appendix; Frame and Casciotti, 2010; Kool et al., 2011; Stein and Klotz, 2011). Under the first pathway, N_2O production is modeled as a linearly related fraction of hydroxylamine decomposition (Frame and Casciotti, 2010). The second pathway simulates the detoxification of accumulated NO_2 as the two steps of nitrification become uncoupled. This decoupling can occur because NOB have a lower affinity for O_2 than the AOB; therefore as O_2 is consumed during nitrification (or in low O_2 environments), the two reactions may become spatially or temporally uncoupled. NO_2 toxicity stimulates a detoxification pathway converting NO_2 to N_2O via NO. This detoxification pathway is potentially the more significant mechanism by which AOB produce N_2O. AOA have recently been shown to produce N_2O (Santoro et al., 2011), although the mechanism has not yet been elucidated. Therefore, in the present version of the model we predict AOA N_2O production using the same relationships as for AOB.

As NO_2 concentrations become toxic to AOO, their growth and NH_3 uptake decline. We represent these transitions by modifying

an organism's affinity for NH_3 as a function of NO_2, NO, and O_2 concentrations:

$$K_M^{NH_3} = K_{Mb}^{NH_3}\left[1 + K_d^{max}\frac{[C]}{[O_2]}\right] \quad (9)$$

where $K_{Mb}^{NH_3}$ is the base NH_3 affinity, K_d^{max} is the affinity constant for NO_2 or NO during detoxification, and [C] represents the concentration (M) of either NO_2 or NO. Energy for detoxification is assumed to come from the degradation of microbial biomass resulting in the output of CO_2.

NUTRIENT POOL TRANSFORMATIONS

The dynamic aqueous NH_3 concentration ($[NH_3]$ (M) depends on a balance between losses from oxidation $\left(V_{NH_3}^E\right)$, uptake into biomass of AOO $\left(V_{NH_3}^B\right)$, and NOB $\left(V_{NH_3}^{NOB}\right)$, and inputs resulting from biomass breakdown during detoxification summed across the total number of AOO guilds (n_A) and NOB guilds (n_N):

$$\frac{d[NH_3]}{dt} = -\sum_{i=1}^{i=n_A}\left(V_{NH_3}^E + V_{NH_3}^B\right) - \sum_{I=1}^{i=n_N} V_{NH_3}^{NOB} + \frac{1}{4}\sum_{i=1}^{i=n_A}\left(D_A^{NO_2} + D_A^{NO}\right) \quad (10)$$

where the 1/4 represents the stoichiometry of the detoxification reaction using biomass for energy. The dynamic NO_2 concentration depends on uptake by NOB to generate energy and losses via detoxification by AOB:

$$\frac{d[NO_2]}{dt} = \sum_{i=1}^{i=n_A} V_{NH_3}^E - \sum_{i=1}^{i=n_N} V_{NO_2}^E - \sum_{i=1}^{i=n_A} D_A^{NO_2} \quad (11)$$

MODEL EVALUATION

Resolution of nitrifier diversity across geochemical gradients

We tested MicroTrait-N by examining how nitrifier diversity varies across geochemical gradients in pH, substrate concentration [i.e., (NH_3)], and temperature and compared predictions of this diversity against published studies. Accuracy of modeled communities was gaged by relating the steady state modeled nitrifier diversity to its likely phylogeny based on literature sources of the derived trait values. In addition, an evenness statistic (J^i) is ascribed to each community;

$$J^i = \sum_{i-1}^{S}\frac{\left[(p_i)\ln(p_i)\right]}{\ln(S)}$$

where represents the relative proportion of the ith species, and S is the species richness (Mulder et al., 2008). The evenness statistic varies between 0 and 1, with 1 indicating an equal contribution of each guild to the total biomass. The model also predicts rates of NH_3 oxidation and N_2O production that we report as 30 days running averages.

Physicochemical impacts on nitrifier diversity and activity

We applied a step-wise approach to analyze the impacts of geochemical variables, temporal dynamics of substrate inputs, and combinations of these variables on nitrifier diversity and activity. The five groups of modeling scenarios include sensitivity analyses of the impacts of (i) pH; (ii) temperature; (iii) decoupling during NO_2 detoxification; and (iv) dynamic substrate inputs. For the fifth modeling scenario, (v) we computed predicted community structure with a limited set of available observations.

pH impacts. pH is a determinant of nitrifier diversity, in part, due to its regulation of NH_3 concentrations. The NH_4:NH_3 ratio increases as pH decreases (Li et al., 2012), possibly selecting for nitrifiers adapted to low substrate concentrations. We performed model simulations across pH gradients spanning neutral to slightly acidic conditions (7.8–4.5). For each guild, the model was run with an integration time of 6 months, which allowed the community biomass to come to a steady state. Simulations were initialized with 1×10^{-5} M NH_3 and non-limiting concentrations of O_2 and CO_2 (both $1\,M \times 10^{-3}$ M). Two further substrate pulses (of 1×10^{-6} NH_3) following 2 and 4 months were necessary to prevent the communities becoming substrate limited and maintain them at steady state.

Temperature impacts. Temperature has also been shown to play an important role in determining the diversity of ammonia-oxidizing communities in terrestrial and aquatic ecosystems (Erguder et al., 2009; Prosser, 2011). We applied in the model a temperature-activity relationship based on previously published data (Ratkowsky et al., 2005; Follows et al., 2007) that accounts for a different temperature optima across the guilds (**Table 1**). We simulated a temperature range of 5 to 30°C in 5°C increments under initial conditions of $NH_3 = 5 \times 10^{-5}$ M and pH = 7.8.

Decoupling nitrification reactions. We simulated the forced reduction of NO_2 to N_2O during AOO detoxification by initializing the model to steady state over 6 months under initial conditions of 1×10^{-5} M NH_3, pH = 7.8 and temperature = 20°C. At steady state, the NOB activity was turned off and then simulations were run for a further 6 months. A simultaneous control experiment extended the steady state for a further 6 months maintaining NOB activity.

Pulsed substrate inputs. NH_3 availability is considered to be a major determinant of AOO diversity (Bouskill et al., 2011; Prosser, 2011) and the rate of N_2O efflux (Elberling et al., 2010). Nitrifiers show wide physiological breadth with respect to enzyme kinetics (V_{max} and K_m) and different communities dominate based on the magnitude of substrate inputs (Mahmood et al., 2006). We tested the impact of NH_3 availability by simulating community diversity and activity in response to pulsed NH_3 input events. Under a constant pH (7.8) and temperature (25°C), NH_3 was initially input at a concentration of 1×10^{-6} M and increased on 2-month cycles to 5×10^{-5} M.

Comparisons with observed data. We tested the baseline MicroTrait-N predictions by comparing against published data from five Alaskan ecosystems (Petersen et al., 2012). That dataset combines nitrification rate measurements with a quantification of the different nitrifier groups (AOB and AOA) facilitating a direct comparison with the output of our model. Petersen et al. (2012) also report a comprehensive list of chemical data, which satisfy the

input requirements of the simulation's initial conditions. Furthermore, in contrast to our earlier simulations evaluating community composition at a fixed substrate concentration and low pH (down to 4.5), this dataset represents low pH soils (4.8–4.3) with high substrate concentrations. For these simulations initial conditions are given in **Table A1** in Appendix with temperature = 15°C and simulations were run for 6 months. The model was initialized with mean trait values and then simulations were replicated using the MC approach and five analogs per guild (with each analog representing a stochastically chosen set of trait values across the uniform probability distribution. For comparison, data from two of the sites are replicated using an MC code with a normal distribution. Using the normalized distribution of traits produces little effect on the model output. See appendix).

RESULTS

PHYSICOCHEMICAL IMPACTS ON NITRIFIER DIVERSITY AND ACTIVITY

In this subsection we describe results from our modeling scenarios and comparison of predicted data with observations.

pH impacts

We simulated a pH gradient from approximately neutral (pH = 7.8) to acidic (pH = 4.5) conditions and recorded diversity and activity (NH_3 oxidation rate and N_2O production). During the hydrolysis reaction of NH_3, the ratio NH_4:NH_3 increased hyperbolically as pH decreased. Thus, at pH < 5, the extremely low [NH_3] encouraged the growth of oligotrophic ammonia oxidizers. Both baseline (i.e., fixed trait values, **Figures 2A,B**) and MC (**Figures 2C,D**) approaches showed a decline in AOB community evenness with decreasing pH. The highest evenness values are predicted around neutral values where AOB guilds 7 [AOB(7)] and 4 [AOB(4)] dominate. As pH decreases, community diversity declines until the AOA guild dominates. Although both simulations had similar trends in diversity, the multiple analog experiments (**Figures 2C,D**) predicted more variability in community diversity, as evidenced by more variable evenness values. Predicted nitrifier activity (as indicated by NH_3 oxidation rates and N_2O production) also declined with decreasing pH from a maximum NH_3 oxidation rate of 1.9 M N day^{-1} to less than 0.1 M

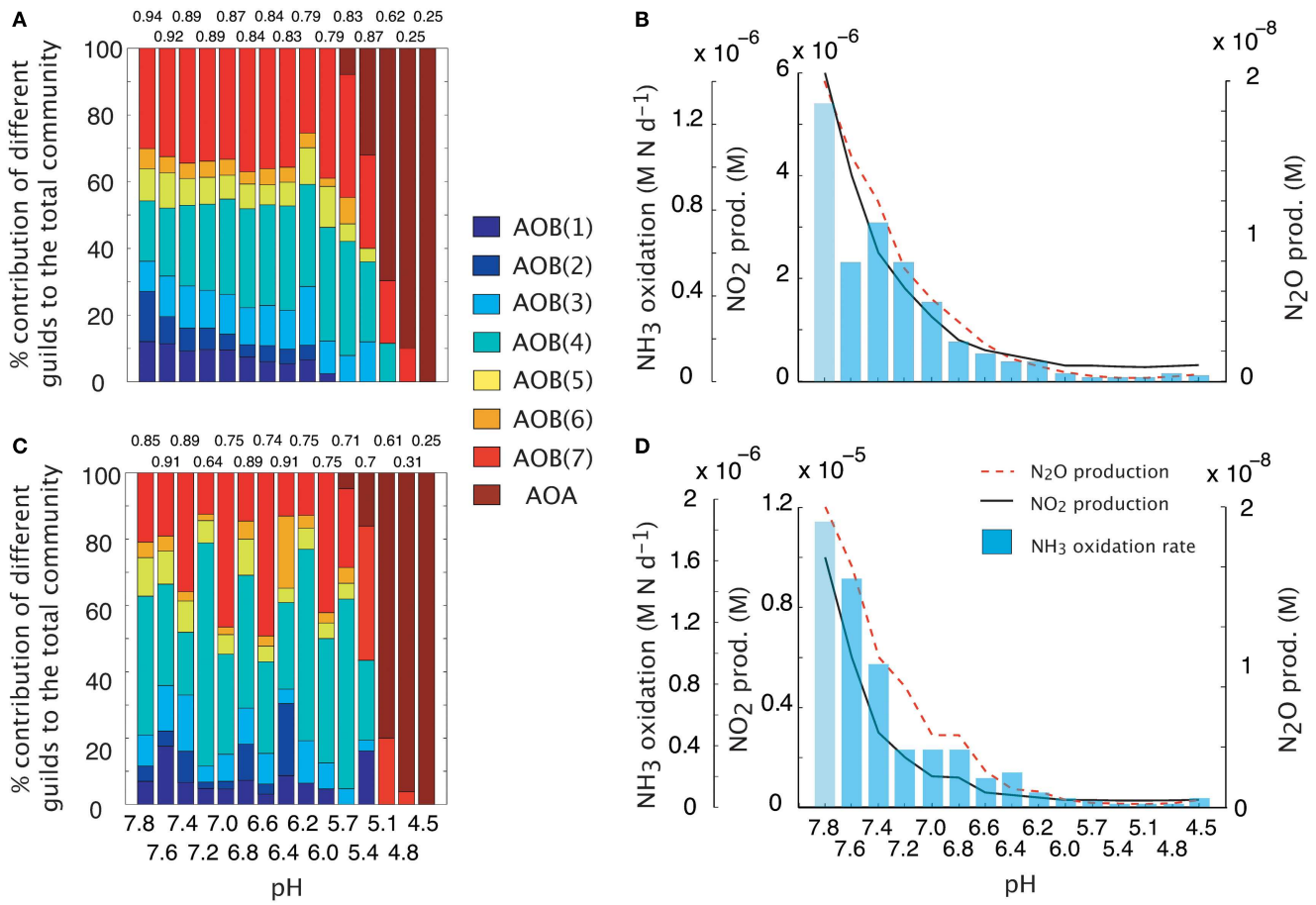

FIGURE 2 | Simulations of AOO diversity and activity across a pH gradient. Community evenness values are given above the stacked bars. **(A)** Community diversity (proportion of total biomass) predictions using mean trait values. **(B)** Simulated nitrifier activity (NH_3 oxidation, NO_2 production, N_2O production) using mean trait values. **(C)** Community diversity (proportion of total biomass) predictions using Monte Carlo simulations of multiple AOO analogs ($n = 5$ analogs per guild). **(D)** Simulated nitrifier activity (NH_3 oxidation, NO_2 production, N_2O production) using Monte Carlo simulations of multiple AOB analogs ($n = 5$ analogs per guild).

N day^{-1}. Predicted N_2O production was linearly related to NH_3 oxidation (data not shown, $r = 0.98$, $p = 0.001$, slope = 0.94) indicating the AOB and NOB reactions were coupled regardless of the pH and N_2O was primarily by hydroxylamine decomposition.

Temperature impacts

Maximal rates of ammonia oxidation were simulated at 25°C (**Figure 3B**). Maximal oxidation rates coincided with the highest community evenness. At low temperature, AOO communities were dominated by the cold-adapted AOB(6) guild (**Table 1**, **Figure 3A**), which represents *Nitrosmonas cryotolerans*. The AOA guild was also important at this temperature (**Figure 3A**). With increasing temperatures up to 25°C, the AOB(3) and AOB(7) guilds became more competitive and began to dominate the community. When the temperature reached 30°C, the AOB(1) guild dominated. N_2O production mirrored that of NH_3 oxidation indicating that N_2O production resulted from hydroxylamine decomposition under these conditions.

Decoupling nitrification reactions

We simulated N_2O production through two pathways described above (**Figure A1** in Appendix). After running the simulations to steady state biomass, the NOB were removed allowing rapid accumulation of NO_2 and invoking a detoxification response in the AOO. NO_2 was rapidly converted to N_2O, via NO, using cellular biomass as an energy source. This conversion resulted in a transient N_2O production rate significantly higher than in the scenarios with a steady state community and when the NOB were present (ANOVA, $p < 0.05$; **Figure 4A**). Despite a higher N_2O production rate in the absence of NOB, cumulative production of N_2O over 6 months was significantly (ANOVA, $p < 0.05$) lower than when NOB were present (**Figure 4B**) due to the creation of an unstable half reaction (lacking NO_2 oxidation) resulting in a rapid crash in AOO community biomass (data not shown).

Pulsed substrate input

We simulated the response of our imposed simple community (seven AOB guilds; one AOA guild; and three NOB guilds) to pulsed input of substrate over a 9-month period (**Figure 5**). Over time, and with evenly spaced pulsed events, the evenness of the community declines slightly from 0.76 to 0.58 as one guild, AOB(7), begins to dominate. Pulses of NH_3 are drawn down more quickly as the biomass of AOB increases. However, the second

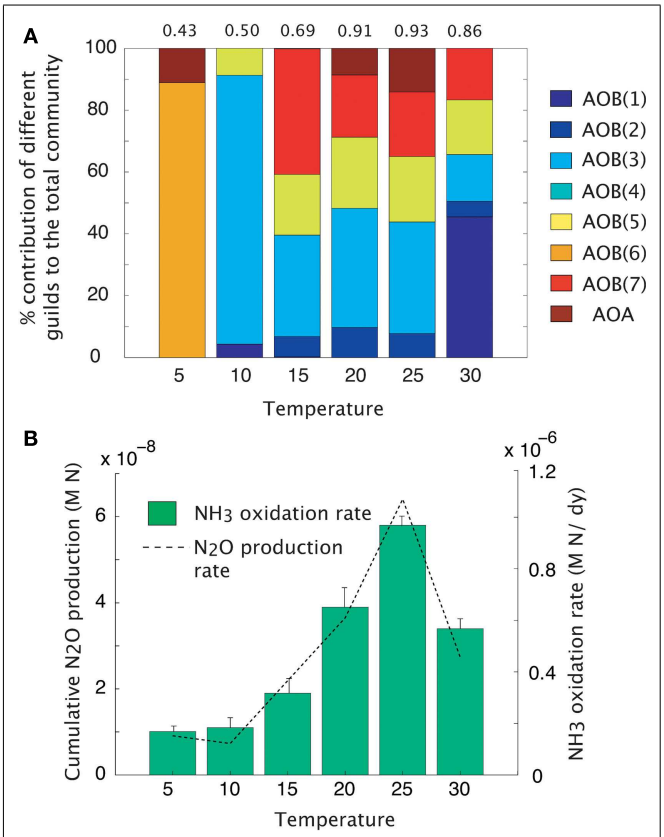

FIGURE 3 | Mean trait-value AOO community diversity and activity across a temperature gradient. (A) Stacked bar chart depicts community diversity as a proportional contribution to the total community biomass. The evenness value is given above the plot. **(B)** Rates of NH_3 oxidation (bar chart) and gross N_2O production (line graph). Error bars are the result of multiple simulations ($n = 3$).

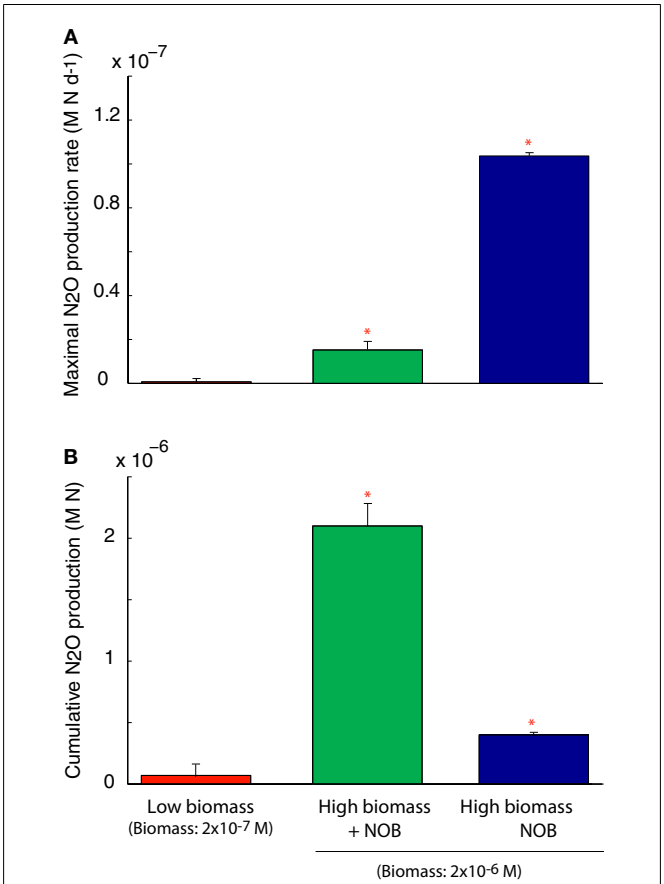

FIGURE 4 | N_2O production under a coupled AOB-NOB nitrification reaction and also as the AOB-NOB reaction becomes uncoupled and the detoxification reaction is activated. (A) Maximal rate of N_2O production **(B)** Cumulative N_2O production over the 6-month simulation. Error bars are the result of three simulations per temperature.

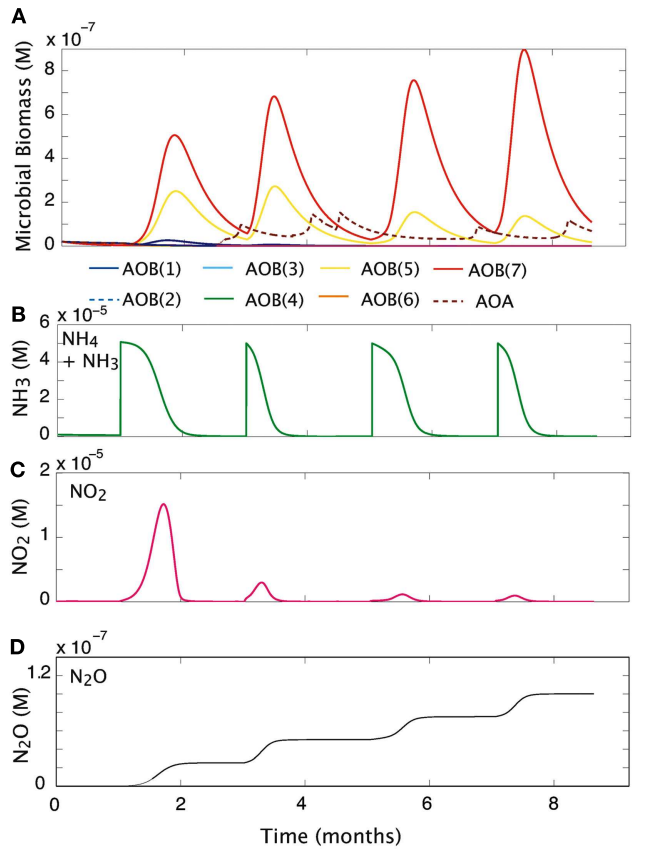

FIGURE 5 | Community response to pulsed substrate input. **(A)** Changes in AOO biomass over time. **(B)** Substrate concentration (M). **(C)** Nitrite dynamics over time. **(D)** Production of N_2O over time.

pulse of NH_3 results in its most rapid drawdown due to a high cumulative biomass and greater diversity of AOO (**Figures 5A,B**). As NOB biomass increases, NO_2 demand increases, and the NO_2 is oxidized as rapidly as it is produced (**Figure 5C**). In the present simulation we did not allow for diffusion, and this resulted in an accumulation of N_2O (**Figure 5D**), nevertheless, the rate at which it is produced reflects the pulses of NH_3 into the system. The initial pulse elevates NH_3 concentrations from 1×10^{-7} to 5×10^{-6} and results in a five-fold increase in the biomass of AOB(7), a four-fold increase in AOB(5), and a small response in AOB(1). As NH_3 is drawn down to lower concentrations ($<1 \times 10^{-6}$ M) AOA briefly become the dominant nitrifiers. While AOA biomass peak when substrate concentrations are low, they are inhibited by subsequent substrate pulses.

Comparison with environmental data

The dataset presented by Petersen et al. (2012) examined AOO community diversity across five-plant community types characteristic of the interior of Alaska. These soils were characterized by high substrate concentrations (range $= 7.3 \times 10^{-3}$ to 0.1 M NH_3) and low pH (4.3–4.8). These observations therefore provide a comparison to our earlier examination of a pH gradient with a fixed substrate concentration. The model predicted that, in contrast to our previous predictions at low pH and NH_3 substrate levels (**Figure 2**), bacteria dominated the AOO community at these sites (**Figure 6A**). Using mean values for traits, the Black Spruce and Bog Birch sites were dominated by AOB(7) and AOB(3) in the case of the Bog Birch site. The Tussock Grassland, Emergent Fen, and Rich Fen also showed lower evenness and were generally dominated by one guild [AOB(1)] accounting for approximately 90% of the total AOB biomass. The AOA guild was never a significant component of the community diversity under these conditions (data not shown). Within-guild diversity was represented using MC simulations that stochastically assigned traits to multiple analogs of each guild. The community composition that emerged when using this approach was different than when traits were represented by their mean values. For example, the AOA became more prominent in the MC simulations, although they were still only a relatively small proportion (2–4%) of the Fen communities and Tussock grassland (**Figure 6A**).

Predicted trends in NH_3 oxidation rates (**Figure 6B**) correlated with the observed data (**Figure 6B**; $r = 0.96$, $p = 0.007$). The highest oxidation rates were associated with the highest NH_3 concentrations at the Emergent Fen site (4.9×10^{-4} M N day^{-1}) and with the lowest rates at the Black Spruce and Bog Birch sites (9×10^{-5} and 9×10^{-6} M N day^{-1} respectively). MicroTrait-N predictions of N_2O production also correlated with NH_3 concentrations and oxidation rates (**Figure 6C**), albeit not significantly ($r = 0.69$, $p = 0.19$), and were 85 times higher at the Emergent Fen site (3.6×10^{-6} M N day^{-1}) than the Black Spruce (4.3×10^{-8} M N day^{-1}).

DISCUSSION

Oxidation of NH_3 to NO_3 is an important process that couples N-inputs and losses via denitrification and influences the availability of N in terrestrial and marine environments (Ward, 2008; Prosser, 2011) with important implications for carbon cycling (Doney et al., 2007). A better understanding of the ecological factors that determine the activity and diversity of the chemoautotrophic nitrifiers will therefore improve our understanding of N-transformations and N-emissions. To that end we describe here a model simulating nitrifier community development as a function of environmental conditions, allowing both community diversity and the rate of nitrification to change across environmental gradients.

GUILD CHARACTERIZATION

MicroTrait-N simulates nitrifier diversity using a guild model loosely based on phylogenetic affiliations (Koops and Pommerening Röser, 2001), with differences in key ecophysiological characteristics (e.g., DON usage, K_M values). Several of the results across gradients showed plausible representation of the dominant nitrifiers guilds emerging on the basis of environmental conditions (discussed below). Our guild characterization recognizes several guilds of the *Nitrosomonas* [AOB(1-6)], one guild of the *Nitrosospira* [AOB(7)] and the AOA, and three guilds of the NOB. The guilds resolve broadly into oligotrophic and copiotrophic groups (Kassen et al., 2000; Lauro et al., 2009). For example, the AOB(5) and AOB(7) guilds have copiotrophic-like characteristics, responding rapidly to substrate pulses (**Figure 5A**), while the

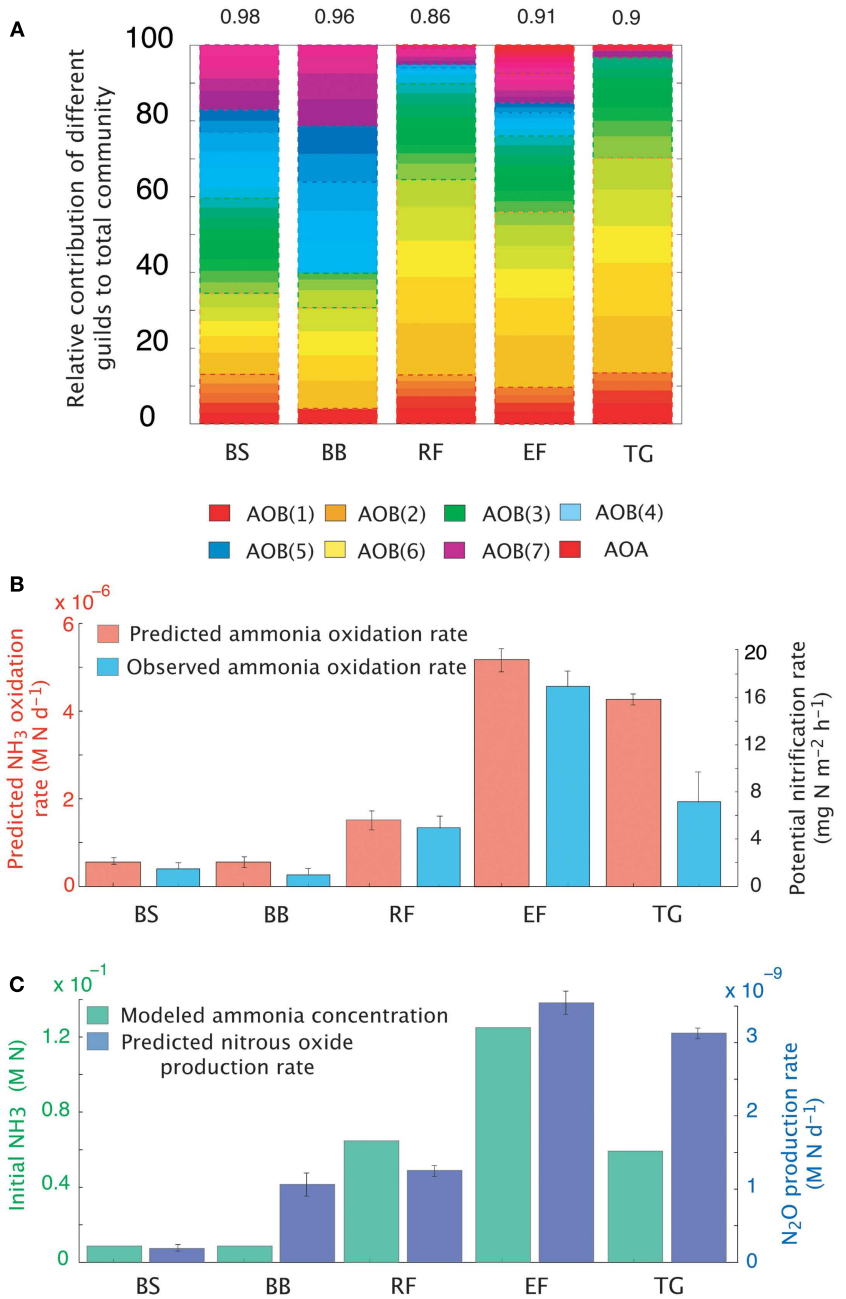

FIGURE 6 | Simulations of the activity and diversity of AOB communities in high-latitude ecosystems. (A) Monte Carlo simulations of multiple AOB analogs ($n = 5$ analogs per guild) across the different sites. Each guild is represented by a distinct color. Subtle differences in the shade of that color demarcate the different analogs/guild. A box outlines the boundaries of each guild's biomass. Evenness statistic given above the bar plots. **(B)** NH_3 oxidation rates from just simulated and observed data. **(C)** Predicted rates of N_2O production and measured NH_3 concentrations. Error bars are the result of multiple simulations ($n = 3$). BS, Black Spruce; BB, Bog Birch; RF, Rich Fen; EF, Emergent Fen; TG, Tussock Grassland.

AOA guild is only competitive as substrate is either drawn down to concentrations $\leq 1\,\mu M$ (**Figure 5A**) or when pH reduces NH_3 availability (**Figure 2**).

The MicroTrait-N model structure is currently weighted in favor of guilds with cultured members and likely under-represents the importance of the AOA. The AOA are known to be in high abundance in both oceanic (Bouskill et al., 2012) and terrestrial (Leininger et al., 2006) environments. However, while it is likely that marine AOA are chemoautotrophic organisms and play an important role in marine nitrification, AOA possibly span a more complicated functional space in terrestrial systems. Attempts to draw correlations between the abundance of terrestrial AOA and NH_3 oxidation rates have produced mixed results (Di et al., 2009); (Jia and Conrad, 2009). In MicroTrait-N, parameterization

of AOA kinetics is extrapolated from a few published cultures (Martens-Habbena et al., 2009; Lehtovirta-Morley et al., 2011). The model consequentially represents the AOA as oligotrophs, dominating nitrifying conditions under low NH_3 concentrations, and becoming outcompeted or possibly inhibited under higher NH_3. The AOA:AOB relationship provides some support for the idea that AOA are oligotrophic, with ratios increasing as substrate concentrations decrease (Mosier and Francis, 2008; Bouskill et al., 2012), while AOA have generally been reported in low abundance within engineered systems of high NH_3 concentrations (Wells et al., 2009). However, the AOA are also abundant in terrestrial ecosystems with high NH_3 concentrations (Verhamme et al., 2011). This diversity might suggest that the physiological breadth of the AOA has yet to be fully uncovered, and that the notion of the AOA as oligotrophic K-strategists might be challenged through isolation of organisms from high NH_3 environments. On the other hand, several studies have demonstrated metabolic diversity of the terrestrial AOA (i.e., mixotrophy; Mußmann et al., 2011), and have proposed that although the abundance of the AOA is high, their contribution to ammonia oxidation is perhaps minimal. Currently, MicroTrait-N is only capable of representing organisms growing autotrophically, and does not represent the abundance of organisms with alternative metabolisms. Therefore, if an appreciable proportion of the AOA community at neutral pH is not actively oxidizing ammonia, they will not be predicted in the current model structure. Further studies into the physiology of the AOA will likely yield data that should help to constrain the models.

GEOCHEMICAL GRADIENT SIMULATIONS

MicroTrait-N attempts to predict trends in community diversity across gradients in substrate concentration, pH, and temperature.

pH impacts

Few studies offer an experimental analog to the simulations presented here, however, Nicol et al. (2008) examined AOA and AOB dynamics along a pH gradient (7.5–4.9) in an agricultural soil. The results of that study did not necessarily support predictions from our simulations (e.g., the AOA were observed to be the numerically dominant nitrifiers across neutral to acidic conditions), however several similarities occurred. Quantification of transcript abundance found the AOA:AOB ratio decreased with increasing pH, suggesting that the relative importance of the AOB to ammonia oxidation increases with increasing pH. Furthermore, Nicol et al. (2008) also noted the taxonomic diversity of AOB to decrease with decreasing pH. This relationship was mainly attributable to the loss of most of the *Nitrosomonas* species and several of the *Nitrosospira* clusters. Additionally, at $pH \leq 5.0$ the *Nitrosospira* were the dominant bacterial nitrifying group. Our simulations reproduced some of these observations, including a drop in bacterial diversity and an increasing prominence of the AOB(7) guild (for which kinetic parameters were derived from the *Nitrosospira*) with decreasing pH.

The dominance of the AOA guild at low pH is supported by several studies (Nicol et al., 2008; Gubry-Rangin et al., 2010). However, there is also evidence of the AOA dominating nitrifier groups across a range of pH (from 8.7 to 3.5; Gubry-Rangin et al., 2011). It is not clear if this dominance is due to a physiological adaptation to low pH or to substrate availability. Nitrification rates have previously been shown to be high at low pH where rates of mineralization (and hence substrate availability) are high (Booth et al., 2005), however, (Gubry-Rangin et al., 2011) did not explicitly measure substrate concentrations in their study.

Temperature impacts

MicroTrait-N also simulates the relationship between temperature and the kinetics of the ammonia-monoxygenase enzyme, which purportedly has a stronger effect on the ammonia oxidation rate than substrate availability (Groeneweg et al., 1994). The MicroTrait-N relationship between temperature and activity (ammonia oxidation) was based on a previously published square-root relationship for the growth rate of bacteria (Ratkowsky et al., 1983, 2005). In the present model, nitrifier diversity and activity was highest at 25°C while the rate of N_2O production tracked the rate of ammonia oxidation. Several laboratory and field experiments have recorded a significant positive relationship between temperature and the activity of nitrifiers (Stark, 1996; Jiang and Bakken, 1999; Avrahami and Bohannan, 2007; Bouskill et al., 2011) with a few studies noting that the relationship continues up to and above 30°C (Stark and Firestone, 1996). Understanding the relationship between temperature and nitrification is crucial to predicting future N_2O effluxes (Avrahami and Bohannan, 2009) and future simulations should account for complex interactions between temperature, substrate, and soil moisture, all of which play a significant role in N_2O fluxes (Avrahami and Bohannan, 2009).

Decoupling nitrification reactions

N_2O is a long-lived greenhouse gas and stratospheric ozone depleting substance (Bange, 2008). The atmospheric mixing ratio of N_2O has increased 20% since 1750 (MacFarling Meure et al., 2006) with terrestrial ecosystems the principle sources of N_2O emissions (Pérez et al., 2001). The annual contribution of nitrification to the global N_2O budget is currently unknown, however, in previous models the ratio of N_2O formed to NH_3 oxidized is generally about 0.1% (Frame and Casciotti, 2010). This relationship does not account for differences in the pathways of N_2O production via nitrification (Frame and Casciotti, 2010).

In the current model, we simulated N_2O production via NO_2 detoxification and hydroxylamine decomposition. The maximal rate of N_2O production was recorded under NO_2 detoxification, and was approximately 150 times higher than it had been directly before NOB removal and seven times higher than the N_2O production rate when NO_2 did not accumulate (i.e., NOB were present and N_2O was produced by hydroxylamine decomposition). This result might suggest that NO_2 detoxification substantially increased N_2O production by ammonia oxidizers upon uncoupling of the nitrification reactions. However, the toxic effect of NO_2 reduces AOO biomass to the point where the populations crash and NH_3 oxidation declines. This biomass change is reflected in the cumulative N_2O production data over the 6 month simulation, which is approximately 5 times lower than that formed during full nitrification (i.e., hydroxylamine decomposition).

These model predictions are supported by previous experimental work. For example, Graham et al. (2007) observed evidence of chaotic instability in the AOB-NOB relationship resulting in significant accumulation of NO_2 in a chemostat experiment. Furthermore, Frame and Casciotti (2010) examined pathways of N_2O production in the marine ammonia oxidizer, *Nitrosomonas marina*. They found that the presence of excess NO_2 in the growth medium increased N_2O yields by an average of 70–87%, while stable isotope and ^{15}N-site preference measurements determined that nitrifier-denitrification (analogous to our detoxification pathway) was responsible for the majority of N_2O production at low oxygen (Frame and Casciotti, 2010).

Comparison with environmental data

We also tested our model against site-collected data from a recent study in a high-latitude site (Petersen et al., 2012). Petersen et al. (2012) sampled five-plant communities characteristic of interior Alaska, and measured the abundance of functional genes affiliated with nitrification (i.e., bacterial and archaeal ammonia monooxygenase) and potential nitrification rates. The sites were characterized by high ammonium concentrations (0.2–2.9 g m^{-2}) and low pH (4.8–4.3). These sites therefore present a contrast to the earlier pH gradient analysis under a lower substrate concentration. In our pH gradient simulation the AOA dominated the low pH possibly due to low substrate availability. Conversely, at higher substrate concentrations Petersen et al. (2012) found AOB to be the dominant nitrifier in these Alaskan soil plots and the AOB *amoA* gene abundance best explained observed nitrification rates. The AOA were only minor components of the AOO communities. Recreating the initial conditions from data collected in Alaska (Carney et al., 2007; Petersen et al., 2012), we resolved plausible trends in both relative community composition (i.e., AOB biomass was higher than that of the AOA) and NH_3 oxidation rates. Predicted NH_3 oxidation rates correlated with NH_3 concentrations. That the AOB dominated these communities over the AOA supports the earlier data suggesting AOO community composition is largely determined by substrate concentrations. N_2O production generally tracked NH_3 oxidation, indicating that N_2O was predominantly produced via hydroxylamine decomposition. The exception was at the Bog Birch site where predicted N_2O production was higher than a rate consistent with hydroxylamine decomposition. This result is significant given predictions of higher N_2O production in high-latitude ecosystems dependent on N-availability (Elberling et al., 2010) and further work is warranted to understand these MicroTrait-N predictions.

In addition to replicating field studies, a major objective of any modeling approach is to test existing hypotheses. For example, our mechanistic model may be used to test existing ecological theory of the controls on ecosystem processes (in this case nitrification). At the present time, two competing hypotheses describe the relationship between community structure and ecosystem processes: The "diversity" hypothesis and the "mass-ratio" hypothesis (Grime, 1998; Green et al., 2008; Laughlin, 2011).

The "diversity hypothesis" postulates that the richness of functional groups determines the rate of ecosystem processes by a complementary association between different functional groups (e.g., Tilman et al., 1996; Laughlin, 2011). On the other hand, the "mass-ratio" hypothesis proposes that ecosystem processes are controlled by the relative abundance of different functional groups.

Our results show that these two hypotheses are both valid but at different stages of the evolving nitrifier ecosystem. Organisms achieving maximal fitness under the initial conditions can rapidly increase their biomass to dominate the nitrification process. Other guilds decline sometimes to extinction. These dynamics seemingly lend support to the "mass-ratio" hypothesis. However, as conditions change (i.e., as substrate concentrations fall), the diversity of the community becomes more important, as guilds more suited to the new conditions become numerically prominent and dominate nitrification. At the present time, we are unaware of any field studies in microbial ecology that exclusively test these theories *in situ*. The functional diversity of microbial communities, and redundancy in those communities, in addition to limitations in current methods limitations, make it difficult to attribute activity to specific groups. These limitations might be overcome in future through continued development of isotope labeling and spectroscopy methods (Hall et al., 2010) and transcriptomics (Moran et al., 2012).

CONCLUSION

Trait-based microbial ecology can potentially link the observations of experimental environmental microbiology, theoretical energy, and mass exchange considerations, and quantitative modeling with an emphasis on depicting microbial diversity across spatial and temporal scales. Previous applications of the microbial trait-based approach have been successful in predicting rates of primary productivity (Follows et al., 2007), heterotrophic activity (Hall et al., 2008), and litter decomposition (Allison, 2012). We demonstrate here that trait-based representation of nitrifiers can be used to connect community diversity with activity, improve understanding of environmental controls on NH_3 oxidation, and test hypotheses centered around the ecology of NH_3-oxidizers and N_2O production, issues that temporal and financial restrictions on field studies are often unable to address. An important avenue for future research is to focus on whether the integration of these microbiological diversity modules into ecosystem models can improve site, regional and global predictions of carbon and nutrient cycling.

ACKNOWLEDGMENTS

This work was supported by Laboratory Directed Research and Development (LDRD) funding from Lawrence Berkeley National Laboratory provided by the Director, Office of Science, Office of Biological and Environmental Research of the US Department of Energy under Contract No. DE-AC02-05CH11231, and by the Next-Generation Ecosystem Experiments (NGEE Arctic) project, supported by the Office of Biological and Environmental Research in the DOE Office of Science under Contract No. DE-AC02-05CH11231.Part of this work was funded through the Department of Energy, Office of Biological and Environmental Research, Genomic Science Program under contract number DE-AC02-05CH11231.

REFERENCES

Allison, S. D. (2012). A trait-based approach for modelling microbial litter decomposition. *Ecol. Lett.* 15, 1058–1070.

Avrahami, S., and Bohannan, B. (2007). Response of *Nitrosospira* sp. strain AF-like ammonia oxidizers to changes in temperature, soil moisture content, and fertilizer concentration. *Appl. Environ. Microbiol.* 73, 1166.

Avrahami, S., and Bohannan, B. J. M. (2009). N_2O emission rates in a California meadow soil are influenced by fertilizer level, soil moisture and the community structure of ammonia-oxidizing bacteria. *Global Change Biol.* 15, 643–655.

Bange, H. B. (2008). "Gaseous nitrogen compounds (NO, N_2O, N_2, NH_3) in the ocean," in *Nitrogen in the Marine Environment*, eds D. G. Capone, D. A. Bronk, M. R. Mulholland and E. J. Carpenter (San Diego: Academic Press), 51–93.

Belser, L. W. (1979). Population ecology of nitrifying bacteria. *Annu. Rev. Microbiol.* 33. 309–333.

Belser, L. W., and Schmidt, E. L. (1979). Serological diversity within a terrestrial ammonia-oxidizing population. *Appl. Environ. Microbiol.* 36. 589–593.

Booth, M. S., Stark, J. M., and Rastetter, E. (2005). Controls on nitrogen cycling in terrestrial ecosystems: a synthetic analysis of literature data. *Ecol. Monogr.* 75, 139–157.

Bouskill, N. J., Eveillard, D., Chien, D., Jayakumar, A., and Ward, B. B. (2012). Environmental factors determining ammonia-oxidizing organism distribution and diversity in marine environments. *Environ. Microbiol.* 14, 714–729.

Bouskill, N. J., Eveillard, D., O'Mullan, G., Jackson, G. A., and Ward, B. B. (2011). Seasonal and annual reoccurrence in betaproteobacterial ammonia-oxidizing bacterial population structure. *Environ. Microbiol.* 13, 872–886.

Brochier-Armanet, C., Boussau, B., Gribaldo, S., and Forterre, P. (2008). Mesophilic Crenarchaeota: proposal for a third archaeal phylum, the Thaumarchaeota. *Nat. Rev. Microbiol.* 6, 245–252.

Caporaso, J. G., Lauber, C. L., Walters, W. A., Berg-Lyons, D., Huntley, J., Fierer, N., et al. (2012). Ultra-high-throughput microbial community analysis on the Illumina HiSeq and MiSeq platforms. *ISME J.* 6, 1621–1624.

Carney, K., Hungate, B., Drake, B., and Megonigal, J. (2007). Altered soil microbial community at elevated CO_2 leads to loss of soil carbon. *Proc. Natl. Acad. Sci. U.S.A.* 104, 4990.

Cébron, A., Berthe, T., and Garnier, J. (2003). Nitrification and nitrifying bacteria in the lower Seine River and estuary (France). *Appl. Environ. Microbiol.* 69, 7091.

De Boer, W., and Kowalchuk, G. (2001). Nitrification in acid soils: micro-organisms and mechanisms. *Soil Biol. Biochem.* 33, 853–866.

Delong, E. F., Preston, C. M., Mincer, T., Rich, V., Hallam, S. J., Frigaard, N.-U., et al. (2006). Community genomics among stratified microbial assemblages in the ocean's interior. *Science* 311, 496–503.

Di, H., Cameron, K., Shen, J., Winefield, C., O'Callaghan, M., Bowatte, S., et al. (2009). Nitrification driven by bacteria and not archaea in nitrogen-rich grassland soils. *Nat. Geosci.* 2, 621–624.

Doney, S., Mahowald, N., Lima, I., Feely, R., Mackenzie, F., Lamarque, J., et al. (2007). Impact of anthropogenic atmospheric nitrogen and sulfur deposition on ocean acidification and the inorganic carbon system. *Proc. Natl. Acad. Sci. U.S.A.* 104, 14580.

Droop, M. R. (1973). Some thoughts on nutrient limitation in algae. *J. Phycol.* 9, 264–272.

Drozd, J. W. (1976). Energy coupling and respiration in Nitrosomonas europaea. *Arch. Microbiol.* 101, 257–262.

Dutkiewicz, S., Follows, M., and Bragg, J. (2009). Modeling the coupling of ocean ecology and biogeochemistry. *Global Biogeochem. Cycles* 23.

Elberling, B., Christiansen, H., and Hansen, B. (2010). High nitrous oxide production from thawing permafrost. *Nat. Geosci.* 3, 332–335.

Erguder, T. H., Boon, N., Wittebolle, L., Marzorati, M., and Verstraete, W. (2009). Environmental factors shaping the ecological niches of ammonia-oxidizing archaea. *FEMS Microbiol. Rev.* 33, 855–869.

Follows, M. J., and Dutkiewicz, S. (2011). Modeling diverse communities of marine microbes. *Annu. Rev. Mar. Sci.* 3, 427–451.

Follows, M. J., Dutkiewicz, S., Grant, S., and Chisholm, S. W. (2007). Emergent biogeography of microbial communities in a model ocean. *Science* 315, 1843–1846.

Frame, C. H., and Casciotti, K. L. (2010). Biogeochemical controls and isotopic signatures of nitrous oxide production by a marine ammonia-oxidizing bacterium. *Biogeosciences* 7, 2695–2709.

Gans, J., Wolinsky, M., and Dunbar, J. (2005). Computational improvements reveal great bacterial diversity and high metal toxicity in soil. *Science* 309, 1387–1390.

Gieseke, A., Purkhold, U., Wagner, M., Amann, R., and Schramm, A. (2001). Community structure and activity dynamics of nitrifying bacteria in a phosphate-removing biofilm. *Appl. Environ. Microbiol.* 67, 1351.

Glover, H. (1985). The relationship between inorganic nitrogen oxidation and organic carbon production in batch and chemostat cultures of marine nitrifying bacteria. *Arch. Microbiol.* 142, 45–50.

Graham, D., Knapp, C., Van Vleck, E., Bloor, K., Lane, T., and Graham, C. (2007). Experimental demonstration of chaotic instability in biological nitrification. *ISME J.* 1, 385–393.

Green, J. L., Bohannan, B. J. M., and Whitaker, R. J. (2008). Microbial biogeography: from taxonomy to traits. *Science* 320, 1039–1043.

Grime, J. P. (1998). Benefits of plant diversity to ecosystems: immediate, filter and founder effects. *J. Ecol.* 86, 902–910.

Groeneweg, J., Sellner, B., and Tappe, W. (1994). Ammonia oxidation in Nitrosomonas at NH_3 concentrations near Km: effects of pH and temperature. *Water Res.* 28, 2561–2566.

Gubry-Rangin, C., Hai, B., Quince, C., Engel, M., Thomson, B. C., James, P., et al. (2011). Niche specialization of terrestrial archaeal ammonia oxidizers. *Proc. Natl. Acad. Sci. U.S.A.* 108, 21206–21211.

Gubry-Rangin, C., Nicol, G. W., and Prosser, J. I. (2010). Archaea rather than bacteria control nitrification in two agricultural acidic soils. *FEMS Microbiol. Ecol.* 74, 566–574.

Hall, E. K., Neuhauser, C., and Cotner, J. B. (2008). Toward a mechanistic understanding of how natural bacterial communities respond to changes in temperature in aquatic ecosystems. *ISME J.* 2, 471–481.

Hall, E. L., Maixner, F., Franklin, O., Daims, H., Richter, A., and Battin, T. (2010). Linking microbial and ecosystem ecology using ecological stoichiometry: a synthesis of conceptual and empirical analysis. *Ecosystems* 14, 261–273.

He, J., Shen, J., Zhang, L., Zhu, Y., Zheng, Y., Xu, et al. (2007). Quantitative analyses of the abundance and composition of ammonia-oxidizing bacteria and ammonia-oxidizing archaea of a Chinese upland red soil under long-term fertilization practices. *Environ. Microbiol.* 9, 2364–2374.

Hutchinson, G. (1961). The paradox of the plankton. *Am. Nat.* 95, 137–145.

Jenkinson, D. S., and Coleman, K. (2008). The turnover of organic carbon in subsoils. Part 2. Modelling carbon turnover. *Eur. J. Soil Sci.* 59, 400–413.

Jia, Z., and Conrad, R. (2009). Bacteria rather than Archaea dominate microbial ammonia oxidation in an agricultural soil. *Environ. Microbiol.* 11, 1658–1671.

Jiang, Q. Q., and Bakken, L. R. (1999). Nitrous oxide production and methane oxidation by different ammonia-oxidizing bacteria. *Appl. Environ. Microbiol.* 65, 2679–2684.

Kassen, R., Buckling, A., Bell, G., and Rainey, P. (2000). Diversity peaks at intermediate productivity in a laboratory microcosm. *Nature* 406, 508–512.

Keen, G., and Prosser, J. (1987). Steady-state and transient growth of autotrophic nitrifying bacteria. *Arch. Microbiol.* 147, 73–79.

Könneke, M., Bernhard, A., José, R., Walker, C., Waterbury, J., and Stahl, D. (2005). Isolation of an autotrophic ammonia-oxidizing marine archaeon. *Nature* 437, 543–546.

Kool, D. M., Dolfing, J., Wrage, N., and Van Groenigen, J. W. (2011). Nitrifier denitrification as a distinct and significant source of nitrous oxide from soil. *Soil Biol. Biochem.* 43, 174–178.

Koops, H., and Pommerening Röser, A. (2001). Distribution and ecophysiology of the nitrifying bacteria emphasizing cultured species. *FEMS Microbiol. Ecol.* 37, 1–9.

Koper, T. E., Stark, J. M., Habteselassie, M. Y., and Norton, J. M. (2010). Nitrification exhibits Haldane kinetics in an agricultural soil treated with ammonium sulfate or dairy-waste compost. *FEMS Microbiol. Ecol.* 74, 316–322.

Kowalchuk, G. A., and Stephen, J. R. (2001). Ammonia-oxidizing bacteria: a model for molecular microbial ecology. *Annu. Rev. Microbiol.* 55, 485–529.

Kujawinski, E. B. (2011). The impact of microbial metabolism on marine dissolved organic matter. *Annu. Rev. Mar. Sci.* 3, 567–599.

Laanbroek, H. J., and Gerards, S. (1993). Competition for limiting amounts of oxygen between Nitrosomonas

europaea and Nitrobacter winogradskyi grown in mixed continuous cultures. *Arch. Microbiol.* 159, 453–459.

Laughlin, D. C. (2011). Nitrification is linked to dominant leaf traits rather than functional diversity. *J. Ecol.* 99, 1091–1099.

Lauro, F., McDougald, D., Thomas, T., Williams, T., Egan, S., Rice, S., et al. (2009). The genomic basis of trophic strategy in marine bacteria. *Proc. Natl. Acad. Sci. U.S.A.* 106, 15527.

Lehtovirta-Morley, L. E., Stoecker, K., Vilcinskas, A., Prosser, J. I., and Nicol, G. W. (2011). Cultivation of an obligate acidophilic ammonia oxidizer from a nitrifying acid soil. *Proc. Natl. Acad. Sci. U.S.A.* 108, 15892–15897.

Leininger, S., Urich, T., Schloter, M., Schwark, L., Qi, J., Nicol, G., et al. (2006). Archaea predominate among ammonia-oxidizing prokaryotes in soils. *Nature* 442, 806–809.

Li, L., Lollar, B. S., Li, H., Wortmann, U. G., and Lacrampe-Couloume, G. (2012). Ammonium stability and nitrogen isotope fractionations for NH_4^+–NH_3(aq)–NH_3(gas) systems at 20–70 °C and pH of 2–13: applications to habitability and nitrogen cycling in low-temperature hydrothermal systems. *Geochim. Cosmochim. Ac.* 84, 280–296.

Litchman, E., Klausmeier, C. A., Miller, J. R., Schofield, O. M., and Falkowski, P. G. (2006). Multi-nutrient, multi-group model of present and future oceanic phytoplankton communities. *Biogeosciences* 3, 585–606.

Litchman, E., Klausmeier, C., Schofield, O., and Falkowski, P. (2007). The role of functional traits and trade-offs in structuring phytoplankton communities: scaling from cellular to ecosystem level. *Ecol. Lett.* 10, 1170–1181.

Litchman, E., and Klausmeier, C. A. (2008). Trait-based community ecology of phytoplankton. *Annu. Rev. Ecol. Evol. Syst.* 39, 615–639.

Loveless, J. E., and Painter, H. A. (1968). The influence of metal ion concentrations and pH value on the growth of a Nitrosomonas strain isolated from activated sludge. *J. Gen. Microbiol.* 52, 1–14.

MacFarling Meure, C., Etheridge, D., Trudinger, C., Steele, P., Langenfelds, R., van Ommen, T., et al. (2006). Law Dome CO_2, CH_4 and N_2O ice core records extended to 2000 years BP. *Geophys. Res. Lett.* 33.

Mahmood, S., Freitag, T. E., and Prosser, J. I. (2006). Comparison of PCR primer-based strategies for characterization of ammonia oxidizer communities in environmental samples. *FEMS Microbiol. Ecol.* 56, 482–493.

Manzoni, S., and Porporato, A. (2009). Soil carbon and nitrogen mineralization: theory and models across scales. *Soil Biol. Biochem.* 41, 1355–1379.

Martens-Habbena, W., Berube, P., Urakawa, H., la Torre De, J., and Stahl, D. (2009). Ammonia oxidation kinetics determine niche separation of nitrifying Archaea and Bacteria. *Nature* 461, 976–979.

McGill, B., Enquist, B., Weiher, E., and Westoby, M. (2006). Rebuilding community ecology from functional traits. *Trends Ecol. Evol. (Amst.)* 21, 178–185.

Monteiro, F. M., Dutkiewicz, S., and Follows, M. J. (2011). Biogeographical controls on the marine nitrogen fixers. *Global Biogeochem. Cycles* 25, GB2003.

Moran, M. A., Satinsky, B., Gifford, S. M., Luo, H., Rivers, A., Chan, L.-K., et al. (2012). Sizing up metatranscriptomics. *ISME J.* doi: 10.1038/ismej.2012.94

Mosier, A., and Francis, C. (2008). Relative abundance and diversity of ammonia-oxidizing archaea and bacteria in the San Francisco Bay estuary. *Environ. Microbiol.* 10, 3002–3016.

Mulder, C. P. H., Bazeley-White, E., Dimitrakopoulos, P. G., Hector, A., Scherer-Lorenzen, M., and Schmid, B. (2008). Specieis evenness and productivity in experimental plant communities. *Oikos* 107, 50–63.

Mußmann, M., Brito, I., Pitcher, A., Damsté, J. S. S., Hatzenpichler, R., Richter, A., et al. (2011). Thaumarchaeotes abundant in refinery nitrifying sludges express amoA but are not obligate autotrophic ammonia oxidizers. *Proc. Natl. Acad. Sci. U.S.A.* 108, 16771–16776.

Nicol, G., Leininger, S., Schleper, C., and Prosser, J. (2008). The influence of soil pH on the diversity, abundance and transcriptional activity of ammonia oxidizing archaea and bacteria. *Environ. Microbiol.* 10, 2966–2978.

Nicol, G., Leininger, S., and Schleper, C. (2011). "Distribution and activity of ammonia-oxidizing archaea in natural environments" in *Nitrification*, eds B. B. Ward, D. J. Arp and M. G. Klotz (Washington: ASM Press), 157–178.

Nishio, T., and Fujimoto, T. (1990). Kinetics of nitrification of various amounts of ammonium added to soils. *Soil Biol. Biochem.* 22, 51–55.

Okabe, S., Satoh, H., and Watanabe, Y. (1999). In situ analysis of nitrifying biofilms as determined by in situ hybridization and the use of microelectrodes. *Appl. Environ. Microbiol.* 65, 3182.

Parton, W. J., Schimel, D. S., Cole, C. V., and Ojima, D. S. (1987). Analysis of factors controlling soil organic matter levels in Great Plains grasslands. *Soil Sci. Soc. Am. J.* 51, 1173–1179.

Pèrez, T., Trumbore, S. E., Tyler, S. C., Matson, P. A., Ortiz-Monasterio, I. Rahn, T. et al. (2001). Identifying the agricultural imprint on the global N_2O budget using stable isotopes. *J. Geophys. Res.* 106, 9869–9878.

Petersen, D. G., Blazewicz, S. J., Firestone, M., Herman, D. J., Turetsky, M., and Waldrop, M. (2012). Abundance of microbial genes associated with nitrogen cycling as indices of biogeochemical process rates across a vegetation gradient in Alaska. *Environ. Microbiol.* 14, 993–1008.

Prosser, J. I. (1989). Autotrophic nitrification in bacteria. *Adv. Microb. Physiol.* 30, 125–181.

Prosser, J. I., Bohannan, B. J. M., Curtis, T. P., Ellis, R. J., Firestone, M. K., Freckleton, R. P., et al. (2007). The role of ecological theory in microbial ecology. *Nat. Rev. Micro.* 5, 384–392.

Prosser, J. (2011). "Soil nitrifiers and nitrification," in *Nitrification*, eds B. B. Ward, D. J. Arp and M. G. Klotz (Washington: ASM Press), 347–383.

Ratkowsky, D. A., Lowry, R. K., McMeekin, T. A., Stokes, A. N., and Chandler, R. E. (1983). Model for bacterial culture growth rate throughout the entire biokinetic temperature range. *J. Bacteriol.* 154, 1222–1226.

Ratkowsky, D. A., Olley, J., and Ross, T. (2005). Unifying temperature effects on the growth rate of bacteria and the stability of globular proteins. *J. Theor. Biol.* 233, 351–362.

Redfield, A. C. (1958). The biological control of chemical factors in the environment. *Am. Sci.* 46, 205–221.

Santoro, A. E., Buchwald, C., McIlvin, M. R., and Casciotti, K. L. (2011). Isotopic signature of N_2O produced by marine ammonia-oxidizing archaea. *Science* 333, 1282–1285.

Schimel, J. P., Firestone, M. K., and Killham, K. S. (1984). Identification of heterotrophic nitrification in a sierran forest soil. *Appl. Environ. Microbiol.* 48, 802–806.

Schneider, T., Keiblinger, K. M., Schmid, E., Sterflinger-Gleixner, K., Ellersdorfer, G., Roschitzki, B., et al. (2012). Who is who in litter decomposition? Metaproteomics reveals major microbial players and their biogeochemical functions. *ISME J.* 6, 1749–1762.

Schramm, A., De Beer, D., Van Den Heuvel, J., Ottengraf, S., and Amann, R. (1999). Microscale distribution of populations and activities of Nitrosospira and Nitrospira spp. along a macroscale gradient in a nitrifying bioreactor: quantification by in situ hybridization and the use of microsensors. *Appl. Environ. Microbiol.* 65, 3690.

Schreiber, F., Loeffler, B., Polerecky, L., Kuypers, M. M. M., and de Beer, D. (2009). Mechanisms of transient nitric oxide and nitrous oxide production in a complex biofilm. *ISME J.* 3, 1301–1313.

Stark, J. (1996). Modeling the temperature response of nitrification. *Biogeochemistry* 35, 433–445.

Stark, J. M., and Firestone, M. K. (1996). Kinetic characteristics of ammonium-oxidizer communities in a California oak woodland-annual grassland. *Soil Biol. Biochem.* 28, 1307–1317.

Stein, L. Y., and Klotz, M. G. (2011). Nitrifying and denitrifying pathways of methanotrophic bacteria. *Biochem. Soc. Trans.* 39, 1826–1831.

Suzuki, I. (1974). Mechanisms of inorganic oxidation and energy coupling. *Ann. Rev. Microbiol.* 28, 85–102.

Suzuki, I., Dular, U., and Kwok, S. (1974). Ammonia or ammonium ion as substrate for oxidation by Nitrosomonas europaea cells and extracts. *J. Bacteriol.* 120, 556.

Tilman, D., Wedin, D., and Knops, J. (1996). Productivity and sustainability influenced by biodiversity in grassland ecosystems. *Nature* 379, 718–720.

Tourna, M., Freitag, T., Nicol, G., and Prosser, J. (2008). Growth, activity and temperature responses of ammonia-oxidizing archaea and bacteria in soil microcosms. *Environ. Microbiol.* 10, 1357–1364.

van der Ploeg, R. R., Bohm, W., and Kirkham, M. B. (1999). On the origin of the theory of mineral nutrition of plants and the law of the minimum. *Soil Sci. Soc. Am. J.* 63, 1055–1062.

Vanparys, B., Spieck, E., Heylen, K., Wittebolle, L., Geets, J., Boon, N., and De Vos, P. (2007). The phylogeny of the genus Nitrobacter based on comparative rep-PCR, 16S rRNA and nitrite oxidoreductase gene sequence analysis. *Syst. Appl. Microbiol.* 30, 297–308.

Verhagen, F., and Laanbroek, H. (1991). Competition for ammonium between nitrifying and heterotrophic bacteria in dual energy-limited chemostats. *Appl. Environ. Microbiol.* 57, 3255.

Verhamme, D. T., Prosser, J. I., and Nicol, G. W. (2011). Ammonia concentration determines differential growth of ammonia-oxidising archaea and bacteria in soil microcosms. *ISME J.* 5, 1067–1071.

Ward, B. B. (2008). "Nitrification in Marine Systems," in *Nitrogen in the Marine Environment*, eds D. G. Capone, D. A. Bronk, M. R. Mulholland and E. J. Carpenter (San Diego: Academic Press), 199–261.

Webb, C. T., Hoeting, J. A., Ames, G. M., Pyne, M. I., and LeRoy Poff, N. (2010). A structured and dynamic framework to advance traits-based theory and prediction in ecology. *Ecol. Lett.* 13, 267–283.

Wells, G., Park, H., Yeung, C., Eggleston, B., Francis, C., and Criddle, C. (2009). Ammonia-oxidizing communities in a highly aerated full-scale activated sludge bioreactor: betaproteobacterial dynamics and low relative abundance of Crenarchaea. *Environ. Microbiol.* 11, 2310–2328.

Wertz, S., Leigh, A. K. K., and Grayston, S. J. (2011). Effects of long-term fertilization of forest soils on potential nitrification and on the abundance and community structure of ammonia oxidizers and nitrite oxidizers. *FEMS Microbiol. Ecol.* 79, 142–154.

Conflict of Interest Statement: The authors declare that the research was conducted in the absence of any commercial or financial relationships that could be construed as a potential conflict of interest.

Received: 03 July 2012; paper pending published: 16 August 2012; accepted: 25 September 2012; published online: 18 October 2012.

Citation: Bouskill NJ, Tang J, Riley WJ and Brodie EL (2012) Trait-based representation of biological nitrification: model development, testing, and predicted community composition. Front. Microbio. ***3****:364. doi: 10.3389/fmicb.2012.00364*

This article was submitted to Frontiers in Aquatic Microbiology, a specialty of Frontiers in Microbiology.

APPENDIX

MATERIALS AND METHODS

Derivation of trait values

Numerical values for five different traits [$K_M(NH_3)$, $K_M(O_2)$, $V_{MAX}(NH_3)$, μmax, $R_{C:N}$] were taken from ecophysiological studies following an extensive literature review (Loveless and Painter, 1968; Suzuki, 1974; Suzuki et al., 1974; Drozd, 1976; Glover, 1985; Belser and Schmidt, 1979; Keen and Prosser, 1987; Prosser, 1989; Nishio and Fujimoto, 1990; Verhagen and Laanbroek, 1991; Laanbroek and Gerards, 1993; Jiang and Bakken, 1999; Schramm et al., 1999; Gieseke et al., 2001; Koops and Pommerening Röser, 2001; Cébron et al., 2003; Martens-Habbena et al., 2009; Schreiber et al., 2009). Where possible the traits were derived from the same study, however, efforts were made to ensure that the similar methodologies were used to calculate trait values (e.g., under similar pH and temperature). The different ecophysiological traits were measured in batch cultures of strains of *Nitrosomonas, Nitrosospira*, *Nitrosopumilus*, *Nitrososphaera* and *Nitrosotalea*.

– $K_M(NH_3)$/$K_M(O_2)$/V_{MAX}: Enzyme kinetics (e.g., affinity constant and uptake) were calculated under substrate saturation conditions (see: Loveless and Painter, 1968; Suzuki et al., 1974; Drozd, 1976; Martens-Habbena et al., 2009). Affinity constants have previously been measured in whole cells as well as cell extracts and oxygen concentrations measured using oxygen electrodes (Suzuki et al., 1974). Enzyme uptake can be calculated using ammonia microprofiles and fitting to the Michaelis–Menton equation (e.g., Schramm et al., 1999). In the case of the AOA, *Nitrosopumilus maritimus*, affinity constants were derived using oxygen microsensors (Martens-Habbena et al., 2009), from multiple oxygen traces. Maximum uptake rate was also calculated under substrate saturation. In general, media with defined ammonia concentrations were sub-sampled over time and substrate concentrations determined fluorometrically. Uptake rates were calculated from oxygen profiles and fitted to a Michaelis Menton equation (Martens-Habbena et al., 2009).
– μmax: Maximum specific growth rate was generally estimated by measuring the evolution of NO_2 as a proxy for growth (e.g., Loveless and Painter, 1968; Keen and Prosser, 1987). NO_2 increases exponentially during growth and the slope of a semi-logarithmic plot of product evolution against substrate concentration is equivalent to specific growth rate.
– $R_{C:N}$: The carbon yield from nitrification was determined in continuous or chemostat cultures (e.g., Belser, 1979; Belser and Schmidt, 1979; Glover, 1985; Keen and Prosser, 1987) by measuring cell number (e.g., using a spectrometric bacterial counter) and the production (AOB), or draw down (NOB), of NO_2.

Table A1 | Initial inputs for model simulation of the Petersen dataset.

Plant community type	pH	NH_3 (g m^3)	Potential nitrification rate	16s bacterial: archaea
Black spruce	4.8	0.2	2	15
Black bog	4.3	0.2	1	37.5
Emergent fen	4.5	2.9	18	10
Rich fen	4.7	1.1	5	3
Tussock grassland	4.7	1.5	7	10

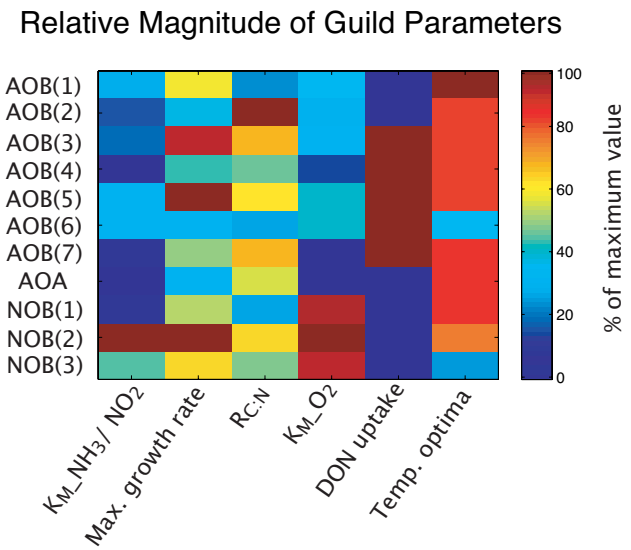

FIGURE A1 | Relative magnitude of guild parameters.

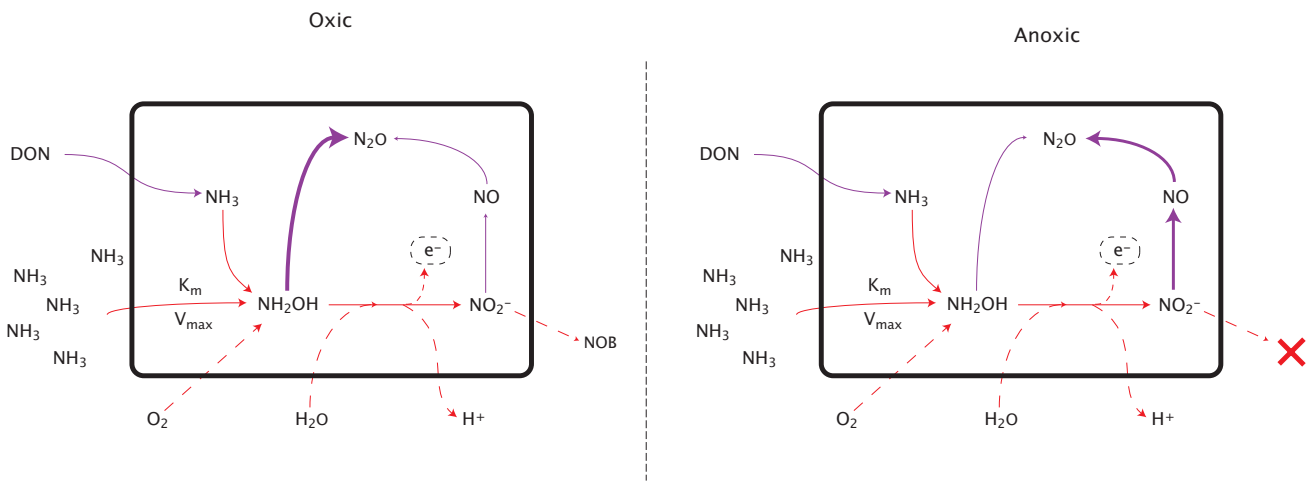

FIGURE A2 | Pathways of nitrous oxide production during nitrification. See text for detailed explanation.

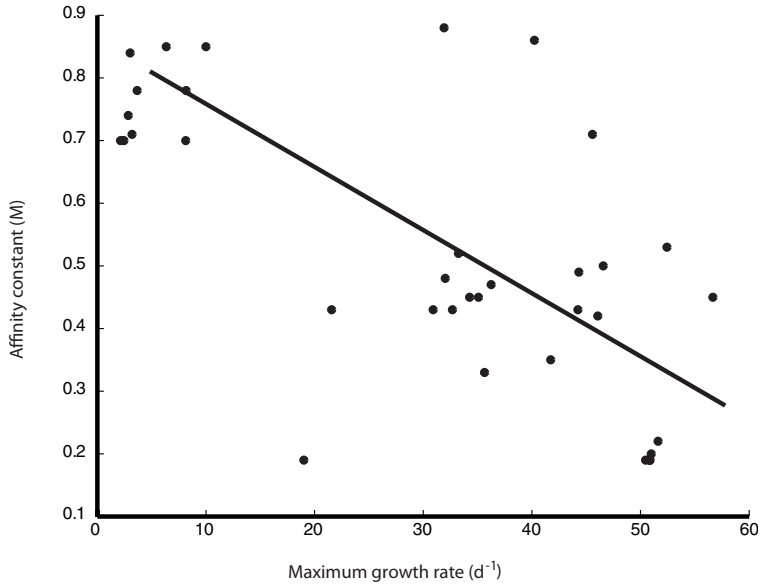

FIGURE A3 | Explicit relationship between trait parameters K_M and μ_{max}.

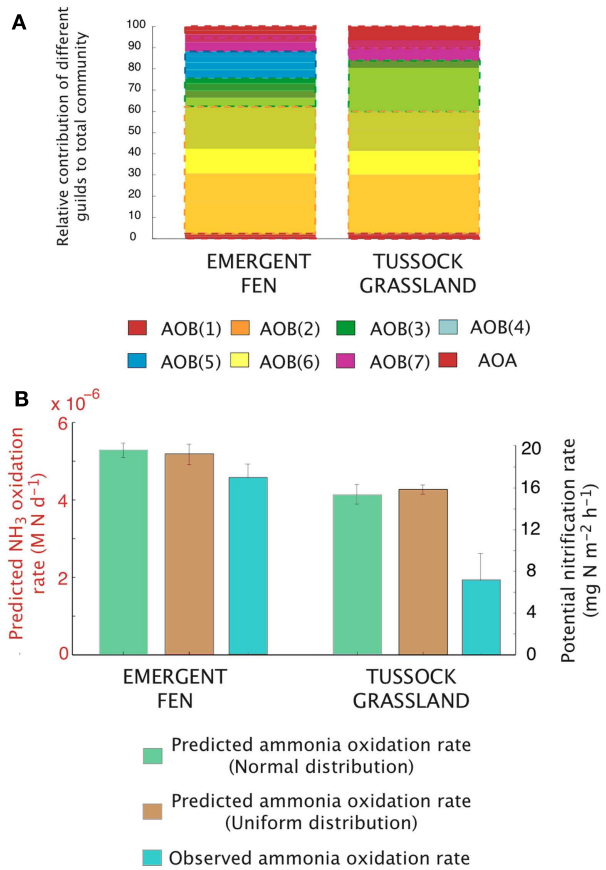

FIGURE A4 | Simulations of the activity and diversity of AOB communities in high-latitude ecosystems. (A) Simulations of multiple AOB analogs ($n = 5$ analogs per guild) across the different sites. These simulations are based on a normalized distribution of trait values. Each guild is represented by a distinct color. Subtle differences in the shade of that color demarcate the different analogs/guild. A box outlines the boundaries of each guild's biomass. Evenness statistic given above the bar plots. **(B)** Experimental observations reproduced from Petersen et al. (2012), showing the trends in potential nitrification rates under a normal distribution, a uniform distribution, and the observed NH_3 oxidation rates.

frontiers in
MICROBIOLOGY

REVIEW ARTICLE
published: 12 October 2012
doi: 10.3389/fmicb.2012.00356

Insights on the marine microbial nitrogen cycle from isotopic approaches to nitrification

***Karen L. Casciotti*[1]* *and Carolyn Buchwald*[2]**

[1] *Department of Environmental Earth System Science, Stanford University, Stanford, CA, USA*
[2] *MIT/WHOI Joint Program in Chemical Oceanography, Woods Hole, MA, USA*

Edited by:
Bess B. Ward, Princeton University, USA

Reviewed by:
Scott D. Wankel, Harvard University, USA
Guang Gao, Chinese Academy of Sciences, China

****Correspondence:***
Karen L. Casciotti, Department of Environmental Earth System Science, Stanford University, Yang and Yamazaki Energy and Environment Building, 473 Via Ortega, Room 140, Stanford, CA 94305, USA.
e-mail: kcasciotti@stanford.edu

The microbial nitrogen (N) cycle involves a variety of redox processes that control the availability and speciation of N in the environment and that are involved with the production of nitrous oxide (N_2O), a climatically important greenhouse gas. Isotopic measurements of ammonium (NH_4^+), nitrite (NO_2^-), nitrate (NO_3^-), and N_2O can now be used to track the cycling of these compounds and to infer their sources and sinks, which has lead to new and exciting discoveries. For example, dual isotope measurements of NO_3^- and NO_2^- have shown that there is NO_3^- regeneration in the ocean's euphotic zone, as well as in and around oxygen deficient zones (ODZs), indicating that nitrification may play more roles in the ocean's N cycle than generally thought. Likewise, the inverse isotope effect associated with NO_2^- oxidation yields unique information about the role of this process in NO_2^- cycling in the primary and secondary NO_2^- maxima. Finally, isotopic measurements of N_2O in the ocean are indicative of an important role for nitrification in its production. These interpretations rely on knowledge of the isotope effects for the underlying microbial processes, in particular ammonia oxidation and nitrite oxidation. Here we review the isotope effects involved with the nitrification process and the insights provided by this information, then provide a prospectus for future work in this area.

Keywords: nitrification, isotopic fractionation, oxygen, nitrogen, nitrate, nitrous oxide

NITRIFICATION IN THE OCEAN—ROLES IN NO_3^- SUPPLY AND N_2O PRODUCTION

Nitrification comprises a key link in the marine nitrogen (N) cycle converting the most reduced form of N (ammonia, NH_3) to the most oxidized (nitrate, NO_3^-). Although sunlight appears to partly inhibit nitrification (Olson, 1981a; Guerrero and Jones, 1996; Merbt et al., 2012), there are many indications that nitrification occurs in the euphotic zone (Ward, 1985, 2005; Wankel et al., 2007; Yool et al., 2007; Clark et al., 2008). Therefore, when reduced organic N is released into solution through cell lysis, grazing and digestion, it can be either reassimilated or oxidized back to NO_3^- in the sunlit surface waters. Also, when particulate organic matter (in the form of detritus, fecal pellets, or marine snow) sinks out of the euphotic zone, it is gradually broken down into its component parts and remineralized into its inorganic forms: CO_2, NH_4^+, and PO_4^{3-}. In oxic water columns, the NH_4^+ released from organic matter remineralization below the euphotic zone is rapidly oxidized to NO_3^-. The distribution of nitrification rates in the ocean is therefore expected to follow the distribution of NH_4^+ supply from organic matter remineralization, which decreases exponentially with depth (Ward and Zafiriou, 1988).

Nitrification is carried out through the combination of two microbial processes: ammonia oxidation to NO_2^- and nitrite oxidation to NO_3^-. Ammonia oxidation is a chemoautotrophic process carried out by ammonia-oxidizing bacteria (AOB) and ammonia-oxidizing archaea (AOA). These organisms use NH_3 as their source of reducing power for CO_2 fixation and energy production. Nitrite oxidation is also a chemoautotrophic process and is carried out by nitrite-oxidizing bacteria (NOB). These bacteria use nitrite (NO_2^-) as their source of reducing power for CO_2 fixation and energy production (Watson, 1965; Bock et al., 1989). Most ammonia and nitrite oxidizers are obligate chemoautotrophs (Watson and Waterbury, 1971), although a few are able to grow mixotrophically (Watson et al., 1986).

Although NO_2^- is an intermediate in the nitrification process, it rarely accumulates in the ocean. NO_2^- can be found at the base of the euphotic zone in a feature termed the primary nitrite maximum (PNM; Wada and Hattori, 1971). The processes contributing to NO_2^- accumulation in the PNM are still debated, but most likely include a combination of ammonia oxidation and nitrite oxidation, as well as assimilatory nitrate and nitrite reduction by phytoplankton (Ward et al., 1982, 1989; Dore and Karl, 1996; Lomas and Lipschultz, 2006; Mackey et al., 2011). The relative contributions of these processes to NO_2^- cycling have different implications for N biogeochemistry and the links between C and N cycling. Net production of NO_2^- through nitrification (decoupling of ammonia and nitrite oxidation) can also have implications for the production of nitrous oxide (N_2O), a climatically important greenhouse gas. It is therefore important to know how the processes contributing to the production and maintenance of the PNM vary in space and time.

NO_2^- also accumulates in oxygen deficient regions of the water column in a feature termed the secondary nitrite maximum

(SNM; Brandhorst, 1959). The SNM is generally assumed to reflect active denitrification in oxygen deficient zones (ODZs), as SNM features are only found in the absence of dissolved oxygen (Brandhorst, 1959; Cline and Richards, 1972; Codispoti and Christensen, 1985). However, recent studies have shown that the presence of a SNM feature may not coincide with the most intense NO_2^- cycling, as active NO_2^- reduction occurs in the Omani upwelling region in the absence of NO_2^- accumulation (Jensen et al., 2011; Lam et al., 2011). NO_2^- consumption in the SNM may occur through many processes, including denitrification (reduction of NO_2^- to N_2), anaerobic ammonia oxidation (reduction of NO_2^- to N_2 and oxidation to NO_3^-), and nitrite oxidation (oxidation of NO_2^- to NO_3^-). Recent studies using natural abundance isotopes (Casciotti, 2009), profile modeling (Lam et al., 2011), isotope tracers (Lipschultz et al., 1990; Füssel et al., 2012), and gene markers (Füssel et al., 2012) suggest that a significant fraction of NO_2^- produced within the SNM may be consumed through oxidation to NO_3^-.

Several questions remain about the roles of AOB and AOA in marine nitrification, the controls on their distribution and activity, and the rates of these processes. These questions relate to the cycling of NO_3^-, NO_2^-, and NH_4^+ in the water column, and the production of N_2O linked to nitrification. These questions can be addressed with a variety of complementary approaches, including molecular community analysis and quantification, instantaneous rate measurements, natural abundance stable isotope measurements, and geochemical modeling.

Examples of applications involving the use of natural abundance stable isotopes to study nitrification include: (1) the role of euphotic zone nitrification in supplying NO_3^- for photosynthetic growth (Wankel et al., 2007; DiFiore et al., 2009), (2) the contributions of nitrification and nitrate reduction to NO_2^- accumulation in the PNM (Buchwald and Casciotti, unpublished), (3) the role of nitrification in near-surface N_2O production (Dore et al., 1998; Santoro et al., 2010, 2011), and (4) the role of nitrite oxidation in recycling NO_3^- in and around ODZs (Sigman et al., 2005; Casciotti and McIlvin, 2007; Casciotti, 2009). Understanding the isotopic systematics for nitrification is also important for tracking the balance of high-latitude and low-latitude productivity and N budget processes (N fixation and denitrification) through NO_3^- isotope distributions in the deep ocean (Sigman et al., 2009). In order to understand these applications we first review the N and O isotopic systematics of the nitrification process, including both ammonia and nitrite oxidation.

ISOTOPE SYSTEMATICS FOR AMMONIA OXIDATION

The $\delta^{18}O$ value of NO_2^- produced during ammonia oxidation ($\delta^{18}O_{NO_2,nit} = ({}^{18}O/{}^{16}O_{NO_2} \div {}^{18}O/{}^{16}O_{VSMOW} - 1) \times 1000$) is dependent on the $\delta^{18}O$ values of the oxygen atom sources (O_2 and H_2O), isotopic fractionation during their incorporation (${}^{18}\varepsilon_{k,O_2}$ and ${}^{18}\varepsilon_{k,H_2O,1}$, respectively), as well as any exchange of oxygen atoms between nitrite and water (x_{AO}) and the corresponding equilibrium isotope effect (${}^{18}\varepsilon_{eq}$) (Equation 1; Casciotti et al., 2011). Throughout this review, kinetic isotope fractionation factors are defined by $\alpha_k = k^l/k^h$ where k^l is the first order rate constant for reaction of the light isotope and k^h is that for reaction of the heavy isotope. Equilibrium fractionation factors are defined as $\alpha_{eq} = R_1/R_2$ where R_1 and R_2 are the isotope ratios of two species in equilibrium. Kinetic and equilibrium isotope effects are defined by $\varepsilon = (\alpha - 1) \times 1000$.

$$\delta^{18}O_{NO_2,nit} = \left[\frac{1}{2}\left(\delta^{18}O_{O_2} - {}^{18}\varepsilon_{O_2}\right) + \frac{1}{2}\left(\delta^{18}O_{H_2O} - {}^{18}\varepsilon_{k,H_2O,1}\right)\right] \times (1 - x_{AO}) + \left(\delta^{18}O_{H_2O} + {}^{18}\varepsilon_{eq}\right)(x_{AO}) \quad (1)$$

Even though oxygen is incorporated enzymatically from O_2 to H_2O in a 1:1 ratio during ammonia oxidation (Andersson and Hooper, 1983), early studies of AOB found that a large amount of oxygen atom exchange with water could be associated with ammonia oxidation (Dua et al., 1979; Andersson et al., 1982; Andersson and Hooper, 1983). The conditions favoring oxygen atom exchange included high cell densities and high NO_2^- concentrations. These findings, as well as the low variation of deep ocean $\delta^{18}O_{NO_3}$ (Casciotti et al., 2002; Sigman et al., 2009) led researchers to assume that the O atoms in oceanic NO_3^- derive primarily from H_2O with little residual signal from dissolved O_2. In more recent studies, however, the amount of biologically-catalyzed exchange has been determined under lower cell densities and substrate concentrations and found to be much lower for marine AOB (Casciotti et al., 2010; Buchwald et al., 2012) and AOA (Santoro et al., 2011). Exchange levels were particularly low (5%) when NO_2^- concentrations were held near 1 μm by co-cultivation with NOB (Buchwald et al., 2012). These results suggested that oxygen isotope exchange during nitrification may be quite low where ammonia and nitrite oxidation are tightly coupled, but may play a role when ammonia and nitrite oxidation become decoupled, such as in the PNM.

Given low amounts of biologically-catalyzed oxygen atom exchange with H_2O, the low $\delta^{18}O$ values of NO_3^- in seawater may be surprising given the high $\delta^{18}O$ values of dissolved O_2 (Kroopnick and Craig, 1976). However, oxygen atom incorporation from O_2 and/or H_2O during ammonia oxidation is associated with isotopic fractionation, such that the ${}^{18}O$:${}^{16}O$ of oxygen atoms incorporated into NO_2^- is significantly lower than the ambient pools of O_2 and H_2O (Casciotti et al., 2010; Santoro et al., 2011). This leads to production of NO_2^- from ammonia oxidation with $\delta^{18}O$ values between −3‰ and 5‰ rather than near 12‰, which would be expected from average $\delta^{18}O_{H_2O}$ and $\delta^{18}O_{O_2}$ values (Casciotti et al., 2010). Furthermore, since oxygen atom exchange occurs with an equilibrium isotope effect (${}^{18}\varepsilon_{eq}$) of 11–14‰ (Casciotti et al., 2007; Buchwald and Casciotti, unpublished), this equilibration would tend to raise the $\delta^{18}O$ value of NO_2^- relative to the initial $\delta^{18}O_{NO_2}$ produced by ammonia oxidation.

Nitrogen isotopic fractionation during ammonia oxidation ranges from 14‰ to 38‰ for AOB (Mariotti et al., 1981; Yoshida, 1988; Casciotti et al., 2003) and 20–22‰ for AOA (Santoro and Casciotti, 2011). These values represent the isotope effect expressed under non-limiting concentrations of NH_4^+. In the ocean NH_4^+ consumption generally goes to completion, so the isotope effect for ammonia oxidation may not be expressed. It may, however, be expressed at the branch point between ammonia assimilation and oxidation in the euphotic zone (Wankel

et al., 2007; DiFiore et al., 2009) or in the production of N_2O by ammonia oxidizers (Yoshida, 1988; Frame and Casciotti, 2010).

ISOTOPE SYSTEMATICS FOR N_2O PRODUCTION

Production of N_2O by AOB occurs through two separate pathways: hydroxylamine decomposition and nitrite reduction, so-called "nitrifier denitrification" (**Figure 1**; Poth and Focht, 1985; Hooper et al., 1990). The isotopic compositions ($\delta^{15}N^{bulk}$, $\delta^{18}O$, $\delta^{15}N^{\alpha}$, $\delta^{15}N^{\beta}$, and site preference (SP) $= \delta^{15}N\alpha - \delta^{15}N^{\beta}$) of the N_2O produced through these pathways may provide insight into the mechanisms of N_2O production under different growth conditions (Frame and Casciotti, 2010; Sutka et al., 2003, 2004). For example, N_2O production through nitrifier denitrification (enhanced by high cell densities, high NO_2^- concentrations, and low O_2 concentrations; Frame and Casciotti, 2010) has low $\delta^{15}N^{bulk}$ and low SPs relative to that produced by hydroxylamine decomposition (**Figure 2**). This is most likely due to the additional steps involved with the production of N_2O from NO_2^- and accumulation of the main product, NO_2^-, which enables fractionation associated with NO_2^- reduction to be expressed.

Oxygen isotopes have been underutilized in determining N_2O sources, primarily because the isotopic systematics are less well understood, but knowledge of the O isotope systematics is increasing (Frame and Casciotti, 2010; Snider et al., 2012). The N_2O produced via nitrifier denitrification has a slightly lower $\delta^{18}O$ value than that produced from hydroxylamine decomposition (**Figure 2**; Frame and Casciotti, 2010). This is most likely because H_2O is incorporated into NO_2^-, leading to lower $\delta^{18}O$ values in NO_2^- relative to NH_2OH. However, going from either NH_2OH or NO_2^- to N_2O involves the loss of O atoms, which can occur with fractionation. This fractionation leads to preferential loss of ^{16}O and retention of ^{18}O in the residual N oxides transferred to N_2O. The net isotopic fractionation for oxygen isotopes in the hydroxylamine decomposition pathway ($^{18}\varepsilon_{NH2OH}$), including both incorporation of O_2 into NH_2OH and production of N_2O from NH_2OH, was 2.9 ± 0.8‰ indicating that N_2O produced from this pathway had a lower ^{18}O:^{16}O than the ambient O_2 (Frame and Casciotti, 2010). The net isotope effect for N_2O production from NO_2^- via nitrifier denitrification ($^{18}\varepsilon_{ND}$) was -8.4 ± 1.4‰ (Frame and Casciotti, 2010). The negative value indicates that the N_2O produced from NO_2^- is enriched in ^{18}O relative to NO_2^-, consistent with branching of O atoms and preferential loss of ^{16}O during this reaction (Casciotti et al., 2007).

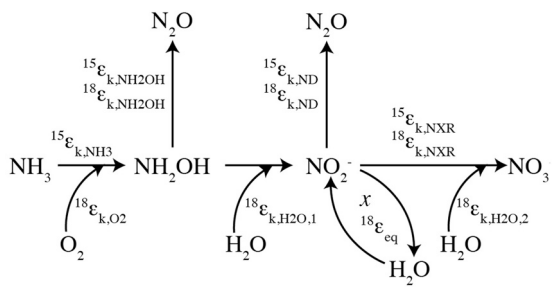

FIGURE 1 | Isotopic systematics for nitrification. A schematic of the isotopic systematics for ammonia oxidation and nitrite oxidation during nitrification. The kinetic isotope effects for ammonia oxidation ($^{15}\varepsilon_{k,NH3}$) and nitrite oxidation ($^{15}\varepsilon_{k,NXR}$ and $^{18}\varepsilon_{k,NXR}$) characterize the isotopic fractionation for the main N transformation processes while isotopic fractionation during oxygen atom incorporation ($^{18}\varepsilon_{k,O_2}$, $^{18}\varepsilon_{k,H_2O,1}$, and $^{18}\varepsilon_{k,H_2O,2}$) controls the oxygen isotopes incorporated by the central pathway. Oxygen isotope exchange during ammonia oxidation and/or post-production abiotic exchange (x) may also play a role through the equilibrium fractionation ($^{18}\varepsilon_{eq}$) associated with it. N_2O production occurs with N and O fractionation through decomposition of hydroxylamine (NH_2OH) and nitrifier-denitrification (ND).

The N_2O site preference (SP) is determined mainly by the enzymatic mechanism, rather than the substrate $\delta^{15}N$ value (Toyoda and Yoshida, 1999; Yoshida and Toyoda, 2000; Schmidt et al., 2004). The SP of N_2O produced during nitrification is +30‰ to +38‰ (**Figure 2**; Sutka et al., 2003, 2004; Frame and Casciotti, 2010), while N_2O produced from denitrification and nitrifier denitrification has a SP of −10‰ to +5‰ (Sutka et al., 2003, 2004; Toyoda et al., 2005; Frame and Casciotti, 2010). The large difference between the SP values of these two primary mechanisms for N_2O production provides a large signal with which to distinguish their contributions. The interpretation of SP values is therefore somewhat simplified relative to bulk $\delta^{15}N$ and $\delta^{18}O$ values that reflect both mechanism and substrate isotope ratios, which change over time. This seemingly simple distinction is complicated, however, by the fact that N_2O consumption during denitrification increases SP (Ostrom et al., 2007; Yamagishi et al., 2007; Koba et al., 2009). Therefore, a high SP value may arise through production of N_2O via nitrification or net N_2O consumption during denitrification. However, the $\delta^{18}O$ signature of these two scenarios is quite different and can enable the scenarios to be distinguished (**Figure 2**).

Recently, the isotopic compositions of N_2O produced by AOA were found to be distinct from AOB (Santoro et al., 2011). In particular, N_2O produced by AOA is enriched in ^{15}N and ^{18}O relative to that produced by AOB, which may explain some of the elevated $\delta^{15}N$ and $\delta^{18}O$ values observed in oceanic N_2O (Santoro et al., 2011). The reasons for the isotopic distinction between AOA and AOB is not known, but may involve a different mechanism of N_2O production involving a unique intermediate or enzymatic pathway. However, the SP of N_2O produced by AOA is similar to that of N_2O produced by hydroxylamine decomposition by AOB (Santoro et al., 2011; Loescher et al., 2012). While it is not yet clear whether N_2O production (or nitrification in general) by AOA involves hydroxylamine, isotopic evidence to date shows that the N_2O produced aerobically by AOA does not have a SP consistent with denitrification or nitrifier-denitrification. $\delta^{18}O$ data also show that the N_2O produced by AOA incorporates O primarily from O_2, rather than from H_2O, which supports production by decomposition of an intermediate, rather than from NO_2^- under the conditions tested (Santoro et al., 2011). It is still unknown whether AOA are able to produce N_2O through a second pathway similar to nitrifier denitrification and thus produce N_2O with a lower SP. Genetic analyses currently suggest that nitrification in AOA may proceed via a NO or HNO intermediate (Walker et al., 2010), which could potentially be converted to N_2O. Further work

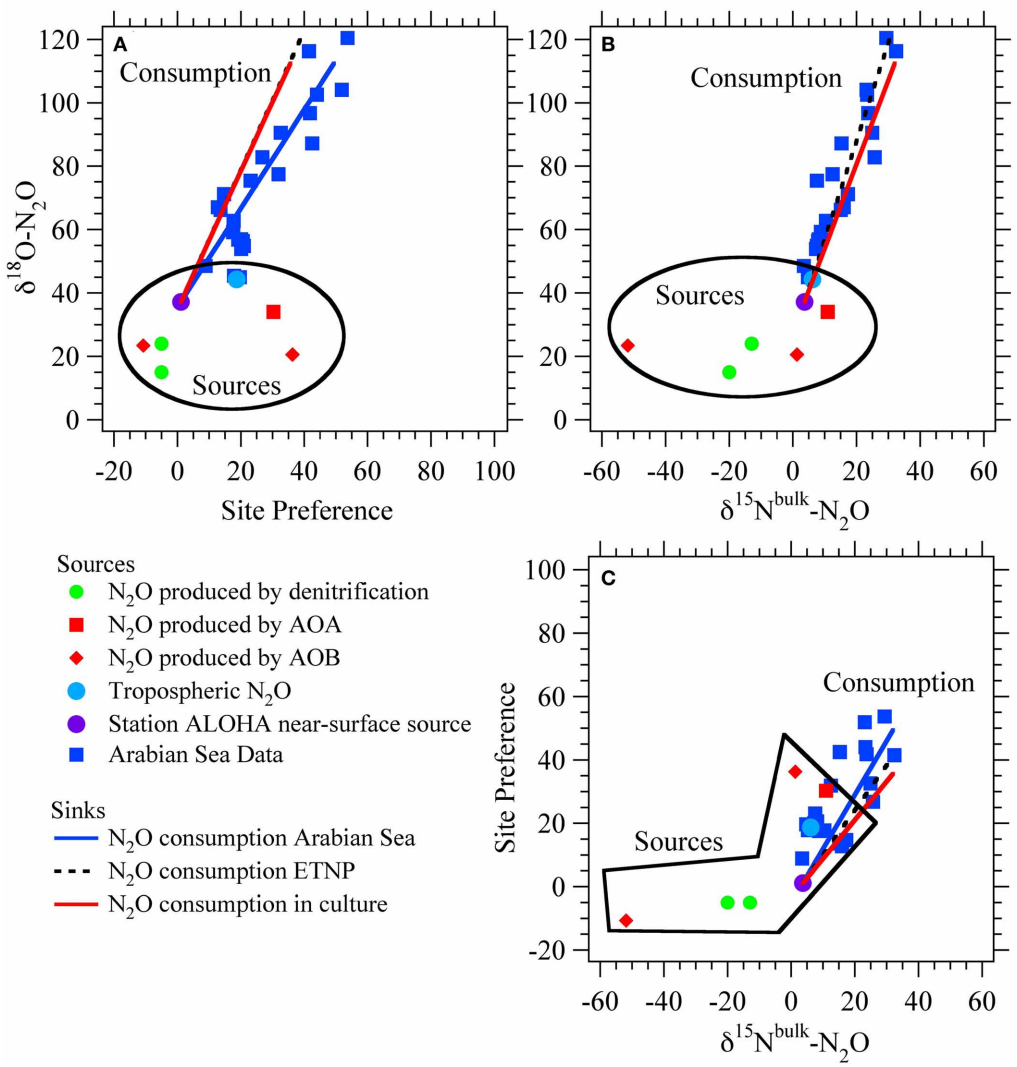

FIGURE 2 | Isotopic signatures for nitrous oxide sources and sinks. Isotope-isotope plots for N_2O sources from ammonia-oxidizing archaea (AOA; Santoro et al., 2011), nitrification and nitrifier-denitrification by ammonia-oxidizing bacteria (AOB; Frame and Casciotti, 2010), and production by denitrification of NO_3^- or NO_2^- (Barford et al., 1999; Casciotti et al., 2007). Also shown are average tropospheric air (Kim and Craig, 1990; Yoshida and Toyoda, 2000; Croteau et al., 2010) and the estimated near-surface source at Station ALOHA in the North Pacific Subtropical Gyre (Popp et al., 2002). The isotopic trends for N_2O consumption by denitrification are based on the Arabian Sea data (McIlvin and Casciotti, 2010), ETNP data (Yamagishi et al., 2007), and culture studies (Ostrom et al., 2007). Sources and sinks are distinguished by their effects on d18O-N_2O vs. SP **(A)**, d18O-N_2O vs. d15Nbulk-N_2O **(B)**, and SP vs. d15Nbulk-N_2O **(C)**.

is required to determine the pathway and intermediates of nitrification and N_2O production by AOA, and to further study its isotope systematics under a variety of growth conditions.

ISOTOPE SYSTEMATICS FOR NITRITE OXIDATION

The isotopic systematics for nitrite oxidation to nitrate have also been studied recently, and were found to occur with extremely unique inverse kinetic isotope effects for N (Casciotti, 2009) and O isotopes (Buchwald and Casciotti, 2010). Because of these inverse isotope effects, when nitrite oxidation is active, the $\delta^{15}N_{NO_2}$ and $\delta^{18}O_{NO_2}$ values are expected to be lower than the NO_2^- initially produced by ammonia oxidation or nitrate reduction. As discussed below, this appears to occur in both primary and secondary nitrite maxima (Casciotti, 2009; Buchwald and Casciotti, unpublished). In most parts of the ocean, however, NO_2^- does not accumulate and the isotope effects associated with nitrite oxidation can only be expressed through a branch point (**Figure 3**). Isotopic separation can occur at a branch point because there is more than one fate for NO_2^- (e.g., NO_2^- is either oxidized to NO_3^- or assimilated into particulate N, PN) and the heavy isotope can be preferentially shunted in one direction vs. the other. This is analogous to the branch point that has been described during the oxidation or assimilation of ammonium (Sigman et al., 2005; Wankel et al., 2007; DiFiore et al., 2009). The

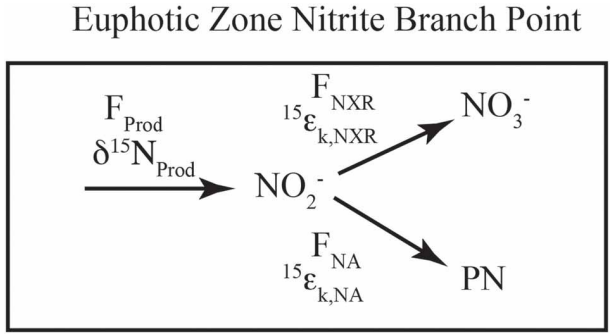

FIGURE 3 | Schematic of euphotic zone nitrite branch point. A schematic of the fluxes and isotope effects involved with NO_2^- consumption in the euphotic zone. NO_2^- is produced (F_{prod}, $\delta^{15}N_{prod}$) from ammonia oxidation and/or nitrate reduction, the mixture of which sets the incoming flux and $\delta^{15}N$ value. NO_2^- consumption can occur through nitrite oxidation (F_{NXR}, $^{15}\varepsilon_{k,NXR}$) or nitrite assimilation by phytoplankton (F_{NA}, $^{15}\varepsilon_{k,NA}$). The relative rates of uptake vs. oxidation dictate the partitioning between NO_2^- and NO_3^- relative to the source(s) of NO_2^-.

equations that describe the steady state N isotopic partitioning between NO_2^- and NO_3^- when nitrite oxidation and assimilation occur concurrently are:

$$\delta^{15}N_{NO_2} = \delta^{15}N_{NO_2,produced} + f_{NA} \times {}^{15}\varepsilon_{k,NA} + f_{NXR} \times {}^{15}\varepsilon_{k,NXR} \quad (2)$$

$$\delta^{15}N_{NO_3,produced} = \delta^{15}N_{NO_2} - {}^{15}\varepsilon_{k,NXR} \quad (3)$$

where f_{NA} and f_{NXR} are the fractions of NO_2^- consumed by assimilation and oxidation, respectively, and $^{15}\varepsilon_{k,NA}$ and $^{15}\varepsilon_{k,NXR}$ are the respective isotope effects. In general, nitrite oxidation will transfer NO_2^- with an elevated ^{15}N:^{14}N ratio to the NO_3^- pool, while nitrite assimilation transfers the residual NO_2^- with a lower ^{15}N:^{14}N ratio into the PN pool. If $^{15}\varepsilon_{k,NA}$ is 1‰ (Waser et al., 1998), $^{15}\varepsilon_{k,NXR}$ is −15‰ (Buchwald and Casciotti, 2010), $\delta^{15}N_{NO_2}$ at steady state will be lower than the source of NO_2^-, unless nitrite assimilation is >95% of the NO_2^- sink. This has the opposite sense of the ammonia oxidation/assimilation branching where ammonia oxidation transfers low ^{15}N:^{14}N material into the NO_2^- and NO_3^- pools and higher ^{15}N:^{14}N material into the PN pool.

When nitrite oxidation is tightly coupled to ammonia oxidation and NO_2^- does not accumulate, the $\delta^{18}O$ value of the NO_3^- produced primarily reflects the $\delta^{18}O$ values of the O atom sources (H_2O and O_2; Kumar et al., 1983) and the incorporation isotope effects for ammonia and nitrite oxidation (Buchwald et al., 2012). The oxygen isotope systematics of nitrite oxidation can be described by Equation 4, while the full oxygen isotope systematics of nitrification starting from NH_4^+, assuming no biologically-catalyzed oxygen atom exchange during nitrite oxidation ($x_{NO} = 0$; DiSpirito and Hooper, 1986; Friedman et al., 1986; Buchwald and Casciotti, 2010), is described by Equation 5.

$$\delta^{18}O_{NO_3,final} = \frac{2}{3}\left[(1-x_{NO})\delta^{18}O_{NO_2} + x_{NO}\left(\delta^{18}O_{H_2O} + {}^{18}\varepsilon_{eq}\right)\right] + \frac{1}{3}\left(\delta^{18}O_{H_2O} - {}^{18}\varepsilon_{k,H_2O,2}\right) \quad (4)$$

$$\delta^{18}O_{NO_3,final} = \left[\frac{2}{3} + \frac{1}{3}x_{AO}\right]\delta^{18}O_{H_2O} + \frac{1}{3}\left[\left(\delta^{18}O_{O_2} - {}^{18}\varepsilon_{k,O_2} - {}^{18}\varepsilon_{k,H_2O,1}\right)(1-x_{AO}) - {}^{18}\varepsilon_{k,H_2O,2}\right] + \frac{2}{3}{}^{18}\varepsilon_{eq}\,(x_{AO}) \quad (5)$$

Equation 5 indicates that the $\delta^{18}O_{NO_3}$ produced by tightly-coupled ammonia and nitrite oxidation should reflect variations in both $\delta^{18}O_{O_2}$ and $\delta^{18}O_{H_2O}$ in a ratio of 1 to 2, with slight modification of this stoichiometry by biologically-catalyzed oxygen atom exchange during ammonia oxidation (Casciotti et al., 2010; Buchwald et al., 2012). As discussed below, when ammonia and nitrite oxidation are not tightly coupled, abiotic equilibration can affect $\delta^{18}O_{NO_2}$ and the final $\delta^{18}O_{NO_3}$ produced. Regardless of whether NO_2^- accumulates, isotopic fractionation during oxygen atom incorporation should lead to an isotopic offset between the substrates (O_2 and H_2O) and the produced NO_3^-. The expected $\delta^{18}O_{NO_3}$ value produced in oxygenated seawater with little exchange is −1‰ to +1‰ (similar to $\delta^{18}O_{H_2O}$), resulting from a complex series of fractionation factors rather than the unfractionated incorporation of and exchange with H_2O (Buchwald et al., 2012).

ABIOTIC EQUILIBRATION OF OXYGEN ATOMS IN NITRITE

As introduced above, abiotic equilibration of oxygen atoms between NO_2^- and H_2O is likely to play a role in setting $\delta^{18}O_{NO_2}$ and $\delta^{18}O_{NO_3}$ values observed in the ocean. This process does not change the concentration of NO_2^- nor it's $\delta^{15}N$ value, only its $\delta^{18}O$ value. Oxygen atom equilibration shifts a $\delta^{18}O_{NO_2}$ value from its biological starting point or "end member," set by the isotopic systematics for biological production and consumption, toward the equilibrated $\delta^{18}O_{NO_2}$ value, dictated by ambient $\delta^{18}O_{H_2O}$ and the equilibrium isotope effect for the exchange ($^{18}\varepsilon_{eq}$), which is dependent on temperature (McIlvin and Casciotti, 2006; Buchwald and Casciotti, unpublished). The relevance of abiotic exchange depends on the rates of biological turnover of nitrite relative to the rate of oxygen atom exchange with water. Where nitrite turns over quickly and does not accumulate, there is little opportunity for abiotic exchange to occur. Where nitrite turns over more slowly (several weeks-months), abiotic exchange can play an important role in $\delta^{18}O_{NO_2}$ and $\delta^{18}O_{NO_3}$ (Buchwald et al., 2012).

The tendency of NO_2^- to exchange oxygen atoms abiotically with H_2O at typical seawater pH and temperature conditions suggests a utility of NO_2^- oxygen isotopes as a tracer for determining the rate of biological turnover of NO_2^- (Buchwald and Casciotti, unpublished). This provides a unique approach to determining rates of biological processes based on static isotope measurements, without bottle incubation and associated perturbations

of the system. Applications such as this move us from laboratory studies of isotope effects to a deeper understanding of the cycling of N in the environment. There are many additional examples of how knowledge of the isotope effects for nitrification has enabled advances in our understanding of the marine N cycle, and we highlight a few below.

IMPLICATIONS FOR UNDERSTANDING N CYCLING IN OXYGEN DEFICIENT ZONES

As mentioned above, processes that occur in ODZs are important for the marine N budget. Both denitrification and anammox can occur in these regions, producing N_2 gas from dissolved inorganic nitrogen (DIN) compounds thereby removing them from the nutrient inventory. The magnitudes of these fluxes have been estimated in many different ways: through isotope tracer experiments (Kuypers et al., 2005; Thamdrup et al., 2006; Hamersley et al., 2007; Lam et al., 2009; Ward et al., 2009; Bulow et al., 2010; Jensen et al., 2011), as well as geochemical techniques based on NO_3^- deficit calculations (Cline and Richards, 1972; Naqvi et al., 1982; Codispoti and Christensen, 1985; Naqvi and Sen Gupta, 1985; Gruber and Sarmiento, 1997; Deutsch et al., 2001) and biogenic N_2 production (Devol et al., 2006; Chang et al., 2010). The ^{15}N experiments in particular showcase a complex series of interacting processes cycling N in and around ODZs that can vary sporadically in space and time. What controls the overall rate of N_2 production is not known with certainty, although it is most likely tied directly or indirectly to organic carbon supply (Ward et al., 2008). Natural abundance stable isotopes provide an integrative longer-term view of the average rates of the major fluxes of N that can be used to complement short-term incubation studies. For example, natural abundance $\delta^{15}N_{NO_3}$ and $\delta^{18}O_{NO_3}$ measurements have been used to estimate the relative rates of N cycle processes such as N fixation and denitrification (Brandes et al., 1998; Sigman et al., 2005).

Another aspect of N cycling in ODZs that is of great interest is the fate of NO_2^- that is produced in ODZs. Once produced, NO_2^- can be consumed through oxidation, regenerating NO_3^-, or reduction to N_2 and loss from the nutrient inventory. Since nitrite oxidation is believed to be an oxygen requiring process, the fate of NO_2^- in the oxygen deficient zone has generally been assumed to be through nitrite reduction. However, it has been shown though a variety of approaches that NO_2^- can also be oxidized to NO_3^- in and around ODZs. For example, early 1-D modeling studies suggested that a large fraction of NO_2^- produced by nitrate reduction is reoxidized to NO_3^-, likely on the fringes of the oxygen deficient zone (Anderson et al., 1982). More recent nutrient profile modeling suggests that NO_2^- could be oxidized to NO_3^- within the oxygen deficient zone itself (Lam et al., 2011). Furthermore, direct evidence for NO_2^- oxidation to NO_3^- within the ODZ comes from short-term ^{15}N incubation experiments (Lipschultz et al., 1990; Füssel et al., 2012).

The importance of nitrite oxidation as a sink of NO_2^- in and around ODZs is supported by natural abundance isotope measurements of NO_3^- and NO_2^-, which integrate over longer periods. Sigman et al. (2005) and Casciotti and McIlvin (2007) found that nitrite oxidation could be an important sink for NO_2^- at the top of the SNM based on $\delta^{15}N_{NO_3}$ and $\delta^{18}O_{NO_3}$ measurements. Casciotti (2009) also showed the need for nitrite oxidation to explain the large $\delta^{15}N$ differences between NO_3^- and NO_2^- ($\Delta\delta^{15}N = \delta^{15}N_{NO_3} - \delta^{15}N_{NO_2}$) observed within ODZs (Casciotti and McIlvin, 2007). Although the isotope effect for NO_3^- reduction to NO_2^- is approximately 25‰ (Brandes et al., 1998; Voss et al., 2001), $\Delta\delta^{15}N$ values within the SNM ranged from 25‰ to 40‰ (Casciotti and McIlvin, 2007). At steady state, $\Delta\delta^{15}N$ is given by equation 6:

$$\Delta\delta^{15}N = \delta^{15}N_{NO_3} - \delta^{15}N_{NO_2} = {}^{15}\varepsilon_{k,NAR} - F_{NXR}/F_{NAR} \times {}^{15}\varepsilon_{k,NXR} - F_{NIR}/F_{NAR} \times {}^{15}\varepsilon_{k,NIR} \quad (6)$$

where F_{NAR}, F_{NXR}, and F_{NIR} are the fluxes from nitrate reduction, nitrite oxidation, and nitrite reduction, respectively, and ${}^{15}\varepsilon_{k,NAR}$, ${}^{15}\varepsilon_{k,NXR}$, and ${}^{15}\varepsilon_{k,NIR}$ are the respective N isotope effects. At steady state, the large $\Delta\delta^{15}N$ values cannot be explained by reductive processes alone since nitrite reduction would be expected to increase $\delta^{15}N_{NO_2}$, thereby decreasing $\Delta\delta^{15}N$ below 25‰. The only known mechanism for increasing $\Delta\delta^{15}N$ above 25‰ is through NO_2^- consumption with an inverse kinetic isotope effect, such as observed in nitrite oxidation (Casciotti, 2009; Buchwald and Casciotti, 2010). If all NO_2^- consumption occurs through oxidation ($F_{NXR}/F_{NAR} = 1$) with a kinetic isotope effect of −15‰, then $\Delta\delta^{15}N$ at steady state should approach 40‰. If all NO_2^- consumption occurs through nitrite reduction ($F_{NXR}/F_{NAR} = 0$) with a kinetic isotope effect of +15‰, then $\Delta\delta^{15}N$ would be expected to approach 10‰ at steady state. The $\delta^{15}N$ difference between NO_3^- and NO_2^- may therefore be diagnostic of NO_2^- sinks in ODZs (Casciotti, 2009).

While nitrite oxidation is generally considered to be an oxygen requiring process, O_2 is not required as an enzymatic substrate for nitrite oxidation. Rather, O_2 is used as an electron acceptor to support the oxidation of NO_2^- to NO_3^-. Therefore, if an alternative electron acceptor could be substituted, nitrite oxidation may proceed in the absence of O_2. The alternate electron acceptors that can be used by NOB for nitrite oxidation remain to be determined, but oxidation of NO_2^- by species such as iodate (IO_3^-), Fe(III), and Mn(IV) would be thermodynamically feasible. Moreover, as mentioned above, there is independent evidence based on ^{15}N incubations for nitrite oxidation occurring within the ODZs in the ETSP (Lipschultz et al., 1990) and Namibian upwelling (Füssel et al., 2012). The presence of nitrite oxidizing bacteria from the genera *Nitrospina* and *Nitrococcus* comprising up to 9% of the microbial community in the Namibian upwelling (Füssel et al., 2012) also gives strong support to their success even in low oxygen environments.

Of course, even if nitrite oxidation is occurring in ODZs, more than one process may contribute, as both bacterial nitrite oxidizers and anammox bacteria can oxidize NO_2^- to NO_3^-. The contribution of anammox to nitrite oxidation can be estimated by comparison of F_{NXR}/F_{NIR} required to explain the isotopic data with that observed during anammox (0.26:1.06; Strous et al., 2006). This ratio places an upper limit on the amount of nitrite oxidation that could be catalyzed by anammox. If the ratio of nitrite oxidation to nitrite reduction necessary to explain

observed $\Delta\delta^{15}N$ values is greater than this, then contributions from bacterial nitrite oxidation would be inferred (Casciotti, 2009). If the ratio of nitrite oxidation to nitrite reduction required to explain the isotopic data is less than this, then nitrite oxidation could potentially all be catalyzed by anammox, although denitrification may be required to explain the additional nitrite reduction. This analysis thus provides a new constraint on the relative rates of anammox and denitrification, integrated over long time periods. However, it assumes that the isotope effects for anammox are similar to denitrification for nitrite reduction and similar to nitrite oxidation for that step. Thus, the approach can be refined with additional information about the isotopic systematics of anammox.

IMPLICATIONS FOR UNDERSTANDING NO_3^- CYCLING AND BUDGETS: Δ(15, 18) REVISITED

Knowing the isotopic systematics of nitrification is critical for interpreting $\delta^{18}O_{NO_3}$, $\delta^{18}O_{NO_2}$, and $\delta^{18}O_{N2O}$ measurements from the ocean. The culture studies described above have advanced our understanding of the oxygen isotope systematics of nitrification; however, there are also constraints from field data (Casciotti et al., 2002; Sigman et al., 2009). Casciotti et al. (2002) used the nitrate $\delta^{18}O$ data to put the first constraints on the $\delta^{18}O$ value of NO_3^- produced in the ocean. These estimates showed that NO_3^- is most likely produced with $\delta^{18}O$ values close to those of seawater (0‰) and were used by Sigman et al. (2005) to constrain the rates of N_2 fixation and nitrite reoxidation from $\delta^{15}N_{NO_3}$ to $\delta^{18}O_{NO_3}$ data. In order to do this, Sigman et al. (2005) introduced a NO_3^- isotope anomaly based on expected enrichments of $\delta^{15}N_{NO_3}$ and $\delta^{18}O_{NO_3}$ due to nitrate assimilation or nitrate reduction during denitrification:

$$\Delta(15,18) = \left(\delta^{15}N_{NO_3} - \delta^{15}N_{NO_3,deep}\right) - {}^{18}5\varepsilon_{k,NAR}/{}^{15}8\varepsilon_{k,NAR} \times \left(\delta^{18}O_{NO_3} - \delta^{18}O_{NO_3,deep}\right) \quad (7)$$

where $\delta^{15}N_{NO_3}$ and $\delta^{18}O_{NO_3}$ are the measured isotopic values of the sample, $\delta^{15}N_{NO_3,deep}$ and $\delta^{18}O_{NO_3,deep}$ are the isotopic values of unaltered deep seawater, which define the starting point for fractionation. ${}^{18}\varepsilon_{k,NAR}$ and ${}^{15}\varepsilon_{k,NAR}$ are the isotope effects for O and N isotopes, respectively, during nitrate reduction. While there is a wide range in the absolute values of ${}^{18}\varepsilon_{k,NAR}$ and ${}^{15}\varepsilon_{k,NAR}$, their ratio is very close to 1 (Granger et al., 2004, 2008, 2010). Therefore, NO_3^- consuming processes generally lead to $\delta^{15}N_{NO_3}$ and $\delta^{18}O_{NO_3}$ values that fall along a 1:1 line and produce samples with $\Delta(15, 18) = 0$‰ (**Figure 4**). Non-zero $\Delta(15, 18)$ values correspond to an enrichment of $\delta^{18}O_{NO_3}$ relative to $\delta^{15}N_{NO_3}$, or a depletion in $\delta^{15}N_{NO_3}$ relative to $\delta^{18}O_{NO_3}$, generally arising from production of NO_3^- with anomalous isotopic signatures. The most likely cause for depletion in $\delta^{15}N$, especially in the nitracline of oligogrophic ocean provinces, is through remineralization of newly fixed N with a $\delta^{15}N$ value near −1‰ (Capone et al., 1997; Karl et al., 1997; Meador et al., 2007). The particulate organic N produced by N fixation is remineralized to NO_3^- in the subsurface, gaining O atoms from nitrification, the same process that sets the oxygen isotopic signature of NO_3^- produced from other N sources. In scenario, the magnitude of

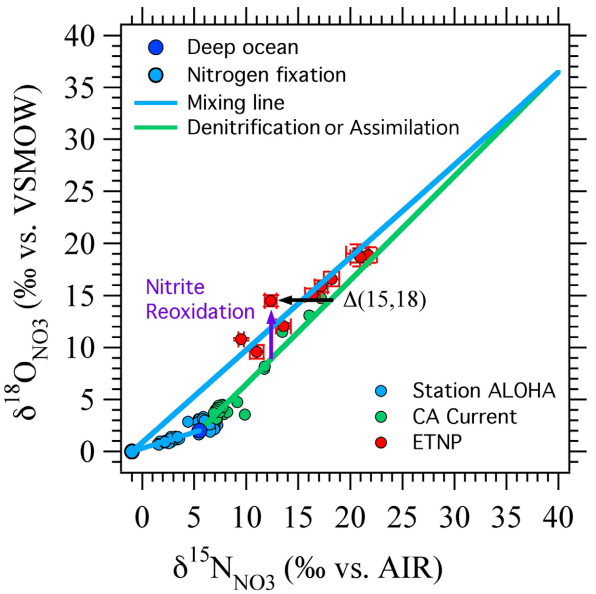

FIGURE 4 | Δ(15, 18) as originally devised. A schematic showing the effects of nitrate reduction, assimilation, and input of NO_3^- from nitrogen fixation linked to nitrification on $\delta^{15}N_{NO_3}$, $\delta^{18}O_{NO_3}$, and the nitrate isotope anomaly, Δ(15, 18) (black arrow). Deep ocean nitrate (dark blue circle) starts with $\delta^{15}N_{NO_3}$ of 5‰ and $\delta^{18}O_{NO_3}$ of 2‰. Nitrate assimilation and denitrification increase $\delta^{15}N$ and $\delta^{18}O$ in a 1:1 ratio ((Granger et al., 2004, 2008, 2010); green line). Remineralization of newly fixed N is assumed to add NO_3^- with $\delta^{15}N_{NO_3}$ of −1‰ and $\delta^{18}O_{NO_3}$ of 0‰ (light blue circle, blue mixing lines). Nitrite reoxidation is expected to generally increase $\delta^{18}O_{NO_3}$ relative to $\delta^{15}N_{NO_3}$ because of the oxygen isotope systematics of nitrate reduction and nitrite oxidation (purple arrow). Data from station ALOHA (Casciotti et al., 2008), California Current (Santoro et al., 2010) and ETNP (Casciotti and McIlvin, 2007) are shown for comparison.

Δ(15, 18) would be proportional to the N fixation flux (Sigman et al., 2005).

A relative enrichment in ^{18}O, especially in the vicinity of oceanic ODZs, could represent the cycling of NO_3^- through the reduction/reoxidation cycle, where the NO_3^- consumed by denitrification has a similar $\delta^{15}N_{NO_3}$ but a lower $\delta^{18}O_{NO_3}$ value than that returned to the NO_3^- pool from nitrite oxidation (Sigman et al., 2005). This formulation was successful at simulating data from regions of the ETNP where NO_2^- did not accumulate (Sigman et al., 2005) and where NO_2^- goes to zero at the top of the SNM (Casciotti and McIlvin, 2007). However, where NO_2^- accumulates, its isotopic composition can vary dramatically within the oxygen deficient zone itself (Casciotti and McIlvin, 2007), and an interpretation including NO_2^- isotope constraints is needed. The relationship between ^{18}O enrichment in NO_3^- and the magnitude of the nitrite reoxidation flux depends critically on the N and O isotope systematics of nitrite oxidation, which we reviewed above. Here we revisit the implications of this new knowledge for interpretations of Δ(15, 18) in euphotic zone and oxygen deficient zones.

Using a simple time-dependent 1-box model of the ODZ N cycle, we have reevaluated the impact of nitrite reoxdiation on $\delta^{15}N_{NO_3}$ and $\delta^{18}O_{NO_3}$ in a hypothetical ODZ (**Figure 5**) and

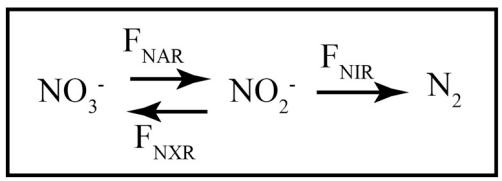

FIGURE 5 | Schematic of ODZ box model. A schematic of the fluxes included in the time-dependent 1-box ODZ model. NO_3^- is reduced to NO_2^- through nitrate reduction (F_{NAR}). NO_2^- can be consumed either through dissimilatory nitrite reduction (F_{NIR}) or nitrite oxidation (F_{NXR}). The rates of these processes are assumed to be first order in NO_3^- or NO_2^-, respectively, and isotope effects control the relative reaction of heavy and light isotopes. **Table 1** gives the values of the parameters used in the model.

show that nitrite oxidation can either raise or lower $\Delta(15, 18)$, depending on the relative $\delta^{15}N$ and $\delta^{18}O$ values of NO_2^- and NO_3^-. Our model focuses on determining the relative rates of NO_2^- reoxidation to NO_3^- (F_{NXR}) and reduction (to NO or NH_4^+; F_{NIR}) from NO_3^- and NO_2^- isotopic data. The oxidative flux is assumed to have the N and O isotopic systematics of bacterial nitrite oxidation (Buchwald and Casciotti, 2010; **Table 1**), regardless of whether it is carried out by bacterial nitrite oxidizers or anammox bacteria, or some mixture of the two. The reductive processes are assumed to have $^{15}\varepsilon = {}^{18}\varepsilon = 15‰$ (**Table 1**) regardless of whether NO_2^- is reduced to N_2 (via anammox or denitrification) or NH_4^+ [via denitrification to ammonium (DNRA)]. Unfortunately, very little information is currently available on the N isotope effects for nitrite reduction by these processes (Bryan et al., 1983) and no information is available for the O isotope effects. In the absence of more specific information, we make the simplifying assumption that the different nitrite reductase enzymes have similar N and O isotope effects. Clearly, this is an important area of future research.

In our model, the processes are all represented as first order, and the rate constants (k's) are given in units of day^{-1} to match measured rates of nitrate reduction, nitrite reduction, and nitrite oxidation in ODZs (**Table 1**). The isotope effects taken from the literature are also given in **Table 1**. We vary the relative rates of nitrite oxidation and nitrite reduction (F_{NXR}/F_{NIR}) between 0 and 3 (F_{NXR} representing 0–75% of NO_2^- consumption) and the rate constant for exchange (k_{EXCH}) between 0 and 1 day^{-1} to evaluate the effects of changes in these parameters on simulated $\delta^{15}N_{NO_3}$ and $\delta^{18}O_{NO_3}$ (**Figure 6**). Maximum rate constants of exchange between NO_2^- and H_2O of 1 day^{-1} appear reasonable based on recent laboratory studies (Casciotti et al., 2007; Buchwald and Casciotti, unpublished). As F_{NXR}/F_{NIR} increases from 0 to 3, the amount of NO_3^- retained in the system increases despite an unchanging rate constant for nitrate reduction. In fact, because the reaction is taken as first order, the higher concentrations of NO_3^- brought about by higher levels of F_{NXR} lead to higher overall rates of nitrate reduction. However, it is clear from the mass balances in the different scenarios that nitrite reoxidation helps buffer against excessive loss of NO_3^-, accumulation of NO_2^-, and production of N_2 (**Figures 6A–D**), and may help explain why NO_3^- is never fully removed in oceanic ODZs.

The magnitude of nitrite oxidation also affects the $\delta^{15}N_{NO_3}$ and $\delta^{18}O_{NO_3}$ patterns. When $F_{NXR}/F_{NIR} = 0$, the $\delta^{15}N_{NO_3}$ and $\delta^{18}O_{NO_3}$ data fall along the 1:1 line prescribed by the isotope effects for nitrate reduction (**Figures 6E–G**). As F_{NXR}/F_{NIR} increases, increasingly negative $\Delta(15, 18)$ values are produced. The strength of this effect is also dependent on the rate of

Table 1 | Parameters used in oxygen deficient zone box model.

Parameter	Description	Value	Reference
$\delta^{15}N_{NO_3,initial}$	Initial nitrate $\delta^{15}N$	5‰	Sigman et al., 2000
$\delta^{18}O_{NO_3,initial}$	Initial nitrate $\delta^{18}O$	2‰	Casciotti et al., 2002
$\delta^{18}O_{H_2O}$	Water $\delta^{18}O$ value	0‰	Craig and Gordon, 1965
k_{NAR}	First order rate constant for nitrate reduction	0.001 day^{-1}	Estimated to achieve a rate of 20 nM day^{-1}; Lam et al., 2011
k_{NXR}	First order rate constant for nitrite oxidation	0–0.003 day^{-1}	Estimated to achieve range of observed nitrite oxidation rates; Füssel et al., 2012; Lipschultz et al., 1990
k_{NIR}	First order rate constant for nitrite reduction	0.001 day^{-1}	Estimated to achieve a rate of 5 nM day^{-1}; Devol et al., 2006
k_{EXCH}	First order rate constant for nitrite/water exchange	0.01 day^{-1}	Buchwald and Casciotti
$^{15}\alpha_{k,NAR}$	N isotope effect for nitrate reduction	1.019	Deutsch et al., 2004; Granger et al., 2008
$^{15}\alpha_{k,NXR}$	N isotope effect for nitrite oxidation	0.985	Casciotti, 2009; Buchwald and Casciotti, 2010
$^{15}\alpha_{k,NIR}$	N isotope effect for nitrite reduction	1.015	Bryan et al., 1983
$^{18}\alpha_{NAR}$	O isotope effect for nitrate reduction	1.019	Granger et al., 2008
$^{18}\alpha_{k,NXR}$	O isotope effect for nitrite oxidation	0.997	Buchwald and Casciotti, 2010
$^{18}\alpha_{k,NIR}$	O isotope effect for nitrite reduction	1.015	Sigman et al., 2005
$^{18}\alpha_{kH_2O,2}$	O isotope effect for H_2O incorporation	1.010	Buchwald and Casciotti, 2010
$^{18}\alpha_B$	Branching O isotope effect during nitrate reduction	0.975	Casciotti et al., 2007
$^{18}\alpha_{eq}$	Equilibrium isotope effect for nitrite/water O exchange	1.014	Casciotti et al., 2007; (Buchwald and Casciotti, unpublished)

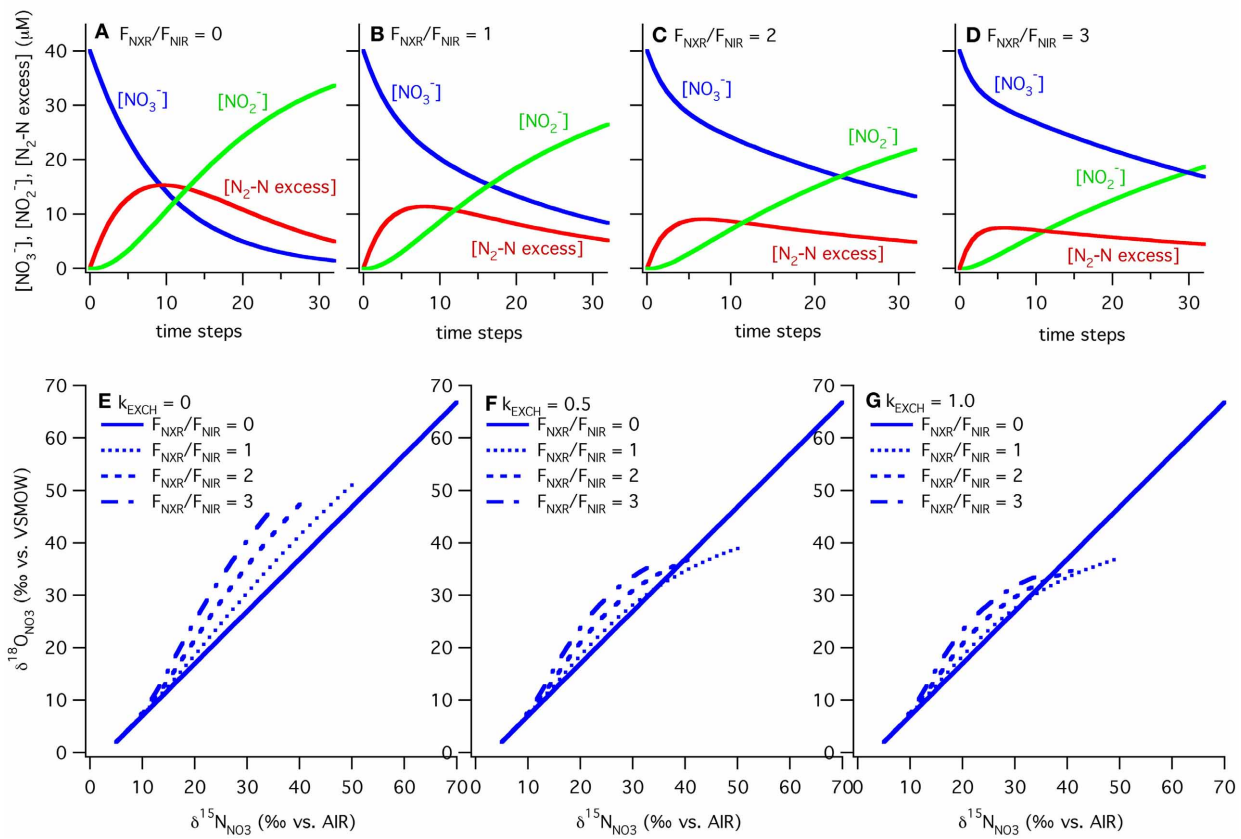

FIGURE 6 | Results of ODZ model for varying ratios of nitrite oxidation to nitrite reduction and rates of exchange. Results from the ODZ box model at different relative rates of nitrite oxidation and nitrite reduction (F_{NXR}/F_{NIR}), ranging from 0 to 3. Mass balance is maintained in the model between NO_3^-, NO_2^- and excess N_2-N with $F_{NXR}/F_{NIR} = 0$ (panel **A**), 1 (panel **B**), 2 (panel **C**) and 3 (panel **D**). NO_2^- accumulation and N_2 production decrease as F_{NXR} increases. The ODZ box model shows that NO_2^- cycling can generate both positive and negative Δ(15, 18) values, depending on the extent of NO_3^- consumption (increasing $\delta^{15}N$, $\delta^{18}O$ values), the relative rates of nitrite oxidation and reduction (F_{NXR}/F_{NIR}), and the rate of oxygen atom exchange between NO_2^- and H_2O (k_{EXCH}). In each case the slope of $\delta^{18}O_{NO_3}$ vs. $\delta^{15}N_{NO_3}$ is equal to 1 when $F_{NXR} = 0$. As F_{NXR}/F_{NIR} increases, the magnitude of the Δ(15, 18) anomaly increases at a given $\delta^{15}N$ value. As NO_2^-/H_2O exchange increases (=0 in panel **E**, 0.5 in panel **F**, and 1.0 in panel **G**), the non-zero levels of nitrite oxidation generate positive Δ(15, 18) values, most likely due to the relative $\delta^{18}O$ values of NO_3^- produced and consumed under these scenarios. All parameters used in the model are reported in **Table 1**.

abiotic NO_2^-/H_2O exchange, with higher exchange rates partly diluting this effect and actually leading to positive Δ(15, 18) values at high extents of NO_3^- consumption (the highest $\delta^{15}N_{NO_3}$ values; **Figure 6**). This interesting phenomenon is most likely due to reversal of the impact of nitrite reoxidation on $\delta^{18}O_{NO_3}$ at high $\delta^{18}O_{NO_3}$ values, with nitrite oxidation returning NO_3^- with a lower $\delta^{18}O_{NO_3}$ value than that removed by nitrite reduction. This would be exacerbated at high rates of exchange, which helps to maintain $\delta^{18}O_{NO_2}$ values at a constant level regardless of $\delta^{18}O_{NO_3}$. Tuning the model to match observed $\delta^{18}O_{NO_2}$ data requires a high rate of exchange relative to biological fluxes, and therefore most closely follows the $k_{EXCH} = 1$ scenario.

Larger ratios of F_{NXR}/F_{NIR} could be imagined, but the model results from such simulations produce unrealistic Δ(15, 18) anomalies at a given $\delta^{15}N_{NO_3}$ value. Furthermore, because excess N_2 does accumulate in ODZs, we know that some NO_2^- is ultimately reduced to N_2. Indeed, we could potentially use the stoichiometry of N_2 production in ODZs to interrogate the importance of nitrite oxidation. If nitrite oxidation is not important, the standard stoichiometry (Richards, 1965; Devol et al., 2006) of 106 CO_2: 55.2 N_2 would be expected, whereas higher amounts of CO_2 would be expected if a significant fraction of the produced NO_2^- is reoxidized to NO_3^-. This may seem counterintuitive because autotrophic nitrite oxidation should fix CO_2 back into organic matter, but the excess NO_3^- reduction required to supply the NO_2^- in the first place should far outweigh the CO_2 fixed by nitrite oxidation.

It is interesting to note that the two scenarios for producing negative Δ(15, 18) values (N_2 fixation and nitrite reoxidation) are each more effective at different points in NO_3^- isotope space (**Figure 7**). N_2 fixation is most effective at generating negative Δ(15, 18) signals at $\delta^{15}N_{NO_3}$ and $\delta^{18}O_{NO_3}$ values less than 10‰, near the base of the euphotic zone. In contrast, nitrite reoxidation is most effective at generating negative Δ(15, 18) signals at intermediate $\delta^{15}N_{NO_3}$ and $\delta^{18}O_{NO_3}$ values and extents of NO_3^-

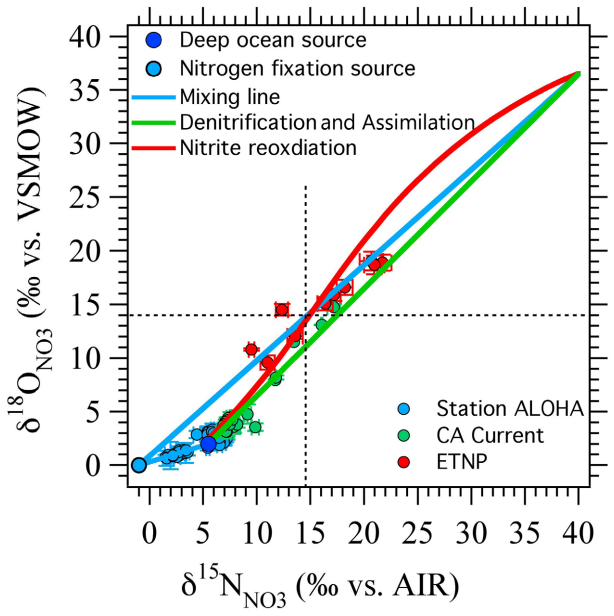

FIGURE 7 | Results from ODZ model compared against published data. Nitrogen fixation (blue circle and blue lines) is efficient at generating negative Δ(15, 18) values at the lower range of $\delta^{15}N_{NO_3}$ and $\delta^{18}O_{NO_3}$ values, while nitrite reoxidation (red line) has a stronger effect at higher $\delta^{15}N_{NO_3}$ and $\delta^{18}O_{NO_3}$ values. The nitrite reoxidation curve shown here was generated from the box model with $k_{EXCH} = 0.5$ and $F_{NXR}/F_{NIR} = 2$ (**Figure 6F**, dashed line). Data from station ALOHA (Casciotti et al., 2008) in the north Pacific subtropical gyre is well explained by an input from N_2 fixation. Data from the California Current (Santoro et al., 2010) falls close to the 1:1 line suggesting little influence of nitrogen fixation or nitrite oxidation in the euphotic zone. Most of the data from the ETNP (Casciotti and McIlvin, 2007) could be explained by either nitrite reoxiation or nitrogen fixation, but two points (which fall in the shallow oxycline at the top of the SNM) require inputs from both nitrite reoxidation and nitrogen fixation.

consumption by denitrification, where N_2 fixation has relatively little effect on the Δ(15, 18). Therefore, we may be able to distinguish between the processes responsible for Δ(15, 18) generation by where the anomaly lies in $\delta^{15}N_{NO_3}$ vs. $\delta^{18}O_{NO_3}$ space, as well as from other water column indicators. For example, using a steady state model, Casciotti and McIlvin (2007) showed that the NO_3^- isotope anomaly at the top of the SNM could not be generated by N_2 fixation alone and was consistent with oxidation of NO_2^- leaking out of the top of the SNM. However, they suggested that a combination of N_2 fixation and nitrite reoxidation may best fit the observations. This conclusion is echoed here where it is difficult to generate large Δ(15, 18) signals at these $\delta^{15}N_{NO_3}$ and $\delta^{18}O_{NO_3}$ values through either N_2 fixation or nitrite reoxidation alone (**Figure 7**).

In addition to oxygen deficient zone and near-surface processes, NO_3^- isotopes have also been used to examine the global ocean cycle and budget of NO_3^- in the ocean interior (Sigman et al., 2009). This was done using an 18-box model of the global ocean where the implications of different assumptions about the oxygen isotopic systematics of nitrification could be tested. Their model was also used to constrain the relative rates of the internal N cycle (NO_3^- uptake, export, and nitrification) and N budget processes (N_2 fixation and denitrification) and the ratio of low latitude productivity, where nutrient consumption goes to completion, to high latitude productivity, where nutrient uptake is incomplete. By comparing model results to $\delta^{15}N_{NO_3}$ and $\delta^{18}O_{NO_3}$ data from a variety of oceanographic profiles representing the major ocean basins, the impacts of partial NO_3^- assimilation in polar regions on the N and O isotopes of NO_3^- in the ocean interior, and of low latitude productivity on the ^{18}O enrichment in preformed NO_3^- was diagnosed. N budget processes (N_2 fixation and denitrification) led to variations in subsurface $\delta^{15}N_{NO_3}$ and $\delta^{18}O_{NO_3}$, but in their absence, the large scale steady state $\delta^{18}O$ value of subsurface NO_3^- was set by nitrate assimilation in polar regions. Nitrate uptake in the southern ocean leads to heavy isotope enrichment in preformed NO_3^-, while nitrate assimilation in low latitudes removes the $\delta^{18}O$ signal of the preformed NO_3^- and replaces it with the nitrification signal (Sigman et al., 2009). Overall, when only internal processes were active in the model, the mean ocean $\delta^{18}O_{NO_3}$ value was 1.1‰ higher than the nitrification source. When the N budget was added to the model, the mean ocean $\delta^{18}O_{NO_3}$ value was 2.4‰ higher than the nitrification source value. This analysis provides additional constraints on the $\delta^{18}O$ value of newly produced NO_3^- in the ocean to fall between −1‰ and +1‰ (Sigman et al., 2009), which is consistent with culture studies that illustrate how these values are controlled biochemically (Buchwald et al., 2012).

NITROGEN CYCLING IN THE EUPHOTIC ZONE

Several studies have now used N and O isotope ratio measurements to study the relative rates of N cycling in the euphotic zone. In particular, knowledge of the isotopic systematics of nitrate uptake (Granger et al., 2004, 2010) and nitrification (Buchwald and Casciotti, 2010; Casciotti et al., 2010, 2011; Buchwald et al., 2012) enables the assessment of the relative rates of nitrification and nitrate uptake from euphotic zone NO_3^- isotope data.

Wankel et al. (2007) used a steady-state box model to interpret the amount of nitrification contributing to nitrate uptake by phytoplankton in Monterey Bay, CA using $\delta^{15}N_{NO_3}$ and $\delta^{18}O_{NO_3}$ variations. Assuming that nitrate assimilation leads to equivalent fractionation of N and O isotopes (Granger et al., 2004), and that $\delta^{18}O_{ntr} = 2.9‰$, they estimated that nitrification could supply up to 30% of NO_3^- assimilated by phytoplankton in Monterey Bay, consistent with intensive isotope tracer incubation studies (Ward, 2005). Because $\delta^{18}O_{ntr}$ was uncertain at that time, they performed sensitivity studies to address the impact of different $\delta^{18}O_{ntr}$ values on their interpretation. We now believe that $\delta^{18}O_{ntr}$ is between −1‰ and +1‰ (Buchwald et al., 2012), and applying this to the model from Wankel et al. (2007), leads to a smaller increase in $\delta^{18}O_{NO_3}$ for the same amount of nitrification. Thus, to achieve the same $\delta^{18}O_{NO_3}$ enrichment in their model requires more nitrification than originally estimated.

DiFiore and colleagues (2009) estimated the amount of nitrification contributing to nitrate uptake in the euphotic zone of the Polar Antarctic Zone using a time-dependent 1-box model. Like Wankel et al. (2007), they assumed that $^{18}\varepsilon_{NR}$=$^{15}\varepsilon_{NR}$ for nitrate

uptake and allowed branching of NH_4^+ (and NO_2^-) between nitrification and assimilation to partition isotopes between the NO_3^- and particulate N pools. One important difference from the Wankel et al. (2007) model is that they assumed $\delta^{18}O_{ntr} = +1.1‰$ based on more recent constraints on this value (Sigman et al., 2009). They inferred that $\delta^{15}N_{NO_3}$ should be lowered slightly due to nitrification (offsetting the isotopic fractionation during uptake) and $\delta^{18}O_{NO_3}$ should be raised (because the $\delta^{18}O$ of newly produced NO_3^- was higher than that removed). Both of these factors should lead to negative $\Delta(15, 18)$ values, as discussed above, but they found that nitrification had a relatively small impact on $\delta^{15}N_{NO_3}$ and $\delta^{18}O_{NO_3}$ values in the Polar Antarctic Zone. They concluded that in the Polar Antarctic Zone less than 1% of NO_3^- assimilated by phytoplankton is likely to have been produced by nitrification in the euphotic zone (DiFiore et al., 2009). This is consistent with other estimates from the southern ocean (Olson, 1981b; Bianchi et al., 1997; Law and Ling, 2001) and quite a bit lower than other regions (Yool et al., 2007; Wankel et al., 2007; Clark et al., 2008). This elegant study provides an excellent example of how NO_3^- isotopes can be used to constrain N cycle processes in an appropriate model framework.

NO_3^- and NO_2^- isotopes have also been used to understand the sources and cycling of NO_2^- in the PNM at the base of the euphotic zone. Mackey et al. (2011) used natural abundance NO_3^- + NO_2^- isotope data and isotope tracer experiments to determine the sources of NO_2^- to the PNM in the Gulf of Aqaba. They found active nutrient regeneration and nitrification throughout the water column. In the transition from well mixed to stratified conditions, NO_2^- was generated by incomplete NO_3^- reduction by light-limited phytoplankton creating a broad band of NO_2^-. After stratification was established, NO_2^- generation by ammonia oxidation contributed to maintenance of the PNM. In both cases, NO_2^- was consumed by nitrite oxidation below the PNM. Once again, nitrification was interpreted to play an important role in NO_3^- isotope dynamics in the upper water column where increases in $\delta^{18}O_{NO_3}$ were much higher than increases in $\delta^{15}N_{NO_3}$.

In another recent study of PNM dynamics, natural abundance $\delta^{18}O_{NO_2}$ and $\delta^{15}N_{NO_2}$ values were used to infer the sources and average age of NO_2^- in the PNM of the Arabian Sea (Buchwald and Casciotti, unpublished). Because the $\delta^{15}N_{NO_2}$ and $\delta^{18}O_{NO_2}$ values produced from ammonia oxidation and nitrate reduction are distinct, the sources can be readily distinguished. Based on natural abundance $\delta^{15}N_{NO_2}$ and $\delta^{18}O_{NO_2}$ data, ammonia oxidation was inferred to be the main source of NO_2^- to the PNM in the Arabian Sea.

IMPLICATIONS FOR INTERPRETING N_2O SOURCES

Uncertainty in the isotopic composition of N_2O produced during ammonia oxidation has hampered the interpretation of near-surface N_2O production rates and fluxes using two-component end member models (Dore et al., 1998; Popp et al., 2002; Santoro et al., 2010). Better understanding of the oxygen isotopic systematics of nitrification can provide further insight into outstanding questions in N_2O oxygen isotope variations, such as why $\delta^{18}O_{N2O}$ in seawater is so high (Ostrom et al., 2000; Popp et al., 2002), what mechanisms of N_2O production operate in oxyclines surrounding oceanic ODZs (Codispoti and Christensen, 1985), and what the mechanisms and controls on N_2O production are in the near-surface ocean (Dore et al., 1998; Popp et al., 2002; Santoro et al., 2011).

For example, N_2O production in the near-surface ocean is largely believed to be the result of nitrification. However, the isotopic composition of N_2O in the near surface and the inferred near surface source (Dore et al., 1998) have higher $\delta^{15}N$ and $\delta^{18}O$ values than are characterized by bacterial ammonia oxidation (Yoshida, 1988; Frame and Casciotti, 2010). Recent evidence suggests that AOA are important for nitrification in such environments (Wuchter et al., 2006; Beman et al., 2008; Mincer et al., 2007; Church et al., 2010; Santoro et al., 2010) and that they produce N_2O with bulk $\delta^{15}N$ and $\delta^{18}O$ values similar to the near-surface source (Santoro et al., 2011). These data support a role for them in near-surface N_2O production. As discussed above, the mechanisms of N_2O production by AOA are currently unknown, and more work is needed to characterize the N_2O production and isotopic composition of marine AOA under a variety of growth conditions. For example, the SP of N_2O produced by AOB varies widely with dissolved oxygen levels (Frame and Casciotti, 2010) but so far the isotopic composition of N_2O produced by AOA has only been examined under aerobic growth conditions (Santoro et al., 2011; Loescher et al., 2012). Therefore, we do not know whether they are capable of producing N_2O with a SP similar to near surface N_2O (Popp et al., 2002).

CONCLUDING REMARKS

Understanding the nitrogen and oxygen isotopic systematics of nitrification can contribute greatly to our understanding of nitrogen cycling in the ocean, as nitrification is involved with transformations between the major pools of DIN (NH_4^+, NO_2^-, NO_3^-, and N_2O). Both ammonia and nitrite oxidation are involved with large and distinctive isotope effects, leading to predictable patterns in the isotope ratios of compounds that they transform. The discovery of AOA and their importance in ocean biogeochemistry necessitates renewed study of the isotopic systematics of nitrification. In preliminary studies, the isotopic systematics of AOA appear similar to AOB for N isotope fractionation and O atom incorporation into NO_2^- (Santoro and Casciotti, 2011; Santoro et al., 2011). However, the production of N_2O and the isotopic systematics of this process need to be further investigated.

ACKNOWLEDGMENTS

We would like to acknowledge the pioneering work of those cited in this review. We have attempted to integrate studies of many authors using various approaches to understand the importance of nitrification in the marine environment, with a focus on the use of natural abundance stable isotope measurements. We thank two anonymous reviewers for their suggestions on an earlier draft of this manuscript. Funding for this work has been provided by NSF/OCE ETSP grants 05-26277, 07-48674, and 11-40404 to Karen L. Casciotti.

REFERENCES

Anderson, J. J., Okubo, A., Robins, A. S., and Richards, F. A. (1982). A model for nitrite and nitrate distributions in oceanic oxygen minimum zones. *Deep Sea Res.* 29, 1113–1140.

Andersson, K. K., and Hooper, A. B. (1983). O_2 and H_2O are each the source of one O in NO_2^- produced from NH_3 by *Nitrosomonas*: ^{15}N-NMR evidence. *FEBS Lett.* 164, 236–240.

Andersson, K. K., Philson, S. B., and Hooper, A. B. (1982). ^{18}O isotope shift in ^{15}N NMR analysis of biological N-oxidations: H_2O-NO_2^- exchange in the ammonia-oxidizing bacterium *Nitrosomonas*. *Proc. Natl. Acad. Sci. U.S.A.* 79, 5871–5875.

Barford, C. C., Montoya, J. P., Altabet, M. A., and Mitchell, R. (1999). Steady-state nitrogen isotope effects of N_2 and N_2O production in *Paracoccus denitrificans*. *Appl. Environ. Microbiol.* 65, 989–994.

Beman, J. M., Popp, B. N., and Francis, C. A. (2008). Molecular and biogeochemical evidence for ammonia oxidation by marine Crenarchaeota in the Gulf of California. *ISME J.* 2, 429–441.

Bianchi, M., Feliatra, F., Treguer, P., Vincendeau, M.-A., and Morvan, J. (1997). Nitrification rates, ammonium and nitrate distribution in upper layers of the water column and in sediments of the Indian sector of the Southern Ocean. *Deep Sea Res. Part II Top. Stud. Oceanogr.* 44, 1017–1032.

Bock, E., Koops, H.-P., and Harms, H. (1989). "Nitrifying bacteria," in *Autotrophic Bacteria*, eds H. G. Schelgel and B. Bowien (Berlin: Springer-Verlag), 81–96.

Brandes, J. A., Devol, A. H., Yoshinari, T., Jayakumar, D. A., and Naqvi, S. W. A. (1998). Isotopic composition of nitrate in the central Arabian sea and eastern tropical North Pacific: a tracer for mixing and nitrogen cycles. *Limnol. Oceanogr.* 43, 1680–1689.

Brandhorst, W. (1959). Nitrification and denitrification in the Eastern Tropical North Pacific. *Journal du Conseil Permanent International l'Exploration de la Mer* 25, 3–20.

Bryan, B. A., Shearer, G., Skeeters, J. L., and Kohl, D. H. (1983). Variable expression of the nitrogen isotope effect associated with denitrification of nitrite. *J. Biol. Chem.* 258, 8613–8617.

Buchwald, C., and Casciotti, K. L. (2010). Oxygen isotopic fractionation and exchange during bacterial nitrite oxidation. *Limnol. Oceanogr.* 55, 1064–1074.

Buchwald, C., Santoro, A. E., McIlvin, M. R., and Casciotti, K. L. (2012). Oxygen isotopic composition of nitrate and nitrite produced by nitrifying co-cultures and natural marine assemblages. *Limnol. Oceanogr.* 57, 1361–1375.

Bulow, S. E., Rich, J. J., Naik, H. S., Pratihary, A. K., and Ward, B. B. (2010). Denitrification exceeds anammox as a nitrogen loss pathway in the Arabian Sea oxygen minimum zone. *Deep Sea Res. Part I Oceanogr. Res. Pap.* 57, 384–393.

Capone, D. G., Zehr, J. P., Paerl, H. W., Bergman, B., and Carpenter, E. J. (1997). *Trichodesmium*, a globally significant marine Cyanobacterium. *Science* 276, 1221–1229.

Casciotti, K. L. (2009). Inverse kinetic isotope fractionation during bacterial nitrite oxidation. *Geochim. Cosmochim. Acta* 73, 2061–2076.

Casciotti, K. L., Böhlke, J. K., McIlvin, M. R., Mroczkowski, S. J., and Hannon, J. E. (2007). Oxygen isotopes in nitrite: analysis, calibration, and equilibration. *Anal. Chem.* 79, 2427–2436.

Casciotti, K. L., Buchwald, C., Santoro, A. E., and Frame, C. (2011). Assessment of nitrogen and oxygen isotopic fractionation during nitrification and its expression in the marine environment. *Methods Enzymol.* 486, 253–280.

Casciotti, K. L., and McIlvin, M. R. (2007). Isotopic analyses of nitrate and nitrite from reference mixtures and application to Eastern Tropical North Pacific waters. *Mar. Chem.* 107, 184–201.

Casciotti, K. L., McIlvin, M. R., and Buchwald, C. (2010). Oxygen isotopic exchange and fractionation during bacterial ammonia oxidation. *Limnol. Oceanogr.* 55, 753–762.

Casciotti, K. L., Sigman, D. M., Galanter Hastings, M., Bohlke, J. K., and Hilkert, A. (2002). Measurement of the oxygen isotopic composition of nitrate in seawater and freshwater using the denitrifier method. *Anal. Chem.* 74, 4905–4912.

Casciotti, K. L., Sigman, D. M., and Ward, B. B. (2003). Linking diversity and stable isotope fractionation in ammonia-oxidizing bacteria. *Geomicrobiol. J.* 20, 335–353.

Casciotti, K. L., Trull, T. W., Glover, D. M., and Davies, D. (2008). Constraints on nitrogen cycling in the subtropical North Pacific Station ALOHA from isotopic measurements of nitrate and particulate nitrogen. *Deep Sea Res. Part II Top. Stud. Oceanogr.* 55, 1661–1672.

Chang, B. X., Devol, A. H., and Emerson, S. R. (2010). Denitrification and the nitrogen gas excess in the eastern tropical South Pacific oxygen deficient zone. *Deep Sea Res. Part I Oceanogr. Res. Pap.* 57, 1092–1101.

Church, M. J., Wal, B., Karl, D. M., and DeLong, E. F. (2010). Abundances of crenarchaeal *amoA* genes and transcripts in the Pacific Ocean. *Environ. Microbiol.* 12, 679–688.

Clark, D. R., Rees, A. P., and Joint, I. (2008). Ammonium regeneration and nitrification rates in the oligotrophic Atlantic Ocean: implications for new production estimates. *Limnol. Oceanogr.* 53, 52–62.

Cline, J. D., and Richards, F. A. (1972). Oxygen deficient conditions and nitrate reduction in the eastern tropical North Pacific Ocean. *Limnol. Oceanogr.* 17, 885–900.

Codispoti, L. A., and Christensen, J. P. (1985). Nitrification, denitrification, and nitrous oxide cycling in the eastern tropical Pacific Ocean. *Mar. Chem.* 16, 277–300.

Craig, H., and Gordon, L. I. (1965). "Deuterium and oxygen 18 variations in the ocean and marine atmosphere," in *Stable Isotopes in Oceanographic Studies and Paleotemperatures,* ed E. Tongiogi (Spoleto, Italy), 9–130.

Croteau, P., Atlas, E. L., Schauffler, S. M., Blake, D. R., Diskin, G. S., and Boering, K. A. (2010). Effect of local and regional sources on the isotopic composition of nitrous oxide in the tropical free troposphere and tropopause layer. *J. Geophys. Res.* 115, D00J11.

Deutsch, C., Gruber, N., Key, R. M., Sarmiento, J. L., and Ganaschaud, A. (2001). Denitrification and N2 fixation in the Pacific Ocean. *Global Biogeochem. Cycles* 15, 483–506.

Deutsch, C., Sigman, D. M., Thunell, R. C., Meckler, A. N., and Haug, G. H. (2004). Isotopic constraints on glacial/interglacial changes in the oceanic nitrogen budget. *Global Biogeochem. Cycles* 18, GB4012.

Devol, A. H., Uhlenhopp, A. G., Naqvi, S. W. A., Brandes, J. A., Jayakumar, D. A., Naik, H., et al. (2006). Denitrification rates and excess nitrogen gas concentrations in the Arabian Sea oxygen deficient zone. *Deep Sea Res. Part I Oceanogr. Res. Pap.* 53, 1533–1547.

DiFiore, P. J., Sigman, D. M., Dunbar, R. B., and Wang, Y. (2009). Upper ocean nitrogen fluxes in the Polar Antarctic zone: constraints from the nitrogen and oxygen isotopes of nitrate. *Geochem. Geophys. Geosyst.* 10. doi: 10.1029/2009GC002468. [Epub ahead of print].

DiSpirito, A. A., and Hooper, A. B. (1986). Oxygen exchange between nitrate molecules during nitrite oxidation by *Nitrobacter*. *J. Biol. Chem.* 261, 10534–10537.

Dore, J. E., and Karl, D. M. (1996). Nitrite distributions and dynamics at station ALOHA. *Deep Sea Res.* 43, 385–402.

Dore, J. E., Popp, B. N., Karl, D. M., and Sansone, F. J. (1998). A large source of atmospheric nitrous oxide from subtropical North Pacific surface waters. *Nature* 396, 63–66.

Dua, R. D., Bhandari, B., and Nicholas, D. J. D. (1979). Stable isotope studies on the oxidation of ammonia to hydroxylamine by *Nitrosomonas europaea*. *FEBS Lett.* 106, 401–404.

Frame, C. H., and Casciotti, K. L. (2010). Biogeochemical controls and isotopic signatures of nitrous oxide production by a marine ammonia-oxidizing bacterium. *Biogeosci. Discuss.* 7, 3019–3059.

Friedman, S. H., Massefski, W., and Hollocher, T. C. (1986). Catalysis of intermolecular oxygen atom transfer by nitrite dehydrogenase of *Nitrobacter agilis*. *J. Biol. Chem.* 261, 10538–10543.

Füssel, J., Lam, P., Lavik, G., Jensen, M. M., Holtappels, M., Gunter, M., et al. (2012). Nitrite oxidation in the Namibian oxygen minimum zone. *ISME J.* 6, 1200–1209.

Granger, J., Sigman, D. M., Needoba, J. A., and Harrison, P. J. (2004). Coupled nitrogen and oxygen isotope fractionation of nitrate during assimilation by cultures of marine phytoplankton. *Limnol. Oceanogr.* 49, 1763–1773.

Granger, J., Sigman, D. M., Lehmann, M. F., and Tortell, P. D. (2008). Nitrogen and oxygen isotope fractionation during dissimilatory nitrate reduction by denitrifying bacteria. *Limnol. Oceanogr.* 53, 2533–2545.

Granger, J., Sigman, D. M., Rhode, M. M., Maldonado, M. T., and Tortell, P. D. (2010). N and O isotope effects during nitrate assimilation by unicellular prokaryotic and eukaryotic plankton cultures. *Geochim. Cosmochim. Acta* 74, 1030–1040.

Gruber, N., and Sarmiento, J. L. (1997). Global patterns of marine nitrogen fixation and denitrification. *Global Biogeochem. Cycles* 11, 235–266.

Guerrero, M. A., and Jones, R. D. (1996). Photoinhibition of marine

nitrifying bacteria. 2. Dark recovery after monochromatic or polychromatic irradiation. *Mar. Ecol. Prog. Ser.* 141, 193–198.

Hamersley, M. R., Lavik, G., Woebken, D., Rattray, J. E., Lam, P., Hopmans, E. C., et al. (2007). Anaerobic ammonium oxidation in the Peruvian oxygen minimum zone. *Limnol. Oceanogr.* 52, 923–933.

Hooper, A., Arciero, D., DiSpirito, A. A., Fuchs, J., Johnson, M., LaQuier, F., et al. (1990). "Production of nitrite and N_2O by the ammonia-oxidizing nitrifiers," in *Nitrogen Fixation: Achievements and Objectives,* eds R. Gresshoff, Stacey, and Newton (New York, NY: Chapman and Hall), 387–391.

Jensen, M. M., Lam, P., Revsbech, N. P., Nagel, B., Gaye, B., Jetten, M. S. M., et al. (2011). Intensive nitrogen loss over the Omani Shelf due to anammox coupled with dissimilatory nitrite reduction to ammonium. *ISME J.* 5, 1660–1670.

Karl, D., Letelier, R., Tupas, L., Dore, J., Christian, J., and Hebel, D. (1997). The role of nitrogen fixation in biogeochemical cycling in the subtropical North Pacific Ocean. *Nature* 388, 533–538.

Kim, K.-R., and Craig, H. (1990). Two-isotope characterization of N_2O in the Pacific Ocean and constraints on its origin in deep water. *Nature* 347, 58–61.

Koba, K., Osaka, K., Tobari, Y., Toyoda, S., Ohte, N., Katsuyama, M., et al. (2009). Biogeochemistry of nitrous oxide in groundwater in a forested ecosystem elucidated by nitrous oxide isotopomer measurements. *Geochim. Cosmochim. Acta* 73, 3115–3133.

Kroopnick, P., and Craig, H. (1976). Oxygen isotope fractionation in dissolved-oxygen in deep-sea. *Earth Planet. Sci. Lett.* 32, 375–388.

Kumar, S., Nicholas, D. J. D., and Williams, E. H. (1983). Definitive N-15 NMR evidence that water serves as a source of O during nitrite oxidation by *Nitrobacter-Agilis*. *FEBS Lett.* 152, 71–74.

Kuypers, M. M. M., Lavik, G., Woebken, D., Schmid, M., Fuchs, B. M., Amann, R., et al. (2005). Massive nitrogen loss from the Benguela upwelling system through anaerobic ammonium oxidation. *Proc. Natl. Acad. Sci. U.S.A.* 102, 6478–6483.

Lam, P., Lavik, G., Jensen, M. M., van de Vossenberg, J., Schmid, M., Woebken, D., et al. (2009). Revising the nitrogen cycle in the Peruvian oxygen minimum zone. *Proc. Natl. Acad. Sci. U.S.A.* 106, 4752–4757.

Lam, P., Jensen, M. M., Kock, A., Lettmann, K. A., Plancherel, Y., Lavik, G., et al. (2011). Origin and fate of the secondary nitrite maximum in the Arabian Sea. *Biogeosciences* 8, 1565–1577.

Law, C. S., and Ling, R. D. (2001). Nitrous oxide flux and response to increased iron availability in the Antarctic Circumpolar Current. *Deep Sea Res. Part II Top. Stud. Oceanogr.* 48, 2509–2527.

Lipschultz, F., Wofsy, S. C., Ward, B. B., Codispoti, L. A., Friedrich, G. J. W., and Elkins, J. W. (1990). Bacterial transformations of inorganic nitrogen in the oxygen-deficient waters of the Eastern Tropical South Pacific Ocean. *Deep Sea Res.* 37, 1513–1541.

Loescher, C. R., Kock, A., Koenneke, M., LaRoche, J., Bange, H. W., and Schmitz, R. A. (2012). Production of oceanic nitrous oxide by ammonia-oxidizing archaea. *Biogeosci. Discuss.* 9, 2095–2122.

Lomas, M. W., and Lipschultz, F. (2006). Forming the primary nitrite maximum: nitrifiers or phytoplankton? *Limnol. Oceanogr.* 51, 2453–2467.

Mackey, K. R. M., Bristow, L., Parks, D. R., Altabet, M. A., Post, A. F., and Paytan, A. (2011). The influence of light on nitrogen cycling and the primary nitrite maximum in a seasonally stratified sea. *Prog. Oceanogr.* 91, 545–560.

Mariotti, A., Germon, J. C., Hubert, P., Kaiser, P., Letolle, R., Tardieux, A., et al. (1981). Experimental determination of nitrogen kinetic isotope fractionation: some principles; Illustration for the denitrification and nitrification processes. *Plant Soil* 62, 413–430.

McIlvin, M. R., and Casciotti, K. L. (2006). Method for the analysis of $\delta^{18}O$ in water. *Anal. Chem.* 78, 2377–2381.

McIlvin, M. R., and Casciotti, K. L. (2010). Fully automated system for stable isotopic analyses of dissolved nitrous oxide at natural abundance levels. *Limnol. Oceanogr.* 8, 54–66.

Meador, T. B., Aluwihare, L. I., and Mahaffey, C. (2007). Isotopic heterogeneity and cycling of organic nitrogen in the oligotrophic ocean. *Limnol. Oceanogr.* 52, 934–947.

Merbt, S. N., Stahl, D. A., Casamayor, E. O., Marti, E., Nichol, G. W., and Prosser, J. I. (2012). Differential photoinhibition of bacterial and archaeal ammonia oxidation. *FEMS Microbiol. Lett.* 327, 41–46.

Mincer, T. J., Church, M. J., Taylor, L. T., Preston, C., Karl, D. M., and DeLong, E. F (2007). Quantitative distribution of presumptive archaeal and bacterial nitrifiers in Monterey Bay and the North Pacific Subtropical Gyre. *Environ. Microbiol.* 9, 1162–1175.

Naqvi, S. W. A., Noronha, R. J., and Reddy, C. V. G. (1982). Denitrification in the Arabian Sea. *Deep Sea Res.* 29, 459–469.

Naqvi, S. W. A., and Sen Gupta, R. (1985). "NO," a useful tool for the estimation of nitrate deficits in the Arabian Sea. *Deep Sea Res.* 32, 665–674.

Olson, R. J. (1981a). Differential photoinhibition of marine nitrifying bacteria: a possible mechanism for the formation of the primary nitrite maximum. *J. Mar. Res.* 39, 227–238.

Olson, R. J. (1981b). ^{15}N tracer studies of the primary nitrite maximum. *J. Mar. Res.* 39, 203–226.

Ostrom, N. E., Pitt, A., Sutka, R., Ostrom, P. H., Grandy, A. S., Huizinga, K. M., et al. (2007). Isotopologue effects during N_2O reduction in soils and in pure cultures of denitrifiers. *J. Geophys. Res.* 112, G02005.

Ostrom, N. E., Russ, M. E., Popp, B., Rust, T. M., and Karl, D. M. (2000). Mechanisms of nitrous oxide production in the subtropical North Pacific based on determinations of the isotopic abundances of nitrous oxide and di-oxygen. *Chemosphere Global Change Sci.* 2, 281–290.

Popp, B. N., Westley, M. B., Toyoda, S., Miwa, T., Dore, J. E., Yoshida, N., et al. (2002). Nitrogen and oxygen isotopomeric constraints on the origins and sea-to-air flux of N_2O in the oligotrophic subtropical North Pacific gyre. *Global Biogeochem. Cycles* 16, 1064.

Poth, M., and Focht, D. D. (1985). ^{15}N Kinetic analysis of N_2O produced by *Nitrosomonas europaea*: an examination of nitrifier denitrification. *Appl. Environ. Microbiol.* 49, 1134–1141.

Richards, F. A. (1965). "Anoxic basins and fjords," in *Chemical Oceanography, Vol. 1*, eds J. P. Riley and G. Skirrow (New York, NY: Academic Press), 611–645.

Santoro, A. E., Buchwald, C., McIlvin, M. R., and Casciotti, K. L. (2011). Isotopic signature of N_2O produced by marine ammonia-oxidizing archaea. *Science* 333, 1282–1285.

Santoro, A. E., Casciotti, K. L., and Francis, C. A. (2010). Activity, abundance, and diversity of nitrifying archaea and bacteria in the central California Current. *Environ. Microbiol.* 12, 1989–2006.

Santoro, A. E., and Casciotti, K. L. (2011). Enrichment and characterization of ammonia-oxidizing archaea from the open ocean: phylogeny, physiology and stable isotope fractionation. *ISME J.* 5, 1796–1808.

Schmidt, H.-L., Werner, R. A., Yoshida, N., and Well, R. (2004). Is the isotopic composition of nitrous oxide an indicator for its origin from nitrification or denitrification? A theoretical approach from referred data and microbiological and enzyme kinetic aspects. *Rapid Commun. Mass Spectrom.* 18, 2036–2040.

Sigman, D. M., Altabet, M. A., McCorkle, D. C., Francois, R., and Fischer, G. (2000). The delta N-15 of nitrate in the Southern Ocean: nitrogen cycling and circulation in the ocean interior. *J. Geophys. Res.* 105, 19599–19614.

Sigman, D. M., DiFiore, P. J., Hain, M. P., Deutsch, C., Wang, Y., Karl, D. M., et al. (2009). The dual isotopes of deep nitrate as a constraint on the cycle and budget of oceanic fixed nitrogen. *Deep Sea Res. Part I Oceanogr. Res. Pap.* 56, 1419–1439.

Sigman, D. M., Granger, J., DiFiore, P. J., Lehmann, M. F., Ho, R., Cane, R., et al. (2005). Coupled nitrogen and oxygen isotope measurements of nitrate along the eastern North Pacific margin. *Global Biogeochem. Cycles* 19, GB4024.

Snider, D. M., Venkiteswaran, J. J., Schiff, S. L., and Spoelstra, J. (2012). Deciphering the oxygen isotope composition of nitrous oxide produced by nitrification. *Global Change Biology* 18, 356–370.

Strous, M., Pelletier, E., Mangenot, S., Rattei, T., Lehner, A., Taylor, M. W., et al. (2006). Deciphering the evolution and metabolism of an anammox bacterium from a community genome. *Nature* 440, 790–794.

Sutka, R. L., Ostrom, N. E., Ostrom, P. H., Gandhi, H., and Breznak, J. A. (2003). Nitrogen isotopomer site preference of N_2O produced by *Nitrosomonas europaea* and *Methylococcus capsulatus* Bath. *Rapid Commun. Mass Spectrom.* 17, 738–745.

Sutka, R. L., Ostrom, N. E., Ostrom, P. H., Gandhi, H., and Breznak, J. A. (2004). Nitrogen isotopomer site preference of N_2O produced by *Nitrosomonas europaea* and *Methylococcus capsulatus* Bath.

Rapid Commun. Mass Spectrom. 18, 1411–1412.

Thamdrup, B., Dalsgaard, T., Jensen, M. M., Ulloa, O., Farias, L., and Escribano, R. (2006). Anaerobic ammonium oxidation in the oxygen-deficient waters off northern Chile. *Limnol. Oceanogr.* 51, 2145–2156.

Toyoda, S., Mutobe, H., Yamagishi, H., Yoshida, N., and Tanji, Y. (2005). Fractionation of N_2O isotopomers during production by denitrifier. *Soil Biol. Biochem.* 37, 1535–1545.

Toyoda, S., and Yoshida, N. (1999). Determination of nitrogen isotopomers of nitrous oxide on a modified isotope ratio mass spectrometer. *Anal. Chem.* 71, 4711–4718.

Voss, M., Dippner, J. W., and Montoya, J. P. (2001). Nitrogen isotope patterns in the oxygen-deficient waters of the Eastern Tropical North Pacific Ocean. *Deep Sea Res. Part I Oceanogr. Res. Pap.* 48, 1905–1921.

Wada, E., and Hattori, A. (1971). Nitrite metabolism in the euphotic layer of the central north Pacific Ocean. *Limnol. Oceanogr.* 16, 766–772.

Walker, C. B., de la Torre, J. R., Klotz, M. G., Urakawa, H., Pinel, N., Arp, D. J., et al. (2010). *Nitrosopumilus maritimus* genome reveals unique mechanisms for nitrification and autotrophy in globally distributed marine crenarchaea. *Proc. Natl. Acad. Sci. U.S.A.* 107, 8818–8823.

Wankel, S. D., Kendall, C., Pennington, J. T., Chavez, F. P., and Paytan, A. (2007). Nitrification in the euphotic zone as evidenced by nitrate dual isotopic composition: observations from Monterey Bay, California. *Global Biogeochem. Cycles* 21, GB2009.

Ward, B. B. (1985). Light and substrate concentration relationships with marine ammonium assimilation and oxidation rates. *Mar. Chem.* 16, 301–316.

Ward, B. B. (2005). Temporal variability in nitrification rates and related biogeochemical factors in Monterey Bay, California, USA. *Mar. Ecol. Prog. Ser.* 292, 97–109.

Ward, B. B., Devol, A. H., Rich, J. J., Chang, B. X., Bulow, S. E., Naik, H., et al. (2009). Denitrification as the dominant nitrogen loss process in the Arabian Sea. *Nature* 461, 78–81.

Ward, B. B., Kilpatrick, K. A., Renger, E., and Eppley, R. W. (1989). Biological nitrogen cycling in the nitracline. *Limnol. Oceanogr.* 34, 493–513.

Ward, B. B., Olson, R. J., and Perry, M. J. (1982). Microbial nitrification rates in the primary nitrite maximum off Southern-California. *Deep Sea Res. Part A Oceanogr. Res. Pap.* 29, 247–255.

Ward, B. B., Tuit, C. B., Jayakumar, A., Rich, J. J., Moffett, J., and Naqvi, S. W. A. (2008). Organic carbon, and not copper, controls denitrification in oxygen minimum zones of the ocean. *Deep Sea Res. Part I Oceanogr. Res. Pap.* 55, 1672–1683.

Ward, B. B., and Zafiriou, O. C. (1988). Nitrification and nitric oxide in the oxygen minimum of the eastern tropical North Pacific. *Deep Sea Res.* 35, 1127–1142.

Waser, N. A. D., Turpin, D. H., Harrison, P. J., Nielsen, B., and Calvert, S. E. (1998). Nitrogen isotope fractionation during the uptake and assimilation of nitrate, nitrite, and urea by a marine diatom. *Limnol. Oceanogr.* 43, 215–224.

Watson, S. W. (1965). Characteristics of a marine nitrifying bacterium, *Nitrosocystis oceanus sp. n. Limnol. Oceanogr.* 10(Suppl.), R274–R289.

Watson, S. W., Bock, E., Valois, F. W., Waterbury, J. B., and Schlosser, U. (1986). *Nitrospira marina* gen. nov. sp. nov.: a chemolithotrophic nitrite-oxidizing bacterium. *Arch. Microbiol.* 144, 1–7.

Watson, S. W., and Waterbury, J. B. (1971). Characteristics of two marine nitrite oxidizing bacteria, *Nitrospina gracilis* nov. gen. nov. sp. and *Nitrococcus* mobilis nov. gen. Nov. sp. *Arch. Microbiol.* 77, 203–230.

Wuchter, C., Abbas, B., Coolen, M. J. L., Herfort, L., van Bleijswijk, J., Timmers, P., et al. (2006). Archaeal nitrification in the ocean. *Proc. Natl. Acad. Sci. U.S.A.* 103, 12317–12322.

Yamagishi, H., Westley, M. B., Popp, B. N., Toyoda, S., Yoshida, N., Watanabe, S., et al. (2007). Role of nitrification and denitrification on the nitrous oxide cycle in the eastern tropical North Pacific and Gulf of California. *J. Geophys. Res. Biogeosci.* 112, G02015.

Yool, A., Martin, A. P., Fernandez, C., and Clark, D. R. (2007). The significance of nitrification for oceanic new production. *Nature* 447, 999–1002.

Yoshida, N. (1988). ^{15}N-depleted N_2O as product of nitrification. *Nature* 355, 528–529.

Yoshida, N., and Toyoda, S. (2000). Constraining the atmospheric N_2O budget from intramolecular site preference in N_2O isotopomers. *Nature* 405, 330–334.

Conflict of Interest Statement: The authors declare that the research was conducted in the absence of any commercial or financial relationships that could be construed as a potential conflict of interest.

Received: 05 August 2012; accepted: 18 September 2012; published online: 12 October 2012.

Citation: Casciotti KL and Buchwald C (2012) Insights on the marine microbial nitrogen cycle from isotopic approaches to nitrification. Front. Microbio. ***3****:356. doi: 10.3389/fmicb.2012.00356*

This article was submitted to Frontiers in Aquatic Microbiology, a specialty of Frontiers in Microbiology.

frontiers in
MICROBIOLOGY

ORIGINAL RESEARCH ARTICLE
published: 01 July 2013
doi: 10.3389/fmicb.2013.00177

Community composition of ammonia-oxidizing archaea from surface and anoxic depths of oceanic oxygen minimum zones

Xuefeng Peng, Amal Jayakumar and Bess B. Ward*

Department of Geosciences, Princeton University, Princeton, NJ, USA

Edited by:
Marlene M. Jensen, University of Southern Denmark, Denmark

Reviewed by:
Marco J. L. Coolen, Woods Hole Oceanographic Institution, USA
Xiang Xiao, Shanghai Jiao Tong University, China
Alyson E. Santoro, University of Maryland Center for Environmental Science, USA

***Correspondence:**
Bess B. Ward, Department of Geosciences, Princeton University, Guyot Hall, Princeton, NJ 08544, USA
e-mail: bbw@princeton.edu

Ammonia-oxidizing archaea (AOA) have been reported at high abundance in much of the global ocean, even in environments, such as pelagic oxygen minimum zones (OMZs), where conditions seem unlikely to support aerobic ammonium oxidation. Due to the lack of information on any potential alternative metabolism of AOA, the AOA community composition might be expected to differ between oxic and anoxic environments. This hypothesis was tested by evaluating AOA community composition using a functional gene microarray that targets the ammonia monooxygenase gene subunit A (*amoA*). The relationship between environmental parameters and the biogeography of the Arabian Sea and the Eastern Tropical South Pacific (ETSP) AOA assemblages was investigated using principal component analysis (PCA) and redundancy analysis (RDA). In both the Arabian Sea and the ETSP, AOA communities within the core of the OMZ were not significantly different from those inhabiting the oxygenated surface waters above the OMZ. The AOA communities in the Arabian Sea were significantly different from those in the ETSP. In both oceans, the abundance of archaeal *amoA* gene in the core of the OMZ was higher than that in the surface waters. Our results indicate that AOA communities are distinguished by their geographic origin. RDA suggested that temperature (higher in the Arabian Sea than in the ETSP) was the main factor that correlated with the differences between the AOA communities. Physicochemical properties that characterized the different environments of the OMZ and surface waters played a less important role, than did geography, in shaping the AOA community composition.

Keywords: ammonia-oxidizing archaea, oxygen minimum zone, Arabian sea, Eastern Tropical South Pacific, community composition, QPCR

INTRODUCTION

Nitrification plays a critical role in the marine nitrogen (N) cycle because it links the major sources (nitrogen fixation) and sinks (denitrification) of fixed reactive N by transforming ammonium to nitrite and subsequently nitrate. The importance of nitrification is also highlighted by its production of regenerated nitrate, which is taken up by phytoplankton, and which has implications for the estimate of export production from the euphotic zone of the ocean (Eppley and Peterson, 1979; Yool et al., 2007). Nitrification consists of two major steps, ammonia oxidation and nitrite oxidation, with ammonia oxidation considered to be the rate-limiting step (Kendall, 1998). Both steps are microbially mediated, although until recently, ammonia oxidation was thought to be accomplished only by ammonia-oxidizing bacteria (AOB). The discovery of the functional gene for ammonia oxidation, ammonia monooxygenase (*amo*), in archaea (Venter et al., 2004; Könneke et al., 2005; Treusch et al., 2005) led to the recognition that ammonia-oxidizing archaea (AOA) are ubiquitous in terrestrial and marine environments (Francis et al., 2005).

In several regions of the ocean, abundance of archaeal ammonia monooxygenase genes subunit A (*amoA*) was one to three orders of magnitude higher than the bacterial *amoA* gene abundance, enumerated by quantitative polymerase chain reaction (QPCR) (Wuchter et al., 2006a; Mincer et al., 2007; Agogue et al., 2008; Beman et al., 2008). Although the number of *amoA* gene copies per cell is reported to vary in the environment (Wuchter et al., 2006a; Agogue et al., 2008), the correlation between Thaumarchaeotal *amoA* and 16S rRNA gene abundances in the Arabian Sea indicates that most of the Thaumarchaeota are AOA (Pitcher et al., 2011). The sheer number of AOA relative to AOB suggests that they might be responsible for most of the ammonia-oxidation in the open ocean. The dominant role of AOA in ammonia-oxidation in the ocean is supported by a positive correlation between their abundance (implied from abundance of *amoA* or 16S rRNA genes) and ammonia-oxidation rates, observed in the Gulf of California (Beman et al., 2008), the North Sea (Wuchter et al., 2006a), and the coastal eastern Pacific (Santoro et al., 2010). Furthermore, there is evidence from the Southern California Bight (Ward, 1987), and the Gulf of California (Beman et al., 2008) that the abundance of AOB is decoupled from nitrification rates in the ocean.

However, a correlation between AOA abundance and ammonia oxidation rate is not always observed. In the Arabian Sea

oxygen minimum zone (OMZ), Newell et al. (2011) found high abundances of AOA ($>10^4$ copies ml^{-1}) both within the oxygen deficient waters and below them ($\geq$900 m depth), where ammonia oxidation rates were barely detectable. At an offshore Eastern Tropical South Pacific (ETSP) station, a local maximum of archaeal *amoA* gene abundance ($>10^4$ copies ml^{-1}) was found at 200 m in the OMZ where ammonia oxidation was not detected (Lam et al., 2009). In the Central California Current, AOA maintained high abundances at depths far below the bottom of the photic zone (on the order of 10^4 *amoA* copies ml^{-1} down to 500 m), where ammonia oxidation rates were very low (10 nM day^{-1}) (Santoro et al., 2010). This is intriguing because all known AOA (and AOB) are obligate aerobes. It is unknown what metabolism might support their growth in the Arabian Sea OMZ where neither oxygen nor ammonium is detectable, or in the deep water below the OMZ where ammonium supply and concentrations are very low, as are the measured ammonium oxidation rates.

Although there is no known alternative metabolism that might allow AOA to thrive in anoxic waters, AOA survival in OMZs could depend on unknown physiological capabilities. Such physiological differences might be reflected by differences in the composition of AOA communities in the anoxic depths of the OMZ relative to oxic waters. In order to assess whether the AOA community compositions within the OMZ differed from those above the OMZ, microarray analysis targeting the *amoA* gene was performed on DNA samples from both the Arabian Sea and the ETSP. Environmental parameters such as temperature and nutrient concentrations at these sites were also investigated using redundancy analysis (RDA) to determine their roles in shaping the AOA habitats. In addition, the abundance of archaeal *amoA* genes was quantified using QPCR.

Besides the environmental effects, the role of geographic separation on determining the community composition of AOA was also considered. A growing body of research has shown that microorganisms vary in community composition and abundance on different spatial scales, such as those summarized by Martiny et al. (2006). A phylogenetic study on AOA has shown that geography has a strong effect on their diversity (Pester et al., 2012). We hypothesized that the community composition of AOA from the Arabian Sea should differ from that from the ETSP, and tested the hypothesis with the microarray data.

MATERIALS AND METHODS

SITE DESCRIPTION

Samples from the Arabian Sea were collected as described by Newell et al. (2011) (**Table 1**). Briefly, in September 2007 on leg KNOX08 aboard the R/V Roger Revelle, samples were collected from above and within the anoxic depths at Stations 1, 2, and 3 in the open ocean OMZ. Stations 1 and 2 were within the permanent OMZ while Station 3 was on the periphery (**Figure 1A**; Newell et al., 2011). Samples from the ETSP were collected as described by Ward et al. (2009), in October 2005 aboard the R/V Knorr. Samples from above and within the anoxic core of the OMZ at six stations (12, 14, 19, 20, 24 and 26) off the coast of Peru were analyzed (**Figure 1B**, **Table 1**). Nutrient data for these sites has been reported previously (Ward et al., 2009; Bouskill et al., 2012).

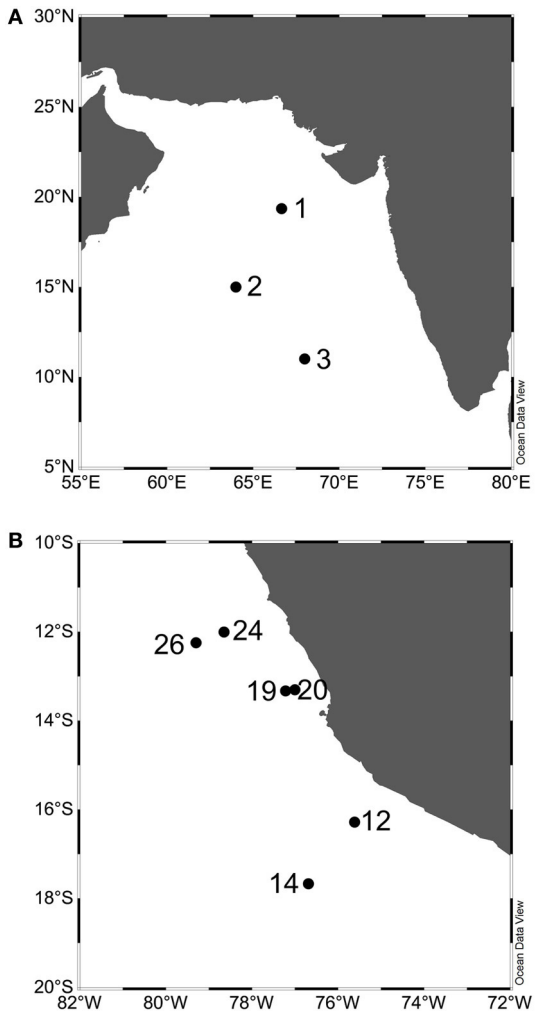

FIGURE 1 | Stations in the Arabian Sea (A) and the Eastern Tropical south Pacific (B). Maps were made using Ocean Data View (Schlitzer, 2012).

MICROARRAY HYBRIDIZATION AND QPCR

Seawater samples (up to 13 L) were filtered onto 0.2 μm pore size Sterivex filters (Millipore, Billerica, MA) using a peristaltic pump, and filters were flash frozen in liquid nitrogen and stored at −80°C. Total DNA was extracted from Sterivex filters using either the Puregene DNA kit (Gentra, Minneapolis, MN) or the AllPrep DNA/RNA Mini Kit (Qiagen Sciences, Maryland, USA) with slight modifications (as in Ward, 2008) to the manufacturer's instructions. The extraction procedures were performed twice on each Sterivex filter in order to maximize the DNA yield.

The archetype array approach used in this study has been published previously (Bulow et al., 2008; Ward and Bouskill, 2011). Using an established algorithm (Bulow et al., 2008), 31 different archetypes were identified representing 1329 archaeal *amoA* sequences from GenBank at the time of probe design (November 2008). Each 90-mer oligonucleotide probe consisted of a 70-mer archetype sequence combined with a 20-mer reference oligo as

Table 1 | Physicochemical data at the Arabian Sea and Eastern Tropical South Pacific stations.

Location	Station code	Latitude/Longitude	Sampling date	Depth (m)	Bottom depth (m)	Depth characteristics	Temp (°C)	Salinity (psu)	DO (μM)	NO_2^- (μM)	NO_3^- (μM)	Volume filtered (ml)
Arabian Sea	Station 1	19° 22.98′ N, 66° 39.35′ E	September 2007	10	3151	Surface	28.77	36.65	203.0	0	0	9,400
				60		Chlorophyll max	23.20	36.10	22.2	0.2	11.4	10,400
				102		Oxycline	20.16	35.95	0.8	0.39	25.22	13,100
				150		Core of OMZ	17.87	35.76	1.1	5.24	15.92	11,610
				175		Core of OMZ	16.95	35.85	0.7	4.6	15.54	14,700
	Station 2	15° 00.00′ N, 64° 00.00′ E		10	3900	Surface	27.98	35.94	185.4	0	0.07	10,820
				150		Oxycline	20.14	35.95	0.6	0.57	22.36	12,800
				200		Core of OMZ	17.26	35.71	0.6	6.37	9.97	12,800
	Station 3	11° 00.00′ N, 68° 00.00′ E		10	4383	Surface	28.32	36.41	195.1	0	0.07	11,300
				110		Oxycline	20.79	35.85	1.2	0.06	25.76	12,600
				150		Core of OMZ	17.60	35.57	0.6	3.78	19.68	12,300
Eastern Tropical South Pacific	Station 12	16° 16.86′ S, 75° 36.76′ W	October 2005	20	4263	Surface	*13.56*	*34.83*	*220.0*	*0.70*	*10*	4,300
				260		Core of OMZ	10.80	34.74	2.0	0.54	22.20	8,600
	Station 14	17° 40.27′ S, 76° 41.27′ W		20	4200	Surface	13.56	34.83	*220.0*	0.00	2.04	4,300
				260		Core of OMZ	*10.80*	*34.74*	2.1	5.20	21.4	8,600
	Station 19	13° 19.99′ S, 77° 13.00′ W		20	1450	Surface	14.50	34.97	115.0	1.38	*19.60*	8,000
				260		Core of OMZ	11.16	34.81	2.0	2.55	*41.40*	8,600
	Station 20	13° 18.38′ S, 76° 59.87′ W		20	788	Surface	14.54	34.96	121.0	1.43	*12.50*	4,300
				260		Core of OMZ	11.49	34.83	2.1	4.38	*23.35*	4,000
	Station 24	12° 14.99′ S, 79° 18.00′ W		20	4930	Surface	16.96	34.96	235.0	0.80	*13.00*	4,300
				260		Core of OMZ	11.75	34.85	1.9	3.58	*26.9*	8,600
	Station 26	12° 00.50′ S, 78° 38.73′ W		20	3490	Surface	16.09	35.03	195.0	1.13	*11.70*	4,300
				260		Core of OMZ	11.20	35.03	2.1	5.21	*22.40*	8,600

Values in italic fonts are interpolated from nearby depths profiles taken at the same stations. DO, dissolved oxygen.

an internal standard. Targets for microarray hybridization were prepared according to Ward and Bouskill (2011), hybridized in duplicate on a microarray slide and washed as described previously (Ward and Bouskill, 2011). Washed slides were scanned using a laser scanner 4200 (Agilent Technologies, Palo Alto, CA) and analyzed with GenePix Pro 6.0 (Molecular Devices, Sunnyvale, CA). All of the original array files are available at NCBI (National Center for Biotechnology Information) GEO (Gene Expression Omnibus; http://www.ncbi.nlm.nih.gov/geo/) database, accession GSE46851.

Archaeal *amoA* abundances were quantified using primers Arch-amoAF (5′-STAATGGTCTGGCTTAGACG-3′) and Arch-amoAR (5′-GCGGCCATCCATCTGTATGT-3′) (Francis et al., 2005). A plasmid containing an archaeal *amoA* fragment was constructed by TOPO TA Cloning (Invitrogen, Grand Island, NY). To make a standard curve, eight serial dilutions of the plasmid DNA were made and quantified using Quant-iT PicoGreen (Invitrogen, Grand Island, NY). Assays in triplicates were performed in a Stratagene Mx3000P QPCR system (Agilent Technologies, La Jolla, CA). Each 25-μl reaction included 12.5 μl of GoTaq qPCR Master Mix (Promega, Madison, WI), 0.4 μM of each primer, 2 mM of $MgCl_2$, and 2 ng of DNA template. The following thermal cycle was used to amplify archaeal *amoA* genes: 5 min of initial denaturation at 95°C, followed by 40 cycles of 94°C for 45 s, 53°C for 45 s, and 72°C for 1 min, and ending with 1 min at 95°C and a final elongation at 72°C for 15 min. All of the reactions were performed in a single 96-well plate. Dissociation curves of the QPCR products were checked to ensure the purity of the products. Cycle thresholds were determined automatically using MxPro QPCR Software (Agilent Technologies, La Jolla, CA). After calculating the number of archaeal *amoA* copies in each reaction, the final result was normalized to copies per milliliter of seawater (necessarily assuming 100% recovery) as:

$$\frac{\text{[archaeal } amoA \text{ copy number } \times \text{ amount of DNA extracted from the Sterivex filter(ng)]}}{\text{[amount of DNA used in the reaction (ng) } \times \text{volume of seawater filtered (ml)]}}$$

DATA ANALYSIS

Quantification of hybridization signals was performed as described previously (Ward and Bouskill, 2011) with the following modifications. For each channel [532 nm (Cy3) and 635 nm (Cy5)], the average background fluorescence was recalculated after excluding background fluorescence values greater than the upper whisker of all the background fluorescence values. The upper whisker was defined as the 75th percentile plus 1.5 times the difference between the 25th and 75th percentiles. Such a filtering process was applied within each block on a microarray to account for variability in background fluorescence between blocks within an array. Another filter was applied to remove anomalous values of Cy3:Cy5 ratios among the triplicate features. This filter excluded any feature with a test statistic Z greater than 1.9 (CI = 80%) where Z is calculated as:

$$Z_i = \frac{r_i}{s/\sqrt{3}}, i = 1, 2, \text{ or } 3,$$

where r_i represents the ratio of Cy3 to Cy5, *s* the standard deviation of the three Cy3:Cy5 ratios. The raw microarray image was checked to ensure that the eliminated features actually exhibited anomalous hybridization signals. Then a normalized fluorescence ratio (FRn) for each archetype was calculated by dividing the fluorescence signal of the archetype by the highest fluorescence signal within the same array. The FRn of each archetype from the duplicate arrays were averaged. The relative fluorescence ratio (RFR) of each archetype was calculated as the contribution of FRn of the archetype to the sum of FRn of all AOA archetypes on the array. All of the data analyses above were performed using Microsoft Excel, and the following multivariate analyses on the array data were performed using R (R Core Team, 2012).

To explore the relationship between AOA communities from different stations and depths, a principal component analysis (PCA) was performed after the community composition data were transformed for chord distance (Legendre and Gallagher, 2001). Redundancy analysis (RDA) was performed using the FRn of each AOA archetype (after chord transformation) as the response variables, and temperature, dissolved oxygen (DO), nitrate and nitrite concentrations, and archaeal *amoA* abundance as explanatory variables. After a square root transformation, all explanatory variables were centered (divided by the standard deviation after the mean of each variable was subtracted). Depth and salinity were not included in the RDA because they had high linear dependence on temperature and dissolved oxygen. Linear dependencies between the environmental variables were examined by calculating variance inflation factors (VIF), and including one or both of these two variables in the RDA largely inflated VIFs of temperature and dissolved oxygen (>16) (Borcard et al., 2011). The VIFs of the five explanatory variables chosen for the RDA were reasonably low (from 2.4 to 4.2). Excluding depth and salinity from the RDA sacrificed a minimal amount of the variance captured by the first two axis of the RDA (<2%).

The hypothesis that the AOA community composition differed between surface depths and OMZ depths, in the Arabian Sea and in the ETSP respectively, was tested using Multi-response Permutation Procedure (MRPP) for its relaxed requirements on the data distribution and the convenience to relate the analysis visually to the biplots from PCA (Zimmerman et al., 1985). MRPP was also used to test the null hypothesis that the AOA community composition in the Arabian Sea was the same as that in the ETSP. A significance level of 5% was chosen.

RESULTS

PHYSICOCHEMICAL PROPERTIES

There was a large temperature gradient (∼10°C) between the surface and the core of the OMZ in the Arabian Sea, while the temperature difference was smaller in the ETSP (**Table 1**). The temperatures at sampled depths in the Arabian Sea were significantly higher than those in the ETSP ($P < 0.001$). The variability in salinity between different depths was small in both the Arabian Sea and the ETSP, but the salinities in the Arabian Sea were significantly higher than those in the ETSP ($P < 0.001$). Dissolved oxygen concentrations were below detection in the core of the OMZ where an accumulation of nitrite (up to 6.4 μM) was observed in both the Arabian Sea and the ETSP.

ARCHAEAL AMOA GENE ABUNDANCE

Archaeal *amoA* gene abundances were lower in the surface (from just over 500 to just under 10,000 copies mL^{-1}) than in the anoxic core of the OMZ (over 10,000 copies mL^{-1} in most samples) at all stations except at Station 1 in the Arabian Sea (**Figure 2**). At Station 1 in the Arabian Sea, archaeal *amoA* gene abundance was the lowest in the chlorophyll maximum (479 copies mL^{-1}), and the highest at the bottom of the oxycline right above the anoxic depths (36,537 copies mL^{-1}, **Figure 2A**). At Stations 2 and 3 in the Arabian Sea, the archaeal *amoA* gene abundance at the oxycline was much higher than that in the surface, reaching >10,000 copies mL^{-1}. At both surface and the anoxic depths of the OMZ, the archaeal *amoA* gene abundances were comparable between the Arabian Sea and the ETSP (**Figure 2**).

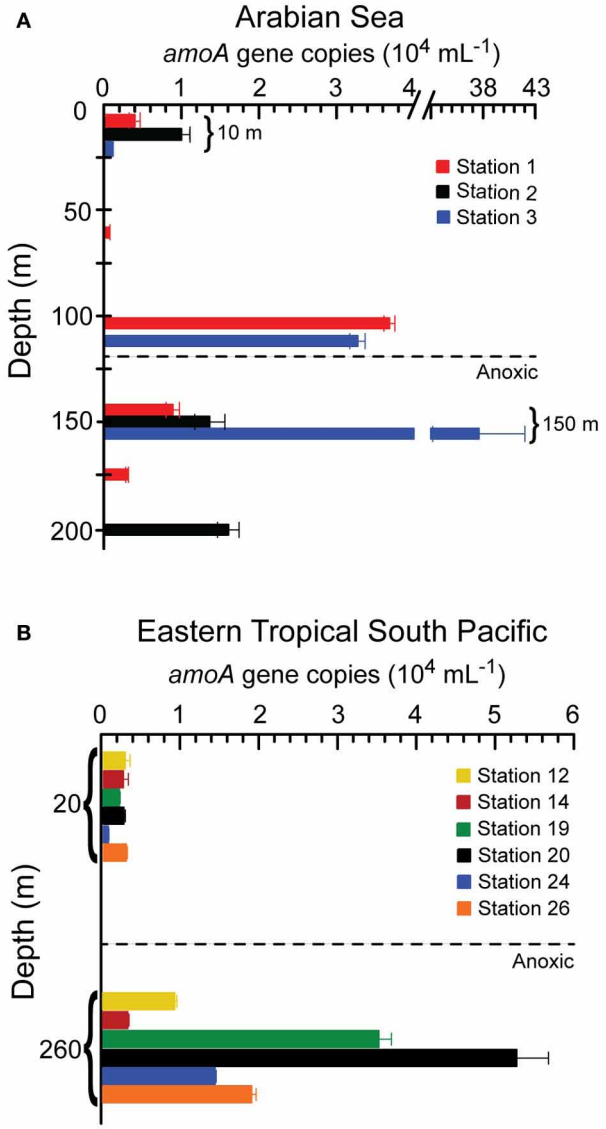

FIGURE 2 | Archaeal *amoA* abundance in copies mL^{-1} at different depths in the Arabian Sea (A) and the Eastern Tropical South Pacific (B). Error bars represent standard deviations of the triplicates in the QPCR run. In some cases the error bars were shorter than the width of the symbol and hence not visible. Different depths were sampled at different stations, so missing bars do not imply zero abundance, rather that samples were not analyzed at those depths.

COMMUNITY COMPOSITION ANALYSIS

In the Arabian Sea, three OMZ AOA assemblages clustered closely (AS1.175 m, AS2.200 m, and AS3.150 m). Nevertheless, the four communities from the anoxic core of the OMZ taken together were not significantly different from the surface communities (**Table 2**) because one OMZ community (AS1.150 m) was very dissimilar from the rest of the OMZ communities (**Figure 3**). AOA assemblages from the oxycline differed significantly from the OMZ assemblages in the Arabian Sea ($P < 0.05$, **Table 2**), even though the measured physicochemical properties in the oxycline were more similar to those in the OMZ than to those in the surface (**Table 1**). The AOA community from the chlorophyll maximum (AS1.60 m) was separated from most of the other AOA communities in the Arabian Sea, and it was ordinated closely to some of the AOA communities in the ETSP such as E24.20 m (**Figure 3**). One surface assemblage in the Arabian Sea (AS2.10 m) was the most similar to ETSP AOA communities (**Figure 3**).

In the ETSP, there was no significant separation between the AOA communities from the core of the OMZ and those from the surface (**Figure 3**, **Table 2**). Most AOA assemblages in the ETSP were characterized by positive values along the first principal component (PC1) (**Figure 3**). The AOA communities in the ETSP OMZ were significantly different from those in the Arabian Sea OMZ, oxycline, and surface, respectively (**Table 2**). Overall, AOA communities in the Arabian Sea were significantly different from those in the ETSP ($P < 0.001$), as evident in the PCA biplot (**Figure 3**). The first two components of PCA, which do not include any environmental variables, captured 76.2% of the variation of the AOA community structure (**Figure 3**).

About a third (11 out of 30) of the AOA archetypes contributed strongly (labeled vectors) to the first two principal components (**Figure 3**). In fact, these 11 AOA archetypes contributed over 70% of the total community RFR in most of the samples (**Figure 4**). Six of them (AOA -4, -10, -17, -19, -21, and -22) contributed to a relatively larger percentage of the total community RFR in the Arabian Sea than in the ETSP (**Figures 3** and **4**). The other five of the 11 important archetypes (AOA -9, -12, -15, -23, and -26) were relatively more abundant in the ETSP than in the Arabian Sea.

Table 2 | Summary of *p* values of Multi-Response Permutation Procedure comparing different AOA communities pairwise.

	AS surface	AS Oxycline	AS OMZ	ETSP surface
AS Oxycline	n.s.			
AS OMZ	n.s.	0.045		
ETSP surface	n.s.	n.s.	0.005	
ETSP OMZ	0.022	0.010	0.003	n.s.

The p value is the probability of a smaller or equal test statistics (Zimmerman et al., 1985). Only the p values smaller than 0.05 were shown. AS: Arabian Sea. ETSP: Eastern Tropical South Pacific. OMZ: oxygen minimum zone, n.s.: not significant.

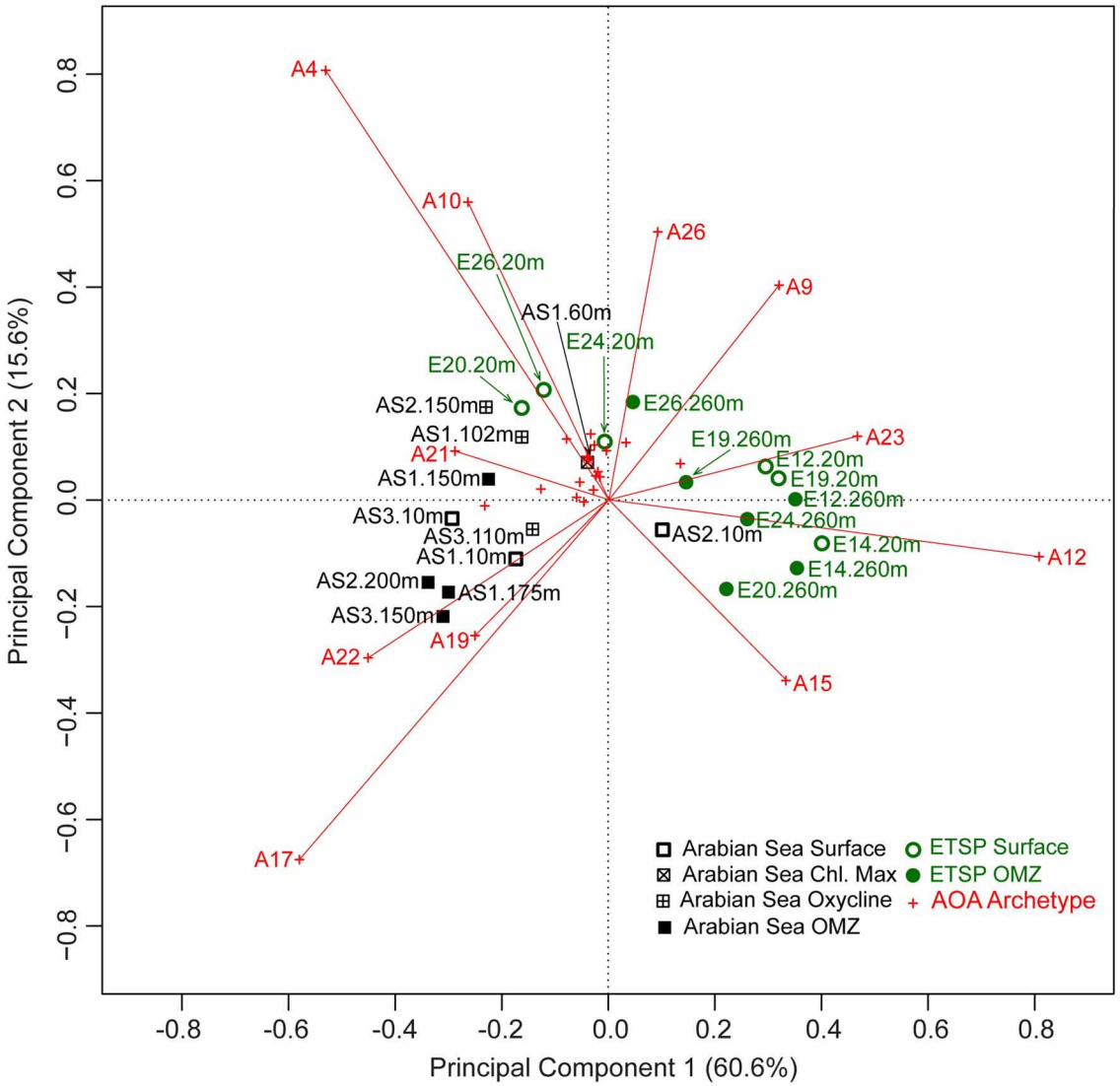

FIGURE 3 | Distance biplot of principal component analysis (PCA) on AOA community composition from the Arabian Sea and the ETSP using chord distance. Each AOA archetype is shown as a red cross. AOA archetypes that had a relatively high contribution to the two principal components plotted were highlighted by labeling them with "A archetype number," and drawing the vector between the origin and the AOA archetype. Circles represent samples from the ETSP (E), and squares represent samples from the Arabian Sea (AS). Hollow symbols represent samples from oxygenated surface waters; filled symbols represent samples from anoxic waters. Squares filled with a vertical cross represent samples from the oxycline, and the square filled with a rotated cross represents the sample from the chlorophyll maximum at Station 1 in the Arabian Sea. Distances among AOA communities are approximations of their Euclidean distance in the multidimensional space (Borcard et al., 2011).

The redundancy analysis (RDA) showed that temperature played an important role in the dispersion of the sites along the first axis (RDA1), which captured 43.2% of the variation of the dataset (**Figure 5**). Most AOA communities in the Arabian Sea were associated with higher temperature compared to AOA communities in the ETSP. The relative abundances of the group of AOA archetypes that were more abundant in the ETSP than in the Arabian Sea (AOA -9, -12, -15, -23, and -26) were positively correlated with dissolved oxygen and nitrate concentration. The group of AOA archetypes with higher RFR in the Arabian Sea than in the ETSP (AOA -4, -10, -17, -19, -21, and -22) were characterized by high temperature. When the number of archaeal *amoA* gene copies was high, archetypes AOA -17 and -22 made up a greater proportion of the AOA community than when the number of archaeal *amoA* gene copies was low. The opposite is true for archetypes AOA -9 and -26 (**Figure 5**).

DISCUSSION

Microarrays offer high throughput compared to other molecular methods such as building clone libraries (Ward and Bouskill, 2011) and therefore facilitate greater sample coverage and replication (Bouskill et al., 2012). In the archetype approach used

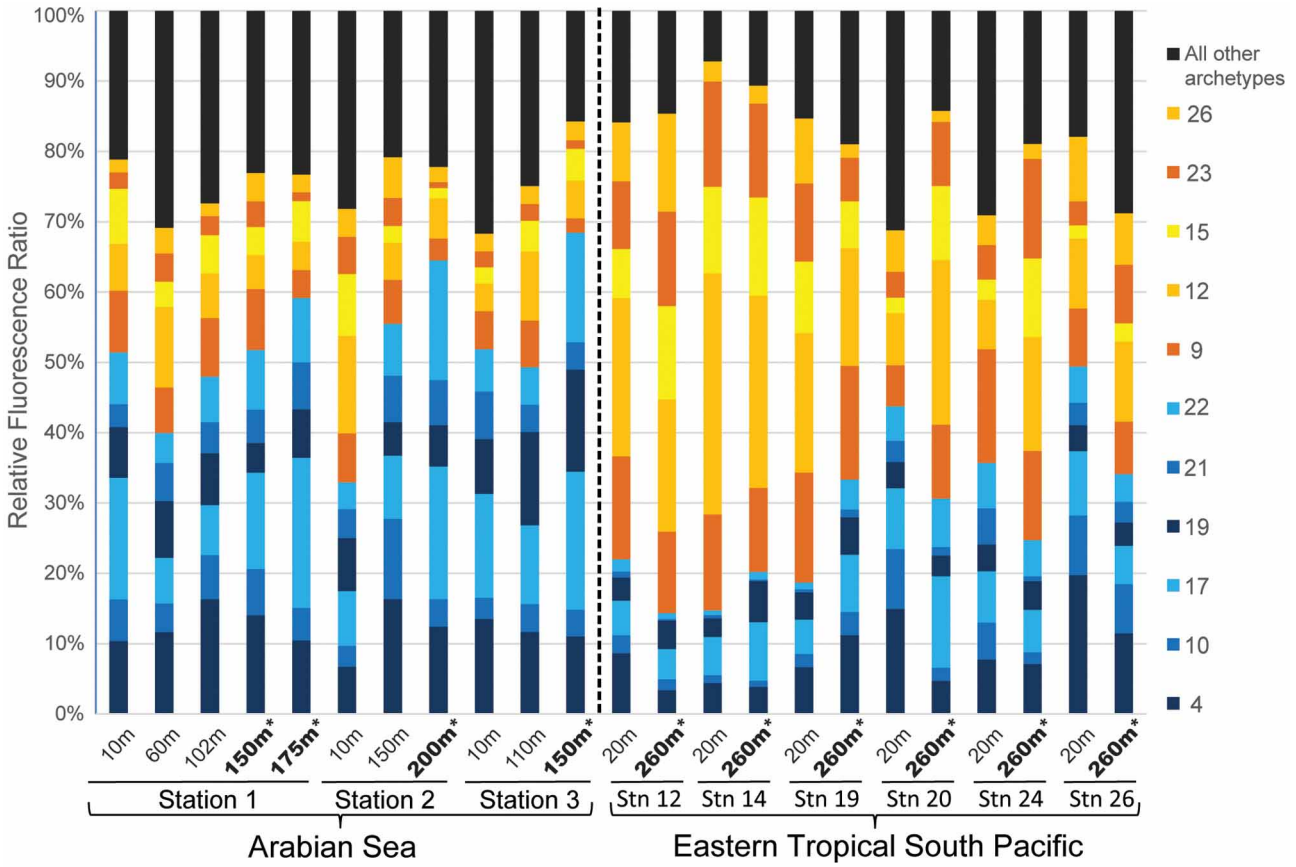

FIGURE 4 | Relative fluorescence ratios (RFR) of archaeal *amoA* archetypes from samples collected in the Arabian Sea and the ETSP. Numbers in the legend represent the AOA archetype identification number. The AOA archetypes that were important constituents of the Arabian Sea communities were shown in blue, while the AOA archetypes that were important constituents of the ETSP communities were shown in orange. The rest of the AOA archetypes were grouped and shown in black. Samples from the anoxic depths were highlighted in bold and with an asterisk.

here, each probe represents all sequences within 87 ± 3% of its 70-mer sequence (Taroncher-Oldenburg et al., 2003). Our knowledge of the ranges of environments that each AOA archetype represents has expanded since the development of the microarray used in this study due to rapid growth of the sequence database (Biller et al., 2012; Pester et al., 2012). The thousands of new AOA *amoA* sequences, which have been reported since the time of the array design, make it clear that the current array cannot represent the entire AOA diversity. Although most of the additional diversity has been reported from soils, there are many archetypes detected in marine samples that are not represented on the array. Therefore, the patterns we observed, based on the limited sequence database available in GenBank in 2009, can still provide valuable insight on AOA community composition and its variation in space and time, but cannot be extrapolated to unrepresented members of the AOA assemblage.

SIMILARITY IN AOA COMMUNITY COMPOSITION BETWEEN THE OXIC AND THE ANOXIC DEPTHS OF THE OMZ

Contrary to our hypothesis, AOA communities from oxic and anoxic depths of OMZs were not significantly different. The oxygen level at the OMZ core depth (260 m) in the ETSP has recently shown to be truly anoxic by highly sensitive STOX oxygen sensors with a detection limit of 10 nM (Thamdrup et al., 2012). Because molecular oxygen is required for aerobic ammonia oxidation, it was unlikely that the AOA communities found in anoxic depths were oxidizing ammonia aerobically. They might be simply inactive at a low energy state, or they might be capable of other metabolisms, which allow them to exist under oxygen-limiting conditions. For example, *Candidatus Nitrosoarchaeum limnia*, an AOA enriched from low salinity environments had a minimum oxygen requirement for growth between 29 and 59 μM (Mosier et al., 2012). The half-saturation concentration (K_m) for oxygen of the only pure marine AOA isolate, *Nitrosopumilus maritimus*, was 3.9 μM (Martens-Habbena et al., 2009). A marine sedimentary AOA in coculture with sulfur-oxidizing bacteria was reported to have a similar K_m, 2.0 μM (Park et al., 2010). Dalsgaard et al. (2013) reported an extremely low K_m (330 nM) for oxygen in a water sample from the anoxic depth in the ETSP. Despite their small genome and apparently restricted metabolic repertoire, AOA might be capable of multiple lifestyles across ecologically significant environmental variation. A recent study on

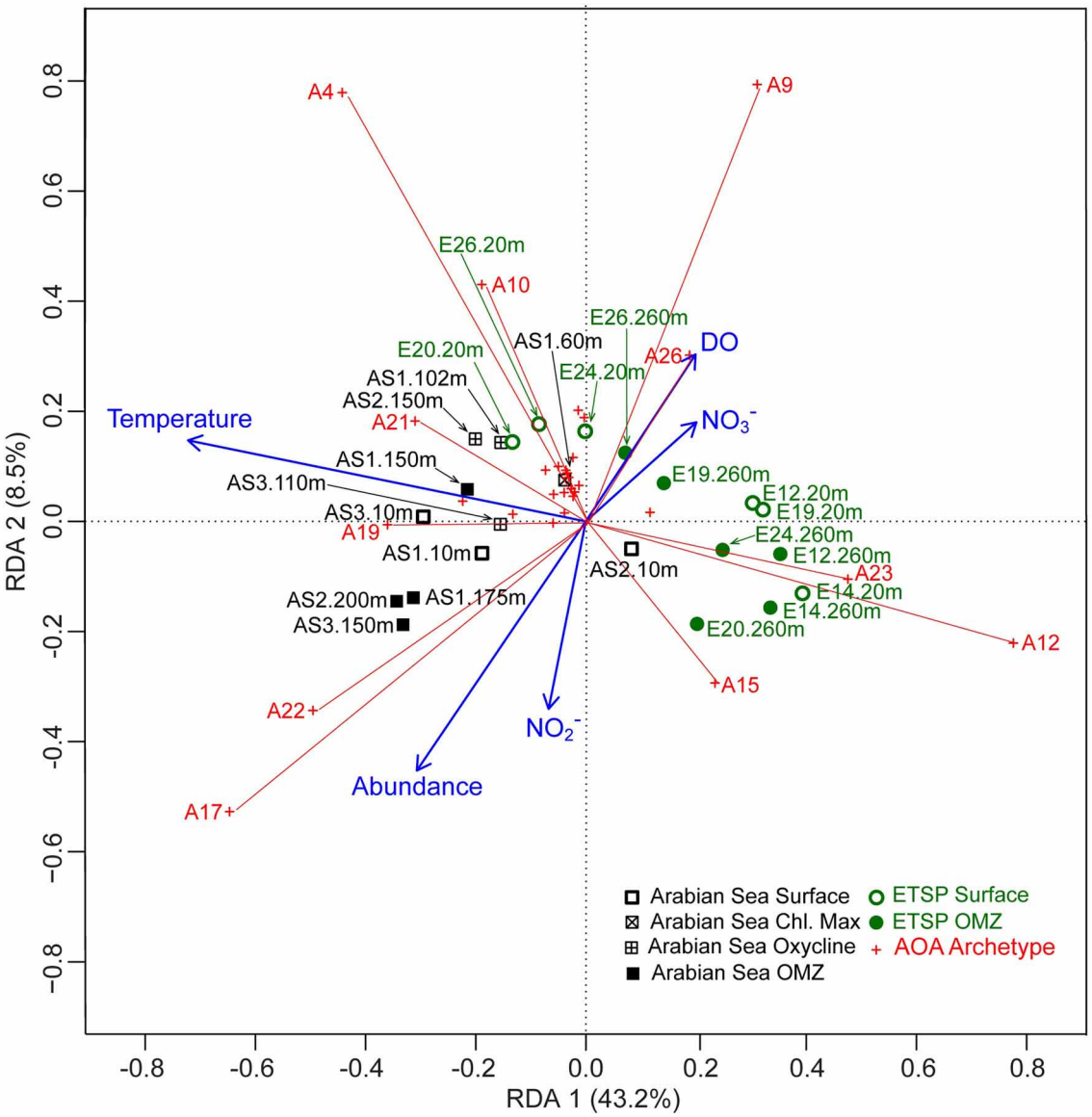

FIGURE 5 | Distance triplot of redundancy analysis (RDA) on AOA community composition from the Arabian Sea and the ETSP, using temperature, dissolved oxygen (DO), archaeal *amoA* abundance, nitrite concentration (NO_2^-), and nitrate concentration (NO_3^-) as explanatory variables. Symbols used here for AOA archetypes and sample stations are the same as described in **Figure 3**. The blue arrows are the vectors of the explanatory variables. Distances among AOA communities are approximation of their Euclidean distance in the multidimensional space. The length of the projection of any sample onto an archetype approximates the RFR of the archetype in that sample. The angles between an environmental variable and an archetype reflect their correlations (Borcard et al., 2011).

the global distribution of AOA using over 6200 archaeal *amoA* gene sequences found no difference between the AOA in oxic and oxygen-limiting environments (Cao et al., 2013).

On the other hand, it is worth noting that differences in microbial diversity have been attributed to selective pressure from physical/chemical conditions at different depths of the water column in the OMZ by other authors. For example, a significant difference between the bacterial community structure of the surface and the anoxic core of the ETSP OMZ was revealed using 16S rRNA clone libraries at the class level (Stevens and Ulloa, 2008). The microarray data suggest that these same selective pressures are not sufficient to differentiate among AOA at the archetype level, which is defined by the most variable 70 bp region of all archaeal *amoA* sequences at the time of the array development. A phylogenetic study on the archaeal *amoA* sequences from the ETSP OMZ showed that although some AOA operational taxonomic units (OTUs) were present in both the well-oxygenated depths and the anoxic depths, a distinct cluster of AOA OTUs were found only in the anoxic depths of the permanent and seasonal OMZ (Molina et al., 2010).

Another possible explanation for the lack of difference between surface and deeper AOA communities is that there was some type of vertical exchange of AOA. Mixing is unlikely due to the strong stratification of the water column in the Arabian Sea and the ETSP (Rao et al., 1989; Fiedler and Talley, 2006). Autonomous movement by AOA is improbable, since most AOA strains reported so far do not exhibit motility (Könneke et al., 2005; Santoro and Casciotti, 2011; Tourna et al., 2011). The only strain reported to have the potential for motility was from low-salinity marine sediments (Mosier et al., 2012). In any case, individual cells simply cannot autonomously travel a distance on the scale of tens or hundreds of meters. There might be particle flux that could bring surface communities down into the OMZ. In the Eastern Tropical North Pacific, another major oceanic OMZ, downward flux of particle-associated bacterial nitrifiers was reported (Karl et al., 1984). It is possible that AOA investigated in this study were also associated with downward particle flux in the OMZs. If this was true, then the samples from the anoxic depths should have included AOA communities from the surface, which would lessen any potential difference in community composition between the oxic and the anoxic depths. In the Arabian Sea glycerol dialkyl glycerol tetraether (GDGT), a lipid produced by marine Crenarchaea, was associated with downward particle flux (Wuchter et al., 2006b). On the other hand, enumeration of AOA with catalyzed reporter deposition fluorescence *in situ* hybridization (CARD-FISH) showed that most of the marine Crenarchaea were free-living (Woebken et al., 2007). It seems likely that preferential association with particles would not be adaptive for the lifestyle of tiny autotrophic microbes, which is selective for the planktonic state. Thus the importance of vertical transport remains questionable.

ARCHAEAL AMOA ABUNDANCE

Although no difference in AOA community structure was found between the surface and the anoxic core of the OMZ, there was a large difference in the abundance of archaeal *amoA* genes between these depths at most stations (**Figure 2**). The low abundance of archaeal *amoA* genes at surface depths was expected because AOA are inhibited by light (Merbt et al., 2012) and ammonia oxidation rates in the upper euphotic zone are usually very low. It is likely that our sampling missed the highest abundances of AOA because we did not sample the depth of the primary nitrite maximum, where local abundance maxima in numbers and rates are often reported (e.g., Beman et al., 2008; Coolen et al., 2007; Newell et al., 2011).

The high abundance of archaeal *amoA* gene in the anoxic core of the OMZs was enigmatic, but consistent with numerous previous reports in OMZs (e.g. Beman et al., 2008; Newell et al., 2011; Pitcher et al., 2011; Bouskill et al., 2012). On the other hand, rates of ammonia oxidation (Newell et al., 2011) at the same stations (different depths) showed the characteristic distribution of highest rates in the oxic layer and low to negligible rates within and below the OMZ. The rate maximum was generally deeper than the depth from which the array sample was collected so no direct comparisons can be made between rates and community composition. Still it is striking that the arrays detected essentially the same community composition across depths that likely varied a great deal in ammonia oxidation rates. The archaeal *amoA* gene abundances in the ETSP measured in this study were consistent with previously reported values in the same region. For example, Station 26 in the ETSP in this study was close to Station 7 from Lam et al. (2009), and the archaeal *amoA* gene abundances in the surface and the core of the OMZ reported in this study were very similar to those from Lam et al. (2009). The archaeal *amoA* gene abundances in the Arabian Sea measured in this study, although similar to those in the ETSP, were generally an order of magnitude lower compared to previous studies (Newell et al., 2011; Pitcher et al., 2011; Bouskill et al., 2012).

BIOGEOGRAPHY

AOA communities differed significantly between the Arabian Sea and the ETSP, suggesting that geographical variation exerts a strong control over the community structure of AOA. Among the four physicochemical variables investigated, temperature was the most important factor that distinguished the AOA communities in the Arabian Sea from those in the ETSP (**Figure 5**). This regional pattern is consistent with the findings of Pester et al. (2012) who analyzed AOA *amoA* genes in soil from Namibia, Costa Rica, Austria, and Greenland. They found that AOA community composition was different among these four locations, and geographic location on the continental scale had a strong effect on the presence or absence of different AOA taxa in individual soils. Pester et al. (2012) identified total nitrogen concentration, organic carbon content, and pH as major driving forces for AOA community structure in soils. However, in a biogeographic study on AOB in soils, temperature was most strongly correlated with AOB community structure among the suite of environmental variables measured (Fierer et al., 2009). Both this study and the study by Pester et al. (2012) lend support to the hypothesis that marine microplankton display biogeographic patterns. In a study that surveyed bacterioplankton communities using clone libraries in nine geographically distinct regions of the world ocean, 69% of the operational taxonomic units were endemic (Pommier et al., 2007).

Biller et al. (2012) investigated the factors correlated with global genotype distribution of AOA *amoA* based on over 8000 *amoA* sequences from literature and public databases. They found that, on the first level, habitat type accounted for the greatest variability in the dataset, separating AOA into 13 groups. On a second level, temperature, latitude, water depth, and salinity were significantly associated with AOA community composition, although the correlation was weak to moderate in the case of temperature and latitude. Their conclusions are consistent with the biogeographic separation between the AOA communities from the two different oceans in our study. All of our samples fell into the "ocean water column" habitat type on the first level, as defined by Biller et al. (2012). On the second level, temperature had the most pronounced influence on the distinction between the AOA communities analyzed in our study. Different types of AOA might each have a temperature optimum for growth, and this could lead to difference in community composition if the temperature optima for different AOA have little overlap. Due to the lack of direct investigation on the effect of temperature

on the AOA community composition, it remains unclear how temperature determines the distribution of AOA. Since both sites in this study were in low latitudes (<23.4°, **Table 1**), the geographic distinction in the AOA communities found between the Arabian Sea and the ETSP indicates that variables other than latitude are important in determining AOA community composition.

A CLOSER LOOK AT COMMUNITY COMPOSITION PATTERNS AT THE ARCHETYPE LEVEL

We found it intriguing that in the Arabian Sea, the AOA communities in the oxycline differed significantly from those in the OMZ, and that AOA communities in the OMZ were more closely related to surface AOA communities (**Figure 3**), even though the oxycline is characterized by physicochemical properties much more similar to the OMZ compared to the surface (**Table 1**). The community composition difference is largely attributable to high RFRs of AOA-4 and -10 but low RFRs of AOA-17, -19, and -22 in the oxycline AOA communities (**Figure 3**). Highest ammonium oxidation rates were reported previously from the oxycline region (Newell et al., 2011), suggesting that archetypes AOA-4 and AOA-10 might represent the most active groups.

The same collection of AOA archetype probes and microarray approach were used to assess AOA diversity in a wide range of marine environments including the Chesapeake Bay, Sargasso Sea, the North Atlantic, as well as the Arabian Sea and the ETSP (Bouskill et al., 2012). Geographic location was also the major factor that distinguished different AOA assemblages in their study. The AOA communities in the Arabian Sea were different from those in the ETSP in their study, but the AOA archetypes that characterized these two geographic locations (AOA-3, -11, -16, -20, -22, -25, -29, and -31 for the Arabian Sea; AOA-1, -2, -8, -10, -21, -23, -28, -30 for the ETSP) were mostly different from the important archetypes in our study. This might be explained by the fact that environmental variables were included in the unconstrained ordination (PCA) in Bouskill et al. (2012), which is not the case in our study where environmental variables were only included in the constrained ordination (RDA) (Legendre and Gallagher, 2001). Nevertheless, the AOA archetypes with the highest RFRs (AOA-9, -12, -4, -26, and -17) found by Bouskill et al. (2012) were also important in defining the community structure of AOA assemblages in the present study (**Figures 3** and **4**).

It is worth noting that archetype AOA-1, which represents the largest number of AOA sequences in GenBank at the time of the microarray development, contributed only minimally to all of the AOA communities in our study. Archetype AOA-1 represents the cultivated marine strain *N. maritimus* and a large number of sequences retrieved with primers designed using *N. maritimus* sequence (e.g., Francis et al., 2005; Beman and Francis, 2006; Santoro et al., 2008; Zhang et al., 2008). The underrepresentation of AOA-1 in our samples suggests that *N. maritimus* is not necessarily representative of the AOA assemblages in the global ocean. This is consistent with the finding that AOA clone libraries constructed with seawater samples from the Gulf of California did not recover any *N. maritimus*-like sequences (Beman et al., 2008). Therefore it is critical to isolate other AOA strains that are typical of marine environments, in order to better understand their physiology and factors that determine their ecology.

The PCR primers used here for quantification of AOA *amoA* were the same ones used by many investigators to build clone libraries, which are often dominated by *N. maritimus*-like sequences. The array targets, however, were prepared from whole DNA, i.e., without PCR amplification. Thus the two assays are apparently detecting different subsets of the overall assemblage.

BEYOND ABIOTIC CONDITIONS

The first two axes of RDA together captured just over half (51.7%) of the variation of AOA community composition. This indicated that factors not included in our ordination should be important in controlling the AOA diversity. Strom (2008) pointed out the inadequacy of explanations of microbial diversity based on "resource availability and abiotic conditions," and she proposed that community interactions such as mortality, allelopathy, and symbiosis warranted more consideration because they have "strong selective pressure on marine microbes." In our study, archaeal *amoA* gene abundance could be regarded as an index for community interaction among AOA. In other words, the interaction among AOA in a community with high AOA abundance should presumably be different than that in a community with low AOA abundance. From our model, we can see that archetypes AOA -17 and -22 were positively correlated with AOA abundance (**Figure 5**). In three samples from the anoxic core of the Arabian Sea with high archaeal *amoA* abundance (175 m at Station 1, 200 m at Station 2, and 150 m at Station 3), archetypes AOA -17 and -22 made up over a third of the total AOA community (**Figure 4**), suggesting that AOA represented by these two archetypes should be important when AOA abundance is high.

A recent study has provided direct evidence for cooperation of AOA with anaerobic ammonia-oxidizing (anammox) bacteria by provision of nitrite and consumption of oxygen (Yan et al., 2012). Lam et al. (2009) argued that a significant portion of the nitrite for anammox in the ETSP OMZ was produced by ammonia oxidizers, implying community interactions between AOA and anammox bacteria, despite the fact that the known nitrite-producing metabolism of AOA is not possible in the extremely low oxygen conditions of the OMZ. On the other hand, a study on the depth distribution of AOA and anammox bacteria in the Arabian Sea OMZ suggested their niches were vertically segregated (Pitcher et al., 2011), so the chance of interaction between AOA and anammox bacteria there was low. Therefore, it is possible that those archetypes (AOA -9, -12, -15, -23 and -26) that had higher RFR in the ETSP than in the Arabian Sea represented AOA that had interactions with anammox bacteria. Conversely, those archetypes (AOA -4, -10, -17, -19, -21 and -22) that had higher RFR in the Arabian Sea than in the ETSP represented AOA that were independent of anammox bacteria. Understandably, these potential interactions between microbial communities were not reflected by the physicochemical data. However, such interactions *in situ* remain speculative and require experimental verification.

ACKNOWLEDGMENTS

We acknowledge helpful discussions with colleagues and use of the Microarray Facility at Princeton University, and George Jackson for the probe algorithm. We thank the chief scientist on R/V Knorr, James Moffet, who also provided nutrient data from the ETSP. We also acknowledge the technical support from Hema Naik and Anil Pratihary who measured the inorganic nutrients in the AS. This project was supported by a first year fellowship from Princeton University (Xuefeng Peng) and NSF grants to Bess B. Ward and Amal Jayakumar.

REFERENCES

Agogue, H., Brink, M., Dinasquet, J., and Herndl, G. J. (2008). Major gradients in putatively nitrifying and non-nitrifying Archaea in the deep North Atlantic. *Nature* 456, 788–791. doi: 10.1038/nature07535

Beman, J. M., and Francis, C. A. (2006). Diversity of ammonia-oxidizing archaea and bacteria in the sediments of a hyper nutrified subtropical estuary: Bahia del Tobari, Mexico. *Appl. Environ. Microbiol.* 72(12), 7767–7777. doi: 10.1128/AEM.00946-06

Beman, J. M., Popp, B. N., and Francis, C. A. (2008). Molecular and biogeochemical evidence for ammonia oxidation by marine Crenarchaeota in the Gulf of California. *ISME J.* 2, 429–441. doi: 10.1038/ismej.2007.118

Biller, S. J., Mosier, A. C., Wells, G. F., and Francis, C. A. (2012). Global biodiversity of aquatic ammonia-oxidizing archaea is partitioned by habitat. *Front. Aquat. Microbiol.* 3:252. doi: 10.3389/fmicb.2012.00252

Bouskill, N. J., Eveillard, D., Chien, D., Jayakumar, A., and Ward, B. B. (2012). Environmental factors determining ammonia-oxidizing organism distribution and diversity in marine environments. *Environ. Microbiol.* 14, 714–729. doi: 10.1111/j.1462-2920.2011.02623.x

Borcard, D., Gillet, F., and Legendre, P. (2011). *Numerical Ecology with R*. New York, NY: Springer. doi: 10.1007/978-1-4419-7976-6

Bulow, S. E., Francis, C. A., Jackson, G. A., and Ward, B. B. (2008). Sediment denitrifier community composition and nirS gene expression investigated with functional gene microarrays. *Environ. Microbiol.* 10, 3057–3069. doi: 10.1111/j.1462-2920.2008.01765.x

Cao, H., Auguet, J., and Gu, J. (2013). Global ecological pattern of ammonia-oxidizing archaea. *PLoS ONE* 8:e52853. doi: 10.1371/journal.pone.0052853

Coolen, M. J. L., Abbas, B., van Bleijswijk, J., Hopmans, E. C., Kuypers, M. M. M., Wakeham, S. G., et al. (2007). Putative ammonia-oxidizing Crenarchaeota in suboxic waters of the Black Sea: a basin-wide ecological study using 16S ribosomal and functional genes and membrane lipids. *Environ. Microbiol.* 9, 1001–1016. doi: 10.1111/j.1462-2920.2006.01227.x

Dalsgaard, T., Stewart, F. J., De Brabandere, L., Thamdrup, B., Revsbech, N. P., Canfield, D. E., et al. (2013). "The effects of oxygen on process rates and gene expression of anammox and denitrification in the Eastern South Pacific oxygen minimum zone," in *ASLO 2013 Aquatic Sciences Meeting*, (New Orleans, LA) abstract ID: 10879.

Eppley, R. W., and Peterson, B. J. (1979). Particulate organic matter flux and planktonic new production in the deep ocean. *Nature* 282, 677–680. doi: 10.1038/282677a0

Fiedler, P. C., and Talley, L. D. (2006). Hydrography of the eastern tropical Pacific: a review. *Prog. Oceanogr.* 69, 143–180. doi: 10.1016/j.pocean.2006.03.008

Fierer, N., Carney, K. M., Horner-Devine, M. C., and Megonigal, J. P. (2009). The biogeography of ammonia of ammonia-oxidizing bacterial communities in soil. *Mirob. Ecol.* 58, 435–445. doi: 10.1007/s00248-009-9517-9

Francis, C. A., Roberts, K. J., Beman, J. M., Santoro, A. E., and Oakley, B. B. (2005). Ubiquity and diversity of ammonia-oxidizing archaea in water columns and sediments of the ocean. *Proc. Natl. Acad. Sci. U.S.A.* 102, 14683–14688. doi: 10.1073/pnas.0506625102

Karl, D. M., Knauer, G. A., Martin, J. H., and Ward, B. B. (1984). Bacterial chemolithotrophy in the ocean is associated with sinking particles. *Nature* 309, 54–56. doi: 10.1038/309054a0

Kendall, C. (1998). "Tracing nitrogen sources and cycling in catchments," in *Isotope Tracers in Catchment Hydrology*, eds C. Kendall and J. J. McDonnell (Amsterdam: Elsevier Science), 519–576. doi: 10.1016/B978-0-444-81546-0.50023-9

Könneke, M., Bernhard, A. E., de la Torre, J. R., Walker, C. B., Waterbury, J. B. and Stahl, D. A. (2005). Isolation of an autotrophic ammonia-oxidizing marine archaeon. *Nature* 437, 543–546. doi: 10.1038/nature03911

Lam, P., Lavik, G., Jensen, M. M., van de Vossenberg, J., Schmid, M., Woebken, D., et al. (2009). Revising the nitrogen cycle in the Peruvian oxygen minimum zone. *Proc. Natl. Acad. Sci. U.S.A.* 106, 4752–4757. doi: 10.1073/pnas.0812444106

Legendre, P., and Gallagher, E. D. (2001). Ecologically meaningful transformations for ordination of species data. *Oecologia* 129, 271–280. doi: 10.1007/s004420100716

Martens-Habbena, W., Berube, P. M., Urakawa, H., de la Torre, J. R., and Stahl, D. (2009). Ammonia oxidation kinetics determine niche separation of nitrifying Archaea and Bacteria. *Nature* 461, 976–981. doi: 10.1038/nature08465

Martiny, J. B. H., Bohannan, B. J. M., Brown, J. H., Colwell, R. K., Fuhrman, J. A., Green, J. L., et al. (2006). Microbial biogeography: putting microorganisms on the map. *Nat. Rev. Microbiol.* 4, 102–112. doi: 10.1038/nrmicro1341

Merbt, S. N., Stahl, D. A., Casamayor, E. O., Marti, E., Nicol, G. W., and Prosser, J. I. (2012). Differential photoinhibition of bacterial and archaeal ammonia oxidation. *FEMS Microbiol. Lett.* 327, 41–46. doi: 10.1111/j.1574-6968.2011.02457.x

Mincer, T. J., Church, M. J., Taylor, L. T., Preston, C., Karl, D. M., and DeLong, E. F. (2007). Quantitative distribution of presumptive archaeal and bacterial nitrifiers in Monterey Bay and the NorthPacific Subtropical Gyre. *Environ. Microbiol.* 9, 1162–1175. doi: 10.1111/j.1462-2920.2007.01239.x

Molina, V., Belmar, L., and Ulloa, O. (2010). High diversity of ammonia-oxidizing archaea in permanent and seasonal oxygen-deficient waters of the eastern South Pacific. *Environ. Microbiol.* 12, 2450–2465. doi: 10.1111/j.1462-2920.2010.02218.x

Mosier, A. C., Lund, M. B., and Francis, C. A. (2012). Ecophisiology of an ammonia-oxidizing archaeon adapted to low-salinity habitats. *Microb. Ecol.* 64, 955–963. doi: 10.1007/s00248-012-0075-1

Newell, S. E. Babbin, A. R., Jayakumar, A., and Ward, B. B. (2011). Ammonia oxidation rates and nitrification in the Arabian Sea. *Global Biogeochem. Cycle* 25:GB4016. doi: 10.1029/2010GB003940

Park, B., Park, S., Yoon, D., Schouten, S., Sinninghe Damste, J. S., and Rhee, S. (2010). Cultivation of autotrophic ammonia-oxidizing archaea from marine sediments in coculture with sulfur-oxidizing bacteria. *Appl. Environ. Microbiol.* 76, 7575–7587. doi: 10.1128/AEM.01478-10

Pester, M., Rattei, T., Flechl, S., Grongroft, A., Richter, A., Overmann, J., et al. (2012). *amoA*-based consensus phylogeny of ammonia-oxidizing archaea and deep sequencing of *amoA* genes from soils of four different geographic regions. *Environ. Microbiol.* 14, 525–539. doi: 10.1111/j.1462-2920.2011.02666.x

Pitcher, A., Villanueva, L., Hopmans, E. C., Schouten, S., Reichart, G., and Damste, J. S. S. (2011). Niche segregation of ammonia-oxidizing archaea and anammox bacteria in the Arabian Sea oxygen minimum zone. *ISME J.* 5, 1896–1904. doi: 10.1038/ismej.2011.60

Pommier, T., Canback, B., Riemann, L., Bostrom, K. H., Simu, K., Lundberg, P., et al. (2007). Global patterns of diversity and community structure in marine bacterioplankton. *Mol. Ecol.* 16, 867–880. doi: 10.1111/j.1365-294X.2006.03189.x

R Core Team. (2012). *R: A Language and Environment for Statistical Computing*. Vienna: R Foundation for Statistical Computing. ISBN 3-900051-07-0, URL http://www.R-project.org/

Rao, R. R., Molinari, R. L., and Festa, J. F. (1989). Evolution of the climatological near-surface thermal structure of the tropical Indian Ocean 1. Description of mean monthly mixed layer depth, and sea surface temperature, surface current, and surface meteorological fields. *J. Geophys. Res.* 94, 10801–10815. doi: 10.1029/JC094iC08p10801

Santoro, A. E., Francis, C. A., de Sieyes, N. R., and Boehm, A. B. (2008). Shifts in the relative abundance of ammonia-oxidizing

bacteria and archaea across physico-chemical gradients in a subterranean estuary. *Environ. Microbiol.* 10, 1068–1079. doi: 10.1111/j.1462-2920.2007.01547.x

Santoro, A. E., Casciotti, K. L., and Francis, C. A. (2010). Activity, abundance and diversity of nitrifying archaea and bacteria in the central California Current. *Environ. Microbiol.* 12, 1989–2006. doi: 10.1111/j.1462-2920.2010.02205.x

Santoro, A. E., and Casciotti, K. L. (2011). Enrichment and characterization of ammonia-oxidizing archaea from the open ocean: phylogeny, physiology and stable isotope fractionation. *ISME J.* 5, 1796–1808. doi: 10.1038/ismej.2011.58

Schlitzer, R. (2012). *Ocean Data View.* http://odv.awi.de

Stevens, H., and Ulloa, O. (2008). Bacterial diversity in the oxygen minimum zone of the Eastern Tropical South Pacific. *Environ. Microbiol.* 10, 1244–1259. doi: 10.1111/j.1462-2920.2007.01539.x

Strom, S. L. (2008). Microbial ecology of ocean biogeochemistry: a community perspective. *Science* 320, 1043–1045. doi: 10.1126/science.1153527

Taroncher-Oldenburg, G., Griner, E., Francis, C. A., and Ward, B. B. (2003). Oligonucleotide microarray for the study of functional gene diversity in the nitrogen cycle in the environment. *Appl. Environ. Microbiol.* 69, 1159–1171. doi: 10.1128/AEM.69.2.1159-1171.2003

Thamdrup, B., Dalsgaaard, T., and Revsbech, N. P. (2012). Widespread functional anoxia in the oxygen minimum zone of the Eastern South Pacific. *Deep Sea Res. Pt. I* 65, 36–45. doi: 10.1016/j.dsr.2012.03.001

Tourna, M., Stieglmeier, M., Spang, A., Könneke, M., Schintlmeister, A., Urich, T., et al. (2011). *Nitrososphaera viennensis*, an ammonia oxidizing archaeon from soil. *Proc. Natl. Acad. Sci. U.S.A.* 108, 8420–8425. doi: 10.1073/pnas.1013488108

Treusch, A. H., Leininger, S., Kletzin, A., Schuster, S. C., Klenk, H. and Schleper, C. (2005). Novel genes for nitrite reductase and Amo-relatedproteins indicate a role of uncultivated mesophilic crenarchaeota in nitrogen cycling. *Environ. Microbiol.* 7, 1985–1995. doi: 10.1111/j.1462-2920.2005.00906.x

Venter, J. C., Remington, K., Heidelberg, J. F., Halpern, A. L., Rusch, D., Eisen, J. A., et al. (2004). Environmental genome shotgun sequencing of the Sargasso Sea. *Science* 304, 66–74. doi: 10.1126/science.1093857

Ward, B. B. (1987). Nitrogen transformations in the Southern California Bight. *Deep-Sea Res.* 34, 785–805. doi: 10.1016/0198-0149(87)90037-9

Ward, B. B. (2008).Phytoplankton community composition and gene expression of functional genes involved in carbon and nitrogen assimilation. *J. Phycol.* 44, 1490–1503. doi: 10.1111/j.1529-8817.2008.00594.x

Ward, B. B., Devol, A. H., Rich, J. J., Chang, B. X., Bulow, S. E., Naik, H., et al. (2009). Denitrification as the dominant nitrogen loss process in the Arabian Sea. *Nature* 461, 78–82. doi: 10.1038/nature08276

Ward, B. B., and Bouskill, N. J. (2011). "The utility of functional gene arrays for assessing community composition, relative abundance, and distribution of ammonia-oxidizing bacteria and archaea," in *Methods in Enzymology*, Vol. 496, eds M. G. Klotz and L. Y. Stein, (Burlington: Academic Press), 373–396.

Woebken, D., Fuchs, B. M., Kuypers, M. M. M., and Amann, R. (2007). Potential interactions of particle-associated anammox bacteria with bacterial and archaeal partners in the Namibian upwelling system. *Appl. Environ. Microbiol.* 73, 4648–4657. doi: 10.1128/AEM.02774-06

Wuchter, C., Abbas, B., Coolen, M. J. L., Herfort, L., van Bleijswijk, J., Timmers, P., et al. (2006a). Archaeal nitrification in the ocean. *Proc. Natl. Acad. Sci. U.S.A.* 103, 12317–12322. doi: 10.1073/pnas.0600756103

Wuchter, C., Schouten, S., Wakeham, S. G., Sinninghe Damste, J. S. (2006b). Archaeal tetraether membrane lipid fluxes in the northeastern Pacific and the Arabian Sea: Implications for TEX86 paleothermometry. *Paleoceanography* 21:PA4208. doi: 10.1029/2006PA001279

Yan, J., Haaijer, S. C. M., Camp, H. J. M. O., van Niftrik, L., Stahl, D. A., Könneke, M., et al. (2012). Mimicking the oxygen minimum zones: stimulating interaction of aerobic archaeal and anaerobic bacterial ammonia oxidizers in a laboratory-scale model system. *Environ. Microbiol.* 14, 3146–3158. doi: 10.1111/j.1462-2920.2012.02894.x

Yool, A., Martin, A. P., Fernandez, C., and Clark, D. R. (2007). The significance of nitrification for oceanic new production. *Nature* 447, 999–1002. doi: 10.1038/nature05885

Zhang, C. L., Ye, Q., Huang, Z., Li, W., Chen, J., Song, Z., et al. (2008). Global occurrence of archaeal *amoA* genes in terrestrial hot springs. *Appl. Environ. Microbiol.* 74, 6417–6426. doi: 10.1128/AEM.00843-08

Zimmerman, G. M., Goetz, H., and Mielke, P. W. (1985). Use of an improved statistical method for group comparisons to study effects of prairie fire. *Ecology* 66, 606–611 doi: 10.2307/1940409

Conflict of Interest Statement: The authors declare that the research was conducted in the absence of any commercial or financial relationships that could be construed as a potential conflict of interest.

Received: 25 January 2013; accepted: 12 June 2013; published online: 01 July 2013.

*Citation: Peng X, Jayakumar A and Ward BB (2013) Community composition of ammonia-oxidizing archaea from surface and anoxic depths of oceanic oxygen minimum zones. Front. Microbiol. **4**:177. doi: 10.3389/fmicb.2013.00177*

This article was submitted to Frontiers in Aquatic Microbiology, a specialty of Frontiers in Microbiology.

frontiers in
MICROBIOLOGY

REVIEW ARTICLE
published: 19 October 2012
doi: 10.3389/fmicb.2012.00375

Influence of vitamin B auxotrophy on nitrogen metabolism in eukaryotic phytoplankton

Erin M. Bertrand and Andrew E. Allen*

Department of Microbial and Environmental Genomics, J. Craig Venter Institute, San Diego, CA, USA

Edited by:
Bess B. Ward, Princeton University, USA

Reviewed by:
Michael R. Twiss, Clarkson University, USA
Kathleen Scott, University of South Florida, USA

****Correspondence:***
Andrew E. Allen, Department of Microbial and Environmental Genomic, J. Craig Venter Institute, 10355 Science Center Drive, San Diego, CA 92121, USA.
e-mail: aallen@jcvi.org

While nitrogen availability is known to limit primary production in large parts of the ocean, vitamin starvation amongst eukaryotic phytoplankton is becoming increasingly recognized as an oceanographically relevant phenomenon. Cobalamin (B_{12}) and thiamine (B_1) auxotrophy are widespread throughout eukaryotic phytoplankton, with over 50% of cultured isolates requiring B_{12} and 20% requiring B_1. The frequency of vitamin auxotrophy in harmful algal bloom species is even higher. Instances of colimitation between nitrogen and B vitamins have been observed in marine environments, and interactions between these nutrients have been shown to impact phytoplankton species composition. This review surveys available data, including relevant gene expression patterns, to evaluate the potential for interactive effects of nitrogen and vitamin B_{12} and B_1 starvation in eukaryotic phytoplankton. B_{12} plays essential roles in amino acid and one-carbon metabolism, while B_1 is important for primary carbohydrate and amino acid metabolism and likely useful as an anti-oxidant. Here we will focus on three potential metabolic interconnections between vitamin, nitrogen, and sulfur metabolism that may have ramifications for the role of vitamin and nitrogen scarcities in driving ocean productivity and species composition. These include: (1) B_{12}, B_1, and N starvation impacts on osmolyte and antioxidant production, (2) B_{12} and B_1 starvation impacts on polyamine biosynthesis, and (3) influence of B_{12} and B_1 starvation on the diatom urea cycle and amino acid recycling through impacts on the citric acid cycle. We evaluate evidence for these interconnections and identify oceanographic contexts in which each may impact rates of primary production and phytoplankton community composition. Major implications include that B_{12} and B_1 deprivation may impair the ability of phytoplankton to recover from nitrogen starvation and that changes in vitamin and nitrogen availability may synergistically impact harmful algal bloom formation.

Keywords: cobalamin, thiamine, S-adenosylmethionine, nitrogen, sulfur, urea cycle, microbial interactions, harmful algal blooms

INTRODUCTION

The rate, magnitude, and species composition of marine primary production has a profound influence of global carbon cycling and therefore climate. As a result, factors controlling the growth of marine primary producers are of considerable interest. While nitrogen and iron availability are often considered the primary bottom-up controls on short-term marine primary productivity, the importance of organic growth factors received considerable early attention (Cowey, 1956; Droop, 1957, 1962; Menzel and Spaeth, 1962; Provasoli, 1963; Gold, 1968; Carlucci and Silbernagel, 1969; Carlucci and Bowes, 1970; Swift and Taylor, 1972; Swift, 1981) and is the subject of renewed interest (e.g., Sañudo-Wilhelmy et al., 2012).

Recent developments in analytical techniques (Okbamichael and Sañudo-Wilhelmy, 2004; Sañudo-Wilhelmy et al., 2012), application of trace metal clean bioassay experiments (Panzeca et al., 2006; Sañudo-Wilhelmy et al., 2006; Bertrand et al., 2007; Gobler et al., 2007; Koch et al., 2011), and culture-based surveys of vitamin requirements (Croft et al., 2005; Tang et al., 2010) have identified B_{12} (cobalamin) and B_1 (thiamine) as highly important growth factors for eukaryotic phytoplankton and suggest that these micronutrients have the potential to broadly influence marine productivity and species composition. Due to the fact that B_{12} and B_1 both play numerous essential roles in cellular biochemistry, starvation for these nutrients has the potential to impact phytoplankton cellular metabolism through a range of mechanisms. The increase in available genome and transcriptome data for relevant organisms has opened doors for new modes of inquiry into the role of these micronutrients in phytoplankton metabolism as well as their potential for interaction with additional states of nutrient deprivation (Croft et al., 2006; Helliwell et al., 2011; Bertrand et al., 2012). Here we review available data to examine potential interactions between B_{12}, B_1, and nitrogen deprivation and sulfur metabolism in eukaryotic phytoplankton communities and provide insight into the potential implications of these interactions for phytoplankton evolutionary trajectories and biogeochemical cycling.

COBALAMIN AND THIAMINE

PRODUCTION, DEMAND, AND BIOCHEMICAL FUNCTION

Cobalamin, B_{12}, is a cobalt-containing organometallic micronutrient that conducts elegant chemistry facilitated by the controlled reactivity of the axial Co-C bond in methyl and adenosylcobalamin (Schrauzer and Deutsch, 1969; Lexa and Savant, 1983; Drennan et al., 1994). The resulting reactivity provides the biochemical capacity for methylation and rearrangement reactions, where a hydrogen atom on one carbon constituent is exchanged for another functional group, typically a methyl, amine, or alcohol group. Cobalamin is believed to be produced only by select bacteria and archaea (Roth et al., 1996; Martens et al., 2002) and is required by humans and other metazoans, by an estimated half of all eukaryotic phytoplankton (Tang et al., 2010) and by some bacteria that are not able to synthesize it (Rodionov et al., 2003; Zhang et al., 2009). Vitamin B_{12} biosynthesis requires over 30 enzymatic steps and significant consumption of cellular energy, carbon, nitrogen, cobalt, zinc, and in some cases iron (Roth et al., 1996; Raux et al., 2000).

Vitamin B_{12} demand by eukaryotic phytoplankton is thought to arise from its role as a cofactor in the enzyme methionine synthase, which catalyzes the conversion of homocysteine and methyl-tetrahydrofolate to tetrahydrofolate and methionine (**Table 1**). The active form of B_{12} in methionine synthase is methylcobalamin. Algae that require B_{12} absolutely posses only the B_{12}-dependant version of this enzyme (MetH), while those that do not have an absolute requirement have the ability to use an alternative B_{12} independent version (MetE) (Croft et al., 2005). Phylogenetic analysis of metE and metH coding sequences support a complex evolutionary history of *metE* gene gain and loss within eukaryotic organisms. In contrast, the phylogeny of *metH* is well resolved and apparently monophyletic in eukaryotes (Helliwell et al., 2011). These analyses suggest that absolute B_{12} requirements in eukaryotic algae have likely arisen as a result of multiple independent loses and acquisitions of *metE* from eukaryotic genomes. Indeed, under high B_{12} concentrations, *metH* is continually expressed by algal strains, whereas *metE*, if present, is repressed until B_{12} is depleted (Croft et al., 2005; Helliwell et al., 2011; Bertrand et al., 2012). These results suggest that B_{12} auxotrophy in eukaryotic algae arose as a function of variable B_{12} availability in the environment. This is supported by observations that the distribution of *metE* in eukaryotic phytoplankton does not follow phylogenetic lines. Importantly, there is strain level variability in whether or not phytoplankton exhibit an absolute requirement for B_{12} (Tang et al., 2010). In addition, B_{12} is a cofactor in the enzyme methylmalonyl coA mutase (mmcM), which is encoded in some but not all B_{12}-requiring phytoplankton genomes (**Table 1**). *mmcM*'s function in eukaryotic phytoplankton remains somewhat unclear, though it likely plays a role in the citric acid cycle as well as fatty acid and propionate metabolism. However, the presence of *mmcM* genes in phytoplankton genomes does not confer a B_{12} requirement under typical laboratory growth conditions (Croft et al., 2006).

Thiamine, B_1, is a cofactor required by all organisms and produced by many prokaryotes as well as by fungi, plants, and some eukaryotic phytoplankton (Webb et al., 2007). It is a sulfur-containing compound, produced though joining of a pyrimidine and a thiazole moiety, and is phosphorylated in its coenzyme form (thiamine diphosphate). In bacterial biosynthetic pathways, thiazole biosynthesis requires six distinct enzymatic steps and pyrimidine synthesis requires two (Rodionov et al., 2002; Jurgenson et al., 2009). While the bacterial thiamine biosynthesis pathway is well characterized, eukaryotic biosynthesis pathways remain poorly understood and appear to be distinct in plants and fungi (Jurgenson et al., 2009). Algal thiamine biosynthesis is even less well-characterized but likely conducted by some enzymes similar to bacterial thiamine biosynthesis genes and some enzymes similar to the yeast and plant pathways (Croft et al., 2006), though this remains to be conclusively demonstrated.

While thiamine was one of the first organic cofactors identified as important for algal growth, early work showed that there are some phytoplankton strains that produce thiamine *de novo*, and some that can scavenge and salvage either the thiazole or pyrimidine moieties from the environment in order to construct a functional cofactor (Droop, 1958; Provasoli and Carlucci, 1974). Preliminary inquiry into eukaryotic phytoplankton genomes conducted via identification of coding sequences similar to those encoding known bacterial, fungi, and plant thiamine biosynthesis enzymes suggests that there are potentially different pathways for thiamine production in stramenopiles versus the green algal lineage (**Table 2**, McRose et al., 2012). The absence of a gene encoding ThiC, a protein involved in pyrimidine biosynthesis, appears to correlate with B_1 auxotrophy in algae with sequenced genomes, regardless of lineage (**Table 2**). This intriguing observation warrants further exploration. Since ThiC is involved in pyrimidine biosynthesis, the relationship between ThiC gene presence and thiamine auxotrophy is likely to hold only for auxotrophs with the ability to synthesize thiamine diphosphate when provided the pyrimidine moiety, not those that can synthesize the vitamin when provided with the thiazole moiety, such as some dinoflagellates and cryptophytes (Droop, 1958). ThiC is an interesting protein; it requires S-adenosyl methionine (SAM) for activity (Chatterjee et al., 2008), is an iron-sulfur cluster protein, and is present in both the plant and bacterial thiamine biosynthesis pathways (Goyer, 2010).

Thiamine catalyzes a number of transformations that are important in carbohydrate and branched amino acid metabolism including those involved in glycolysis, the pentose phosphate pathway, and the tricarboxylic acid pathway. These notably include 2-oxoglutarate dehydrogenase (ODG), pyruvate dehydrogenase/decarboxylase, branched-chain α-ketoacid dehydrogenase, as well as transketolases, acetolactate synthase, and alpha-keto acid dehydrogenase. The chemistry involved in these reactions often includes two carbon group transfers or dehydrogenation reactions (Frank et al., 2007). There is mounting evidence that thiamine may play additional, non-cofactor roles as well. In plants, thiamine has been tied to cellular responses to oxidative stress and disease. Plants subjected to hydrogen peroxide, salt stress, and high light stress, for example, all showed enhanced thiamine production and increased thiamine biosynthesis protein transcripts, such as ThiC (reviewed in Goyer, 2010; Rapala-Kozik et al., 2012). It is possible that this increase

Table 1 | Vitamin B_{12} related genes in sequenced eukaryotic phytoplankton genomes and select marine prokaryotic genomes.

	Auran	Phatr	Thaps	Psemu	Fracy	Emihu	Ostta	Ostlu	MicPu	Chlre	ChlNC	Syn 8102	Pro 9313	P. ubique
MetH	34875	23399	693	213031	207237	423073	16287	45056	148156	76715	36916	SYNW 1238	PMT0729	x
MetE	x	28056	x	x	228154	x	x	x	x	154307	141995	x	x	x
MmcM	26280	51830	33685	261420	273786	120906 417351	x	x	x	x	18280	x	x	x
CBA1	63075	48322	11697	235642	241429, 246327, 273295, 269995	x	x	x	x	x	x	x	x	x
RNR Class 2 B_{12}	x	x	x	x	x	x	x	x	x	x[#]	x	SYNW 1147	PMT 0793	x
RNR Class 1 Fe; small	65685 59025	39306 17523	32555 8522 3367	67342 252139	268008 206256	470988 469622 200748	22908 8886	32923 39468	155636 174818	188785 144621	34102 10712 57791	x	x	PB7211_ 302
RNR Class 1 Fe; Large	30730, 37557, 24558	42726, 45529	370, 268807	223844 319245	260490, 262570, 205957	449248, 212824	22667	48569	167892	185583	32953	x	x	PU1002_ 00625
B_{12} biosynthesis	No	No	No	No	No	No	No	No	No	No	No	Yes	Yes	No
B_{12} Aux. by genome	Yes	No	Yes	Yes	No	Yes	Yes	Yes	Yes	No	No	No	No	No
B_{12} Aux. by culture	Yes (Tang et al., 2010)	No (Droop, 1958)	Yes (Guillard and Ryther, 1962)	Yes (Tang et al., 2010)*	No (Helliwell et al., 2011)	See (Helliwell et al., 2011)	Yes (Helliwell et al., 2011)		Yes (Helliwell et al., 2011)	No (Provasoli and Carlucci, 1974)	No (Shihira and Krauss, 1965)			

The hypothesized vitamin requirements of each strain are also given, along with whether culture-based confirmation of auxotophic status is available. This table represents an expansion of information given in Croft et al., 2006 and Helliwell et al., 2011. No eukaryote is known to make vitamin B_{12}; B_{12} auxotrophy in eukaryotic algae appears to depend on the presence or absence of B_{12}-independent methionine synthase (Croft et al., 2005; Helliwell et al., 2011). Auran, Aureococcus anophagefferans; Phatr, Phaeodactylum tricornutum; Thaps, Thalassiosira pseudonanna; Psemu, Pseudo-nitzschia multiseries CLN-47; Fracyl, Fragilariopsis cylindrus; Chlre, Chlamydomonas reinhardtii (v4; filtered or best proteins); Emihu, Emiliania huxleyi; Ostta, Ostreococcus taurii; Ostlu, Ostreococcus lucimarinus V2 filtered model proteins MicPu, Micromonas pusilla CCMP1545 c3.0, filtered model proteins. ChlNC, Chlorella sp. NC64A filtered proteins; Syn8102, Synechococcus sp. WH8102; Pro9313, Prochlorococcus marinus MIT 9313; P. ubique, Candidatus Pelagibacter ubique SAR11 HTCC1002.

**Auxotrophy tested in culture of a different strain.*

[#]Has a protein with substantial sequence similarity but missing active site: (154521).

Table 2 | Vitamin B_1 (Thiamine) related genes in sequenced eukaryotic phytoplankton genomes.

	Auran	Phatr	Thaps	Psemu	Fracy	Emihu	Ostta	Ostlu	MicPu 1545	MicPu 299	Chlre	ChlNC
ThiC	x	38085	41733	255053	225659	x	x	x	x	x	192720	136333
thiD+thiE/ Thi6/TenI	x	47293	262964-3	320126	153126, 161112	102278	20618, 6224	17535	52893	x	390684	58425
ThiF*	31873, 32858	34373, 20318	261602, 35049	207357, 293997	194811, 275015	68584	19906	38170	51160	113992	138485	22673
dsx	59650	bd1689	574	65889	206898	440786	15650	48774	121145	107366	196568	59788
ThiG[%]	x	PhtrCp129	ThpsCp126, bd1620	–	Scaffold 95, 27066–27869	Emhu Cp072	x	–	x	–	x	x
ThiS[%]	AuanCp078	PhtrCp091	ThpsCp091	–	Scaffold 95, 5640–5849	x	x	–	x	–	x	x
ThiO/H**	72208	31544	263655	230060	241529	53832	x	x	x	x	196226	30311
Thi4	x	x	x	x	x	x	20276^	x	52894^	x	185190	22703
TPK	20636	5423	262503[@]	264355	86232	56054	10431	12109	163134	109022	72868	11702
ThiM/10	x	x	x	x	x	x	x	x	x	x	126905[$]	53510
B1 Aux. by culture	Yes (Tang et al., 2010)	No (Droop, 1958)	No (Guillard and Ryther, 1962)	No (Tang et al., 2010)***	No (Bertrand, unpublished)	Yes (Carlucci and Bowes, 1970)***			Yes (McRose et al., 2012)	Yes (McRose et al., 2012)	No (Provasoli and Carlucci, 1974)	No (Shihira and Krauss, 1965)

The hypothesized vitamin requirements of each strain are also given, along with whether culture-based confirmation of auxotophic status is available. This table expands information given in Croft et al. (2006). Auran = Aureococcus anophagefferans; Phatr = Phaeodactylum tricornutum; Thaps = Thalassiosira pseudonanna; Psemu = Pseudo-nitzschia multiseries CLN-47; Fracyl = Fragilariopsis cylindrus; Chlre = Chlamydomonas reinhardtii (v14; filtered or best proteins); Emihu = Emiliania huxleyi; Ostta = Ostreococcus taurii; Ostlu = Ostreococcus lucimarinus V2 filtered model proteins; MicPu = Micromonas pusilla CCMP1545 c3.0, filtered model proteins. ChlNC = Chlorella sp. NC64A filtered proteins.

x = not found, "–" = search not possible (chloroplast genome not available)

**ThiF is not easily assigned because of similarities with MoeB/Z*

[%] ThiG and ThiS are often chloroplast encoded

^ unclear, potential Thi4 (similarity to tenA proteins too)

[@] uncertain assignment

[$] mutants of this are thiamine auxotrophs

***The diatoms appear to have ThiO, Chlre and ChlNC have thiH*

****Auxotrophy tested in culture of a different strain.*

in thiamine under stress results from demand for transketolase activity in the pentose phosphate pathway which regenerates NADPH required for activity of some antioxidants (Goyer, 2010). However it is also possible that thiamine itself functions as an antioxidant in these cells, as thiamine compounds have antioxidant capacities, likely through the transfer of H+ from amino groups on the thiazole and pyrimidine rings to reactive species (Hu et al., 1995; Lukienko et al., 2000; Bettendorff and Wins, 2009). While there has been comparatively little study of these potential roles of thiamine in algae, available evidence suggests that thiamine biosynthesis per cell in diatoms increases as a function of increasing cell density and nutrient depletion, which may be caused by the increase in oxidative stress (Pinto et al., 2003).

Thiamine auxotrophy is strikingly different from B_{12} auxotrophy in algae; while B_{12} requirements are determined by the ability of a phytoplankton strain to replace B_{12}-requiring metabolisms (**Table 1**), B_1 auxotrophy is defined by whether or not an algal strain is able to synthesize the vitamin *de novo* (**Table 2**). Considering that the enzymes for B_1 biosynthesis are not yet completely elucidated in algae, it is difficult to discern, through analysis of protein coding sequences, the evolutionary origin of B_1 auxotrophy. However, observations concerning the phylogenetic distribution of thiamine auxotrophy support the notion that biosynthesis potential may have also been lost and acquired multiple times. For instance, in the case of two strains of the same species of dinoflagellate, isolated from the same site, one is a B_1 auxotroph and one is not (Tang et al., 2010). Among *Micromonas* spp. strains with thiamine requirements, one is missing more of the biosynthetic pathway than the other (McRose et al., 2012; **Table 2**). These data suggests that like B_{12}, B_1 auxotrophy in algae has likely arisen numerous times though gene loss events. Such loss events could be driven by chronically high thiamine availability coupled to transcriptional repression and associated loss of purifying selection and gene erosion. While this repression is yet to be documented, eukaryotic phytoplankton genomes encode thiamine riboswitches (Croft et al., 2007; Worden et al., 2009); which offer a mechanism by which high thiamine bioavailability can regulate gene transcription.

OCEANOGRAPHIC DISTRIBUTIONS AND CYCLING

In the ocean, dissolved (0.2 μm) vitamin B_{12} and B_1 show variable but often nutrient-like depth profiles and are thought to be present in sub-picomolar quantities to up to 30 pM for B_{12} and 500 pM for B_1 (Sañudo-Wilhelmy et al., 2012). Concentrations of these vitamins in coastal waters are generally higher than in open ocean regions (Panzeca et al., 2009). Measurement techniques for B vitamins in seawater remained restricted to bioassays (Menzel and Spaeth, 1962; Carlucci, 1966) until solid phase extraction, high pressure liquid chromatography methods were developed (Okbamichael and Sañudo-Wilhelmy, 2004; Okbamichael and Sanudo-Wilhelmy, 2005). Development of these techniques, coupled with mass spectrometry, has fostered more efficient and accurate methods for vitamin detection and quantitation in seawater. Such methods however still require inconveniently large volumes and are not currently optimized to detect B_{12} with different α or β axial groups or differentially phosphorylated forms of thiamine, which may be present in seawater and could be important for bioactivity as well as biogeochemical cycling. In addition, concentration measurements alone may not be an informative measure of the impact of vitamins on marine biogeochemical processes since their concentrations are low and they may be cycled and regenerated rapidly in the euphotic zone as a function of biological production and consumption as well as abiotic processing. The halflife of B_{12} in the surface ocean with respect to photodegradation alone is approximately 4 days, while B_1 is more resistant to abiotic transformations in seawater (Gold et al., 1966; Carlucci et al., 1969). This, along with differences in production and consumption of vitamins by different components of marine microbial communities, may explain the observation that B_{12} and B_1 concentrations and cycling may be decoupled in the water column (Panzeca et al., 2008; Sañudo-Wilhelmy et al., 2012). It remains a challenge to reconcile the interesting observation that B vitamin abundance patterns are associated with basin-scale water mass origin (Sañudo-Wilhelmy et al., 2012) with the likely rapid changes in production and consumption of these vitamins. To address this question, continued efforts to measure these vitamins, along with assessments of microbial community composition and vitamin acquisition rates, should include assessments of variability on short (hours to days) as well as seasonal timescales.

Either through dissolved organic matter exudation and cell lysis via the cycling of the microbial loop, (Azam, 1998; Karl, 2002; Droop, 2007) or through direct symbiotic interaction (Croft et al., 2005), some portion of the bacterial and archaeal community must be the ultimate source of vitamin B_{12} to eukaryotic phytoplankton. The genetic potential for vitamin B_{12} production remains largely uncharacterized in any marine environment (Bertrand et al., 2011a). This is in part because the occurrence of the biosynthesis pathway among bacterial and archaeal lineages is extremely variable and is not easily queried using typical phylogenetic profiling techniques. An exception to this is the marine cyanobacteria, where all sequenced genomes appear to contain the B_{12} biosynthetic pathway (Rodionov et al., 2003), and numerous strains have been shown to produce significant amounts of B_{12} (Bonnet et al., 2010). The identity of other groups that contribute significantly to oceanic B_{12} production remains unclear, however, and is of particular importance in regions with scarce cyanobacterial populations such as the polar oceans (Caron et al., 2000; Marchant, 2005). The extremely abundant SAR11 group appears to neither synthesize nor require the vitamin (**Table 1**). In addition, there are examples from many sequenced marine bacterioplankton genomes of strains that either cannot produce the vitamin themselves but require it for various metabolisms, or those that can salvage degraded B_{12} for repair and reuse (Bertrand et al., 2011a). In sum, B_{12} uptake by marine bacteria and archaea can be as significant as uptake by eukaryotic phytoplankton (Bertrand et al., 2007; Koch et al., 2011). This results in a scenario in which eukaryotic phytoplankton likely compete for B_{12} resources with some components of the prokaryotic community (Bertrand et al., 2011b; Sañudo-Wilhelmy et al., 2012).

Thiamine sources to eukaryotic phytoplankton include *de novo* production, uptake or salvage from bacterial production, or uptake and salvage of thiamine produced by other algae (Carlucci and Bowes, 1970; Provasoli and Carlucci, 1974). Similar to B_{12}, competition likely occurs for B_1 amongst microalgae as well as between algal and bacterial groups since not all prokaryotes have the ability to produce thiamine (Rodionov et al., 2002). It remains unclear, however, what the relative importance of these uptake vectors are and how this varies across oceanic regions. A striking difference between B_{12} and B_1 auxotropy is that B_1 requirements in algae could potentially be supplied by growth with B_1 producing algal strains as well as with some bacteria (**Table 2**). This is in contrast to B_{12} where the only potential source of B_{12} to auxotrophic algae is bacterial and archaeal production. This opens interesting avenues for exploration of species succession and potential commensalism between not only algae and bacteria but also between different algal strains.

Bottle incubation bioassay experiments have suggested that availability of B_{12} and to some degree B_1 influence overall rates of primary production as well as phytoplankton community composition in regions ranging from the Southern Ocean to temperate coastal environments (Panzeca et al., 2006; Sañudo-Wilhelmy et al., 2006; Bertrand et al., 2007; Gobler et al., 2007; Koch et al., 2011). In many cases, addition of B vitamins to communities resulted in the proliferation of diatoms or dinoflagellates and larger groups of eukaryotic phytoplankton (**Table 3**). This may have important implications for carbon and nitrogen export as well as silica cycling, since larger phytoplankton tend to support a higher percentage of organic matter export. In addition, coastal and open ocean North Atlantic studies revealed that regions with higher B_{12} concentrations correlated with regions with high bacterioplankton productivity or density (Gobler et al., 2007; Panzeca et al., 2008), though it remains unclear whether these correlations are due to bacterial production of the vitamin or enhanced bacterial abundance as a result of higher B_{12} availability. In the Ross Sea of the Southern Ocean, bacterial abundance was shown to be low where primary production was stimulated by B_{12}, meaning that where bacterioplankton communities were more numerous, B_{12} was less likely to limit primary production (Bertrand et al., 2011b). This suggests that bacterioplankton have an important impact on B_{12} supply to eukaryotic phytoplankton, at least in polar regions. However, intimate associations between bacteria and eukaryotic phytoplankton are known to occur (**Figure 1**; Cole, 1982; Grossart et al., 2005); the importance of these associations to B vitamin cycling and availability to phytoplankton in the marine environment are just beginning to be explored and offer numerous exciting avenues for continued research.

THE IMPORTANCE OF NITROGEN TO EUKARYOTIC PHYTOPLANKTON

Nitrogen is an essential component of all life. The availability of nitrogen is thought to limit the productivity of marine microbial communities in large portions of the ocean (McCarthy and Carpenter, 1983; Hecky and Killam, 1988; Moore et al., 2004). Oceanic dissolved nitrogen distributions are driven in

Table 3 | Results of B-vitamin supplementation in published marine bottle incubation bioassays.

Location	Experiments with stimulation of Chl a production by a B vitamin	B vitamin changed community composition?	Size class or functional group with biggest response	Notes	Interactions with N	References
Long Island embayments	1/1	1/1	>5 μm	Observed correlation between dissolved B_{12}, B_{12} drawdown and growth of large phytoplankton	Yes	Sañudo-Wilhelmy et al., 2006
Antarctic Peninsula	1/1	1/1	nd	Primary and secondary limitation by B_1 + B_{12}	nd	Panzeca et al., 2006
Ross Sea	2/3	3/3	Diatoms	–	nd	Bertrand et al., 2007
Long Island embayments	4/14	–	>5 μm	Fall experiments: large size fraction B vitamin limited	Yes	Gobler et al., 2007
Ross Sea	2/5	5/5	Diatoms	B_{12} uptake rates Fe limited	nd	Bertrand et al., 2011a,b
Gulf of Alaska	1/2	2/2	Dinoglagellates in coastal, diatoms in upwelling	N and Fe co-limitation with B_{12}	Yes	Koch et al., 2011

nd = no data.

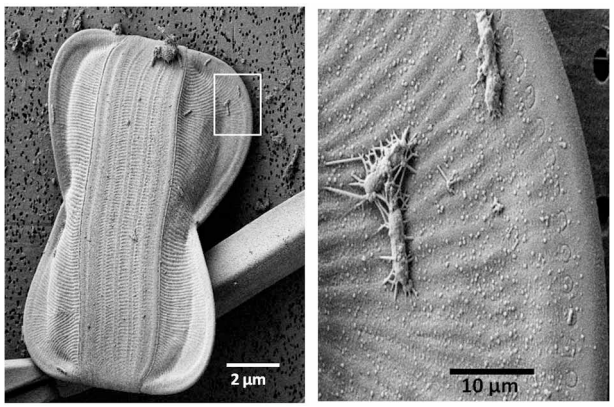

FIGURE 1 | Bacteria can be intimately associated with diatoms. This sea ice *Amphiprora* diatom cell has bacterial cells attached through an apparently tight association likely via the use extracellular polymeric substances (EPS). SEM micrographs were collected at the UC Riverside Center for Nanoscale Science and Engineering. Samples were filtered, critical point dried to preserve cellular structures, coated with Pt:Pd to prevent charging, and imaged at 2 kv on a Zeiss 1540 FE-SEM.

large part by coupled biological processing and large scale patterns in ocean circulation. Dissolved inorganic nitrogen (DIN) is generally considered to be the major source of nitrogen to marine microbial communities; the availability of these compounds (nitrate, nitrite, and ammonia), particularly in the oligotrophic ocean, can be depleted below 0.03 µM (Capone, 2000). Phytoplankton growth limitation by inorganic nitrogen availability has also been observed in coastal and upwelling environments (Kudela and Dugdale, 2000). The availability of this inorganic nitrogen has long been used, via nitrogen balancing calculations, to estimate organic matter export from the surface ocean (Eppley and Peterson, 1979), a concept which has profoundly influenced the field of biogeochemical oceanography. Models of the role of different nitrogen sources to phytoplankton and their microbial transformations have evolved to include additional processes, yet this conceptualization of balance between dissolve nitrate upwelled into the euphotic zone and export of biogenic and dissolved organic nitrogen (Bronk et al., 1994) continues to shape our understanding of controls on marine primary production and carbon cycling.

The relative availability of different N sources is now known to play a role in structuring phytoplankton species composition. Though reduced N compounds require less energy to assimilate, there are differences between taxonomic groups in terms of the impact of these differences on growth rate and the impact of ammonia availability on oxidized N acquisition (Dortch, 1990). In addition, differences in the ability of varying phytoplankton functional groups to respond to variable nitrogen concentrations and sources can create important niche dimensions. For instance, diatoms are a particularly successful group of eukaryotic phytoplankton that tend to dominate in coastal and upwelling regions. These locations are often characterized by highly variable nitrogen sources and concentrations. The ability of diatoms to respond quickly to pulsed nitrogen additions can, in part, explain a portion of their success in such environments. Their successful responses to these pulsed additions are partially explained by their ability to tightly couple anabolic and catabolic nitrogen transformations through incorporation of a complete urea cycle into central metabolism (Allen et al., 2011). Diatoms also tend to exhibit their maximal growth rates when grown on reduced nitrogen sources such as ammonia and urea (Dortch, 1990; Bender et al., 2012), but also in some cases dominate environments when nitrate is the dominant source of DIN. Their ability to take up and flexibly utilize a range of nitrogen sources also likely contributes to their role as a dominant phytoplankton group. We suggest that B vitamin deprivation may impair the ability of diatoms to effectively respond to and recover from nitrogen deprivation and that this may have important implications for interactions between marine microbial groups. This results from the fact that metabolisms impacted by B_1 and B_{12} have important roles in pathways and mechanisms for allocation of cellular N recovery from N starvation.

B VITAMIN AND N INTERACTIONS IN OCEANIC ENVIRONMENTS

It is clear that marine bacterial communities, in some cases, compete with eukaryotic phytoplankton for inorganic nitrogen sources, including nitrate (Kirchman and Wheeler, 1998; Kirchman, 2000; Allen et al., 2001, 2005). These heterotrophic bacterial communities also conduct the canonical transformation of organic N sources to ammonia and dissolved organic nitrogen via cycling within the microbial loop. As a result, bacterial communities can be either net sources or net sinks of available N to phytoplankton communities (Kirchman, 2000; Zehr and Ward, 2002). This may vary as a function of the C:N ratio of available organic matter as well as the community composition of microbial assemblages (Kirchman, 2000). There are clear parallels between N and B vitamin availability in the ocean; the interaction between marine microbial groups plays a key role in shaping the influence these chemicals have on productivity. As a result, the implications of combined nitrogen starvation and B vitamin deprivation for eukaryotic phytoplankton will clearly be interactively impacted by bacterial communities. Intimately associated bacterial communities, such as those shown in **Figure 1**, have the potential to impact vitamin availability as well as nitrogen resources to phytoplankton; interactions between B vitamin and N dynamics in algal bacterial associations have yet to be explored, but are intriguing areas for research.

There have been two studies examining interactive impact of DIN and B vitamin addition on phytoplankton communities. In Long Island embayments, shifts from dinoflagellate dominated, primarily N limited communities in summer to diatom dominated blooms in fall coincided with decreases in B_{12} and B_1 availability and increases in chlorophyll production upon B vitamin additions, suggesting that N and B vitamin availability both influence coastal phytoplankton species succession and biomass. Interestingly, in several instances, B_{12} or B_1 and nitrate, when added together, stimulated chlorophyll production to a greater degree than adding either nutrient alone (Gobler et al., 2007). This interactive effect has yet to be mechanistically explored, but could be a function of vitamins being independently

secondarily limiting, or could be explained by biochemical interactions between nitrogen and B vitamin production or demand (Saito et al., 2008). In a series of bottle incubation studies in the coastal, nitrogen limited region of the Gulf of Alaska, the addition of nitrate alone yielded enhanced productivity, and a shift from a dinoflagellate to diatom dominated community. In contrast, the addition of B_{12} and nitrate together yielded a community dominated by dinoflagellates (Koch et al., 2011). This striking result suggests that B vitamin availability severely impacted the response of the coastal phytoplankton community to nitrogen availability. This response suggests that the dinoflagellate community could not respond to nitrogen addition under B_{12} starvation conditions, either due to secondary, independent limitation of dinoflagellate growth by B_{12} availability or due to biochemical interactions between nitrogen and B_{12} metabolism leading to co-limitation. Since a higher proportion of dinoflagellates are B_{12} auxtrophs (90%) than are diatoms (60%) (Tang et al., 2010), this response may be expected. However, diatom ability to respond to nitrogen additions over dinoflagellates under low B_{12} availability may not be entirely explained by differences in auxotrophy and warrants further exploration. Here we examine potential biochemical mechanisms for interaction between B vitamin and nitrogen metabolism.

MOLECULAR RESPONSES OF EUKARYOTIC PHYTOPLANKTON TO B VITAMIN STARVATION

There is some information available concerning the molecular responses of eukaryotic phytoplankton to B-vitamin starvation. While studies that examine the response of phytoplankton to B_1 deprivation have not been described in detail (McRose et al., 2012), there has been comparatively extensive inquiry into the molecular response of phytoplankton to B_{12} deprivation. An important consequence of B_{12} deprivation in eukaryotic phytoplankton appears to be impaired methionine synthase activity and the use of B_{12}-independant MetE over dependent MetH (Croft et al., 2005; Helliwell et al., 2011; Bertrand et al., 2012). Methionine serves not only as a protein-building amino acid but as the precursor to S-adenosylmethionine (AdoMet or SAM), an important methylating agent, propylamine donor, and radical source. Indeed, there is evidence that SAM deprivation is an important consequence of low B_{12} availability in diatoms (Bertrand et al., 2012; **Figure 2**). Notably, ThiC, an important algal thiamine biosynthesis protein, is SAM-dependant and responds to B_{12} deprivation in diatom cultures, suggesting that there may be consequences of B_{12} deprivation for thiamine production. In addition, dinoflagellate transcriptome and metatranscriptome sequencing studies reveal that SAM cycling genes are among the most highly expressed transcripts in multiple dinoflagellate species (Lidie et al., 2005; Moustafa et al., 2010; Toulza et al., 2010). These data, along with the high percentage of surveyed dinoflagellates that exhibit an obligate B_{12} requirement (>90%; Tang et al., 2010) suggest that B_{12} availability may have important implications for dinoflagellate SAM metabolism; perhaps a disproportionately important process relative to diatoms. This could potentially result from extensive dinoflagellate DNA methylation or increased demand due to toxin production, which has a high SAM requirement (Lin, 2011). In addition, impaired

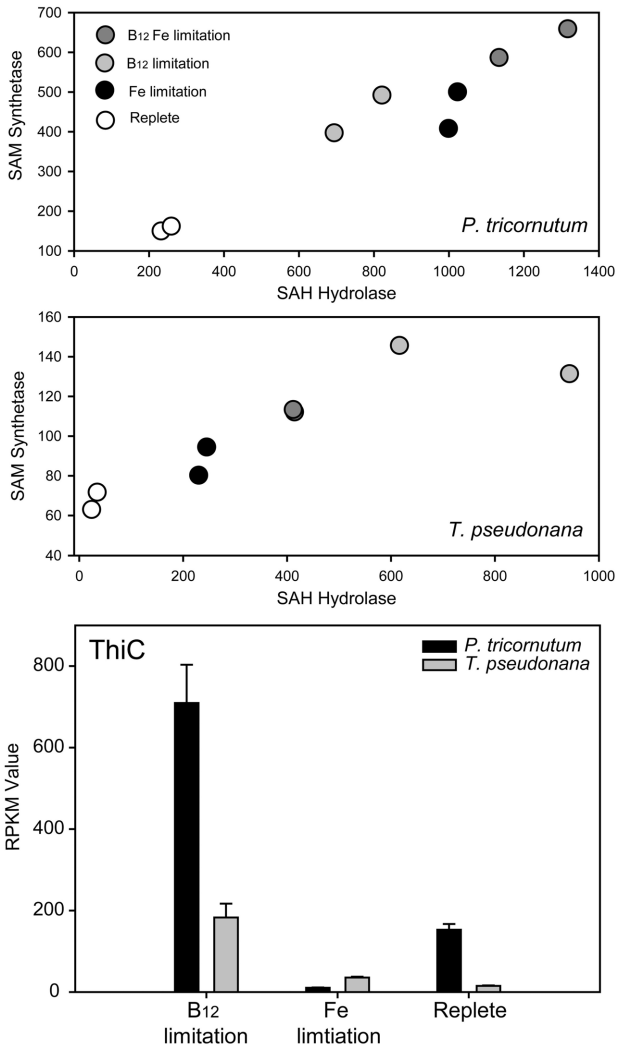

FIGURE 2 | Evidence from Bertrand et al., 2012 that AdoMet SAM starvation is an important consequence of B_{12} deprivation, with implications for thiamine biosynthesis. SAM synthetase (Tp 39946, Pt 18319) converts methionine and ATP to SAM. SAM, after use for methylation reactions, is converted to S-adenosylhomocysteine (SAH). SAH can act as an inhibitor to methylation reactions because of its high affinity for most methyltranserfases. SAH hydrolase (Tp 28496; Pt bd 913) catalyzes the reversible interconversion of SAH to homocysteine and adenosine. The expression of the genes encoding these proteins in two diatoms appears to correlate. RPKM (Reads Per Kilobase of exon model per Million mapped reads) gene expression values are plotted against each other for each of eight samples in two diatoms, duplicates of replete, low B_{12}, low B_{12} with low iron, and low iron alone. Expression under iron limited conditions was examined along with B_{12} to verify whether changes induced were likely a general stress response or more specific to the vitamin. In both diatoms, cells grown under nutrient replete conditions express these genes at the lowest level. Iron and B_{12} availability both influence the expression of these genes, with B_{12} having a greater impact of gene expression the B_{12} requiring diatom *T. pseudonana*. ThiC is a SAM-dependent protein required for pyrimidine moiety synthesis in thiamine biosynthesis. The expression of genes encoding ThiC in both these diatoms is elevated low B_{12} availability and not under low iron availability, suggesting that thiamine biosynthesis, and B_{12} availability may be linked in these diatoms, potentially through B_{12} impacts on SAM availability.

methionine synthase activity prevents efficient folate recycling, which has important implications for nucleic acid biosynthesis (Scott and Weir, 1981; Croft et al., 2005). Molecular evidence for altered folate metabolism has also been documented as a significant component of the diatom response to B_{12} deprivation (Bertrand et al., 2012). This likely holds true for other algal groups as well since the diatom response is similar to distantly related organisms such as humans and other metazoans (e.g., Scott and Weir, 1981).

Molecular aspects of acquisition of these vitamins in eukaryotic algae remains poorly understood. An important result of these inquiries into the molecular response of algae to vitamin deprivation has been the identification of proteins that are potentially involved in B_{12} or B_1 acquisition. Bertrand et al. (2012) identified a previously uncharacterized protein, deemed CBA1, that is directly involved in B_{12} acquisition by diatoms and that is much more abundant in diatoms when they are experiencing B_{12} deprivation. This protein, however, appears to be restricted to the stramenopile lineage, suggesting that other eukaryotic algal groups utilize different, as of yet unidentified, pathways for B_{12} uptake (Bertrand et al., 2012). Several candidate proteins involved in thiamine trafficking have been identified in whole genome sequencing projects (Worden et al., 2009) and transcriptomic analyses of *Micromonas* cultures under thiamine deprivation have also resulted in identification of additional putative thiamine transporters in this B_1 auxotrophic group (McRose et al., 2012).

Examination of transcripts encoding CBA1, ThiC, MetE, and MetH in natural Antarctic diatom communities revealed that all these transcripts are relatively abundant and therefore that B vitamin metabolism is likely an important component of the molecular physiology of field communities (**Figure 3**). These expression patterns suggest that Antarctic diatom communities are experiencing B_{12} deprivation (expressing MetE and CBA1) and that some subset of the community is able to potentially utilize B_{12} for methionine regeneration (MetH expression). This suggests that there are potentially different B_{12} quotas for different diatom species, with species experiencing starvation at varying intersections of cellular demand relative to ambient B_{12} availability. Additionally, there may be a subset of diatoms with localized B_{12} sources, such as intimately attached bacteria (**Figure 1**). These results suggest, however, that examining the distribution of B_{12}—responsive transcripts in field populations will yield important insights into the impact of vitamin availability on community

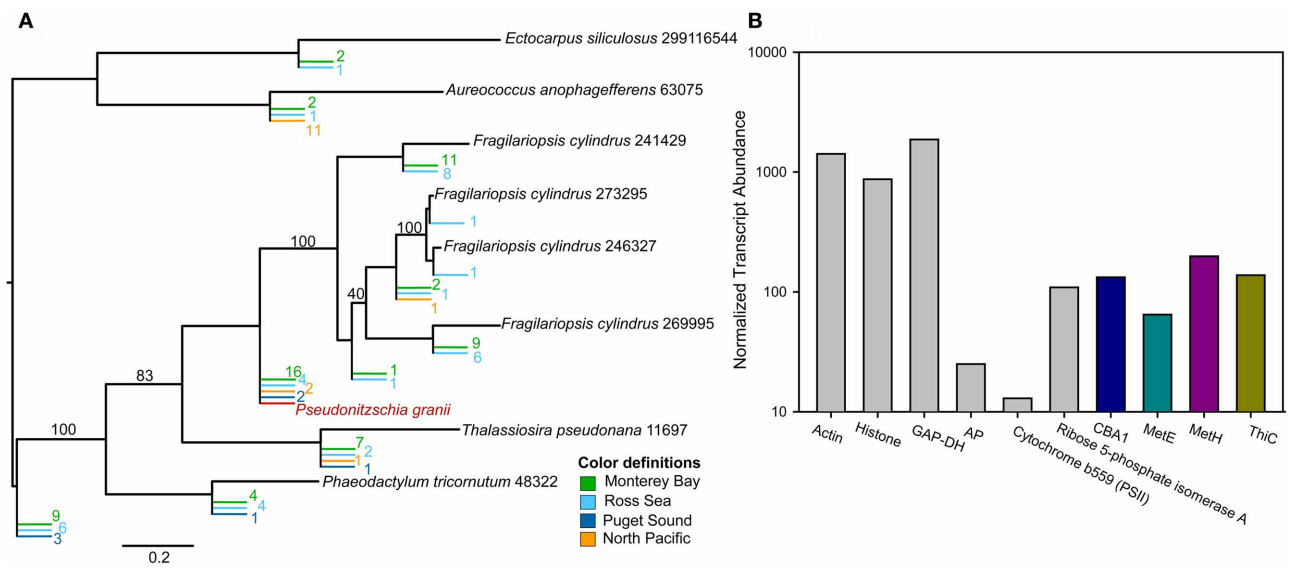

FIGURE 3 | The abundance and diversity of CBA1, B_{12} starvation indicator, and the abundance of ThiC, MetH, and MetE transcripts attributable to diatoms in Antarctic transcriptomic datasets, compared to the expression of transcripts encoding other well-characterized proteins (modified from Bertrand et al., 2012). (A) Phylogenetic tree containing CBA1 sequences from 454 metatranscriptomic (cDNA) libraries from the Ross Sea of the Southern Ocean, Monterey Bay, Puget Sound, and the North Pacific. Reference sequences from *Phaeodactylum tricornutum*, *Fragilariopsis cylindrus*, *Thalassiosira pseudonana*, *Aureococcus anophagefferenas*, and *Ectocarpus siliculosus* genomes were used to construct these trees and are shown in black. CBA1-like sequences from environmental samples are shown in color, as described in the key. CBA1 transcripts were detectable in diverse marine environments, suggesting that cobalamin acquisition is an important component of diatom molecular physiology. **(B)** The normalized abundance of Open Reading Frames (ORFs) assigned to CBA1 from within the Ross Sea is shown in blue, MetE: PF01717 is shown in green, MetH:PF02965 is shown in purple, ThiC:PF01964 in yellow, while the abundance of read counts assigned to diatom ORFs containing well-characterized pfam domains for comparison [Actin: PF00022, Histone:PF00125, GAP-DH: PF02800, Alkaline Phosphatase: PF00245, Flavodoxin: PF00258, Cytochrome b559 (PSII): PF00283, Ribose 5-phosphate isomerase A: PF06026] are shown in gray. Read counts for each ORF where summed across six libraries from Ross Sea samples and RPKM values were calculated. RPKMs were then summed across all diatom ORFs that contained that a domain of interest. CBA1, MetE, MetH, and ThiC are not among the extremely abundant transcripts (e.g., those encoding Actin, GAP-DH, Histone) but are comparable to those encoding Calvin Cycle protein Ribose 5-phosphate isomerase A, and are more abundant than the transcripts encoding a cytochrome required for photosystem II activity (b559) as well as alkaline phosphatase (AP), suggesting that they are of importance to the molecular physiology of natural diatom communities.

structure and primary productivity. For these analyses, it would be useful to know what percentage of the eukaryotic phytoplankton community possesses the ability to produce MetE; this would allow for more extensive interpretation of MetE and MetH transcript expression patterns. Similar analyses may be possible with thiamine—responsive genes in the future. Potential candidates for this include the recently identified putative transporters as well as ThiC, which appears to be present in genomes that are not auxotrophs and absent from genomes of organisms that require exogenous thiamine (**Table 2**).

POTENTIAL B_{12} AND B_1 METABOLIC INTERACTIONS WITH NITROGEN IN EUKARYOTIC PHYTOPLANKTON

B VITAMIN AND N STARVATION IMPACTS ON OSMOLYTE PRODUCTION AND UTILIZATION

Osmolytes are molecules that serve roles in osmoregulation. In eukaryotic phytoplankton, these include proline, glycine betaine (GBT), dimethylsulfonium propionate (DMSP), homarine, and isethionic acid (Boroujerdi et al., 2012). There are potentially important roles for B_{12}, B_1, methionine, SAM, and nitrogen metabolism in osmolyte production that likely result in interactive biochemical effects. One example is that methionine and SAM are both required for DMSP production, which is used by a subset of diatoms possibly as a cryoprotectant, osmolyte (Stefels, 2000), or antioxidant (Sunda et al., 2002), and is the precursor to the climatically important gas dimethylsulfide (Charlson et al., 1987). SAM recycling genes appear to play a role in the response of diatoms to low nitrogen, suggesting that there may be synergistic impacts of nitrogen and B_{12} depletion on SAM availability (**Table 4**). This observation is intriguing and warrants further exploration via SAM metabolite analysis under conditions of varying B_{12} and nitrogen availability.

In addition, nitrogen limitation has been previously identified as an important factor driving DMSP and DMS produced by phytoplankton populations. Nitrogen deprivation, more than any other nutrient starvation scenario tested, led to enhanced DMSP production per cell in an important oceanic diatom (Bucciarelli and Sunda, 2003; Sunda et al., 2007). A possible explanation for this trend is that under nitrogen starvation, N-containing osmolytes such as proline, homarine, and GBT are replaced by DMSP, which does not contain nitrogen (Bucciarelli and Sunda, 2003). There is some evidence that under N-replete conditions, GBT and homarine replace DMSP in *T. pseudonana* and that GBT concentrations increase upon addition of N to N-starved cultures of diatoms and coccolithophores (Keller et al., 1999). If DMSP is in fact used to replace N-containing osmolytes, B_{12} starvation coupled with N-limitation has the potential to negatively impact that substitution in at least two ways. The first is by potentially limiting the amount of DMSP produced due to restricted methionine availability. The second is again through SAM deprivation, which has been hypothesized to play an important role in diatom metabolism under low B_{12} conditions (**Figure 3**; Bertrand et al., 2012). These metabolic connections suggest that there may be synergistic impacts of B_{12} and N starvation on DMSP-producing algal strains. Alternatively, if the primary function for DMSP is as an antioxidant, increases in DMSP as a function of nitrogen starvation could be due to elevated demand for DMSP under the oxidative stress induced by nitrogen deprivation (Sunda et al., 2002, 2007). If DMSP in fact serves an important antioxidant role and if thiamine is shown to be an important algal antioxidant as well, this suggests that there could be potentially important interactions between B_1, B_{12}, and N availability in algal cells in response to oxidative stress.

Synthesis of GBT, in many organisms, also requires SAM as a methyl group donor. Also like DMSP, there is evidence that GBT production is tied to nitrogen metabolic status of individual cultures, (Keller et al., 1999, 2004). Since GBT synthesis requires nitrogen and is likely SAM dependent, B_{12} starvation may prompt substitution of other osmolytes, such as proline, for GBT as well as DMSP. This may have important implications for cellular nitrogen cycling. Notably, proline is generated from ornithine via activity of ornithine cyclodeaminase. Ornithine is an important metabolite in the urea cycle, which is a major pathway for nitrogen recycling in diatoms and potentially other algae (Fernie et al., 2012). If the proline balance were significantly impacted as a result of a metabolic cascade resulting from changes in the osmolyte balance, this could have significant impacts on overall cellular nitrogen metabolism.

B_{12} AND B_1 STARVATION IMPACTS ON AMINO ACID AND POLYAMINE BIOSYNTHESIS

The major organic constituent of diatom silica frustules are a series of long chain polyamines (LCPAs). Different diatoms synthesize different suites of LCPAs (Kroger et al., 2000). These molecules, along with silica deposition proteins called silafins and silafin-like girdle band and nanopattern-associated proteins call cingulins (Scheffel et al., 2011), induce biomineralization, and are responsible for differences in frustule morphology between diatom groups. LCPAs vary in chain length and degree of methylation, but appear to all be synthesized from putricine, spermidine, or spermine precursors. These precursors are synthesized sequentially from ornithine, with spermidine, and spermine production both requiring SAM as a propylamine donor. Subsequent steps in LCPA formation likely require SAM as well (Kroger and Poulsen, 2008). LCPAs recovered in net tows are mostly putracine-based, with varying degrees of methylation, suggesting that SAM is an important component of LCPA production for field diatom populations as well (Bridoux et al., 2012). Conceivably, reduced SAM production through B_{12} starvation could induce changes in silica frustule formation by decreasing the pool of available LCPAs. Indeed, reduction of LCPA production as a result of the addition of an inhibitor for ornithine decarboxylase, which is known to be involved in polyamine biosynthesis, dramatically reduced biogenic silica formation in *T. pseudonana* (Frigeri et al., 2006). In diatoms, possible LCPA biosynthesis genes have been identified. These are potentially gene fusions of bacterially derived polyamine biosynthetic enzymes S-adenosylmethionine decarboxylase (SAM DC) and an aminopropyltransferase (Michael, 2011), which require input of SAM. The Met salvage pathway would need to be efficient, and if SAM starvation does result from B_{12} deprivation, there could be substantial implications of low B_{12} for LCPA biosynthesis. Ornithine represents a significant component of the carbon and nitrogen pool within phytoplankton cells and is a centrally important

Table 4 | B_{12} and B_1 related genes from published *P. tricornutum* EST libraries.

	Original standard	Si−	Si+	Low Fe	n replete chemostat	N-starved	Urea, low N	Ammonia, low N	Description
	os	sm	sp	fl	nr	ns	ua	aa	
B_{12}-RELATED									
G18319	0	0	1	9	4	15	20	33	s-adenosyl homocysteine hydrolase
G48322	3	2	0	0	1	0	2	3	CBA1
G18665	1	0	1	1	1	3	10	11	Glycine hydroxymethyltransferase
G28056	0	7	11	0	0	2	0	1	MetE
G913.1	1	0	0	5	2	3	0	1	S-adenosylmethionine synthetase
G54015	0	0	1	4	1	6	0	0	Glycine hydroxymethyltransferase
G23399	1	0	0	9	0	1	5	5	MetH
G51830	4	0	3	0	0	3	7	4	Methylmalonyl co a mutase
G30471	0	0	1	0	0	0	4	2	Methylenetetrahydrofolate reductase
B_1 USE									
G20183	2	0	1	0	0	2	0	0	Transketolase
G20360	0	0	0	0	0	3	0	0	Pyruvate dehydrogenase e1 component beta subunit
G12375	0	0	0	0	0	2	1	0	Pyruvate dehydrogenase e1 component alpha subunit
G29016	2	0	0	0	0	4	0	2	2-oxoglutarate dehydrogenase e1 oxoglutarate alpha-ketoglutaric
G37341	2	1	3	0	0	0	2	7	Acetolactate synthase
G48444	0	0	1	0	0	1	1	1	2-oxoglutarate dehydrogenase e1 component
G46387	0	0	0	0	1	0	0	0	Dehydrogenase, E1 component
G36257	0	0	0	0	0	0	0	1	Fructose-6-phosphate phosphoketolase
G9476	1	2	4	2	0	1	0	0	2-oxoisovalerate dehydrogenase alpha, mitochondrial expressed
G41856	14	0	2	1	2	3	12	3	Plastid transketolase
G29260	5	0	0	2	1	2	11	6	Probable transketolase
G11021	0	3	2	3	1	0	0	0	Branched-chain alpha-keto acid decarboxylase e1 beta subunit
B1 SYNTHESIS									
G34373	0	0	0	1	0	0	0	0	Possible ThiF
G1689.1	3	0	0	2	2	5	1	0	Possible Dsx
G31544	4	2	0	1	0	4	3	2	Possible ThiO
G38085	9	1	0	0	1	1	3	4	ThiC
G47293	0	0	0	0	0	0	0	0	Possible ThiD/E
G5423	1	0	0	0	0	0	0	0	TPK
LCPA BIOSYNTHESIS									
G7617	0	0	1	0	0	3	4	0	s-adenosylmethionine decarboxylase proenzyme
G7910	0	0	0	0	0	0	0	1	Spermine synthase
G3362	0	2	0	0	0	4	9	0	S-adenosylmethionine decarboxylase
G7621	0	0	0	0	0	0	1	0	s-adenosylmethionine decarboxylase proenzyme

Treatment descriptions and labels can be found in Maheswari et al. (2010).

metabolite in the ornithine urea cycle (OUC), which is the major distribution hub for nitrogen in diatom cells (Allen et al., 2011; Bender et al., 2012). If SAM starvation results in major changes in ornithine balance through alterations in polyamine biosynthesis, this would hold substantial ramifications for the impact of B_{12} deprivation on nitrogen cycling.

Overall, it seems that N starvation could induce up-regulation in pathways that demand B_{12}, such as methionine and SAM synthesis. This would potentially be reflected in elevated expression of B_{12} acquisition proteins under nitrogen limitation, and elevation of proteins required to generate methionine.

LINKS BETWEEN N, B_1 AND B_{12} THROUGH SULFUR METABOLISM IN EUKARYOTIC PHYTOPLANKTON

Connections between nitrate reduction and sulfur assimilation are well known. Sulfate reduction is thought to be regulated by nitrogen nutrition in plants (Koprivova et al., 2000; Takahashi et al., 2011); this may also be true for phytoplankton, as sulfur uptake and assimilation genes in diatoms appear to be responsive to nitrogen availability. Both B_1 and B_{12} have important ties to sulfur metabolism, since B_{12} is important for sulfur amino acid cycling and DMSP synthesis and B_1 is produced from thiazole, a sulfur containing moiety. Indeed, in plants, methionine synthesis and other aspects of sulfur metabolism are very tightly regulated by SAM availability. If the B_{12} dependence of SAM availability hypothesized for phytoplankton is verified (Bertrand et al., 2012), this suggests that B_{12} availability may influence additional aspects of sulfur and nitrogen metabolism.

INFLUENCE OF B_{12} AND B_1 STARVATION ON THE DIATOM UREA CYCLE THROUGH IMPACTS ON THE CITRIC ACID CYCLE AND AMINO ACID CYCLING

Important impacts of vitamins on amino acid and amine cycling include the previously discussed impact of B_{12} on cysteine and methionine cycling and the impact of B_1 on branched amino acid synthesis. B_1 contributes to the first step in valine synthesis as well as important steps in amino acid degradation and recycling via keto acid dehydrogenase activity (Binder et al., 2007). In addition, B_1 appears to impact nitrogen assimilation and amino acid recycling though the dependence of 2-oxoglutarate dehydrogenase (OGDHC) on the cofactor (Bunik and Fernie, 2009). For instance, potato OGDHC inhibition causes reductions in nitrate assimilation as well as increases in glutamate and GABA accumulation (Araujo et al., 2008). This suggests that disturbances in B_1 metabolism may have profound affects for nitrogen assimilation and amino acid recycling, though this has yet to be confirmed for phytoplankton.

The OUC is of central importance to diatoms and potentially other phytoplankton as a nitrogen assimilation and repackaging hub. The OUC and the citric acid (TCA) cycles are linked (Allen et al., 2011). Mitochondrial amino acid catabolism yield carbon skeletons for the TCA cycle as well as ammonia and bicarbonate that is shunted into the OCU. This connection is supported by metabolic data suggesting that fumarate and malate, important TCA cycle intermediates, display similar patterns as OUC metabolites in diatom cell lines with altered urea cycle pathways (CPS knockdowns; Allen et al., 2011). Both B_{12} and B_1 play important roles in the citric acid (TCA) cycle. For example, B_{12} is a cofactor for mmcM which generates succinyl coA from methylmalonyl coA, an amino acid degradation product. Expression of the gene encoding mmcM is upregulated under—N conditions in *P. tricornutum* EST libraries (**Table 4**), suggesting that there could be consequences of reduced mmcM activity for cells experiencing nitrogen deprivation. B_{12} availability does not appear to influence mmcM expression (Bertrand et al., 2012). It is notable that mmcM expression levels are not insignificant in diatom transcriptome studies, suggesting that this gene product may be of utility to phytoplankton despite the fact that the presence of this gene in phytoplankton genomes does not confer an absolute B_{12} demand (**Table 1**). There are numerous connections between B_1 and the citric acid cycle. B1 is required for the generation of acetyl CoA from pyruvate via the pyruvate dehydrogenase complex. The enzyme ODG is also thiamine-dependent and plays a important role in the citric acid cycle. This enzyme is also thought to be a important player in plant nitrogen assimilation though its impact on glutamine stores (Bunik and Fernie, 2009). Interestingly, the reactant consumed by this protein, 2-oxoglutarate, accumulates strongly in diatom cell lines with impacted urea cycle (Allen et al., 2011). These data suggest that B_1- and B_{12}-dependent metabolisms play key roles in steps that maintain cellular carbon and nitrogen recycling; synergistic impacts of B vitamin deprivation and N starvation are therefore likely.

SYNTHESIS AND IMPLICATIONS FOR EUKARYOTIC PHYTOPLANKTON ECOLOGY

Many of the interactions between B vitamins and N metabolism described above have the potential to profoundly influence eukaryotic phytoplankton ecology and are summarized in **Figure 4**. From these interactions, we can hypothesize that nitrogen limitation, experienced by phytoplankton in much of the ocean, may induce enhanced demand for B_{12} and B_1 via a variety of mechanisms. These include substitution of N-containing osmolytes with DMSP, substituting N-containing antioxidants and DMSP with thiamine, and effectively recycling amino acids and glutamine stores utilizing high amounts of B_1. There are also interactions discussed above that would result in B vitamin deprivation leading to impaired nitrogen recycling which could conceivably increase nitrogen demand in phytoplankton cells. These include impaired glutamine recycling due to reduced 2-oxogultarate dehydrogenase and pyruvate dehydrogenase activity and impaired ornithine and proline cycling due to B_1 and B_{12} impacts on the TCA cycle as well as through potential imbalances in the methyl cycle due to B_{12} deprivation. These mechanisms all suggest that biochemical interactions between B vitamin and N limitation have the potential to lead to interactive colimitation and thus that the B vitamin and N colimitations observed in field studies (Koch et al., 2011; Gobler et al., 2007) may be due to both independent secondary limitation or dependent colimitation scenarios (Saito et al., 2008).

These biochemical dependencies have the potential to impart changes in phytoplankton species composition based on differences in B_1 and B_{12} demand between phytoplankton groups. Diatoms are thought to rely on an efficient urea cycle for distributing and recycling nitrogen (Allen et al., 2011; Bender et al., 2012). The impacts of B_{12} and B_1 deprivation on the efficiency of the urea cycle, therefore, may disproportionately impact diatoms. In addition, if dinoflagellate SAM demand is indeed elevated over other phytoplankton as hypothesized, it is possible that B_{12} deprivation could disproportionately impact dinoflagllate strategies for coping with nitrogen deprivation, such as the use of DMSP to replace N-containing osmolytes. These impacts may be of particular importance to harmful algal bloom species, which are known to have disproportionately high instances of B_1 and B_{12} auxotrophy (Tang et al., 2010). Additionally, toxin production by some dinoflagellate species has been shown to

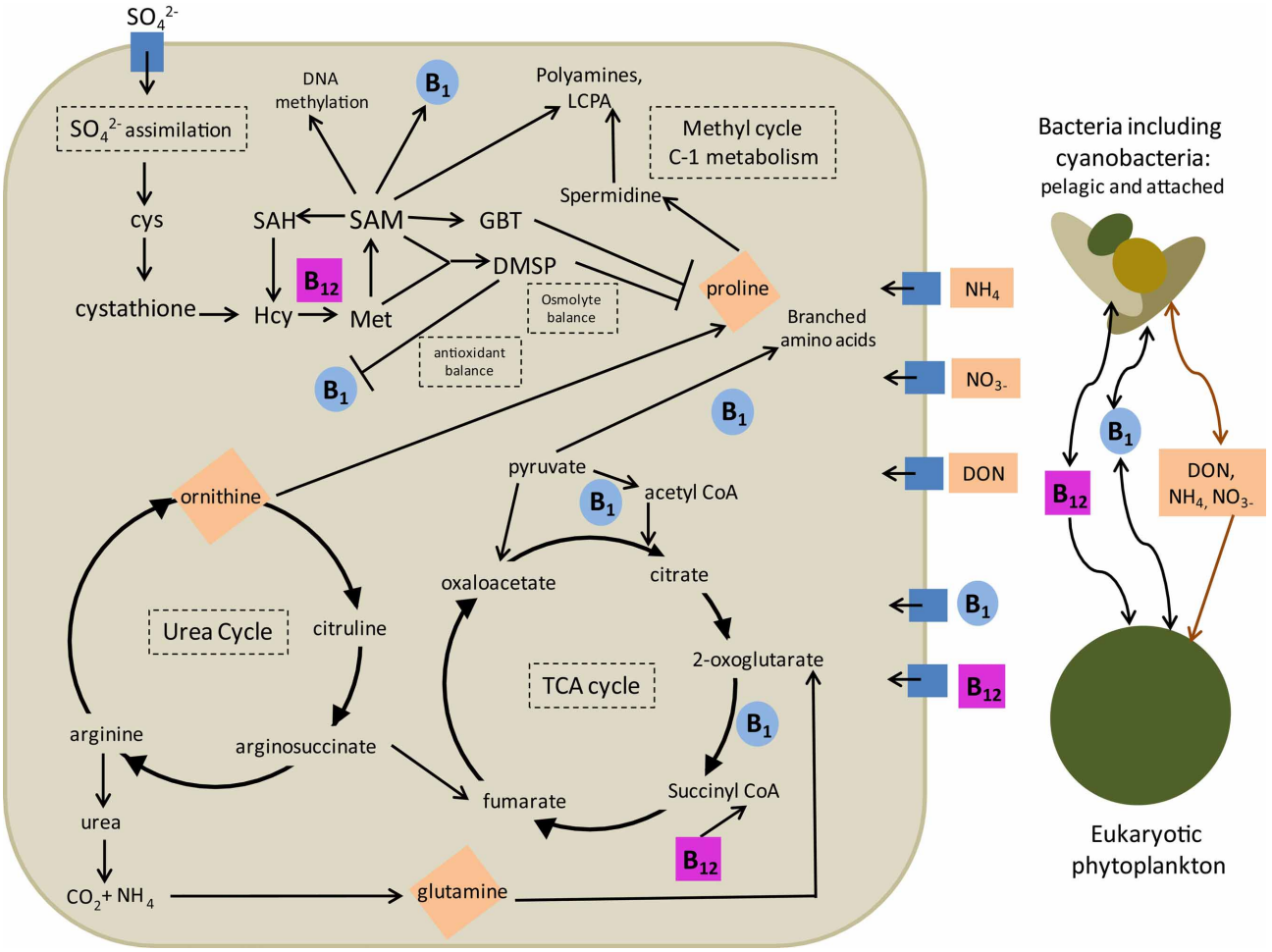

FIGURE 4 | An overview of B_{12} and B_1 interactions with nitrogen metabolism in eukaryotic phytoplankton. Four major intracellular mechanisms are outlined: (1) impacts on osmolyte and antioxidant production and utilization and (2) impacts on polyamine biosynthesis via the methyl cycle, (3) impacts on the urea cycle and amino acid recycling through impacts on the citric acid cycle, and (4) impacts of nitrogen balance on sulfur assimilation. Major cellular nitrogen stores impacted by B_1 and B_{12} availability are shown in orange diamonds. Arrows denote direction of reaction, production, or consumption. Bars denote potential negative feedbacks, where increases in originating compound may decrease abundance or importance of the connected compound. Also described are major interactions with other microbial groups outside the cell in terms of production and consumption of B_1, B_{12}, and nitrogen sources. Groups considered include pelagic and attached bacteria, including cyanobacteria (brown) and other eukaryotic algae (green). Relevant acquisition pathways are denoted by blue boxes. Cys, cysteine; Hcy, homocysteine; SAH, S-adenosyl homocysteine; SAM, S-adenosyl methionine; GBT, glycine betaine; DMSP, dimethylsulfonium propionate.

increase under N-limitation (Ransom Hardison et al., 2012); synthesis pathways of many dinoflagellate toxins such as saxitoxin and brevetoxin are thought to be SAM-dependent (Lin, 2011). Together, these data suggests that HAB species may be more susceptible than others to impacts of these dependent colimitations between N and B vitamins and that these colimitations may additionaly impact toxin production rates. This is further evidence that B vitamin dynamics should be considered when predicting and evaluating potential for harmful algal bloom scenarios.

Given that B_{12}, B_1, and nitrogen availability to eukaryotic phytoplankton all have potential to be impacted by bacterial community composition and activity, the bacterial community is likely an important driver of when and where instances of these dependent colimitations may be important. This may be especially true when considering timing and species composition in spring bloom scenarios, which is an active area of continued research today (Mahadevan et al., 2012). Swift and Guillard (1978) determined that spring bloom diatom species, though not B_{12} auxotrophs, grew faster and experienced shorter lag phases in the presence of the vitamin, suggesting that possible interactions between N and S metabolism, and B_{12} utilization could be important for bloom timing and species composition. Recent work also suggests that bacterioplankton respond to various phases in spring blooms by changing both metabolic potential and species composition over time (Teeling et al., 2012). This could have important impacts for B_{12} and B_1 production and consumption as well as for nitrogen availability and recycling. Mounting evidence

suggests that there could be synergistic interactions of these impacts on eukaryotic phytoplankton that could influence not only species composition but also bloom timing and overall productivity. This suggests that time series measurements, over both day to week and seasonal timescales, which include B_{12}, B_1, and nitrogen species concentration measurements and uptake rates as well as protein or transcript-based indicators of nitrogen and vitamin deprivation, would be useful, particularly in conjunction with bacterioplankton community composition assessments and implementation of B vitamin biosynthesis indicators. Locations where this would be of considerable interest include high latitude ecosystems, which largely lack B_{12} producing cyanobacteria, coastal locations with HAB blooming dinoflagellates, and diatoms as well as the North Atlantic, before during and after bloom scenarios.

ACKNOWLEDGMENTS

We thank Greg Wanger for the use of his electron microscopy images. We are indebted to Mak Saito, Peter Lee, Ruben Valas, Stephane Lefebvre, James McCarthy, Jeff McQuaid, and Karen Beeri for helpful discussions. This work was funded by an NSF Office of Polar Programs Postdoctoral Fellowship to Erin M. Bertrand (ANT-1103503) and NSF-MCB-1024913, NSF-ANT-1043671, and DOE-DE-SC0006719 (Andrew E. Allen).

REFERENCES

Allen, A., Dupont, C. L., Obornik, M., Horak, A., Nunes-Nesi, A., McCrow, J. P., et al. (2011). Evolution and metabolic significance of the urea cycle in photosynthetic diatoms. *Nature* 473, 203–206.

Allen, A. E., Booth, M. G., Frischer, M. E., Verity, P. G., Zehr, J. P., and Zani, S. (2001). Diversity and detection of nitrate assimilation genes in marine bacteria. *Appl. Environ. Microbiol.* 67, 5343–5348.

Allen, A. E., Booth, M. G., Verity, P. G., and Frischer, M. E. (2005). Influence of nitrate availability on the distribution and abundance of heterotrophic bacterial nitrate assimilation genes in the Barents Sea during summer. *Aquat. Microb. Ecol.* 39, 247–255.

Araujo, W. L., Nunes-Nesi, A., Trenkamp, S., Bunik, V. I., and Fernie, A. R. (2008). Inhibition of 2-oxoglutarate dehydrogenase in potato tuber suggests the enzyme is limiting for respiration and confirms its importance in nitrogen assimilation. *Plant Physiol.* 148, 1782–1796.

Azam, F. (1998). Microbial control of oceanic carbon flux: the plot thickens. *Science* 280, 694–696.

Bender, S. J., Parker, M. S., and Armbrust, E. (2012). Coupled effects of light and nitrogen source on the urea cycle and nitrogen metabolism over a diel cycle in the marine diatom *Thalassiosira pseudonana*. *Protist* 163, 232–251.

Bertrand, E. M., Allen, A. E., Dupont, C. L., Norden-Krichmar, T. M., Bai, J., Valas, R. E., et al. (2012). Influence of cobalamin scarcity on diatom molecular physiology and identification of a cobalamin acquisition protein. *Proc. Natl. Acad. Sci. U.S.A.* 109, E1762–E1771.

Bertrand, E. M., Saito, M. A., Jeon, Y. J., and Neilan, B. A. (2011a). Vitamin B_{12} biosynthesis gene diversity in the Ross Sea: the identification of a new group of putative polar B_{12}-biosynthesizers *Environ. Microbiol.* 13, 1285–1298.

Bertrand, E. M., Saito, M. A., Lee, P. A., Dunbar, R. B., Sedwick, P. N., and DiTullio, G. R. (2011b). Iron limitation of a springtime bacterial and phytoplankton community in the Ross Sea: implications for vitamin B_{12} nutrition. *Front. Aquat. Microbiol.* 2:160. doi: 10.3389/fmicb.2011.00160

Bertrand, E. M., Saito, M. A., Rose, J. M., Riesselman, C. R., Lohan, M. C., Noble, A. E., et al. (2007). Vitamin B12 and iron co-limitation of phytoplankton growth in the Ross Sea. *Limnol. Oceanogr.* 52, 1079–1093.

Bettendorff, L., and Wins, P. (2009). Thiamin diphosphate in biological chemistry: new aspects of thiamin metabolism, especially triphosphate derivatives acting other than as cofactors. *FEBS J.* 76, 2917–2925.

Binder, S., Knill, T., and Schuster, J. (2007). Branched-chain amino acid metabolism in higher plants. *Physiol. Plant.* 129, 68–78.

Bonnet, S., Webb, E. A., Panzeca, C., Karl, D. M., Capone, D. G., and Sanudo-Wilhelmy, S. A. (2010). Vitamin B_{12} excretion by cultures of the marine cyanobacteria *Crocosphaera* and *Synechococcus*. *Limnol. Oceanogr.* 55, 1959–1964.

Boroujerdi, A. F. E., Lee, P. A., DiTullio, G. R., Janech, M. G., Vied, S. B., and Bearden, D. W. (2012). Identification of isethionic acid and other small molecule metabolites of *Fragilariopsis cylindrus* with nuclear magnetic resonance *Anal. Bioanal. Chem.* 404, 777–784.

Bridoux, M. C., Keil, R., and Ingalls, A. E. (2012). Analysis of natural diatom communities reveals novel insights into diversity of long chain polyamine structures involved in silica precipitation. *Org. Geochem.* 47, 9–21.

Bronk, D. A., Glibert, P. M., and Ward, B. B. (1994). Nitrogen uptake, dissolved organic nitrogen release, and new production. *Science* 265, 1843–1846.

Bucciarelli, E., and Sunda, W. G. (2003). Influence of CO2, nitrate, phosphate, and silicate limitation on intracellular DMSP in batch cultures of the coastal diatom *Thalassiosira pseudonana*. *Limnol. Oceanogr.* 48, 2256–2265.

Bunik, V. I., and Fernie, A. R. (2009). Metabolic control exerted by the 2-oxoglutarate dehydrogenase reaction: a cross-kingdom comparison of the crossroads between energy production and nitrogen assimilation. *Biochem. J.* 422, 405–421.

Capone, D. G. (2000). "The marine microbial nitrogen cycle," in *Microbial Ecology of the Oceans*, ed D. Kirchman (New York, NY: Wiley Liss), 455–494.

Carlucci, A. F. (1966). Bioassay of seawater. II. Methods for the determination of vitamin B1 in seawater. *Can. J. Microbiol.* 12, 1079–1089.

Carlucci, A. F., and Bowes, P. M. (1970). Production of vitamin B_{12}, thiamine, and biotin by phytoplankton. *J. Phycol.* 6, 351–357.

Carlucci, A. F., and Silbernagel, S. B. (1969). The effect of viamin concentrations on growth and development of vitamin-requiring algae. *J. Phycol.* 5, 64–67.

Carlucci, A. F., Silbernagel, S. B., and McNally, P. M. (1969). The influence of temperature and solar radiation on persistence of vitamin B_{12}, thiamine, and biotin in seawater. *J. Phycol.* 5, 302–305.

Caron, D. A., Dennett, M. A., Lonsdale, D. J., Moran, D. M., and Shalapyonok, L. (2000). Microzooplankton herbivory in the Ross Sea, Antarctica. *Deep Sea Res. II* 47, 3249–3272.

Charlson, R. J., Lovelock, J. E., Andreae, M. O., and Warren, S. G. (1987). Oceanic phytoplankton, atmospheric sulphur, cloud albedo, and climate. *Nature* 326, 655–661.

Chatterjee, A., Li, S., Zhang, Y., Grove, T. L., Lee, M., Krebs, C., et al. (2008). Reconstitution of ThiC in thiamine pyrimidine biosynthesis expands the radical SAM superfamily. *Nat. Chem. Biol.* 4, 758–765.

Cole, J. J. (1982). Interactions between bacteria and algae in aquatic systems. *Annu. Rev. Ecol. Sys.* 13, 291–314.

Cowey, C. B. (1956). A preliminary investigation of the variaton of vitamin B-12 in oceanic and coastal waters. *J. Mar. Biol. Assoc. U.K.* 35, 609–620.

Croft, M. T., Lawrence, A. D., Raux-Deery, E., Warren, M. J., and Smith, A. G. (2005). Algae acquire vitamin B12 through a symbiotic relationship with bacteria. *Nature* 438, 90–93.

Croft, M. T., Moulin, M., Webb, M. E., and Smith, A. G. (2007). Thiamine biosynthesis in algae is regulated by riboswitches. *Proc. Natl. Acad. Sci. U.S.A.* 104, 20770–20775.

Croft, M. T., Warren, M. J., and Smith, A. G. (2006). Algae need their vitamins. *Eukaryot. Cell* 5, 1175–1184.

Dortch, Q. (1990). The interaction between ammonium and nitrate uptake in phytoplankton. *MEPS* 61, 183–201.

Drennan, C. L., Matthews, R. G., and Ludwig, M. L. (1994). Cobalamin-dependent methoionine synthase: the structure of a methylcobalamin-binding fragment and implicatiosn for other B_{12}-dependent enzymes. *Curr. Opin. Struct. Biol.* 4, 919–929.

Droop, M. R. (1957). Vitamin B_{12} in marine ecology. *Nature* 180, 1041–1042.

Droop, M. R. (1958). Requirement for thiamine among some marine and supralittoral protists. *J. Mar. Biol. Assoc. U.K.* 37, 323–329.

Droop, M. R. (1962). "Organic micronutrients," in *Physiology and Biochemistry of Algae*, ed R. A. Lewin (New York, NY: Academic Press), 141–159.

Droop, M. R. (2007). Vitamins, phytoplankton and bacteria: symbiosis or scavenging? *J. Plankton Res.* 29, 107–113.

Eppley, R. W., and Peterson, B. J. (1979). Particulate organic matter flux and planktonic new production in the deep ocean. *Nature* 282, 677–680.

Fernie, A. R., Obata, T., Allen, A. E., Araújo, W. L., and Bowler, C. (2012). Leveraging metabolomics for functional investigations in sequenced marine diatoms. *Trends Plant Sci*. 17, 395–403.

Frank, R., Leeper, F., and Luisi, B. (2007). Structure, mechanism and catalytic duality of thiamine-dependent enzymes. *Cell. Mol. Life Sci.* 64, 892–905.

Frigeri, L. G., Radabaugh, T. R., Haynes, P. A., and Hildebrand, M. (2006). Identification of Proteins from a cell wall fraction of the diatom *Thalassiosira pseudonana*. *Mol. Cell. Proteomics* 5, 182–193.

Gobler, C. J., Norman, C., Panzeca, C., Taylor, G. T., and Sanudo-Wilhelmy, S. A. (2007). Effect of B-vitamins and inorganic nutrients on algal bloom dynamics in a coastal ecosystem. *Aquat. Microb. Ecol.* 49, 181–194.

Gold, K. (1968). Some factors affecting the stability of thiamine. *Limnol. Oceanogr.* 13, 185–188.

Gold, K., Roels, O. A., and Bank, H. (1966). Temperature dependent destruction of thiamine in seawater. *Limnol. Oceanogr.* 12, 410–413.

Goyer, A. (2010). Thamine in plants: aspects of its metabolism and functions. *Phytochemistry* 71, 1615–1624.

Grossart, H., Levold, F., Allgaier, M., and Brinkhoff, S. M. (2005). Marine diatom species harbour distinct bacterial communities. *Environ. Microbiol.* 7, 860–873.

Guillard, R. R. L., and Ryther, J. H. (1962). Studies of marine planktonic diatoms 1. *Cyclotella nana Hustedt*, and *Detonula confervacea* (cleve) Gran. *Can J. Microbiol.* 8, 229–239.

Hecky, R. E., and Killam, (1988). Nitrogen limitation of phytoplankton in freshwater and marine environments: a review of recent evidence on the effects of enrichment. *Limnol. Oceanogr.* 33, 796–822.

Helliwell, K. E., Wheeler, G. L., Leptos, K. C., Goldstein, R. E., and Smith, A. G. (2011). Insights into the evolution of vitamin B_{12} auxotrophy from sequenced algal genomes. *Mol. Biol. Evol*. 28, 2921–2933.

Hu, M., Chen, Y., and Lin, Y. (1995). The antioxidant and prooxidant activity of some B vitamins and vitamin-like compounds. *Chem. Biol. Interact.* 97, 63–73.

Jurgenson, C. T., Begley, T. P., and Ealick, S. E. (2009). The structural and biochemical foundations of thiamine biosynthesis. *Annu. Rev. Biochem.* 78, 569–603.

Karl, D. M. (2002). Nutrient dynamics in the deep blue sea. *Trends Microbiol.* 10, 410–418.

Keller, M. D., Keine, R. P., Matrai, P. A., and Bellows, W. K. (1999). Production of glycine betaine and DMSP in marine phytoplankton 1. Batch cultures. *Mar. Biol.* 135, 237–248.

Keller, M. D., Matrai, P. A., Keine, R. P., and Bellows, W. K. (2004). Responses of coastal phytoplankton populations to nitrogen addition: dynamics of cell-associated DMSP, GBT and homarine. *Can. J. Fish. Aquat. Sci.* 61, 685–699.

Kirchman, D. (2000). "Uptake and regeneration of inorganic nutrients by marine heterotrophic bacteria," in *Microbial Ecology of the Oceans*, ed D. Kirchman (New York, NY: Wiley Liss), 261–288.

Kirchman, D. L., and Wheeler, P. A. (1998). Uptake of ammonium and nitrate by heterotrophic bacteria and phytoplankton in the sub-Arctic Pacific. *Deep Sea Res. I* 45, 347–365.

Koch, F., Marcoval, M. A., Panzeca, C., Bruland, K. W., Sanudo-Wilhelmy, S. A., and Gobler, C. J. (2011). The effect of vitamin B_{12} on phytoplankton growth and community structure in the Gulf of Alaska. *Limnol. Oceanogr.* 56, 1023–1034.

Koprivova, A., Suter, M., Op den Camp, R., Brunold, C., and Kopriva, S. (2000). Regulation of sulfate assimilation by nitrogen in Arabadopsis. *Plant Physiol.* 122, 737–746.

Kroger, N., Deutzmann, R., Bergsdorf, C., and Sumper, M. (2000). Species-specific polyamines from diatoms control silica morphology. *Proc. Natl. Acad. Sci. U.S.A.* 97, 14133–14138.

Kroger, N., and Poulsen, N. (2008). Diatoms- from cell wall biogeneisis to nanotechnology. *Annu. Rev. Genet.* 42, 83–107.

Kudela, R. M., and Dugdale, R. C. (2000). Nutrient regulation of phytoplankton productivity in Monterey Bay, CA. *Deep Sea Res. II* 47, 1023–1053.

Lexa, D., and Savant, J. M. (1983). The electrochemistry of vitamin B12. *Acc. Chem. Res.* 16, 235–243.

Lidie, K. B., Ryan, J. C., Barbier, M., and Van Dolah, F. M. (2005). Gene expression in Florida red tide dinoflagellate *Karenia brevis*. *Mar. Biotechnol.* 7, 481–493.

Lin, S. (2011). Genomic understanding of dinoflagellates. *Res. Microbiol.* 162, 551–569.

Lukienko, P. I., Melnichenko, N. G., Zverinskii, I. V., and Zabrodskaya, S. V. (2000). Antioxidant properties of thiamine. *Bull. Exp. Biol. Med.* 130, 874–876.

Mahadevan, A., D'Asaro, E., Lee, C., and Perry, M. J. (2012). Eddy-driven stratification initiates North Atlantic spring phytoplankton blooms. *Science* 337, 54–58.

Maheswari, U., Jabbari, K., Petit, J. L., Porcel, B. M., Allen, A. E., Cadoret, J. P., et al. (2010). Digital gene expression profiling of novel diatom transcripts provides insight into their biological functions. *Genome Biol.* 11, R85.

Marchant, H. J. (2005). "Cyanophytes," in *Antarctic Marine Protists,* eds F. J. Scott and H. J. Marchant (Hobart: Australian Biological Resources Study), 324–325

Martens, J. H., Bargv, H., Warren, M. J., and Jan, D. (2002). Microbial production of vitamin B_{12}. *Appl. Microbiol. Biotechnol.* 58, 275–285.

McCarthy, J. J., and Carpenter, E. J. (1983). "Nitrogen cycling in the near surface waters of the open ocean," in *Nitrogen in the Marine Environment,* eds E. J. Carpenter and D. G. Capone (New York, NY: Academic Press), 487–572.

McRose, D., Yan, S., Reistetter, E., and Worden, A. Z. (2012). "Vitamin biosynthesis and regulation in marine algae," in *Genomics Science Contractors-Grantees Meeting*, (Bethesda, MD).

Menzel, D. W., and Spaeth, J. P. (1962). Occurrence of vitamin B_{12} in the Sargasso Sea. *Limnol. Oceanogr.* 7, 151–154.

Michael, A. J. (2011). Molecular machines encoded by bacterially-derived multidomain gene fusions that potentially synthesize N-methylate and tranfer long chain polyamines in diatoms. *FEBS Lett.* 585, 2627–2634.

Moore, J. K., Doney, S. C., and Lindsay, K. (2004). Upper ocean ecosystem dynamics and iron cycling in a global three-dimensional model. *Glob. Biogeochem. Cycles* 18, 4028–4049.

Moustafa, A., Evans, A. N., Kulis, D. M., Hackett, J. D., Erdner, D. L., Anderson, D. M., et al. (2010). Transcriptome profiling of a toxic dinoflagellate reveals a gene-rich protist and a potential impact on gene expression due to bacterial presence. *PLoS ONE* 5:e9688. doi: 10.1371/journal.pone.0009688

Okbamichael, M., and Sañudo-Wilhelmy, S. A. (2004). A new method for the determination of Vitamin B_{12} in seawater. *Anal. Chim. Acta* 517, 33–38.

Okbamichael, M., and Sanudo-Wilhelmy, S. A. (2005). Direct determination of vitamin B1 in seawater by solid phase extraction and high performance liquid chromatography quantification. *Limnol. Oceanogr. Methods* 3, 241–246.

Panzeca, C., Beck, A., Leblanc, K., Taylor, G. T., Hutchins, D. A., and Sañudo-Wilhelmy, S. A. (2008). Potential cobalt limitation of vitamin B_{12} synthesis in the North Atlantic Ocean. *Glob. Biogeochem. Cycles* 22, 2029–2036.

Panzeca, C., Beck, A. J., Tovar-Sanchez, A., Segovia-Zavala, J., Taylor, G. T., Gobler, C. J., et al. (2009). Distributions of dissolved vitamin B12 and Co in coastal and open-ocean environments. *Estuar. Coast. Shelf Sci.* 85, 223–230.

Panzeca, C., Tovar-Sanchez, A., Agusti, S., Reche, I., Duarte, M., Taylor, G. T., et al. (2006). B vitamins as regulators of phytoplankton dynamics. *EOS* 87, 593–596.

Partensky, F., Hess, W. R., and Vaulot, D. (1999). *Prochlorococcus*, a marine photosynthetic prokaryote of global significance. *Microbiol. Mol. Biol. Rev.* 63, 106–127.

Pinto, E., Nieuwerburgh, L., Barros, M., Pedersen, M., Colepicolo, P., and Snoeijs, P. (2003). Density dependant patterns in thiamine and pigment production in the diatom *Nitzschia microcephala*. *Phytochemistry* 63, 155–163.

Provasoli, L. (1963). "Organic regulation of phytoplankton fertility," in *The Sea*, ed M. N. Hill (New York, NY: Interscience), 165–219.

Provasoli, L., and Carlucci, A. F. (1974). "Vitamins and growth regulators," in *Algal Physiology and Biochemistry*, ed W. P. D Stewart (Oxford: Blackwell), 741–787.

Ransom Hardison, D., Sunda, W. G., Litaker, R. W., Shea, D., and Tester, R. A. (2012). Nitrogen limitation increases brevetoxins in *Karenia brevis*: implications for bloom toxicity. *J. Phycol.* 48, 844–858.

Rapala-Kozik, M., Wolak, N., Kujda, M., and Banas, A. K. (2012). Upregulation of thiamine biosynthesis in *A. thaliana* seedlings under salt and osmotic stress conditions is mediated by abscisic acid at the early stages of this stress response. *BMC Plant Biol.* 12:2. doi: 10.1186/1471-2229-12-2

Raux, E., Schubert, H. L., and Warren, M. J. (2000). Biosynthesis of cobalamin (vitamin B_{12}): a bacterial conundrum. *Cell. Mol. Life Sci.* 57, 1880–1893.

Rodionov, D. A., Vitreschak, A. G., Mironov, A. A., and Gelfand, M. S. (2002). Comparative genomics of thiamine biosyntheisis in prokaryotes. *J. Biol. Chem.* 277, 48949–48959.

Rodionov, D. A., Vitreschak, A. G., Mironov, A. A., and Gelfand, M. S. (2003). Comparative genomics of the Vitamin B_{12} metabolism and regulation in prokaryotes. *J. Biol. Chem.* 278, 41148–41159.

Roth, J. R., Lawrence, J. G., and Bobik, T. A. (1996). Cobalamin (coenzyme B_{12}): synthesis and biological significance. *Annu. Rev. Microbiol.* 50, 137–181.

Saito, M. A., Goepfert, T. J., and Ritt, J. T. (2008). Some thoughts on the concept of colimitation: three definitions and the importance of bioavailability. *Limnol. Oceanogr.* 53, 276–290.

Sañudo-Wilhelmy, S. A., Cutter, L., Durazo, R., Smail, E., Gomez-Consarnau, L., Webb, E. A., et al. (2012). Multiple B-vitamin deficiency in large areas of the coastal ocean. *Proc. Natl. Acad. Sci. U.S.A.* 109, 14041–14045.

Sañudo-Wilhelmy, S. A., Okbamichael, M., Gobler, C. J., and Taylor, G. T. (2006). Regulation of phytoplankton dynamics by vitamin B12. *Geophys. Res. Lett.* 33, LO4604.

Scheffel, A., Poulsen, N., Shian, S., and Kroger, N. (2011). Nanopatterned protein microrings from a diatom that direct silica morphognesis. *Proc. Natl. Acad. Sci. U.S.A.* 108, 3175–3180.

Schrauzer, G. N., and Deutsch, E. (1969). Reactions of cobalt(I) supernucleophiles. the alkylation of vitamin B12s, cobaloximes (I), and related compounds. *J. Am. Chem. Soc.* 91, 3341–3350.

Scott, J. M., and Weir, D. G. (1981). The methyl folate trap: a physiological response in man to prevent methyl group deficiency in kwashiorkor (methionine deficiency) and an explanation for folic-acid-induced exacerbation of subacute combined degeneration in pernicious anaemia. *Lancet* 318, 337–340.

Shihira, I., and Krauss, R. W. (1965). *Chlorella: Physiology and Taxonomy of 41 Isolates.* College Park, PA: University of Maryland Press.

Stefels, J. P. (2000). Physiological aspects of the production and conversion of DMSP in marine algae and higher plants. *J. Sea Res.* 43, 183–197.

Sunda, W., Kieber, D. J., Kiene, R. P., and Huntsman, S. (2002). An antioxidant function for DMSP and DMS in marine algae. *Nature* 418, 317–320.

Sunda, W. G., Hardison, R., Kiene, R., Bucciarelli, E., and Harada, H. (2007). The effect of nitrogen limitation on cellular DMSP and DMS release in marine phytopankton: climate feedback implications. *Aquat. Sci.* 69, 341–351.

Swift, D. (1981). Vitamin levels in the Gulf of Maine and ecological significance of vitamin B12 there. *J. Mar. Res.* 39, 375–403.

Swift, D. G., and Guillard, R. R. (1978). Unexpected response to vitamin B12 of dominant centric diatoms from the spring bloom in the Gulf of Maine. *J. Phycol.* 14, 377–386.

Swift, D. G., and Taylor, W. R. (1972). Growth of vitamin B12 - limited cultures: *Thalassiosira pseudonana, Monochyrsis lutheri*, and *Isochrysis galbana*. *J. Phycol.* 10, 385–391.

Takahashi, H., Kopriva, S., Giordano, M., Saito, K., and Hell, R. (2011). Sulfur assimilarion in photosynthetic organisms: molecular function and regulation transporters and assimilatory proteins. *Annu. Rev. Plant Biol.* 62, 157–184.

Tang, Y. Z., Koch, F., and Gobler, C. J. (2010). Most harmful algal bloom species are vitamin B1 and B_{12} auxotrophs. *Proc. Natl. Acad. Sci. U.S.A.* 107, 20756–20761.

Teeling, H., Fuchs, B. M., Becher, D., Klockow, C., Gardebrecht, A., Bennke, C. M., et al. (2012). Substrate-controlled succession of marine bacterioplankton populations induced by a phytoplankton bloom. *Science* 336, 608–611.

Toulza, E., Shin, M. S., Blanc, G., Audic, S., Laabir, M., Collos, Y., et al. (2010). Gene expression in proliferating cells of the dinoflagellate *Alexandrium catenella*. *Appl. Environ. Microbiol.* 76, 4521–4529.

Webb, M., Marquet, A., Mendel, R., Rebeille, F., and Smith, A. (2007). Elucidating biosynthetic pathways for vitamins and cofactors. *Nat. Prod. Rep.* 24, 988–1008.

Worden, A. Z., Lee, J. H., Mock, T., Rouzé, P., Simmons, M. P., Aerts, A. L., et al. (2009). Green evolution and dynamic adaptations revealed by genomes of the marine picoeukaryotes *Micromonas*. *Science* 324, 268–274.

Zehr, J. P., and Ward, B. B. (2002). Nitrogen cycling in the ocean: new perspectives on processes and paradigms. *Appl. Environ. Microbiol.* 68, 1015–1024.

Zhang, Y., Rodionov, D. A., Gelfand, M. S., and Gladyshev, V. N. (2009). Comparative genomics analysis of nickel, cobalt, and vitamin B_{12} utilization. *BMC Genomics* 10:78. doi: 10.1186/1471-2164-10-78

Conflict of Interest Statement: The authors declare that the research was conducted in the absence of any commercial or financial relationships that could be construed as a potential conflict of interest.

Received: 07 August 2012; paper pending published: 12 September 2012; accepted: 02 October 2012; published online: 19 October 2012.

*Citation: Bertrand EM and Allen AE (2012) Influence of vitamin B auxotrophy on nitrogen metabolism in eukaryotic phytoplankton. Front. Microbio. **3**:375. doi: 10.3389/fmicb.2012.00375*

This article was submitted to Frontiers in Aquatic Microbiology, a specialty of Frontiers in Microbiology.